



Document Number: ICT-317669-METIS/D3.3

Project Name:  
Mobile and wireless communications Enablers for the Twenty-twenty Information  
Society (METIS)

## Deliverable D3.3

Final performance results and consolidated view on the  
most promising multi-node/multi-antenna transmission  
technologies

Date of delivery: 28/02/2015  
Start date of Project: 01/11/2012

Version: 1  
Duration: 30 months



# Deliverable D3.3

## Final performance results and consolidated view on the most promising multi-node/multi-antenna transmission technologies

<b>Project Number:</b>	ICT-317669
<b>Project Name:</b>	Mobile and wireless communications Enablers for the Twenty-twenty Information Society

<b>Document Number:</b>	ICT-317669-METIS/D3.3
<b>Document Title:</b>	Final performance results and consolidated view on the most promising multi-node/multi-antenna transmission technologies
<b>Editor(s):</b>	P. Baracca (ALU), D. Aziz (ALU)
<b>Author(s):</b>	D. Aziz (ALU), P. Baracca (ALU), E. de Carvalho (AAU), R. Fantini (TI) and N. Rajatheva (UOULU) P. Popovski, J. H. Sørensen, H. Thomsen (AAU) T. Svensson, J. Li, T. R. Lakshmana, Y. Sui (CTH) A. Benjebbour, S. Suyama (DOCOMO) R. Abrahamsson, G. Fodor (EAB) A. Jaziri, D.T. Phan Huy, H. Khanfir, R. Visoz, Y. Yuan, Y. Lejosne, A. Mohamad, A.Saadani, S. Smirani (FT) M. Kurras, L. Thiele (HHI) M. Castañeda, N. Vucic, M. Iwanow (HWDU) S. Ben Slimane, H. Ghauch, M. Skoglund, S. M. Kim, M. Bengtsson, R. Mochaourab (KTH) T. Ihalainen (NOKIA) W. Zirwas (NSN) P. Sroka, K. Ratajczak, K. Bąkowski (PUT) K. Guo (RWTH) G. Dell'aera, B. Melis, M. Caretti (TI) C. Bockelmann, F. Lenkeit (UB) A. Tölli, K. S. Jayasinghe (UOULU) S. Roger, D. Calabuig, J. F. Monserrat (UPVLC) M. Sternad (CTH/UU)
<b>Dissemination Level:</b>	Public



<b>Contractual Date of Delivery:</b>	28/02/2015
<b>Status/Issue:</b>	Final
<b>Version:</b>	1
<b>File Name:</b>	METIS_D3.3_v1

### Revision History:

Revision	Date	Issued by	Description
1	28/02/2015	METIS	D3.3 release v1

### Abstract:

This document provides the most recent updates on the technical contributions and research challenges focused in WP3. Each Technology Component (TeC) has been evaluated under possible uniform assessment framework of WP3 which is based on the simulation guidelines of WP6. The performance assessment is supported by the simulation results which are in their mature and stable state. An update on the Most Promising Technology Approaches (MPTAs) and their associated TeCs is the main focus of this document. Based on the input of all the TeCs in WP3, a consolidated view of WP3 on the role of multinode/multi-antenna transmission technologies in 5G systems has also been provided. This consolidated view is further supported in this document by the presentation of the impact of MPTAs on METIS scenarios and the addressed METIS goals.

### Keywords:

Multi-antenna, Massive-MIMO, inter-node coordination, relay, multi-hop communication, wireless network coding, mm-waves



## Executive summary

This document presents the final performance results and consolidated view on the most promising multi-node/multi-antenna transmission technologies proposed and investigated by Work Package 3 (WP3). These proposals on the multi-node/multi-antenna transmission technologies serve as one of the essentials for achieving the METIS project goals, which are 1000x data volume, 10-100x user data rate, 10-100x number of devices, 10x longer battery life, 5x E-E reduced latency and energy efficiency and cost.

The WP3 is structured into tasks, research clusters, and technology components. Each task focuses on an aspect of multi-node/multi-antenna transmission. There are three tasks in WP3. Each partner in the work package has presented research work (to achieve METIS goals) in terms of one or more technology components. The research proposals are assessed with the help of a common evaluation framework based on research clusters (as reported in [METIS14-D32]). Using these results, we were able to identify the most promising technology approaches in each task. In addition to that, we have also reported the consolidated statements based on the results of all the technology components in WP3. The main part of this document presents the impact of WP3 contributions on the development of 5G-METIS system concept. Further details of achievements and performance results of each technology component are reported in the appendix.

Task 3.1 (T3.1) has identified that Massive MIMO as in-band backhaul is a significant enabler of ultra dense networks and an essential feature for the goal of capacity increase in 5G systems. The results have shown that with low complexity techniques proposed in this approach we can achieve up to 200% gain in spectral efficiency on backhaul. Another high potential approach that has been identified is Massive MIMO for access. According to the performance analysis, our proposed resource allocation and 3D beamforming techniques allow us to achieve 10 times higher spectral efficiency than LTE-A.

Task 3.2 (T3.2) has identified two main approaches as very promising ones for 5G systems. First, the use of UEs with advanced capabilities which can alleviate the coordination complexity at the network side. Then, CoMP with limited backhaul capabilities which addresses the issues of backhaul bottleneck and provides solutions for the realization of the gains of CoMP in 5G systems. The research work in this task enables us to achieve compared to the baseline up to 50% transmit power saving and up to 55% gain in spectral efficiency when constrained backhaul is considered.

Task 3.3 (T3.3) has identified in-band backhaul and access for its most promising technologies. Here, the technology components consider heterogeneous networks at lower frequencies (<10GHz) and also mesh networks at mm-waves for indoor scenarios. The results have shown that with these approaches we can achieve user rates in the order of Gbps which also allow us to serve very high number of devices in a given coverage area.

The performance results reported in this document show that the focus of WP3 on multi-node/multi-antenna transmission is very well positioned in the project. These results show a good mixture of short-term and long-term impact of WP3 contributions on the development of 5G systems.



## Contents

1	Introduction .....	1
2	Task 3.1: Multi-antenna/Massive-MIMO .....	3
2.1	General overview .....	3
2.2	Most Promising Technology Approach 1: Massive MIMO for Backhaul .....	5
2.3	Most Promising Technology Approach 2: Massive MIMO for Access .....	10
2.4	Impact on METIS system.....	25
2.5	Overview of achieved results .....	25
2.6	Conclusion .....	26
3	Task 3.2: Advanced inter-node coordination.....	27
3.1	General overview .....	27
3.2	Most Promising Technology Approach 1: CoMP with advanced UE capabilities .....	29
3.3	Most Promising Technology Approach 2: CoMP with limited backhaul capabilities ..	42
3.4	Impact on METIS system.....	51
3.5	Overview of achieved results .....	52
3.6	Conclusion .....	53
4	Task 3.3: Multi-hop communications/wireless network coding .....	55
4.1	General overview .....	55
4.2	Most Promising Technology Approach 1: Heterogeneous network at lower frequencies .....	56
4.3	Most Promising Technology Approach 2: Indoor dense mesh network at mm-waves	65
4.4	Impact on METIS system.....	69
4.5	Overview of achieved results .....	70
4.6	Conclusion .....	70
5	Conclusion .....	71
6	References.....	72
7	Appendix A: Final results for Task 3.1 .....	77
7.1	T3.1 TeC 1 MIMO communications with large aperture massive array systems [AAU]	77
7.2	T3.1 TeC 1b: DFT based spatial multiplexing and maximum ratio transmission for mm-wave large MIMO [AAU, FT, UOULU] .....	77
7.3	T3.1 TeC 1c: MIMO communications with large aperture massive array systems [AAU]	84
7.4	T3.1 TeC 2: Coordinated resource and power allocation for pilot and data signals in multicell massive SIMO systems [EAB] .....	89
7.5	T3.1 TeC 3: Modelling with spherical waves, linear precoding [HHI].....	98
7.6	T3.1 TeC 4: Multi-cell MU-MIMO in real world scenarios – performance evaluation of EVD-based channel covariance feedback and multi-path extraction in massive MIMO systems [NOKIA] .....	98
7.7	T3.1 TeC 5: Model based channel prediction [NSN].....	98
7.8	T3.1 TeC 6: Adaptive large MISO Downlink with predictor antenna array for very fast moving vehicles [FT, CTH, UU] .....	107
7.9	T3.1 TeC 7: Massive MIMO transmission using higher frequency bands based on measured channels with CSI error and hardware impairments [DOCOMO] .....	115
7.10	T3.1 TeC 8: Massive MIMO and ultra-dense networks [ALU].....	122
7.11	T3.1 TeC 9: Eigenvalue decomposition (EVD) based channel estimation for MU-MIMO [RWTH] .....	122
7.12	T3.1 TeC 9b: Uplink power control with MMSE receiver in multi-cell MU-Massive-MIMO [RWTH] .....	122
7.13	T3.1 TeC 10: Decentralized coordinated transceiver design with large antenna arrays [UOULU] .....	128
7.14	T3.1 TeC 11: Massive SDMA with a LSAS exploiting elevation and azimuth beamforming [HHI].....	134



8 Appendix B: Final results for Task 3.2 ..... 144

8.1 T3.2 TeC 1: Multi-node resource allocation under imperfect feedback and backhaul channels [CTH]..... 144

8.2 T3.2 TeC 1b: Non-coherent joint processing CoMP for energy-efficient small cell networks [CTH]..... 144

8.3 T3.2 TeC 1c: Precoder design with limited information in CoMP networks [CTH]... 151

8.4 T3.2 TeC 2: Exploiting temporal channel correlation to reduce feedback in CoMP scheme [FT]..... 155

8.5 T3.2 TeC 2b: DoF and net DoF of recent schemes for the MIMO IC and BC with delayed CSIT and finite coherence time [FT] ..... 155

8.6 T3.2 TeC 3: Distributed precoding in multicell multiantenna systems with data sharing [HWDU]..... 160

8.7 T3.2 TeC 4: Real world interference alignment [ALU] ..... 171

8.8 T3.2 TeC 5: Semi-distributed IA algorithm for MIMO-IC channel, with power control convergence speed up [FT]..... 180

8.9 T3.2 TeC 5b: Distributed interference alignment techniques under imperfect channel state information [FT]..... 180

8.10 T3.2 TeC 6: Distributed low-overhead schemes for MIMO Interference Channels [KTH] 187

8.11 T3.2 TeC 7: Dynamic clustering with multiple receive antennas in downlink CoMP systems [ALU]..... 195

8.12 T3.2 TeC 8: Studies on non-orthogonal multiple access (NOMA) [DOCOMO] ..... 202

8.13 T3.2 TeC 9: Coordination scheme for medium range interference with message splitting to facilitate efficient SIC [EAB]..... 210

8.14 T3.2 TeC 10: Hierarchical precoding for ultra dense networks with enhanced multi-antenna receive processing [HHI]..... 210

8.15 T3.2 TeC 11: Decentralized interference aware scheduling [NOKIA]..... 220

8.16 T3.2 TeC 12: Network-assisted interference suppressing/cancelling receivers and ultra-dense networks [NOKIA] ..... 220

8.17 T3.2 TeC 13: Extension of IMF-A interference mitigation framework to small cell scenarios and Massive-MIMO – The OP CoMP concept [NSN]..... 226

8.18 T3.2 TeC 14: Joint dynamic clustering and coordinated scheduling for relaying with physical layer network coding [PUT]..... 234

8.19 T3.2 TeC 15: Adaptive and energy efficient dense small cells coordination [TI] ..... 240

8.20 T3.2 TeC 16: Non-coherent communication in coordinated systems [UPVLC] ..... 247

8.21 T3.2 TeC 17: Bidirectional signalling for dynamic TDD [UOULU]..... 252

9 Appendix C: Final results for Task 3.3 ..... 259

9.1 T3.3 TeC 1: Coordinated multi-flow transmission for wireless backhaul [AAU] ..... 259

9.2 T3.3 TeC 2: Interference aware routing and resource allocation in a millimetre-wave ultra-dense network [EAB] ..... 266

9.3 T3.3 TeC 3: Virtual full-duplex buffer-aided relaying [KTH] ..... 274

9.4 T3.3 TeC 4: Distributed coding for the multiple access multiple relay channel [FT] 283

9.5 T3.3 TeC 5: Bi-directional relaying with non-orthogonal multiple access [UB] ..... 290

9.6 T3.3 TeC 6 MIMO physical layer network coding based underlay D2D communication [UOULU] ..... 297

9.7 T3.3 TeC 6b: MIMO PLNC based D2D communication [UOULU]..... 297

9.8 T3.3 TeC 7: Cooperative D2D communications [KTH] ..... 303

9.9 T3.3 TeC 8: Open-loop techniques in a network with D2D relaying [UPVLC] ..... 311

9.10 T3.3 TeC 9a: Studies of deploying moving relay nodes [CTH] ..... 311

9.11 T3.3 TeC 9b: Uplink enhancement of vehicular users by using D2D communications [CTH] 320

9.12 T3.3 TeC 10: MIMO techniques for TDD wireless systems with relaying [PUT]..... 325

10 Appendix D: List of Specific METIS Abbreviations..... 331

10.1 List of METIS WP3 partners ..... 331



---

**Document:** FP7-ICT-317669-METIS/D3.3

**Date:** 25/02/2015

**Security:** Public

**Status:** Final

**Version:** 1

---

10.2	List of METIS Horizontal Topics.....	331
10.3	List of METIS Test Cases .....	331

## List of Abbreviations, Acronyms, and Definitions

3GPP	Third Generation Partnership Project
5G	Fifth Generation
ABS	Almost Blank Subframe
AgN	Aggregation Node
AMC	Adaptive Modulation and Coding
AN	Access Node
AP	Access Point
ARQ	Automatic Repeat Request
ARTIST4G	Advanced Radio Interface Technologies for 4G Systems
ASCIC	Advanced Successive Corrected Interference Cancellation
AWCSCGN	Additive White Circular Symmetric Complex Gaussian Noise
AWGN	Additive White Gaussian Noise
BB	BaseBand
BC	Broadcast Channel
BD	Block Diagonalization
BDIA	Block Diagonalization Interference Alignment
BER	Bit Error Rate
BF	BeamForming
BLER	Block Error Rate
BPSK	Binary Phase Shift Keying
BR	Buffer-Aided Relaying
BS	Base Station
BSOS	Border Switch Off Scheme
BVDM	Building Vector Data Map
CA	Carrier Aggregation
CBR	Constant Bit Rate
CC	Component Carrier
CCI	Co-Channel Interference
CD2DC	Cooperative Device-to-Device Communication
CDF	Cumulative Distribution Function
CIR	Channel Impulse Response
CMP	Coordinated Multi-Cell Precoder
CoMP	Coordinated Multi Point
CQI	Channel Quality Indicator
CRC	Cyclic Redundancy Checks
CRE	Cell Range Extension
CRS	Common reference signal
CS	Coordinated Scheduling

CSI	Channel State Information
CSI-RS	Channel State Information Reference Signal
CSIT	Channel State Information at the Transmitter
CU	Central Unit
CUE	Cellular User Equipment
D2D	Device-to-Device
DAS	Distributed Antenna System
DBSCAN	Density-Based Spatial Clustering of Applications with Noise
DC	Dynamic Clustering
DCMR	Dynamic Clustering with Multiantenna Receivers
DCSIT	Delayed CSIT
DF	Decode and Forward
DFT	Discrete Fourier Transform
DIA	Destructive Interference Addition
DIAS	Decentralized Interference Aware Scheduling
DL	Downlink
DMRS	Demodulation reference signal
DoF	Degrees of Freedom
DPC	Dirty Paper Coding
DPS/B	Dynamic Points Selection with Blanking
DUSTM	Differential Unitary Space-Time Modulation
EARTH	Energy Aware Radio and neTwork technologies
EFZF	Effective Zero Forcing
EM	EigenMode
EQPA	Equal Power Allocation
ETU	Extended Typical Urban
F-B	Forward-Backward
FBCP	Fixed BF and CSI-based Precoding
FCFB	Foresighted Channel Feedback
FD	Full-Duplex
FDD	Frequency-division Duplexing
FDMA	Frequency Division Multiple Access
felCIC	Further enhanced Inter-Cell Interference Coordination
FER	Frame Error Rate
FRN	Fixed Relay Node



FRoI	Finite Rate of Innovation
FSPA	Full Search Power Allocation
FTP	File Transfer Protocol
GBR	Guaranteed Bit Rate
GFNC	Galois Field Network Coding
GoB	Grid of Beams
GRA	Greedy Rate Approximation
HD	Half-Duplex
HetNet	Heterogeneous Network
HPBW	Half Power Beam Width
HT	Horizontal Topic
IA	Interference Alignment
IAR	Interference Aware Routing
IBLER	Individual Block Error Rate
IC	Interference Channel
ICI	Inter-Cell Interference
IDMA	Interleave Division Multiple Access
IF	Intermediate Frequency
IGI	Inter Group Interference
IMF	Interference Mitigation Framework
IRA	Irregular Repeat Accumulate
IRC	Interference Rejection Combiner
IRI	Inter-Relay Interference
IS	Interference Suppression
ISD	Inter Site Distance
ITU	International Telecommunication Union
JGP	Joint Group Precoding
JNCC	Joint Network Channel Coding
JNCD	Separate Network Channel Decoding
JP	Joint Processing
JSDM	Joint Spatial Division and Multiplexing
JT	Joint Transmission
KPI	Key Performance Indicator
L2S	Link-to-System
LM	Leakage Minimization
LOS	Line Of Sight
LS	Least Square
LSAS	Large Scale Antenna System
LTE	Long Term Evolution
LTE-A	LTE - Advanced
MA	Multiple Access
MAC	Multiple Access Channel
MAMRC	Multiple Access Multiple Relay Channel
MBCP	Model Based Channel Prediction

mBS	Micro Base Station
MBS	Macro Base Station
MCS	Modulation and Coding Scheme
MET	Multiuser Eigenmode Transmission
METIS	Mobile and wireless communications Enablers for Twenty-twenty Information Society
MF	Matched filter
MIMO	Multiple Input Multiple Output
MISO	Multiple Input Single Output
ML	Maximum Likelihood
M-MIMO	Massive MIMO
MMSE	Minimum Mean Square Error
mmW	millimetre Wave
MN	Moving Networks
MPC	Multi Path Component
MPTA	Most Promising Technology Approach
MRC	Maximum Ratio Combining
MRN	Moving Relay Node
MRT	Maximum Ratio Transmission
MS	Mobile Station
M-SDMA	Massive SDMA
MSE	Mean-Square-Error
MU	Multi-User
MU-BDBF	Multi User Block Diagonalization Beamforming
MUD	Multi-User Detection
MUI	Multi User Interference
MUICIA	Multi User Inter Cell Interference Alignment
NA	Network Assistance
NA&C	Nodes Activation and Clustering techniques
NC	Network Coding
NCJP	Non-Coherent Joint Processing
NLOS	Non Line Of Sight
NMSE	Normalized Mean Square Error
NOMA	Non-Orthogonal Multiple Access
O&M	Operation and Maintenance
OFDM	Orthogonal Frequency Division Multiplexing
OMA	Orthogonal Multiple Access
OMAC	Orthogonal Multiple Access Channel
OP	Outage Probability
OSI	Open Systems



	Interconnection
OSTBC	Orthogonal Space-Time Block Code
PAPC	Per Antenna Power Constraint
PBZF	Projection Based Zero Forcing
PC	Pilot Contamination
PDP	Power Delay Profile
PDPR	Pilot-to-Data Power Ratio
PF	Proportional Fair
PGP	Per Group Precoding
PHY	PHYSical layer
PI	Polynomial Interpolation
PLNC	Physical Layer Network Coding
PMI	Precoding Matrix Indicator
PRB	Physical Resource Block
PSO	Particle Swarm Optimization
QoS	Quality of Service
QOSTBC	Quasi-Orthogonal Space-Time Block Code
QuaDRiGa	Quasi-Deterministic Radio Channel Generator
RA	Resource Allocation
RB	Resource Block
RC	Research Cluster
RF	Radio Frequency
RIA	Retrospective Interference Alignment
RN	Relay Node
RR	Round Robin
RSCC	Recursive Systematic Convolutional Code
RSOS	Random Switch Off Scheme
RSSI	Received Signal Strength Indicator
RU	Resource Utilization
RV	Regularization Value
RZF	Regularized ZF
SBS	Small cell BS
SC	Small Cell
SCIC	Successive Corrected Interference Cancellation
SCP	Single Cell Processing
SDMA	Spatial Division Multiple Access
SE	Spectral efficiency
SFBC	Space Frequency Block Coding
SIC	Successive Interference Cancellation
SIMO	Single Input Multiple Output

SINR	Signal to Interference plus Noise Ratio
SISO	Single Input Single Output
SLIC	Symbol-level interference cancellation
SLNR	Signal to Leakage Interference plus Noise Ratio
SM	Spatial Multiplexing
SNR	Signal to Noise Ratio
SOC	Second Order Cone
SOCP	Second Order Cone Programming
SO-MAMRC	Semi Orthogonal Multiple Access Multiple Relay Channel
SON	Self-Optimizing Network
SOS	Switch Off Scheme
SotA	State of the Art
SRTA	Separate Receive and Training Antenna
S-SDMA	Sparse SDMA
STC	Space-Time Code
STIA	Space Time Interference Alignment
ST-RRM	Short Term Radio Resource and Interference Management
SU	Single-User
SUS	Semi-orthogonal User Selection
SVD	Singular Value Decomposition
TC	Test Case
TDD	Time Division Duplex
TDMA	Time Division Multiple Access
TeC	Technology Component
TM	Transmission Mode
TP	ThroughPut
TTI	Transmission Time Interval
TWR	Two Way Relaying
UDN	Ultra Dense Network
UE	User Equipment
UFMC	Universal Filtered Multi Carrier
UL	Uplink
ULA	Uniform Linear Array
ULPwrCtrl	Uplink Power Control
UMa	Urban Macro
UPA	Uniform Planar Array
UPC	Uncoordinated Power Control
URC	Ultra Reliable Communications
UTP	User Throughput



VFD	Virtual Full-Duplex
VLA	Very Large Aperture
VPL	Vehicular Penetration Loss
VUE	Vehicular User Equipment
WEW	Wireless Emulated Wire
WINNER	Wireless world INitiative NEw Radio

WLBH	Wireless Backhaul
WMMSE	Weighted MMSE
WNC	Wireless Network Coding
WUS	Without User Selection
ZF	Zero-Forcing
ZFBF	Zero-Forcing BeamForming

## 1 Introduction

The document at hand is the Deliverable (D3.3) on the final performance assessment of the Technology Components (TeCs) proposed by the partners in WP3. The D3.3 is the final step in continuation with the previous deliverables [METIS13-D31] and [METIS14-D32]. The major objective in [METIS14-D32] was to provide preliminary results on TeCs and to define the alignment strategies along WP3 with respect to the evaluation of the TeCs. These alignment strategies were based on adopting WP6 simulation guidelines, using channel models from WP1, common parameters and assumptions, TeC complementary analysis within WP3 and evaluating the impact on Test Cases (TCs). As a result of this alignment campaign in [METIS14-D32], we were able to come up with an identification of a first set of TeCs that defines the Most Promising Technology Approaches (MPTAs) in WP3. Specifically, we have defined two MPTAs in each of the three tasks in WP3 (see also Figure 1-1).

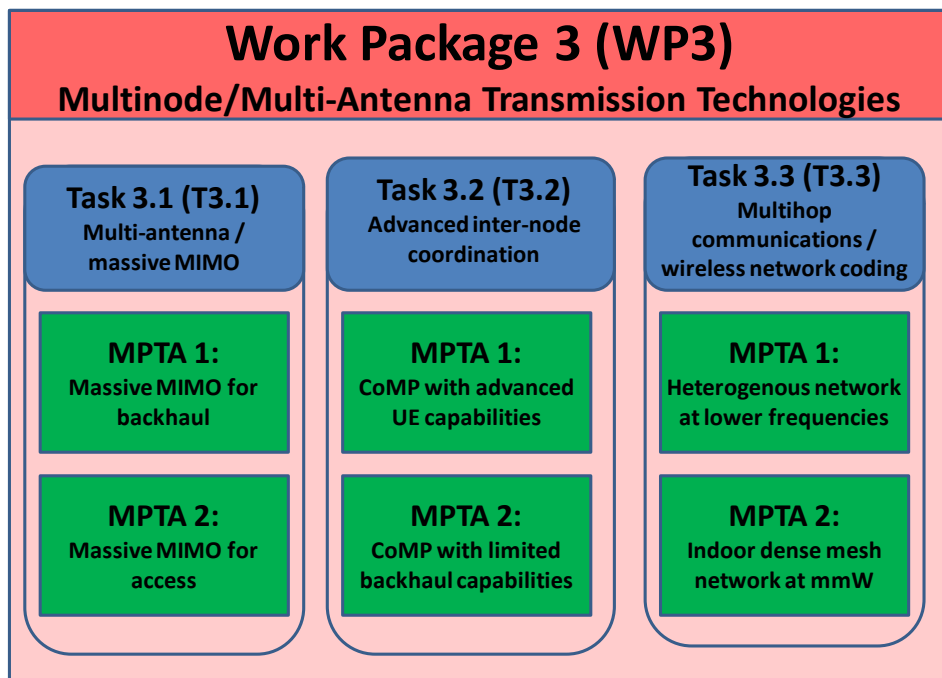


Figure 1-1: WP3 structure

In D3.3, we report the performance assessment of all the TeCs under the alignment framework of [METIS14-D32]. This includes the reporting of performance evaluation of each TeC in the most possibly aligned simulation scenarios. As a result of the new, aligned and intensive technical evaluation, we have to revise the set of TeCs constituting MPTAs in each task of WP3. In particular, in Task 3.1 we have added new TeCs in MPTAs. Based on the new and promising results from the partners, in Task 3.2 we have introduced a new MPTA.

Task 3.1 (T3.1) focuses on the role of Massive MIMO for high spectral and energy efficiency in 5G systems. Major research in this task has been done to enable the theoretical gains of Massive MIMO in practical scenarios. The contributions provide solutions to alleviate the practical limitations of massive antenna arrays and to realize the potential gains. The key problems that have been addressed are pilot and data power allocation, RF-chain management, acquisition of channel state information, transmit and receive processing optimization. As the potential of massive antenna arrays can easily be exploited for backhaul, therefore, the research in this task targets not only the enablement of Massive MIMO for access but also for in-band backhauling. Moreover, the contributions consider both legacy frequencies and frequencies above 6 GHz.



Task 3.2 (T3.2) envisions 5G as a ultra dense network of nodes. The purpose of this task is to target the high spectral efficiency, increase in average user throughput, higher number of served users as well as energy efficiency. The technical contributions are based on the exploitation of multiple antennas and inter node cooperation techniques. One of the focuses is to enable the CoMP technologies for 5G. This leads to the evolution of CoMP transmission techniques considering also limited backhaul and channel state information. In addition to this, the research in this task provides solutions that exploit the advanced UE capabilities (e.g. multiple antennas) for interference cancellation techniques. These techniques help to achieve high spectral and energy efficiency for 5G systems.

Task 3.3 (T3.3) considers different aspects of multi node and multi hop heterogeneous networks. The performance metrics targeted here are spectral efficiency, user throughput and number of served users. One of the major research focuses is to enable in-band backhaul and access especially for relaying scenarios. The solutions are based on virtual-full duplex relaying and wireless network coding. The task also addresses the exploitation of mmW for indoor scenarios to serve a high density of users and increase the average user throughput. Moreover, solutions for efficient device to device communications are provided.

This deliverable is organized as follows. Sections 2, 3 and 4 are dedicated respectively to Task 3.1, 3.2 and 3.3. For the sake of a self-contained document, each section initiates with a general overview of the task. Following the task overview, we introduce the MPTAs. Each MPTA section contains an introduction and performance results from the associated TeCs. Then we provide the METIS goals addressed by this MPTA. Each task section ends with a description of the impact on METIS system concept, an overview of achieved results and conclusion. Using these subsections, we have reported the consolidated statements based on the results of all the TeCs in WP3. Finally, the main part of the document is concluded with an overview of the solutions and achieved results in WP3 as well as some open research challenges.

Another important part of this report is the appendix where a more thorough technical description of TeCs and their results are included. The reader is advised to refer to the appendix for the details of any TeC in order to obtain a better understanding of the consolidated statements.

Finally, note that some new TeCs have appeared in D3.3 and some TeCs were completed during the course of [METIS14-D32], where we associated each TeC in each task to one of the Research Clusters (RCs) in the task. The RC based alignment framework is still used for evaluation in D3.3. However, here we have not used RC based classification, as per the description of work we comply to provide MPTAs for the development of 5G-METIS system concept.

## 2 Task 3.1: Multi-antenna/Massive-MIMO

### 2.1 General overview

Multi-antenna/Massive-MIMO plays an increasingly important role in the research conducted for 5G systems around the world. In Task 3.1 this is expected to be more crystallized with concrete contributions addressing different aspects of massive-MIMO with many publications to date. The work is carried out in two research clusters (RCs) as defined in [METIS13-D31] under different TeCs. RC1 looks into more realistic scenarios, whereas RC2 aims at making more fundamental investigations. In both clusters TDD is considered. The current TeCs in RC1 comprise of large aperture, mm-wave, pilot/data trade offs, channel prediction and moving network applications. In RC2 we consider uplink and downlink resource allocation schemes. Among all the TeCs from both RCs, two main most promising technology approaches (MPTAs) are identified:

- massive-MIMO for backhaul (MPTA 1);
- massive-MIMO for access (MPTA 2).

These are expected to be incorporated into the final METIS 5G system architecture.

From T3.1 one of the key areas considered to contribute to a 5G system is backhaul. This may prove to be very significant due to anticipated proliferation of ultra dense networks and vehicular networks with high capacity. Therefore, one of the MPTAs is Massive MIMO for in-band backhaul. This is investigated in TeC 1b which utilizes mm-waves and symmetric MIMO, and also in TeC 6 which focuses on high mobility. Energy saving and improvement in spectral efficiency are expected as direct outcomes.

One of the most significant aspects in a 5G network is access. Here we consider how massive-MIMO access TeCs chosen as MPTAs contribute to achieve METIS goals in specific test case scenarios. The TeCs come from both research clusters and investigate mm-waves and CSI error as well as general resource allocation and beamforming methods. For better understanding of the access scenario investigated by the TeCs in this approach, a typical multi-cell configuration is considered with massive-MIMO base stations.

In the following the details of the TeCs comprising MPTAs are given. However, in Table 2.1 we have listed all the TeCs (along with their short description) that have been proposed within T3.1. For the detailed assessment of the TeCs in T3.1 we refer to the appendix and references therein.

**Table 2.1: Full List of TeCs in Task 3.1**

TeC #	Short Title	Short description	MPTA
TeC 1	Large aperture massive MIMO	Development of low-complexity and energy-efficient multi-antenna transceiver techniques for Large Aperture Massive Array Systems.	—
TeC 1b	DFT-SM-MRT	Discrete Fourier Transform (DFT) based spatial multiplexing (SM) and maximum ratio transmission (MRT) for mm-wave large MIMO.	MPTA 1
TeC 1c	Very Large Aperture Massive MIMO	Random access scheme to very large aperture massive array systems.	—
TeC 2	Coordinated Resource and Power Allocation for Massive MIMO	This TeC enables multicell massive SIMO/MIMO systems to coordinate the resources used for pilot and data transmission. The goal of the coordination is to mitigate or avoid pilot contamination and maximize spectrum efficiency	MPTA 2



		by smart allocation of resources to pilot and data transmission.	
TeC 3	Modelling with spherical waves, Linear precoding	The influence on spectral efficiency caused by spherical instead of planar waves is considered in the channel model. The spherical model is necessary due to the increased aperture size, which is linked with the large number of antennas when assuming fixed antenna spacing.	---
TeC 4	EVD-based blind channel covariance estimation	Analyse the performance of eigenvalue decomposition (EVD) based blind channel covariance estimation methods and compare them with ideal multi-path extraction, also to investigate the feasibility of massive MIMO systems with non-reciprocal duplex channels.	---
TeC 5	Model Based Channel Prediction (MBCP)	Interference mitigation based on tight cooperation like JT CoMP as well as massive MIMO are very sensitive to accurate knowledge of channel state information for transmitter sided precoding. Channel prediction can be seen as main enabler for such advanced schemes as it robustifies the system performance, releases latency requirements for backhaul networks – especially important for integration of small cells – and reduces the required feedback rate in case of full division duplex (FDD) systems. Novel extensions like bandwidth enlargement, virtual beamforming, massive MIMO and model based channel prediction are proposed to enhance state of the art performance in this area.	---
TeC 6	Predictor antenna array for fast moving vehicles	Adaptive Large MISO Downlink with Predictor Antenna Array for very fast moving vehicles.	MPTA 1
TeC 7	M-MIMO-MMW	Massive MIMO (M-MIMO) transmission using higher frequency bands based on measured channels with CSI error and hardware impairments.	MPTA 2
TeC 8	Massive MIMO and ultra dense networks	Study of a TDD based network architecture with the aim of integrating a massive MIMO macro network with a dense layer of small cells (SCs).	---
TeC 9	Eigenvalue decomposition (EVD) based channel estimation for MU-MIMO	Analytical and simulation based study on the use of an improved EVD-based channel estimation (widely linear algorithm) in multi-cell MU-Massive-MIMO systems.	---
TeC 9b	Uplink power control for massive MIMO (ULPwrCtrl)	Uplink per-user pilot and data transmit power control satisfying per-user power and SINR constraints.	MPTA 2
TeC 10	Decentralized coordinated transceiver design with large	Decouples the precoder optimization subproblems at different BSs for a minimum power beamforming by utilizing a large dimension approximation for inter-cell interference (ICI) terms	MPTA 2

	antenna arrays	as the coupling variables.	
TeC 11	Interference aware massive SDMA with massive MIMO	This TeC exploits the multiplexing and beamforming gain offered by large antenna systems with massive space-division multiple access combining interference aware user clustering, user grouping and interference aware precoding.	MPTA 2

## 2.2 Most Promising Technology Approach 1: Massive MIMO for Backhaul

### 2.2.1 Introduction

It is expected that mm-wave communication will enable the utilization of a large chunk of the spectrum in 5G networks. Channel measurements in these frequency regions are being conducted in WP1 T1.2. In TeC 1b we look at backhaul possibilities with mm-wave. Wireless inband backhaul can be considered as a key direction with massive-MIMO. Indeed, massive arrays of hundreds of antennas at both the transmitter and the receiver sides can be used to multiplex hundreds of data streams in the spatial domain. Massive MIMO for in-band backhaul has been explored in TeC 1b to provide a huge spectral efficiency in the order of hundreds of bits/s/Hz. As mm-wave transmission is very sensitive to mobility, this TeC targets a static scenario (for instance a link between base stations). In TeC 6, a new scheme, called “Polynomial Interpolation” (PI), is proposed specifically for large MISO downlink beamforming in TDD. The objective is to provide a robust wireless backhaul for fast moving vehicular relays, with high energy efficiency at the network side.

### 2.2.2 TeC 1b: DFT based spatial multiplexing and maximum ratio transmission for mm-wave large MIMO

Massive MIMO systems, with both transmitter and receiver equipped with arrays of hundreds of antennas, can potentially deliver massive spectral efficiencies of hundreds of bits/s/Hz, and therefore Gbit/s throughput. For the particular application of backhauling in ultra dense network using short range communications (10-100 meters), one can consider the use of mm-waves. Advantageously, very compact antenna elements can be used to build the massive array. Depending on the spacing between antennas and the distance between the transmitter and the receiver, the MIMO channel matrix is likely to be ill-conditioned. Singular value decomposition (SVD) is the obvious solution to perform spatial multiplexing. However, it has a complexity in the order of  $N^3$ , where  $N$  is the number of antennas. We here propose a new system called discrete Fourier transform based spatial multiplexing (DFT-SM) with maximum ratio transmission (DFT-SM-MRT). It has a complexity in the order of  $N^2 \log_2(N)$ . When the DFT-SM scheme alone is used, the data streams are either mapped onto different angles of departures in the case of aligned linear arrays (as illustrated in Figure 2-1 a)), or mapped onto different orbital angular momentums (OAM) in the case of aligned circular arrays (as illustrated in Figure 2-1 b)). Maximum ratio transmission pre-equalizes the channel and compensates for arrays misalignments. The proposed scheme performs better in line of sight configuration and if misalignments remain slight.

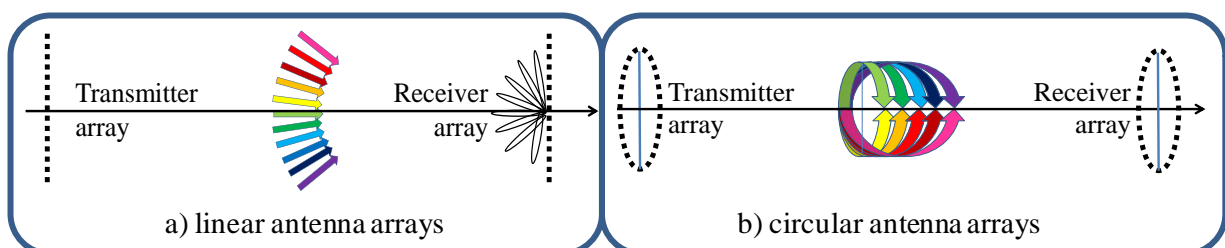
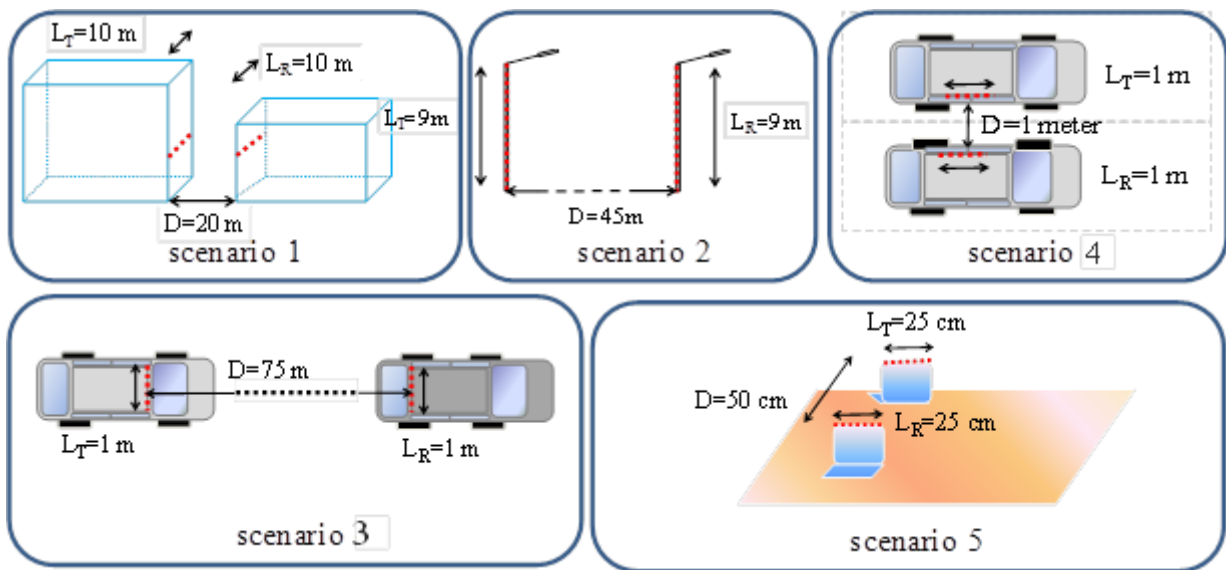


Figure 2-1: Mapping of streams onto a) angles for linear arrays, b) OAMs on circular arrays

## Performance Results

In [METIS14-D32], simulation results have shown that massive spectral efficiencies could be reached with DFT-SM-MRT, for particular values of  $R$ ,  $D$  and  $f$ , where  $R$  is the radius of the circular array ( $R$  being also half of the length of the linear array),  $D$  is the transmitter-receiver distance and  $f$  is the carrier frequency. For example, for  $R=3$  m,  $D=45$  m and  $f=60$  GHz, (assuming no phase noise) massive spectral efficiencies of 189 to 1000bits/s/Hz is attained depending on the type of array, the level of misalignment and the presence of reflectors. It has been shown that, DFT-SM-MRT achieves 1/3 to 1/14 of SVD performance, with a complexity  $N^2 \log_2(N)$ , i.e., around  $3 \cdot 10^4$  times lower than the one of SVD for  $N=512$  antennas. Compared to a mm-wave SISO system (achieving 6bits/s/Hz with 64QAM), the proposed system reaches a spectral efficiency up to  $1000/6=166$  times higher. These results have been fully described in [PTRC+14].



**Figure 2-2: Five scenarios. N°1: building to building. N°2: lamp post to lamp post. N°3 and N°4: back-to-front and side-to-side, car-to-car in a parking lot. N°5: laptop to laptop**

In this deliverable, we do not restrict ourselves to one configuration and one carrier frequency. We provide new results which help to better understand in which deployment scenarios DFT-SM-MRT should be used, and especially with which carrier frequency. For this particular study, the focus is on Uniform Linear Arrays (ULAs). Based on the theoretical work done in [BOO06] on line of sight MIMO with aligned ULAs, we derive the following condition on the carrier frequency  $f = \frac{cD}{L_T L_R} N$ , where  $c$  is the speed of light,  $N$  is a given number of antennas (corresponding to a given cost and complexity budget),  $D$  is the distance between the ULAs,  $L_T$  and  $L_R$  are the lengths of transmit and receive ULAs, respectively. According to [BOO06], this condition guarantees that the MIMO channel matrix  $H$  has  $N$  equal eigenvalues and hence  $N$  streams can be spatially multiplexed with equal rate to maximize the capacity. Therefore, for a given geometry of the system (given values of  $L_T$ ,  $L_R$  and  $D$ ) and for a given cost and complexity budget (given value of  $N$ ), there is an optimum carrier frequency  $f = \frac{cD}{L_T L_R} N$ , which maximises the capacity. We will now determine on some practical examples, the optimum carrier frequency to be used. The five scenarios illustrated in Figure 2-2 are studied. Figure 2-3 plots the optimum carrier frequency as a function of the number of antennas  $N$  for each of the five studied scenarios. One can observe that for front-to-back car-to-car communication (scenario 3) and laptop-to-laptop communication (scenario 5), large MIMO systems (i.e. with  $N > 50$ ) will be sub-optimum even for sub-millimeter waves. One can note that for all other scenarios the optimum carrier frequency corresponds to mm-waves.

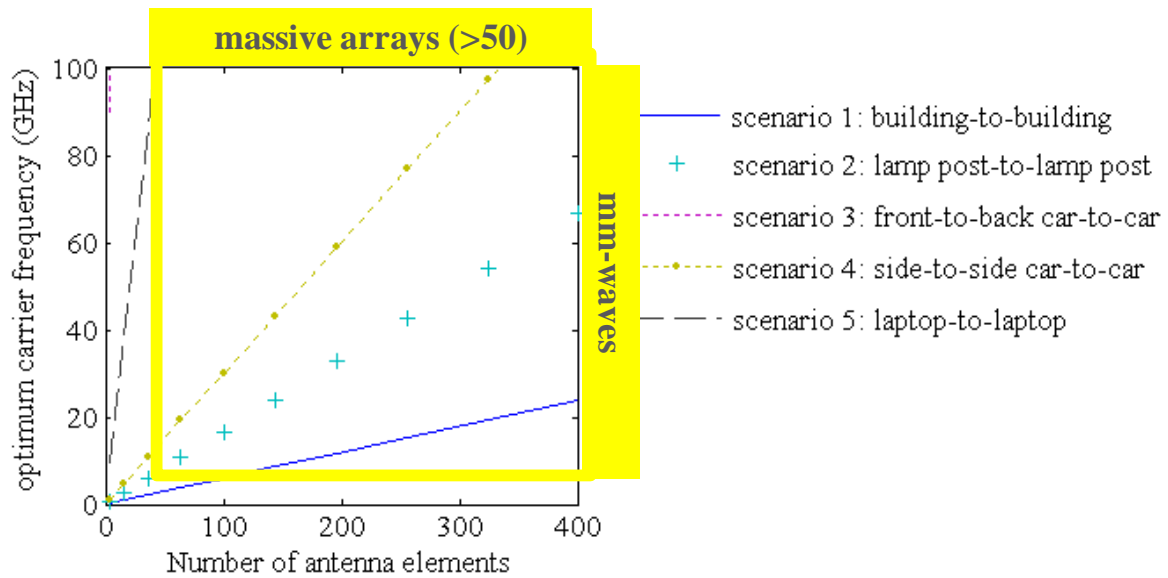


**Figure 2-3: Optimum frequency as a function of the number of antennas (these configurations guarantees that the eigen values of the MIMO matrix are equal)**

In conclusion, in this deliverable we have provided new results which do not impact the performance bounds reported in [METIS14-D32]. However, they help us better understand in which deployment scenarios and more specifically with which carrier frequencies DFT-SM-MRT should be used. One of the main results of this deliverable, is that, for a given geometry and a given complexity budget, mm-waves can be optimum. Therefore, mm-waves might be usefull not only because they offer compact antenna solutions but also because they maximise the capacity.

### 2.2.3 TeC 6: Adaptive large MISO downlink with predictor antenna array for very fast moving vehicles

A new scheme called “Polynomial Interpolation” (PI) is proposed specifically for large MISO downlink beamforming in TDD. The objective is to provide a robust wireless backhaul for fast moving vehicular relays, with a high energy efficiency at the network side. Beamforming mispointing occurs at high speed, due to outdated channel state information at the BS. An array of aligned predictor antennas, placed upon the roof of the vehicle periodically sends pilots to the BS, to provide a very dense pattern of channel measurements in space. The BS interpolates the measurements to predict the channel between the BS and the receive antenna, accurately. The Polynomial Interpolation scheme is compared to several less complex prediction techniques derived from the Separate Receive and Training Antenna (SRTA) scheme [PHH13], namely a Random Switch Off Scheme (RSOS), the Border Switch Off Scheme (BSOS) and a Reference System (RS). See Appendix C section 9.1.6 of [METIS14-D32], and [PHH13][PHS+13] for further details. The RS, SRTA, SRTA-BSOS and SRTA-PI schemes are illustrated in the Figure 2-4 a), b), c) and d) respectively.

#### Performance Results

In this deliverable, we present new results on TeC6 using WP6 mobility models ([METIS13-D61] and [METIS14-D63]) at 2 GHz carrier frequency. These new results do not change the minimum and maximum values of the gains reported in [METIS14-D32]. These new results provide estimated gains in very particular scenarios: cars and pedestrians in urban environment. In this deliverable, we consider pedestrians as well as cars. Indeed, in the future, machines or robots equipped with antennas may move at pedestrian speeds. In this deliverable, we are therefore exploring the possibility to extend the field of application of this TeC from wireless backhaul only to both backhaul and access.

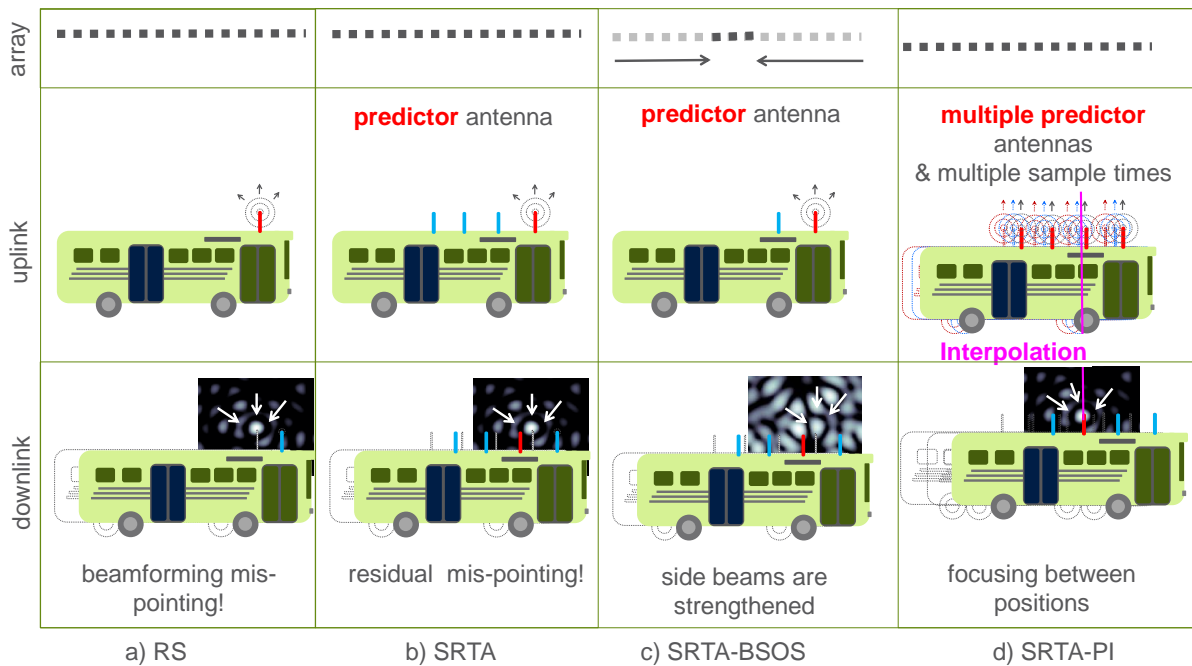


Figure 2-4: Studied schemes

In [METIS14-D32], the BLER and the energy saving metrics have been measured as the function of the vehicle speed (0-300 km/h), by simulation. We recall that the energy saving is the ratio of the power required with a SISO system over the power required with a large MISO system and adaptive beamforming. It was shown that SRTA-PI improves:

- the BLER by a factor of up to x100 when compared to RS/SRTA/SRTA-BSOS/SRTA-RSOS;
- the energy saving by a factor of up to x30 when compared to SRTA-RSOS/SRTA-BSOS.

In this new study we have used these BLER versus speed, and energy saving versus speed look up tables and combined them with WP6 mobility models to better estimate the gain from TeC6 in the particular case of a typical urban environment with typical values of speed. WP6 mobility models provide traces of the positions of 460 cars and 1500 pedestrians, every second, during one hour, in an urban environment. We have post processed these traces and computed the speed of each car, each pedestrian, every second, for one hour. Using our look up tables from [METIS14-D32], we have then computed the BLER of each car, each pedestrian, every second, for one hour. Finally, we have computed the following CDF curve for cars (see Figure 2-5) and pedestrians (see Figure 2-6) separately:  $y(x)$  = ratio of mobiles for which the BLER is guaranteed to be lower than  $x$  during 95% of the time (total time of 1hour). As [PHS+13] has shown a slightly higher performance for SRTA-RSOS compared to SRTA-BSOS, we will focus on SRTA-RSOS performance in this deliverable.

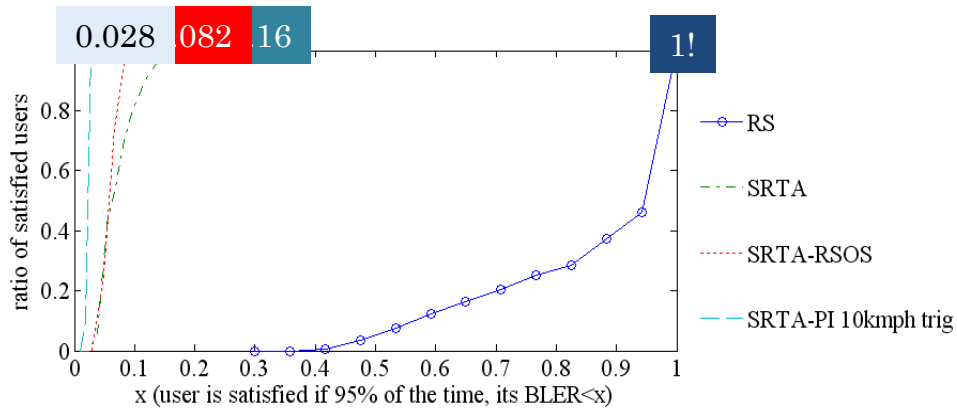


Figure 2-5: Performance of 460 cars in urban environment, during one hour

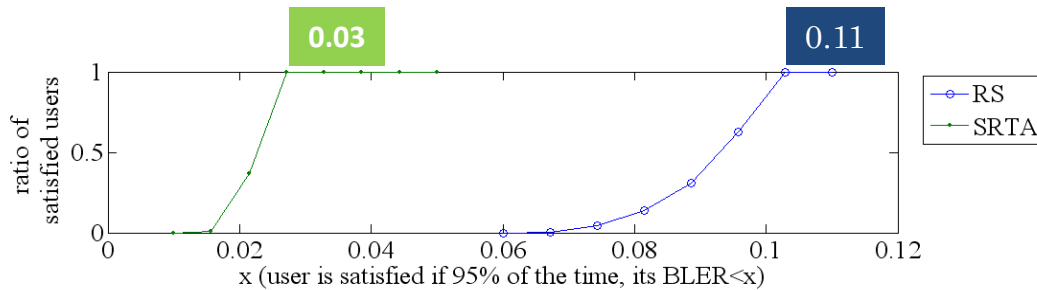


Figure 2-6: Performance of 1500 pedestrians in urban environment, during one hour

Based on these curves, we can derive the “guaranteed BLER for all cars”, and the “guaranteed BLER for all pedestrians”. This is the value  $x$  for which, 95% of the cars have the BLER lower than  $x$  during 95% of the time. This exercise helps us determine which technique can guarantee services with delay requirements similar to infotainment (around 10% BLER at initial transmission) and services with extremely low latency requirements (around 1% BLER at initial transmission), such as drones for instance. The guaranteed BLER values and the corresponding supported services are given in the Table 2.2, for all studied schemes.

Table 2.2: Performance (gains are given relatively to the RS performance)

Scheme =>		RS		SRTA		SRTA-RSOS		SRTA-PI	
		value	gain	value	gain	value	gain	value	gain
Cars	Guaranteed BLER	1	x1	0.16	x6.25	0.082	x12	0.03	x33
	Supported service	none		Infotainment		Infotainment		Ultra low latency	
Pedestrians	Guaranteed BLER	0.11	x1	0.03	x3.6	Not necessary			
	Supported service	none		Ultra low latency					

In conclusion, our new simulation results, based on WP6 mobility model, do not change the minimum and maximum values of the gains reported in [METIS14-D32]. However, they show the performance and gain of TeC6 in very particular scenarios. They also show that TeC6 might be useful *also for slow moving* devices. Indeed, services requiring *Ultra Low Latency* (1% BLER at initial transmission) might need SRTA even for pedestrian speeds. To achieve such performance with a low pilot overhead one must rely on smart channel measurement techniques such as the ones investigated in WP2 TeC6.4 [METIS15-D24].

## 2.2.4 Addressed METIS Goals

**1000x data volume:** This approach focuses on wireless backhaul and TeC 1b targets very high data rates and spectral efficiencies, in the order of hundreds of bits/s/Hz, achieved by low-complexity transceivers.

**5x E-E reduced latency:** For vehicles from 0 to 300kmph TeC 6 provides x100 improvement of BLER, whereas for pedestrians in urban environment TeC 6 provides x3.6 improvement of BLER. Corresponding values of latency reduction are for further study.

**Energy efficiency and cost:** Energy efficiency is improved by TeC 6 at the network side, thanks to SRTA-PI beamforming and the use of massive arrays at the BS.

## 2.3 Most Promising Technology Approach 2: Massive MIMO for Access

### 2.3.1 Introduction

One of the significant drivers of 5G is the access where modifications to existing LTE waveforms are investigated in WP2. Wireless access would without any doubt form the main thrust in any proposed 5G system. This is where main impacts are expected in terms of capacity increase, low latency, increased energy efficiency, etc. In T3.1 we consider massive-MIMO for access as the other MPTA. The issues investigated are as follows. In TeC 2 smart allocation of resources to pilot and data is investigated. In order to activate massive-MIMO with high performance, a precoder requires accurate CSI at the transmitter as identified in TeC 7. In addition, massive-MIMO handles an extremely large number of radio frequency (RF), intermediate frequency (IF) and base band (BB) circuits, and thus it is more important to compensate for impairments and imbalances of the RF, IF and BB circuits including the antennas. The advantages of uplink power control have not been addressed in previous massive-MIMO work, since equal uplink power allocation among users has always been assumed, thus the general case is addressed in TeC 9b. For the downlink scenario investigated in TeC 10, the sub-problems at different base stations (BS) for a minimum power beamforming are decoupled by utilizing a large dimension approximation for inter-cell interference (ICI), which allows developing a simplified near optimal algorithm. TeC 11 considers the feedback from the user equipment (UE) to the BS providing information about the ICI situation at the UE. In addition user clustering targeting densely crowded scenarios, to reduce the amount of feedback in FDD or required complexity in TDD systems, is investigated.

### 2.3.2 TeC 2: Coordinated resource and power allocation for pilot and data signals in multicell massive SIMO/MIMO systems

In massive MIMO systems, the quality of channel estimation can be severely degraded by the interference caused by uplink pilot (reference signal) transmissions in neighbouring cells. This problem, known as *pilot contamination* (PC), has been identified and analysed by the research community, see for example [Mar10]. Methods to combat pilot contamination typically involve multicell cooperation that, for example, helps to identify spatially well separated users who do not cause excessive interference to one another and can therefore reuse identical pilot sequences, see for example [YGF+13]. Multicell cooperation, however, may suffer from excessive signalling or inter-cell information exchange and high computational complexity.

The key idea of T3.1 TeC2 is to employ (1) a low complexity multicell coordination scheme operating on the large time scale (applicable for implementation by operation and maintenance (O&M) system or self-optimizing network (SON) algorithms) and (2) assigning the time-frequency and power resources within a cell to pilot and data signal transmission in such a way that the spectral efficiency within the cell is maximized. Thus T3.1 TeC2 is the combination of two main components operating together such that it (1) effectively avoids pilots contamination and (2) manages the pilot and data resources within a cell in a close to optimum fashion (Figure 2-7). The advantage of the joint operation of (1) and (2) is that the

spectral efficiency potential of massive MIMO systems can be effectively harvested without introducing excessive complexity and signalling overhead due to the typical cooperation needs of multicell massive MIMO systems. Parts of the performance analysis of T3.1-TeC2 are described in [FT14], [GGF+14] and [FDT14].

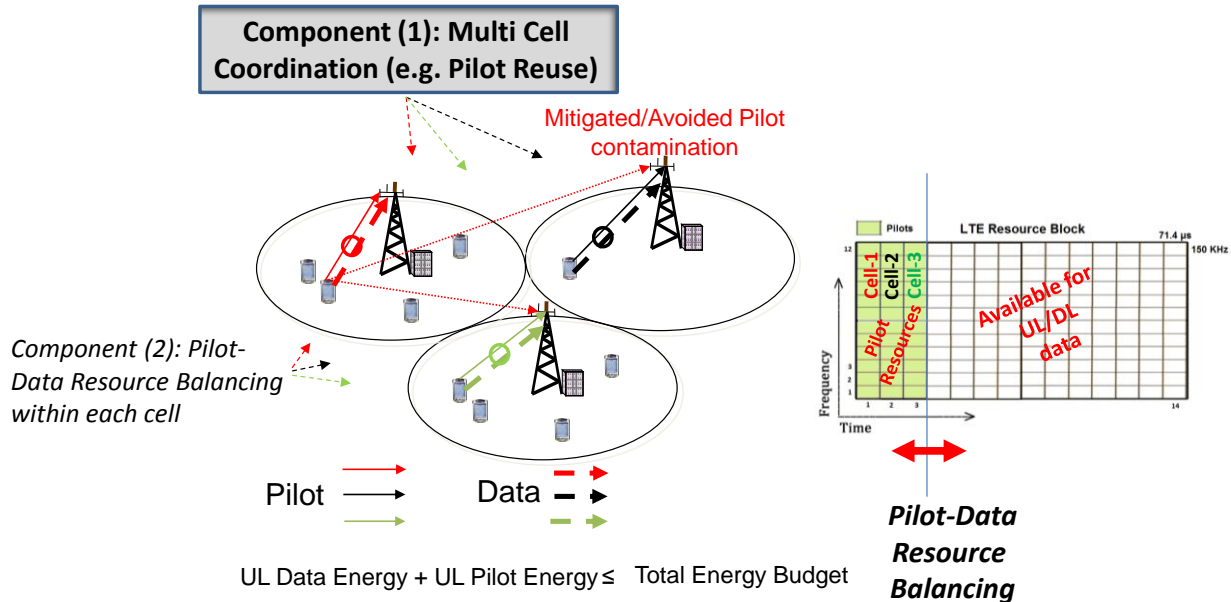


**Figure 2-7: The two components of T3.1 TeC2: (1) multicell coordination to avoid pilot contamination and (2) managing the time-frequency and power resources within a cell work jointly in a multicell massive MIMO system**

As illustrated in Figure 2-7, TeC2 intertwines the two components of (1) assigning resource elements to cells (effectively a pilot reuse) and (2) UL pilot power control, also called Pilot-to-Data Power Ratio (PDPR) balancing [KA05], within a cell. Pilot reuse operates on a coarse time scale applicable in O&M Systems. The O&M system can also facilitate pilot reuse configuration as part of a centralized or distributed SON solution, similarly to existing SON features such as coverage and capacity optimization. Pilot reuse configuration collects input data, such as traffic load information, number of served UEs, installed antenna infrastructure, system bandwidth and carrier frequency, etc, from all cells of a geographical area. Based on these input data, it configures the reuse pattern to be used in the cells belonging to the geographical area under the control of the O&M System. Although such functionality is not explicitly supported by today's O&M systems, the introduction of such pilot pattern control is feasible due to its slow time scale operation and its similarity to traditional reuse pattern schemes.

PDPR balancing operates at a finer time scale, ideally at the time scale of reference signal measurement and reporting (i.e. ~200 ms), and at the level of individual UEs within a cell. Its main inputs are the large scale fading (path loss) measurements performed by the UE on downlink reference signals. TeC2 contains algorithms that compute the optimum PDPR in terms of the mean square error (MSE) of the equalized uplink received data symbols for a given number of resource elements available for pilot and data symbols [FT14]. PDPR balancing can thus rely on existing (mobility and handover) measurements and can operate jointly with pilot reuse.

### Performance Results

To evaluate the performance of T3.1 TeC2, we consider a multicell multiuser MIMO (MU-MIMO) system with single antenna user equipment and multiantenna base stations according to the T3.1 simulation guidelines of [METIS14-D32, Appendix B]. The main simulation

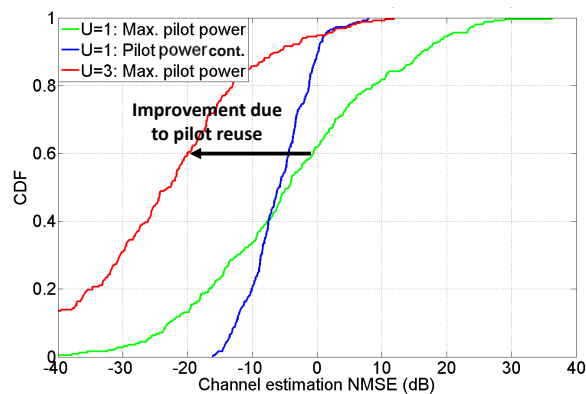
parameters are summarized in Table 2.3. We assume saturated (full) buffers and perfect synchronization between the BSs and their respective served users.

Figure 2-8 shows the performance improvement due to controlling pilot reuse in terms of the channel estimation quality (measured in normalized channel estimation as proposed by [YGF+13]). With pilot reuse-3, the pilot contamination is reduced at the expense of reserving more time-frequency resources for channel state information acquisition. However, reducing pilot contamination results in dramatically improved channel estimation performance.

**Table 2.3: Main system simulation parameters used for the evaluation of T3.1 TeC 2**

Network Deployment	21-cell hexagonal grid
Inter-site distance	500 m
Exclusion radius	35 m
Terminals per cell ( $K$ )	{3, 6, 12, 24}
Terminal speed	60 kmph
BS transmit power ( $P_{BS}$ )	0.067W per subcarrier
Max. terminal transmit power ( $P_T$ )	23 dBm over 20 MHz
Carrier Frequency ( $f_c$ )	2 GHz
Subcarrier spacing	15 KHz
BS array	100-antenna uniform linear array (ULA)
Tilt	11°
BS antenna	Fitted Kathrein, Vertically Polarized
Antenna spacing	0.7 $\lambda_c$
Max. antenna gain	18 dBi
3dB horizontal beamwidth	65°
3dB vertical beamwidth	6.5°
BS antenna noise figure	5 dB
Terminal antenna	Omnidirectional, Vertically Polarized
Terminal antenna noise figure	9 dB

Figure 2-9 shows that the average NMSE achieved by low complexity LS channel estimation becomes lower than that of MMSE estimation when using pilot power control according to TeC2. Although the average NMSE using MMSE estimation improves with increasing number of base station antennas, pilot power control yields superior NMSE performance even with 100 antennas.



**Figure 2-8: Comparing the improvement of the NMSE using LS estimation due to pilot power control and pilot reuse of U=3**

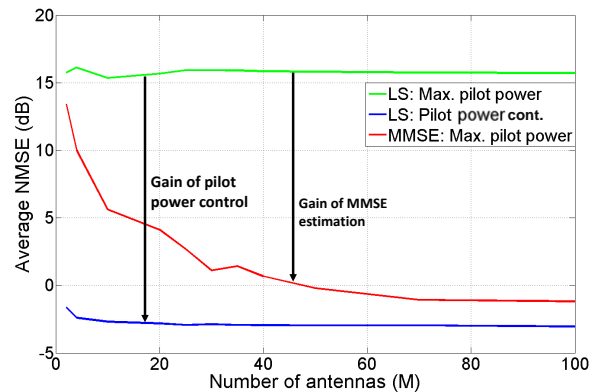


**Figure 2-9: Comparing the improvement of the average NMSE using LS estimation with pilot power control or MMSE channel estimation (U=3)**

Figure 2-10 shows that improving the quality of CSI by reducing pilot contamination pays off in terms of DL per-cell sum rate, even though pilot reuse-3 ( $U=3$ ) requires more resources for CSI acquisition purposes (see Figure 2-7). As shown in Figure 2-10, the DL sum-rate improvement depends on the DL precoding method (MRT or ZF) but is beneficial for any number of antennas in the examined range.

Figure 2-11 shows the beneficial impact of pilot power control alone or pilot reuse ( $U=3$ ) without pilot power control. Pilot reuse ( $U=3$ ) alone can practically achieve the SINR performance of a system in which perfect CSI would be available. Notice that the SINR is somewhat lower with full pilot reuse due to pilot contamination.

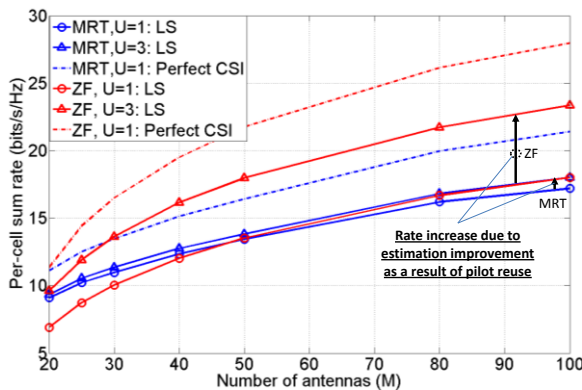


Figure 2-10: Per-cell DL sum-rate when employing MRT or ZF transmission without ( $U=1$ ) and with pilot reuse ( $U=3$ ) according to Component (1) of TeC2

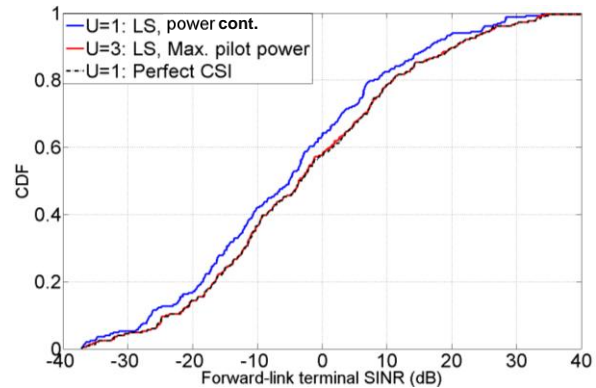


Figure 2-11: DL achieved SINR under full pilot reuse ( $U=1$ ) employing pilot power control and using pilot reuse-3 ( $U=3$ ) with full pilot power

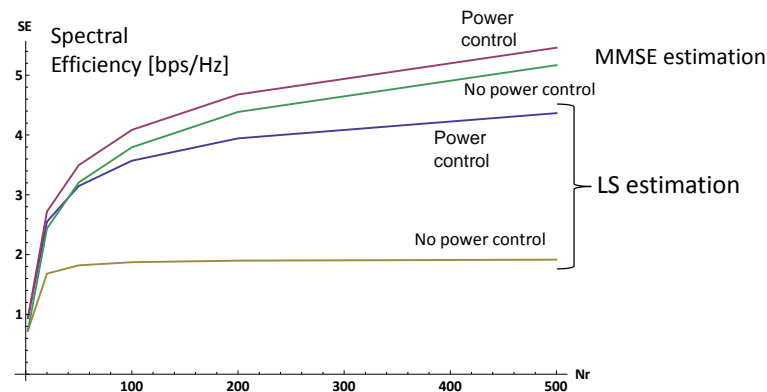


Figure 2-12: UL spectral efficiency (per UE) against the number of receive antennas ( $N_r$ ) when using LS and MMSE channel estimation with and without pilot power control (PDR balancing). In practice, PDR balancing could be implemented by means of a table that associates the optimal pilot and data power setting with the large scale geometry of the system. In its simplest form PDR balancing could be performed on the basis of path loss measurements and reporting of individual UEs.

Finally, Figure 2-12 shows the uplink spectral efficiency per UE when using LS and MMSE channel estimation without and with pilot power control in a pilot contamination free system (achieved by pilot reuse). As expected, MMSE estimation shows superior performance, but it requires the availability of the channel covariance matrices. Therefore, LS estimation can be more practical, although as shown in Figure 2-12, LS estimation needs pilot power control to have an acceptable performance in a massive MIMO system.

### 2.3.3 TeC 7: Massive MIMO transmission using higher frequency bands based on measured channels with CSI error and hardware impairments

In order to tackle the rapidly increasing data traffic, usage of higher frequency bands that can easily expand signal bandwidth has been widely studied for 5G mobile communication systems. NTT DOCOMO has successfully achieved 10 Gbps packet transmission employing 11 GHz band 8×16 MIMO with 400 MHz bandwidth by field experiments in partnership with Tokyo Institute of Technology in December 2012 [NDP13], [SSO13]. Moreover, mobile services using the higher frequency bands can be flexibly introduced by a Phantom Cell concept where the control plane is supported by a lower frequency band, such as 800 MHz or 2 GHz, and only the user plane is provided by the higher frequency bands, as high as several tens GHz [IKT12]. In the higher frequency bands, the number of antenna elements can be drastically increased compared to the 2 GHz band because the size of one antenna element can be miniaturized, and it is expected that Massive MIMO can provide the higher data rate and transmission quality. However, in order to activate Massive MIMO with high performance, a Massive MIMO precoder requires accurate CSI at the transmitter. In addition, Massive MIMO handles an extremely large number of radio frequency (RF), intermediate frequency (IF) and base band (BB) circuits. Therefore, it is more important to compensate for impairments and imbalances of the RF, IF and BB circuits including the antennas.

As the prior step of this research, we evaluated performances of 30 Gbps 24×24 MIMO-OFDM eigenmode (EM) transmission by link level simulations using both channel data that are measured in the 11 GHz propagation experiments [SSS+14] and channel model based on the Kronecker model. The computer simulations followed the specifications of the 11 GHz band 8×16 MIMO transmission and 24×24 MIMO propagation experiments [SSO+13], [KKG+11]. However, the required total transmission power is over 30 dBm for applying such an enhanced MIMO technique to 20 GHz band small cells that provide a super high bit rate of 20 Gbps [SSB+14]. Thus, in order to reduce the total transmission power to 30 dBm by exploiting a BF effect of Massive MIMO, we employed Massive MIMO of uniform planar array (UPA) with 256 transmitter antennas for the 20 GHz band 20 Gbps transmission in [METIS14-D32]. Spatially multiplexing 16 streams with the 400 MHz bandwidth achieves the bit rate of 23.5 Gbps. It was shown that Massive MIMO with 256 antennas can drastically improve the throughput performance by the 3D BF effect compared to the typical MIMO with 16 antennas. However, this investigation assumed a fully-digital Massive MIMO that requires 256 RF and BB chains.

Here, to reduce the cost of the Massive MIMO transceiver, a hybrid BF that consists of analog BF and digital precoding is employed, because the analog BF with RF phase shifters can drastically reduce the number of the up-converters and BB chains in the hybrid BF as shown in Figure 2-13. As a new precoding scheme for the Massive MIMO OFDM with the hybrid BF, we propose fixed BF and CSI-based precoding (FBCP) [OSS+14]. The proposed FBCP consists of  $N_T$  transmitter antennas and  $L$  RF and BB chains for  $M$  data streams as shown in Figure 2-13. Moreover, the FBCP employs a successive two-stage algorithm;  $L$  analog fixed BF weights are firstly selected from some analog fixed BF weight candidates based on the steering vector for arbitrary 2D angles. The  $L$  analog fixed BF weights denoted by  $\mathbf{W}$  are selected on the maximum total received power criterion. In the second stage, a precoding matrix  $\mathbf{P}(n)$  at the  $n$ -th subcarrier is calculated by singular value decomposition (SVD) using an equivalent channel matrix  $\mathbf{H}(n)\mathbf{W}$  where  $\mathbf{H}(n)$  is the channel matrix. Note that  $\mathbf{H}(n)\mathbf{W}$  is accurately estimated by exploiting a reference signal with the selected analog fixed BF.

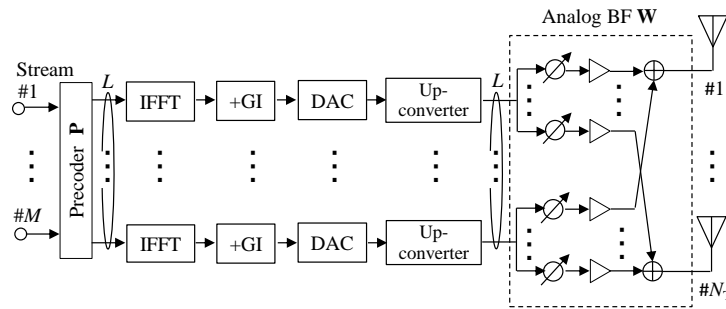


Figure 2-13: Massive MIMO OFDM transmitter employing FBCP

### Performance Results

Link level simulations are performed to evaluate throughput performances of the 20 GHz band Massive MIMO employing the proposed FBCP. The same simulation baseline as [METIS14-D32] is employed here. The parameters used for the simulations are given in Table 2.4.  $N_T$  is set to 16 or 256, and the number of receiver antennas,  $N_R$ , is fixed to 16. The receiver detects the spatially multiplexed streams by using a postcoding matrix that is calculated from the SVD of the equivalent channel matrix  $\mathbf{H}(n)\mathbf{W}$ . Both the transmitter and the receiver employ the 2D UPA as the antenna array structure in Figure 2-14. The number of the streams,  $M$ , is fixed to 16. The maximum bit rate reaches 31.4 Gbps according to the parameters set where the modulation and coding scheme is 256QAM with coding rate,  $R$ , of 3/4 in the turbo code. AMC is used ideally. Channel model was based on the Kronecker model including LOS and NLOS components. Rician factor,  $K$ , is assumed to be 10 dB for the Nakagami-Rice fading channel.

Table 2.4: Simulation parameters of Massive MIMO

Transmission scheme	Downlink Massive MIMO OFDM
Signal bandwidth	400 MHz
Active subcarriers	Pilot: 32, data: 2000
No. of antennas	Transmitter, $N_T$ : 16, 256 Receiver, $N_R$ : 16
No. of data streams, $M$	16
Modulation scheme	QPSK, 16QAM, 64QAM, 256QAM (w/ AMC)
Channel coding	Turbo code, $R = 1/2, 2/3, 3/4$ (w/ AMC)
Maximum bit rate	31.4 Gbps (256QAM, $R = 3/4$ )
Antenna array structure	UPA
Angular power spectrum	$\theta$ : Laplacian distribution $\phi$ : wrapped Gaussian distribution
Average angle ( $\theta, \phi$ )	Departure: (90 deg, 90 deg) Arrival: (90 deg, 90 deg)
Angular spread ( $\theta, \phi$ )	Departure: (5 deg, 5 deg) Arrival: (20 deg, 20 deg)
Channel model	Kronecker model
Fading channel	Nakagami-Rice ( $K = 10$ dB), 16-path

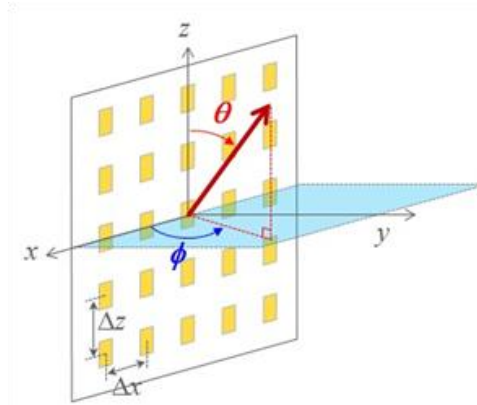


Figure 2-14: UPA for 3D BF

Figure 2-15(left) shows throughput performance of the FBCP for different values of  $L$ . Ideal channel estimation is assumed. Search angular intervals for the analog BF in zenith and azimuth,  $\Delta\phi$  and  $\Delta\theta$ , are fixed to 5 degrees. For comparison, throughput performances of the EM precoding which employs the fully-digital Massive MIMO of  $L = N_T$ , are also plotted in Figure 2-15(left). It is shown that as  $L$  increases, the throughput of the FBCP approaches to that of the EM by improvement of the BF gain, and that the convergence value of  $L$  is 32 for  $N_T = 256$ . Since the EM requires the same number of the RF and BB chains as  $N_T$ , FBCP is the much cost-effective scheme. Moreover, in comparison with the conventional fully digital MIMO with  $N_T = 16$ , the FBCP with  $N_T = 256$  and  $L = 32$  can reduce the required SNR at the 20 Gbps throughput by 14 dB by exploiting the higher BF and diversity gains.

Figure 2-15(right) shows throughput performance of the FBCP with the CSI error. For comparison, throughput performance of the fully digital EM precoding is also plotted in Figure 2-15(right). In both schemes, the CSI error is generated by complex Gaussian distribution with zero mean and variance of  $\sigma_e^2$ . Let  $\sigma_n^2$  denote noise power per antenna, and  $\sigma_e^2$  is set to  $\sigma_n^2 - 10$  dB or  $\sigma_n^2 - 20$  dB. This setting is based on the assumption that the reference signals with additional gain are transmitted and accurate channel estimation can be performed by using them. Figure 4 demonstrates that as the CSI error increases, the throughput of the EM drastically degrades while the FBCP is robust to the CSI error. It is also found that when  $\sigma_e^2 = \sigma_n^2 - 20$  dB, the FBCP can achieve the same throughput as the EM in spite of the significantly low complexity.

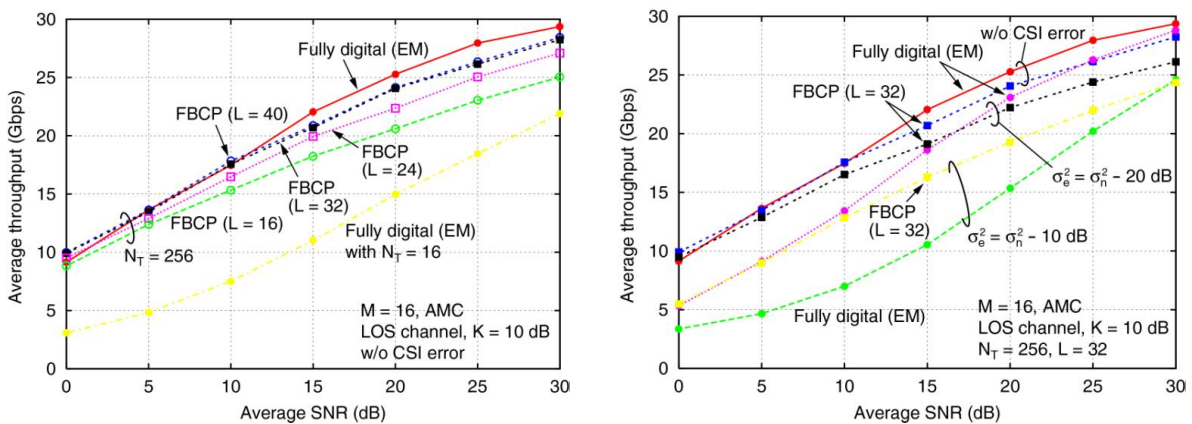


Figure 2-15: Left: Optimization of  $L$  for FBCP. Right: Throughput of FBCP with CSI error.

### 2.3.4 TeC 9b: Uplink power control with MMSE receiver in multi-cell MU-Massive-MIMO

Multi-cell uplink power control has been illustrated to largely improve the energy efficiency in conventional MIMO systems [FJS10]-[SKZ10]. With perfect CSI and multi-cell coordination,

the optimal solution of jointly assigning interference-plus-noise ratio (SINR) targets and transmit power can substantially reduce the uplink power consumption [FJS10]; while with imperfect CSI but free of pilot contamination, the authors in [SKZ10] have exploited the interdependency between pilot and data transmissions to adjust pilot power in the context of existing data power control, such that total power saving is achieved subject to the per-user SINR constraint. However, these advantages of uplink power control have not been addressed in previous massive MIMO work [Mar10]-[NLM13b], since equal uplink power allocation among users has always been assumed. Therefore, we are motivated to investigate the potential of uplink pilot and data power control in multi-cell MU-Massive-MIMO systems.

The standard MMSE receiver based on the practical channel estimates with pilot contamination [JAM+11] is applied at the BS. In order to minimize the sum pilot and data transmit power of all users under the per-user SINR and per-user power constraints, we first derive the closed-form lower bound on the average uplink SINR (instead of directly computing the average SINR which in general has intractable form [HBD13]) for a very large but finite number of BS antennas, which takes the individual power allocation among different users into account. Based on the lower bound, we then propose a joint iterative pilot and data power control algorithm which embeds the pilot power minimization into a standard data power control process [CAH+07]. The existence and uniqueness of the optimal solution are proved for single-user setup, while the convergence in multi-user case is guaranteed by an extra monotone decreasing constraint [GGF+14]. Simulation results demonstrate the tightness of the lower bound as well as the large gain of applying multi-cell uplink power control together with massive MIMO technique to further improve the energy efficiency.

The general idea of the joint iterative algorithm is to perform the pilot power control with a given data power value which is acquired from previous data power control, if the per-user power constraint is currently satisfied. Based on the obtained pilot power allocation, the standard data power control converges to a unique optimal solution which is used as updated input for the subsequent pilot power control. For the details of the algorithm please refer to [GGF+14].

## Performance Results

We consider a MU-Massive-MIMO system consisting of  $L = 3$  hexagonal cells which have a radius of 1000 meters. Each BS located in the cell centre serves  $K = 5$  users at the same time-frequency resource. All users are distributed uniformly inside the cell and have at least a distance of 100 meters away from the BS. The path-loss exponent is selected to be 4 and the large-scale fading is modelled as a zero mean log-normal distribution with a standard deviation of 8 dB. Throughout the simulations in this section, normalized additive Gaussian noise with variance of 1 is assumed; the same target SINR and power allowed for uplink transmission are applied for all users in the system, i.e.  $\gamma_{lk} = \gamma$ ,  $p_{lk} = p = 200$  mW,  $\forall(l, k)$ ; referring to [SKZ10], around 1/6 of the transmit power is assigned initially to the uplink training.

Next we illustrate the performance of the proposed joint iterative power control based on the previous user placement and initial power. In the upper part of Figure 2-16, e.g. for  $M = 100$ , the optimal assigned sum pilot power is larger than the sum data power except for very low target SINRs, which coincides with the fact that only data transmission takes advantage of massive BS antennas (i.e. power-scaling law), while uplink training does not, since it is performed on a per-receive antenna basis [NLM13a]. Due to the same reason, for  $\gamma$  up to 10.7 dB, the obtained data power allocation leads to a sum data power varying from 12.6 to 17.4 dBm as the pursued SINR rises, which is much smaller than the increment from 11.4 to 27 dBm in sum pilot power. In contrast, in the high target SINR region with  $\gamma \geq 10.7$  dB, the inner loop for pilot power control is terminated by the monotone decreasing constraint only after 1 iteration, because the pilot contamination confines the impact of pilot power control. As a result, the joint power control reduces to a simple data power control with fixed (initial) pilot power. On the other hand, as  $M$  grows, the lower limit of high target SINR region also increases, which extends the region where power saving can be obtained through joint power

control. In addition, as depicted in both parts of Figure 2-16, the joint algorithm becomes infeasible when the target SINR is above a certain value, e.g. 15 dB for  $M = 100$ , due to the per-user power constraint. However, as  $M$  becomes large, this upper limit increases as well, which reflects the potential of combining the joint uplink power control with massive MIMO technique to attain a higher SINR target with less sum transmit power, hence improving the energy efficiency.

In Figure 2-17, we demonstrate the advantage in power saving of the proposed joint algorithm comparing to a simple data power control where the pilot power allocation is fixed to the initial value as in the joint algorithm, i.e.  $\frac{1}{6}p$  for all users. Here the y-axis represents the ratio of obtained sum power saving (between simple data power control and the proposed algorithm) w.r.t. the result when the simple data power control is applied. It is obvious that a power saving up to 95% can be achieved with joint algorithm in low target SINR region. The advantage disappears however when the target SINR exceeds the lower limit of high SINR region. It is especially worth noting that the benefit of deploying a large number of BS antennas tends to become marginal as  $M$  keeps growing, since the ultimate SINR performance is exclusively limited by the pilot contamination and transmit power control.

Finally we evaluate the infeasibility of the joint algorithm which is caused by either the per-user power constraint or the unattainable per-user SINR target. The latter is checked based on the obtained pilot power prior to the data power control to avoid unnecessary computations if the SINR target is infeasible. The results in the upper part of Figure 2-18 verify that the significant infeasibility (>5%) first occurs due to the per-user power limit. However as the target SINR increases, it tends to be simply unachievable with the joint power control, thus  $\lambda_{\max}(\Psi C) \geq 1$  starts to become the dominant cause of infeasibility. Besides, Figure 2-18 also illustrates that by deploying a larger number of BS antennas the achievable target SINR is increased, e.g. 3 dB gain from 100 to 200 BS antennas.

The above results has demonstrated the attainable power saving of the joint algorithm comparing to a simple data power control with fixed pilot power, which comes with the trade-off in a bit higher infeasibility. Nevertheless, if combined with a very large number of BS antennas, the joint uplink power control can achieve a higher target SINR with less sum transmit power and hence significantly improve the system energy efficiency.

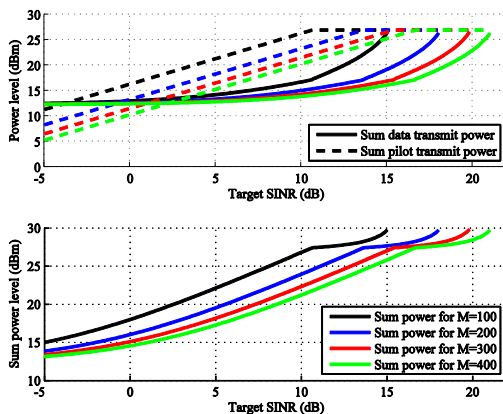


Figure 2-16: Joint iterative pilot and data power control vs. target SINRs

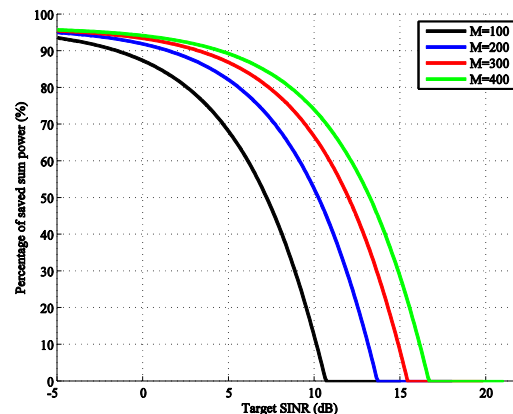


Figure 2-17: Percentage of power saving vs. target SINRs

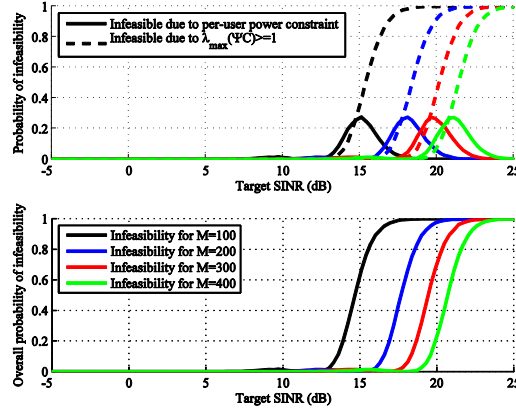


Figure 2-18: Probability of infeasibility over random user placements

### 2.3.5 TeC 10: Decentralized coordinated transceiver design with large antenna arrays

A minimum power beamforming problem is considered here. The centralised problem is decoupled and decentralised among the base stations (BSs) via fixing the inter-cell interference (ICI) terms per user. A large dimension approximation is applied such that the ICI terms depend only on the statistical properties of the channel vectors (large-scale fading characteristics and antenna correlation). This results in a simplified near optimal algorithm with smaller exchange rate and processing load compared to the optimal centralized solution.

#### System model

The cellular system consists of  $N_B$  BSs and  $K$  single antenna users; each BS has  $N_T$  transmitting antennas. Users allocated to BS<sub>*b*</sub> are in set  $U_b$ . The signal for user  $k$  consists of the desired signal, intra-cell and inter-cell interference. Assuming  $w_{b,k}$  as transmit beamformer, we solve following optimization problem [TPK11]

$$\begin{aligned} & \text{Min} \sum_{b \in B} \sum_{k \in U_b} |w_{b,k}^H h_{b,k}|^2 \\ & \text{subject to} \frac{|w_{b,k}^H h_{b,k}|^2}{\sigma^2 + \sum_{l \in U_{b_k} \setminus k} |w_{b,l}^H h_{b,l,k}|^2 + \sum_{b \neq b_k} \varepsilon_{b,k}^2} \geq \gamma_k \quad \forall k \in U, b \in B \\ & \sum_{l \in U_b} |w_{b,l}^H h_{b,l,k}|^2 \leq \varepsilon_{b,k}^2 \quad \forall k \neq U_b, b \in B \end{aligned}$$

where the optimization variables are  $w_{b,k}$ , the inter-cell interference is constrained by  $\varepsilon_{b,k}$ , and  $h_{b,k}$  denotes the channel between BS  $b$  and user  $k$

#### Description of the proposed solution and Analysis

We extended the results derived in [METIS14-D32] for i.i.d channel scenario to a *generic per user channel correlation model*  $h_{b,k} = \theta_{b,k}^{\frac{1}{2}} g_{b,k}$ , where  $\theta_{b,k}^{\frac{1}{2}}$  is the correlation matrix of user  $k$  and  $g_{b,k}$  is a vector with i.i.d complex entries with variance  $\frac{1}{N_t}$ . This per-user channel correlation model can be applied to various propagation environments.

We have shown that the approximately optimal uplink powers  $\tilde{\lambda}_l$  for the generic model are given by [ATR14b, ATR14a], i.e.  $\tilde{\lambda}_k = \frac{\gamma_k}{m_{B_k, \theta_{b_k, k}}(-1)}$ , where  $m_{B_k, \theta_{b_k, k}}(z)$  is defined for  $z \in \mathbb{C} \setminus \mathbb{R}^+$  by [ATR14b], i.e.  $m_{B_k, \theta_{b_k, k}}(z) = \frac{1}{N_t} \text{tr} \theta_{b_k, k} \left( \frac{1}{N_t} \sum_l \frac{\tilde{\lambda}_l \theta_{b_k, l}}{1 + \tilde{\lambda}_l m_{B_k, \theta_{b_k, l}}(-1)} - z I_{N_t} \right)^{-1}$ . The approximation for downlink powers can be derived similarly, see [ATR14b, ATR14a] for details. The above

approximations result in an algorithm that gives near optimal uplink and downlink powers based on local CSI and statistics of other BS channels. However, the error in approximations causes variations in the resulted SINRs/rates. Thus, the SINR constraints cannot be guaranteed and those might be higher or lower than the target SINRs.

Next, we propose a novel approach for decoupling the sub-problems at base stations. Following the same logic as in [TPK11], ICI is considered as the principal coupling parameter among BSs and the large dimension approximation for ICI term based on statistics of the

channels is derived as [ATR14b], i.e.  $\varepsilon_{b,k}^2 \approx \sum_{l \in U_b} \sqrt{\delta_{b,l}} \frac{1}{N_T} \frac{a_{b,j}^2 a_{b,i}^2 m'_{b,k} \theta_{b,k,k} (-1)}{\mu_{b,k,l}^2 \mu_{b,k,k}^2}$  and  $\mu_{b,l} = 1 + \lambda^0 m_{b,\theta_{b,l}} (-1)$ , where  $\varepsilon_{b,k}^2$  is downlink interference from  $BS_b$  to user  $k$ . This approximation allows derivation of approximately optimal ICI terms based on statistics of the user channels. Each BS needs the knowledge about user specific average statistics, i.e., user specific correlation properties and pathloss values from other BSs (these statistics can be exchanged over the backhaul between coordinating network nodes). Based on the statistics, each BS can locally and independently calculates the approximately optimal ICI values. Plugging the approximate ICI into the primal problem decouples the sub-problems at BSs and the resulting SINRs satisfy the target constraints with slightly higher transmit power compared to the optimal method. Dependency of the coupling parameters on channel statistics results in reduced backhaul exchange rate and processing load. Moreover, the algorithm can be applied to fast fading scenario as the channel statistics (pathloss, correlation properties) change slower than the instantaneous channel realizations.

## Performance Results

Two algorithms, developed [ATR14a, ATR14b] and briefly summarized in the previous section, provide good approximations even when the dimensions of the problem (i.e. the number of users and antennas) are practically limited. We present however here only the results for the algorithm based on ICI approximation. This algorithm satisfies the target SINRs for all users; however, the error in approximations leads to higher transmit power at the BSs. A network with 7 cells is considered and users are equally distributed between cells. Exponential pathloss model is used for assigning the pathloss to each user, i.e.  $a_{b,k} = (\frac{d_0}{d_{b,k}})^2$ , where  $d_{b,k}$  is distance between BS  $b$  and user  $k$ . The pathloss exponent is 2.3 and the reference distance ( $d_0$ ) is 1m. The pathloss from a base station to the boundary of the reference distance of the neighboring base station is fixed to 60dB. The correlation among channel entries is introduced using a simple exponential model  $[\theta_{b,k}]_{i,j} = \rho^{|i-j|}$ , where  $\rho$  represents the correlation coefficient which is 0.8 for the following simulations. The users are dropped randomly for each trial and in total 1000 user drops are used for calculating the average transmit power. The number of antennas at each BS varies from 14 to 84 and the total number of users is equal to half the number of antennas at each BS. Thus, *the spatial loading is fixed as the number of antennas is increased.*

Figure 2-19 and Figure 2-20 illustrate the transmit powers versus the number of antennas for 0 dB and 10dB SINR target respectively. It is clear that the gap between the approximated and optimal algorithm (denoted as SOCP [TPK11]) diminishes as the number of antennas and users increase. Small gap in small dimensions indicates that the *approximate algorithm can be applied to the practical scenarios with a limited number of antennas and users.* From the results it is clear that the SOCP algorithm and the approximated ICI algorithm outperform the ZF method. Note that the number of antennas at each BS per number of served users is increasing while the gap between ZF and optimal and approximated method is fixed which is due to the fixed ratio of the number of antennas to the total number of users. The gap in performance is mainly due to the fact that the ZF algorithm wastes a degree of freedom for nulling the interference towards the distant users while the SOCP algorithm finds the optimal balance between interference suppression and maximizing the desired signal level. MF beamforming must be dealt with more care since it completely ignores the interference (both

intra- and inter-cell) and hence the SINR target is below the target SINR indicated by magenta plots in Figure 2-19 and Figure 2-20. Note that MF beamforming can satisfy the target SINR only asymptotically in a very special case, i.e., when the ratio of the number of antennas to the number of users approaches infinity.

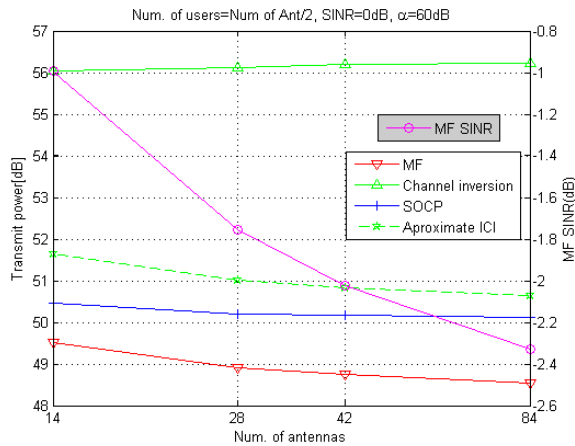


Figure 2-19: Comparison of required transmit power for 0 dB SINR target

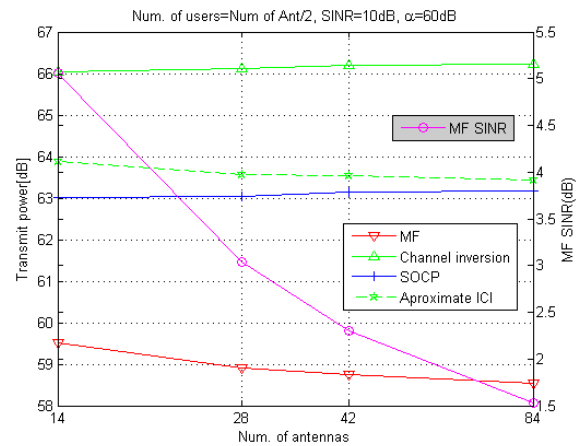
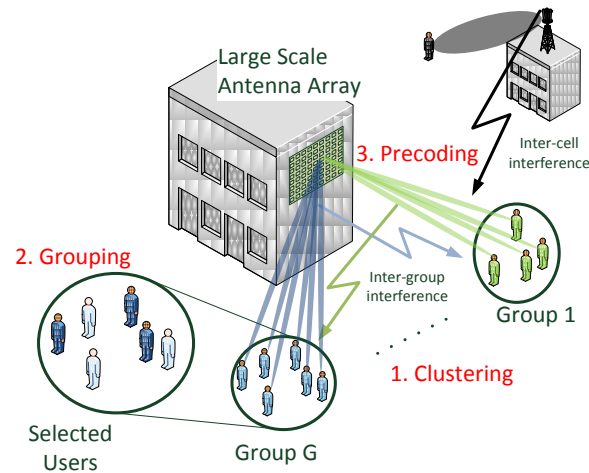


Figure 2-20: Comparison of required transmit power for 10 dB SINR target

### 2.3.6 TeC 11: Massive SDMA with a LSAS exploiting elevation and azimuth beamforming

This TeC exploits the advantages of massive MIMO, in particular the spatial multiplexing and array gain offered by the use of large antenna system at the base station (BS). In theory the sum-throughput  $R$  scales linear with the number of spatial multiplexed users  $R \sim K_c$ , and logarithmic with the number of antennas  $R \sim \log_2(N)$ . Following the METIS test case 2 “Dense urban information society” [METIS13-D11] trading the forecast increase of devices, we load the system in this TeC with many users. The transmission strategy is depicted in Figure 2-21, and can be divided into the following three parts applying a two-stage beamforming:

1. Inter-group interference aware clustering of co-located users into groups
  - I. First beamforming
2. Per group: User selection for downlink transmission on same time-frequency resource
3. Per group: Inter-cell interference aware precoder design for selected user
  - II. Second beamforming



**Figure 2-21: Inter-group interference clustering, user-grouping and inter-cell-interference aware precoding with massive MIMO antenna arrays**

In the first step (the user-clustering), we divide the set of users  $\mathcal{K}$  into  $G$  groups of users with similar second-order channel statistics. We use the joint spatial division multiplexing (JSDM) concept of pre-beamforming from [ANAC13] to spatially separate the channels of each user-group. We adapted a density based clustering algorithm from [EKS+96], called DBSCAN (density-based spatial clustering of applications with noise). This algorithm clusters an adaptive number of groups with respect to a certain user density which we adapted to the level of inter-group interference.

In the second step, which is done independently for each group, we use semi-orthogonal user selection (SUS) based grouping [YG06] to find a subset of users for simultaneously downlink transmission on the same time-frequency resource. In this work SUS algorithm is adapted with the maximum sum-rate objective using projection based rate approximation according to [TKBH12]. With this we ensure that the limited available transmit power split to an increasing number of spatial resources doesn't result in a loss of sum-throughput [KRTT13].

In the third step, after the users are clustered in groups and in each group a subset of users is scheduled, the precoder used for beamforming at the BS is designed. Due to out-of cell interference from BSs with a low number of antennas, e. g. current LTE base stations, this so called inter-cell interference has to be considered to balance signal, multi-user interference and inter-cell interference in the right way [KTH14]. We use regularized zero-forcing where inter-cell interference can be taken into account in the regularization values. Therefore, we introduce a scalar broadband power-value of the interference-covariance matrix at the users which needs to be feedback from the users to the base station in a time division duplex system.

Note that step one is based on slowly-varying statistical channel information (second order statistics) which is assumed to be constant over several transmission time intervals (TTIs). In contrast to this step, two and three are performed on a TTI level taking into account the effective channel feedback either from downlink training and feedback in FDD or uplink estimation in TDD.

Combining all these three concepts we showed that large performance gains in terms of sum-throughput up to 10 times can be achieved compared to baseline scenarios with 8 antennas, e.g. in LTE-A (3GPP Release 12) utilizing:

1. Spatial multiplexing gain serving many users on the same time-frequency resource;
2. Beamforming gain of a large antenna array;
3. Power gain of pool power constraint over all antennas.

## Performance Results

To evaluate the first step of our approach, we assume a single sector with an [1x256] antenna array and 6 physical nearby located clusters of users, each consisting of 6 users. This clustering into space-orthogonal groups has to be done with respect to inter-group interference. The clustering with the well-known K-means++ algorithm with the joint spatial division multiplexing scheme as in [NAAC14] is not practical for this task because the number of groups  $G$  is required as input which is not known a-priori. An exhaustive search for the optimal  $G$  of each user constellation is hardly feasible. Therefore, we looked into the class of density based clustering algorithms adapting the DBSCAN algorithm.

The simulation assumptions and further details are provided in the appendix. In Figure 2-22 we compare the K-means++ and DBSCAN algorithm with the LTE baseline scenario. For the baseline we assume 8 antennas and zero-forcing multi-user beamforming.

To evaluate the second and third step of our approach we use the more realistic QUADIRGA (quasi deterministic radio channel generator) [JRB+14]. Again more details are provided in the appendix.

Assuming perfect channel knowledge of the downlink user channels at the BS, Figure 2-23 shows the multiplexing gain increasing the number of user candidates  $K = |\mathcal{K}|$  from 40 to 120. Thereby we consider two following user grouping modes:

1. WUS: Without user selection (WUS) the set of scheduled users is  $\mathcal{K}_{WUS} = \mathcal{K}$
2. SUS: With semi-orthogonal user selection (SUS) the set of scheduled user is  $\mathcal{K}_{SUS} \subset \mathcal{K}$

Red lines with upper triangles in Figure 2-23 consider interference aware regularized zero-forcing precoding. With this we observe a gain of 150 and 20% at  $K = 120$  for mode 1 and 2, respectively. The effect utilized is that multi-user interference is only reduced to the same level as the constant noise and out of cell interference resulting in higher signal power per user and smaller loss due to precoder normalization.

In Figure 2-24 the per antenna power constraint from LTE is relaxed to a pool power constraint due to reduced requirements on amplifiers by the power distribution over 128 instead of 2 and averaging effects from many spatial layers.

The gain we can achieve from the pool power relaxation is shown in Figure 2-24 together with the LTE-A baseline scenario for comparison considering 8 antennas and maximum sum-throughput multi-user scheduling.

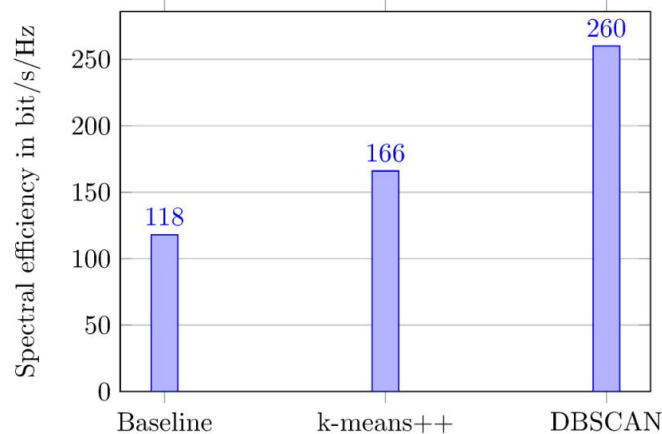


**Figure 2-22: JSDM per group precoding comparing LTE-baseline  $N_{LTE} = 8$  antennas with massive MIMO  $N_{LSAS} = 256$  antennas for state-of-the-art k-means++ and new adapted DBSCAN user clustering**

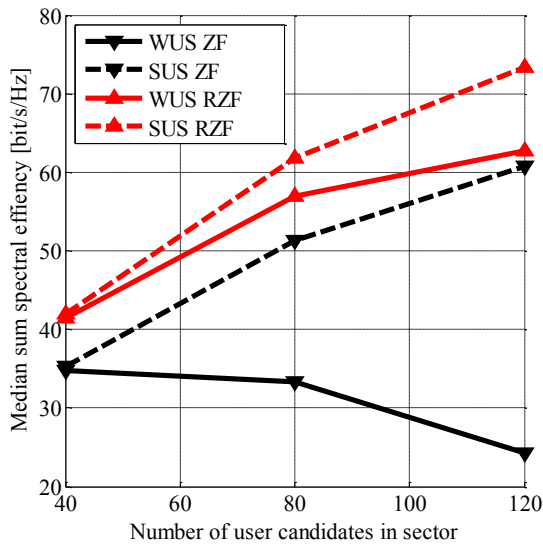


**Figure 2-23: Performance over users with and without user selection comparing zero-forcing and regularized zero-forcing with interference power feedback**

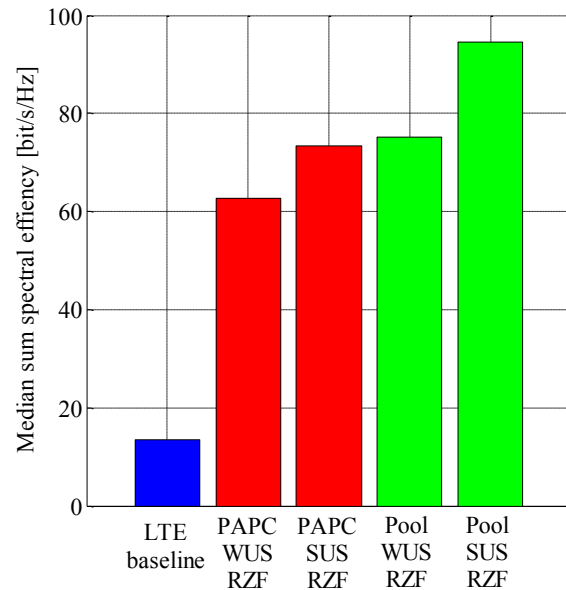


**Figure 2-24: Performance comparison at 120 users with and without user selection for per antenna and pool power constraint**

### 2.3.7 Addressed METIS Goals

**1000x data volume:** Massive MIMO inherently boosts the data volume by increasing the density of active users. With the help of TeC 2, optimum power allocation between pilot and data enables co-scheduling of multiple users on the same time-frequency resource, which supports the achievement of high data rates and spectral efficiencies. In addition to that, TeC 7 shows that massive MIMO at higher frequencies provides more than 10 times higher throughput compared to LTE-A baseline with 8 antennas. With the help of coordinated transceiver design as proposed by TeC 10, large beamforming gains are available to improve spectral efficiency. The solution of TeC 11, which is based on user clustering and SDMA with massive MIMO, provides 4-7 times higher throughput when compared to a LTE-A baseline with 8 antennas.

**10-100 user data rate:** The user data rates are also increased by the TeCs of this approach by enabling hundreds of antennas (TeCs 7, 10 and 11) and harvesting the increased gains due to the mitigation of pilot contamination (TeC 2).

**10-100x number of devices:** Ideally, by increasing the number of antennas at the BS by a factor X, we may increase the number of devices by the same factor. However, due to practical limitations such as pilot allocation, the number of users supported per time-frequency resource can be increased by 10-20 times (TeCs 2, 10 and 11).

**10x longer battery life:** TeC 2 enables the UEs to use lower pilot+data power for a target SNR, thereby the battery life is extended. Moreover, the solution in TeC 9b for uplink power control directly influences the battery lifetime and improves it to a considerable extent.

**Energy efficiency and cost:** The solution in TeC 2 allows the UE to reduce the sum power level for a predefined UL spectral efficiency (rate) target and, therefore, to improve the UL (UE) energy efficiency. Moreover, the uplink power control scheme in TeC 9b provides a saving up to 95% with respect to the current power control.

## 2.4 Impact on METIS system

All TeCs report significant amount of results and impact mainly the horizontal topic UDN as well as most of the METIS goals. A couple of TeCs contribute to MN and URC.

The TeCs in MPTA1 aim to improve the proposed 5G backhaul as the technological power of massive MIMO makes it implicitly attractive for backhaul technologies. We consider both scenarios where we require backhaul for static nodes as well as for moving nodes. The example of static nodes is considered under the UDN scenario where small cells require robust and economic wireless backhaul. TeC 1b is a spectrally efficient and low complex backhaul solution using frequencies corresponding to mmW. The proposed scheme can be applied to almost line of sight links and between slightly misaligned large antenna arrays. In case of mobile nodes, e.g. in MN scenarios, mobility-robust high data-rate links for mobile terminals and moving relays to enable broadband as well as real-time services is required. For this purpose, TeC 6 provides methods which use advanced channel prediction techniques based on a predictor antenna array. These methods provide x100 improvement of BLER for a vehicle speed from 0 to 300kmph by using large arrays at the BS and beamforming.

MPTA2 topics are based on massive MIMO and aim to improve the proposed 5G access. This approach mainly targets the UDN scenario, but some focus has been given also to MN and URC scenarios. In case of conventional MIMO with legacy frequencies, TeC 10 provides advanced coordinated transceiver design with minimal required information exchange between the transmitting nodes. In addition to that, we also address in TeC 9b the uplink power control issue for both data and pilot transmission to operate in a given transmit power budget. The fusion of massive MIMO with mmW frequencies has been considered by TeC 7, which, with the help of 3D beamforming and by using more than 100 antenna elements, improves the received signal power to the desired user and reduce the interference power to other users. This allows us to realize mmW pico cells in a UDN scenario. The MN scenario can also be supported with the help of massive MIMO BSs if coordinated resource and power allocation for pilot and data signals is done as per TeC 2. With the help of massive and sparse spatial division multiple access schemes we also support the URC scenario. For this purpose, TeC 11 provides a solution which can guarantee a target SINR or a target rate for user with low geometry factor.

Finally, TeC 1c considers large aperture massive array systems which impacts on UDN scheduling a dense population with random access protocol. TeC 5 targets mainly the 1000 times capacity also impacting on UDN.

## 2.5 Overview of achieved results

In terms of results and contributions, TeC 1 and TeC 1c consider the following: the size of the massive array matters more than the number of antennas to create a large number of degrees of freedom (DoF) and large diversity order. The line of sight multi-user MIMO channel offers superior user decorrelation properties. In crowd scenarios, a strategy based on random access enables efficient joint pilot and data communication protocols.

TeC 1b provides a spectral efficiency of hundreds of bits/s/Hz for wireless backhaul in ultra dense networks, with very low complexity, thanks to the naturally huge degrees of freedom of short range MIMO in line of sight. TeC 2 considers coordinated resource and power allocation for pilot and data signals in massive MIMO Systems. Balancing the power and time-frequency resources between pilot and data signals shows spectral efficiency gains both in single cell and multi-cell massive MIMO systems. In particular, feasible low-rate multi-cell coordination techniques include pilot reuse and open loop path loss compensation based pilot power control schemes. Channel prediction considered in TeC 5 can be seen as main enabler for joint transmission CoMP, massive MIMO and integration of small cells as well as reduction of the required feedback rate in case of frequency division duplex (FDD) systems. Novel



extensions like bandwidth enlargement, virtual beamforming, massive MIMO and model based channel prediction are able to enhance state of the art performance considerably. TeC 6 provides robust and energy efficient wireless backhaul for fast moving vehicles thanks to arrays of predictor antennas. A proposed hybrid beamforming scheme for massive MIMO provides extremely high bit rates of more than 10 Gbps in higher frequency bands (TeC 7).

Multi-cell uplink power control has been illustrated to largely improve the energy efficiency in conventional MIMO systems. Tec 9b jointly controls the pilot and data transmit powers in multi-cell multi-user massive MIMO system subject to per-user SINR and power constraints. Two algorithms developed in the coordinated transceivers provide good approximations even when the dimensions of the problem (i.e. the number of users and antennas) are practically limited (TeC 10). This algorithm satisfies the target SINRs for all users; however, the error in approximation results in higher transmit powers at BSs. TeC 11 proposes to fully utilize the spatial multiplexing gain of massive MIMO in TDD, inter-cell interference at the receivers has to be taken into account for precoder design.

For a more detailed analysis of the synergies among the TeCs developed within Task 3.1, for instance which TeCs can be combined together to further enhance the performance, please refer also to [METIS14-D32, Sections 2.2.3-2.3.3].

## 2.6 Conclusion

The TeCs in this massive-MIMO/multi-antenna task T3.1 are now quite mature with distinct contributions in backhaul, access, mm-wave, channel prediction as well as moving networks. Many TeCs report better throughput, spectral efficiencies, SNR gains, coordination and resource allocation methods compared to LTE-A type scenario. The number of antennas goes up into hundreds with a variety of non-ideal aspects taken into account in the system. The main focus has been in the UDN which is expected to meet the capacity targets in a 5G system. Two MPTAs have been identified, i.e, massive-MIMO for backhaul and access. The TeCs under these are expected to contribute to METIS system architecture supported also by the other TeCs.

### 3 Task 3.2: Advanced inter-node coordination

#### 3.1 General overview

Inter-cell interference has been acknowledged as one of the limiting factors in nowadays cellular networks. One of the most promising approaches in dealing with interference has been the introduction of coordination between the elements of the network. Several studies were conducted, and the very large gains that were theoretically claimed are still difficult to be found when a realistic scenario is considered. Truth is that this kind of solution requires a careful design in order to reach the impressive gains that are expected, in particular when a joint transmission coordination is considered, where high performance backhauling with limited latency, and extensive and reliable channel knowledge are needed.

One of the outcomes of the research activities in Task 3.2 was that some of the issues that usually arise with full blown Joint Transmission CoMP approaches can be alleviated if non-dummy UEs are considered. Different technology components that exploit advanced UEs have been proposed and collected in Most Promising Technology Approach 1 “CoMP with advanced UE capabilities”. It was identified that assuming UEs with interference suppression capabilities allows for less complex coordination schemes at the BSs, and that fundamental enablers like channel prediction should be considered in order to overcome the limitation due to feedback delays. Cancellation capabilities can be even enhanced if the network assists the UEs in this task. Moreover, a joint optimization of BS clustering, beamforming design and UE receive processing can be exploited to achieve higher spectral and energy efficiency. A detailed description of these techniques is provided in Section 3.2.

Still it is possible that in certain situations the advanced infrastructure requested for joint transmission is not available. In this case the technologies described in Section 3.3 for Most Promising Technology Approach 2 “CoMP with limited backhaul capabilities” become viable solutions. All these approaches assume a limited exchange of information (or even none) between the transmitting nodes, but still can provide improved performance compared to SotA solutions by exploiting advanced schemes based on the capability to design transmitter/receiver filters that align/suppress the perceived interference at the UE.

Other studies were also performed in the task, some more theoretical which aimed to provide performance bounds for coordination techniques, other dealing with new network architectures (e.g. including relays or ultra dense deployments) or based on new access scheme (e.g. NOMA or non-coherent transmission), that tried to extend these novel approaches including coordination between the nodes. The full list of activities in Task 3.2 is reported in Table 3.1, while a comprehensive description of the results achieved in every technology component is collected in the appendix.

**Table 3.1: Full List of TeCs in Task 3.2**

TeC #	Short Title	Short description	MPTA
TeC 1	CoMP Resource Allocation	Investigation of the impact of feedback and backhaul links on the performance of different multi-node transmission schemes. Multi-node resource allocation is proposed under imperfect feedback and backhaul channels.	—
TeC 1b	NCJP CoMP for HetNets	Jointly optimize the precoding, load balancing, and BS operation mode (active or sleep) for improving the energy efficiency of heterogeneous networks. Multiple BSs can serve the users by joint non-coherent multiframe beamforming.	MPTA 1
TeC 1c	Precoder design with	The precoder design with limited information	—



	limited information in CoMP	can be improved using the long term channel statistics already available in legacy networks.	
TeC 2	Exploiting temporal channel correlation to reduce feedback in CoMP	An optimal feedback period is derived such that it guarantees same spectrum efficiency as using a conventional feedback scheme.	---
TeC 2b	DoF of MIMO BC and IC with delayed CSIT	Theoretical analysis of the Degree of Freedom (DoF) and net DoF of recent schemes for the MIMO IC and BC with delayed CSIT (DCSIT) and finite coherence time.	---
TeC 3	Distributed Precoding with Data Sharing	Precoding scheme for interference mitigation in multi-cell multi-antenna systems based on local CSI and data sharing.	MPTA 2
TeC 4	Multi-User Inter-Cell Interference Alignment (MUICIA)	Design of multi-user selection algorithms in an OFDM based closed loop downlink transmission system. The transmit-precoding scheme is based on interference alignment in a multi-user multi cell network where both the transmitters and the users are equipped with multiple antennas.	---
TeC 5	Semi-distributed IA with PC convergence speed up	Semi-distributed algorithm to find the optimal filters at the BSs and UEs that achieve a target SINR at each UE, with power control (PC) to reduce the number of iterations and check the existence of the optimal solution at the beginning.	---
TeC 5b	IA with Imperfect CSI	Study of distributed iterative interference alignment based techniques for MIMO interference channel with imperfect effective channel state information.	---
TeC 6	Distributed Low-Overhead Schemes for sum-rate maximization in MIMO Interfering Networks	Algorithms relying on the use of UL / DL pilots and forward-backward iterations to gradually refine both transmit and receive filters, in a fully distributed manner, to maximize the sum-rate. The proposed schemes only require a handful of such F-B iterations, to deliver high spectral-efficiency.	MPTA 2
TeC 7	Dynamic Clustering with Multiantenna Receivers (DCMR)	Develop a dynamic BS clustering and UE scheduling for downlink CoMP systems where the resource allocation scheme explicitly considers that UEs are equipped with multiple antennas.	MPTA 1
TeC 8	NOMA	Non Orthogonal Multiple Access (NOMA) with multi-antenna transmission schemes.	---
TeC 9	Coordination scheme for medium range interference with message splitting to facilitate efficient SIC	The work investigates a Han-Kobayashi like coordination scheme that pursues the generalized degree of freedom of the system by splitting each user message into two separate parts. One part is designed not to significantly interfere with the other message receiver, but rate adapted to the desired receiver, and another part is power-set and rate adapted to be decodable at the interfered receiver, to give a good likelihood of successful interference	---

		cancellation.	
TeC 10	Hierarchical Precoding for UDN	This work develops a hierarchical precoding solution which mitigates the inter-cell interference from the macro-cells caused at the users mainly served by the small-cells.	MPTA 1
TeC 11	DIAS	Decentralized interference aware scheduling (DIAS) approach suitable for D2D communication, based on the transmission of a reverse beacon to signal interference.	—
TeC 12	NA IS/IC receivers and ultra-dense networks	Network-assisted co-channel interference robust receivers for dense cell deployments.	MPTA 1
TeC 13	Interference mitigation based on JT CoMP and massive MIMO	In ARTIST4G a powerful interference mitigation framework has been developed based on CoMP-JT beside others for a 4x2 MIMO scenario. Identified limitations like limited coverage for indoor users and rank deficiencies in case of many simultaneously served users are overcome by proper inclusion of small cells and massive MIMO. Coded reference signals (CSI-RS) allow estimation of some tens of relevant out of hundreds of potential channel components, enabling the novel framework in frequency division duplex (FDD) systems.	MPTA 1
TeC 14	Coordinated scheduling for two-way relaying with NC.	In this work we apply the coordinated scheduling approach for the two-way relaying with NC and MIMO in TDD systems.	—
TeC 15	Adaptive and energy efficient dense small cells coordination	Define coordination schemes that allow to switch off unnecessary small cells when traffic request is low.	—
TeC 16	Non-coherent communication in coordinated systems	This work investigates non-coherent communication in systems where the users can be connected to multiple transmission points.	—
TeC 17	Interference management for dynamic TDD transmission/reception	Coordinated precoder/decoder optimization in multicell multiuser dynamic TDD system in order to maximize network utilities.	MPTA 2

### 3.2 Most Promising Technology Approach 1: CoMP with advanced UE capabilities

#### 3.2.1 Introduction

The huge spread of UEs with advanced capabilities, for instance smartphones and tablets equipped with multiple antennas, high-speed processors or high-storage capacity, needs to be taken into account when designing cellular networks in the next years. In TeC 1b multiframe transmission is assumed by a set of coordinated BSs, which allows each UE to receive different data streams from multiple BSs by performing successive interference cancellation on its own information symbols. Dynamic clustering solutions for downlink CoMP are then investigated in TeC 7 by explicitly considering UEs equipped with multiple antennas that exploit these degrees of freedom to suppress the interference and to detect multiple streams of data. Moreover, channel prediction algorithms at the UEs are implemented in TeC 10 to reduce the feedback requirements. In TeC 12 a network providing additional interference

information to the UEs is studied with the aim of allowing the UEs to better exploit their interference suppression capabilities. Finally, TeC 13 can exploit better interference estimation at the UEs to improve the performance achieved when CoMP-JT is applied by macro BSs and small cells.

### **3.2.2 TeC 1b: Non-coherent joint processing CoMP for energy-efficient small cell networks**

The concept of heterogeneous dense networks, which is based on the idea of dense deployment of low-cost and low-power access points coexisting with the traditional macro BSs, has been considered as a key technique to increase the spectral efficiency and energy efficiency for future wireless communication systems. By creating a large number of small cells, these low-power access points have the potential to offload traffic from macro BSs, reduce the average distance between users and transmitters, increase the system capacity and reduce the transmission power.

Different from the traditional cellular system, the densely deployed access points will be heterogeneous in the number of transmit antennas, transmit power, and coverage area, etc. Moreover, the knowledge of the CSI at each BS is highly likely to be different and imperfect. In this complex scenario, a major research problem is to design low-complexity and robust multi-BS cooperative schemes that improve the overall energy efficiency, at the same time, satisfying QoS expectations of the users.

This TeC studies the joint precoding and load balancing problem in the downlink of a heterogeneous network, as illustrated in Figure 3-1. The network consists of different types of BSs serving single-antenna users randomly deployed in the network. We assume that the BSs are connected via backhaul links, and all BSs are able to transmit to all users at the same time and frequency resources. However, motivated by the fact that tight phase synchronization between BSs is extremely difficult to achieve in practice, only linear non-coherent joint transmission is allowed: that is, each user can be served by a set of BSs using superposition coding. This scheme can be referred to as spatial multiframe transmission and requires each user to perform successive interference cancellation on its own information symbols in order to receive different data streams from multiple BSs. In addition, it is assumed that the channels are imperfectly known to the users and the BSs.

The following important system design questions are investigated in this work: a) How to design precoding matrix for each BS with imperfect CSI? b) How to select the transmission nodes for each user? c) How to decide the operation mode (active or sleep) for each BS? d) How to reduce the energy consumption, at the same time, satisfying QoS expectations of the users?

These issues can be formulated into a joint resource optimization problem, which minimizes the weighted total power consumption of the system, while satisfying a set of per-user SINR constraints (rate constraints) and a set of per-BS transmit power constraints. The optimization problem is not convex. In particular, when taking BS operation mode (active or sleep) selection into account, the power consumption function leads to a hard combinatorial problem. However, we show that for each fixed combination of BS operation modes, the optimization problem can be reformulated to a convex problem. Then, the global optimum can be found by an exhaustive combinatorial search over these  $2^M$  convex problems, where  $M$  is the number of BSs in the network. Moreover, in order to reduce the complexity, we propose a heuristic algorithm, which resolves the non-convex problem by iterative convex approximations of the power consumption functions.

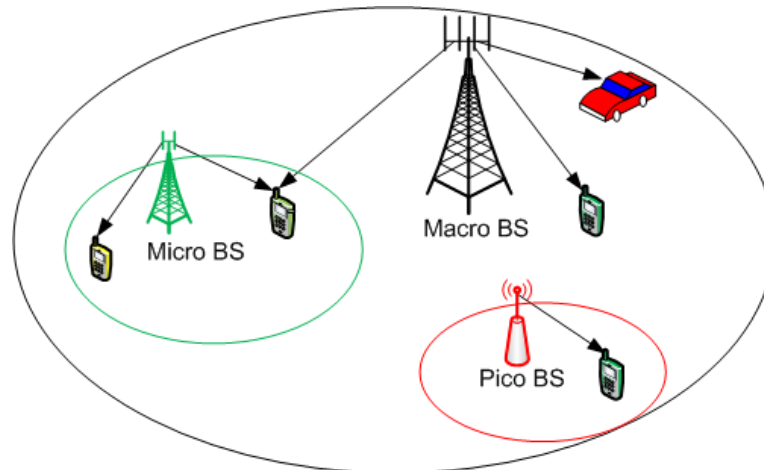


Figure 3-1: Illustration of a downlink heterogeneous network consisting of macro, micro and pico BSs

### Performance Results

System level simulation is performed to illustrate our analytical results and test our proposed algorithms. The environment model is a simplified version of the dense urban information society model (TC2) used in the METIS project, as illustrated in Figure 3.4 of [METIS13-D61], consisting of four square shaped buildings of 120m×120m, each with 6 floors. A macro BS (MBS) is complemented with 4 small cell BSs (SBSs). The MBS has 4 transmit antennas, and the SBS has 2 transmit antennas each. Five users are randomly and uniformly dropped in the network, with 80% are indoor users and 20% are outdoor users. Here, we adopt the indoor and outdoor propagation models, PS#1-PS#4, identified in METIS. More details regarding network deployment and propagation modes can be found in Table 3.7 and Section 8.1 of [METIS13-D61]. We assume independent Rayleigh small-scale fading.

The total power consumption of the network is modelled with a static part that depends on the transceiver hardware and a dynamic part which is proportional to the transmit signal power. Adding more low-power BSs or more transmit antennas can reduce the dynamic power consumption, but require more hardware, thus, it will increase the static part. Note that the static power consumption also depends on the operation mode of each BS, i.e., whether the BS is active or in the sleep mode. In particular, we adopt the linear approximated power consumption model proposed in the EU EARTH project [EAR12D23, Table 6 and Table 8].

Three different joint precoding and load balancing schemes are compared in this scenario. We name these three schemes as “Optimal”, “Heuristic” and “All Active” respectively. The “Optimal” scheme obtains the global optimal solution by an exhaustive search over all  $2^5$  possible BS mode combinations. The “Heuristic” scheme follows the proposed iterative heuristic algorithm. The “All Active” scheme is used as our performance baseline, which solves the optimization problem by assuming that all BSs are active. For each scheme, the performance is averaged over 1000 independent user drops that provide feasible solutions for our optimization problem. For each user drop, the algorithms are evaluated over 50 independent channel realizations. Define the dynamic part of the total power consumption as the total RF power and the remaining part of the total power consumption as the circuit power. Figure 3-2 demonstrates the total RF power and the total power consumption as a function of target spectral efficiency per user. As expected, the total power consumption and the RF power increase as the target spectral efficiency increases. Figure 3-2 (left) shows that the RF power for the “All Active” scheme is less than that of the “Heuristic” and “Optimal” schemes. This is expected since all BSs are active in the “All Active” scheme, whereas for the “Heuristic” and “Optimal” schemes, some BSs are put into the sleep mode. With more BSs being active, the “All Active” scheme provides better energy-focusing and less propagation losses between

the users and the transmitters, and will therefore reduce the total RF power. However, as can be seen from Figure 3-2 (right), compared to the “All Active” scheme, the “Heuristic” and “Optimal” schemes can substantially reduce the total power consumption, especially when the target QoS is small. This is because the circuit power consumption under the sleep mode is much lower compared to the one under the active mode. For the “All Active” scheme, the increase in the circuit part from the extra power consumed by activating BSs clearly outweighs the decrease in the dynamic part. This implies that putting a BS into sleep mode by proper load balancing is an important solution for energy savings in heterogeneous networks.

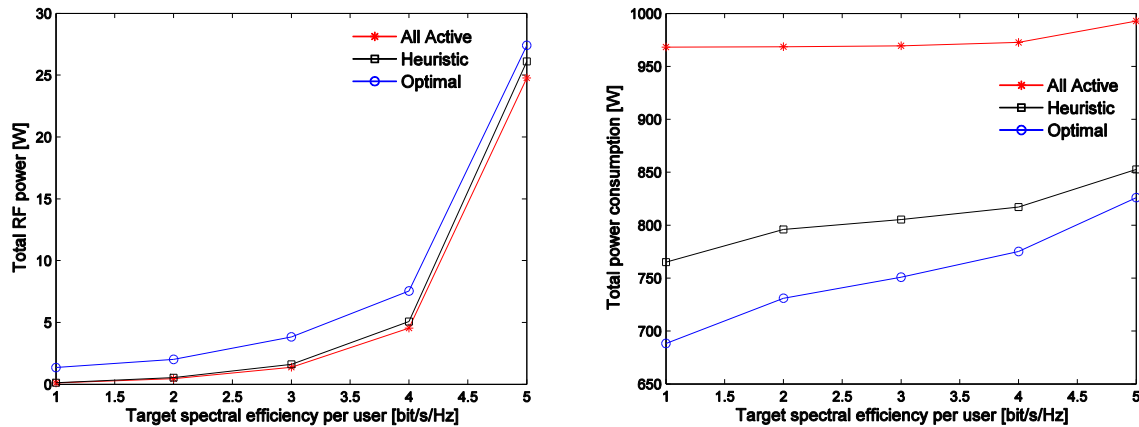


Figure 3-2: Total RF power (left) and total power consumption (right) vs. target spectral efficiency per user

### 3.2.3 TeC 7: Dynamic clustering with multiple receive antennas in downlink CoMP systems

Most of the works on CoMP focus on systems where UEs are equipped with only one antenna, although already with LTE-Advanced UEs may be equipped with up to eight antennas [BCG+12]. Although this number seems rather optimistic, the technological innovation may allow in the near future manufacturing smartphones and tablets equipped with several antennas. Moreover, different types of UEs will be served by the cellular networks in 2020: for instance, vehicles will probably be part of the cellular infrastructure, and, due to their size, they can be quite easily equipped with multiple antennas [METIS14-D62]. Hence, the importance of developing algorithms for CoMP-JP has been recognized which that these additional UE capabilities explicitly take into account [HCL+13].

This TeC considers a downlink CoMP-JP scenario, i.e., a scenario where CSI and data to be sent to the UEs are shared among the BSs. We assume that a central unit (CU) coordinates the BSs and the backhaul links have zero latency and are error free. In this setup, we propose an algorithm to jointly perform dynamic BS clustering and UE scheduling, under the assumption of multi-antenna UEs. We assume that UEs perform successive interference cancellation (SIC) with interference rejection combining (IRC). By observing that most of the interference at each UE comes from the closest BSs and with the aim of reducing the implementation complexity of the algorithm, we assume that only a set of candidate BS clusters, which depends on the large scale fading, is considered by the CU. As this candidate BS cluster selection depends on the large scale fading component of the channel, the list of candidate BS clusters is updated on a long-term time interval, for instance every hundreds of milliseconds.

Then, depending on the fast-fading component of the channel, i.e., every few milliseconds, the CU organizes BS clusters and schedules UEs in each cluster by applying the following two-step scheme.

1. For each candidate BS cluster, a weighted sum-rate is estimated by optimizing precoders, powers, transmission ranks and scheduled UEs. In particular, we use the multiuser eigenmode transmission (MET) scheme [BH07], with equal power allocation among the streams and a greedy iterative eigenmode selection algorithm.
2. Once the weighted sum rate has been computed for all the candidates, the CU selects the set of non-overlapping BS clusters to be used for transmission by maximizing the system weighted sum rate. As the optimization problem is shown to be NP-hard, we propose a greedy iterative algorithm to reduce the implementation complexity.

More details about this TeC can be found in [BBB14].

## Performance Results

We consider the WP3 task 3.2 simulation baseline where 3 macro sectors and 18 micro sectors, for a total of 21 BSs, are deployed in a grid of 3x3 buildings and serve 210 outdoor UEs [METIS14-D32, Fig. 8.1]. Details regarding the position of the BSs and the model for the large scale fading component of the channel can be found in [METIS14-D32, Section 8.2]. Regarding the fast fading, we consider (a) a MIMO Rice model with a Rice factor of 10 dB for the LOS case and (b) a MIMO Rayleigh model for the NLOS case. Moreover, we assume that each macro BS is equipped with 4 antennas with a maximum transmit power of 46 dBm, whereas each micro BS is still equipped with 4 antennas but with a maximum transmit power of 30 dBm. The carrier frequency is 2.6 GHz and the system bandwidth is 10 MHz. Then, we implement proportional fair scheduling to provide fairness among the UEs, which employ SIC with IRC. Perfect detection is also assumed.

We compare the developed scheme based on dynamic clustering (DC) by assuming a maximum cluster size of 3 BSs against a baseline denoted single cell processing (SCP), where each UE is served by its anchor BS and no cooperation is allowed among the BSs in the network.

In Figure 3-3 we report in terms of the number  $N$  of UE antennas the average cell rate and the 5th percentile of the UE rate, respectively. By adding antennas at the UE, we observe an important performance improvement. For instance, with SCP by increasing  $N$  from 1 to 4 there is an improvement of about 80% in terms of 5th percentile of the UE rate. Two factors mainly contribute to this gain: (a) UEs with lower SINR use IRC to limit the impact of residual ICI not managed at the transmit side and (b) UEs with higher SINR can be served by multiple streams of data. From Table 3.2, where we report the distribution of the transmission rank with  $N = 4$ , we note that with SCP more than 80% of the transmissions are rank-1. On the other hand, with DC, as the interference level suffered by the UEs is lower, about 35% of transmissions are multi-stream. This shows that in general most of the gain is due to the IRC and multi-stream transmission plays a non-negligible role only with DC. Moreover, we also observe that the performance gain achieved by DC over SCP decreases by adding more antennas at the UE side. In fact, as the gain of using multiple antenna UEs is mainly due to the IRC which cancels ICI, the benefits of increasing  $N$  are seen more in a non-cooperative scenario, where the residual ICI is higher with respect to DC. In detail, the performance gain in terms of the average cell rate achieved by DC over SCP drops from about 70% with  $N = 1$  to about 25% with  $N = 4$ , while the performance gain in terms of the 5th percentile of the UE rate achieved by DC over SCP drops from about 160% with  $N = 1$  to about 100% with  $N = 4$ .

Then, two important comments should be made when we compare these results with the ones already shown in a homogeneous hexagonal scenario [BBB14, Fig.s 5-6]. First, we observe that much higher rates are achieved in the WP3 task 3.2 simulation baseline considered here: for instance, the average cell rate is almost doubled. Second, we observe that the gain achieved by CoMP over the baseline are much higher here than in the homogeneous hexagonal scenario: for instance, in terms of the 5<sup>th</sup> percentile of the UE rate, in [BBB14] this gain varies from about 15% when  $N=4$  to about 50% when  $N=1$ , whereas here this gain varies from about 100% when  $N=4$  to about 160% when  $N=1$ . These two effects can be explained by

observing that the WP3 task 3.2 simulation baseline is a heterogeneous scenario with an higher density of BSs. Therefore, those UEs closer to their anchor BS measure a better SINR and, as a consequence, achieve higher rates. Then, in heterogeneous networks the *structure* of the interference is typically different with respect to the one in a homogeneous scenario: in heterogeneous networks the interference comes mainly from few strong interferers, typically the macro BSs. Hence, CoMP schemes provide more benefits in this setup, even if the maximum cluster size is rather small (only 3 BSs).

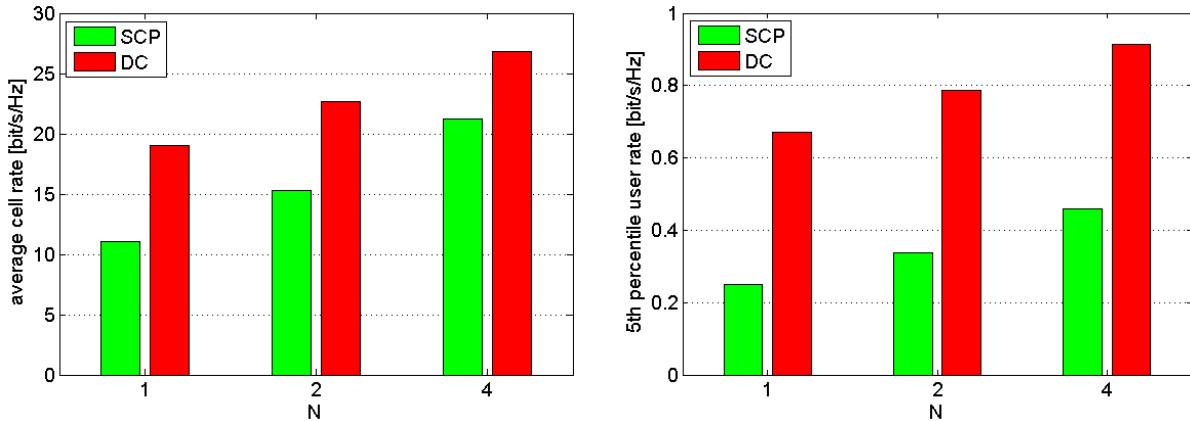


Figure 3-3: Average cell rate (left) and 5th percentile of the UE rate (right) with respect to the number N of UE antennas

Table 3.2: Distribution (%) of the transmission rank with N=4

	Rank-1	Rank-2	Rank-3	Rank-4
SCP	82.0	15.6	2.2	0.2
DC	65.2	22.3	9.2	3.3

### 3.2.4 TeC 10: Hierarchical precoding for ultra dense networks with enhanced multi-antenna receive processing

The need for cell densification leads to inter-cell interference mitigation techniques known as CoMP transmission and reception. In this TeC, we demonstrate the limits of joint regularized zero-forcing precoding within a cluster of several macro and small-cell base stations. While studying the effects of heterogeneous power constraints in such a cluster of transmission nodes, we develop a hierarchical precoding solution which mitigates the inter-cell interference from the macro-cells caused mainly at the users served by the small-cells. Due to significantly reduced transmission power, inter-cell interference between small-cells as well as interference caused at the macro users is not significant and hence is not taken into account within the precoding algorithm. This assumption is justified by using a cell-range extension (CRE) factor of 6 dB which ensures that users connected to the macro are not located close to the small-cell BS. In [METIS13-D31, METIS14-D32] we showed that feedback delays up to 20 ms can be compensated approximately without performance loss for user with 3km/h velocity using channel prediction.

#### Performance Results

Here we consider a coordinated cluster to constitute three macro-sectors and the respective small cells, which are allocated within the coverage area of the macro BS. The set of users within the cluster  $c$  are divided into macro users and small-cell users as illustrated in Figure 3-4. For more details on the simulation assumptions and setup we refer to the appendix.

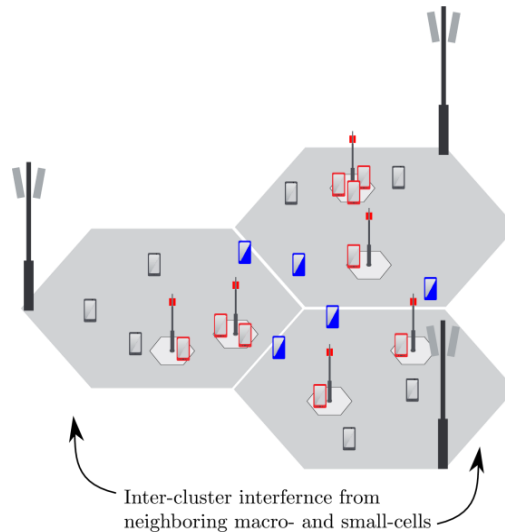


**Figure 3-4: Inter-site CoMP of macro-sectors facing to each other. In addition, we add 2 small-cells per macro sector footprint. Red UEs are attached to small-cells, blue UEs will benefit most from the joint transmission of macro sectors, and gray UEs may be served independently from all others.**

Based on the idea from [DKTH14] where BD is combined with the iterative IA algorithm from [ABW12, APJ12] we are using MMSE optimization in the iterative pre- and post-coder design. In [DKTH14] no results on data rates are provided leaving an open question on quantifying the overall system efficiency by reducing the interference at the small-cell users and at the same time sacrificing efficiency for the macro users. Here we compare the schemes from [DKTH14] and an extended approach with MMSE optimization for the post- and pre-coders. The following acronyms correspond to the three cases:

1. BD: Uncoordinated case where each node uses the BD precoding independently
2. BDIA: Hierarchical precoding as in [DKTH14] where small cell users are protected from macro-cell interference
3. BDIA MMSE: Extension of the scheme shown in [DKTH14] with MMSE transmit and receive filter design.

In the third case, also the channels between the small-cell users and small-cell BSs have to be known at the macro BS, but there is no joint precoding, i.e., no user data are shared among the macro and small-cell BSs.

The effect on the interference from the macro BS received at the small-cell users after post-coder is shown in Figure 3-5 (a). We assume that two users at the macro BS and one user per small-cell BS are served. Here we observe an average gain of more than 20 dB using the IA techniques with and without the MMSE modification in the single-cell scenario, labeled with 'SC'. However, in the multi-cell scenario labeled with 'MC' there is a lower bound from inter-cell interference (ICI) which limits the gains achieved in the single-cell scenario. The impact on signal power received at the macro users is given in Figure 3-5 (b) where we observe the expected loss for both IA schemes compared to 'BD' which maximizes the signal power.

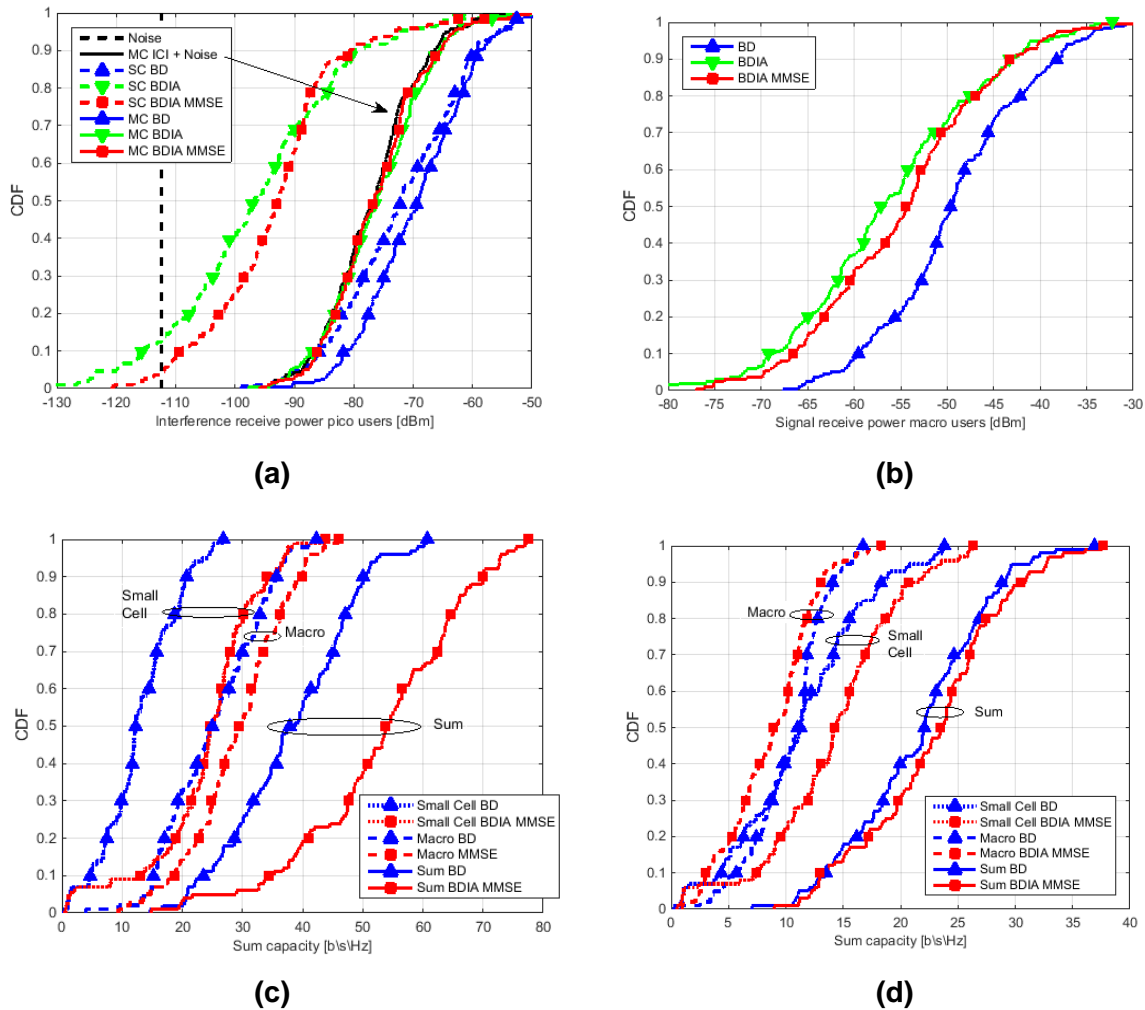


**Figure 3-5: (a) Impact of interference coordination on perceived macro-cell interference at small-cell users. (b) Impact of signal power perceived at macro-cell users. (c) Results in sum spectral efficiency for a single macro-sector and its corresponding 2 small-cells. (d) Results in sum spectral efficiency in multi-cell environment.**

The results on capacity in the single-cell scenario are shown in Figure 3-5 (c). Compared to the uncoordinated case we can achieve a gain of 16 bit/s/Hz with the joint BDIA MMSE approach by increasing the performance for interference limited small-cell users. The gain achieved at the macro users despite the loss in the receive signal is caused by the interference suppression from small cells. In Figure 3-5 (d) the corresponding multi-cell results are shown where the overall gain is reduced to 3 bit/s/Hz originating from the small cells.

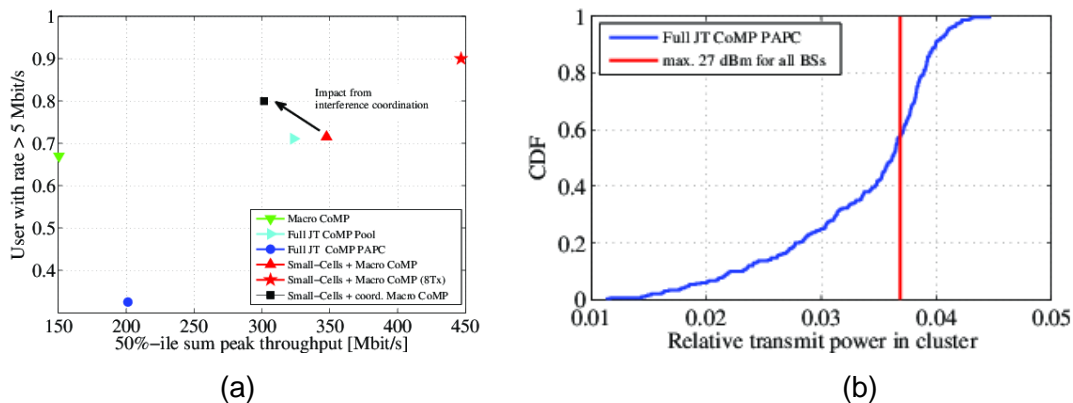
We expect another improvement by using channels weighted with the transmit power to further optimize the SINR, especially for small-cell UE. Future work will study this algorithm in presence of remaining multi-cell interference on system-level.

Figure 3-6 shows the system-level simulation results for different assumptions on the infrastructure side: First we show (green triangle) the performance of a system where only macro-cells are available and 3 sectors perform the joint transmission. In this case, we can only guarantee the given bit rate target for 67% of users.

As next step, we add small-cells into the coverage area and assume a full joint transmission among all nodes in the cluster, i.e. 3 macro sectors and 6 small-cells in total (right-pointing triangle and circle) as indicated in Figure 3-4. We observe severe degradation in peak and user rates under a realistic PAPC. This is attributed to the small power budget at small cells which results in the fact that also macro BS transmit with 27 dBm instead of 46 dBm. As a

proof, Figure 3-6 shows the CDF of the distributed transmit power budget in the cluster. 100% attributes to  $3 \times 46$  dBm +  $6 \times 27$  dBm and is achieved in the non-feasible pool power constraint (light blue) case, where all BS can share their transmit power budget. The red bound is based on the assumption of  $9 \times 27$  dBm transmit power allocation.

Next, we compare these results with the assumption that 3 macro-sectors perform joint transmission and small-cells operate independently in the same band (red triangle), which improves the the peak performance significantly. However, user satisfaction is only slightly better. Finally, we provide the results of macro-interference coordination and highlight that coordination trades peak performance with higher user satisfaction ratio (black square).



**Figure 3-6: (a) The x-axis depicts the 50%-ile sum data rates under a full-buffer assumption for user data traffic. Therefore, we call it peak data rate. The y-axis plots the fraction of users achieving their bit rate target of 5 Mbit/s (the higher the better). Note, we cannot achieve both metrics at the same time. The data point (red star) assumes  $N_t=8$  at the macro sites and  $N_r=4$  elements at UE, while all other results assume  $N_t=4$  and  $N_r=2$ . (b) Depicts the power allocation in the joint precoding case, i.e. Full JT CoMP PAPC.**

### 3.2.5 TeC 12: Network-assisted interference suppressing/cancelling receivers and ultra-dense networks

In cellular networks, particularly in those targeting high system spectral efficiency by deploying frequency reuse 1, the user data rates, especially on the cell border areas, can be severely degraded by the interference caused by the transmissions in neighbouring cells. This co-channel inter-cell interference (ICI) problem has been identified by the research community as a key limiting factor for reaching increased capacity in cellular networks.

Network-centric approaches to resolve the ICI problem include techniques such as the 3GPP Rel-10 enhanced inter-cell interference coordination (eICIC) mechanism [DMW+11, LVD+11], which involves multi-cell resource management function that takes into account information (e.g., the status of traffic load and resource usage) in multiple cells, such that different cells coordinate use of resources in frequency (coordinating resource block allocation) and time (coordinating subframe utilization across cells in time through so called almost blank subframe (ABS) patterns) domains. In Rel-11, the eICIC operation for heterogeneous deployments was further enhanced by providing a UE with assistance information on cell-specific reference symbols (CRS) of the aggressor (interferer) cells to enable the victim UE to cancel interference on common control channels of ABSs caused by CRS of high power macro cells. Two aspects in this further enhanced ICIC (feICIC) scheme are worth noting, namely (1) the active role of the UE receiver (w.r.t. Rel-10 eICIC operation) and (2) the employment of non-linear interference cancellation.

Another approach to cope with the co-channel interference issue, targeting boost in network capacity, is to increase the UE receiver role in system design. This path was taken when Release 11 specified UE performance requirements for interference rejection combining (IRC)

receiver [3GPP12-36829]. The obtained results were promising showing notable performance gain compared to receivers treating co-channel interference as additive white Gaussian noise (AWGN) [PIB+13, 3GPP12-36829].

The core idea of this TeC is to make a UE receiver aware of information related to the key parameters characterizing the transmission in the neighbouring cells causing co-channel interference to the victim UE. Depending on the transmission scheme, these interference parameters may include, e.g., (but are not limited to) cell ID, reference signal ports, power offset values, precoder selection, transmission rank, modulation order. With the aid of network assistance (NA) (implemented by means of eNB-to-UE higher-layer signalling), the accuracy of the co-channel interference estimation and mitigation performance in terms of suppression (IS) or cancellation (IC) at UE receiver can be improved [3GPP13-RP130404, 3GPP13-36866]. An example of NA-enabled advanced non-linear receiver structures is a receiver that performs symbol-level IC, and is referred to as SLIC. The SLIC receiver performs the following additional processing, in comparison to that of the baseline IRC: interferer parameter extraction (obtained through eNB-to-UE NA signalling and/or blind detection at UE receiver), interferer channel estimation, interferer detection, and interference reconstruction and cancellation at symbol-level. The concept of network-assisted co-channel interference mitigation is depicted in Figure 3-7.

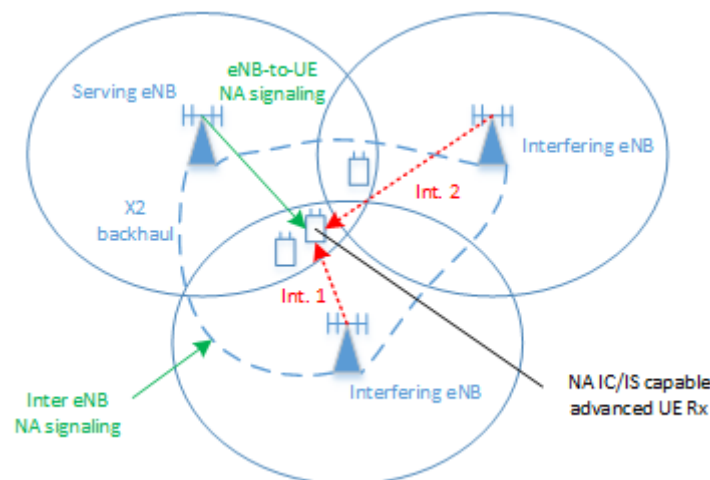


Figure 3-7: Overview concept picture showing the higher-layer NA signaling components

## Performance Results

To evaluate the performance of this TeC, we consider a multi-cell multi-user MIMO system assuming 2Tx – 2Rx antenna configuration ( $\setminus$ w cross-polarization). For the system-level evaluations, a drop based simulation methodology is adopted. To model the links between cells and UEs, channel realizations are generated according to model in [3GPP10-36814] with the geometry-based stochastic ITU-R Advanced model for fast fading. Quasi-static simulations are assumed, that is, within a given drop the large scale propagation parameters (e.g., path loss and shadowing) remain unchanged whereas Doppler related multi-path parameters change according to UE speed, which is assumed as 3 km/h. Overall, a few tens of drops, each covering a period of few thousand transmission time intervals (TTI), are simulated.

The simulations are carried out assuming homogeneous network deployment and ITU UMa (Urban macro) environment. Regarding the network topology, a hexagonal grid with inter-site distance (ISD) of 500m is assumed and two tiers (7 sites with co-located 3–sectorized antennas / 3 cells each) are modelled. Bursty (non-full buffer) traffic is modelled using a FTP traffic model characterized by a fixed packet size of 0.5 Mbytes and Poisson distributed packet arrival process with average arrival rate of 1.5 packets/sec/eNB. PF scheduling algorithm is

applied. The performance is measured in terms of the mean and 5%-tile user throughputs (UTP), where user throughput is given by the ratio between the amount of data (file size) and the time needed to download data [3GPP10-36814].

The system-level performance of a network-assisted genie-aided SLIC receiver is evaluated and compared to that of the Rel-11 baseline IRC receiver by carrying out simulations under the following assumptions. We consider a carrier frequency of 2 GHz and a system bandwidth of 10 MHz. A 2x2 SU-MIMO operation based on transmission mode (TM) 10 with rank adaptation is assumed as transmission scheme. Practical channel and covariance estimation (associated to both serving and interfering cells) required for demodulation as well as for CSI feedback purposes are assumed. Further, regarding UE feedback we assume subband CQI and wideband PMI reporting and consider 5 ms reporting interval and 6 ms delay in the evaluations. Moreover, HARQ process with maximum of 5 re-transmissions is modelled. Overhead due to reference symbols (incl. 2 CRS Rel-8 legacy overhead, DMRS and CSI-RS) and control channel (assuming 3 OFDM symbols) are taken into account. A BLER target of 10% is set for CQI selection as well as for outer-loop link-adaptation. For SLIC receiver, we have considered the link-to-system (L2S) modelling from [3GPP13-36866].

The obtained system-level results are summarized in Table 3.3, showing the 5%-tile and mean user throughput numbers in Mbps for the Rel-11 baseline IRC receiver and the NA genie-aided SLIC receiver assuming Rel-11 CQI feedback. SLIC receiver can be observed to provide relative gains of 8.7 % and 3.0 % in cell edge and cell average throughputs, respectively.

**Table 3.3: The system-level gains of network-assisted SLIC receiver in homogeneous macro scenario in case of moderate network load (resource utilization ~40%)**

	<b>5%-tile UTP [Mbps]</b>	<b>Mean UTP [Mbps]</b>
<b>Rel-11 IRC</b>	3.60 (baseline)	18.25 (baseline)
<b>SLIC /w Rel-11 CQI</b>	3.91 (+8.7 %)	18.80 (+3.0 %)

### **3.2.6 TeC 13: Extension of IMF-A interference mitigation framework to small cell scenarios and Massive-MIMO – The OP CoMP concept**

Interference mitigation, massive MIMO and small cells (SCs) are expected to be main drivers to an increased spectral efficiency in future mobile radio networks. Based on joint transmission cooperative multipoint (JT CoMP) the so called Interference Mitigation Framework (IMF-A) has been developed in the FP7 project ARTIST4G [ARTD14] and laid the foundation to notable performance gains with respect to coverage and average spectral efficiency. For achieving a further step to higher performance one has to overcome the outdoor to indoor penetration loss and to increase the rank and condition of the channel matrices characterizing each single cell of the network. Theoretical and simulation results indicate that massive MIMO and small cells in combination with JT CoMP provide significant performance gains. For UDN networks very high number of small cells per macro cell can be expected, which makes a full and tight integration challenging. For that reason it is proposed to limit the cooperation to those small cells bringing significant benefit for the macro layer, while the rest of the small cells is operating in a different SC frequency band completely independent of the macro layer.

The overall scheme is called opportunistic CoMP (OP CoMP) as it opportunistically selects suitable small cells and beams depending on the user locations as well as other criteria like backhaul availability, channel estimation performance, load conditions etc. The full potential of OP CoMP is still under evaluation, but it is expected to reduce the otherwise high complexity to a reasonable level.

Massive MIMO assumes as baseline time division duplex (TDD), where exploitation of channel reciprocity allows channel estimation of massive number of channel components with a single/few sounding reference signals (SRS) per UE. For OP CoMP we assume frequency

division duplex (FDD) requiring CSI estimation and according uplink reporting per antenna element.

The here assumed baseline concept is a combination of enlarged cooperation areas formed over e.g. three sites with three cells each, where each of the nine macro cells is equipped with a massive MIMO antenna array. A typical massive MIMO configuration will be a 16x16 or 32x16 square linear array (SLA), meaning 16 or 32 columns of 16 vertically stacked antenna elements. This would lead to 256 or even 512 overall antenna elements per massive MIMO array. This number of physical antenna elements can be significantly reduced by forming for example eight effective channel components by a suitable fixed precoder generating eight equally spaced beams per cell sector. This is typically called a grid of beam (GoB) concept and downscales the number of channel components per cell from 256 to 8. As there are 9 macro cells, there will be overall 72 macro cell beams or channel components. Assuming furthermore 70 small cells per cooperation area with 6 beams each, the CSI for additional 420 small beams will have to be estimated.

Investigations like ray-tracing simulations in Munich city centre as well as other system level simulations reveal that a single UE will see only a very limited set of these channel components, i.e. the overall channel matrix will be sparse. OP COMP exploits this for example to reduce the size of the precoding matrix. More importantly a novel CSI-RS reference signal scheme has been developed, being termed 'Coded-CSI' reference signals. While for 3GPP LTE CSI RSs are allocated individually per antenna port, in case of Coded CSI each CSI-RS is being transmitted from a carefully chosen subset of antenna ports. In addition each antenna port transmits at least two different CSI-RSs. For reconstruction of the per antenna element CSI, the UEs perform typically a pseudo inverse on all received CSI-RSs. That way, N out of  $N^2$  channel components can be reconstructed, allowing for N=40 CSI RSs - as provided by LTE - the reconstruction of 40 UE individual out of overall 400 channel components. Important to note is that each UE can reconstruct a different set of relevant channel components.

From WP3 perspective, Coded CSI is a game changer as it enables a low overhead FDD massive MIMO solution – potentially including CoMP as well as high number of small cells - with limited overhead. It is a way to solve the well known pilot contamination issue and exploits the inherent beamforming gains of the GoB concept.

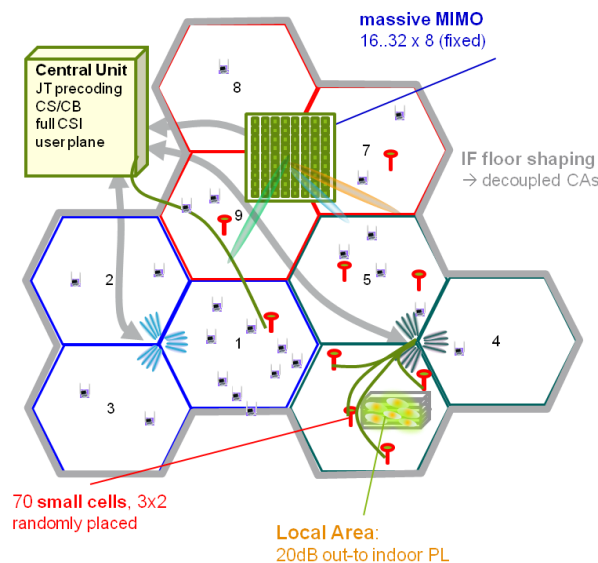


**Figure 3-8: Single cooperation area consisting of nine cells enhanced by massive MIMO array of size 16x16 as well as 70 randomly placed small cells**

## Performance Results

First analysis and simulations have been performed for a better understanding of the benefits of massive or more importantly of large scale MIMO in the context of future 5G wide area concepts. A single cooperation area as illustrated in Figure 3-8 consisting of nine cells enhanced by massive MIMO arrays of size 16x16 as well as 70 randomly placed small cells has been evaluated. All vertical macro antenna elements are standard Kathrein antennas as typically being used in today's wide area networks consisting of a row of 8/16 antenna elements and are placed in a height of 35m. Beamforming is limited in this case to the horizontal plane according to precoding of the 16 antenna elements forming a uniform linear array (ULA). 70 small cells are placed randomly in the cooperation area and are down selected e.g. to the 40 most relevant small cells.

At least for lower RF-frequencies of around 2 to 3GHz and reasonable number of antenna elements in real world scenarios there will be a strong inter beam interference. A powerful interference mitigation technique joint transmission CoMP is performed in the central processing unit connected to all relevant radio stations over fibre. So far the backhaul connections are assumed to be ideal, but one of the main targets for OP CoMP is to relax these requirements in terms of required capacity as well as latency as far as possible. This will be investigated in more detail in the future.

Figure 3-9 is the typical resulting power normalization loss (PNL) for increasingly higher number of simultaneously served users. The PNL is the sum precoding power divided by the sum Tx power of all participating radio stations and therefore characterizing the performance of the overall solution. Ideally the PNL should be close to 0dB to avoid any SNR degradations for the UEs.

In case of 'macro only' all small cells are being switched off and accordingly the number of supportable UEs limited to 50 users. Even in the case of 50 users the PNL is already at about 4 to 5dB. For 80 users the PNL is even higher and in addition the system will be overloaded so that there are further performance degradations. Contrarily activating all or a suitable subset of small cells allows serving up to 80 or even 90 UEs per cooperation area with high modulation and coding schemes (MCS) as well as high signal to interference and noise ratio (SINR). Based on further improvements some first results indicate that raw spectral efficiencies of 45 to 50bit/s/Hz might be possible for OP CoMP like schemes, which would be a factor of about 8 over LTE Release 10 4x2 MU MIMO. For massive MIMO stand alone solutions replacing 4 passive by 16 active antenna elements the performance gain is in the range of a factor of 3. A factor for 8 for massive MIMO plus JT CoMP and small cells is a good motivation to look further such more advanced solutions.

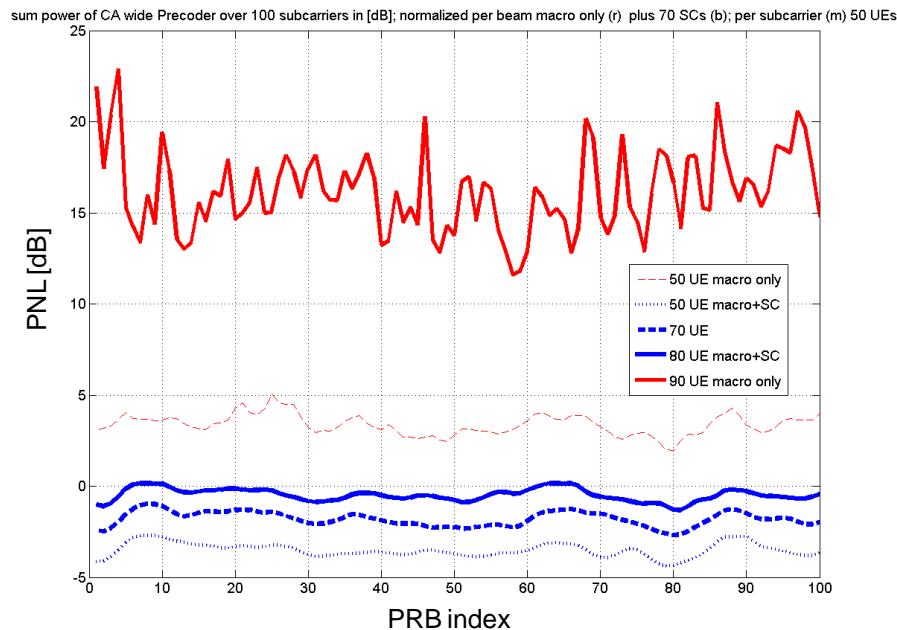


Figure 3-9: PNL in [dB] for macro cells only (red) and macro plus small cells (blue) versus the PRB index: the thickness of the lines indicates the number of UEs (50, 60, 70, 80) per cooperation area (fat line)

### 3.2.7 Addressed METIS Goals

**1000x data volume:** CoMP schemes with advanced UE capabilities provided by TeC 7 and TeC 10 provide a gain in the achieved cell throughput and spectral efficiency of 70% and 200%, respectively, when compared to LTE Release 11. This ultimately supports the increase of the data volume per area, especially in UDN. A gain factor of 8 can be achieved by allowing coordination among small cells and massive MIMO macro BSs in TeC 13.

**10-100 user data rate:** The user data rates highly benefit from the CoMP schemes, in particular for the users at the cell edge. The results based on TeC 7 show a gain in the fifth percentile of the user rate up to 160%. Similarly TeCs 10, 12 and 13 provide important gains in user rates.

**10-100x number of devices:** Increase in data rates and system throughput can be translated to an increase in the number of connected and served UEs in a given time. A higher number of devices also improves the UE selection diversity.

**Energy efficiency and cost:** The solution provided by TeC 1b mainly focuses on the energy efficiency aspect. With the help of sleep modes and proper load balancing, higher energy efficiency is achieved, especially in UDN scenarios.

## 3.3 Most Promising Technology Approach 2: CoMP with limited backhaul capabilities

### 3.3.1 Introduction

The imperfect backhaul is recognized as one of the key issues in fast multi-cell cooperation, especially in the context of small cells and ultra-dense networks. This implies the assumption of CSI exchange between cooperating transmitting nodes (BSs) might not always hold in practice due to backhaul limitations. Hence, approaches which consider only local or distributed CSI become relevant in such scenarios. Assuming for instance (smart) caching at the cooperating BSs, new techniques on distributed precoding with solely local CSI at the BSs

and with (almost) no fast information exchange between nodes provide gains (larger DoF) with respect to the SotA approaches (TeC 3). In addition, when considering both links of a TDD system, *forward-backward* (F-B) iterations between UL and DL enable to iteratively optimize transmit/receive filters without any CSI exchange between the nodes. By taking into account the interference-plus-noise and signal subspace, iterative algorithms requiring small number of F-B iterations lead to superior performance compared to schemes with orthogonal access (TeC 6). This concept of F-B iterations also referred to as bi-directional training between UL/DL can further be applied in a TDD network with asymmetric UL/DL allocation among adjacent cells. In this case, bi-directional signalling allows to iteratively optimize transmit/receive filters by considering cross-link interferences without any CSI exchange between nodes or additional special training. Results indicate that a small number of iterations suffice to achieve a better performance than an uncoordinated scheme (TeC 17).

### 3.3.2 TeC 3: Distributed precoding in multicell multiantenna systems with data sharing

The concept of precoders utilizing data sharing (e.g., by caching) and local channel knowledge has been introduced in [METIS13-D31], and further developed in [METIS14-D32] (cf. also [LVS14]). The main goal has been to enable a form of “light” coordinated multi-point (CoMP) transmission, by significantly reducing the requirements on the backhaul links’ latencies. The proposed scheme benefits from the envisaged possibility of smart end-user data sharing/caching in future wireless access networks (cf. e.g. [GMD+13]). The precoding is distributed with respect to the channel state information (CSI) availability, which is assumed to be local for a time-division-duplex (TDD) system. The interference at the users is cancelled by a predefined, offline agreement among the base stations (BSs) and hence, the proposed approach is referred to as destructive interference addition (DIA).

For this TeC, the mathematical background was developed and the evaluations were performed in a simplified (normalized Rayleigh channels), two cell setting in [METIS13-D31, METIS14-D32]. We focus in this deliverable on further evaluations regarding the performance improvement achieved by increasing the cluster size and the use of more sophisticated system-level simulators.

#### Performance Results

Although DIA is able to guarantee no intra-cluster interference, it provides no constructive addition of the desired signal components like distributed MRT or cooperative multicell precoding (CMP) [BZG+10]. Increasing the number of cooperating BSs, however, will lead to a diversity gain for the desired signal, since it will consist of a larger number of components. Nonetheless, the DoF, i.e. the slope of the curves at high SNR, would be able to remain unchanged. For instance, extending the previous setting [METIS14-D32, LVS14] involving three single-antenna users in an isolated cluster with two cooperating BSs, each equipped with two antennas, to a cluster size consisting of three, four, and ten cooperating BSs leads to a gain in the average sum rate at high SNR of 1.2, 1.8 and 3.5 bpcu, respectively with respect to two cooperating BSs.

To align our results with the task-baseline, a further evaluation is performed using two simulation environments:

- MIDAS: A Winner/3GPP-like deployment (developed at the Huawei ERC) consisting of hexagonal sectors with three co-located BSs at a site as shown in Figure 3-10 (left hand side). In the figure, the red circles represent the sites’ positions, while the numbers represent the index of the hexagonal sector. To better reflect the given hexagonal deployment, we assume a cluster consisting of the three closest BSs belonging to different sites, such that the cluster’s coverage area is given by a triangle as depicted in Figure 3-10 (left hand side). The triangular clusters result from assuming that each user is connected to the three closest sites.
- METIS TC2 model: The WP6 TC2 model is modified for the purpose of testing advanced multi-node cooperation algorithms in [METIS14-D32]. We apply a simple “pie-based”

clustering scheme for this model, shown in Figure 3-10 (right-hand side), and study both the homogeneous dense case (only micro BSs turned on) and the heterogeneous case (macro and micro BSs turned on), with the results for the latter case given in the appendix. This clustering scheme results from grouping those micro BSs which are in the same macro sector. Other clustering approaches were analyzed, but the “pie-based” clustering scheme achieved the best performance.

We plot in Figure 3-11 the average sum rate of an isolated cluster as a function of the cell edge SNR for the MIDAS model from Figure 3-10 (left). We assume the BSs to be equipped with two antennas, an ISD of 50 meters and three single-antenna users uniformly distributed in the cluster. Cell edge SNR refers to the average SNR of a user in the middle of the cluster. For a comparison we also include the performance with distributed MRT, distributed ZF and CMP [BZG+10], which represent the SotA assuming only local CSI at each cooperating BSs. We can clearly observe that while the other schemes saturate due to the interference, DIA outperforms all of them at high SNR. In the figure, we also include the performance of DIA-UPC (DIA with Uncoordinated Power Control), which is a variant of DIA which relaxes the interference nulling condition in the DIA algorithm. Hence, our results obtained previously with normalized Rayleigh channels [METIS14-D32, LVS14] can be translated into a more realistic scenario. At low SNR, DIA is outperformed by distributed MRT and CMP, since the optimum strategy is to maximize the desired signal magnitude and not to null out the interference. Although the other distributed schemes could drop one user to avoid the sum rate saturation at high SNR, DIA would still outperform them at high SNR since it achieves a higher DoF.

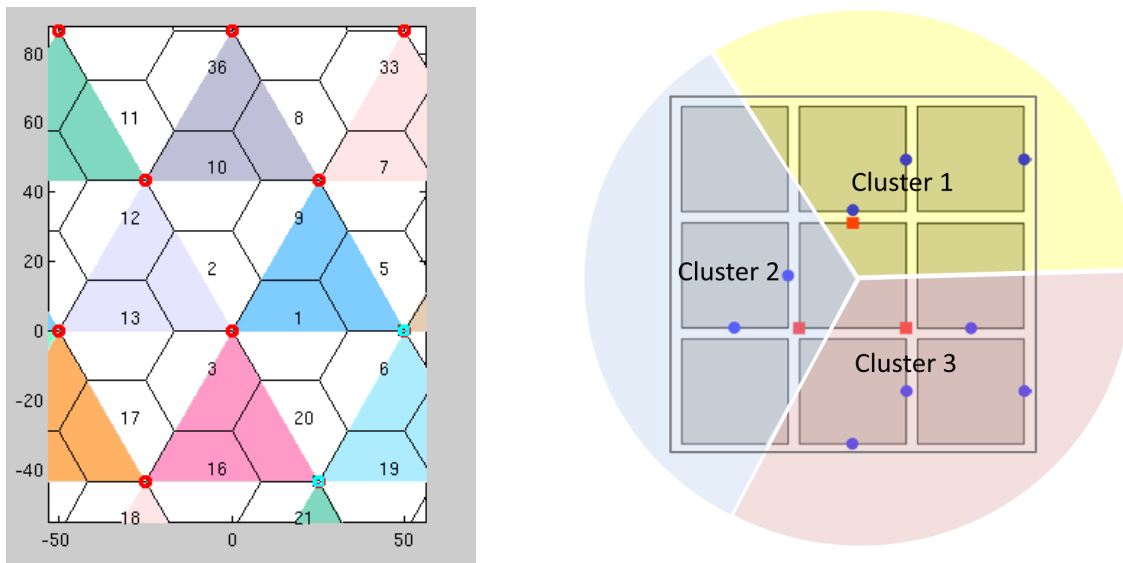


**Figure 3-10: Network Deployment and Pattern of Simultaneously Active Clusters in the MIDAS simulator (left hand side). METIS TC2 model and the applied clustering scheme (right hand side).**

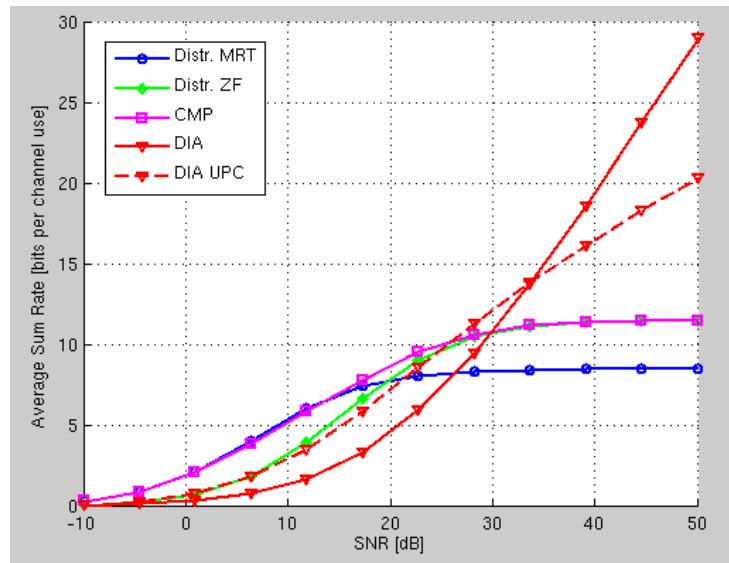


Figure 3-11: Average Sum Rate for Different Schemes with Distributed CSI

In Table 3.4, we show the numerical results for the METIS TC2 model with the clustering scheme depicted in Figure 3-10 (right). Following the model specification, each BS sector and micro BS is equipped with 4 antennas. In all clusters, the number of supported users per RB is 5 (underdetermined system). It can be seen that all distributed precoding schemes with data sharing significantly outperform the basic MRT scheme (the latter also being able to support underdetermined systems directly). DIA boosts the performance for the higher percentiles (depending on the scenario), while CMP is generally better for guaranteeing (lower) data rates, so the techniques can be used in a complementary fashion. Compared with the MRT approach, the gains of the best decentralized strategy (DIA or CMP) range from 195% until 212%. DIA outperforms the CMP for 7.3% and 19% for the 50<sup>th</sup> and the 90<sup>th</sup> percentile, respectively, in the homogeneous dense case.

Table 3.4: Percentiles for area/cell spectral efficiency (bits per channel use) in the homogeneous small cell case for the 4 analyzed schemes in the METIS TC2 model

Homogeneous Case (micro BSs turned on)				
Percentile	MRT	CMP	DIA	DIA-UPC
10 <sup>th</sup>	18.70	61.02	55.13	45.86
50 <sup>th</sup>	28.43	82.65	88.67	66.44
90 <sup>th</sup>	41.88	101.92	121.11	86.83

### 3.3.3 TeC 6: Distributed low-overhead schemes for MIMO Interference Channels

The main focus of this TeC is to greatly enhance the spectral efficiency of DL and UL transmission in dense heterogeneous networks. The proposed schemes advocate the use of *training via UL / DL pilots in a TDD network (also known as forward-backward (F-B) iterations) to iteratively optimize transmit / receive filters, in a fully distributed manner*. In the DL phase of each F-B iteration, users estimate their effective signal and interference covariance matrix (using DL pilots), and optimize their receive filters based on this local CSI only. Similarly, in the UL phase, micro base stations (mBSs) estimate their effective signal and interference covariance matrix using UL pilots, and optimize their transmit filters employing this local CSI. The latter algorithm is an extension to our earlier proposed method in [METIS14-D32] (described in [GKB+15]), where we now *accommodate multiple users within each cell*.

In contrast to previous works employing this F-B iterations structure (e.g. [GCJ08]) and which require a significant number of iterations, in this work we consider relatively small number of F-B iterations (i.e. less than 5), resulting in algorithms with small overhead. Note that each F-B iteration consists of one subframe, and perfect channel estimation at BSs and UEs is assumed: though static users are used in the simulations, the results are still relevant for slow-moving UEs. The chief advantage of such schemes is that they alleviate the need for feedback (while keeping a low overhead), and for a backhaul (since only local CSI is needed at each mBSs). As opposed to “pure IA” schemes that are only aimed at reducing/suppressing interference, the proposed schemes optimize both the signal and interference, thus resulting in far better performance than pure IA methods.

### Performance Results

We follow standard baseline for TC2, outlined in [METIS14-D32, Section 8.2], consisting of 210 outdoor users of the “reduced Madrid Grid”. Exploiting the fact that each mBS has two sectors, we assign 4 orthogonal resource blocks to the area in question, resulting in every two mBS sectors covering a specific area, that we dub super-cell as shown in Figure 3-12.  $K_u = 26$  users are dropped randomly in each sector (following a uniform distribution), for a total of approximately 210 outdoor users. The path loss value at each user location was computed using the supporting material provided in [M13].

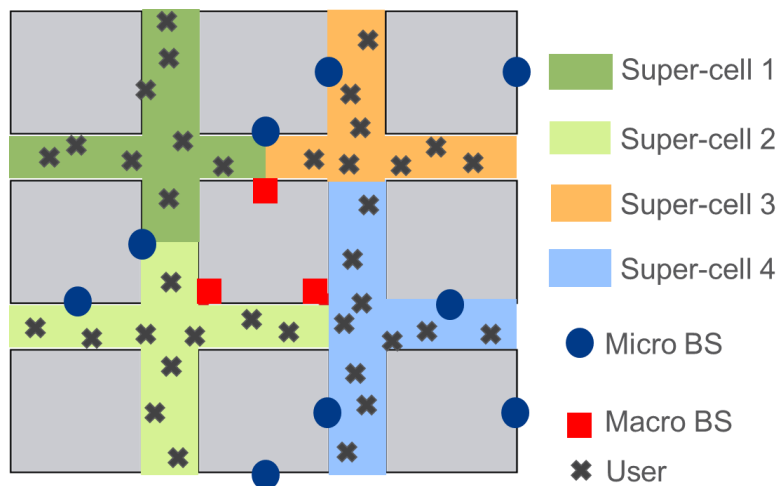


Figure 3-12: Simulation Setup

Since the channels are unknown and scheduling is not considered here, we do not use any channel specific scheduling and thus use a round robin scheduler. In each of the two sectors,  $K < K_u$  users are scheduled, such that all  $K_u$  users are served in  $K_u/K$  blocks. For each group of  $K$  users we run our proposed algorithm to optimize the filters at the mBS and users. As a baseline scheme to compare our algorithm, we consider one using orthogonal access (e.g. TDMA), where each user in each sector is assigned a separate transmission block, thereby removing interference from any transmission. Capacity-achieving single user eigenbeamforming based on the SVD of the channel is used for the latter transmission (we assume the channel is known perfectly for that case).

To evaluate our algorithm, we depict in Figure 3-13 the complementary CDF  $Prob[R > \gamma]$  of the downlink rate  $R$  of a random user, for both our proposed schemes and the benchmark. To this end, we assume SNR=10 dB,  $N=4$  antennas at the users,  $d=2$  streams and different number  $M$  of antennas at the mBSs. As we can see, there is a significant gap between the proposed schemes and the benchmark. In addition, when the number of mBSs antennas is gradually increased, the performance of our proposed scheme increases massively (around 200% gain for  $M=10$ ), while improvement of the benchmark scheme is quite insignificant. Furthermore, we note that for  $M=10$ , the 3.75 bps/Hz threshold (shown as dashed vertical line)

is satisfied around 97% of the time. This implies the main KPI of TC2, i.e. user data rate of 300 Mbps in DL should be maintained for 95% of the time, is met.

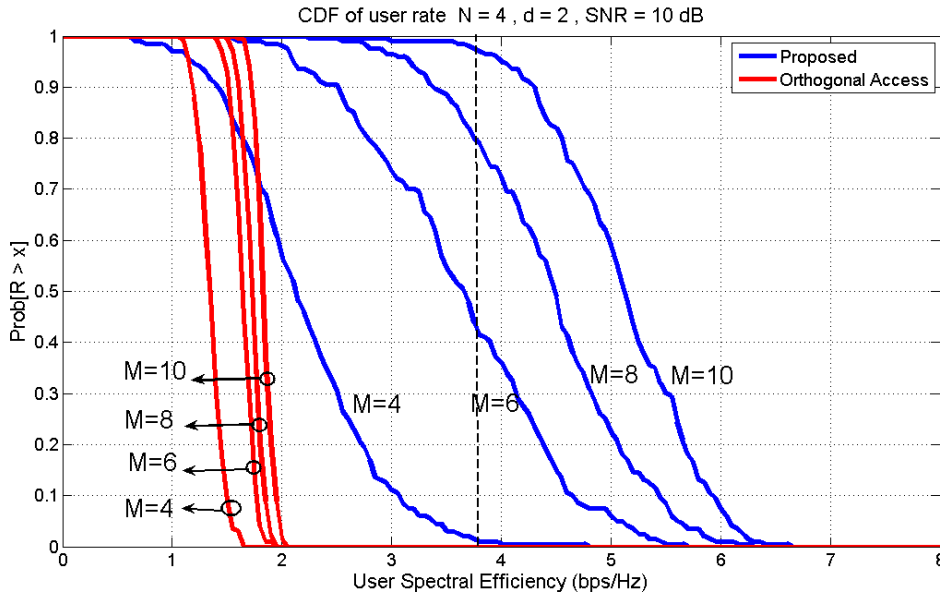


Figure 3-13: CDF of user rate as function of number of transmit antenna (N=4, d=2)

In Figure 3-14 and Figure 3-15, we provide the 5<sup>th</sup>, 50<sup>th</sup> and 90<sup>th</sup> percentile of a given user’s spectral efficiency for both schemes. We can see that although our scheme has slightly less robustness in performance than the benchmark, it does offer significantly better performance (2-3 times better).

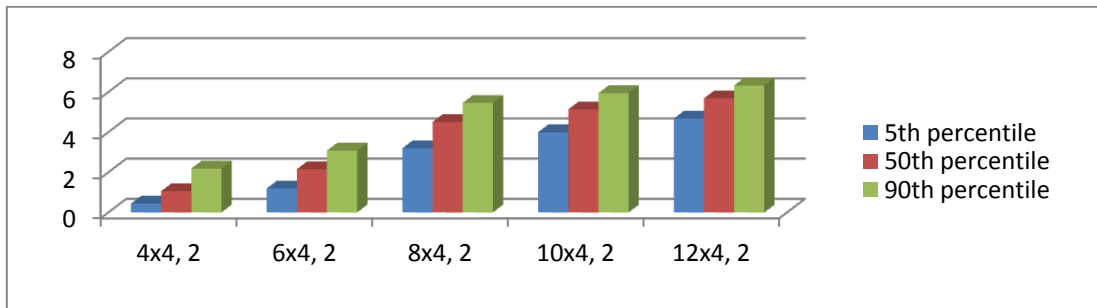


Figure 3-14: Statistics of user rate for proposed scheme

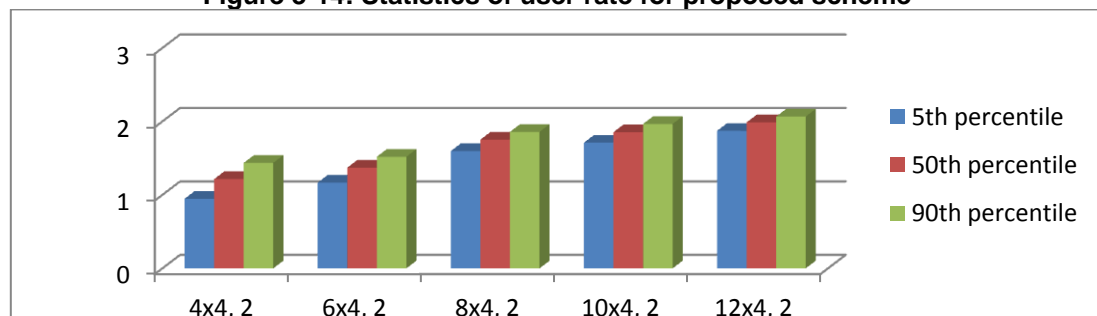


Figure 3-15: Statistics of user rate for benchmark scheme

Next, we evaluate some area-wide performance statistics such as the mean (in bps/Hz) and standard deviation of the user rate, for both the proposed scheme and the benchmark (note that all the results are divided by the number of used resource blocks, i.e. 4). As we can see from Table 3.5, though the performance delivered by our schemes seems to have more variability than the benchmark, the average area-wide performance is largely superior.

**Table 3.5: Mean and Standard deviation of area spectral efficiency**

		<i>Area spectral efficiency (bps/Hz)</i>				
<b>Prop.</b>	<i>mean</i>	14.233	20.947	26.474	29.964	32.501
	<i>std. dev.</i>	0.262	0.377	0.304	0.331	0.305
<b>Orth.</b>	<i>mean</i>	8.583	9.611	10.336	10.847	11.327
	<i>std. dev.</i>	0.0534	0.0401	0.0331	0.0337	0.0338
		<b>4x4, 2</b>	<b>6x4, 2</b>	<b>8x4, 2</b>	<b>10x4, 2</b>	<b>12x4, 2</b>

Finally, we investigate the net effect of the schemes by comparing the increase in average area spectral efficiency of our proposed scheme with respect to the benchmark against the corresponding increase in overhead. Interestingly, as it can be seen from Figure 3-16, the gains in spectral efficiency will offset the required increase in overhead.

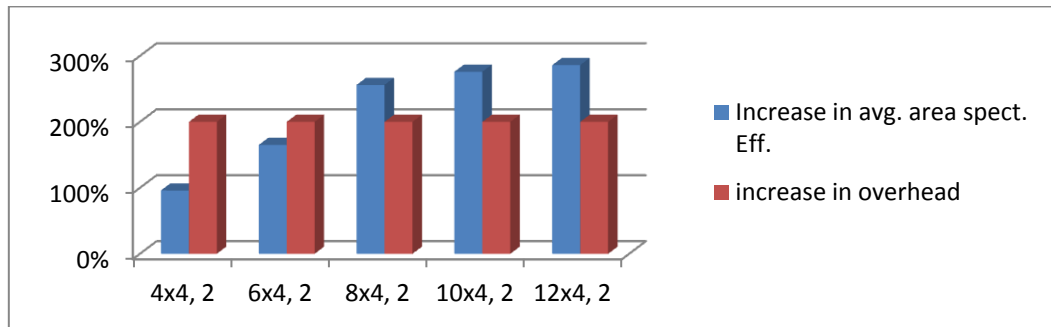


**Figure 3-16: Gain in area spectral efficiency vs increase in overhead**

### 3.3.4 TeC 17: Bidirectional signalling for dynamic TDD

In small cell scenarios, the UL and DL traffic may vary significantly with time and among the adjacent cells. In such cases, dynamic TDD allows adapting resources between UL and DL, and thus provides vastly improved overall resource utilization. The main challenge in designing dynamic TDD system is handling cross-link interferences (user-to-user and BS-to-BS) generated by the asymmetry between the cells. In the literature numerous studies consider time-slot allocation algorithms to minimize the cross-link interference in dynamic TDD. In this research, we aim at jointly optimizing the allocation of resources (space, frequency and time, including the allocation to UL and DL) and coordinated beamformer (CB CoMP) design across the entire network to maximize various system performance measures.

We assume each TDD frame is allocated either to UL or DL depending on the instantaneous traffic load of the cell, similarly to the METIS frame structure specified in [Figure 2-1, METIS14-D23]. For the given UL/DL allocation, we propose coordinated iterative algorithms to find precoders/decoders in all the network and corresponding signaling concepts of effective CSI for weighted sum rate (WSR) maximization [KTJ13] with per transmitter power constraints. Further, bi-directional signaling/training is performed for each TDD frame [SBH14, KTJ13], allowing for *iterative precoder/decoder optimization to be carried out independently* for each frame. In this way, the optimized receivers from the previous F-B iteration can be used as precoded pilots for the next iteration. At the same time it can be *used to carry out implicit user selection* at each frame by letting the iterative algorithm decide the optimal set of users/streams to be served. Finally, *backhaul information exchange is not anymore required to carry out the precoder coordination*. There is a clear trade-off between the achievable throughput gains from the iterations and the training overhead caused the bidirectional signaling. The training should be large enough to come up with efficient precoder/decoders

while short enough to guarantee sufficient resources for the actual data transmission.

### Performance Results

The numerical analysis is carried out for two and three cell scenarios with 4 users in each cell. The power constraint for the DL transmission is fixed to  $P_i=10$  dB and for the UL user power transmission  $P_{j,i}=4$  (UL transmit power constraint is selected such that the maximum sum power of the UL users is equal to the power constraint of the DL BS). All the priority weights are assumed to be 1. The number of antennas at each BS is  $M_i = 4$  and the number of antennas at each user terminal is  $N_k = 2$ . The simulation environment is defined by three types of terminal separations: The path loss between the two DL cell edge users is  $\alpha$ , UL user to DL user is  $\beta$ , and UL BS to DL BS is  $\delta$ . Also, the path loss from a BS to in-cell users is normalized to be 0 dB.

The actual sum rate for transmit SNRs 10 dB and 20 dB, versus the total overhead for two cell DL only case is shown in Figure 3-17. One BIT iteration is assumed to take two OFDM symbols. Thus,  $\gamma= 0.01$  and  $\gamma = 0.02$  correspond to frame lengths 200 and 100, respectively. Also, uncoordinated beamformer design is considered as the reference case (beamformers calculated locally without considering the inter-cell interference). Algorithm from [KTJ13, Algorithm 3] with the bi-directional signaling can be seen to obtain the peak data rate with less than 10% and 15% overhead for the frame length  $\gamma = 0.01$  and  $\gamma = 0.02$ , respectively. Now, the total signaling overhead is  $\rho = \text{BIT} \times \gamma$ . Thus, the actual achievable WSR can be obtained as  $(1-\rho)R$ , where  $R$  is the achieved WSR from [KTJ13, Algorithm 3].

The actual sum rate improves significantly compared to the uncoordinated system when cell separation is equal to  $\alpha=0$  dB, and it provides considerable performance gain even for larger signaling overhead. However, for the low inter-cell interference scenarios (lower transmit SNR with larger cell separation), the uncoordinated system starts to outperform the proposed beamformer design.

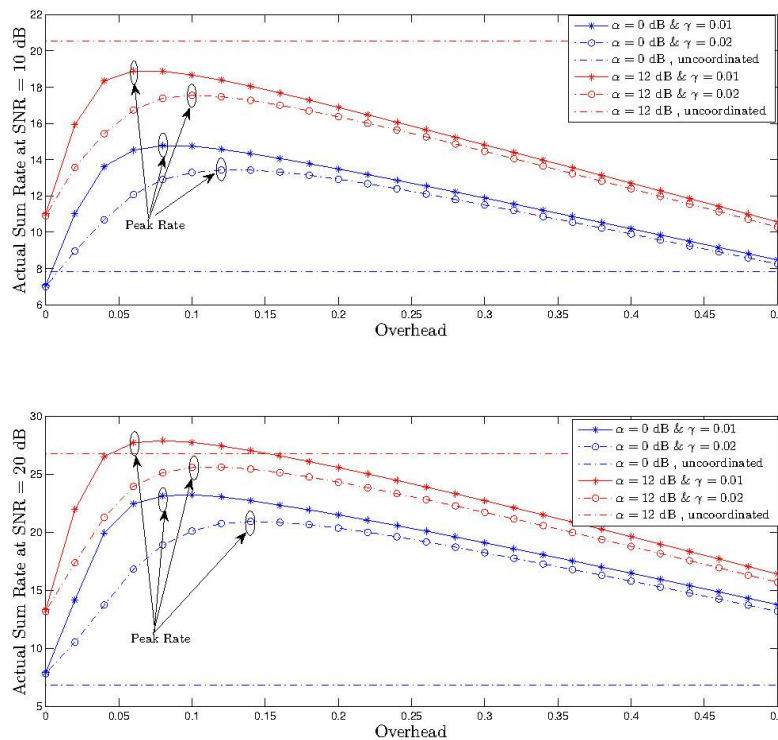


Figure 3-17: Actual Sum rate vs bidirectional signalling overhead with different SNR (10, 20 dB) values

Figure 3-18 demonstrates the actual sum rate versus the total overhead of the three cell network with two DL BSs and one UL BS. We consider the TDD frame length 200 ( $\gamma=0.01$ ), and different  $\alpha$ ,  $\beta$  and  $\delta$  values. Similarly to Figure 3-17, the actual sum rate improves significantly for lower  $\alpha$ ,  $\beta$  and  $\delta$  values compared to the uncoordinated system. The peak rate is obtained with less than 12% overhead for all the scenarios and the sum rate improves even with 30% signaling overhead. Therefore, the proposed algorithm performs very well when complex interference conditions are present. Figure 3-19 illustrates the average sum rate of the system versus the transmit SNR with similar BS allocation as Figure 3-18. We vary  $\beta$  (3, 6, 9, 12 dB), while  $\alpha$  and  $\delta$  are fixed, to observe the impact of the UL user transmission on the sum rate. For lower  $\beta$  and high transmit SNR, UL users dominate the sum rate. This is due to the high UL-to-DL interference, which degrades the DL user SINR. However, for large  $\beta$  DL user dominates due to less UL-to-DL interference.

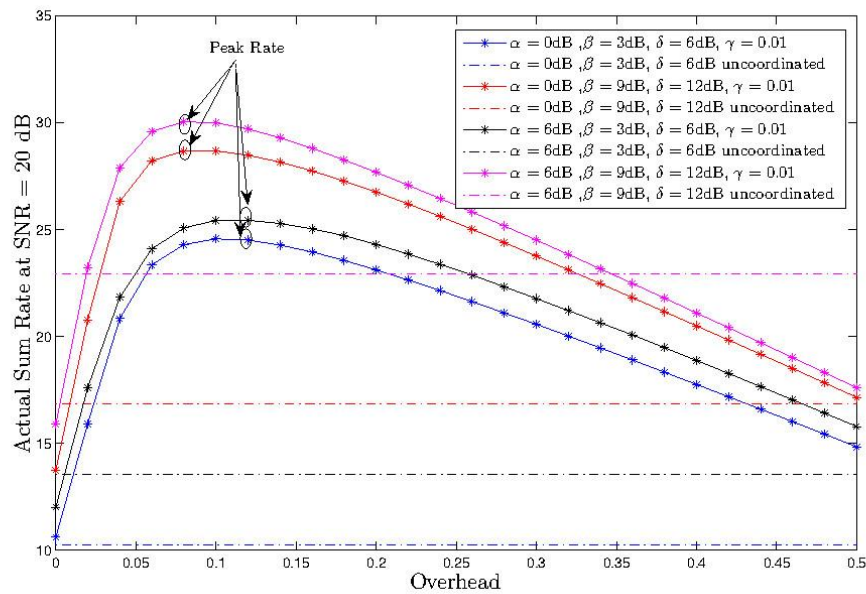


Figure 3-18: Actual sum rate vs overhead at SNR = 20 dB, with different  $\alpha$ ,  $\beta$  and  $\gamma$

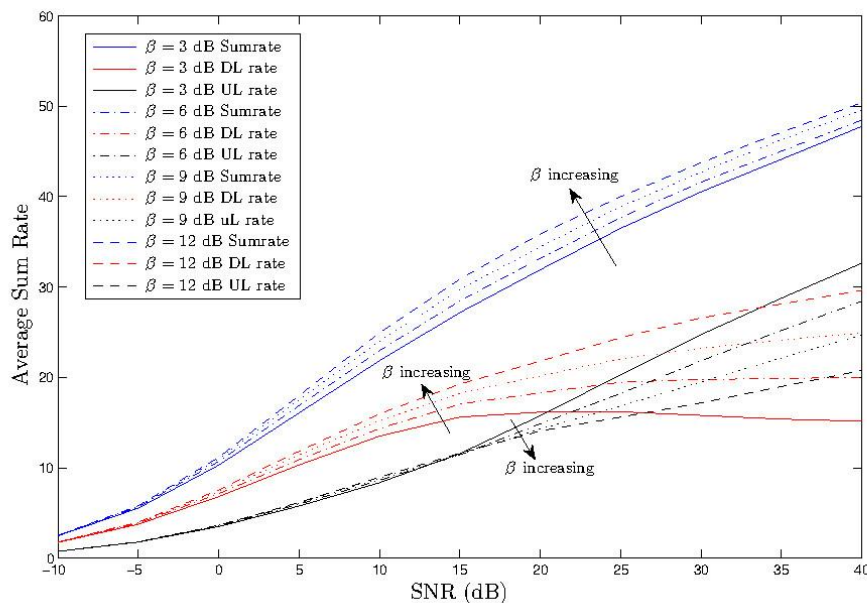


Figure 3-19: Average sum rate vs SNR for different  $\beta$  values

### 3.3.5 Addressed METIS Goals

**1000x data volume:** Although the solutions in this approach are based on limited backhaul capabilities, however, as shown in the results, TeC 3 still achieves a cluster sum-rate gain of 30%, 45% and 54%, in the 10th percentile, 50th percentile and 90th percentile, respectively, with respect to the baseline solution. In addition to that, large gains are also achieved by TeC 17.

**10-100 user data rate:** The solutions are based on clustering and higher user data rates are achieved, especially for cell edge users. In particular, TeC 6 provides 2-3 times increase in average user data rates.

**Energy efficiency and cost:** The solution based on TeC 3 provides approximately a 50% transmit power saving when compared with baseline methods.

## 3.4 Impact on METIS system

The solutions in Task 3.2 mainly address increased data volume, user data rate, and served number of devices.

In particular for MPTA 1, the solutions are based on the exploitation of the enhancements in the device technology. Therefore, they can be applied to any scenario which considers UEs with advanced capabilities. The advancements at the UEs in terms of multiple antennas and high processing power allow the network to employ advanced CoMP solutions. Especially in a Ultra Dense Network (UDN) scenario, with high density of transmission nodes as well as mobile users, the joint optimization of clustering (cell selection), beamforming and user selection is done to achieve higher spectral (TeC 7) and energy efficiency (TeC 1b). The coordination of nodes in UDN also allows using network assistance for interference estimation and cancellation at the UEs (TeC 12). In cases where UDN is supported by the macro layer, TeC 13 provides a solution which combines CoMP with massive MIMO. Enhanced UE processing capabilities and multiple antennas are also used in TeC 10 to implement adaptive linear channel prediction with the aim of reducing feedback and increasing robustness against CSI aging.

MPTA 2 is based on the solutions which enable the coordination of the nodes with limited backhaul capabilities, thus addressing UDN core aspect for small cell integration and interaction. In UDN it is necessary to realize fair provision of services with practical (non-ideal) backhauling, irrespective of the user's geographic location. In TeC 3 interference mitigation is applied with relaxed backhauling requirements by an offline agreement on the placement of the interference components. Moreover, TeC 6 exploits the densification feature of UDN to propose simple coordination schemes which promise higher throughput. In addition to that, backhaul information exchange in UDN is minimized in TeC 17 by using a minimal set of bi-directional training to compute optimal transceiver weights which allow higher spectral efficiencies. The proposed solution is also shown to be robust in case of CSI uncertainty.

In general, solutions presented in the whole task provide a tighter control of interference in the system and higher quality in the communication link. Thus, these solutions can be beneficial to provide Ultra Reliable Communications (URC) [METIS14-D62, Section 2.5], having an impact in particular on Reliability Aspect 1 (decreased power of the useful signal) and Reliability Aspect 2 (reducing uncontrollable interference). Moreover, the proposed solutions allow better management of resource competitions (Reliability Aspect 3).

The improved data rates offered by the TeCs in Task 3.2 can be beneficial to provide wireless backhauling to a Moving Network (MN) [METIS14-D62, Section 2.3], in particular for flexible network deployment based on nomadic network nodes (mobility aspect MN-N). MPTA 1 approaches in particular can benefit from the higher capabilities that can be available on

nomadic nodes, while MPTA 2 proposes schemes that can be provided also with a flexible network deployment. The non-coherent transmission scheme studied in TeC 16 enable the use of multi-user MIMO techniques for vehicular scenarios in an efficient manner as a result of reduced pilot contamination and immunity against outdated channel estimates, and is well suited for broadcasting transmissions as described in TC12. Because of this, the TeC has been considered in the context of clusters MN-M and MN-V.

### 3.5 Overview of achieved results

Results presented by the TeCs in MPTA 1 showed that, by exploiting advancements in future UEs, it is possible to overcome some of the practical impairments that so far limited performance gains with realistic joint transmission schemes.

With a careful design of joint transmission including smart clustering approaches, UEs equipped with more antennas, interference suppression algorithms and channel prediction capabilities, improvements in the range from 70% to 100% in the mean cell throughput have been reported, with even better results for cell edge users, since for 5th percentile user throughput gains up to 160% have been also shown.

Results in the baseline scenario derived from TC2 “dense urban information society” highlight how the interference scenario in this more realistic environment allows to better exploit the proposed coordination schemes. This is due to the fact that a lower number of dominant interferers impair the received signal compared to a traditional hexagonal and homogeneous macro deployment.

A complex framework including heterogeneous networks with massive MIMO enhanced BS has been also proposed, that, by assuming an ideal backhaul, is able to provide 8 times better average spectral efficiency compared to LTE Release 10, making a spectral efficiency of 48 bit/s/Hz/cell possible. Use of coordination in a heterogeneous scenario has been studied also from an energy consumption point of view, showing how exploiting joint transmission (even non-coherent) allows providing the same quality to users with a reduced number of active base stations, thus improving the overall energy efficiency.

The second set of MPTA has investigated the potentiality of novel distributed precoding/filtering design schemes that can be used when only limited backhauling is available. The presented solutions showed how distributed approaches can still be considered to manage interference effectively, in particular when the system is mainly interference limited: in scenarios where the deployment is rather dense, so that they would exhibit good SNR in the cell-edge, but that are impaired by the inter-cell interference. Gains from 35% to 55% in spectral efficiency have been shown, without the need to deploy high performance backhauling in the network. A solution based on UL / DL pilots and forward-backward iterations to gradually refine both transmit and receive filters, in a fully distributed manner, has been presented. It has been shown that using 10 transmitting antennas it is able to provide, in the TC2 simplified scenario considered in Task 3.2, more than 3.75 bps/Hz spectral efficiency for around 97% of the time, thus satisfying the challenging requirements (envisaged for TC2) of a user data rate of 300 Mbps in DL, maintained for 95% of the time. The overall additional overhead that could be needed for this kind of solution has been also analyzed, investigating the trade-off between the throughput gains achievable from the forward-backward iterations and the training overhead caused by the bidirectional signaling.

For a more detailed analysis of the synergies among the TeCs developed within Task 3.2, for instance which TeCs can be combined together to further enhance the performance, please refer also to [METIS14-D32, Sections 3.2.3-3.3.3-3.4.3].

### 3.6 Conclusion

Activities in Task 3.2 have shown that there is still large potential for coordination schemes, especially in future heterogeneous scenarios. However it should be stressed out that coordination approaches, in particular coherent joint transmission, require a careful design in order to reach the impressive gains that are promised.

Some of the issues that usually arise with full DL Joint Transmission CoMP can be alleviated if smarter UEs are considered. It was shown that UEs with interference suppression capabilities allow for less complex coordination schemes at the BSs (TeC 7), and that with the aid of network assistance (NA), implemented by means of eNB-to-UE higher-layer signalling, the accuracy of co-channel interference estimation and suppression (IS) or cancellation (IC) at the UE receiver can be improved (TeC 12). Channel prediction in the UE also emerged as an important tool to solve feedback delays (TeC 1, TeC 10, TeC 13).

In general, the evaluations performed in an heterogeneous scenario, including macro and micro BS, as for example in the WP3 task 3.2 simulation baseline [METIS14-D32, Section 8.2] derived from the dense urban information society model (TC2), have shown that gain achieved by CoMP is higher in heterogeneous networks, since the interference comes mainly from few strong interferers and is more easily tackled by CoMP (TeC 7, TeC 10, TeC 13). However particular care should be taken in the design of the cooperation scheme, due to possible issues with power imbalance between macro and micro BSs. It was also proved that massive MIMO and small cells in combination with JT CoMP can provide significant performance gains (TeC 10, TeC 13).

When the advanced infrastructure required by JT CoMP is not available, solutions that require a limited exchange of information (or even none) are also possible: a "light" form of CoMP was introduced in TeC 3 by means of distributed precoding based on local CSI at each cooperating BS, such that the interference at the users is (approximately) cancelled by a predefined, offline agreement among the BSs. TeC 17 studied coordinated precoder/decoder optimization in multicell multiuser dynamic TDD system in order to maximize network utilities. The use of Interference Alignment in a multi-user multi cell network where both the transmitters and the users are equipped with multiple antennas (TeC 4) has proved to provide significant gains. Low-overhead algorithms that iteratively refine the filter at BSs and UEs to maximize the spectral efficiency, in a fully distributed manner, using uplink-downlink pilots (no coordination, no feedback) have been introduced (TeC 6), and it was shown that to ameliorate the system performance and reduce the overhead with distributed interference alignment, it is more preferable to reliably estimate the channel first by allocating more power for pilot transmission than continuing over-the-air iterations (TeC 5b). It was also shown that the sum rate achieved with limited CSI in a CoMP scenario for cell-edge users can be improved by using side information, such as RSSI, in the precoder design (TeC 1c).

Coordination approaches can be used also to achieve higher energy efficiency: precoding, load balancing, and BS operation mode (active or sleep) can be optimized for improving the energy efficiency of heterogeneous networks (TeC 1b), and CoMP scheme can be designed to reduce energy consumption when traffic is low, exploiting sleep mode in base stations (TeC 15). The Destructive Interference Addition (DIA) scheme presented in TeC 3 provides also significant transmit power savings (approximately 60% in the homogenous hexagonal scenario).

Approaches with new access schemes or architectures have been also investigated: it was shown that non-coherent reception can provide higher throughput than pilot-based reception in high SNR scenarios and/or with a medium to high number of transmit and receive antennas (TeC 16), and that system level performance of two-way relaying scheme in dense deployment is highly degraded due to D2D-like interference, therefore it requires proper interference management scheme to achieve gains (TeC 14). TeC 8 combines Non-Orthogonal Multiple Access (NOMA) schemes with multi-antenna transmission schemes, so that spectrum efficiency, system capacity, cell-edge user performance can be improved and



**Document:** FP7-ICT-317669-METIS/D3.3

**Date:** 25/02/2015

**Security:** Public

**Status:** Final

**Version:** 1

---

the number of simultaneously served users can be almost doubled, even in high mobility scenarios.

The different TeCs in Task 3.2 have provided solid results with highly detailed system level simulations, considering realistic impairments and still showing significant improvements both in cell-edge and average cell throughput.

## 4 Task 3.3: Multi-hop communications/wireless network coding

### 4.1 General overview

The research activities in T3.3 have focused on consolidating the results in each technology component. Most of the TeCs have adopted the baseline simulation set-up defined in WP3 T3.3 for TC2 Dense Urban Information Society and involving a simplified Madrid grid.

In T3.3, two technologies have been identified as most promising:

- Heterogeneous network at lower frequencies (MPTA 1): The goal of this technology is a spectrally efficient network densification. In TeC 1 (Section 4.2.2), the principle of network coding is applied to increase the spectral efficiency of wireless backhauling to achieve performance that is close to a deployment based on a wired backhaul. Spectral efficiency is further improved by exploiting non-orthogonal transmission techniques as in TeC 5 (Section 4.2.4) as well as buffer-aided relaying as in TeC 3 (Section 4.2.3).
- Indoor dense mesh network at mm-waves (MPTA 2): TeC 2 (Section 4.3) has simulated a practical deployment of an indoor dense mesh network supported by a wireless backhaul, with a realistic ray tracing based channel modelling and specific placement of the access points. Based on this set-up, low-complexity routing and resource allocation schemes are devised and achievable throughput are provided.

In addition to the MPTAs, other studies have been carried out within the task: In Table 4.1 we have listed all the TeCs that have been developed in T3.3. We refer to the appendix for a detailed assessment of all these TeCs.

Table 4.1: Full List of TeCs in Task 3.3

TeC #	Short Title	Short description	MPTA
TeC 1	Wireless-Emulated Wired (WEW)	Devise a transmission scheme in a heterogeneous network for efficient wireless backhaul. The scheme is based on the principle of wireless network coding and emulates a wired backhaul connection.	MPTA 1
TeC 2	IAR and RA in a mmW UDN	Enabler for ultra-densification by wireless access nodes enhancing spectral efficiency by providing practical interference aware routing (IAR) and resource allocation (RA) for several multi-hop flows.	MPTA 2
TeC 3	Virtual Full-Duplex Buffer-aided Relaying (VFD-BR)	In order to overcome multiplexing gain loss of HD relaying, this TeC allows concurrent transmissions of the source and a relay exploiting more than two relays with buffer.	MPTA 1
TeC 4	Distributed coding for MAMRC.	This work investigates the design of joint channel-network codes for different multiple access multiple relay channel (MAMRC) access schemes.	—
TeC 5	IDMA-based bi-directional relaying	The impact of interleave division multiple access (IDMA) is analysed in combination with network coding to identify efficient strategies regarding MAC/BC structuring, resource allocation and channel coding for bi-directional communication.	MPTA 1
TeC 6	MIMO PLNC to expand D2D coverage	A relay assisted D2D communication is considered with all nodes having multiple antennas, where the relay performs physical layer network coding (PLNC). The D2D transmission uses the same frequency spectrum as cellular communication.	—

TeC 6b	Secure beamforming design for PLNC based MIMO D2D communication	Secure beamforming design is proposed to prevent eavesdropping on the MIMO D2D communication. Devices communicate via trusted relay node which performs PLNC, and multiple eavesdroppers are trying to intercept the device information. At the devices, the CSI of the channel between the device and eavesdropper is imperfect. A robust secure beamforming design is proposed to enhance D2D communication while preventing eavesdropping.	—
TeC 7	Cooperative D2D Communications (CD2DC)	The main objective behind the proposed scheme is to allow cooperation between cellular links and direct device-to-device communication links to increase the spectral efficiency, the cell throughput, the number of connected devices within the cell, and the cell coverage.	—
TeC 8	Open-loop D2D relaying	This work extends the concept of multi-functional MIMO transmission to implement distributed space-time coding in networks with UE relays of limited capabilities.	—
TeC 9a	Initial studies of moving relay nodes (MRNs)	Power outage probability and energy efficiency studies of fixed and moving relays.	—
TeC 9b	D2D communications to Enhance VUE uplink	By using D2D communication and cooperating with each other, less energy is required to send the same amount of data of each active vehicular user equipment (VUE) in the cooperative transmission than the individual VUE-to-BS communications.	—
TeC 10	MIMO in TDD system with relaying	In the following TeC the two-phase two-way relaying scheme is investigated. The information exchange occur between one BS and two MSs. Advanced interference cancellation receivers are used to decode data signals intended for these stations.	—

## 4.2 Most Promising Technology Approach 1: Heterogeneous network at lower frequencies

### 4.2.1 Introduction

The principles of wireless network coding (WNC) are applied to cellular architectures with small cells in order to regain the loss due to half duplex relaying (performed by the small cell base stations). The target is to obtain a performance that is close to a wired backhaul solution taking into account the interference potentially created by the wireless backhaul transmission (TeC 1). Beside the use of WNC, this scheme combines special ZF and beamforming for its wireless backhaul solution. The spectral efficiency of those new transmission methods can be further enhanced using the techniques developed in TeC 5 and TeC 3. A practical multiple access scheme used in conjunction with WNC, named IDMA-based bi-directional relaying, is developed in TeC 5. Buffer-aided relaying is investigated in TeC 3 for the specific purpose of mimicking full-duplex relaying. The concept of buffer-aided relaying can be generalized and used to improve the spectral efficiency of the methods developed in TeC 1.

### 4.2.2 TeC 1: Coordinated multi-flow transmission for wireless backhaul

The proposed wireless backhaul scenario of this TeC is depicted in Figure 4-1(a). The novelty of the proposed TeC appears in employing a wireless backhaul BS-SBS<sub>*i*</sub> instead of a conventional wired backhaul. The uplink  $R_U$  and downlink  $R_D$  rates are assumed the same as

in the wired backhaul case. The exchange of information takes place over two phases with the help of WNC. This is possible because in Phase 1,  $MS_i$  and BS transmit to  $SBS_i$ , while in Phase 2,  $SBS_i$  decodes the received signals, and broadcasts the XOR of those signals. The BS and  $MS_i$  can then decode the XOR-ed signal, to obtain the desired signal. The scheme is designed under the assumption that the  $MS_i$  should not undergo any change in the PHY/baseband - it only needs to XOR the received packet with its previously sent packet.

There are two important aspects of the wireless-emulated wired (WEW) scheme: First, the BS partitions the downlink data for each MS into two parts, a private and a common part as shown in Figure 4-2. In Figure 4-2(a), the BS transmits the data to the SBS using only spatial ZF. This scheme is referred to as private data since each SBS receives only its own data. In Figure 4-2(b), the BS concatenates the data for both MSs, and transmits them using a common beam-former. The WEW scheme, shown in Figure 4-2(c), is a hybrid of the former two, and we find the optimal partitioning of data into a private and a common part.

The private part for each MS is sent using spatial ZF, so that each SBS can only decode the message intended for it. The common parts for both MSs are concatenated, before being transmitted to both SBSs.

Second, to have a transparent operation of the scheme to the MS, we assume that the MS transmits a rate equal to the capacity of the MS-SBS link. Then, in Phase 1, the SBS receives three signals, the private and common data (which is the downlink data), and the uplink data from the MS. The SBS first decodes the private and common data, while treating the MS's uplink data as noise. After this decoding is done, the SBS decodes the uplink data, without any residual interference from the downlink data.

We find the optimal transmission power at the BS, the optimal beam-former for the common parts of the data.

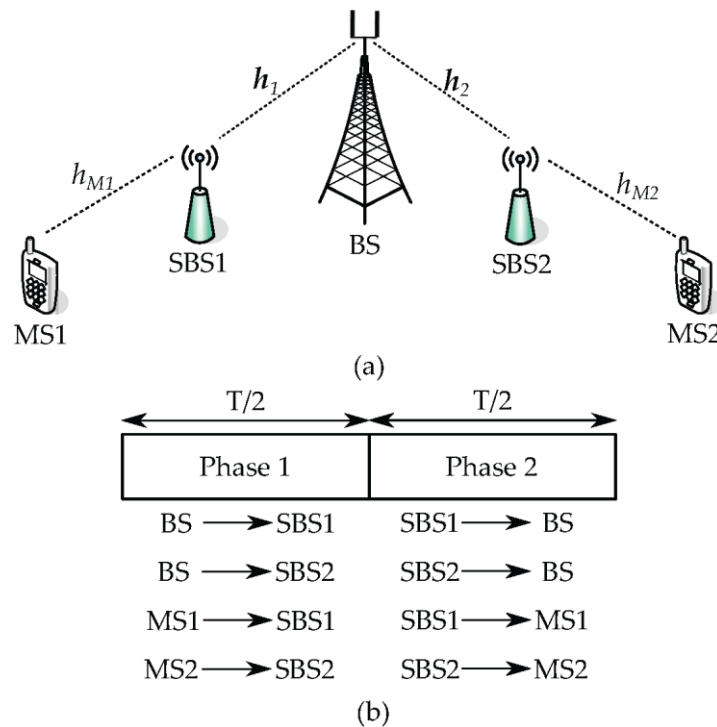


Figure 4-1: The wireless backhaul system model (a) and the transmissions phases (b)

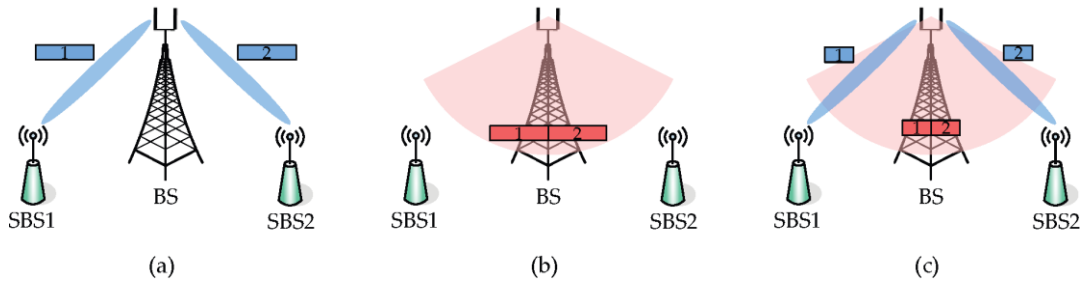


Figure 4-2: The three transmission methods considered in the wireless backhaul solution

### Performance Results

The simulation baseline considered is the WP3 Task 3.3 simulation baseline, consisting of nine square buildings arranged in a square grid [METIS14-D32 Sec. 8.3]. In the model, there are three macro BSs, and nine micro BSs. In our simulations, we select one micro BS as the transmitting BS in the WEW scheme. The other micro BS does not transmit. The remaining micro BSs and the three macro BSs are interferers in our scheme. All nodes use the same transmission frequency of 2.6 GHz. The transmission power of the interferers are 42 dBm for Macro and 37 dBm for the micro BSs. Background noise power is set at -95 dBm. Two SBSs are deployed on floor 3. The MSs are deployed randomly on the same floor of the building. The simulations include path loss as well as small-scale fading. The results are averaged over a sufficient number of fading realizations, and are given in terms of minimal transmission power required by the BS to satisfy the MSs' uplink and downlink rate requirements.

The optimization problem is solved using the software CVX [GB-CVX], where the path-loss, rates and small scale fading are given as parameters. The formulation of the optimization problem is given below:

$$\begin{aligned} & \min P_1 + P_2 + |\mathbf{w}_C|^2 \\ & s. t. R_{Pi} \leq \log \left( 1 + \frac{\gamma_{Pi}}{1 + \gamma_{Ui} + \frac{I}{\sigma^2}} \right), \\ & R_C \leq \log \left( 1 + \frac{\gamma_{Ci}}{1 + \gamma_{Ui} + \frac{I}{\sigma^2}} \right), R_{Pi} + R_C \leq \log \left( 1 + \frac{\gamma_{Pi} + \gamma_{Ci}}{1 + \gamma_{Ui} + \frac{I}{\sigma^2}} \right) \end{aligned}$$

Here, the rate of the downlink packet to SBS $i$  is  $R_i = R_{Pi} + R_{Ci}$ , where  $R_{Pi} = \alpha_i R_{Di}$  and  $R_{Ci} = (1 - \alpha_i) R_{Di}$ .  $R_{Di}$  is the rate of the downlink packet sent to SBS $i$ , and  $0 \leq \alpha_i \leq 1$  is the splitting factor of the packet.

The optimization variables are the transmission powers  $P_1, P_2$  for the ZF beamformers, and  $|\mathbf{w}_C|^2$  for the common beamformer, and the splitting factors  $\alpha_1, \alpha_2$ . The constraints mean that each SBS $i$  must decode the entire private packet at rate  $R_{Pi}$ , and the entire concatenated packet at rate  $R_C = R_{C1} + R_{C2}$ . Recalling that the SBS $i$  needs to decode the downlink signals while treating the uplink signal as noise, we divide by the equivalent SNR  $\gamma_{Ui}$  of the MS $i$ -SBS $i$  link. The last term  $I$  in the denominators is the aggregated interference from all interfering nodes in the scenario.

The simulation results are illustrated in Figure 4-3, where we compare WEW with three other methods. The uplink rates of the MSs are fixed, while the downlink rates vary over the interval shown on the x-axis. The first is when BS transmits using only spatial ZF, the second one when using only the common beam approach, while the third is when we select the partitioning of the data randomly for each MS.

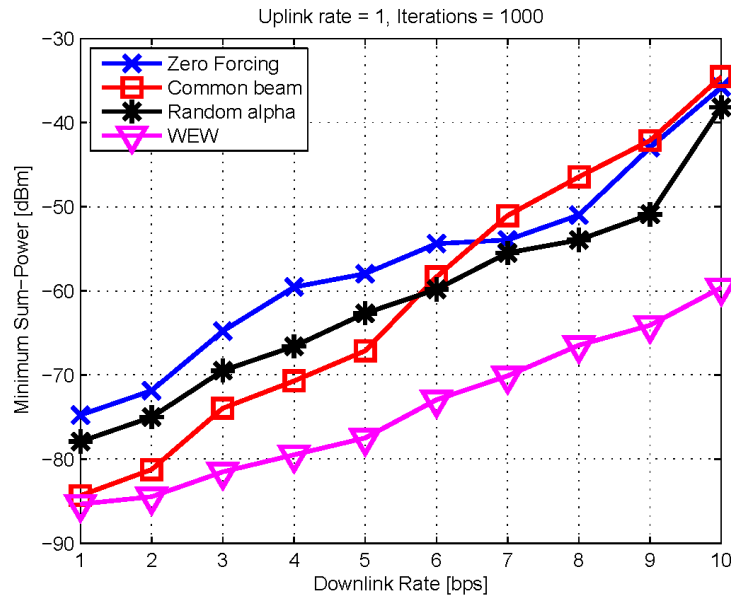


Figure 4-3: Comparison of our proposed method

It is observed that the performance of ZF is generally the worst, however the gap in performance between ZF and common beam decreases as the downlink rate requirement (related to the size of the packet) increases. Because high rate requirements translate into high SINR requirements, this is related to the fact that ZF has an advantage at higher SINRs. We also see that the method using the common beam is quite good at low rates (equals small packets), but is not so good at high rates. Recalling that in the Common-only scheme the receivers need to decode the entire concatenated packet, this gives a rather large overhead for the large rates. Furthermore, the optimization of the splitting factors gives an advantage, compared to choosing them at random. This also justifies the optimization of the splitting factors. The WEW scheme is the best of the schemes in terms of transmission power.

#### 4.2.3 TeC 3: Virtual full-duplex buffer-aided relaying

A virtual full-duplex (FD) relaying exploiting more than two half-duplex (HD) relays with buffer is proposed in this TeC. More specifically, one relay receives new data from the source while another relay forwards previously received data stored in its buffer to the destination. The main goal is to approach the average end-to-end rate of ideal FD relaying even in the presence of inter-relay interference (IRI). To this end, we propose transmission schemes based on a joint relay selection and beamforming (BF) design utilizing multiple buffer-aided relays and multiple antennas at the relays [KB13], [KB14]:

1. *SINR-based relay selection with BF neglecting IRI* – beam-formers are determined without consideration of IRI (i.e., MRC at the receiving relay and MRT at the transmitting relay) and then an SINR measure is used at the receiving relay for relay selection.
2. *ZFBF-based relay selection* – transmit beam-former is determined so that the IRI is perfectly cancelled at the receiving relay while receive beam-former is determined by MRC. Then, effective SNR measures after applying beam-formers are used for relay selection.
3. *MMSE BF-based relay selection* – receive beam-former is determined so that the received SINR is maximized at the receiving relay while transmit beam-former is determined by MRT. Then, effective SNR measures after applying beam-formers are used for relay selection. This scheme has been developed after [METIS14-D32] and newly included in this report.

4. *Optimal BF-based relay selection* – transmit and receive beam-formers are optimized through an iterative algorithm between transmitting and receiving relays so that the end-to-end rate is maximized. Then, effective SNR measures after applying beam-formers are used for relay selection.

## Performance Results

The simulation is based on the WP3 T3.3 simulation baseline for TC2 Dense Urban Information Society. Figure 4-4 shows the SINR map of a serving Pico BS in our simulation setup. The left most Pico BS serves an edge UE placed at inside corner of the building. We place two relays (RS1 and RS2 in Figure 4-4) in medium SINR range between the serving Pico BS and UE. While our algorithm is not restricted to special deployment of the relays and can support more than two relays, we choose in the considered setting the position of the two relays to be in similar interference ranges in order to avoid that one relay plays a more significant role in forwarding the messages and thus de-emphasising the relay selection mechanism. Otherwise, the simulation results are qualitatively similar to the ones we present later. The small scale fading of links of interest is generated by [ITU09-2135] model referred in [METIS13-D61]. For serving Pico-relay and serving Pico-UE links, the small scale fading follows Urban Micro O2I (UMi O2I) model and for relay-UE and relay-relay links, it follows Indoor Hotspot (InH) model.

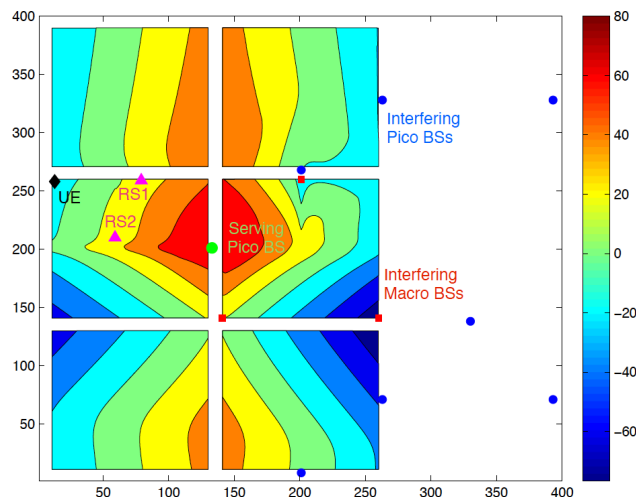


Figure 4-4: Simulation environment and SINR map

The simulation parameters follow the WP3 T3.3 simulation baseline. Since we consider a resource block (RB) based relay selection, bandwidth, transmit power, and noise are taken into account as per subcarrier (e.g., 15 kHz in LTE). We assume that a single RB is used for serving the UE in Figure 4-4. Although multiple UEs can be scheduled using multiple RBs, we consider a single user supported by relays at this moment. The BF is applied for each subcarrier and the relay selection is performed in unit of RB based on the effective transmission rate for an RB. We assume that the serving Pico BS has always data to transmit and perfect channel state information is available at the transmitters.

The performance is evaluated in terms of average end-to-end rate in [bps/Hz], which corresponds to spectral efficiency in KPI. Our scheme is compared to five benchmarks:

- *Upper Bound (UB)*: This bound is obtained assuming no IRI. MRC and MRT beam-formers for the receiving and transmitting relays are used and then the best relay pair is selected through an exhaustive search.
- *Space FD max-max relay selection (SFD-MMRS)*, which does not assume IRI using highly directional antennas at relays [IKS12].

- *HD best relay selection (HD-BRS)* which it does not consider buffer at relay and thus the best relay is selected based on a maximum of minimum of channel gains for source-relay and relay-destination links [BKR+06].
- *HD max-max relay selection (HD-MMRS)* which considers buffer at relay and the best relay is determined as a relay with maximum channel gain of source-relay link at first time slot and a relay with maximum channel gain of relay-destination link at second time slot [IMS12].
- *Direct communication* between the serving Pico BS and UE.

Figure 4-5 (left) shows the spectral efficiency for varying transmission power of the serving Pico BS and relays in case of two relays ( $K=2$ ) with four antennas ( $M=4$ ). It is observed that the conventional SFD-MMRS has always worse performance than the HD relaying schemes due to no consideration of IRI in relay selection. The HD relaying schemes do not suffer from IRI due to orthogonal transmissions but it has one-half performance degradation due to the orthogonal transmissions, compared to the UB. The proposed ZFBF-based relay selection and MMSE-based relay selection schemes significantly outperform the HD relaying schemes. Even if they have some gap with the UB, the slopes of curves are similar to that of the UB. In this simulation setup, the proposed ZFBF-based relay selection scheme always outperforms the MMSE-based relay selection scheme. The proposed ZFBF-based relay selection scheme achieves average gains from 80% to 85% as compared to the HD-MMRS scheme and from 210% to 460% as compared to the SFD-MMRS scheme.

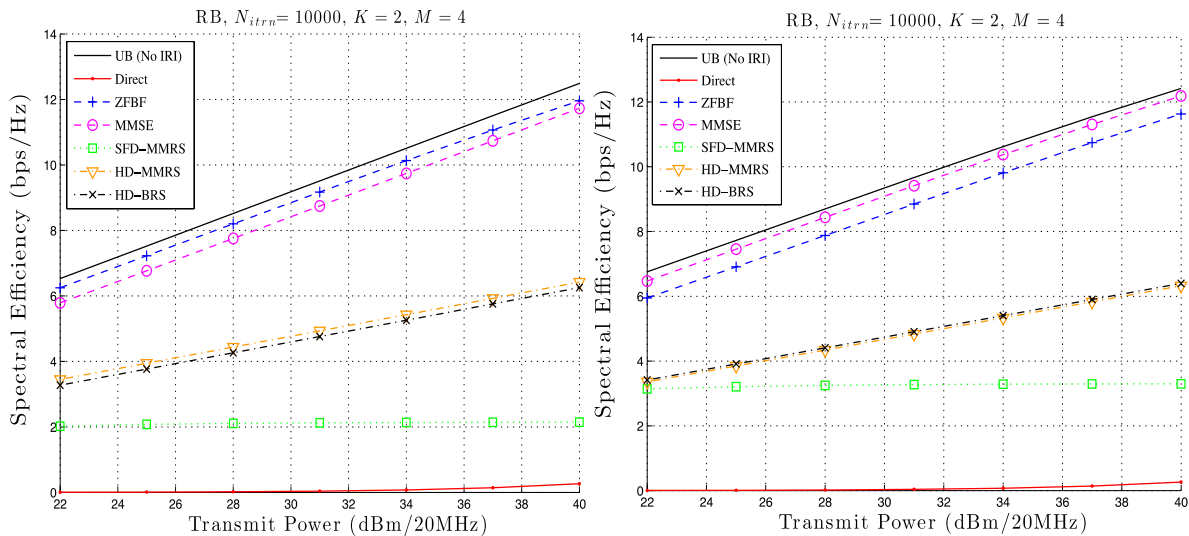


**Figure 4-5: Spectral efficiency for two buffer-aided relays ( $K=2$ ) with four antennas ( $M=4$ ) when relays are placed to be closer to the destination (left) and when relays are placed closer to source (right)**

Figure 4-5 (right) shows the spectral efficiency for  $K=2$  and  $M=4$  when the relays are placed closer to the source. The obtained results show that the MMSE-based relay selection scheme always outperforms the ZFBF-based relay selection scheme. In the ZFBF-based relay selection scheme, the bottleneck link becomes the relay-to-destination link since it causes a loss in the effective rate of the link due to IRI cancellation while the other source-to-relay link can achieve the maximum rate by MRC. On the contrary, in the MMSE-based relay selection scheme, the bottleneck link is the source-to-relay link due to a loss in the effective rate of the link for suppressing IRI at the receiving relay.

Basically, the average end-to-end rate is limited by the minimum of average effective rates of both links. Hence, for the ZFBF-based relay selection scheme, a deployment scenario, where the relay-to-destination link qualities are better than the source-to-relay link qualities, is better because it can provide an extra budget for IRI cancellation at the transmitting relay. On the other hand, for the MMSE-based relay selection scheme, another relay deployment scenario,

where the source-to-relay link qualities are better than the relay-to-destination link qualities, is better since it can provide an extra budget for IRI suppression at the receiving relay.

In principle, the proposed VFD-BR schemes can recover the loss of multiplexing gain caused by HD relaying as both/either the number of relays and/or the number of antennas increases. In practice, more than three relays supporting one source-destination pair could be unavailable in many realistic scenarios. However, through the WP3 T3.3 baseline simulation, it is shown that only two relays are enough to recover the loss of multiplexing gain if increasing the number of antennas is available. Compared between the proposed ZFBF-based and MMSE-based relay selection schemes, the ZFBF-based relay selection scheme is more efficient when relays are closer to the destination and the MMSE-based relay selection scheme is more efficient when relays are closer to the source. Therefore, we could selectively use one of the proposed schemes according to relay deployment scenarios.

#### **4.2.4 TeC 5: Bi-directional relaying with non-orthogonal multiple access**

Relaying has been an extensively investigated research topic over the last decades as it allows coping with path loss and fading in mobile radio systems. The main drawback of relaying, however, is the loss in spectral efficiency due to the half-duplex constraint. To overcome this drawback, bidirectional relaying has been investigated considering both transmission directions between two nodes jointly. Applying techniques like network coding (NC) [ACL+00] [FBW06] in the second phase, where the relay broadcasts to both nodes, the overall number of required transmission slots is reduced and, thus, the spectral efficiency is increased.

In order to obtain a highly flexible system concept, especially when considering multiple communication pairs with different rate requirements, non-orthogonal medium access based on IDMA [PLW+06] is applied. The combination of NC with IDMA offers great flexibility in terms of designing MAC and BC phase. Further considering resource allocation and channel coding leads to a system concept supporting high device densities and high spectral efficiencies, which is the foundation for a high end user throughput.

One of the crucial parameters of the proposed system is the applied channel code. In [METIS14-D32] Irregular Repeat Accumulate (IRA) codes [JKM00] have been proposed as they allow for a very flexible design at moderate complexity. A code design framework for IRA codes has been developed and IRA codes have been implemented into the general simulation framework. Details regarding the code design framework can be found in [METIS14-D32] and initial performance results have been published in [LBW+13].

In order to get more meaningful results, the simple channel models used thus far have been dropped in favour of more realistic modelling assumptions. Specifically, a concrete simulation model has been developed in which effects as path losses and more realistic small scale fading are incorporated. Within the simulation model, a specific scenario has been investigated which is described in more detail in the following section. Furthermore, an OFDMA-based four-way relaying simulation framework has been developed. In conjunction with LTE-A parameters, this system serves as a legacy solution benchmark for the proposed IDMA-based scheme.

### **Performance Results**

The principle system and code optimization assuming a simplified system model has already been presented in [METIS14-D32]. The novelty in the results presented here lie in the adoption of the T3.3 simulation baseline. Figure 4-6 shows the investigated setup within the simplified Madrid grid agreed upon within T3.3. One single relay (orange triangle) is placed indoor 10m apart from the outdoor facing wall to increase outdoor-to-indoor coverage as well as to facilitate indoor device to device communication. In the specific investigated setup the relay supports the communication from an outdoor Pico base station (green dot) to an indoor user UE1 (green rectangle) as well as the communication between two indoor users UE2,

UE3 (yellow rectangles). Indoor users are uniformly distributed within a circle of radius  $R$  around the relay.

The overall communication experiences background interference which is caused by Macro base stations (red squares) and Micro base stations (blue circles) which are deployed as indicated in the figure. The overall background interference and noise pattern is indicated by the underlying colour map. It depends on the positions of the interferers, as well as their transmit powers.

Node transmission powers as well as channel models follow the simulation guidelines described in [METIS13-D61]. Specifically, the Macro BSs transmit with 42dBm, whereas Micro/Pico BSs transmit with 37dBm. The transmit power of the indoor relay is set to 20dBm and the users transmit power to 24dBm. The path loss between Pico BS and relay as well as relay and UEs is calculated using path loss model PS#4 for outdoor-to-indoor and PS#7 for indoor-to-indoor communication, respectively. Additionally, small scale fading is introduced which is calculated based on the WINNER models using parameters agreed on within T3.3.

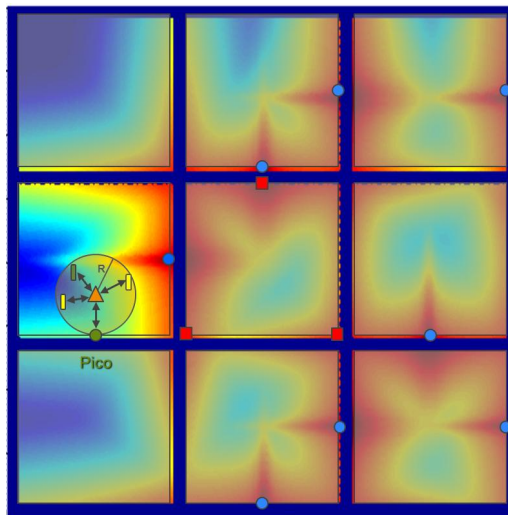


**Figure 4-6: Simplified TC2 simulation model with investigated placement of nodes**

In order to achieve a meaningful comparison of the proposed IDMA system with an OFDMA based legacy solution we choose  $R_{WP} = 10m$  as our working point. That means we optimize the system for a distribution of users within a circle of radius  $R = 10m$  around the fixed position of the relay. The distance between the Pico BS and the relay is fixed and set to  $d_{PR} = 10m$ . This working point is chosen arbitrarily. A different working point might lead to different throughputs due to lower or higher path losses. This, however, affects the proposed IDMA system as well as the OFDMA based legacy solution equally.

The IDMA system is now optimized according to the chosen working point and the code optimization process as described in detail in [METIS14-D32]. As benchmark we investigate an OFDMA-based four-way relaying system. Figure 4-7 depicts the average end-to-end-throughput of the optimized two way relaying (TWR) IDMA system and the legacy OFDMA-based solution for different modulation and coding schemes. In this figure, the distance between the relay and UE is  $d_{RU} \leq R_{max}$ . The distance between Pico BS and relay is fixed as  $d_{PR} = 10m$ . For every investigated scheme, two curves are shown. The solid line depicts the average throughput (up- and downlink) of the pico-UE1 communication and the dashed line the average throughput (up- and downlink) of the UE2-UE3 communication. Up- and downlink here are to be understood with respect to the end users and not with respect to the relay. That means, e.g. for the Pico-UE1 transmission, if the link between Pico and relay is in outage, the throughput between Pico and UE1 is zero and the depicted average is the average between zero and the throughput of the transmission from UE1 to Pico. Furthermore, the throughput

curves for Pico-UE1 and UE2-UR3 communication are not necessarily identical, since the distance between Pico and relay is fixed and, thus, does not vary with  $R_{max}$ .

For the optimized IDMA system the achieved throughput at the working point of  $R_{WP} = 10m$  is approximately  $TP = 0.5$  bit/s/Hz for both links. Increasing the distance between relay and UEs leads to a significant drop in throughput. As can be seen, the throughput of the UE2-UE3 link decreases faster than the throughput of the Pico-relay link. This is due to the fixed distance between Pico BS and relay and is independent of the actual transmission scheme but is due to the chosen setup. The OFDMA-based schemes experience the same behaviour, as can be seen in the figure.

The performance results for the OFDMA-based legacy solution are given for two different modulation schemes and two different code rates. Specifically, QPSK and 16-QAM modulation are shown. Higher order modulation schemes as 64-QAM already fail after a few meters distance between relay and UEs and are, hence, omitted here. The applied code is the LTE turbo code with base code rate of  $R_c = 1/3$  and a punctured version of this code with code rate  $R_c = 2/3$ . As can be seen, the QPSK-based transmission as well as the 16-QAM-based transmission with the base code rate achieve a significantly lower throughput than the optimized IDMA system. At the working point, the throughput of the IDMA system is approximately 50% higher than the best OFDMA-based solution, the 16-QAM-based system with base code rate. The 16-QAM-based system with the punctured code of rate  $R_c = 2/3$  achieves a higher throughput than the IDMA system for the UE2-UE3 link, but already fails at the desired working point. Clearly, the IDMA system could then be optimized for a new working point  $R_{WP} = 5m$ , again outperforming the OFDMA system. Note that for most depicted schemes the throughput curves start at the same point for both communication pairs, e.g.  $TP = 0.5$  bits/s/Hz for the IDMA system. For the OFDMA-based solution with 16QAM and the punctured code of rate  $R_c = 2/3$  this is not the case. Here the throughput of the Pico-UE1 transmission is only half of the throughput of the UE2-UE3 transmission. The reason for this behaviour is the fixed distance between Pico and relay of  $d_{PR} = 10m$ . For this distance the combination of modulation and coding fails for the chosen transmit power of the relay of 20dBm such that the transmission from UE1 to Pico is always in outage. The transmit power of the Pico of 37dBm, however, is higher than the transmit power of the relay, such that the transmission from Pico to UE1 is not in outage for small  $R_{max}$ . Hence, the average throughput of both directions for the Pico-UE1 pair is only half of the average throughput of the UE2-UE3 pair for 16QAM,  $R_c = 2/3$  and small  $R_{max}$ .

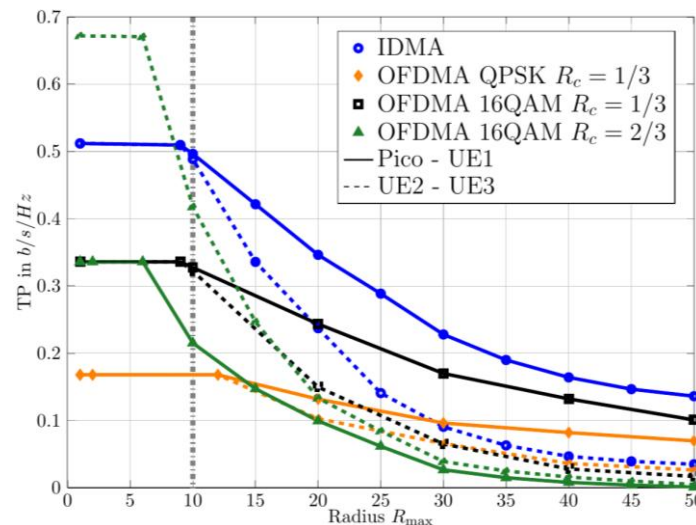


Figure 4-7: Average end-to-end throughput in bits/s/Hz of optimized TWR IDMA vs. legacy OFDMA-based solution over the distance of the UEs to the relay. Random distance  $d_{UR} \leq R_{max}$

It is important to point out, that the investigated system highly favours the OFDMA-based solutions as no impairments as, e.g., timing and frequency offsets, Doppler effects, etc. are considered. The IDMA solution is much more robust against these effects and, hence, more realistic simulations would likely lead to even higher gains for the IDMA system compared to the OFDMA solution.

#### 4.2.5 Addressed METIS Goals

**1000x data volume:** The combination of network coding and IDMA in TeC 5 provides a factor 2 gain with respect to SotA, which can be translated into higher data volumes. A gain of about 100% is also achieved by TeC 1 and TeC 3.

**10-100 user data rate:** The solutions in this approach mainly target the increase in user data rates, especially for the cell edge users. In detail, TeC 3 provides an increase of edge user data rate supported by relays up to 85%. Moreover, layered transmission enabled by IDMA in TeC 5 helps to increase user data rate.

**10-100x number of devices:** By deploying relays and small cells, an increase in the coverage area is achieved and, in turn, also an increase of the number of served devices.

### 4.3 Most Promising Technology Approach 2: Indoor dense mesh network at mm-waves

#### 4.3.1 Introduction

Communications at mm-wave frequencies are of primary interest to METIS concept as this is where opportunities for wide spectrum are most likely. Foreseen traffic volumes and propagation conditions of mm-waves will in significant cases imply dense deployments where backhaul in sufficient amount can only be economically motivated to be wireless and native inband. Practical deployments in diverse topologies will require mesh-like solutions on a general level. This is what TeC 2 is focusing on by considering the problem of routing and resource allocation schemes for multi-hop backhaul using access nodes as inband relays. More specifically, low complexity schemes have been developed and studied in the complex scenarios that practical mesh deployments constitute and which are hard to analyse in terms of optimality.

It should be noted that several of the TeCs in MPTA 1, see section 4.2, could be applicable as solutions to particular bottleneck scenarios within specific problematic areas of the general meshes when those areas fulfil the models assumed of respective TeC.

As this MPTA is an enabler targeting mmW spectrum, it deviates from the TC2 2.6GHz T3.3 baseline and is simulated using a proprietary ray-traced and stochastic combined channel model. This MPTA is, after the initial evaluations- and results-phase in a TeC specific scenario, now shifting towards closer adherence to TC1 which appears more tailored for a mmW solution than the TC2 scenario used for the T3.3 baseline.

#### 4.3.2 TeC 2: Interference aware routing and resource allocation in a millimetre-wave ultra-dense network

This technology component considers the problem of multi-hop wireless routing and resource allocation and should be considered as a medium term radio resource management component in the following context [HA13, METIS14-D32]. The resources are taken from a resource pool that is assumed to have been provided by a longer term inter-UDN coordinator (see TeC9 of WP5 [METIS14-D53, Section 3.1.2]). Several simultaneous flows are managed, associated with active users communicating through a UDN comprising many wireless access nodes and a limited number of wired aggregation nodes. The flows are assumed having full buffer traffic in one direction, the other direction, or both of them. The resulting routes and

allocations are then to be handed off (potentially after some further classification e.g. based on inter route interference) to a faster MAC based RRM operating on individual hops to harvest statistical multiplexing gains when the flows deviate from the full buffer assumption causing local load and interference fluctuations in parts of the UDN (see TeCC#12.3 of WP2 [METIS14-D23, Section 2.12.3]).

The routing scheme operates by using an expected throughput metric taking interference of previous laid out routes and hops into account and trading a tuneable fraction of the metric for latency (number of hops). Subsequently routes are alternately widened in frequency and/or time based on their performance relative to what they would achieve if they comprised a sole flow in the UDN. By prioritizing the flow with the worst *relative* performance in the iterative scheme, degrees of fairness can be achieved without wasting excessive amount of resources on users that will anyway suffer due to poor channel gains. For more details on the proposed routing/resource allocation scheme we refer to [METIS14-D32].

The increment as compared to previous reports is mainly the new scenario and deployment comparisons as well as the inclusion of the new fairness aspect.

## Performance Results

In these evaluations we adhere to the cubicle office environment scenario of TC1: *Virtual reality office* described in [METIS13-D61] Section 4.1 and Section 9.1. The simulated room is 12m x 25m (see Figure 4-8, for the used access point locations and user positions possible in the random drops, left, and the used access node antennas, right).

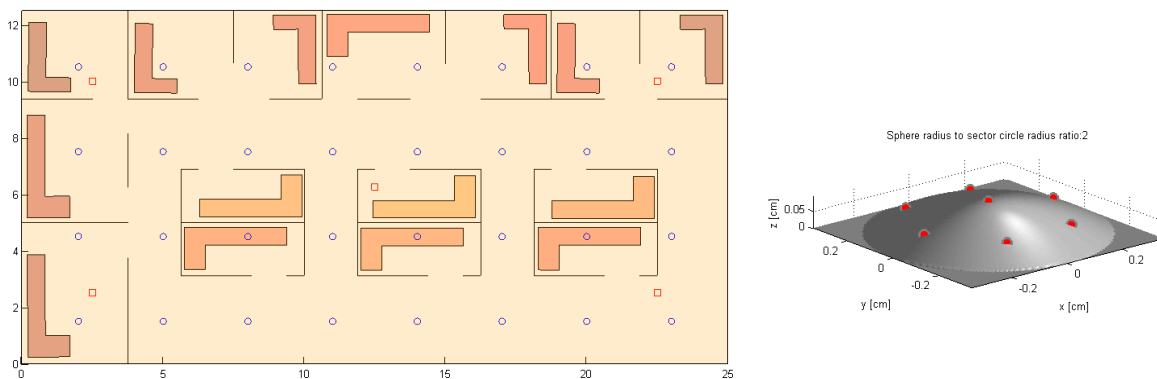


**Figure 4-8: Left: Top view of TC1 layout used. Red squares: AN locations, Blue circles: UE drop positions. Right: AN antenna layout (flip vertically for a ceiling mounted antenna).**

In Figure 4-9 we provide system level results assuming full buffer traffic, 7 AN antennas, 2 UE antennas, 20mW TX power of AN, and 10mW on the user side. For simulation efficiency, only 200MHz bandwidth as opposed to the envisioned 2GHz is used. The carrier frequency used is 60GHz and the propagation channel is simulated using an up to two reflection ray-tracing model with a 5.6dB reflection loss plus a stochastic channel component 11dB below the ray-tracing component. More details can be found in the appendix description of this TeC.

The left plot of Figure 4-9 illustrates system throughput performance at various loads for the case of a single *wired* access node (the Aggregation Node (AgN)) with zero, two or four additional *wireless* access nodes (WL ANs). The *central* red square of Figure 4-8 illustrates the ceiling located wired AgN providing the connection to/from the core network. With an interference *unaware* version of the TeC (dotted lines), adding wirelessly backhauled access nodes lowers system performance unless load is very low. With interference *aware* routing, the cost to users close to the AgN of sharing the access medium with WLBN for WL AN is more than compensated for by the higher data rate coverage for users further away from the wired AgN. The reason for the difference between interference aware and unaware routing also for a single AN (the AgN) is that spatially multiplexed users in UL do not see the MU-MIMO inter-user interference and are hence co-scheduled irrespective of how well they can be

spatially separated by the RX beamforming. Simultaneous UL/DL interference is still avoided by the restriction of not having simultaneous UL and DL in any node that typically would lead to RX saturation.

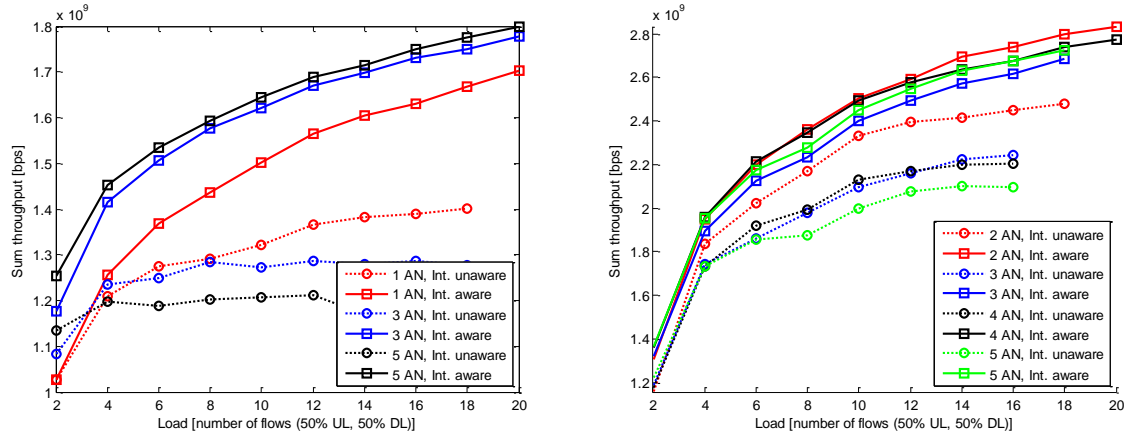


**Figure 4-9: System throughput versus load with increasing number of wireless access nodes for single (left plot) or two (right plot) wired aggregation nodes**

If we turn to the right plot of Figure 4-9, system performance is illustrated when the lower left and upper right AN's of Figure 4-8 (left) are serving as 2 wired AgNs and the effect of adding one WL AN in the middle, two WL AN in the other corners or all three of them. The fact that there are now two connections to the Core Network significantly increases the general throughput level. The limited directivity of the antennas (aperture of 1/3 wavelength in one random orientation at the UE side and approximately 1/2 and 1.5 wavelengths in elevation and azimuth respectively on the Access node side) is causing a blocking effect in the routing resource allocation when WL access nodes are added to better cover users further from the wired AgNs. Ignoring the interference in the scheme in this case gives a smaller penalty but is still worse than the interference aware version.

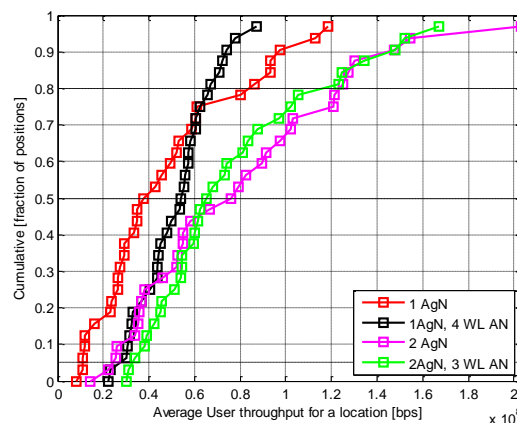


**Figure 4-10: Fraction of the user positions where average user throughput is less than x-axis value. This is for load point of 10 flows in Figure 4-9. Red and black shows the average throughput spatial coverage for a central AgN only and for the AgN + 4 corner WL AN's, respectively. Magenta and green is with two aggregation nodes and two aggregation nodes + 3 WL AN, respectively (compare Figure 4-9, right plot).**

In Figure 4-10 we get an overview of the distribution of average throughputs over user positions. We observe that adding WL ANs increases the fairness. It can also be observed that interference between access and backhaul is significantly reducing individual performance for users close to the AgN(s).

More specifically, adding 4 wireless ANs improves the 95% availability throughput over the single AgN by 145%. With 2 AgNs and 3 WL ANs, the corresponding improvement is 195% (out of which 118% can be attributed to the increase of wired AgNs from 1 to 2). The corresponding improvement in median over location is 42% and 71%. Note though that the 20% best performance is reduced significantly under the used simulation assumptions as resources otherwise used for central UE access is given to the WL BH.

Translating the TC1 KPIs of 0.5Gbps average TP per user during busy hour and 100Mbps/m<sup>2</sup> traffic density to the office area of 312.5m<sup>2</sup>, this gives 62.5 users active on average in both UL and DL. Now, assuming 2GHz spectrum rather than the simulated 200MHz, this would translate to a load point of 12.5 flows in Figure 4-9, assuming links are interference limited rather than power limited. With a single aggregation node we can then read out a system spectral efficiency 170Mbps/200MHz = 0.9bps/Hz and 1.7Gbps/12.5flows = 136Mbps/user in UL and DL respectively, if 4 WL ANs are added, and 120Mbps/user without the WL ANs, i.e. a 13% improvement. Similarly, for 2 aggregation nodes, we can read out 1.3bps/Hz and 2.6Gbps/12.5flows = 208Mbps/user in UL and DL respectively on average. With this setup we conclude that we only reach between 27% and 42% of the targeted average user data rate. We further reflect on the fact that the office is busy indeed. During these busy hours we have more than 4 users per desk each consuming 1Gbps, *on average*. In this scenario, where all ANs are in mutual line of sight and with most UE positions as well, WL BH with this limited beamforming directivity is a challenge compared to the previously studied scenario with rooms and a corridor providing some means of isolation between routes. We expect however that increasing the antenna apertures, in particular at the ANs, will dramatically improve the situation, but likely, a higher density of both AgN and WL AN will be needed to meet the TC1 targets and will be studied next.

Regarding Latency, we finally do the following reflection: TeCC#1 of WP2 [METIS14-D23, Section 2.1] on flexible air interface, TTI is expected to be scaled down from corresponding LTE numerology in a similar way as carrier frequency is scaled up. Assuming 1ms-1.5ms latency in the core network in either direction and a similar latency in UL as in DL within the UDN, a 10ms total latency requirement leaves slightly more than 3ms for the multiple hops for each flow. With 3-4 hops that would mean approximately 1ms per hop. In our simulation, a subframe duration of 25 $\mu$ s is used, but even if that is increased to 50 $\mu$ s or 100 $\mu$ s there will be several TTI's of time for processing and potential hop-level re-transmissions. Hence we conclude that a round trip latency of 10ms is not expected to be a problem even with multi-hop WL BH for mmW UDN.

### 4.3.3 Addressed METIS Goals

**1000x data volume:** The main goal addressed by TeC 2 is the increase in the data volume, and TeC 2 provides a traffic volume per area of 100Mbps/m<sup>2</sup> UL/DL.

**10-100 user data rate:** The increase in the traffic volume per area is the result of an increased user rate, and TeC 2 guarantees an experienced user rate 95% above 1Gbps, and 20% above 5Gbps.

**10-100x number of devices:** The increase in the user rate can be translated into an increased number of active users.

**10x longer battery life:** Longer battery-life results from faster user data transfer and thereby hopefully longer sleep cycles. Furthermore, the enabled densification will likely allow for a larger fraction of the network to enter sleep states at low load than an already sparse network of high power nodes that still need to provide coverage at low load.

**5x E-E reduced latency:** Shortened OFDM symbols in mmW, and thereby frame structure and TTI, will allow reducing latency to less than 10ms even if multi-hop backhauling is used.

**Energy efficiency and cost:** By enabling native inband backhauling with single radio will reduce costs as compared to wired installations or outband backhauling. Further, many small highly integrated access nodes will enjoy larger economy of scale and hence further contribute to cost target.

#### 4.4 Impact on METIS system

The TeCs developed within T3.3 have their main impact in horizontal topics UDN and D2D. One TeC targets horizontal topic MN.

In **UDN**, T3.3 targets network densification based on **wireless backhaul** for cost efficiency and deployment flexibility compared to a wired backhaul. The overall goals are: spectral efficiency, interference management caused by the wireless backhaul and coverage.

One ambitious goal of the wireless backhaul solution is to obtain performance approaching the one given by a wired backhaul in terms of spectral efficiency. This goal is achieved by exploiting the principles of wireless network coding along with new broadcast techniques at the macro base station, in a setting with multiple small cells where each user in a small cell has a two-way traffic. Non-orthogonal access via IDMA in combination with network coding allows for a very flexible design of the MAC and BC phase in order to support a dense node deployment and flexible rate requirements.

Another solution for network densification relies on UEs acting as small cell BSs and relaying the uplink traffic to the BS. The solution builds upon advanced relaying protocols based on non orthogonal multiple access techniques and optimized joint network-channel coding designs.

At millimeter wave frequencies, a very dense mesh network of access points connected by a wireless backhaul along with an interference aware routing enables very high data rates and coverage for large amount of users

An increased coverage at the cell edge is enabled relying on multi-antenna relays. Spectral efficiency of edge users is increased by exploiting buffers at the relays. Moreover, concurrent transmission and reception at the relays is optimised through joint relay-pair selection.

In **D2D**, T3.3 targets **D2D communications through a relay**. The overall goals involve efficient transmission methods through a relay as well as transmission methods providing coexistence or cooperation between the cellular and D2D traffic.

Two-way traffic through a relay between 2 UEs is employed to provide increased spectral efficiency. Also proposed for UDN, IDMA as a non-orthogonal channel access scheme in combination with network coding provides support for a dense node deployment operating on very wide bands and flexible rate requirements in order to increase throughput and capacity. Multiple antenna capabilities at the different nodes are exploited for an efficient two-way communication, where a system level interference management is needed to achieve performance gain. In a cellular system, multiple antenna based methods are exploited with two different goals: suppressing the interference between the cellular and the two-way D2D traffic and providing secure communications.

A cooperative D2D communications scheme allows coexistence of cellular users and D2D communications without the need for extra radio resources. Important gains are observed, such as an increase in the number connected devices within the cell, an increase in the cell throughput and the data volume.

In **MN**, T3.3 targets the **deployment of relays in moving networks**.

By using moving relay networks to serve vehicular UEs, both the power outage probability at the vehicular UEs can be lowered at a fixed transmit power, or significant RF energy savings can be observed at a given power outage probability at the vehicular UEs. Furthermore, via cooperation between vehicular UEs enabled by D2D communication, all the VUEs that

participate in the cooperation can save energy when the vehicle is moving away from the BS, and the communication is affected by high vehicular power loss.

#### 4.5 Overview of achieved results

T3.3 explores innovative solutions to improve spectral efficiency of a wireless network based on the deployment of relays and wireless network coding. Most of the results are produced using the baseline simulation set-up defined in WP3 T3.3 for TC2 Dense Urban Information Society and based on a simplified Madrid grid. The results obtained in T3.3 show that relays offer a wide range of functionalities that can be exploited in 5G networks for network densification, spectral efficiency improvement, D2D communications, moving networks and coverage extension.

As the first of the most promising technologies, relaying with bi-directional traffic exploiting the principles of wireless network and non-orthogonal access is shown to be a promising tool to enable network densification with deployment of small cells. Buffering at the relays is also shown to further compensate for the loss due to the half duplex nature of the relays.

For the second most promising technology, very thorough simulation results are provided based on a practical deployment of an indoor dense mesh network supported by a wireless backhaul in mm-wave frequencies. An interference aware routing is proposed for which the impact of the number of wired access nodes and number of wireless access nodes is demonstrated.

Relaying is also shown to be a powerful tool for D2D communications where the relay carries the D2D traffic and simultaneously insures co-existence between cellular and D2D traffic. Cellular and D2D traffic are also designed as cooperative flows to enhance the overall spectral efficiency. At last, an extensive study on relaying in moving networks is provided where performance is shown given a practical set-up.

For a more detailed analysis of the synergies among the TeCs developed within Task 3.3, for instance which TeCs can be combined together to further enhance the performance, please refer also to [METIS14-D32, Sections 4.2.3-4.3.3].

#### 4.6 Conclusion

The research in T3.3 has been consolidated by adopting a common simulation baseline corresponding to a representative 5G scenarios defined by the METIS project. The results show the significant gains that relaying provides in such a scenario. Furthermore, T3.3 shows that relaying offers many functions that 5G networks can advantageously exploit. Bi-directional traffic along with wireless network coding, non-orthogonal access as well as buffering at the relay enables efficient network densification with wireless backhaul. In mm-wave frequencies, propagation loss motivates the use of many wireless access nodes relaying the traffic and interference aware routing. In D2D, relaying serves to manage the cellular and D2D traffic either as competitive or cooperative flows. At last, relaying serves as a tool for coverage extension or as an access point in a moving network.



## 5 Conclusion

This document has provided the final performance assessment of the TeCs that are proposed by WP3. The assessment is mostly based on a uniform framework that was developed within WP3. As a result of the assessment, this document has provided an update on the MPTAs and the TeCs associated with each MPTA. Most of the TeCs provide solutions that can be applied to many scenarios. However, the specific targets are the improvements in wireless backhaul and wireless access in the scenarios like UDN, MN, D2D and in some cases URC.

The results provided in this document give an insight on how the WP3 TeCs impact the METIS system concept. Moreover, we have also presented a short analysis for each MPTA (in the main part) as well as each TeC (in appendix) showing in what ways WP3 contributions influence the METIS goals and create impact on final system architecture. Based on the reported results, we see that Massive MIMO, CoMP, In-Band Backhaul and Access are the key technologies for achieving 5G targets and requirements.

The results have shown that with the proposals of WP3 we can realize the gains of Massive MIMO in METIS 5G systems for both access and backhaul scenarios. If we focus on the achieved results, we can see that WP3 has provided solutions which shift the performance gains towards the achievable limits. However, there is still some room for improvements which require further research. For example, 3D-beamforming proposed in WP3 helps to achieve a spectral efficiency 10 times higher than LTE-A. However, considering the future demand for capacity and number of connected devices, further research is required to elevate this factor.

Enabling CoMP technologies for 5G systems is another important achievement of WP3. The contributions in WP3 have shown that CoMP techniques have high potential to achieve higher spectral efficiency and higher average user throughput. In particular, the focus of WP3 is to exploit the gains of JT-CoMP a) in constrained backhaul scenarios and b) with the help of advanced UE capabilities. For example, the results have shown that gains up to 55% in spectral efficiency can be achieved with respect to LTE-A, even with limited backhaul capabilities. However, further research is still required, for instance to find the theoretical and practical gains with the combination of Massive MIMO and CoMP techniques.

Not only access technologies but also efficient backhaul solutions are required for 5G. It is a very difficult task to provide wired backhaul to the nodes in a ultra dense future network. Therefore, WP3 has also focused on the problem of backhaul and provided revolutionary concepts on in-band backhauling. For example, one of the solutions is based on the principle of wireless network coding and emulates a wired backhaul connection. This helps to achieve up to 100% spectral efficiency on access and backhaul. However, further research is required to realize these gains in practical systems.

## 6 References

- [3GPP10-36814] 3GPP TR 36.814, "Further advancements for E-UTRA physical layer aspects," Release 9, v9.0.0 (2010-03).
- [3GPP12-36829] 3GPP TR 36.829, "Enhanced performance requirements for LTE user equipment (UE)," Release 11, v11.1.0 (2012-12).
- [3GPP13-36866] 3GPP TR 36.866, "Network-assisted interference cancellation and suppression for LTE," Release 12, v1.1.0 (2013-11).
- [3GPP13-RP130404] RP-130404, "Study on network-assisted interference cancellation and suppression for LTE," Mediatek, Renesas Mobile Europe, Broadcom Corporation, Vienna, Austria, Feb. 2013.
- [ABW12] D. Aziz, F. Boccardi, and A. Weber, "System-level performance study of interference alignment in cellular systems with base-station coordination", 23rd IEEE Intern. Symp. on Personal, Indoor and Mobile Radio Communications (PIMRC 2012), Sep. 2012.
- [ACL+00] R. Ahlswede, M. Cai, S.-Y. Li and R. Yeung, "Network Information Flow", IEEE Transactions on Information Theory, vol. 46, no. 4, pp. 1204-1216, Jul. 2000.
- [ANAC13] A. Adhikary, J. Nam, J.-Y. Ahn and G. Caire, "Joint Spatial Division and Multiplexing: The Large-Scale Array Regime", Information Theory, IEEE Transactions on, vol. 59, pp. 6441-6463, 2013.
- [APJ12] O. El Ayach, S. W. Peters, and R. W. Heath Jr., "The practical challenges of interference alignment", CoRR, abs/1206.4755, 2012.
- [ARTD14] ARTIST4G consortium, "D1.4 – Interference Avoidance techniques and system design," project report, July, 2012.
- [ATR14a] H. Asgharimoghaddam, A. Tölli, and N. Rajatheva, "Decentralizing the optimal multi-cell beamforming via large system analysis," in Proc. IEEE ICC, Sydney, Australia, Jun. 2014.
- [ATR14b] H. Asgharimoghaddam, A. Tölli, and N. Rajatheva, "Decentralized Multi-cell Beamforming via Large System Analysis in Correlated Channels", in Proc. EUSIPCO, Lisbon, Portugal, 2014.
- [AV07] D. Arthur and S. Vassilvitskii, "k-means++: The advantages of careful seeding", Proceedings of the eighteenth annual ACM-SIAM symposium on Discrete algorithms, pp. 1027-1035, 2007.
- [BBB14] P. Baracca, F. Boccardi, and N. Benvenuto, "A dynamic clustering algorithm for downlink CoMP systems with multiple antenna UEs," EURASIP journal on wireless communications and networking, 2014:125, Aug. 2014.
- [BCG+12] F. Boccardi, B. Clercks, A. Ghosh, E. Hardouin, K. Kusume, E. Onggosanusi and Y. Tang, "Multiple-Antenna Techniques in LTE-advanced", IEEE Communications Magazine, vol. 50, no. 3, pp.114-121, Mar. 2012.
- [Ber06] P. Berkhin, "A survey of clustering data mining techniques", Grouping multidimensional data, Springer, pp. 25-71, 2006.
- [BG92] D. P. Bertsekas and R.G. Gallager, "Data Networks," 2nd Edition, Prentice Hall, 1992.
- [BH07] F. Boccardi and H. Huang, "A near-optimum technique using linear precoding for the MIMO broadcast channel," in Proc. IEEE International Conference on Acoustics, Speech and Signal Processing (ICASSP), Honolulu (HI), Apr. 2007.

[BKR+06] A. Bletsas, A. Khisti, D. P. Reed, and A. Lippman, "A simple cooperative diversity method based on network path selection," *IEEE J. Sel. Areas Commun.*, vol. 24, no. 3, pp. 659 – 672, Mar. 2006.

[BOO06] F. Bohagen, P. Orten, and G. E. Oien, "Optimal Design of Uniform Planar Antenna Arrays for Strong Line-of-Sight MIMO Channels," *Signal Processing Advances in Wireless Communications*, 2006. SPAWC '06. IEEE 7th Workshop on, pp.1-5, 2-5 Jul. 2006.

[BZG+10] E. Björnson, R. Zakhour, D. Gesbert and B. Ottersten, "Cooperative Multicell Precoding: Rate Region Characterization and Distributed Strategies with Instantaneous and Statistical CSI," *IEEE Trans. on Signal Processing*, vol. 58, no. 8, pp. 4298-4310, Aug 2010.

[CAH+07] R. Chen, J. Andrews, R. Heath, and A. Ghosh, "Uplink power control in multi-cell spatial multiplexing wireless systems," *IEEE Trans. Wireless Commun.*, vol. 6, no. 7, pp. 2700-2711, Jul. 2007.

[DKTH14] J. Dommel, P.-P. Knust, L. Thiele, and T. Haustein. Massive MIMO for interference management in heterogeneous networks. In *Sensor Array and Multichannel Signal Processing Workshop (SAM)*, 2014 IEEE 8th, pag. 289–292, June 2014.

[DMW+11] A. Damnjanovic, J. Montojo, Y. Wei, T. Ji, T. Luo, M. Vajapeyam, T. Yoo, O. Song and D. Malladi, "A survey on 3GPP heterogeneous networks," *IEEE Wireless Commun. Mag.*, 18(3), pp. 10-21, Jun. 2011.

[EAR12D23] INFISO-ICT-247733 EARTH, Deliverable D2.3, "Energy efficiency analysis of the reference systems, areas of improvements and target breakdown," Jan. 2012.

[EKS+96] M. Ester, H.-P. Kriegel, J. Sander and X. Xu, "A density-based algorithm for discovering clusters in large spatial databases with noise", *Proceedings of 2nd International Conference on Knowledge Discovery and Data Mining (KDD)*, vol. 96, pp. 226-231, 1996.

[FBW06] C. Fragouli, J. Boudec and J. Widmer, "Network Coding: An Instant Premier", *ACM SIGCOMM Computer Communication Review*, vol. 36, no. 1, pp. 63-68, Mar. 2006.

[FDT14] G. Fodor, P. Di Marco and M. Telek, "Performance Analysis of Block and Comb Type Channel Estimation in Massive MIMO Systems", *1st International Conference on 5G for Ubiquitous Connectivity*, Levi, Finland, Nov. 2014.

[FJS10] G. Fodor, M. Johansson, and P. Soldati, "Near optimum power control and precoding under fairness constraints in network MIMO systems," *EURASIP International Journal of Digital Multimedia Broadcasting*, vol. 2010, pp. 1-17, Mar. 2010.

[FT14] G. Fodor and M. Telek, "On the Pilot-Data Power Trade-Off in Single Input Multiple Output Systems", *20<sup>th</sup> European Wireless Conference*, Barcelona, 14-16 May 2014.

[GB-CVX] M. Grant and S. Boyd, "CVX: Matlab software for disciplined convex programming," available at <http://cvxr.com/cvx/>.

[GCJ08] K. S. Gomadam, V. R. Cadambe and S. A. Jafar, "Approaching the Capacity of Wireless Networks through Distributed Interference Alignment", *Proceedings of IEEE GLOBECOM*, New Orleans, LA, Dec. 2008.

[GGF+14] K. Guo, Y. Guo, G. Fodor and G. Ascheid, "Uplink Power Control with MMSE Receiver in Multicell Multi-User Massive MIMO Systems," in *Proc. IEEE International Conference on Communications (ICC)*, Jun. 2014, pp. 5184-5190.

[GKB+15] H. Ghauch, T. Kim, M. Bengtsson, M. Skoglund, "Distributed Low-Overhead Schemes for Multi-stream MIMO Interference Channels", *IEEE Trans. on Signal Processing*, accepted for publication, Jan. 2015.

[GMD+13] N. Golrezaei, A. F. Molisch, A. G. Dimakis, and G. Caire, "Femtocaching and device-to-device collaboration: A new architecture for wireless video distribution," *IEEE Comm. Magazine*, vol. 51, no. 4, pp. 142-149, Apr. 2013.

[HA13] D. Hui and J. Axnäs, "Joint Routing and Resource Allocation for Wireless Self-Backhaul in an Indoor Ultra-Dense Network," Personal Indoor and Mobile Radio Communications (PIMRC), 2013 IEEE 24th International Symposium on, London, UK, Sept. 2013.

[HBD13] J. Hoydis, S. ten Brink, and M. Debbah, "Massive MIMO in the UL/DL of cellular networks: How many antennas do we need?" *IEEE J. Sel. Areas Commun.*, vol. 31, no. 2, pp. 160-171, Feb. 2013.

[HCL+13] I. Hwang, C.-B. Chae, J. Lee, and R. W. Heath, "Multicell cooperative systems with multiple receive antennas," *IEEE Wireless Commun. Mag.*, vol. 20, no. 1, pp. 50–58, Feb. 2013.

[IKS12] A. Ikhlef, J. Kim, and R. Schober, "Mimicking full-duplex relaying using half-duplex relays with buffers," *IEEE Trans. Veh. Technol.*, vol. 61, no. 7, pp. 3025 – 3037, Sept. 2012.

[IKT12] H. Ishii, Y. Kishiyama, and H. Takahashi, "A novel architecture for LTE-B :C-plane/U-plane split and Phantom Cell concept," in *Proc. IEEE Globecom Workshops*, pp. 624-630, Dec. 2012.

[IMS12] A. Ikhlef, D. S. Michalopoulos, and R. Schober, "Max-max relay selection for relays with buffers," *IEEE Trans. Wireless Commun.*, vol. 11, no. 3, pp. 1124 – 1135, Mar. 2012.

[ITU09-2135] "Guidelines for Evaluation of Radio Interface Technologies for IMT Advanced", International Telecommunication Union-R, M.2135-1, Dec. 2009.

[JAM+11] J. Jose, A. Ashikhmin, T. Marzetta, and S. Vishwanath, "Pilot contamination and precoding in multi-cell TDD systems," *IEEE Trans. Wireless Commun.*, vol. 10, no. 8, pp. 2640-2651, Aug. 2011.

[JKM00] H. Jin, A. Khandekar and R. McEliece, "Irregular Repeat Accumulate Codes", Second International Symposium on Turbo Codes, Brest, France, Sep. 2000.

[JRB+14] S. Jaeckel, L. Raschkowski, K. Borner and L. Thiele, "QuaDRiGa: A 3-D Multi-Cell Channel Model With Time Evolution for Enabling Virtual Field Trials", *IEEE Transactions on Antennas and Propagation*, vol. 62, pp. 3242-3256, Jun. 2014.

[KA05] T. Kim and J. Andrews, "Optimal Pilot to Data Power Ratio for MIMO OFDM", in *Proc. IEEE Globecom '05*, pp. 1481-1485, Dec. 2005.

[KB13] S. M. Kim and M. Bengtsson, "Virtual full-duplex buffer-aided relaying – relay selection and beamforming," in *Proc. IEEE PIMRC*, Sept. 2013.

[KB14] S. M. Kim and M. Bengtsson, "Virtual full-duplex buffer-aided relaying in the presence of inter-relay interference," *IEEE Trans. Wireless Commun.*, Aug. 2014 (Submitted).

[KKG+11] Y. Konishi, M. Kim, M. Ghoraiishi, J. Takada, S. Suyama, and H. Suzuki, "Channel sounding technique using MIMO software radio architecture," in *Proc. the 5<sup>th</sup> EuCAP*, pp. 2546-2550, Apr. 2011.

[KRTT13] M. Kurras, L. Raschkowski, M. Talaat and L. Thiele, "Massive SDMA with Large Scale Antenna Systems in a Multi-Cell Environment", *AFRICON*, 2013.

[KTH14] M. Kurras, L. Thiele and T. Haustein, "Interference Aware Massive SDMA with a Large Uniform Rectangular Antenna Array", *European Conference on Networks and Communications (EUCNC)* Bologna, 2014.

[KTJ13] P. Komulainen, A. Tölli, and M. Juntti, "Effective CSI signaling and decentralized beam coordination in TDD multi-cell MIMO systems", *IEEE Transactions on Signal Processing*, vol. 61, no. 9, pp. 2204-2218, Feb. 2013.

[LBW+13] F. Lenkeit, C. Bockelmann, D. Wübben and A. Dekorsy, "IRA Code Design for IDMA-based Multi-Pair Bidirectional Relaying Systems", *International Workshop on*



Broadband Wireless Access (BWA 2013) co-located with IEEE Globecom 2013, Atlanta, GA, USA, 9.-13. Dec. 2013.

[LVD+11] D. Lopez-Perez, A. Valcarce, G. De La Roche, J. Zhang, "Enhanced intercell interference coordination challenges in heterogeneous networks," *IEEE Wireless Commun. Mag.*, 18(3), pp. 22-30, Jun. 2011.

[LVS14] Y. Long, N. Vucic, and M. Schubert, "Distributed precoding in multicell multi-antenna systems with data sharing," *Proc. EW'14*, Barcelona, Spain, May 2014.

[M13] METIS test cases following the simulation guidelines, <https://www.metis2020.com/documents/simulations/>.

[Mar10] T. Marzetta, "Noncooperative cellular wireless with unlimited numbers of base station antennas," *IEEE Trans. Wireless Commun.*, vol. 9, no. 11, pp. 3590-3600, Nov. 2010.

[METIS13-D11] METIS D1.1, "Scenarios, requirements and KPIs for 5G mobile and wireless system", Apr. 2013.

[METIS13-D31] METIS D3.1, "Positioning of multi-node/multi-antenna transmission technologies", Jun. 2013.

[METIS13-D61] METIS D6.1, "Simulation Guidelines", Oct. 2013.

[METIS14-D23] METIS D2.3, "Components of a new air interface - building blocks and performance", Apr. 2014.

[METIS14-D32] METIS D3.2, "First performance results for multi-node/multi-antenna transmission technologies", Apr. 2014.

[METIS14-D53] METIS D5.3, "Description of the spectrum needs and usage principles", Aug. 2014.

[METIS14-D62] METIS D6.2, "Initial report on horizontal topics, first results and 5G system concept," Mar. 2014.

[METIS14-D63] METIS D6.3, "Intermediate system evaluation results", Jul. 2014.

[METIS15-D24] METIS D2.4, "Proposed solutions for new radio access", Feb. 2015.

[NAAC14] J. Nam, A. Adhikary, J.-Y. Ahn and G. Caire, "Joint Spatial Division and Multiplexing: Opportunistic Beamforming, User Grouping and Simplified Downlink Scheduling", *Selected Topics in Signal Processing*, IEEE Journal of, vol. PP, pp. 1-1, 2014.

[NDP13] NTT DOCOMO press releases, "DOCOMO and Tokyo Institute of Technology achieve world's first 10 Gbps packet transmission in outdoor experiment," [http://www.nttdocomo.co.jp/english/info/media\\_center/pr/2013/0227\\_00.html](http://www.nttdocomo.co.jp/english/info/media_center/pr/2013/0227_00.html), Feb. 2013.

[NLM13a] H. Q. Ngo, E. G. Larsson, and T. L. Marzetta, "Energy and spectral efficiency of very large multiuser MIMO systems," *IEEE Trans. Commun.*, vol. 61, no. 4, pp. 1436-1449, Apr. 2013.

[NLM13b] H. Ngo, E. G. Larsson, and T. Marzetta, "The multicell multiuser MIMO uplink with very large antenna arrays and a finite-dimensional channel," *IEEE Trans. Commun.*, vol. 61, no. 6, pp. 2350-2361, Jun. 2013.

[OSS+14] T. Obara, S. Suyama, J. Shen, and Y. Okumura, "Joint fixed beamforming and eigenmode precoding for super high bit rate massive MIMO systems using higher frequency bands," in *Proc. IEEE PIMRC2014*, Sept. 2014.

[PDN05] D. T. Pham, S. S. Dimov and C. Nguyen, "Selection of K in K-means clustering", *Proceedings of the Institution of Mechanical Engineers, Part C: Journal of Mechanical Engineering Science*, SAGE Publications, vol. 219, pp. 103-119, 2005.

- [PHH13] D.T. Phan Huy, M. H elard, "Large MISO Beamforming For High Speed Vehicles Using Separate Receive & Training Antennas," in *Proc. IEEE International Symposium on Wireless Vehicular Communications (WiVEC)*, Dresden, Germany, 2-3 Jun. 2013.
- [PHS+13] D.-T. Phan-Huy, M. Sternad, T. Svensson, "Adaptive Large MISO Downlink with Predictor Antenna Array for very fast moving vehicles," in *Proc. 2013 International Conference on Connected Vehicles & Expo*, Las Vegas, USA, 2-6 Dec. 2013.
- [PIB+13] P. Papadimitriou, T. Ihalainen, H. Berg and K. Hugel, "Link-level performance of an LTE UE receiver in synchronous and asynchronous networks," *WCNC2013*, Shanghai, China, Apr. 2013.
- [PLW+06] L. Ping, L. Liu, K. Wu and W. Leung, "Interleave-Division Multiple Access", *IEEE Transactions on Wireless Communications*, vol. 5, no. 4, pp. 938-947, Apr. 2006.
- [PTRC+14] D.-T. Phan-Huy, A. T olli, N. Rajatheva, E. De Carvalho, "DFT based spatial multiplexing and maximum ratio transmission for mm-wave large MIMO," *IEEE WCNC 2014*, Istanbul, Turkey, 6-9 Apr. 2014.
- [RH09] C. v. Rensburg and P. Hoesin, "Interference Coordination through Network-Synchronized Cyclic Beamforming", *Vehicular Technology Conference Fall (VTC 2009-Fall)*, 2009 IEEE 70th, pp. 1-5, Sep. 2009.
- [SBH14] C. Shi, R. A. Berry, and M. L. Honig, "Bi-Directional Training for Adaptive Beamforming and Power Control in Interference Networks," *Signal Processing*, *IEEE Transactions on*, vol. 62, no. 3, pp. 607-618, Feb. 2014.
- [SKZ10] Y.-K. Song, D. Kim, and J. Zander, "Pilot power adjustment for saving transmit power in pilot channel assisted DS-CDMA mobile systems," *IEEE Trans. Wireless Commun.*, vol. 9, no. 2, pp. 488-493, Feb. 2010.
- [SRL11] Q. Shi; M. Razaviyayn, Z.-Q. Luo and C. He, "An Iteratively Weighted MMSE Approach to Distributed Sum-Utility Maximization for a MIMO Interfering Broadcast Channel," *Signal Processing*, *IEEE Transactions on*, vol.59, no.9, pp.4331,4340, Sept. 2011.
- [SSB+14] S. Suyama, J. Shen, A. Benjebbour, Y. Kishiyama, and Y. Okumura, "Super high bit rate radio access technology for small cells using higher frequency bands," in *Proc. IEEE IMS2014*, Jun. 2014.
- [SSO+13] S. Suyama, J. Shen, Y. Oda, H. Suzuki, and K. Fukawa, "11 GHz band 8x16 MIMO-OFDM outdoor transmission experiment for 10 Gbps super high bit rate mobile communications," in *Proc. IEEE PIMRC2013*, Sept. 2013.
- [SSS+14] S. Suyama, J. Shen, H. Suzuki, K. Fukawa, and Y. Okumura, "Evaluation of 30 Gbps super high bit rate mobile communications using channel data in 11 GHz band 24x24 MIMO experiment," in *Proc. IEEE ICC2014*, June 2014.
- [TKBH12] L. Thiele, M. Kurras, K. B orner, and T. Haustein, "User-aided sub-clustering for CoMP transmission: Feedback overhead vs. data rate trade-off," *46th Asilomar Conference on Signals, Systems and Computers*, Nov. 2012.
- [TPK11] A. T olli, H. Pennanen, and P. Komulainen, "Decentralized Minimum Power Multi-cell Beamforming with Limited Backhaul Signalling", *IEEE Trans. on Wireless Comm.*, vol. 10, no. 2, pp. 570 - 580, Feb. 2011.
- [YG06] T. Yoo and A. Goldsmith, "On the Optimality of Multiantenna Broadcast Scheduling Using Zero-Forcing Beamforming", *IEEE Journal on Selected Areas in Communications*, vol. 24, pp. 528 - 541, Mar. 2006.
- [YGF+13] H. Yin, D. Gesbert, M. Filippou and Y. Liu, "A Coordinated Approach to Channel Estimation in Large Scale Multiple-Antenna Systems", *IEEE Journal of Selected Areas in Communications*, Vol. 31, No. 2, pp. 264-273, Feb. 2013.

## 7 Appendix A: Final results for Task 3.1

### 7.1 T3.1 TeC 1 MIMO communications with large aperture massive array systems [AAU]

The work on this TeC is completed. Please refer to [METIS14-D32] for the most updated results.

### 7.2 T3.1 TeC 1b: DFT based spatial multiplexing and maximum ratio transmission for mm-wave large MIMO [AAU, FT, UOULU]

#### 7.2.1 General Overview

By using large point-to-point multiple input multiple output (MIMO), spatial multiplexing of a large number of data streams in wireless communications using millimeter-waves (mm-waves) can be achieved. However, according to the antenna spacing and transmitter-receiver distance, the MIMO channel is likely to be ill-conditioned. In such conditions, highly complex schemes such as the singular value decomposition (SVD) are necessary. In this TeC, we propose a new low complexity system called discrete Fourier transform based spatial multiplexing (DFT-SM) with maximum ratio transmission (DFT-SM-MRT). When the DFT-SM scheme alone is used, the data streams are either mapped onto different angles of departures in the case of aligned linear arrays, or mapped onto different orbital angular momentums in the case of aligned circular arrays. Maximum ratio transmission pre-equalizes the channel and compensates for arrays misalignments. Simulation results show that, although the DFT-SM-MRT scheme has a much lower complexity than the SVD scheme, it still achieves high spectral efficiencies and is robust to misalignment and reflection.

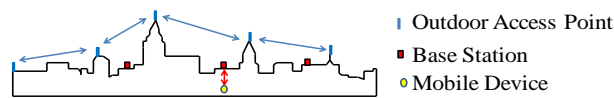


Figure 7-1: mm-wave for both backhaul and direct links

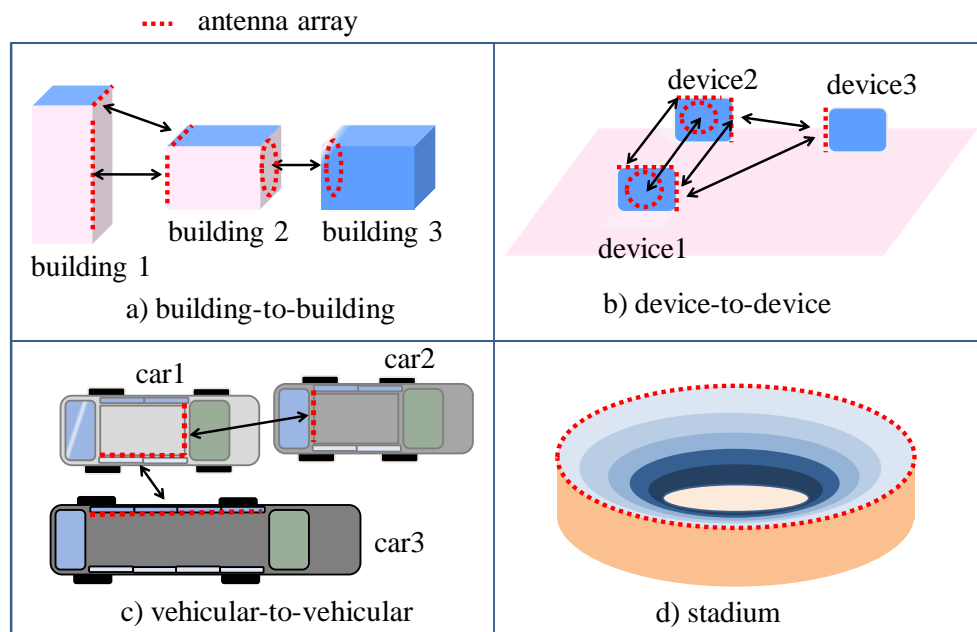


Figure 7-2: Wireless backhaul links using mm-waves and massive MIMO

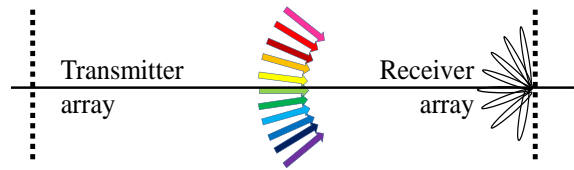


Figure 7-3: With linear arrays, data streams are mapped onto angles of arrivals



Figure 7-4: With circular arrays data streams are mapped onto vortices of various orbital angular momentums

## 7.2.2 Performance Results

### Reminder on [METIS14-D32] results

The spectral efficiencies achieved by Discrete Fourier Transform based spatial multiplexing and maximum ratio transmission (DFT-SM-MRT) are assessed for particular values of the following parameter derived from the diffraction theory in optics:  $m = \frac{R^2}{\lambda D}$ , where  $R$  is the radius of the circular array ( $R$  being also half of the length of the linear array),  $D$  is the transmitter-receiver distance and  $f$  is the carrier frequency. These values are chosen so that they correspond to mm-waves short range communications.

Table 7.1 summarizes the results for two different array arrangements linear array and circular array as shown in Figure 7-3 and Figure 7-4 respectively with  $m = 40$ . Here are two examples of scenarios with  $m = 40$ :  $R = 3$  m,  $D = 45$  m and  $f = 60$  GHz, or  $R = 3$  m,  $D = 75$  m and  $f = 100$  GHz.

The three following effects are assessed separately and also combined, to assess the robustness of DFT-SM-MRT with respect to misalignment and NLOS: a slight translation of the arrays, a slight rotation of the arrays, one reflection over a roof.

Depending on the scenario, DFT-SM-MRT achieves hundreds of bits/s/Hz. In comparison with SVD, DFT-SM-MRT achieves 1/3 to 1/14 of SVD performance, with a complexity which is around  $3 \times 10^4$  times lower, for the considered number of antennas ( $N = 512$ ).

Table 7.1: DFT-SM-MRT performance at  $m = 40$

Effects	DFT-SM-MRT spectral efficiency (bits/s/Hz)		Ratio between DFT-SM-MRT and SVD spectral efficiencies	
	Circular Array	Linear Array	Circular Array	Linear Array
Translation	770	224	>1/3	~3/4
Rotation	1000	215	~1/3	~5/7
Reflection	440	135	>1/7	~4/9
All	215	189	>1/14	~5/8

Compared to a mm-wave SISO system (achieving 6bits/s/Hz with 64QAM), the gain of the proposed system, in terms of spectral efficiency, reaches around  $1000/6$ , i.e. 166.

To conclude this section, DFT-SM-MRT provides high spectral efficiency without inter-antenna spacing optimization with respect to the distance, and is more robust than DFT-SM to the two following effects: misalignment of the transmit array and the receive array and the multi-path propagation due to one reflector.

This results have been fully described in the conference paper [PTRC+14].

### **New results on suitable deployment scenarios and carrier frequencies**

In this deliverable, we try to better understand in which deployment scenarios DFT-SM-MRT should be used. For this particular study, we will first concentrate on Uniform Linear Arrays (ULAs), for which there exist some exploitable theoretical results. Indeed, in [BOO06], the authors have found the optimum configuration in terms of capacity, for two ULAs with a given geometry. The geometry is given by the distance  $D$  between the ULAs, the length  $L_T$  of the transmit ULA and the length  $L_R$  of the receive ULA. Assuming that the two ULAs are in the same plan, the angles  $\theta_T$  and  $\theta_R$  of the transmit and the receive ULAs, respectively, can be defined as in Figure 7-5.

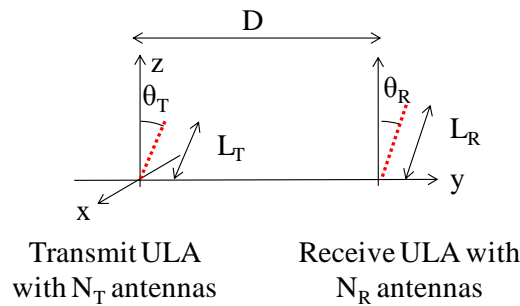


**Figure 7-5: Communication between two ULAs in Line-Of-Sight**

Let  $N_T$  and  $N_R$  be the number of antenna elements at the transmitter side, and the receiver side, respectively. One can define the antenna separation at the receiver side  $d_R = L_R/N_R$  and the antenna separation at the transmitter side  $d_T = L_T/N_T$ . Let  $\lambda$  be the wavelength. According to [BOO06], the optimum capacity is attained when the following equation is verified:

$$d_R d_T = \frac{|\cos(\theta_T)\cos(\theta_R)|\lambda D}{N_R} \quad (1)$$

We define  $f$  as the carrier frequency and  $c$  as the light speed, we therefore have  $\lambda = c/f$ . One can therefore re-write (1) as follows:

$$f = \frac{|\cos(\theta_T)\cos(\theta_R)|cD}{L_T L_R} N_T \quad (2)$$

The geometry of the system is given by the parameters  $\theta_T$ ,  $\theta_R$ ,  $D$ ,  $L_T$  and  $L_R$  whereas the number of transmit antennas  $N_T$  is linked to the cost and the complexity of the system. As a consequence, for a given system *geometry* and for a given number of antennas and RF chains (therefore for a given *cost and complexity* budget), there is an *optimum carrier frequency*  $f$ .

The aim of this paper is to estimate on some practical examples of Large MIMO in line of sight deployments, the optimum carrier frequency to be used. The following scenarios are studied:

- scenario 1, illustrated in Figure 7-6, involves the communication between two buildings;
- scenario 2, illustrated in Figure 7-7, involves the communication between two lamp posts;
- scenario 3 and scenario 4, illustrated in Figure 7-8 and Figure 7-9, respectively, involve the communication between two cars. Such a configurations could happen in a parking lot for instance;

- scenario 5, illustrated in Figure 7-10, involves the communication between two computers. Such a configuration could happen in an office for instance.

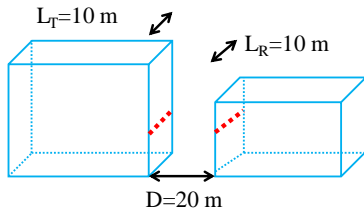


Figure 7-6: Scenario 1: communicating buildings, using ULAs

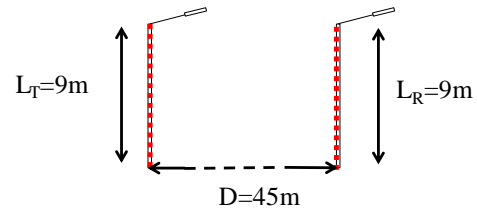


Figure 7-7: Scenario 2: communicating lamp posts (These are heights and separations in France), using ULAs

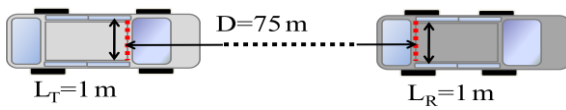


Figure 7-8: Scenario 3: front-to-back communicating cars (non moving), using ULAs

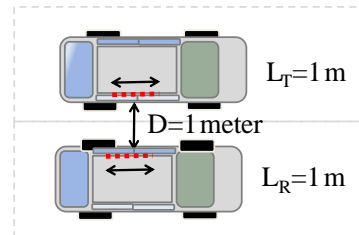


Figure 7-9: Scenario 4: side-to-side communicating cars (non moving), using ULAs

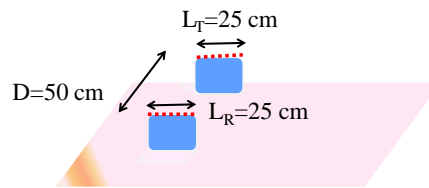


Figure 7-10: Scenario 5: communicating laptops (devices)

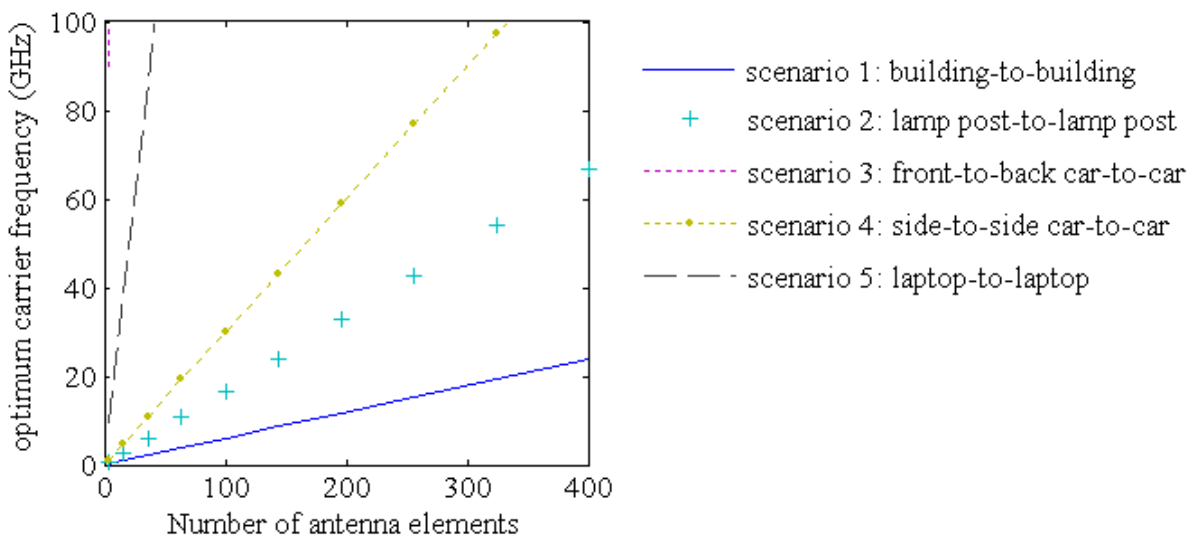


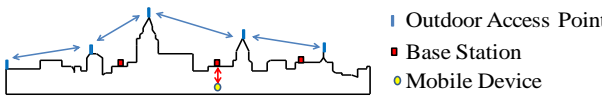
Figure 7-11: Optimum frequency as a function of the number of antennas

Figure 7-11 plots the optimum carrier frequency as a function of the number of antenna  $N$  for each of the 5 studied scenarios. This curve is obtained by using equations (2). One can observe that for front-to-back car-to-car communication (scenario 3) and laptop-to-laptop communication (scenario 5), large MIMO systems (i.e. with  $N > 50$ ) will be sub-optimum even for a carrier frequency as high as 100GHz. One can note that for building-to-building (scenario

1), with ULAs, millimeter waves will be necessary. For lamp post-to-lamp post (scenario 2) and side-to-side car-to-car (scenario 4) communications, millimeter waves will also be needed to achieve high rank large MIMO.

**Conclusion**

In this deliverable we have provided new results which **do not impact the performance bounds reported in [METIS14-D32]**. However, these new results help to better understand in which **deployment scenarios and with which carrier frequencies** DFT-SM-MRT could be used.

T3.1 TeC 1b – DFT-SM-MRT	
 <p>mm-wave for both backhaul and direct links</p>  <p>With linear arrays, data streams are mapped onto angles of arrivals.</p>  <p>With circular arrays data streams are mapped onto vortices of various orbital angular momentums.</p>	<p style="text-align: center;"><b>Main Idea</b></p> <p>According to the antenna spacing and transmitter-receiver distance, the large MIMO channel in mm-wave communications is likely to be ill-conditioned. In such conditions, highly complex schemes such as the singular value decomposition (SVD) are necessary. We propose a new low complexity system called discrete Fourier transform based spatial multiplexing (DFT-SM) with maximum ratio transmission (DFT-SM-MRT). When the DFT-SM scheme alone is used, the data streams are either mapped onto different angles of departures in the case of aligned linear arrays, or mapped onto different orbital angular momentums in the case of aligned circular arrays. Maximum ratio transmission pre-equalizes the channel and compensates for arrays misalignments.</p>
Considered SoA solution	<ul style="list-style-type: none"> <li>mm-wave single input single output (SISO) system for spectral efficiency, SVD scheme for complexity.</li> </ul>
KPIs considered and achieved gain	<p>Spectral Efficiency: x166 [bits/s/Hz] compared to SISO.</p> <p>Complexity reduction with N antennas <math>\approx O(N^2/\log_2(N))</math>: <math>\times 3 \cdot 10^4</math> (for N=512) compared to SVD.</p>
Performance evaluation approach	Link level simulation
System model considered	WP3 Task Simulation Baseline/Other
Deviation compared to Simulation Baseline	<p>Not Applicable:</p> <ul style="list-style-type: none"> <li>Model of environment: dense urban</li> <li>Spectrum assumptions: mm-waves, 10GHz-100GHz carrier frequencies</li> <li>Propagation model: line of sight, or near to line of sight</li> </ul>



	<ul style="list-style-type: none"> <li>• Deployment model: outdoor mesh network.</li> <li>• User/Device distribution: none</li> <li>• Traffic model: full buffer</li> </ul>
Brief update of the results with respect to D3.2	Initially in [METIS14-D32], TeC 1b was proposed for roof top to roof top communication. This deliverable proposes to extend the use of TeC 1b to, building to building, lamp post to lamp post, laptop to laptop, car-to-car (non moving) communications.
Association to the TeC Approach	Tech Approach 1: Massive MIMO for Backhaul
Targeted TCs	TC 2 Dense Urban society
Impacted HTs	Ultra Dense Networks (wireless backhaul link for UDN), D2D
Required changes for the realization with respect to LTE Rel. 11	Major: mm-waves spectrum.
Trade-off required to realize the gains	Near to line of sight propagation. Aligned or very slightly misaligned arrays.

### 7.2.3 Impact on Horizontal Topics

T3.1 TeC 1b - HT.UDN, HT.D2D	
Technical challenges	Low complexity, spectrally efficient wireless backhauling, in the case where the UDN consists of very close devices operating as a mesh network.
TeC solution	TeC 1b achieves spectral efficiencies is in the order of hundreds of bits/s/Hz, with low complexity transceivers and receivers, for the wireless backhaul.
Requirements for the solution	TeC 1b only applies to near to line of sight links between slightly misaligned and large arrays: typically outdoor and indoor mesh networks.
KPIs addressed and achieved gain	Spectral Efficiency: x166 [bits/s/Hz] compared to SISO.  Complexity reduction with N antennas $\approx O(N^2/\log_2(N))$ : x $3 \cdot 10^{-4}$ (for N=512) compared to SVD.
Interaction with other WPs	WP6: mm-wave spectrum is needed.

### 7.2.4 Addressing the METIS Goals

T3.1 TeC 1b	
1000x data volume	TeC 1b achieves spectral efficiencies is in the order of hundreds of bits/s/Hz, with low complexity transceivers and receivers, for the wireless backhaul.
10-100 user data rate	
10-100x number of devices	



10x longer battery life	
5x E-E reduced latency	
Energy efficiency and cost	

### 7.2.5 References

[RSM+13] T.S. Rappaport, Shu Sun; R. Mayzus, Hang Zhao, Y. Azar, K. Wang, G.N. Wong, J.K. Schulz, M. Samimi, F. Gutierrez, "Millimeter Wave Mobile Communications for 5G Cellular: It Will Work!," Access, IEEE vol.1, no., pp.335-349, 2013.

[YYH+10] D. Yang, L.-L. Yang, L. Hanzo, "DFT-Based Beamforming Weight-Vector Codebook Design for Spatially Correlated Channels in the Unitary Precoding Aided Multiuser Downlink," in Proc. IEEE Int. Conf. Comm. (ICC), pp.1-5, 23-27 May 2010.

[EJ+12 ] O. Edfors, A.J. Johansson, "Is Orbital Angular Momentum (OAM) Based Radio Communication an Unexploited Area?," IEEE Trans. on Antennas and Propagation , vol.60, no.2, pp.1126-1131, Feb. 2012.

[PTRC+14] D.-T. Phan-Huy, A. Tölli, N. Rajatheva, E. De Carvalho, "DFT based spatial multiplexing and maximum ratio transmission for mm-wave large MIMO," IEEE WCNC 2014, Istanbul, Turkey, 6-9 Apr. 2014.

[BOO06] Bohagen, F.; Orten, P.; Oien, G.E., "Optimal Design of Uniform Planar Antenna Arrays for Strong Line-of-Sight MIMO Channels," IEEE 7th Workshop on Signal Processing Advances in Wireless Communications (SPAWC) 2006, pp.1-5, 2-5 July 2006.

[METIS14-D32] METIS D3.2, "First performance results for multi-node/multi-antenna transmission technologies", Apr. 2014.

## 7.3 T3.1 TeC 1c: MIMO communications with large aperture massive array systems [AAU]

### 7.3.1 General Overview

We target the deployment of Very Large Aperture (VLA) arrays with a very large number of antennas in hotspots, where the VLA massive arrays serve as access points to a crowd of users and are designed as part of a new infrastructure. Referring to the METIS scenarios, VLA arrays can be deployed along walls or ceiling of a shopping mall or airport, around the structure of a football stadium or along the facade of a building. We have previously described the channel characteristics of such a multi-user scenario in line-of-sight conditions highlighting the acute discrimination capability between users, especially beneficial in crowd scenarios.

In a crowd scenario, a coordinated scheduling would result in a prohibitive signalling overhead. In particular, scheduling of groups of users with orthogonal training sequences becomes infeasible. Instead, a random access method clearly surfaces as extremely pertinent. The communication protocol involves first an uplink phase, i.e. the access phase, followed by the downlink phase, once access is granted to a given user.

Given a pool of pilot sequences shared by all the users, each user transmits during a given transmission slot with probability  $p_a$  and selects randomly one pilot sequence. Since the users are not coordinated, pilot contamination will happen. The pilot contamination problem can be cast as a collision in a specific form of random access problem. We adopt the framework of coded random access [Liv11, SPV12] and boost the performance by applying successive interference cancellation (SIC). When a collision happens, the colliding users retransmit using a different pilot sequence (please note, there is no collision detection at the BS: one user is active in a given time slot with probability  $p_a$  and transmits the same data in several time slots within a given frame). Transmissions over a sufficiently large time horizon form a space-time code that is decoded using the SIC principle. Once a collision has been resolved, the user is granted downlink access using the CSI acquired in the uplink phase (we assume channel reciprocity). In more details, the solution can be viewed as a two-stage processing approach:

*Matched filter.* The received uplink pilot and data signals are processed using matched filters, which are constructed from the contaminated channel estimates. The filtered signals contain linear combinations of the pilots (in the pilot phase) and of the data (in the data phase) transmitted by the users contributing to the contaminated estimate. This is a result of near orthogonality of the involved channels, when the number of antennas,  $M$ , is high.

*Successive interference cancellation:* The coefficients of the linear combinations arising from the matched filtering are the two-norms of the involved channels. In a massive MIMO system, with hundreds of antennas, this can be assumed slowly fading, contrary to the fast fading channel coefficients. Hence, successive interference cancellation can be reliably applied on the filtered signals in order to reduce the linear combinations to data signals from individual users. SIC does not suffer from outdated CSI stemming from decoding delay.

This last point is a fundamental aspect here. SIC-enhanced random access has been mostly restricted to machine-to-machine communications in a slowly varying environment. Mobility resulting in outdated CSI hinders its use in a mobile environment. Remarkably, channel hardening brought by massive MIMO enables its extension to a mobile environment.

Consider the simple example of two users, A and B, sharing two uplink transmission time slots, denoted 1 and 2. The users are active with a certain probability in each time slot, whereby a user may transmit in multiple time slots. The resulting received pilot signals,  $Y_1^{pu}$  and  $Y_2^{pu}$ , are expressed in (1) and (2) in Figure 7-12, where  $h_{1A}$  and  $h_{2A}$  are the  $M \times 1$  channel vectors associated with user A, similarly for user B. The channel estimates arising from these signals are as expressed in (3) and (4), where pilot contamination occurs in (3). (5) and (6) expresses the matched filtering step, where the result is a linear combination of the (same) pilot sequence with coefficients being the channel norms. These can be assumed constant,

when  $M$  is high, which allows successive interference cancellation across time slots. We subtract (6) from (5) and utilize knowledge of the pilot sequence to find the channel norm for user A. The data signals,  $Y_1^u$  and  $Y_2^u$ , also reflect the interference. Again the matched filter is applied, in (9) and (10), resulting in linear combination of the messages,  $x_A^u$  and  $x_B^u$ , again with the channel norms as coefficients. Subtracting (10) from (9) and utilizing knowledge of the channel norm of user A, we resolve the collision and achieve the message from user A. More details can be found in [SCP14].

$$Y_1^{pu} = \mathbf{h}_{1A}\mathbf{s}^T + \mathbf{h}_{1B}\mathbf{s}^T + z_1^{pu}, \quad (1)$$

$$Y_2^{pu} = \mathbf{h}_{2B}\mathbf{s}^T + z_2^{pu}, \quad (2)$$

$$\phi_1 = (\mathbf{s}_j^H \mathbf{s})^{-1} \mathbf{s}^H Y_1^{puT} = \mathbf{h}_{1A} + \mathbf{h}_{1B} + z_1^{pu'}, \quad (3)$$

$$\phi_2 = (\mathbf{s}_j^H \mathbf{s})^{-1} \mathbf{s}^H Y_2^{puT} = \mathbf{h}_{2B} + z_2^{pu'}, \quad (4)$$

$$\phi_1^H Y_1^{puT} = \|\mathbf{h}_{1A}\|^2 \mathbf{s}^T + \|\mathbf{h}_{1B}\|^2 \mathbf{s}^T + z_1^{pu'}, \quad (5)$$

$$\phi_2^H Y_2^{puT} = \|\mathbf{h}_{2B}\|^2 \mathbf{s}^T + z_2^{pu'}, \quad (6)$$

$$Y_1^u = \mathbf{h}_{1A}\mathbf{x}_A^u + \mathbf{h}_{1B}\mathbf{x}_B^u + z_1^u, \quad (7)$$

$$Y_2^u = \mathbf{h}_{2B}\mathbf{x}_B^u + z_2^u, \quad (8)$$

$$\phi_1^H Y_1^u = \|\mathbf{h}_{1A}\|^2 \mathbf{x}_A^u + \|\mathbf{h}_{1B}\|^2 \mathbf{x}_B^u + z_1^u, \quad (9)$$

$$\phi_2^H Y_2^u = \|\mathbf{h}_{2B}\|^2 \mathbf{x}_B^u + z_2^u. \quad (10)$$

**Figure 7-12: Example of the steps of matched filtering and successive interference cancellation**

### 7.3.2 Performance Results

The proposed scheme is simulated and compared to framed slotted ALOHA in terms of uplink throughput and block error rate at a single access point. The proposed scheme is based on an assumption that the channel coefficients in different time slots are i.i.d., while their two-norms remain constant within a period of  $\beta$  time slots. In the numerical evaluations, we challenge these assumptions by simulating with fading channels. A rich scattering environment is assumed, such that the channel coefficients can be modelled using Clarke's model, with parameters as found in Table 7.2.

**Table 7.2: Simulation parameters**

Parameter	Value	Description
$f_c$	1.8 GHz	Carrier frequency
$v$	3 km/h	User mobility
$N_s$	20	Number of scatterers
$\sigma_n^2$	0.1	Relative noise power
$\tau$	5 bits	Length and number of pilot sequences
$t_s$	0.01 s	Length of a time slot
$L$	1000 bits	Length of uplink data messages
$\beta$	$1.2N/\tau$	Number of time slots

Figure 7-13 shows the normalized goodput, i.e. throughput with erroneous messages discarded, as a function of the number of users accessing the base station. It is seen that the proposed scheme clearly outperforms the conventional method of framed slotted ALOHA. The gap between the two schemes increases with  $N$  (the number of users), since the proposed scheme benefits from a larger number of messages to code across. An increase in  $N$  can be viewed as an increase in the block length, which improves the coding efficiency.

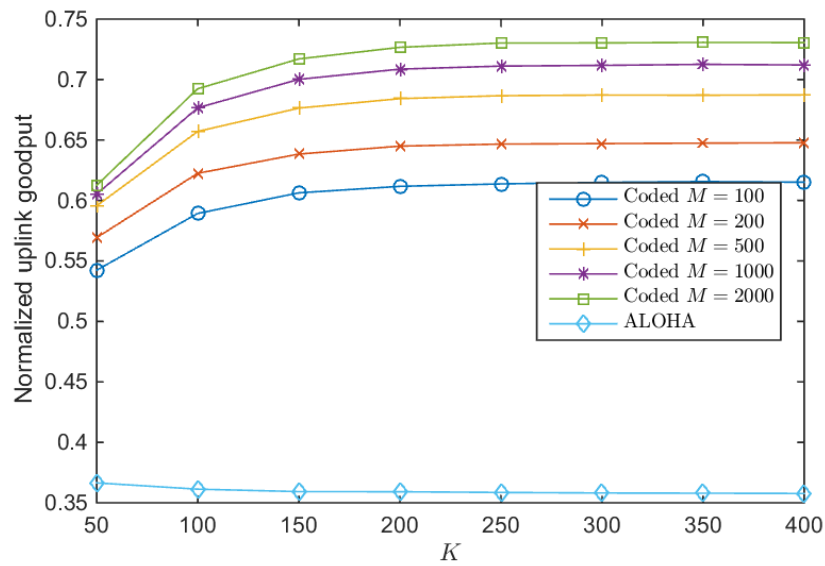


Figure 7-13: Goodput as a function of the number of users

The coding gain comes at the price of an increased error rate. Whenever SIC is performed, noise and estimation errors are accumulated, which may lead to errors. At higher N, it is more common to see high degrees in the code graph, even if the average degree remains constant. Moreover, SIC is performed across a larger time span, which leads to larger errors in the norm estimation. As a result, we experience an increased error rate for increasing N, which is illustrated in Figure 7-14. The figure also shows that the error rate drops significantly, when the number of base station antennas (M) is increased. The reason is that the norm stabilizes for increasing M, such that the assumption of a constant norm is increasingly valid.

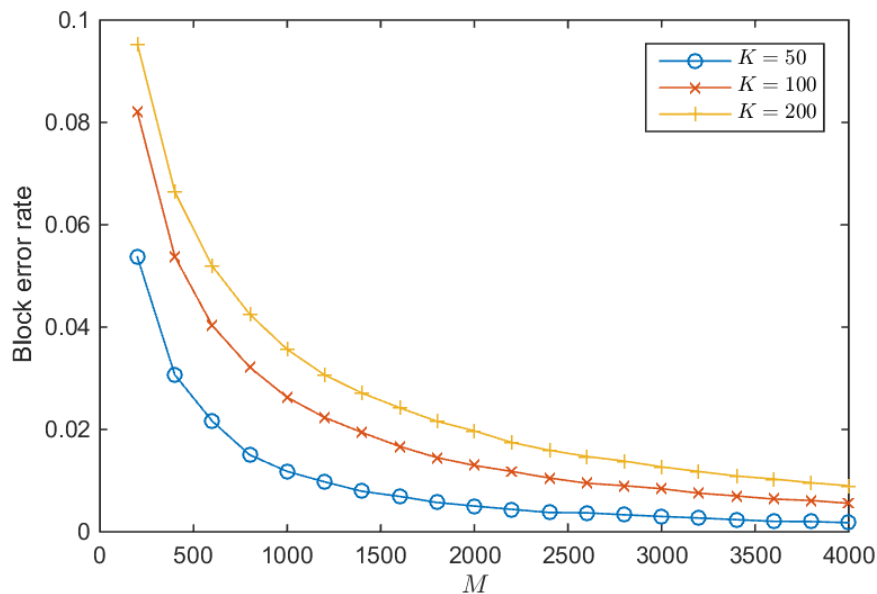
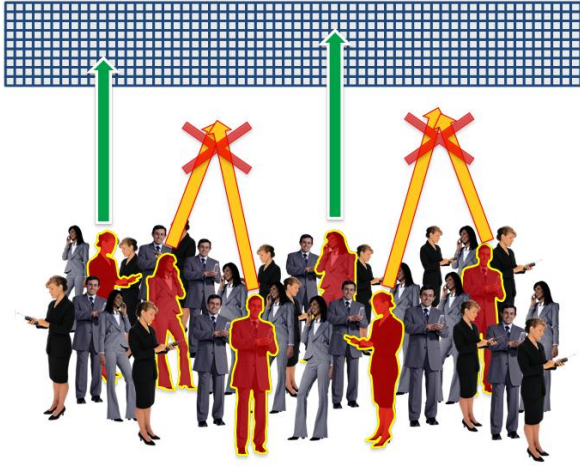


Figure 7-14: Block error rate as a function of the number of access point antennas

### T3.1 TeC 1c – MIMO Communications with Very Large Aperture Massive Array Systems



**Main Idea**

We propose the deployment of massive arrays of very large aperture in a hotspot to serve as access points to a crowd of users. Coordinated scheduling is infeasible due to heavy signal overhead. Instead, we propose a communication protocol based on random access. In the uplink phase, collisions, due to pilot contamination, are resolved using advanced methods based on successive interference cancellation. Once access is granted to a given user, it is allowed to transmit in downlink.

Considered SoA solution	ALOHA random access
KPIs considered and achieved gain	Spectral efficiency (comprising signalling overhead), 50%-100% gain
Performance evaluation approach	Analytical / Simulation-based (Simulation Type) (see Note 4)
System model considered	Gaussian channel model.
Deviation compared to Simulation Baseline	We do not consider the simulation baseline.
Brief update of the results with respect to D3.2	We introduce a new idea for a communication protocol adapted to a dense population of users.
Association to the TeC Approach	Asking to reconsider this TeC to be included in most promising technology.
Targeted TCs	TC2, TC3, TC4, TC9
Impacted HTs	UDN
Required changes for the realization with respect to LTE Rel. 11	Major
Trade-off required to realize the gains	Requires a sufficient number of degrees of freedom in the massive channel.

#### 7.3.3 Impact on Horizontal Topics

T3.1 TeC 1c – HT.UDN	
Technical challenges	Scheduling a dense population of users in a massive MIMO system
TeC solution	Random access protocol
Requirements for the solution	Sufficient number of degrees of freedom in the massive channel.
KPIs addressed and achieved gain	Spectral efficiency (comprising signalling overhead), 50%-100% gain



Interaction with other WPs

### 7.3.4 Addressing the METIS Goals

T3.1 TeC 1c	
1000x data volume	Efficient communication protocol to serve a crowd of users
10-100 user data rate	Use of massive MIMO
10-100x number of devices	Crowd of users is specifically targeted.
10x longer battery life	Use of massive MIMO
5x E-E reduced latency	
Energy efficiency and cost	Use of massive MIMO

### 7.3.5 References

[Liv11] G. Liva, "Graph-Based Analysis and Optimization of Contention Resolution Diversity Slotted ALOHA," Communications, IEEE Transactions on, vol. 59, pp. 477 –487, Feb. 2011.

[SPV12] C. Stefanovic, P. Popovski, and D. Vukobratovic, "Frameless ALOHA protocol for Wireless Networks," IEEE Comm. Letters, vol. 16, pp. 2087–2090, Dec. 2012.

[SCP14] J. H. Sørensen, E. de Carvalho, and P. Popovski, "Massive MIMO for Crowd Scenarios: A Solution Based on Random Access", IEEE International Workshop on Massive MIMO: From theory to practice, In Proc. IEEE Globecom 2014.

## 7.4 T3.1 TeC 2: Coordinated resource and power allocation for pilot and data signals in multicell massive SIMO systems [EAB]

### 7.4.1 General Overview

In massive MIMO systems, the quality of channel estimation can be severely degraded by the interference caused by uplink pilot (reference signal) transmissions in neighbouring cells. This problem, known as *pilot contamination* (PC), has been identified and analysed by the research community, see for example [Mar 10]. Methods to combat pilot contamination typically involve multi-cell cooperation that, for example, helps to identify spatially well separated users who do not cause excessive interference to one another and can therefore reuse identical pilot sequences, see for example [YGF+ 13]. Multi-cell cooperation, however, may suffer from excessive signalling or inter-cell information exchange and high computational complexity.

The key idea of T3.1 TeC2 is to employ (1) a low complexity multi-cell coordination operating on the large time scale (applicable for implementation by O&M system or SON algorithms) and (2) assigning the time- frequency and power resources within a cell to pilot and data signal transmission in such a way that the spectral efficiency within the cell is maximized. Thus T3.1 TeC2 is the combination of two main components operating together such that it (1) effectively avoids pilots contamination and (2) manages the pilot and data resources within a cell in a close to optimum fashion (Figure 7-15). The advantage of the joint operation of (1) and (2) is that the spectral efficiency potential of massive MIMO systems can be effectively harvested without introducing excessive complexity and signalling overhead due to the typical cooperation needs of multi-cell massive MIMO systems. Parts of the performance analysis of T3.1-TeC2 are described in [FT14], [GGF+14], and [FDT14].

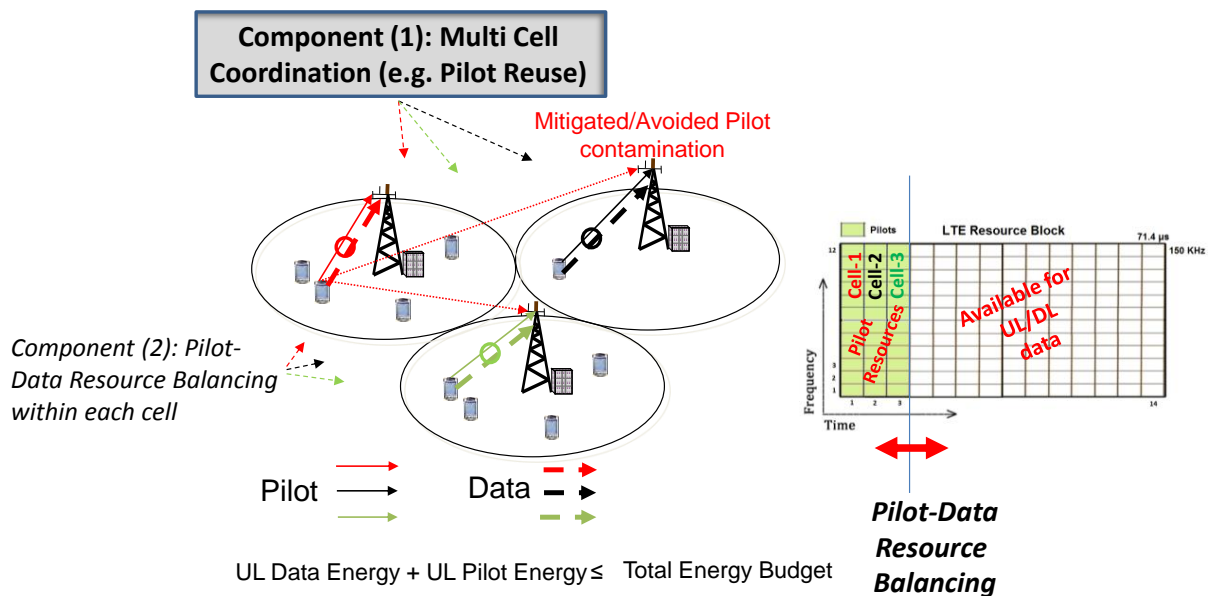


**Figure 7-15: The two components of T3.1 TeC2 (1) multicell coordination to avoid pilot contamination and (2) managing the time- frequency and power resources within a cell work jointly in a multicell massive MIMO system**

As illustrated in Figure 7-15, TeC2 intertwines the two components of (1) assigning resource elements to cells (effectively a pilot reuse) and (2) UL pilot power control -- also called Pilot-to-Data Power Ratio (P DPR) balancing [KA05] -- within a cell. Pilot reuse operates on a coarse time scale applicable in Operation and Management (O&M) Systems. The O&M system can also facilitate pilot reuse configuration as part of a centralized or distributed self-optimizing network (SON) solution, similarly to existing SON features such as coverage and capacity optimization. Pilot reuse configuration collects input data, such as traffic load information, number of served UEs, installed antenna infrastructure, system bandwidth and carrier frequency, etc, from all cells of a geographical area. Based on these input data, it configures

the reuse pattern to be used in the cells belonging to the geographical area under the control of the O&M System. Although such functionality is not explicitly supported by today's O&M systems, the introduction of such pilot pattern control is feasible due to its slow time scale operation and its similarity to traditional reuse pattern schemes.

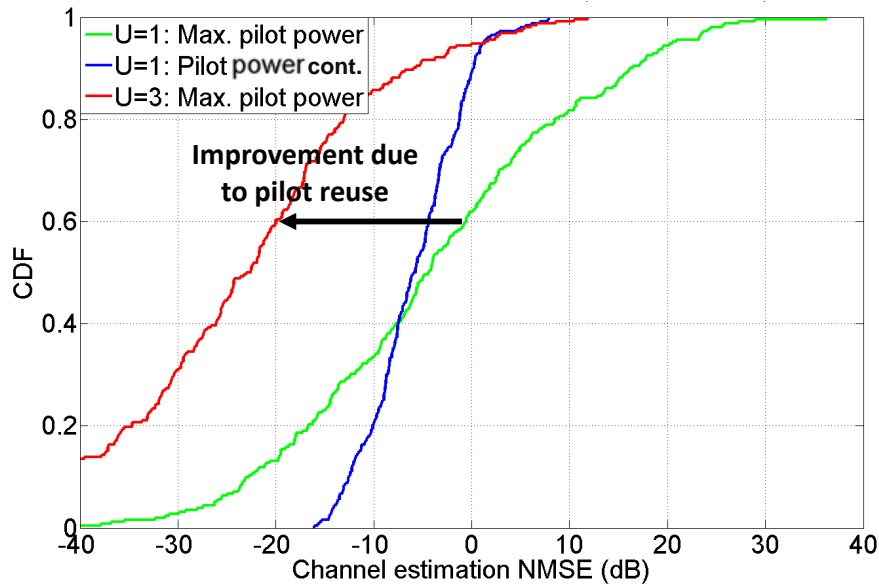
PDPR balancing operates at a finer time scale, ideally at the time scale of reference signal measurement and reporting (i.e.  $\sim 200$  ms), and at the level of individual UEs within a cell. Its main input is the large scale fading (path loss) measurements performed by the UE on downlink reference signals. TeC2 contains algorithms that compute the optimum PDPR in terms of the mean square error of the equalized uplink received data symbols for a given number of resource elements available for pilot and data symbols [FT 14]. PDPR balancing can thus rely on existing (mobility and handover) measurements and can operate jointly with pilot reuse.

#### 7.4.2 Performance Results

To evaluate the performance of T3.1 TeC2, we consider a multi-cell multiuser MIMO (MU-MIMO) system with single antenna user equipment and multi-antenna bases stations according to the T3.1 simulation guidelines of [METIS D3.2, Appendix B]. The main simulation parameters are summarized in Table 7.3. We assume saturated (full) buffers and perfect synchronization between the BSs and their respective served users.

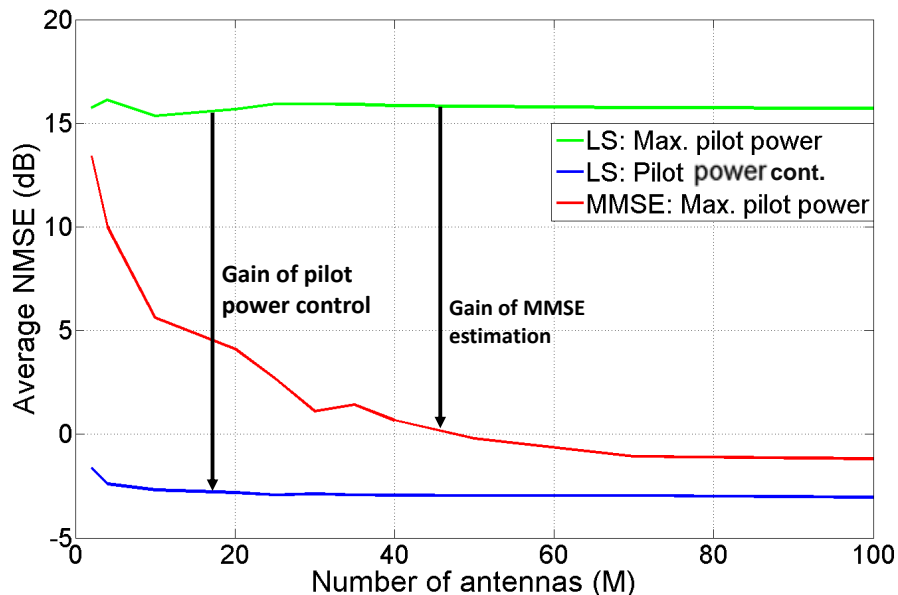
**Table 7.3: Main system simulation parameters used for the evaluation of T3.1 TeC2**

Network Deployment	21-cell hexagonal grid
Inter-site distance	500 m
Exclusion radius	35 m
Terminals per cell ( $K$ )	{3, 6, 12, 24}
Terminal speed	60 kmph
BS transmit power ( $P_{BS}$ )	0.067W per subcarrier
Max. terminal transmit power ( $P_T$ )	23 dBm over 20 MHz
Carrier Frequency ( $f_c$ )	2 GHz
Subcarrier spacing	15 KHz
BS array	100-antenna uniform linear array (ULA)
Tilt	$11^\circ$
BS antenna	Fitted Kathrein, Vertically Polarized
Antenna spacing	$0.7 \lambda_c$
Max. antenna gain	18 dBi
3dB horizontal beamwidth	$65^\circ$
3dB vertical beamwidth	$6.5^\circ$
BS antenna noise figure	5 dB
Terminal antenna	Omnidirectional, Vertically Polarized
Terminal antenna noise figure	9 dB



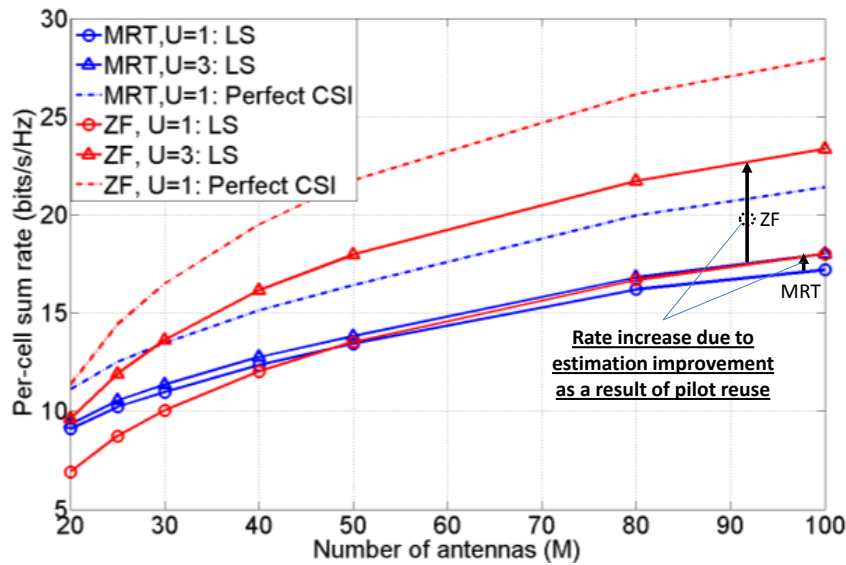
**Figure 7-16: Comparing the improvement of the normalized channel estimation error (NMSE) due to pilot power control and pilot reuse of U=3. The NMSE improves due to pilot reuse in the entire region of the NMSE CDF.**

Figure 7-16 shows the performance improvement due to controlling pilot reuse in terms of the channel estimation quality (measured in normalized channel estimation as proposed by [YGF+13]). With pilot reuse-3, the pilot contamination is reduced at the expense of reserving more time-frequency resources for channel state information acquisition. However, reducing pilot contamination results in dramatically improved channel estimation performance.

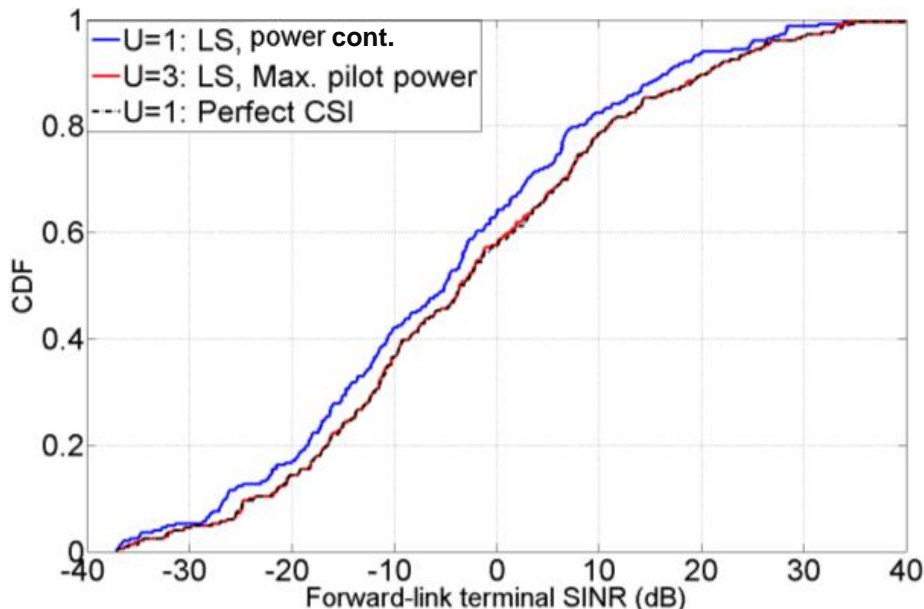


**Figure 7-17: Comparing the improvement of the average normalized channel estimation error (NMSE) using Least Square estimation due to pilot power control or MMSE channel estimation. Pilot power control with a low complexity LS channel estimation provided superior average NMSE performance.**

Figure 7-17 shows that the average NMSE achieved by a low complexity LS channel estimation becomes lower than that of MMSE estimation when using pilot power control according to TeC2. Although the average NMSE using MMSE estimation improves with increasing number of base station antennas, pilot power control yields superior NMSE performance even with 100 antennas.

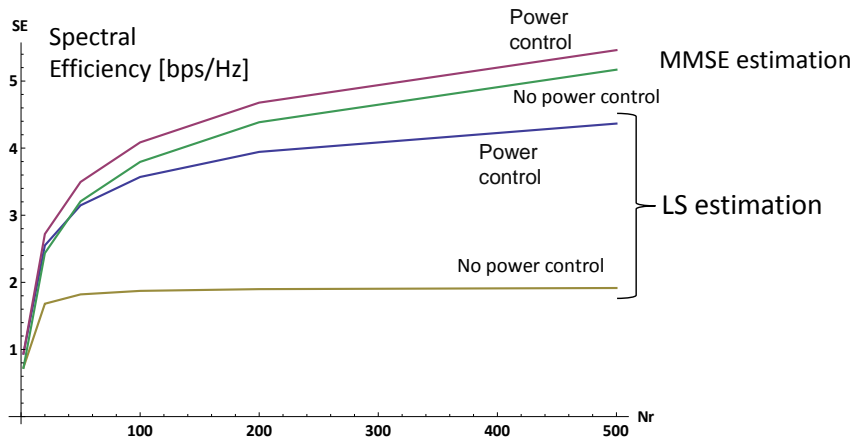


**Figure 7-18: Per-cell DL sum-rate when employing MRT or ZF transmission without ( $U=1$ ) and with pilot reuse ( $U=3$ ) according to Component (1) of TeC2. Although pilot reuse ( $U=3$ ) requires more pilot resources, the DL spectral efficiency increases due to improved channel estimates. Figure 7-18 shows that improving the quality of CSI by reducing pilot contamination pays off in terms of DL per-cell sum rate, even though pilot reuse-3 ( $U=3$ ) requires more resources for CSI acquisition purposes (see Figure 7-15). As shown in Figure 7-18, the DL sum-rate improvement depends on the DL precoding method (MRT or ZF) but is beneficial for any number of antennas in the examined range.**



**Figure 7-19: DL achieved SINR under full pilot reuse ( $U=1$ ) employing pilot power control and using pilot reuse-3 ( $U=3$ ) with full pilot power.  $U=3$  pilot reuse achieves nearly the same SINR performance of a system with perfect CSI.**

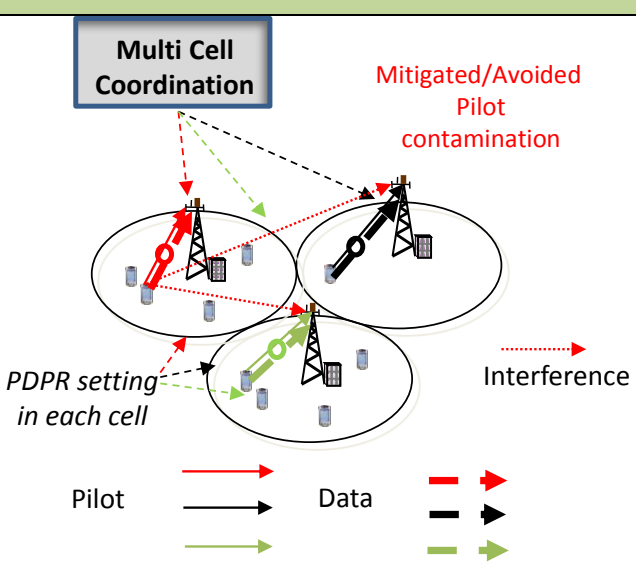
Figure 7-19 shows the beneficial impact of pilot power control alone or pilot reuse ( $U=3$ ) without pilot power control. Pilot reuse ( $U=3$ ) alone can practically achieve the SINR performance of a system in which perfect CSI would be available. Notice that the SINR is somewhat lower with full pilot reuse due to pilot contamination.



**Figure 7-20: UL spectral efficiency (per UE) when using LS and MMSE channel estimation with and without pilot power control (PDPR balancing). In practice, PDPR balancing could be implemented by means of a table that associates the optimal pilot and data power setting with the large scale geometry of the system. In its simplest form PDPR balancing could be performed on the basis of path loss measurements and reporting of individual UEs.**

Figure 7-20 shows the uplink spectral efficiency per UE when using LS and MMSE channel estimation without and with pilot power control in a pilot contamination free system (achieved by pilot reuse). As expected, MMSE estimation shows superior performance, but it requires the availability of the channel covariance matrices. Therefore, LS estimation can be more practical, although as shown in Figure 7-20, LS estimation needs pilot power control to have an acceptable performance in a massive MIMO system.

Finally, we observe that the multicell resource and power allocation for pilot and data symbols studied here can be applied jointly with the uplink pilot/data power control scheme developed in T3.1 – TeC 9b (which runs on a short time scale) to achieve a proven optimality with respect to some QoS (SINR targets), while minimizing the sum transmit power.

T3.1 TeC 2 – Coordinated Resource and Power Allocation for Pilot and Data in Massive MIMO	
<div style="border: 1px solid black; padding: 5px; margin-bottom: 10px;"> <p style="text-align: center;"><b>Multi Cell Coordination</b></p>  </div>	<p style="text-align: center;"><b>Main Idea</b></p> <p>In multi-cell massive MIMO systems, pilot contamination depends on the resources and transmit-power levels used for the pilot signals. On the other hand, there is an inherent trade-off between the resources used for pilot and data signals. The main idea is to use (1) low rate multi-cell coordination to avoid or mitigate pilot contamination and (2) a single cell pilot-to-data-power-ratio (PDPR) setting that maximizes the spectral efficiency. These two components together ensure avoiding the negative impact of pilot contamination and the near optimal allocation of pilot and data transmit power resources.</p>
<p>Considered SoA solution</p>	<p>System without multi-cell coordination and without pilot-data power balancing, such as an LTE Advanced (3GPP Release 10) system.</p>



KPIs considered and achieved gain	<ul style="list-style-type: none"> <li>• Spectral efficiency 100-200 % depending on the deployed number of antennas and employed transmission modes;</li> <li>• User throughput 100-200 % depending on the deployed number of antennas and employed transmission modes;</li> </ul> <p>Spectral efficiency as well as the user throughput are improved by requiring lower pilot and data power for a prescribed mean square error (MSE) of the equalized data symbols or decreasing the MSE with a predefined pilot+data power budget. Avoiding pilot contamination and setting the capacity optimal PDR boost the performance especially when the number of base station antennas grows large. Also, for a given target user throughput, the sum pilot+data power can be reduced which contributes to the energy efficiency.</p>
Performance evaluation approach	Analytical and simulation-based (hybrid) approach. Analytical approach is used to determine the MSE and spectral efficiency for an arbitrary pilot + data power setting as a function of the number of base station antennas without pilot contamination. Detailed system simulation is used to evaluate the impact of the low rate pilot coordination component.
System model considered	ITU Urban Macro [ITU09-2135] like environment adjusted according to [METIS D3.2, Appendix B] System Simulation Guidelines using a modified Spatial Channel Model [3GPP12-25996] suitable for >100 BS antennas in terms of channel covariance matrix dimensions.
Deviation compared to Simulation Baseline	The link model does not capture the METIS 3D model. Static simulations are used.
Brief update of the results with respect to D3.2	Component (1) coordinating the system-wise pilot reuse factor are new compared with [METIS D3.2]. Also, the analytical calculations of Component (2) compute the spectral efficiency rather than MSE only. We also implemented antenna correlation models to capture the impact of correlated antennas on the MSE and spectral efficiency performance. New channel estimation techniques include coordinated pilot assignment by [YGF+ 13] as benchmark, MMSE and LS for comparison purposes.
Association to the TeC Approach	T3.1 Tech Approach 2: Massive MIMO for Access. The two intertwined components of T31. TeC2 are studied jointly and new simulation results are presented.
Targeted TCs	TC2 with the specific challenge of increasing the spectral efficiency with low complexity and with relaxed feedback and backhauling requirements.
Impacted HTs	HT <i>Moving Networks</i> serving a large number of users.
Required changes for the realization with respect to LTE Rel. 11	Major: (1) The resources used for uplink reference signals should be adaptive rather than fixed



	(standardized) and (2) the transmit power levels used to transmit pilot and data symbols should be able to be set differently.
Trade-off required to realize the gains	Component (1) Multicell Coordination requires slow (couple of 100 ms or seconds) periodic measurements from multiple cells and a low rate signalling to BSs. Alternatively, Component (1) needs to be included in a suitable SON implementation. Component (2) requires a new algorithm in the UE and transmit power setting for pilot and data symbols.

### 7.4.3 Impact on Horizontal Topics

T3.1 TeC 2 – HT.MN	
Technical challenges	A large number of users moving with vehicular speed with respect to a macro base station, whose coherence time and frequency can support only a few hundred symbols. This coherence budget must be spent on channel state information acquisition and uplink/downlink data transmission. At the same time, massive MIMO technology should be taken advantage of for spatially multiplexing multiple users. The technical challenges include accurate CSI acquisition and achieving high UL/DL spectral efficiency and thereby high UL/DL data rates.
TeC solution	T3.1 TeC2 is especially useful in scenarios in which the trade-off between pilot-data resources is critical, especially when spectral efficiency is to be maximized. The solution of TeC2 is to avoid pilot contamination that can otherwise be a major source of poor channel estimations and to find the trade-off between pilot and data power that maximizes spectral efficiency.
Requirements for the solution	In the basic implementation, TeC2 assumes the availability of a central entity operating on a coarse time scale, such as an O&M entity that continuously receives measurements from cells (base stations) on the current load situation that allows the central entity to determine the time-frequency resources that should be made available in each cell. Also, within each cell, UEs need to estimate their large scale fading (path loss) values which is a necessary input to determine the pilot and data power levels.
KPIs addressed and achieved gain	Spectral efficiency and user throughput
Interaction with other WPs	WP4: The proposed scheme targets interference limited-scenarios and a close alignment is needed with WP4 where interference management is an important topic.



**7.4.4 Addressing the METIS Goals**

T3.1 TeC 2	
1000x data volume	Massive MIMO inherently boosts the data volume by enabling increasing the density of active users. TeC2 then specifically enables MU MIMO by allowing multiple co-scheduled multiple users on the same time-frequency resource to avoid pilot contamination and thereby acquire accurate CSI, see Figure 7-16 and Figure 7-17.
10-100 user data rate	As illustrated in Figure 7-18 and Figure 7-20, the DL and UL (respectively) spectral efficiency is boosted by TeC2. Thereby the user data rates are increased, due to enabling 100s of antennas and enabling harvesting the increasing gains due to eliminating pilot contamination.
10-100x number of devices	TeC2 enables a large number of antennas and specifically designed for MU MIMO support. Thereby, the number of users supported per time-frequency resource can be increased by 10-20x.
10x longer battery life	The pilot-data power ratio (PDPR) tuning (Component 2 of this TeC) enables the UEs to use lower pilot+data power for a target SNR, thereby the battery life is extended.
5x E-E reduced latency	Not applicable.
Energy efficiency and cost	PDPR optimization allows the UE to reduce the sum power level for a predefined UL spectral efficiency (rate) target. Therefore, TeC contributes to the UL (UE) energy efficiency.

**7.4.5 References**

[FT14] G. Fodor and M. Telek, "On the Pilot-Data Power Trade-Off in Single Input Multiple Output Systems", *20<sup>th</sup> European Wireless Conference*, Barcelona, 14-16 May 2014.

[GGF+14] K. Guo, Y. Guo, G. Fodor and G. Ascheid "Uplink Power Control with MMSE Receiver in Multicell Multi-User Massive MIMO Systems", *IEEE International Conference on Communications (ICC)*, June 2014, Sydney, Australia.

[FDT14] G. Fodor, P. Di Marco and M. Telek, "Performance Analysis of Block and Comb Type Channel Estimation in Massive MIMO Systems", *1st International Conference on 5G for Ubiquitous Connectivity*, Levi, Finland, Nov. 2014.

[Mar 10] T. L. Marzetta, "Non-Cooperative Cellular Wireless with Unlimited Numbers of Base Station Antennas", *IEEE Transactions on Wireless Communications*, Vol. 9, No. 11, pp. 3590-3600, November 2010.

[YGF+ 13] H. Yin, D. Gesbert, M. Filippou and Y. Liu, "A Coordinated Approach to Channel Estimation in Large Scale Multiple-Antenna Systems", *IEEE Journal of Selected Areas in Communications*, Vol. 31, No. 2, pp. 264–273, February 2013, 2013.

[Hug87] D. Hughes-Hartog, "Ensemble modem structure for imperfect transmission media", US patent 4 679 227, July 7, 1987.

[KA05] T. Kim and J. Andrews, "Optimal Pilot to Data Power Ratio for MIMO OFDM", *IEEE Globecom '05*, pp. 1481-1485, December 2005.

[METIS D3.2] "First Performance Results for Multi-Node Multi-Antenna Transmission Technologies", METIS Deliverable 3.2, April 2014.



**Document:** FP7-ICT-317669-METIS/D3.3

**Date:** 25/02/2015

**Security:** Public

**Status:** Final

**Version:** 1

---

[PPS07] S. Pfletschinger, A. Piątyszek and S. Stiglmayr, "Frequency-selective Link Adaptation using Duo-Binary Turbo Codes in OFDM Systems", IST Mobile and Wireless Communications Summit, Budapest, July 2007.

[WIN207-D61314] IST-4-027756 WINNER II, Deliverable D6.13.14 Version 1.0 "WINNER II system concept description", November 2007.

[3GPP09-36913] "Requirements for further advancements for Evolved Universal Terrestrial Radio Access (E-UTRA) (LTE-Advanced) (Release 9)", 3GPP Technical Report, 36.913, Oct. 09.

[ITU09-2135] "Guidelines for Evaluation of Radio Interface Technologies for IMT Advanced", International Telecommunication Union-R, M.2135-1, Dec. 2009.

[3GPP12-25996] "Spatial Channel Model for Multiple Input Multiple Output (MIMO) Simulations (Release 11)", 3GPP Technical Report, 25.996, V11.0.0, Sept. 2012.

## 7.5 T3.1 TeC 3: Modelling with spherical waves, linear precoding [HHI]

Please refer to [METIS13-D31] for the most updated results. The work in T3.1 on modelling spherical waves for near field effects in massive MIMO was removed from the TeCs in T3.1 since [METIS14-D32]. These activities on the channel model are done in T1.2.

## 7.6 T3.1 TeC 4: Multi-cell MU-MIMO in real world scenarios – performance evaluation of EVD-based channel covariance feedback and multi-path extraction in massive MIMO systems [NOKIA]

The work on this TeC has been stopped. Please refer to [METIS14-D32] for the most updated results.

## 7.7 T3.1 TeC 5: Model based channel prediction [NSN]

### 7.7.1 General Overview

‘1000 times capacity’ is the main target of this innovation even so in this case in a more indirect way, i.e. in form of providing a main enabler to support advanced solutions like the interference mitigation framework (IMF-A) from Artist4G enhanced by massive MIMO macro cells and integrated small cell layers (see for more details Task 3.2 TeC13, [JMZ+14]).

The benefit of channel prediction in the context of tight cooperation like joint transmission CoMP has been verified by several research groups as can be concluded for example from [TKO+13] as well as the results from the Artist4G project [ARTD14]. Here the focus is on improving state of the art channel prediction by making use of the design freedom for a novel 5G air interface.

A closer look to available results for channel prediction reveals that relatively good performance can be achieved for fully artificial radio channels, while for typical measured channels the prediction horizon often shrinks to few tenth of  $\lambda$ , the according RF wavelength. Note  $0.1 \lambda$  means about 1 cm for here interesting RF frequencies of two to three GHz, which significantly limits its applicability to either low prediction time of few ms or to very low mobile speeds.

One main reason for the limited predictability of state of the art solutions like Wiener or Kalman filtering is the discrepancy between the low degree of freedom of the predictor versus a high number of multi path components (MPC) in real world scenarios with several interactions points like transmissions, reflections or diffractions. A special further challenge poses diffuse scatterers, for example esteeming from the leaves of a tree moving in the wind.

Parameter estimation solutions like model based channel prediction (MBCP) tries to identify the number of MPCs and to estimate all relevant according parameters like amplitude, phase, angle of arrival, angle of departure, etc. with most possible accuracy. MBCP means to have a certain model of the surrounding of a radio station like an eNB in form of a building vector data map (BVDM), but typical BVDMs are not accurate enough to allow for direct channel estimation. Therefore a combination with measurement based estimation algorithms like ESPRIT [RT89], SAGE [FH94] or RiMAX [HTR04] is envisaged. In a first step the number of relevant MPCs has to be estimated, for example by minimum description length (MDL) principles. Afterwards parameters per MPC are estimated either step by step for different subsets of the parameters by expectation maximization or sometimes even in a single stage.

Especially the RiMAX algorithm relies on iterative optimization of one MPC after the other based on the Levenberg Marquardt algorithm. These algorithms have some well known challenges for global optimization and there is always the risk to be tracked by a local instead of the global optimum. The likelihood for missing the global optimum increases with number of MPCs as well as with the ‘distance’ of the start from the real parameters. Furthermore MPCs with very similar parameters might be seen as one single MPC or two MPCs with opposite phase values might add up to one single real world MPC. For channel prediction it is sufficient

to have a proper evolution of the estimated MPCs, in case of MBCP it is further desirable to really find and map the estimated MPC to the BVDM for example to proper update and learn the BVDM.

The main goal is to find out general physical limitations for channel prediction and ways to overcome or stretch these limits. Previous results with ray tracing compared to real world measured single input single output (SISO) channels had already indicated that for a prediction horizon in the order of about one  $\lambda$  with high accuracy few to several hundreds of MPCs have to be estimated with high accuracy.

This leads to the follow up question how far real world channels are deterministic or fully random. In most system level simulations radio channels are generated as random variables with statistical parameters mapped to certain scenarios like urban macro, micro or indoor. Real world channels are definitely the result of a deterministic process, but due to the high dimension of this process the final measurements behave most of the time similar to a random variable and it is often claimed that there are according physical limits to the performance of channel prediction.

Fortunately for real world channels one can expect an upper bound of relevant MPCs, as with increasing number of reflections and diffractions for a single ray there will be some losses per interaction point as well as higher pathloss just due to the increasing path length. This can be easily observed from the typical power delay profiles (PDP) of radio channels with an exponential decrease in Rx power for linearly increasing excess delay. From ray tracing simulations compared to similar real world measurements the number of relevant paths - allowing accurate prediction with a normalized mean square error (NMSE) of about -20dB - seems to be in the order of 100 to several hundred MPCs. This is quite a high number, but at the same time it is definitely a limited number.

The goal of a proper 5G system design is two-fold, i.e. to i) reduce the number of relevant MPCs from a SISO channel as far as possible and ii) to improve the system capabilities for identification of single MPCs.

Reduction of relevant MPCs for a certain channel component can be achieved in different ways:

**Massive MIMO beamforming** at the eNB will limit transmission of Tx-power into a narrow sub-sector of the whole served sector so that MPCs with a higher angle of departure (AoD) will be not excited.

**Real or virtual beamforming** at the UE down-selects MPCs to those coming from a certain direction. Beamforming at UE side can be very powerful as angle of arrival (AoA) spreads are known to be large for UEs surrounded by buildings.

**Small Cells:** small cells are typically placed below rooftop and due to the lower cell size with higher line of sight (LOS) probability. For that reason these channels have a smaller number of relevant MPCs with typically shorter delays.

**Higher RF frequencies** have typically higher transmission, reflection and diffraction losses. For that reason path loss per MPC should be stronger for higher RF frequencies and accordingly more MPCs will fall below a certain threshold.

Improving resolution for a given number of MPCs is possible by:

**Bandwidth Enlargement** has been proposed already in previous deliverables and extends the channel state information (CSI) measurements from a single LTE carrier of e.g. 18MHz to larger bandwidth of 100 or several hundreds of MHz. This decreases the tap delay spacing  $\Delta t=1/F$  – with F as the according bandwidth - by a factor of N. Here N is the bandwidth

extension factor. A lower  $\Delta\tau$  results in accordingly less MPCs per tap for the channel impulse response (CIR) thereby reducing the number of unobservable MPCs per tap.

Certainly there will be limitations on PHY level from different other reasons which provide different other upper performance bounds:

- Diffuse scatterers are as such not predictable as these are the results from many moving small objects like leaves of a tree. Fortunately there are mechanical limitations so that typical movements can be expected to be in the range of few Hz promising prediction horizons in the order of some 100ms.
- Another source limiting prediction performance are cluster effects for reflections or diffractions, i.e. collocated objects of similar size as the RF wavelength, which might lead to fast changes of the reflection coefficients. For higher RF frequencies with shorter wavelengths one has to expect limitations at least for some of the MPCs.
- Moving objects might pose some problem, but in case of a few strong reflections an estimation of their Doppler frequency might be still possible to some extent
- The high number of MPCs has already been discussed above. A high number of unobservable MPCs makes it difficult to estimate all parameters of all MPCs with sufficient accuracy even so it should be theoretically possible from analysis of the Fisher information.

The focus of the work in this TeC has been mainly on the last bound, i.e. the high number of MPCs. As mentioned above it is assumed that the overall estimation as well as optimization problem will be large but limited.

For a novel 5G air interface the above mentioned techniques like **massive MIMO**, **virtual beamforming**, **small cells**, **higher RF frequencies** and **bandwidth enlargement** can be easily combined or are anyway planned as a main part of a future 5G system. Massive MIMO is seen as one of the main improvements for supporting by factors higher capacity, coverage and energy efficiency. Number of UE antennas is expected to grow gradually to potentially something like four antennas per UE. A combination with virtual beamforming combining Rx signals over several time steps to e.g. a virtual  $4 \times 4 = 16$  antenna element uniform linear array (ULA) will provide already significant beamforming gains. Small cells are expected to be an integral part of 5G and larger bandwidth of 100 or several hundreds of MHz have already been proposed for LTE Release 13.

In the following the benefits of virtual beamforming with massive MIMO have been assessed based on ray-tracing simulations for a typical macro cellular outdoor scenario (see Figure 7-21) as well as for an indoor office scenario based on measurements with different number of moving persons and activities of the persons. A schematic of the office room is provided in Figure 7-22. In both cases it will be shown below that even with state of the art Kalman filtering (or higher order singular value decomposition) promising prediction horizons of about 10ms seems to be possible. While for the macro outdoor scenarios we have to apply above-mentioned techniques like massive MIMO and virtual beamforming, indoor SISO channels have already such a low number of relevant Channel Components (CCs) that prediction can be applied directly with good results. It proves that radio channels are deterministic, at least for some well behaving scenarios.

The integration of model based channel prediction and the evaluation of further performance gains is for further study (ffs). Similarly the potential contribution of bandwidth enlargement for real world channel estimation is expected to be significant, but needs further confirmation in the future.

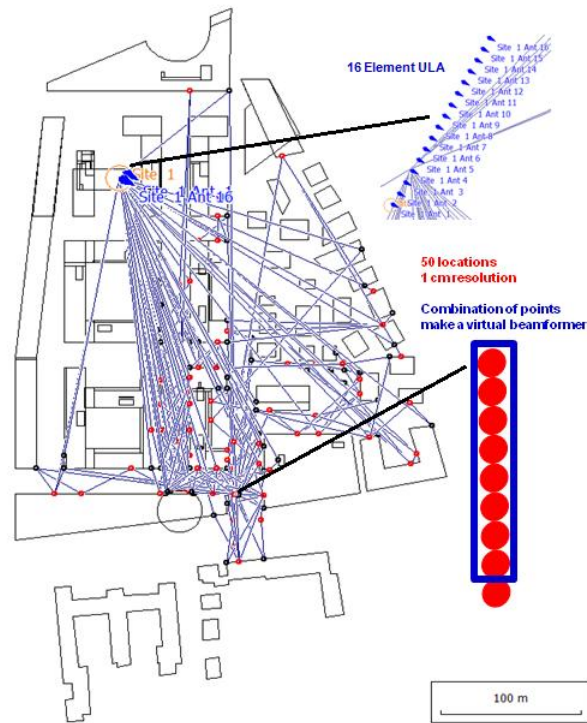


Figure 7-21: Typical urban macro outdoor scenario being investigated by raytracing and measurements

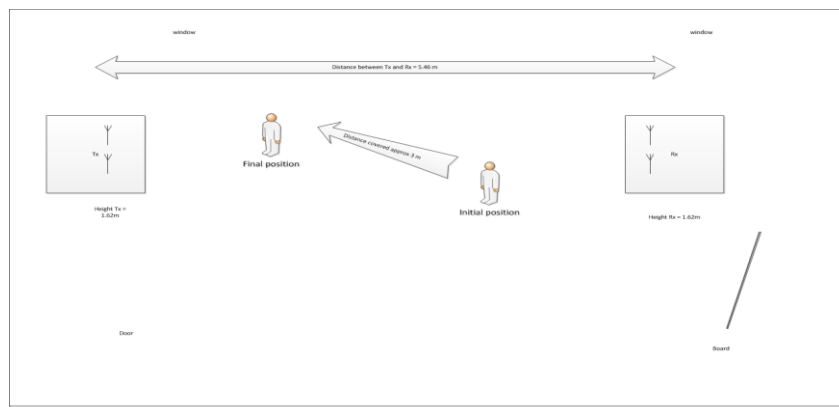


Figure 7-22: Typical indoor office scenario investigated with and without moving persons as well as a waving plate

### 7.7.2 Performance Results

The following simulation results demonstrating the potential performance of channel prediction for both outdoor and indoor office scenarios and the benefits of massive MIMO and virtual beamforming are done for the scenarios according to Figure 7-21 and Figure 7-22.

Some main simulation parameters for macro outdoor are:

- height eNB / UE = 35 / 1.5m
- antennas eNB / UE = 16x16...32 / 1...32 (virtually or real beamforming)
- RF frontends per macro cell = 16 allowing horizontal beamforming
- single polarization only

- GoB eNB = strongest beam selected from 8 beams equally spaced over 120°
- RF frequency = 2.6GHz
- RF bandwidth = 18 MHz plus 2 MHz guard band
- Channel = raytracing of NSN campus area in Munich
- Scheduler = remove 25% of PRBs with worst channel prediction performance

The achievable NMSE over an increasing prediction horizon measured in the distance the UE has moved away from the point of channel estimation can be found in Figure 7-23. Obviously the combination of virtual beamforming together with massive MIMO at the eNB significantly outperforms the prediction horizon for single SISO channels by about 10 to 20dB. At least for a prediction over  $\lambda/10^{\text{th}}$  a NMSE close to -20dB seems to be possible.

Another observation indicates that increasing the size of the virtual beamforming array at UE side will provide some further improvements in the range of 3 to 5dB.

Important is that measured and raytraced prediction matches relatively good for similar system setups, especially for the 1cm prediction horizon. For large prediction horizons measurements seem to suffer from either higher number of MPCs compared to that in a raytracing scenario or due to other effects like diffuse scatterers. Due to this good match also measured radio channels are expected to benefit from massive MIMO GoB beamforming. Note so far measurements are available for two cross polarized Tx antennas only.

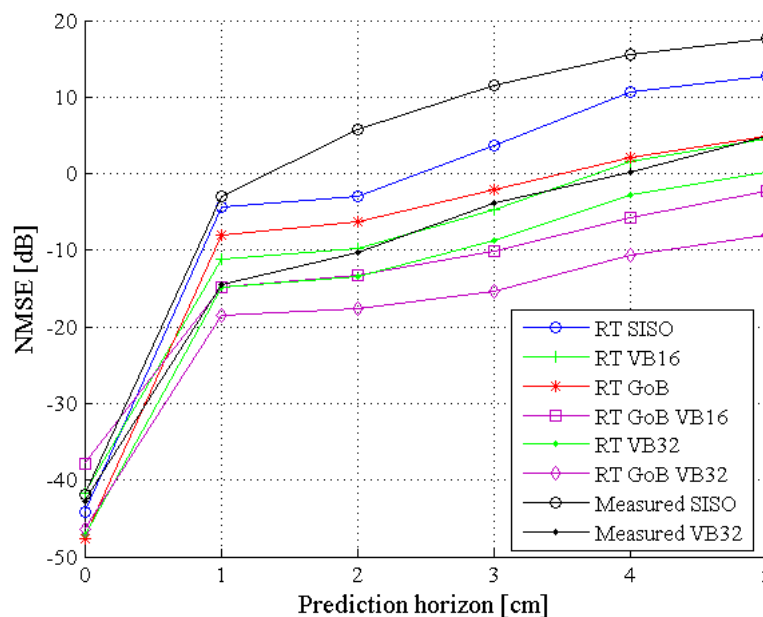


**Figure 7-23: Prediction horizon with and without virtual beamforming and with and without massive MIMO at eNB, which generates a grid of beam consisting of 8 beams (8 GoB) for raytraced and measured radio channels. The abbreviations are RT for ray tracing, GoB for grid of beam, VBxx for virtual beamforming with xx virtual antennas.**

Some main simulation parameters for measured indoor office scenario:

- height AP / UE = 2 / 1.5m
- antennas eNB / UE = 2 / 2 ULA with  $\lambda/2$  spacing
- RF frequency = 2.6GHz

- RF bandwidth = 18 MHz plus 2 MHz guard band
- Channel = typical indoor office room
- Measurement time about 1s

In Figure 7-24 the achievable NMSE is depicted over time (instead of location) in this case as the UE is for these measurements static. The different colors in the figure indicate that furthermore the environment is static as well (blue line), one person is moving in the room (red line) or one person is waving a metallic moveboard (black line). As expected the static scenario provides the best prediction performance, but for a single moving person the degradation is minimal. In case of the moveboard scenario there is a significant performance reduction increasing the NMSE for an intended prediction horizon from -20 to about -10dB, so an adaptation to varying conditions might be needed. Furthermore there might be similar benefits of MIMO as discussed above for outdoor macro scenarios.

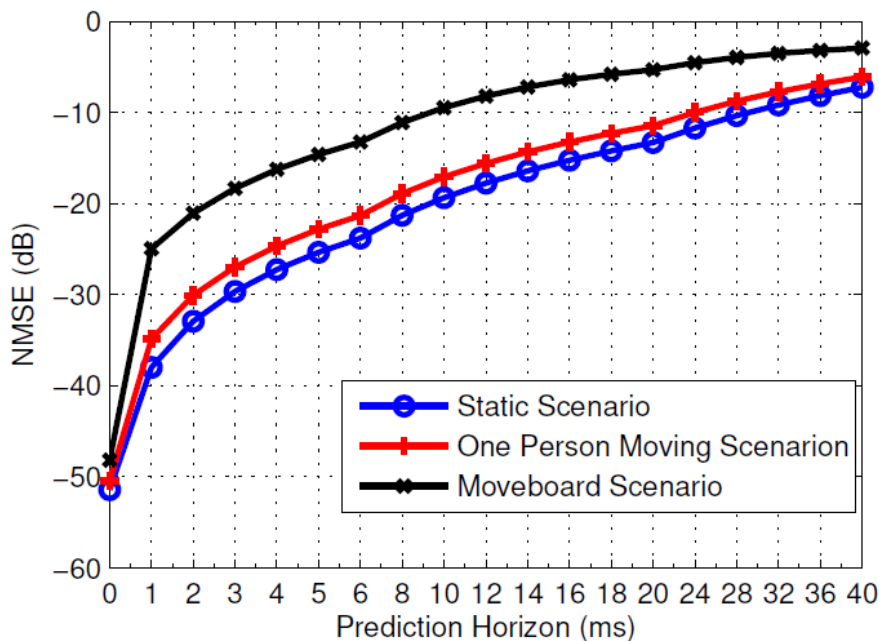
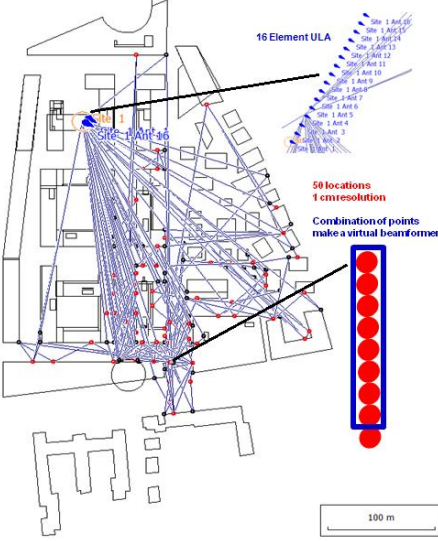


Figure 7-24: prediction horizon for measured indoor office scenario for static access point and UE, but moving persons or a person waving with a moveboard

T3.1 TeC 5 - Model Based Channel Prediction	
	<p style="text-align: center;"><b>Main Idea</b></p> <p>The main idea is to apply and combine massive MIMO, virtual beamforming, bandwidth extension, small cells, model based channel prediction etc. to reduce the complexity of radio channels – i.e. the number of relevant MPCs - to the point where more or less conventional channel prediction techniques can provide a large prediction horizon of about 10ms with an NMSE of about -20dB. Channel prediction can be seen as the potential main differentiator to current LTE evolution as it is a main enabler for advanced</p>

	<p>massive MIMO solutions and for joint transmission coordinated multi point (JT CoMP). From system level simulations assuming ideal channel knowledge large performance gains could be achieved for the combination of massive MIMO together with effective interference mitigation. Application of state of the art channel prediction keeps a significant portion of the performance gains, at least up to mobile speeds of few kmh. Improved channel prediction will extend the applicability to more use cases and higher mobile speed.</p>
<p>Considered SoA solution</p>	<p>Comparison with SISO Kalman filter performance as provided e.g. by Artist4G</p>
<p>KPIs considered and achieved gain</p>	<ul style="list-style-type: none"> <li>• Prediction horizon: NMSE over distance (or time)</li> <li>• Final KPI is CoMP and massive MIMO performance, which are known to significantly improve with increasing prediction quality</li> </ul>
<p>Performance evaluation approach</p>	<p>Evaluation is done for parametric channel models like lImprop [GMM+04], raytracing and measurements, depending on the goals of the evaluation</p>
<p>System model considered</p>	<p>Other</p>
<p>Deviation compared to Simulation Baseline</p>	<p>Some:</p> <ul style="list-style-type: none"> <li>• The channel are generated for some deterministic ray tracing and/or measurement scenarios</li> <li>• Channel models like Winner, Quadriga or SCMe are known to be unsuitable to cover the real challenges of channel prediction</li> </ul>
<p>Brief update of the results with respect to D3.2</p>	<ul style="list-style-type: none"> <li>• Simulation results for the combination of massive MIMO plus virtual beamforming as well as for indoor office scenarios with new implementation of Kalman filtering</li> </ul>
<p>Association to the TeC Approach</p>	<p>CoMP and massive MIMO</p>
<p>Targeted TCs</p>	<p>TC2 (Dense urban information society)</p>
<p>Impacted HTs</p>	<p>UDN</p>
<p>Required changes for the realization with respect to LTE Rel. 11</p>	<p>To be checked:</p> <ul style="list-style-type: none"> <li>• Feedback: from codebook to predicted radio channels</li> <li>• Massive MIMO related changes</li> </ul>



	<ul style="list-style-type: none"> <li>• Potentially reference signal design</li> <li>• Control information</li> </ul>
Trade-off required to realize the gains	A 5G system is assumed consisting of massive MIMO, multiple UE antennas, larger bandwidth (with and without carrier aggregation), novel CSI feedback schemes, ...

### 7.7.3 Impact on Horizontal Topics

T3.1 TeC 5 - HT.UDN	
Technical challenges	Significantly reducing the number of relevant multi path components (MPC) for real world outdoor macro radio channels, so that the residual MPCs can be predicted with high accuracy over a large prediction horizon
TeC solution	Apply massive MIMO, virtual beamforming, bandwidth enlargement, model based channel principles etc. to reduce number of MPCs per channel component as well as to minimize the number of unobservable MPCs
Requirements for the solution	<ul style="list-style-type: none"> <li>• Massive MIMO</li> <li>• Multiple UE antennas and/or storage of measured CSI over several sub frames or frames</li> <li>• Large bandwidth for CSI measurement (typically larger than that used for user data transmission)</li> </ul>
KPIs addressed and achieved gain	<ul style="list-style-type: none"> <li>• Prediction horizon: more than 10dB improvement over direct application of Kalman filtering, which is seen as upper bound for state of the art prediction.</li> <li>• -20dB NMSE achievable up to a prediction horizon of about <math>\lambda/10^{\text{th}}</math></li> <li>• As a rule of thumb, a NMSE of -20dB maintains about 70 to 80% of the CoMP or massive MIMO performance achievable with perfect CSI [DBZ+14]</li> </ul>
Interaction with other WPs	<ul style="list-style-type: none"> <li>• WP2/WP4: having a reliable channel prediction available might simplify many D2D and interference coordination schemes</li> <li>• WP6: For system level evaluations and integration of channel prediction into the system level concept</li> </ul>

### 7.7.4 Addressing the METIS Goals

T3.1 TeC 5	
1000x data volume	Increase in the achieved cell throughput and spectral efficiency (target is factor of 8...10)



	based on CoMP, massive MIMO and small cells. Accurate and reliable channel prediction is seen for these techniques as main enabler for a real world implementation as it relaxes backhaul requirements as well as allows for certain signal processing delays and overcomes CSI outdateding.
10-100 user data rate	Indirectly supporting CoMP and massive MIMO gains
10-100x number of devices	
10x longer battery life	Indirectly supporting CoMP and massive MIMO gains
5x E-E reduced latency	
RF power reduction can be set as target. It remains open how far there would be overall battery gains	Indirectly by CoMP and massive MIMO

### 7.7.5 References

[TR36814] 3GPP, "Further Advancements for E-UTRA - Physical Layer Aspects," TR 36.814, V 9.0.0, March 2010.

[ARTD14] ARTIST4G consortium, "D1.4 – Interference Avoidance techniques and system design," project report, July, 2012.

[JMZ+14] Volker Jungnickel, Konstantinos Manolakis, Wolfgang Zirwas, Berthold Panzner, Volker Braun, Moritz Lossow, Mikael Sternad, Rikke Apelfröjd, Tommy Svensson, The Role of Small Cells, Coordinated Multi-point and Massive MIMO in 5G, IEEE Communications Magazine, special issue on 5G, May 2014.

[TKO+13] Lars Thiele, Martin Kurras, Michael Olbrich, Kai Borner, On Feedback Requirements for CoMP Joint Transmission in the Quasi-Static User Regime, Vehicular Technology Conference (VTC Spring), 2013 IEEE 77<sup>th</sup>.

[RT89] R. Roy and T. Kailath, "ESPRIT-Estimation of Signal Parameters via Rotational Invariance Techniques," IEEE transactions on acoustic, Speech and Signal Processing, Vol. 37. No. 7, July 1989.

[FH94] J. A. Fessler and A. O. Hero, Space-Alternating Generalized Expectation-Maximization Algorithm. IEEE Transactions on Signal Processing, pp. 2664-2675, 1994.

[HTR04] M. Haardt, R. S. Thomä, and A. Richter, "Multidimensional high-resolution parameter estimation with applications to channel sounding," in High-Resolution and Robust Signal Processing (Y. Hua, A. Gershman, and Q. Chen, eds.), pp. 255-338, Marcel Dekker, New York, NY, Chapter 5, invited paper, 2004.

[DBZ+14] Stefan Dierks, Muhammad Bilal Amin, Wolfgang Zirwas, Martin Haardt, Berthold Panzner, The Benefit of Cooperation in the Context of Massive MIMO, InOWo 2014, August 2014, Essen, Germany.

[GMM+04] G. Del Galdo, M. Milojevic, M. Haardt, and M. Hennhöfer, "Efficient channel modelling for frequency-selective MIMO channels," in Proc. IEEE/ITG Workshop on Smart Antennas, (Munich, Germany), Mar. 2004.

## 7.8 T3.1 TeC 6: Adaptive large MISO Downlink with predictor antenna array for very fast moving vehicles [FT, CTH, UU]

### 7.8.1 General Overview

A new scheme called “Polynomial Interpolation” (PI) is proposed specifically for large MISO downlink beamforming in TDD. The objective is to provide a highly efficient wireless backhaul, in terms of energy consumption, for fast moving vehicular relays. Beamforming mis-pointing occurs at high speed, due to outdated channel state information at the BS. An array of aligned predictor antennas, placed upon the roof of the vehicle periodically sends pilots to the BS, to provide a very dense pattern of channel measurements in space. The BS interpolates the measurements to predict the channel between the BS and the receive antenna, accurately. The Polynomial Interpolation scheme is compared to several less complex prediction techniques derived from the Separate Receive and Training Antenna (SRTA) scheme [PHH13], namely a Random Switch Off Scheme (RSOS), the Border Switch Off Scheme (BSOS) and a Reference System (RS). See Appendix C section 9.1.6 of [METIS14-D32], and [PHH13][PHS+13] for further details.

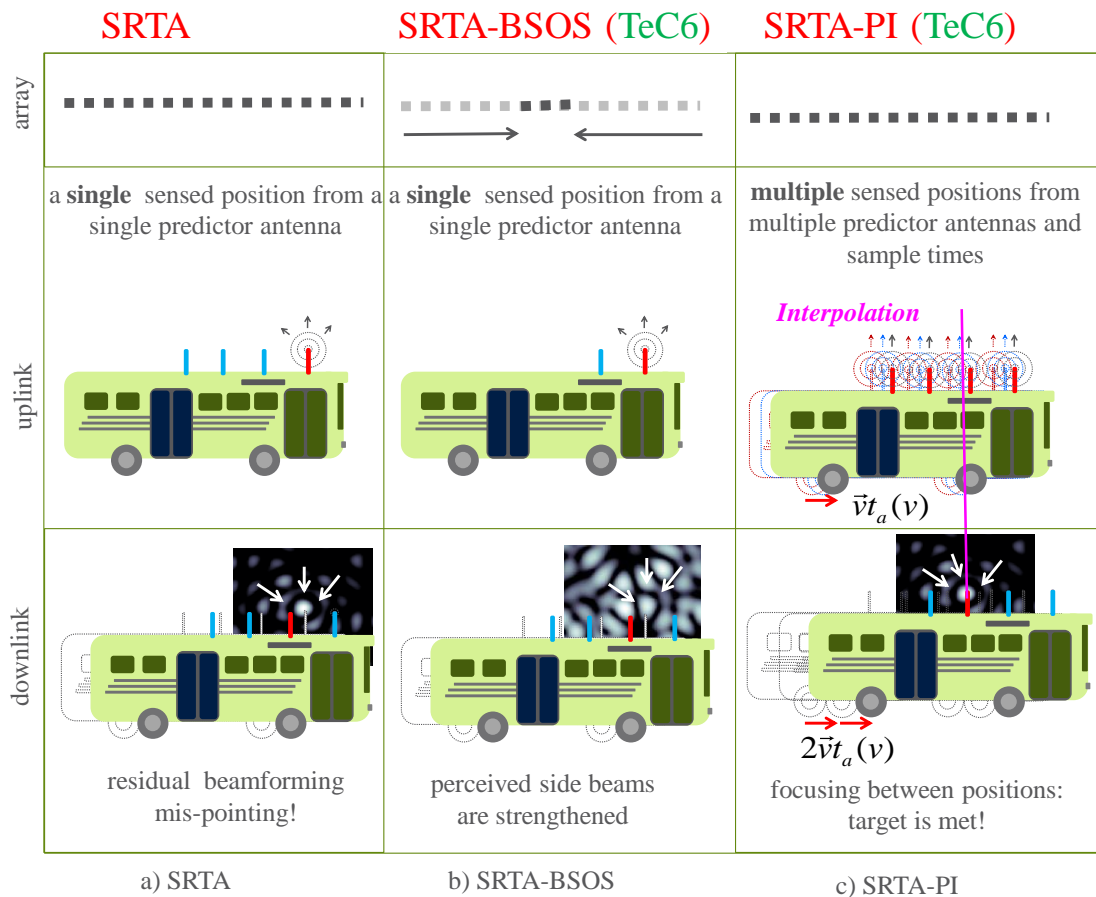


Figure 7-25: Studied schemes

### 7.8.2 Performance Results

In this deliverable, we present new results on TeC6 using WP6 mobility models (<https://www.metis2020.com/confluence/display/MET/Simulation+Models>). These new results do not change the min and max values of the gains reported in [METIS14-D32]. These new results provide estimated gains in very particular scenarios: cars and pedestrians in urban environment. In this deliverable, we consider pedestrians as well as cars. Indeed, in the future, machines or robots equipped with antennas may move at pedestrian speeds.

First, let us recall the results from [METIS14-D32]. The two figures below present link level simulation results where the BLER and the energy saving metrics are plotted as the function of the vehicle speed. We recall that the energy saving  $e_s$  is the ratio of the power required with a SISO system over the power required with a large MISO system and adaptive beamforming. These are the same curves as for [METIS14-D32], except for the SRTA-PI. For SRTA-PI, simulations have been re-run, to trigger the PI operation at the speed threshold of 10kmph instead of 50kmph.

RS and SRTA use all antennas at the Base Station to focus the energy onto the vehicle and therefore achieve the maximum energy saving (which is around 20dB). SRTA-BSOS/RSOS mute some antennas to compensate mis-pointing, and therefore save less energy. The proposed SRTA-PI achieves the target BLER of 0.01 and reaches the maximum energy saving (20dB) at the same time.

Compared to RS/SRTA/SRTA-BSOS/SRTA-RSOS, the BLER is improved by a factor of x100, and the energy saving by a factor of x30. These gains have been reported in [METIS14-D32].

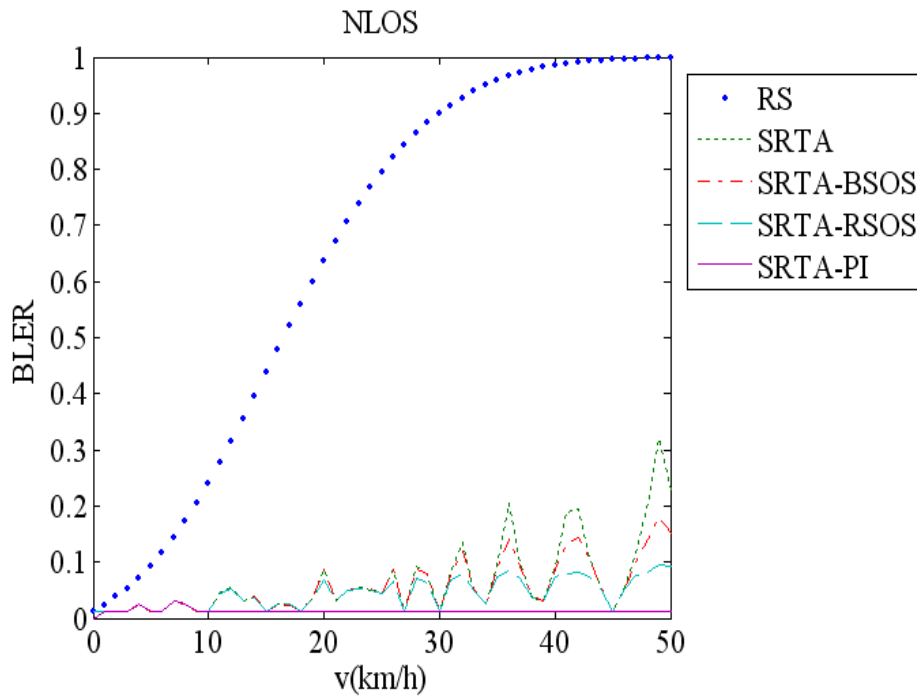


Figure 7-26: BLER versus speed Look Up Table

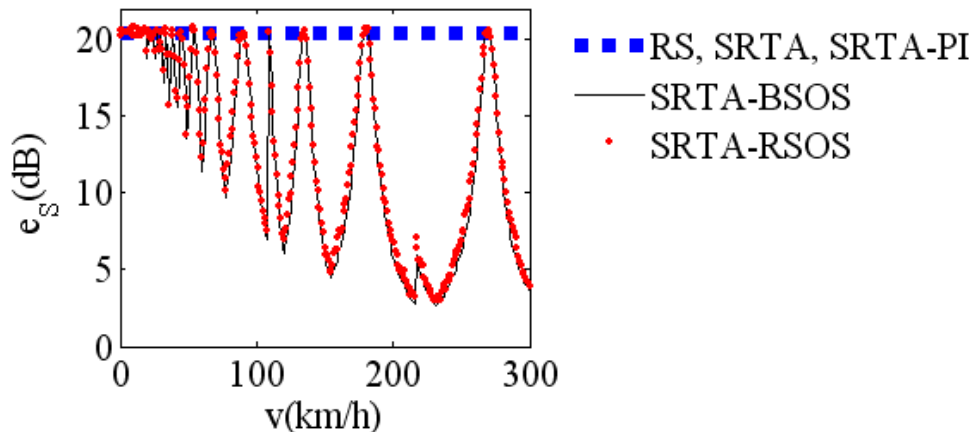
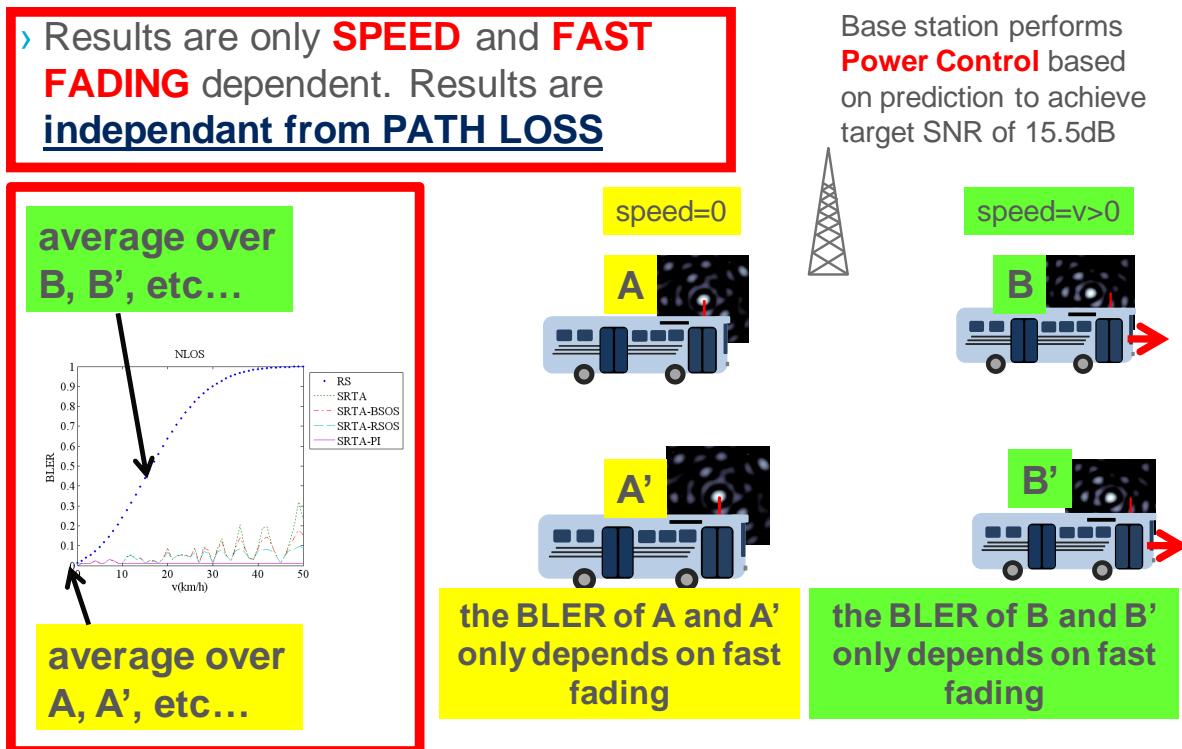


Figure 7-27: Energy Saving versus speed Look Up Table

In this new study we have used these BLER vs. speed, and energy saving vs. speed look up tables and combined them with WP6 mobility models to better estimate the gain from TeC6 in the particular case of a typical urban environment.

First, we need to recall that the look up table is independent from the BS-vehicle pathloss. As illustrated in the figure below, the mispointing effect and the resulting BLER is independent from the pathloss, in a power controlled system.



**Figure 7-28: Look Up Tables are independent from BS-vehicle pathloss**

We will now present our methodology to produce new results using WP6 mobility models. WP6 mobility models provide traces of the positions of 460 cars and 1500 pedestrians, every second, during one hour, in a urban environment. As illustrated below, we have post processed these traces and computed the speed of each car, each pedestrian, every second, for one hour. Using our look up tables from [METIS14-D32], we have then computed the BLER of each car, each pedestrian, every second, for one hour.

Finally, we have computed the following CDF curve for cars and pedestrians separately:

$y(x)$ =ratio of mobiles for which the BLER is guaranteed to be lower than  $x$  during 95% of the time (total time of 1hour).

WP6 mobility model

Mobiles position and time traces: 3600 samples, 1 sample per second, per mobile

post processing

Mobiles speed traces: 3600 samples, 1 sample per second, per mobile

post processing

BLER vs speed Look Up Tables (LUT)

Mobiles BLER traces: 3600 samples, 1 sample per second, per mobile

post processing

**Statistics:**  $x$  and  $y(x)$ ,  $y(x)$ =ratio of mobiles for which the BLER is guaranteed to be lower than  $x$  during 95% of the time (total time of 1 hour)

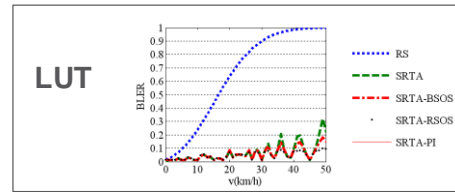


Figure 7-29: Methodology

The  $y(x)$  is plotted below, for cars.

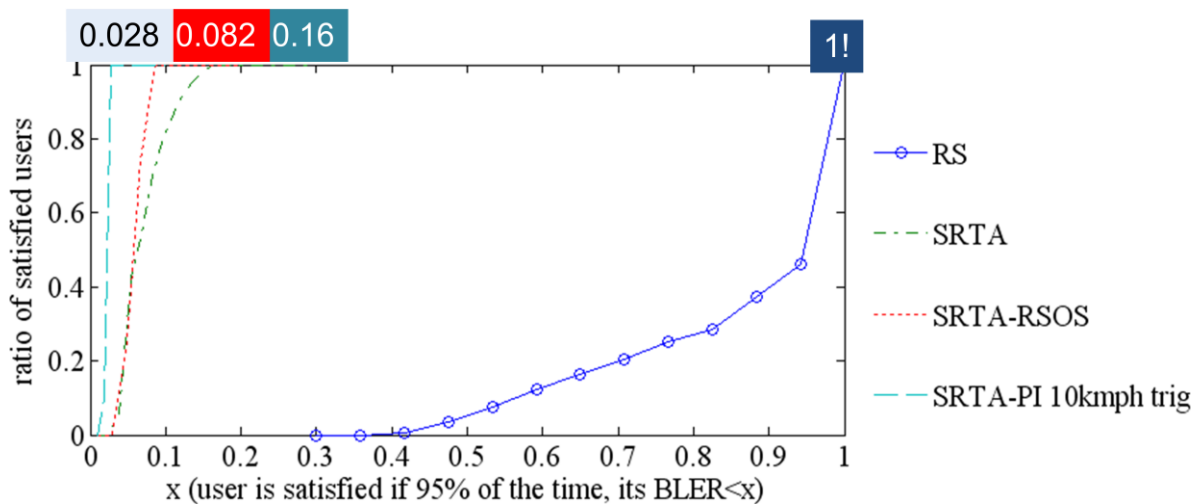


Figure 7-30: Performance of 460 cars in urban environment, during one hour

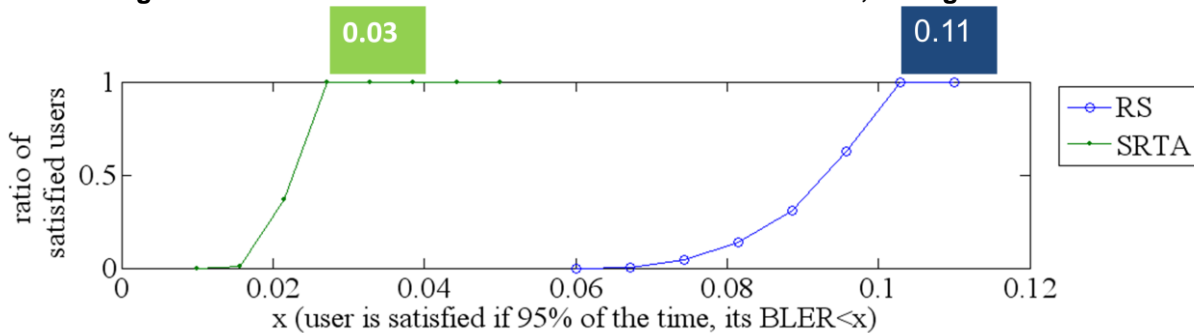


Figure 7-31: Performance of 1500 pedestrians in urban environment, during one hour

Based on these curves, we can derive the “guaranteed BLER for all cars”, and the “guaranteed BLER for all pedestrians”. This is the value  $x$  for which, 95% of the cars have the BLER lower than  $x$  during 95% of the time.

This exercise helps us determine which technique can guarantee services with delay requirements similar to infotainment (around 10% BLER at initial transmission) and services with extremely low latency requirements (around 1% BLER at initial transmission), such as drones for instance.

**Table 7.4: Performance gain 460 cars in urban environment, during one hour**

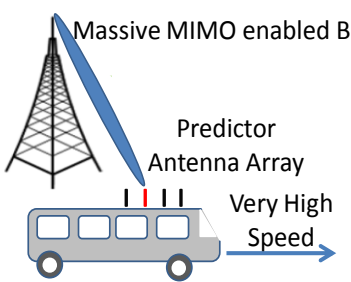
Scheme	SRTA-PI TeC6		SRTA-RSOS TeC6		SRTA SoA		RS SoA	
	Value	Gain	Value	Gain	Value	Gain	Value	Gain
Guaranteed BLER For all Cars	0.03	<b>x33</b>	0.082	<b>x12</b>	0,16	<b>x6.25</b>	1 (no guarantee!)	x1
Supported service	Ultra Low Latency (drones)		Infotainment		Infotainment		None	

**Table 7.5: Performance gain 1500 pedestrians in urban environment, during one hour**

Scheme	SRTA		RS	
	Value	Gain	Value	Gain
Guaranteed BLER For all Pedestrians	0,03	<b>X3.6</b>	0.11	x1
Supported service	Ultra Low Latency Link (drones)		Infotainment	

In conclusion, our new simulation results, based on WP6 mobility model, **do not change the minimum and maximum values of the gains reported in [METIS14-D32]**. However, they show the performance and gain of TeC6 in very particular scenarios. They also show that TeC6 might be useful **also for slow moving** devices. Indeed, services requiring **Ultra Low Latency** (1% BLER at initial transmission) might need SRTA even for pedestrian speeds.

**T3.1 TeC 6 – Adaptive large MISO downlink with predictor antenna array for very fast moving vehicles**

 <p>Massive MIMO enabled BS</p> <p>Predictor Antenna Array</p> <p>Very High Speed</p> <p>Vehicle with very high speed served by a massive-MIMO enabled BS using very narrow beams. The vehicle is equipped with a predictor antenna array.</p>	<p style="text-align: center;"><b>Main Idea</b></p> <p>A new scheme called “Polynomial Interpolation” (PI) is proposed specifically for large MISO downlink beamforming in TDD. The objective is to provide a highly efficient wireless backhaul, in terms of energy consumption, for fast moving vehicular relays.</p> <p>Beamforming miss-pointing occurs at high speed, due to outdated channel state information at the BS.</p> <p>An array of aligned predictor antennas, placed upon the roof of the vehicle periodically sends pilots to the BS, to provide a very dense pattern of channel measurements in space. The BS interpolates the measurements to predict the channel between the BS and the receive antenna, accurately.</p> <p>The Polynomial Interpolation scheme is compared to several less complex prediction techniques derived from the Separate Receive and Training Antenna (SRTA) scheme</p>
---	---



	[PHH13], namely a Random Switch Off Scheme (RSOS), the Border Switch Off Scheme (BSOS) and a Reference System (RS). See Appendix C section 9.1.6 of [METIS14-D32] for further details.
Considered SoA solution	DL MISO MRT BF TDD system called Reference System (RS) with 64 antennas at the BS & power control to meet a target SNR for 64QAM, coding rate $\frac{3}{4}$ and 1% target BLER.
KPIs considered and achieved gain	<ul style="list-style-type: none"> <li>TX Energy Saving: x1 to x30</li> <li>BLER: x1 to x100</li> </ul>
Performance evaluation approach	Simulation-based (Simulation Type: Not Applicable")
System model considered	Other.
Deviation compared to Simulation Baseline	Not Applicable: <ul style="list-style-type: none"> <li>Link level simulations: 2GHz carrier frequency, NLOS propagation, Rayleigh fading.</li> <li>Traffic model: Fixed rate and QoS (64QAM, coding rate <math>\frac{3}{4}</math>, target BLER 1%).</li> <li>Statistical results for particular scenarios: WP6 mobility model for cars and pedestrians in urban environment.</li> </ul>
Brief update of the results with respect to D3.2	WP6 mobility models have been used to derive the BLER that can be guaranteed for cars/pedestrians in a urban environment, using WP6 mobility model.
Association to the TeC Approach	Tech Approach 1: Massive MIMO for Backhaul
Targeted TCs	Test Case 8 "Real-time remote computing for mobile terminals"
Impacted HTs	Moving Networks mainly (cars, buses, trains) Possibly: Ultra Reliable Communications and Machine-to-Machine, if the devices are moving and need ultra low latency.
Required changes for the realization with respect to LTE Rel. 11	Major: <ol style="list-style-type: none"> <li>For SRTA-BSOS and SRTA-RSOS: Elastic frame (For SRTA-PI: a fixed frame is sufficient).</li> <li>"Predictor antenna array and associated signalling.</li> </ol>
Trade-off required to realize the gains	Proposed schemes in increasing order of complexity and signalling: SRTA, SRTA-RSOS (or BSOS) and SRTA-PI.

### 7.8.3 Impact on Horizontal Topics

T3.1 TeC 6 - HT.MN	
Technical challenges	Cluster #1: Mobility-robust high-data rate communication links for mobile terminals and moving relays to enable broadband as well as real-time services. Key Requirements: high-data rate and low latency communication links.
TeC solution	TeC6 uses advanced channel prediction techniques based on a predictor antenna array to



	provide a robust and guaranteed BLER at initial transmission whatever the vehicle speed, and still achieve energy savings at the network side at the same time, by using large arrays on the BS and beamforming.
Requirements for the solution	The adequate architecture for moving cells and nodes.
KPIs addressed and achieved gain	<ul style="list-style-type: none"> <li>• TX Energy Saving: x1 to x30</li> <li>• BLER: x1 to x100</li> </ul>
Interaction with other WPs	WP2. MRT BF and therefore TeC6 is compatible with a new waveform (OFDM/OQAM) [DHS+14].

T3.1 TeC 6 - HT.URC	
Technical challenges	Cluster URC over a long term (URC-L) >10 ms and URC in a short term (URC-S) <10 ms: Mobility-robust high-data rate communication links for mobile terminals and moving relays to enable broadband as well as real-time services with a delays larger or lower than 10ms.
TeC solution	Regarding Cluster URC-L: TeC6 variants called 'SRTA' and 'SRTA-SOS' offer a BLER of 10-20% at initial transmission for 0-300kmph speeds, and can therefore achieve a total delay after retransmissions of 10ms, by using the predictor antenna concept. Regarding cluster URC URC-S: TeC6 variant called 'SRTA-PI' can achieve 1% BLER at initial transmission for any speed in the 0-300kmph range, and can therefore achieve a delay of lower than 10ms, by using the predictor antenna array concept. Key Requirements: high-data rate and low latency communication links.
Requirements for the solution	The adequate architecture for moving cells and nodes.
KPIs addressed and achieved gain	<ul style="list-style-type: none"> <li>• BLER: x1 to x100</li> <li>• Latency reduction: x1 to infinite</li> </ul>
Interaction with other WPs	WP2. MRT BF and therefore TeC6 is compatible with a new waveform (OFDM/OQAM) [DHS+14].

#### 7.8.4 Addressing the METIS Goals

T3.1 TeC 6	
1000x data volume	
10-100 user data rate	
10-100x number of devices	
10x longer battery life	
5x E-E reduced latency	For vehicles from 0 to 300kmph: x1-x100 improvement of BLER at initial transmission. For pedestrians in urban environment: x3.6 BLER



	improvement at initial transmission. Corresponding values of latency reduction = $(1 - \text{BLER}_{\text{TeC6}}) / (1 - \text{BLER}_{\text{RS}})$ , where $(1 - \text{BLER}_{\text{TeC6}})$ ranges between 0.99 and 0.5 and $(1 - \text{BLER}_{\text{RS}})$ ranges between 0.99 and 1. Based on simulation results, the latency reduction ranges between x1 (no reduction of latency at 0 speed) and infinite (at speeds larger than 30kmph with TeC6 variant called 'SR TA-PI' for instance).
Energy efficiency and cost	Energy efficiency is improved at the network, thanks to BS MRT BF and the use of massive arrays at the BS.

### 7.8.5 References

[PHH13] D.T. Phan Huy, M. H elard, "Large MISO Beamforming For High Speed Vehicles Using Separate Receive & Training Antennas," in *Proc. IEEE International Symposium on Wireless Vehicular Communications (WiVEC)*, Dresden, Germany, 2-3 June 2013.

[PHS+13] D.-T. Phan-Huy, M. Sternad, T. Svensson, "Adaptive Large MISO Downlink with Predictor Antenna Array for very fast moving vehicles," in *Proc. 2013 International Conference on Connected Vehicles & Expo*, Las Vegas, USA, 2-6 December 2013.

[DHS+14] Dubois, Thierry; Helard, Maryline; Siohan, Pierre; Crussiere, Matthieu; Chapelain, Laurent; Jahan, Bruno, "Efficient MISO system combining Time Reversal and OFDM/OQAM," in; *Proceedings of 20th European Wireless Conference (EW 2014)*, pp.1,5, 14-16 May 2014.

[METIS14-D32] METIS D3.2, "First performance results for multi-node/multi-antenna transmission technologies", Apr. 2014.

## 7.9 T3.1 TeC 7: Massive MIMO transmission using higher frequency bands based on measured channels with CSI error and hardware impairments [DOCOMO]

### 7.9.1 General Overview

In order to tackle the rapidly increasing data traffic, usage of higher frequency bands that can easily expand signal bandwidth has been widely studied for 5G mobile communication systems. NTT DOCOMO has successfully achieved 10 Gbps packet transmission employing 11 GHz band 8×16 MIMO with 400 MHz bandwidth by field experiments in partnership with Tokyo Institute of Technology in December 2012 [NDP13],[SSO13]. Moreover, mobile services using the higher frequency bands can be flexibly introduced by a Phantom Cell concept where the C-plane is supported by a lower frequency band, such as 800 MHz or 2 GHz, and only the U-plane is provided by the higher frequency bands, as high as several tens GHz [IKT12]. In the higher frequency bands, the number of antenna elements can be drastically increased compared to the 2 GHz band because the size of one antenna element can be miniaturized, and it is expected that Massive MIMO can provide the higher data rate and transmission quality.

However, in order to activate Massive MIMO with high performance, a Massive MIMO precoder requires accurate CSI at the transmitter. In addition, Massive MIMO handles an extremely large number of RF, IF and BB circuits, and thus it is more important to compensate for impairments and imbalances of the RF, IF and BB circuits including the antennas. For example, IQ imbalance in the higher-frequency-band RF circuit, different antenna patterns and mutual coupling among antenna elements may degrade the Massive MIMO capability.

As the prior step of this research, we evaluated performances of 30 Gbps 24×24 MIMO-OFDM eigenmode (EM) transmission by link level simulations using both channel data that are measured in the 11 GHz propagation experiments [SSS+14] and channel model based on the Kronecker model. The computer simulations followed the specifications of the 11 GHz band 8×16 MIMO transmission and 24×24 MIMO propagation experiments [SSO+13],[KKG+11]. However, the required total transmission power is over 30 dBm for applying such an enhanced MIMO technique to 20 GHz band small cells that provide a super high bit rate of 20 Gbps [SSB+14]. Thus, in order to reduce the total transmission power to 30 dBm by exploiting a BF effect of Massive MIMO, we employed Massive MIMO of UPA with 256 transmitter antennas for the 20 GHz band 20 Gbps transmission in [METIS14-D32]. Spatially multiplexing 16 streams with the 400 MHz bandwidth achieves the bit rate of 23.5 Gbps. It was shown that Massive MIMO with 256 antennas can drastically improve the throughput performance by the 3D BF effect compared to the typical MIMO with 16 antennas. However, this investigation assumed a fully-digital Massive MIMO transceiver that requires 256 RF and BB chains.

Here, to reduce the cost of the Massive MIMO transceiver, a hybrid BF that consists of analog BF and digital precoding is employed, because the analog BF with RF phase shifters can drastically reduce the number of the up-converters and BB chains in the hybrid BF as shown in Figure 7-32. As a new precoding scheme for the Massive MIMO OFDM with the hybrid BF, we propose fixed BF and CSI-based precoding (FBCP) [OSS+14]. The proposed FBCP consists of  $N_T$  transmitter antennas and  $L$  RF and BB chains for  $M$  data streams as shown in Figure 7-32. Moreover, the FBCP employs a successive two-stage algorithm;  $L$  analog fixed BF weights are firstly selected from some analog fixed BF weight candidates based on the steering vector for arbitrary 2D angles. The  $L$  analog fixed BF weights denoted by  $\mathbf{W}$  are selected on the maximum total received power criterion. In the second stage, a precoding matrix  $\mathbf{P}(n)$  at the  $n$ -th subcarrier is calculated by singular value decomposition (SVD) using an equivalent channel matrix  $\mathbf{H}(n)\mathbf{W}$  where  $\mathbf{H}(n)$  is the channel matrix. Note that  $\mathbf{H}(n)\mathbf{W}$  is accurately estimated by exploiting a reference signal with the selected analog fixed BF.

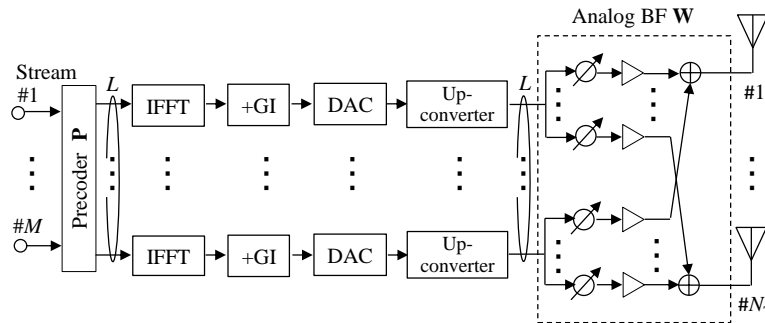


Figure 7-32: Massive MIMO OFDM transmitter employing FBCP

### 7.9.2 Performance Results

Link level simulations are performed to evaluate throughput performances of the 20 GHz band Massive MIMO employing the proposed FBCP. The same simulation baseline as [METIS14-D32] is employed here. The parameters used for the simulations are given in Table 7.6.  $N_T$  is set to 16 or 256, and the number of receiver antennas,  $N_R$ , is fixed to 16. The receiver detects the spatially multiplexed streams by using a postcoding matrix that is calculated from the SVD of the equivalent channel matrix  $\mathbf{H}(n)\mathbf{W}$ . Both the transmitter and the receiver employ the 2D UPA as the antenna array structure in Figure 7-33. The number of the streams,  $M$ , is fixed to 16. The maximum bit rate reaches 31.4 Gbps according to the parameters set where the modulation and coding scheme is 256QAM with coding rate,  $R$ , of 3/4 in the turbo code. AMC is used ideally. Channel model was based on the Kronecker model including LOS and NLOS components. Rician factor,  $K$ , is assumed to be 10 dB for the Nakagami-Rice fading channel. Note that computer simulations using the measured channel data will be performed in the near future.

Table 7.6: Simulation parameters of Massive MIMO

Transmission scheme	Downlink Massive MIMO OFDM
Signal bandwidth	400 MHz
Active subcarriers	Pilot: 32, data: 2000
No. of antennas	Transmitter, $N_T$ : 16, 256 Receiver, $N_R$ : 16
No. of data streams, $M$	16
Modulation scheme	QPSK, 16QAM, 64QAM, 256QAM (w/ AMC)
Channel coding	Turbo code, $R = 1/2, 2/3, 3/4$ (w/ AMC)
Maximum bit rate	31.4 Gbps (256QAM, $R = 3/4$ )
Antenna array structure	UPA
Angular power spectrum	$\theta$ : Laplacian distribution $\phi$ : wrapped Gaussian distribution
Average angle ( $\theta, \phi$ )	Departure: (90 deg, 90 deg) Arrival: (90 deg, 90 deg)
Angular spread ( $\theta, \phi$ )	Departure: (5 deg, 5 deg) Arrival: (20 deg, 20 deg)
Channel model	Kronecker model
Fading channel	Nakagami-Rice ( $K = 10$ dB), 16-path

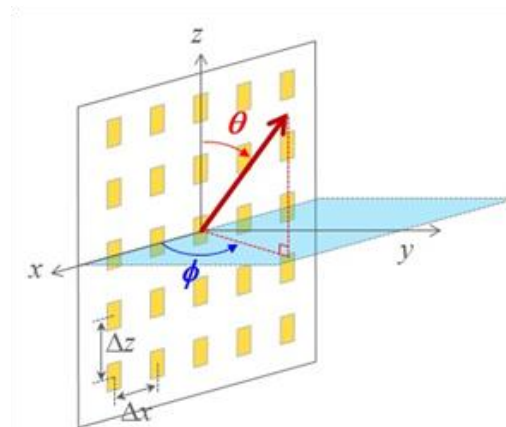


Figure 7-33: UPA for 3D BF

Figure 7-34 shows throughput performance of the FBCP with  $L$ . Ideal channel estimation is assumed. Search angular intervals for the analog BF in zenith and azimuth,  $\Delta\phi$  and  $\Delta\theta$ , are fixed to 5 degrees. For comparison, throughput performances of the EM precoding which employs the fully-digital Massive MIMO of  $L = N_T$ , are also plotted in Figure 7-34. It is shown that as  $L$  increases, the throughput of the FBCP approaches to that of the EM by improvement of the BF gain, and that the convergence value of  $L$  is 32 for  $N_T = 256$ . Since the EM requires the same number of the RF and BB chains as  $N_T$ , FBCP is the much cost-effective scheme. Moreover, in comparison with the conventional fully digital MIMO with  $N_T = 16$ , the FBCP with  $N_T = 256$  and  $L = 32$  can reduce the required SNR at the 20 Gbps throughput by 14 dB by exploiting the higher BF and diversity gains.

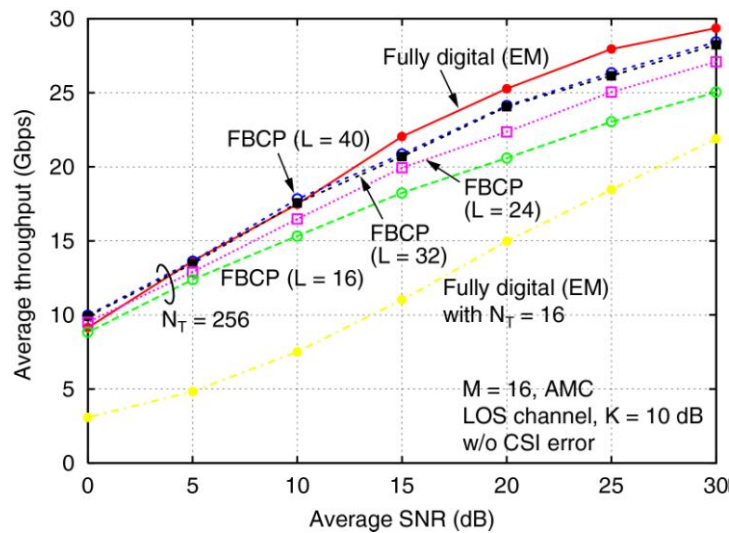


Figure 7-34: Optimization of  $L$  for FBCP

Figure 7-35 shows throughput performance of the FBCP with the CSI error. For comparison, throughput performance of the fully digital EM precoding is also plotted in Figure 7-35. In both schemes, the CSI error is generated by complex Gaussian distribution with zero mean and variance of  $\sigma_e^2$ . Let  $\sigma_n^2$  denote noise power per antenna, and  $\sigma_e^2$  is set to  $\sigma_n^2 - 10$  dB or  $\sigma_n^2 - 20$  dB. This setting is based on the assumption that the reference signals with additional gain are transmitted and accurate channel estimation can be performed by using them. Figure 7-35 demonstrates that as the CSI error increases, the throughput of the EM drastically degrades while the FBCP is robust to the CSI error. It is also found that when  $\sigma_e^2 = \sigma_n^2 - 20$  dB, the FBCP can achieve the same throughput as the EM in spite of the significantly low complexity.

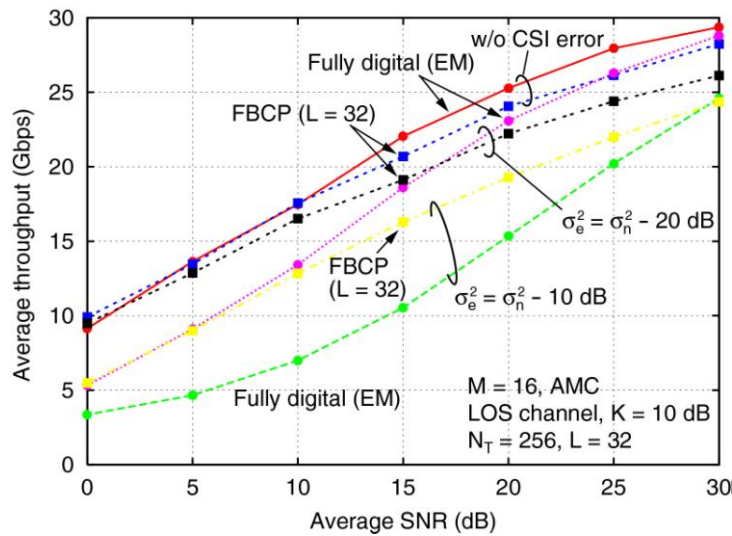


Figure 7-35: Throughput performance of FBCP with CSI error

Finally, throughput performance of the FBCP with the phase error is shown in Figure 7-36. The phase error is considered as the hardware impairment in the RF phase shifters of the FBCP and is generated by Gaussian distribution with zero mean and variance of  $\sigma_p^2$ . Standard deviation  $\sigma_p$  is set to 3 degrees or 5 degrees. From Figure 7-36, it can be seen that the FBCP achieves the same throughput irrespective of the phase error and is the robust precoding scheme to the hardware impairment. Since the analog BF weights are searched on the maximum received power criterion and the searching algorithm depends on the relative 2D angles, the FBCP is insusceptible to the phase error.

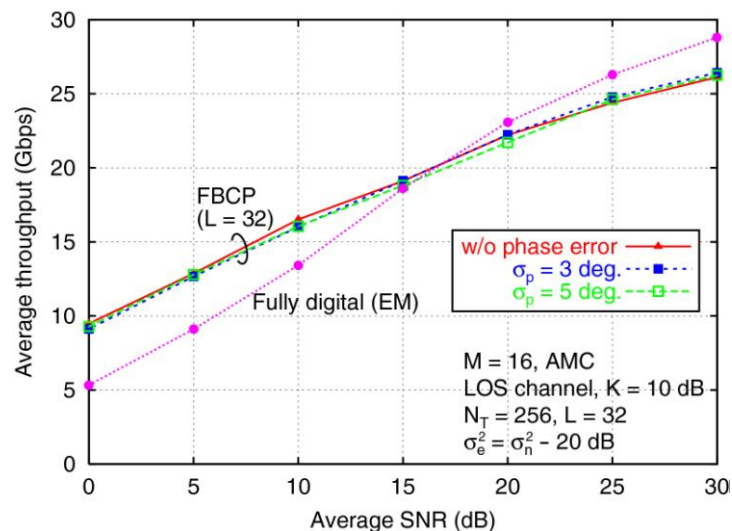
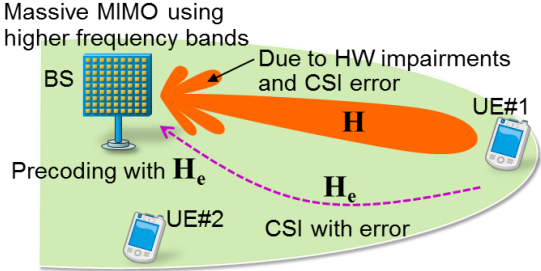


Figure 7-36: Throughput performance of FBCP with phase error

**T3.1 TeC 7 – Massive MIMO transmission using higher frequency bands based on measured channels with CSI error and hardware impairments**

**Main Idea**

20 GHz band Massive MIMO transmission using 2D UPA with 256 transmitter antennas was investigated, and by spatially multiplexing 16

 <p style="text-align: center;"><b>System Model</b></p> <p>Massive MIMO transmission using higher frequency bands based on measured channels with CSI error and hardware impairments</p>	<p>streams with 400 MHz bandwidth it achieves the super high bit rate of more than 20 Gbps. However, this investigation assumed a fully-digital Massive MIMO transceiver. Here, to reduce the cost and provide the realistic architecture of the Massive MIMO transceiver, fixed BF and CSI-based precoding (FBCP) is proposed as a new precoding scheme for the Massive MIMO which employs a hybrid BF consisting of the analog BF and the digital one. Simulation results show that FBCP can achieve almost the same throughput performance as the fully-digital Massive MIMO using the eigenmode precoding in spite of the significantly low complexity, and that the FBCP is the more robust precoding scheme to the CSI error than the fully-digital eigenmode precoding.</p>
<p>Considered SoA solution</p>	<p>20 Gbps 16x16 MIMO transmission with 400 MHz bandwidth and 16 streams</p>
<p>KPIs considered and achieved gain</p>	<p>Experienced user throughput and energy efficiency: Average SNR to achieve 20 Gbps throughput can be reduced by 14 dB at same transmitter power.</p>
<p>Performance evaluation approach</p>	<p>Simulation-based: link level evaluation for single link</p>
<p>System model considered</p>	<p>Other</p>
<p>Deviation compared to Simulation Baseline</p>	<ul style="list-style-type: none"> <li>• Model of environment: Single user scenario</li> <li>• Spectrum assumptions: CM/MM-waves (currently, 20 GHz band)</li> <li>• Propagation model: LOS channel with Rician factor of 10 dB and generated by the Kronecker model</li> <li>• Deployment model: None</li> <li>• User/Device distribution: Single user scenario and SNR is changed</li> <li>• Traffic model: Full buffer</li> </ul>
<p>Brief update of the results with respect to D3.2</p>	<p>New precoding scheme for a low complexity Massive MIMO transceiver is proposed and it is shown that the performance of the proposed scheme is almost the same as that of the conventional one in [METIS14-D32] in spite of low complexity in the same simulation alignment /KPI/TC.</p>
<p>Association to the TeC Approach</p>	<p>T3.1 Tech Approach 2: Massive MIMO for Access</p>
<p>Targeted TCs</p>	<p>TC2</p>
<p>Impacted HTs</p>	<p>UDN</p>
<p>Required changes for the realization with respect to LTE Rel. 11</p>	<p>Major</p> <ul style="list-style-type: none"> <li>• New frame structure</li> <li>• Support of larger number of streams</li> <li>• Support of larger number of antennas</li> <li>• Wider bandwidth</li> <li>• New precoding scheme</li> </ul> <p>Support of CSI feedback / utilization of channel reciprocity</p>



Trade-off required to realize the gains	The gains achieved for this TeC are obtained by deployment of many antennas and accurate CSI.
---	---

### 7.9.3 Impact on Horizontal Topics

T3.1 TeC 7 - HT.UDN	
Technical challenges	Increase the spectral efficiency by multiplexing a large number of data streams and reduce both the transmitter power and interference power to other users.
TeC solution	<ul style="list-style-type: none"> <li>• 3D BF by Massive MIMO using more than 100 antenna elements can improve the received signal power to the desired user and reduce the interference power to other users</li> <li>• Massive MIMO can spatially multiplex the larger number of data streams by exploiting the freedom of multiple antennas</li> </ul>
Requirements for the solution	Explicit CSI for precoding scheme
KPIs addressed and achieved gain	<ul style="list-style-type: none"> <li>• More than 10 times throughput compared to LTE-A baseline with 8 antennas</li> <li>• Average SNR to achieve 20 Gbps throughput can be reduced by 14 dB at same transmitter power</li> </ul>
Interaction with other WPs	

### 7.9.4 Addressing the METIS Goals

T3.1 TeC 7	
1000x data volume	More than 10 times throughput compared to LTE-A baseline with 8 antennas
10-100 user data rate	More than 10 times throughput compared to LTE-A baseline with 8 antennas
10-100x number of devices	
10x longer battery life	
5x E-E reduced latency	
Energy efficiency and cost	Proposed FBCP drastically reduces cost of Massive MIMO transceiver compared to fully-digital one

### 7.9.5 References

[NDP13] NTT DOCOMO press releases, “DOCOMO and Tokyo Institute of Technology achieve world’s first 10 Gbps packet transmission in outdoor experiment,” [http://www.nttdocomo.co.jp/english/info/media\\_center/pr/2013/0227\\_00.html](http://www.nttdocomo.co.jp/english/info/media_center/pr/2013/0227_00.html), Feb. 2013.

[SSO+13] S. Suyama, J. Shen, Y. Oda, H. Suzuki, and K. Fukawa, “11 GHz band 8x16 MIMO-OFDM outdoor transmission experiment for 10 Gbps super high bit rate mobile communications,” in Proc. *IEEE PIMRC2013*, Sept. 2013.



[IKT12] H. Ishii, Y. Kishiyama, and H. Takahashi, "A novel architecture for LTE-B :C-plane/U-plane split and Phantom Cell concept," in Proc. *IEEE Globecom Workshops*, pp. 624-630, Dec. 2012.

[KKG+11] Y. Konishi, M. Kim, M. Ghoraiishi, J. Takada, S. Suyama, and H. Suzuki, "Channel sounding technique using MIMO software radio architecture," in Proc. the *5<sup>th</sup> EuCAP*, pp. 2546-2550, Apr. 2011.

[SSS+14] S. Suyama, J. Shen, H. Suzuki, K. Fukawa, and Y. Okumura, "Evaluation of 30 Gbps super high bit rate mobile communications using channel data in 11 GHz band 24x24 MIMO experiment," in Proc. *IEEE ICC2014*, June 2014.

[SSB+14] S. Suyama, J. Shen, A. Benjebbour, Y. Kishiyama, and Y. Okumura, "Super high bit rate radio access technology for small cells using higher frequency bands," in Proc. *IEEE IMS2014*, June 2014.

[OSS+14] T. Obara, S. Suyama, J. Shen, and Y. Okumura, "Joint fixed beamforming and eigenmode precoding for super high bit rate massive MIMO systems using higher frequency bands," in Proc. *IEEE PIMRC2014*, Sept. 2014.

[METIS14-D32] METIS D3.2, "First performance results for multi-node/multi-antenna transmission technologies", Apr. 2014.

### 7.10 T3.1 TeC 8: Massive MIMO and ultra-dense networks [ALU]

The work on this TeC is completed. Please refer to [METIS14-D32] for the most updated results.

### 7.11 T3.1 TeC 9: Eigenvalue decomposition (EVD) based channel estimation for MU-MIMO [RWTH]

The work on this TeC is completed. Please refer to [METIS14-D32] for the most updated results.

### 7.12 T3.1 TeC 9b: Uplink power control with MMSE receiver in multi-cell MU-Massive-MIMO [RWTH]

#### 7.12.1 General Overview

Multi-cell uplink power control has been illustrated to largely improve the energy efficiency in conventional MIMO systems [FJS10]-[SKZ10]. With perfect CSI and multi-cell coordination, the optimal solution of jointly assigning interference-plus-noise ratio (SINR) targets and transmit power can substantially reduce the uplink power consumption [FJS10]; while with imperfect CSI but free of pilot contamination, the authors in [SKZ10] have exploited the interdependency between pilot and data transmissions to adjust pilot power in the context of existing data power control, such that total power saving is achieved subject to the per-user SINR constraint. However, these advantages of uplink power control have not been addressed in previous massive MIMO work [Mar10]-[NLM13b], since equal uplink power allocation among users has always been assumed. Therefore, we are motivated to investigate the potential of uplink pilot and data power control in multi-cell MU-Massive-MIMO systems.

The standard MMSE receiver based on the practical channel estimates with pilot contamination [JAM+11] is applied at the BS. In order to minimize the sum pilot and data transmit power of all users under the per-user SINR and per-user power constraints, we first derive the closed-form lower bound on the average uplink SINR (instead of directly computing the average SINR which in general has intractable form [HBD13]) for a very large but finite number of BS antennas, which takes the individual power allocation among different users into account. Based on the lower bound, we then propose a joint iterative pilot and data power control algorithm, which embeds the pilot power minimization into a standard data power control process [CAH+07]. The existence and uniqueness of the optimal solution are proved for single-user setup, while the convergence in multi-user case is guaranteed by an extra monotone decreasing constraint. Simulation results demonstrate the tightness of the lower bound as well as the large gain of applying multi-cell uplink power control together with massive MIMO technique to further improve the energy efficiency.

The general idea of the joint iterative algorithm is to perform the pilot power control with prior data power output, if the per-user power constraint is currently satisfied. Based on the obtained pilot power allocation, the standard data power control converges to a unique optimal solution, which is used as updated input for the subsequent pilot power control. For the details of the algorithm please refer to [GGF+14].

#### 7.12.2 Performance Results

We consider a MU-Massive-MIMO system consisting of  $L = 3$  hexagonal cells which have a radius of 1000 meters. Each BS located in the cell centre serves  $K = 5$  users at the same time-frequency resource. All users are distributed uniformly inside the cell and have at least a distance of 100 meters away from the BS. The path-loss exponent is selected to be 4 and the large-scale fading is modelled as a zero mean log-normal distribution with a standard deviation of 8 dB. Throughout the simulations in this section, normalized additive Gaussian noise with variance of 1 is assumed; the same target SINR and power allowed for uplink transmission are applied for all users in the system, i.e.  $\gamma_{lk} = \gamma$ ,  $p_{lk} = p = 200$  mW,  $\forall (l, k)$ ; referring to [SKZ10], around 1/6 of the transmit power is assigned initially to the uplink training.

Next we illustrate the performance of the proposed joint iterative power control based on the previous user placement and initial power. In the upper part of Figure 7-37, e.g. for number of BS antennas ( $M = 100$ ), the optimal assigned sum pilot power is larger than the sum data power except for very low target SINRs, which coincides with the fact that only data transmission takes advantage of massive BS antennas (i.e. power-scaling law), while uplink training does not, since it is performed on a per-receive antenna basis [NLM13a]. Due to the same reason, for  $\gamma$  up to 10.7 dB, the obtained data power allocation leads to a sum data power varying from 12.6 to 17.4 dBm as the pursued SINR rises, which is much smaller than the increment from 11.4 to 27 dBm in sum pilot power. In contrast, in the high target SINR region with  $\gamma \geq 10.7$  dB, the inner loop for pilot power control is terminated by the monotone decreasing constraint only after 1 iteration, because the pilot contamination confines the impact of pilot power control. As a result, the joint algorithm reduces to a simple data power control with fixed (initial) pilot power. On the other hand, as  $M$  grows, the lower limit of high target SINR region also increases, which extends the region where power saving can be obtained through joint power control. In addition, as depicted in both parts of Figure 7-37, the joint algorithm becomes infeasible when the target SINR is above a certain value, e.g. 15 dB for  $M = 100$ , due to the per-user power constraint. However, as  $M$  becomes large, this upper limit increases as well, which reflects the potential of combining the joint uplink power control with massive MIMO technique to attain a higher SINR target with less sum transmit power, hence improve the energy efficiency.

Moreover, as shown in Figure 7-38, we demonstrate the advantage in power saving of the proposed joint algorithm comparing to a simple data power control where the pilot power allocation is fixed to the initial value as in the joint algorithm, i.e.  $\frac{1}{6}p$  for all users. Here the y-axis represents the ratio of obtained sum power saving (between simple data power control and the proposed algorithm) w.r.t. the result when the simple data power control is applied. It is obvious that a power saving up to 95% can be achieved with joint algorithm in low target SINR region. The advantage disappears however when the target SINR exceeds the lower limit of high SINR region. It is especially worth noting that the benefit of deploying a large number of BS antennas tends to become marginal as  $M$  keeps growing, since the ultimate SINR performance is exclusively limited by the pilot contamination and transmit power control.

Finally we evaluate the infeasibility of the joint algorithm which is caused by either the per-user power constraint or the unattainable per-user SINR target. The latter is checked based on the obtained pilot power prior to the data power control to avoid unnecessary computations if the SINR target is infeasible. The results in the upper part of Figure 7-39 verify that the significant infeasibility (>5%) first occurs due to the per-user power limit. However as the target SINR increases, it tends to be simply unachievable with the joint power control, thus  $\lambda_{\max}(\Psi\mathbf{C}) \geq 1$  starts to become the dominant cause of infeasibility. In particular, the overall probability in the lower part of Figure 7-39 has a decreasing behaviour (e.g. around 10 dB for  $M = 100$ ) due to the fact that the joint algorithm reduces to a simple data power control. Although the joint power control has a large gain in power saving, the inner loop of pilot power control may result in a case where some of the cell edge users are infeasible to attain the target SINR, which can be however achieved at the expense of higher sum transmit power, if only the data power control with fixed initial pilot power is applied. Besides, Figure 7-39 also illustrates that by deploying a larger number of BS antennas the achievable target SINR is increased, e.g. 3 dB gain from 100 to 200 BS antennas.

The above results has demonstrated the attainable power saving of the joint algorithm comparing to a simple data power control with fixed pilot power, which comes with the trade-off in a bit higher infeasibility. Nevertheless, if combined with a very large number of BS antennas, the joint uplink power control can achieve a higher target SINR with less sum transmit power and significantly improve the system energy efficiency.

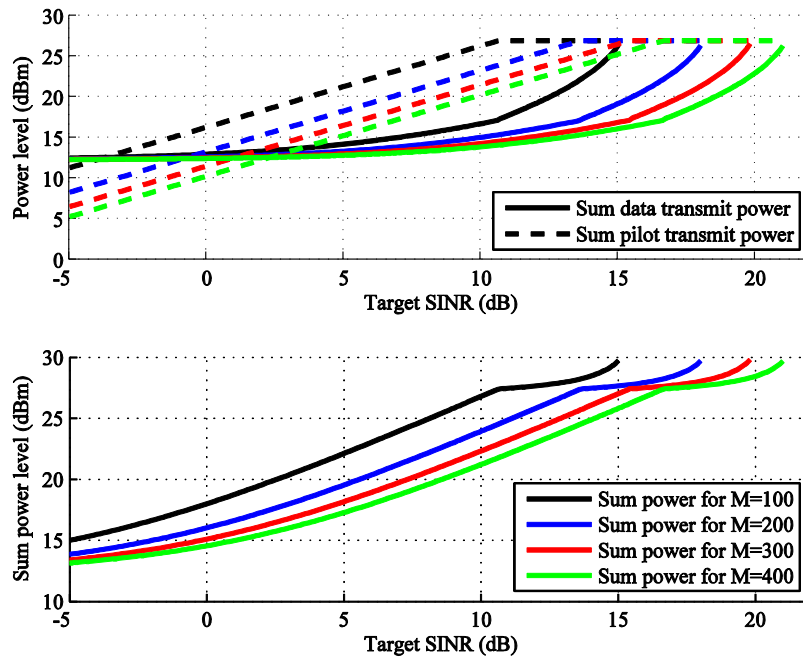


Figure 7-37: Joint iterative pilot and data power control vs. target SINRs

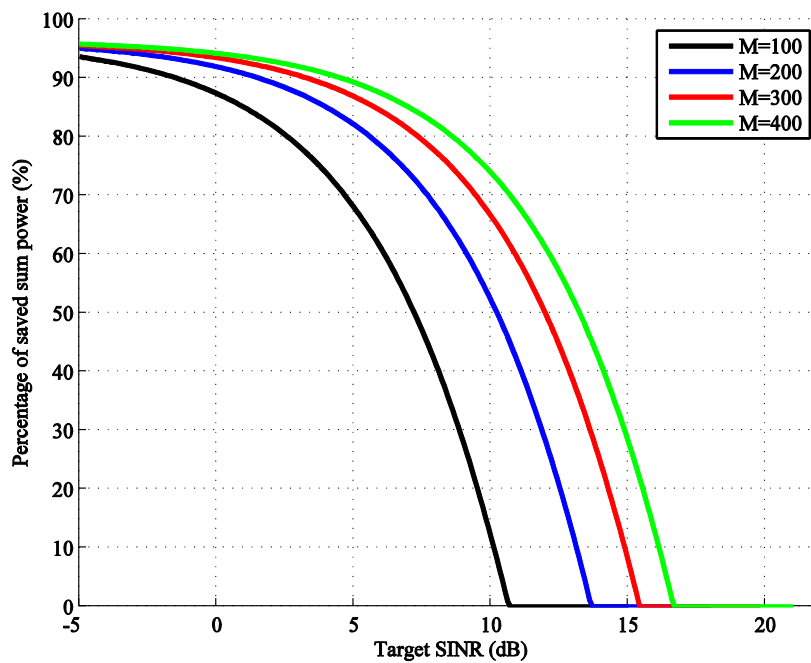


Figure 7-38: Percentage of power saving vs. target SINRs

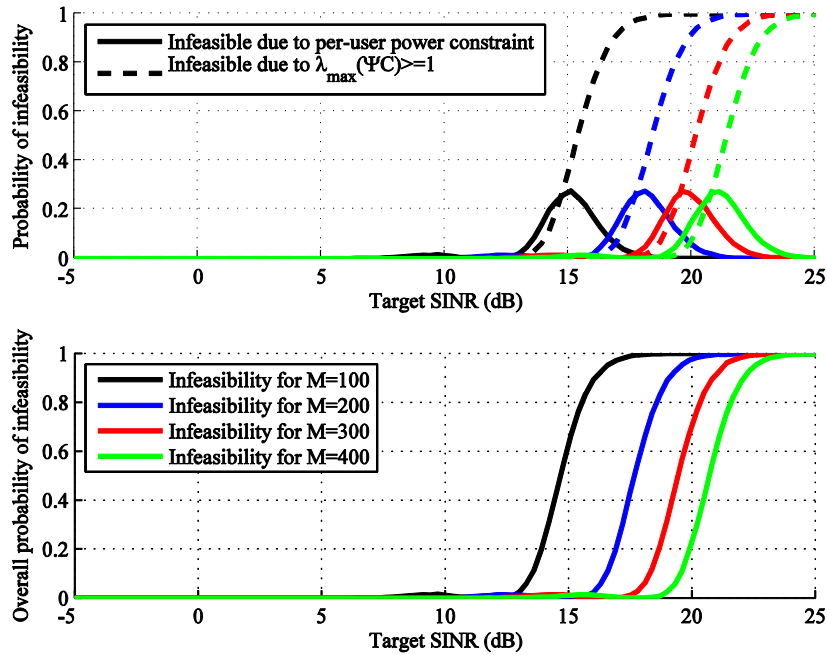
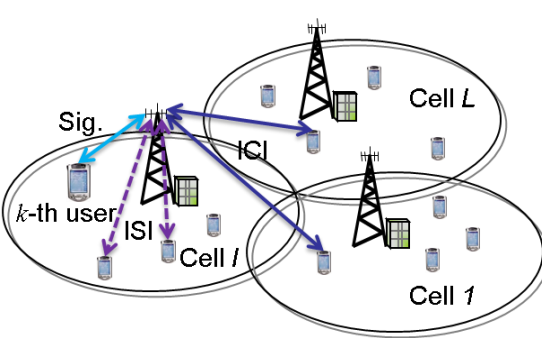


Figure 7-39: Probability of infeasibility over random user placements

T3.1 TeC 9b – Uplink power control for massive MIMO (ULPwrCtrl)	
	<p style="text-align: center;"><b>Main Idea</b></p> <p>We apply multi-cell uplink power control, assuming the MMSE receiver based on the pilot contaminated channel estimation and a very large but finite number of antennas at the base station. We derive the lower bound on the average post-processing uplink SINR with individual power assignment between pilot and data transmissions for each user, which facilitates a joint iterative uplink pilot and data power control strategy that minimizes the sum transmit power of all users subject to the per-user SINR and per-user power constraints</p>
Considered SoA solution	Simple data transmit power control [CAH+07]
KPIs considered and achieved gain	Transmit power saving: up to 95%
Performance evaluation approach	Analytical / Simulation-based (System level evaluation)
System model considered	WP3 task 3.2 simulation baseline
Deviation compared to Simulation Baseline	<p>Some:</p> <ul style="list-style-type: none"> <li>• Propagation model: <ul style="list-style-type: none"> <li>○ The channel is modelled using distance-dependent path-loss and uncorrelated quasi-static Rayleigh fading components.</li> <li>○ For both own and cross channels, the path-loss exponent is set to 4 and the large-scale fading is drawn from a zero mean log-normal</li> </ul> </li> </ul>

	<p>distribution with a 8 dB standard deviation.</p> <ul style="list-style-type: none"> <li>• Deployment model: <ul style="list-style-type: none"> <li>○ We consider a 3 hexagonal cell system with a radius of 1000 m. Each cell contains 5 users, which are uniformly placed but at least 100 meters away from the serving macro BS.</li> <li>○ We assume that the inter-cell interference of each cell comes exclusively from the other two neighboring cells.</li> </ul> </li> </ul>
Brief update of the results with respect to D3.2	This update is another important (separate) aspect w.r.t. the previous results
Association to the TeC Approach	Massive MIMO for Access
Targeted TCs	TC2 (Dense urban information society)
Impacted HTs	UDN
Required changes for the realization with respect to LTE Rel. 11	None
Trade-off required to realize the gains	Feedback channel from BS to UE during uplink

### 7.12.3 Impact on Horizontal Topics

T3.1 TeC 9b - HT.UDN	
Technical challenges	Uplink power control for both pilot and data transmissions
TeC solution	Iterative joint pilot/data power control scheme
Requirements for the solution	Feedback channel from BS to UE during uplink
KPIs addressed and achieved gain	Transmit power saving: up to 95%
Interaction with other WPs	Not Applicable

### 7.12.4 Addressing the METIS Goals

T3.1 TeC 9b	
1000x data volume	
10-100 user data rate	
10-100x number of devices	
10x longer battery life	Yes
5x E-E reduced latency	
Energy efficiency and cost	Power saving up to 95% of current power control

### 7.12.5 References

[FJS10] G. Fodor, M. Johansson, and P. Soldati, "Near optimum power control and precoding under fairness constraints in network MIMO systems," EURASIP International Journal of Digital Multimedia Broadcasting, vol. 2010, pp. 1-17, Mar. 2010.



[SKZ10] Y.-K. Song, D. Kim, and J. Zander, "Pilot power adjustment for saving transmit power in pilot channel assisted DS-CDMA mobile systems," *IEEE Trans. Wireless Commun.*, vol. 9, no. 2, pp. 488-493, Feb. 2010.

[Mar10] T. Marzetta, "Noncooperative cellular wireless with unlimited numbers of base station antennas," *IEEE Trans. Wireless Commun.*, vol. 9, no. 11, pp. 3590-3600, Nov. 2010.

[RPL+13] F. Rusek, D. Persson, B. K. Lau, E. Larsson, T. Marzetta, O. Edfors, and F. Tufvesson, "Scaling up MIMO: Opportunities and challenges with very large arrays," *IEEE Signal Process. Mag.*, vol. 30, no. 1, pp. 40-60, Jan. 2013.

[NLM13a] H. Q. Ngo, E. G. Larsson, and T. L. Marzetta, "Energy and spectral efficiency of very large multiuser MIMO systems," *IEEE Trans. Commun.*, vol. 61, no. 4, pp. 1436-1449, Apr. 2013.

[GA13] K. Guo and G. Ascheid, "Performance analysis of multi-cell MMSE based receivers in MU-MIMO systems with very large antenna arrays," in *Proc. IEEE Wireless Communications and Networking Conference (WCNC)*, Apr. 2013, pp. 3175-3179.

[JAM+11] J. Jose, A. Ashikhmin, T. Marzetta, and S. Vishwanath, "Pilot contamination and precoding in multi-cell TDD systems," *IEEE Trans. Wireless Commun.*, vol. 10, no. 8, pp. 2640-2651, Aug. 2011.

[HBD13] J. Hoydis, S. ten Brink, and M. Debbah, "Massive MIMO in the UL/DL of cellular networks: How many antennas do we need?" *IEEE J. Sel. Areas Commun.*, vol. 31, no. 2, pp. 160-171, Feb. 2013.

[NLM13b] H. Ngo, E. Larsson, and T. Marzetta, "The multicell multiuser MIMO uplink with very large antenna arrays and a finite-dimensional channel," *IEEE Trans. Commun.*, vol. 61, no. 6, pp. 2350-2361, Jun. 2013.

[CAH+07] R. Chen, J. Andrews, R. Heath, and A. Ghosh, "Uplink power control in multi-cell spatial multiplexing wireless systems," *IEEE Trans. Wireless Commun.*, vol. 6, no. 7, pp. 2700-2711, Jul. 2007.

[GGF+14] K. Guo, Y. Guo, G. Fodor and G. Ascheid, "Uplink Power Control with MMSE Receiver in Multicell Multi-User Massive MIMO Systems," in *Proc. IEEE International Conference on Communications (ICC)*, Jun. 2014, pp. 5184-5190.

## 7.13 T3.1 TeC 10: Decentralized coordinated transceiver design with large antenna arrays [UOULU]

### 7.13.1 General Overview

A minimum power beamforming problem is considered here. The centralised problem is decoupled and decentralised among the base stations (BSs) via fixing the inter-cell interference (ICI) terms per user. A large dimension approximation is applied such that the ICI terms depend only on the statistical properties of the channel vectors (large-scale fading characteristics and antenna correlation). This results in a simplified near optimal algorithm with smaller exchange rate and processing load compared to the optimal centralized solution.

#### System model

The cellular system consists of  $N_B$  BSs and  $K$  single antenna users; each BS has  $N_T$  transmitting antennas. Users allocated to BS<sub>*b*</sub> are in set  $U_b$ . The signal for user  $k$  consists of the desired signal, intra-cell and inter-cell. Assuming  $w_{b,k}$  as transmit beamformer, we solve following optimization problem [TPK11]

$$\begin{aligned} & \text{Min} \sum_{b \in B} \sum_{k \in U_b} \|w_{b,k}\|^2 \\ & \text{subject to} \frac{|w_{b_k,k}^H h_{b_k,k}|^2}{\sigma^2 + \sum_{l \in U_{b_k} \setminus k} |w_{b,l}^H h_{b,l,k}|^2 + \sum_{b \neq b_k} \varepsilon_{b,k}^2} \geq \gamma_k \quad \forall k \in U, b \in B \\ & \sum_{l \in U_b} |w_{b,l}^H h_{b,l,k}|^2 \leq \varepsilon_{b,k}^2 \quad \forall k \neq U_b, b \in B \end{aligned}$$

#### Description of the proposed solution and Analysis

We extended the results derived in [METIS14-D32] for i.i.d channel scenario to a *generic per user channel correlation model*

$$h_{b,k} = \theta_{b,k}^{\frac{1}{2}} g_{b,k}$$

where  $\theta_{b,k}^{\frac{1}{2}}$  is the correlation matrix of user  $k$  and  $g_{b,k}$  is a vector with i.i.d complex entries with variance  $\frac{1}{N_t}$ . This per-user channel correlation model can be applied to various propagation environments.

We have shown that the approximately optimal uplink powers  $\lambda^o_l$  for the generic model are given by [ATR14b, ATR14a]

$$\lambda_k = \frac{\gamma_k}{m_{B_k, \theta_{b_k,k}}(-1)}$$

where  $m_{B_k, \theta_{b_k,k}}(z)$  is defined for  $z \in \mathbb{C} \setminus \mathbb{R}^+$  by [ATR14b],

$$m_{B_k, \theta_{b_k,k}}(z) = \frac{1}{N_t} \text{tr} \theta_{b_k,k} \left( \frac{1}{N_t} \sum_l \frac{\lambda_l \theta_{b_k,l}}{1 + \lambda_l m_{B_k, \theta_{b_k,k}}(-1)} - z I_{N_t} \right)^{-1}$$

The approximation for downlink powers can be derived similarly, see [ATR14b, ATR14a] for details. The above approximations result an algorithm that gives the approximately optimal uplink and downlink powers based on local CSI and statistics of other BS channels. However, the error in approximations causes variations in the resulted SINRs/rates. Thus, the SINR constraints cannot be guaranteed and those might be higher or lower than the target SINRs.

Next, we propose a novel approach for decoupling the sub-problems at base stations. Following the same logic as in [TPK11], ICI is considered as the principal coupling parameter

among BSs and the large dimension approximation for ICI term based on statistics of the channels is derived as [ATR14b],

$$\varepsilon_{b,k}^2 \approx \sum_{l \in U_b} \sqrt{\delta_{b,l}} \frac{1}{N_T} \frac{a_{b,j}^2 a_{b,j,i}^2 m'_{b_k, \theta_{b_k,k}}}{\mu_{b_k,l}^2 \mu_{b_k,k}^2} \quad (-1)$$

$$\mu_{b,l} = 1 + \lambda^o_{l,m_{b,\theta_{b,l}}} (-1)$$

Where,  $\varepsilon_{b,k}^2$  is downlink interference from  $BS_b$  to user  $k$ . This approximation allows derivation of approximately optimal ICI terms based on statistics of the user channels. Each *BS needs the knowledge about user specific average statistics*, i.e., user specific correlation properties and pathloss values from other BSs (these statistics can be exchanged over the backhaul between coordinating network nodes). Based on the statistics, each BS can locally and independently calculates the approximately optimal ICI values. Plugging the approximate ICI into the primal problem decouples the sub-problems at BSs and the resulted SINRs satisfies the target constraints with slightly higher transmit power compared to the optimal method. Dependency of the coupling parameter just on channel statistics results in reduced backhaul exchange rate and processing load. Moreover, the algorithm can be applied to fast fading scenario as the channel statistics (pathloss, correlation properties) change slower than the instantaneous channel realizations.

### 7.13.2 Performance Results

Two algorithms developed in the previous section for multi-cell system with large dimensions provide good approximations even when the dimensions of the problem (i.e. the number of users and antennas) are practically limited. In order to show the performance of the approximate algorithms, some numerical examples are presented in this section. Due to lack of space, we just present the results for the algorithm based on ICI approximation. This algorithm satisfies the target SINRs for all users; however, the error in approximations results a somewhat higher transmit power at BSs. A network with 7 cells is considered and users are equally distributed between cells. Exponential pathloss model is used for assigning the pathloss to each user,

$$a_{b,k} = \left(\frac{d_0}{d_{b,k}}\right)^2$$

Where  $d_{b,k}$  is distance between base station  $b$  and user  $k$ . The pathloss exponent is 2.3 and the reference distance ( $d_0$ ) is 1m. The pathloss from a base station to the boundary of the reference distance of the neighboring base station is fixed to 60dB. The correlation among channel entries is introduced using a simple exponential model

$$[\theta_{b,k}]_{i,j} = \rho^{|i-j|}$$

where,  $\rho$  represents the correlation coefficient which is 0.8 for the following simulations. The users are dropped randomly for each trial and in total 1000 user drops are used for calculating the average transmit power. The number of antennas at each BS varies from 14 to 84 and the total number of users is equal to half the number of antennas at each BS. Thus, *the spatial loading is fixed as the number of antennas is increased*. Figure 7-40 and Figure 7-41 illustrate the transmit powers versus the number of antennas for 0 dB and 10dB SINR target respectively. It is clear that the gap between the approximated and optimal algorithm (denoted as SOCP [TPK11]) diminishes as the number of antennas and users increase. Small gap in small dimensions indicates that the *approximate algorithm can be applied to the practical scenarios with a limited number of antennas and users*. From the results it is clear that SOCP algorithm and the approximated ICI algorithm outperform the ZF method. Note that the number of antennas at each BS per number of served users is increasing while the gap between ZF and optimal and approximated method is fixed which is due to the fixed ratio of the number of antennas to the total number of users. The gap in performance is mainly due to

the fact that the ZF algorithm wastes a degree of freedom for nulling the interference towards the distant users while the SOCP algorithm finds the optimal balance between interference suppression and maximizing the desired signal level. MF beamforming must be dealt with more care since it completely ignores the interference (both intra- and inter-cell) and hence the SINR target is below the target SINR indicated by magenta plots in Figure 7-40 and Figure 7-41. Note that MF beamforming can satisfy the target SINR only asymptotically in a very special case, i.e., when the ratio of the number of antennas to the number of users approaches infinity.

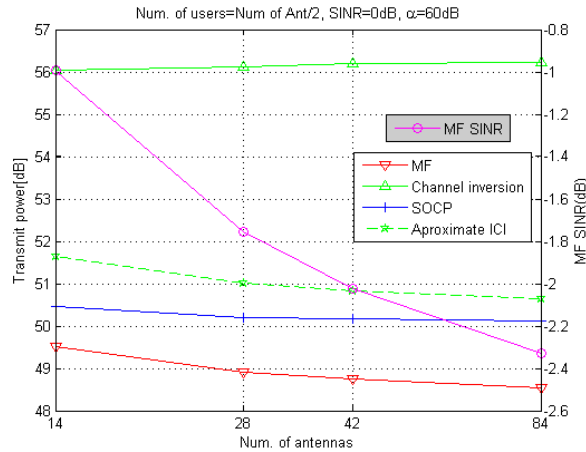


Figure 7-40: Comparison of required transmit power for 0 dB SINR target

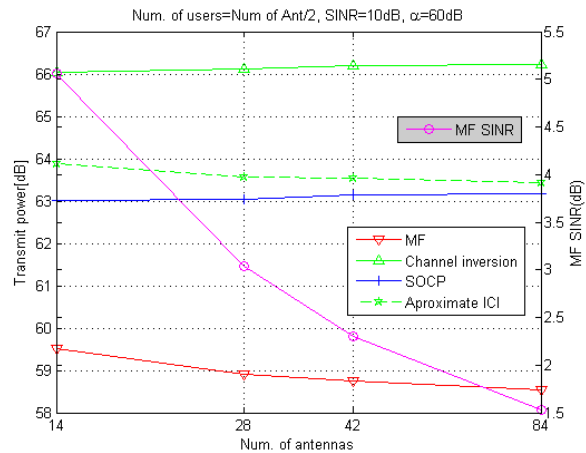
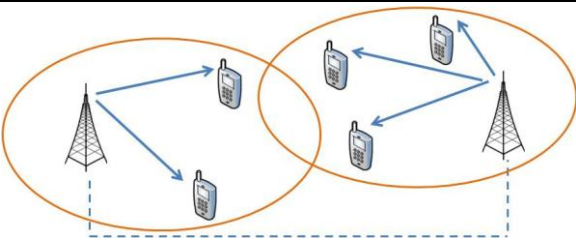


Figure 7-41: Comparison of required transmit power for 10 dB SINR target

T3.1 TeC 10 - Decentralized coordinated transceiver design with large antenna arrays	
	<p><b>Main Idea</b></p> <p>MIMO interfering broadcast channel (IBC) and interfering multiple access channel (IMAC) are considered. Each BS serves its own set of user terminals and co-channel transmissions from each BS cause interference to the user terminals of other cells. Inter-cell interference (ICI) is a key parameter in the design of distributed beamforming algorithm as it couples the sub-</p>
<p>A decentralized beamforming algorithm is</p>	



considered with backhaul signaling among BSs.	problems at BSs. In this work, a large dimension approximation based on the channel statistics (correlation, pathloss) for the optimal ICI is considered. According to this approximation an algorithm is proposed for decoupling the sub-problems at BSs which results in a significant reduction in backhaul information exchange rate and processing load. This algorithm guarantees the target SINRs without any major loss of performance as compared to the optimal centralized design as the dimensions of the system grow large.
Considered SoA solution	
KPIs considered and achieved gain	Transmit power reduction Reduced signalling between network nodes (backhaul traffic)
Performance evaluation approach	Analytical and Simulation-based
System model considered	Multi-cell, multiple users with interferences considered in frequency flat fading.
Deviation compared to Simulation Baseline	Minor: <ul style="list-style-type: none"> <li>• Model of environment: N/A (Per user channel model)</li> <li>• Spectrum Assumptions: Frequency agnostic</li> <li>• Propagation model: N/A (Per user channel model)</li> <li>• Deployment model: 7 cell wrap around</li> <li>• User/Device Distribution: 14-42 users dropped to random locations in cells</li> <li>• Traffic model: No traffic model</li> </ul>
Brief update of the results with respect to D3.2	Extension of results from i.i.d model to a generic per user channel model and evaluation of performance based on MC simulations.
Association to the TeC Approach	Tech Approach 2: Massive MIMO for Access
Targeted TCs	TC 1,2 and 4: Specific Challenge: Reduce energy consumption, backhaul signalling and cost of infrastructure and UEs. Increase availability and reliability. Solution: Transceiver complexity is reduced with minimal information exchange between transmitter nodes to realise the proposed algorithm based on random matrix theory for large antenna regime Requirements: Exchange path loss values and correlation properties of active users between coordinating BSs in the network, i.e. improved x2 type interface is required. Expected Gain: Transmit power reduction. Reduced signalling between network nodes (backhaul traffic).
Impacted HTs	UDN
Required changes for the realization with respect to LTE Rel. 11	Major, improved x2 type interface is required.
Trade-off required to realize the gains	Exchange path loss values and correlation properties of



	active users between coordinating BSs in the network lead to somewhat more signalling as compared to non-cooperative baseline
--	---

### 7.13.3 Impact on Horizontal Topics

T3.1 TeC 10 - HT.UDN	
Technical challenges	Coordination in multiple user environment
TeC solution	Reduced complexity transceiver solution with minimal information exchange between transmitter nodes. Only statistics of active users need to be exchanged between coordinating BSs
Requirements for the solution	Sufficient information exchange mechanisms between network nodes to realise the proposed algorithm which relies on random matrix theory for large antenna regime, i.e., improved x2 type interface is required.
KPIs addressed and achieved gain	Transmit power reduction, reduced signalling between network nodes.
Interaction with other WPs	WP4: The proposed scheme targets interference limited-scenarios and a close alignment is needed with WP4 where interference management is an important topic.

### 7.13.4 Addressing the METIS Goals

T3.1 TeC 10	
1000x data volume	Large beamforming gains are available to improve the user rates accordingly, interference control benefits especially the cell edge users
10-100 user data rate	Large beamforming gains are available to improve the user rates accordingly, interference control benefits especially the cell edge users
10-100x number of devices	By increasing the number of antennas at the BS by X may increase the number of devices by the same factor.
10x longer battery life	
5x E-E reduced latency	
Energy efficiency and cost	Large transmit power reduction is achieved for fixed QoS targets, reduced signalling between network nodes, signal processing is distributed among multiple serving nodes

### 7.13.5 References

[TPK11] A. Tölli, H. Pennanen, and P. Komulainen, "Decentralized Minimum Power Multi-cell Beamforming with Limited Backhaul Signalling", IEEE Trans. on Wireless Comm., vol. 10, no. 2, pp. 570 - 580, February 2011.

[ATR14a] H. Asgharimoghaddam, A. Tölli, and N. Rajatheva, "Decentralizing the optimal multi-cell beamforming via large system analysis," Sydney, Australia, Jun. 2014.



[ATR14b] H. Asgharimoghaddam, A. Tölli, and N. Rajatheva, “Decentralized Multi-cell Beamforming via Large System Analysis in Correlated Channels” Lisbon, Portugal, 2014.

[LHDA10] Subhash Lakshminarayana, Jakob Hoydis, Mérouane Debbah, Mohamad Assaad. Asymptotic analysis of distributed multi-cell beamforming. PIMRC 2010, 26-29 September 2010, Istanbul, Turkey. pages 2105-2110, IEEE, 2010.

[DY10] Dahrouj H. & Yu W. (2010) Coordinated beamforming for the multicell multiantenna wireless system. IEEE Transactions on Wireless Communications 9, pp. 1748–1759.

[WCMD12] Sebastian Wagner, Romain Couillet, Merouane Debbah, Dirk T. M. Slock “Large System Analysis of Linear Precoding in Correlated MISO Broadcast Channels under Limited Feedback”. IEEE Trans. Inf. Theory, vol. 58, no. 7, pp. 4509 - 4537, Jul. 2012.

[METIS14-D32] METIS D3.2, “First performance results for multi-node/multi-antenna transmission technologies”, Apr. 2014.

## 7.14 T3.1 TeC 11: Massive SDMA with a LSAS exploiting elevation and azimuth beamforming [HHI]

### 7.14.1 General Overview

This technical component exploits the advantages of massive (MIMO) in particular the spatial multiplexing and array gain offered by the use of large antenna system at the base station (BS). In theory the sum-throughput  $R$  scales linear with the number of spatial multiplexed users  $R \sim K_c$  and logarithmic with the number of antennas  $R \sim \log_2(N)$ . Following the METIS test case 2 “Dense urban information society” [METIS11] treading the forecast increase of devices we load the system in this technology component with many users. The transmission strategy is depicted in Figure 7-42 and can be divided into the following three parts applying a two-stage beamforming:

1. Inter-group interference aware clustering of co-located users into groups
  - I. First beamforming
2. Per group: User selection for downlink transmission on same time-frequency resource
3. Per group: Inter-cell interference aware precoder design for selected user
  - II. Second beamforming

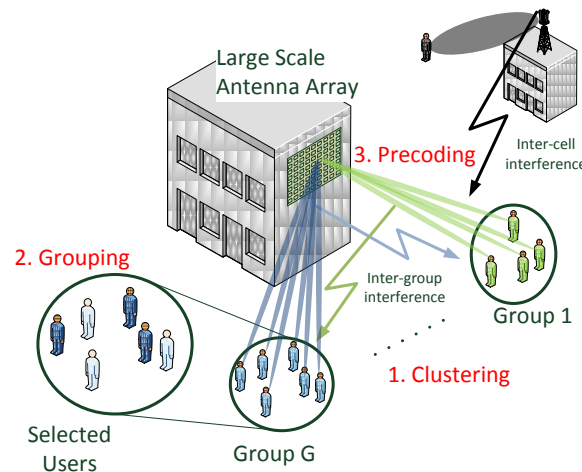


**Figure 7-42: Inter-group interference clustering, user-grouping and inter-cell-interference aware precoding with massive MIMO antenna arrays**

In the first step the user-clustering, we divide the set of users  $\mathcal{K}$  into  $G$  groups of users with similar second-order channel statistics. We use the joint spatial division multiplexing (JSDM) concept of pre-beamforming from [ANAC13] to spatially separate the channels of each user-group. We adapted a density based clustering algorithm from [EKX96], called DBSCAN (density-based spatial clustering of applications with noise). This algorithm clusters an adaptive number of groups with respect to a certain user density which we adapted to the level of inter-group interference.

In the second step, which is done independently for each group we use semi-orthogonal user selection (SUS) based grouping [YG06] to find a subset of users for simultaneously downlink transmission on the same time-frequency resource. In this work SUS algorithm is adapted with the maximum sum-rate objective using projection based rate approximation according to [TKBH12]. With this we ensure that the limited available transmit power split to an increasing number of spatial resources doesn't result in a loss of sum-throughput [KRTT13].

In the third step, after the users are clustered in groups and in each group a subset of users is scheduled the precoder used for beamforming at the BS is designed. Due to out-of cell interference from BSs with a low number of antennas, e. g. current LTE base stations, this so called inter-cell interference has to be considered to balance signal, multi-user interference and inter-cell interference in the right way [KTH14]. We use regularized zero-forcing where inter-cell interference can be taken into account in the regularization values. Therefore, we introduced a scalar broadband power-value of the interference-covariance matrix at the users which to be feedback from the users to the base station in a time division duplex system.

Note that step one is based on slowly-varying statistical channel information (second order statistics) which is assumed to be constant over several transmission time intervals (TTIs). In contrast to this step, two and three are performed on a TTI level taking into account the effective channel feedback either from downlink training and feedback in FDD or uplink estimation in TDD.

Combining all these three concepts we showed that large performance gains in terms of sum-throughput up to 10 times can be achieved compared to baseline scenarios with 8 antennas, e.g. in LTE-A release 11 [3GPP14-36213] utilizing:

1. Spatial multiplexing gain serving many users on the same time-frequency resource
2. Beamforming gain of a large antenna array and the
3. Power gain of pool power constraint over all antennas.

### 7.14.2 Performance Results

To evaluate the first step of our approach we assume a single sector with an [1x256] antenna array and 6 physical nearby located clusters of users, each consisting of 6 users shown in Figure 7-43. This clustering into space-orthogonal groups has to be done with respect to inter-group interference. The clustering with the well-known K-means++ algorithm with the joint spatial division multiplexing scheme as in [NAAC14] is not practical for this task because the number of groups  $G$  is required as input which is not known a-priori. An exhaustive search for the optimal  $G$  of each user constellation is hardly feasible. Therefore, we looked into the class of density based clustering algorithms [KKSZ11] adapting the DBSCAN algorithm from [EK SX96].

The input parameters  $\delta$  and  $P_{min}$  define the density which is required to form a group and given by

1.  $P_{min}$ : minimum number of users to form a group;
2.  $\delta_{i,j} = \left\| U_i^* U_j^* \right\|_F^2$ : Frobenius norm of the dominant eigenvectors of the transmit correlation matrices of user  $i$  and  $j$  [ANAC13].

With  $P_{min} = 1$  this results in the extreme cases  $\delta = 1$  only users with the same transmit correlation matrix are in the same group and  $\delta = 0$  all users are in the same group. With this  $\delta$  can be interpreted as a measure of the interference among users. We assume perfect knowledge of the transmit correlation matrix and the dominant eigenvectors are obtained by singular value decomposition.

In Figure 7-44 we compare the K-means++ and DBSCAN algorithm with the LTE baseline scenario. For the baseline we assume 8 antennas and zero-forcing multi-user beamforming. The number of groups for the K-means++ algorithm is set to  $G_{Kmeans} = 6$  according to the placement in Figure 7-43. The parameters for the DBSCAN algorithm are  $P_{min} = 1$  and  $\delta = 4 \cdot 10^{-4}$ . Note that  $\delta$  is a system design parameter and can be obtained by offline optimization or measurements and adjusted in the run time. The simulation parameters are summarized in Table 7.7.

In Figure 7-45 the multi-user interference is depicted as the receive power per user for all spatial streams where we see cross-interference as blocks from group 1 to 2, 2 to 3, 5 to 4 and 6 to 5. The interference inside of a group is mitigated by the second beamforming per group, zero-forcing precoding. Note, that the channel is not symmetric so inter-group interference doesn't have to be symmetric between groups.

**Table 7.7: Simulations assumptions**

Parameters part 1: Clustering		Parameters part 2 and 3: User grouping and interference aware precoding	
Channel model	One-ring []	Channel model	QUADRIGA [JRBT14]
Deployment	Single cell	Deployment	Multi cell hexagonal
Number BS antennas	256	Number of BS antennas	$[8 \times 16] = 128$
Number users	64	Number users	40...120
Number MS antennas	1	Number MS antennas	1
Transmit power	70 dB	Transmit power	43 dBm
Clustering: K-means++	$G_{Kmeans} = 6$	User distribution	Uniform random
Clustering: DBSCAN	$P_{min} = 1,$ $\delta = 4 \cdot 10^{-4}$	User grouping	WUS or SUS
Beamforming 1	Eigenbeamforming	Beamforming 1	-
Beamforming 2	Per group zero-forcing	Beamforming 2	Regularized zero-forcing

To evaluate the second and third step of our approach we use the more realistic QUADRIGA (quasi deterministic radio channel generator) [JRBT14]. Furthermore we set  $\delta = 0$  resulting in 1 group due to the uniform user distribution in the sector. We also consider a rectangular antenna array of size  $[8 \times 16]$  with practical patch antennas from [BH07a] which is deployed in the sector of interest surrounded by 2-antenna LTE base stations shown in Figure 7-46. The main simulation assumptions are summarized in Table 7.7 and further details can be found in [KTH14].

Assuming perfect channel knowledge of the downlink user channels at the BS Figure 7-47 shows the multiplexing gain increasing the number of user candidates  $K = |\mathcal{K}|$  from 40 to 120. Thereby we consider two following modes user grouping modes:

1. WUS: Without user selection (WUS) the set of scheduled users  $\mathcal{K}_{WUS} = \mathcal{K}$
2. SUS: With semi-orthogonal user selection (SUS) the set of scheduled user  $\mathcal{K}_{SUS} \subset \mathcal{K}$

In the second mode the selection of subset  $\mathcal{K}_{SUS}$  is done by semi-orthogonal user selection with maximum sum-throughput objective as in [TKBH12].

For multi-user precoding we consider regularized zero-forcing given from [PHS05]. The regularization value  $RV$  of user  $k$  is obtained by

$$RV_k = \frac{1}{N_{RB}} \sum_{i=1}^{N_{RB}} \text{trace}(\mathbf{z}_{k,i}), \quad (1)$$

where  $N_{RB}$  is the number of resource blocks in frequency and  $\mathbf{Z}_{k,i}$  is the interference covariance matrix on resource block  $i$  and user  $k$ . Further details of our proposed feedback are given in [KTH14]. This low rate feedback is a wideband scalar power value of the interference observed at the users which is not known at the BS in time division duplex from channel estimation. Due to the averaging in frequency and space the feedback interval can be several resource blocks.

To clearly show the value of user-grouping we force  $RV_k = 0$  for black lines with lower triangles in Figure 7-47 resulting in “classical” zero-forcing precoding from [YG06]. Applying mode 1 we observe that distributing the transmit power to more users decreases the signal while the noise out of cell interference is constant, leading to a turning point where the multiplexing gain no longer leads to increased sum-throughput. In contrast to this mode 2 stops to increase  $K_c = |\mathcal{K}_c|$  at a certain point and increasing  $K$  further provides only a diversity gain for the user selection.

Red lines with upper triangles in Figure 7-47 consider the regularization values from Equation (1). With this we observe a gain of 150 and 20% at  $K = 120$  for mode 1 and 2, respectively. The effect utilized is that multi-user interference is only reduced to the same level as the constant noise and out of cell interference resulting in higher signal power per user and smaller loss due to precoder normalization.

In Figure 7-48 the per antenna power constraint from LTE is relaxed to a pool power constraint for the following two reasons:

1. The same transmit power of 2 antennas in LTE is now distributed over 128 antennas resulting in reduced constraints for amplifiers with  $PAPC_2 = 200 \text{ mW} \gg PAPC_{128} = 1.6 \text{ mW}$  per resource block.
2. The peak to average power ration of the transmitted power per antennas is less than 2 dB because of averaging effects over the number of antennas and served users depicted in Figure 7-49.

The gain we can achieve from the pool power relaxation is shown in Figure 7-48 together with the LTE-A baseline scenario for comparison considering 8 antennas and maximum sum-throughput multi-user scheduling.

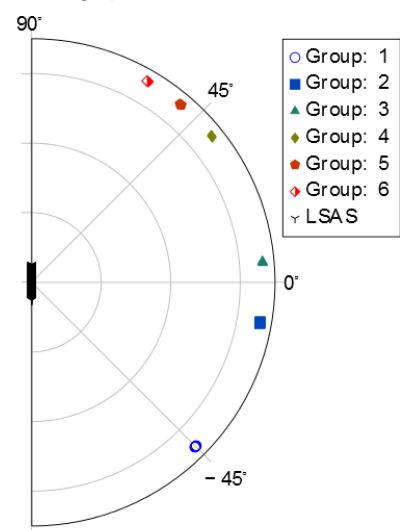


Figure 7-43: User placement for clustering with 6 users per group

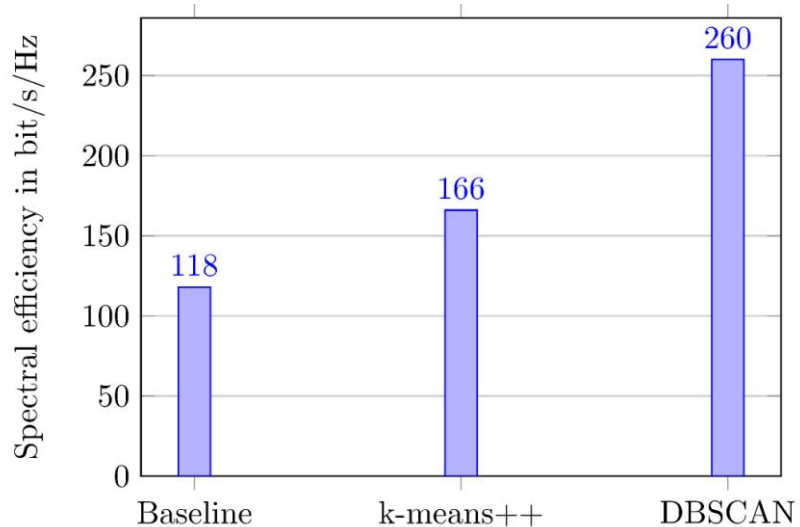


Figure 7-44: JSDM per group precoding comparing LTE-baseline  $N_{LTE} = 8$  antennas with massive MIMO  $N_{LSAS} = 256$  antennas for state-of-the-art k-means++ and new adapted DBSCAN user clustering

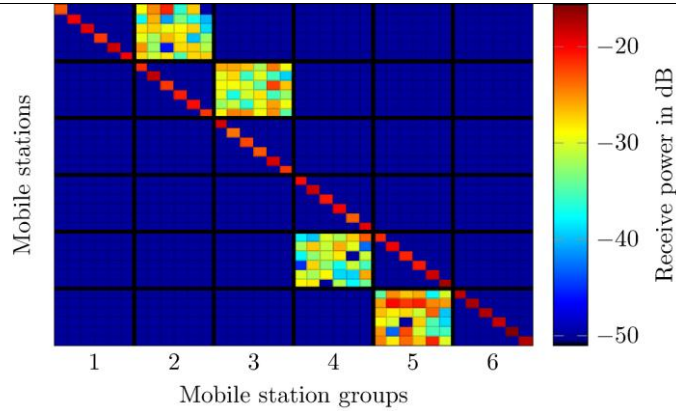


Figure 7-45: Mobile stations receive power per spatial stream

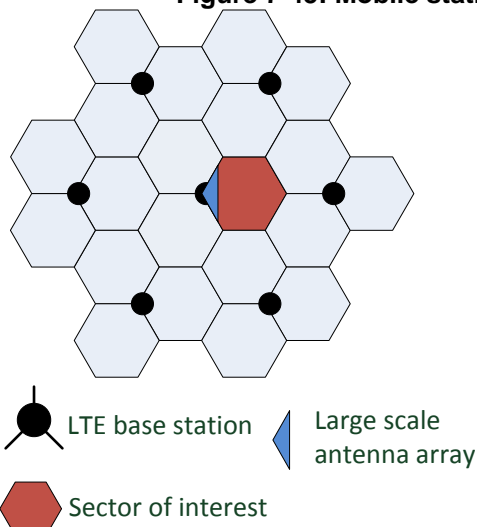


Figure 7-46: Base station deployment for user grouping and interference aware precoding

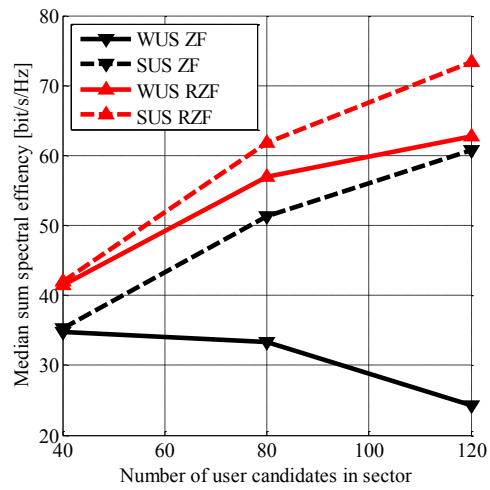


Figure 7-47: Performance over users with and without user selection comparing zero-forcing and regularized zero-forcing with interference power feedback

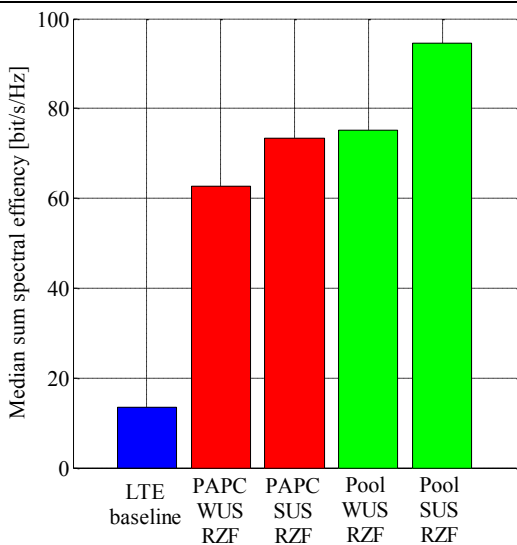


Figure 7-48: Performance comparison at 120 users with and without user selection for per antenna and pool power constraint

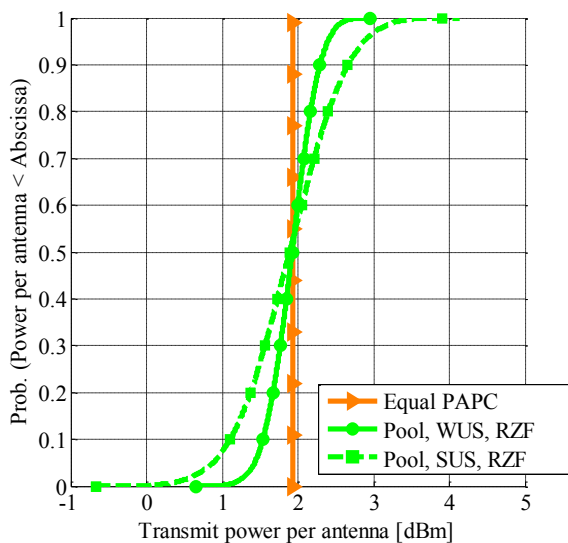
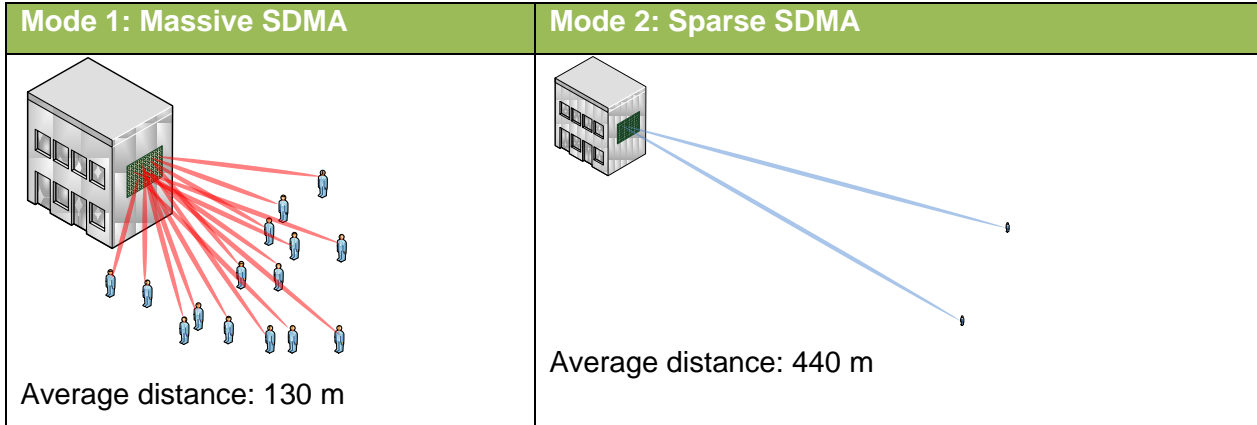


Figure 7-49: Power distribution per antenna with a [8,16] antenna array, pool power constraint with and without user selection

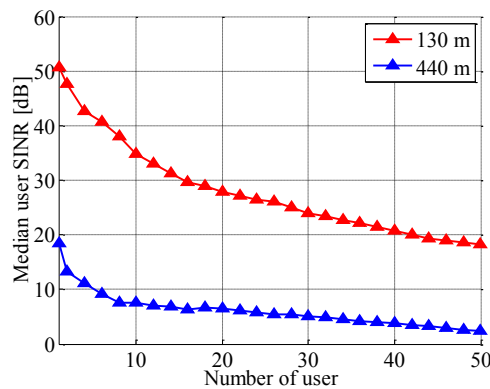
**Flexible use of large antenna array**

- User at cell center (moderate - high SNR): massive spatial multiple access (M-SDMA)
- User at cell edge (low – moderate SNR): sparse spatial multiple access (S-SDMA)



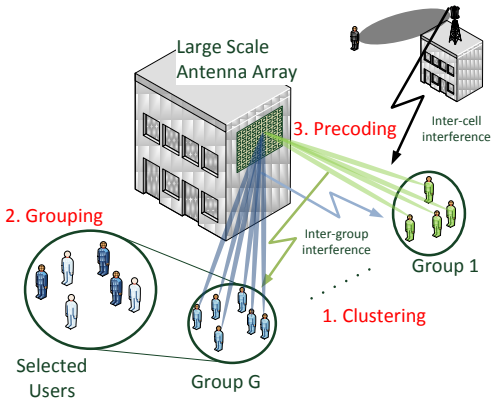
Assumptions for suitability study same as for T3.1 TeC 11 in [METIS31] expect the user selection and only the massive antenna BS is considered. The noise level for all user is selected such that user in mode 1 have a SNR=30 dB.

Figure 7-50 shows the median SINR of user in mode 1 and mode 2 varying the number of user. It is intuitive that the more user are multiplexed with the same amount of transmit power the SINR is decreasing. To guarantee a minimum SINR even for user far away with low SNR the BS can switch on the mode 2 “sparse SDMA” and reduce the number of served user until the target SINR is achieved. For example if the target SINR is 5 or 10 dB than 30 or 4 user can be served in the low SNR region, respectively. On mode 1 more than 50 user can be served.



**Figure 7-50: SINR over number of user, mode switching**

### T3.1 TeC 11 – Massive SDMA with Large Scale Antenna Systems

	<p style="text-align: center;"><b>Main Idea</b></p> <p>To utilize the gains of large antenna arrays and many users, we developed a transmission framework consisting of the following three parts applying a two-stage beamforming:</p> <ol style="list-style-type: none"> <li>1. Inter-group interference aware clustering of co-located users into groups             <ol style="list-style-type: none"> <li>a. First beamforming</li> </ol> </li> <li>2. Per group: User selection for downlink transmission on same time-frequency resource</li> <li>3. Per group: Inter-cell interference aware precoder design for selected user             <ol style="list-style-type: none"> <li>a. Second beamforming</li> </ol> </li> </ol>
<p>Considered SoA solution</p>	<p>LTE-A baseline using 8 antennas and multi-user MIMO with sum-throughput maximizing scheduler.</p>
<p>KPIs considered and achieved gain</p>	<p>Median cell throughput gain:</p> <ul style="list-style-type: none"> <li>• <b>User clustering with JSMD and per group precoding</b> <ul style="list-style-type: none"> <li>○ Kmeans++ clustering: 40 %;</li> <li>○ DBSCAN clustering: 130%</li> </ul> </li> <li>• <b>Interference aware precoding and pool power constraint:</b> <ul style="list-style-type: none"> <li>○ Without user selection: 430 %;</li> <li>○ With user selection: 700 %</li> </ul> </li> </ul>
<p>Performance evaluation approach</p>	<p>Simulation based: system level evaluation</p>
<p>System model considered</p>	<p>WP 3 task 3.1 simulation baseline</p>
<p>Deviation compared to Simulation Baseline</p>	<p>Minor:</p> <ul style="list-style-type: none"> <li>• Model of environment: WINNER urban macro</li> <li>• Center frequency: 2.6 GHz</li> <li>• Propagation model: Fast fading and 100% NLOS with QUADRIGA channels [JRBT14]</li> <li>• Deployment model: 3 sites per BS in a hexagonal grid with an inter site distance ISD=500m</li> <li>• User distribution: uniform random</li> <li>• Traffic model: full buffer</li> </ul>
<p>Brief update of the results with respect to D3.2</p>	<p>Final results on inter-group interference aware user-clustering, user grouping and inter-cell interference aware precoding.</p>
<p>Association to the TeC Approach</p>	<p>T3.1: Massive MIMO for Access</p>
<p>Targeted TCs</p>	<p>TC2 (Dense urban information society)</p>



Impacted HTs	Ultra Reliable Communications (URC)
Required changes for the realization with respect to LTE Rel. 11	Major: <ul style="list-style-type: none"> <li>• New low rate feedback about the ICI (single wide-band power value on a long term time interval)</li> <li>• Effective CSI of the downlink channel at the BS</li> <li>• Deployment of many active antennas</li> </ul>
Trade-off required to realize the gains	The gains achieved for this TeC are obtained by deployment of many active antennas and accurate CSI from many users at the BS.

### 7.14.3 Impact on Horizontal Topics

T3.1 TeC 11 - HT.URC	
Technical challenges	Guarantee a target SINR/rate for user with low geometry factor or SNR
TeC solution	Flexible use of large antenna array with mode switching: <ul style="list-style-type: none"> <li>• Mode 1: Massive spatial division multiple access (M-SDMA) for a lot of user with high SNR</li> <li>• Mode 2: Sparse spatial division multiple access (S-SDMA) for only a few user with low SNR to guarantee a certain target SINR</li> </ul>
Requirements for the solution	Indicator of minimum SINR requirement
KPIs addressed and achieved gain	See results below Table.
Interaction with other WPs	<ul style="list-style-type: none"> <li>• WP2: TeC developed by assuming OFDM, no major change expected when other air interfaces like UFMC are employed</li> <li>• WP4: Interference is taken into account for beamforming by new feedback.</li> <li>• WP5: TeC targets frequencies below 6 GHz</li> </ul>

### 7.14.4 Addressing the METIS Goals

T3.1 TeC 11	
1000x data volume	4-7 times compared to LTE-A baseline with 8 antennas
10-100 user data rate	4-7 times compared to LTE-A baseline with 8 antennas
10-100x number of devices	Up to 10 times the number of devices
10x longer battery life	
5x E-E reduced latency	



Energy efficiency and cost

### 7.14.5 References

- [3GPP14-36213] 3GPP TR 36.213, "Physical layer procedures (Release 11)", Jul. 15.
- [ANAC13] A. Adhikary, J. Nam, J.-Y. Ahn and G. Caire, "Joint Spatial Division and Multiplexing: The Large-Scale Array Regime", *Information Theory, IEEE Transactions on*, vol. 59, pp. 6441-6463, 2013.
- [AV07] D. Arthur and S. Vassilvitskii, "k-means++: The advantages of careful seeding", *Proceedings of the eighteenth annual ACM-SIAM symposium on Discrete algorithms*, pp. 1027-1035, 2007.
- [BH07a] T. Biedermann and F. Hirtenfelder, "A dual-polarized patch antenna with high decoupling", *ITG-Fachbericht-INICA 2007, VDE VERLAG GmbH*, vol. 1, pp. 1-5, 2007.
- [EKX96] M. Ester, H.-P. Kriegel, Jö. Sander and X. Xu, "A density-based algorithm for discovering clusters in large spatial databases with noise", *Proceedings of 2nd International Conference on Knowledge Discovery and Data Mining (KDD)*, vol. 96, pp. 226-231, 1996.
- [JRBT14] S. Jaeckel, L. Raschkowski, K. Borner and L. Thiele, "QuaDRiGa: A 3-D Multi-Cell Channel Model With Time Evolution for Enabling Virtual Field Trials", *Antennas and Propagation, IEEE Transactions on*, vol. 62, pp. 3242-3256, June. 2014.
- [KKSZ11] H.-P. Kriegel, P. Kröger, Jö. Sander and A. Zimek, "Density-based clustering", *Wiley Interdisciplinary Reviews: Data Mining and Knowledge Discovery, Wiley Online Library*, vol. 1, pp. 231-240, 2011.
- [KRTT13] M. Kurras, L. Raschkowski, M. Talaat and L. Thiele, "Massive SDMA with Large Scale Antenna Systems in a Multi-Cell Environment", *AFRICON*, 2013.
- [KTH14] M. Kurras, L. Thiele and T. Haustein, "Interference Aware Massive SDMA with a Large Uniform Rectangular Antenna Array", *European Conference on Networks and Communications (EUCNC) Bologna*, 2014.
- [METIS11] METIS consortium "D1.1 - Scenarios, requirements and KPIs for 5G mobile and wireless system", project report, Apr. 2013.
- [METIS31] METIS consortium, "D3.1 – Positioning of multi-node/multi-antenna transmission technologies," project report, Jun. 2013.
- [METIS32] METIS consortium, "D3.2 – First performance results for multi-node/multi-antenna transmission technologies," project report, Apr. 2014.
- [METIS62] METIS consortium, "D6.2 – Initial report on horizontal topics, first results and 5G system concept," project report, Mar. 2014.
- [NAAC14] J. Nam, A. Adhikary, J.-Y. Ahn and G. Caire, "Joint Spatial Division and Multiplexing: Opportunistic Beamforming, User Grouping and Simplified Downlink Scheduling", *Selected Topics in Signal Processing, IEEE Journal of*, vol. PP, pp. 1-1, 2014.
- [OCB05] H. Ozelik, N. Czink and E. Bonek, "What makes a good MIMO channel model?", *Vehicular Technology Conference (VTC) IEEE 61st*, vol. 1, pp. 156-160 Vol. 1, May. 2005.
- [PDN05] D. T. Pham, S. S. Dimov and C. Nguyen, "Selection of K in K-means clustering", *Proceedings of the Institution of Mechanical Engineers, Part C: Journal of Mechanical Engineering Science, SAGE Publications*, vol. 219, pp. 103-119, 2005.
- [PHS05] C. Peel, B. Hochwald and A. Swindlehurst, "A vector-perturbation technique for near-capacity multiantenna multiuser communication-part I: channel inversion and regularization", *Communications, IEEE Transactions on*, vol. 53, pp. 195-202, 2005.



**Document:** FP7-ICT-317669-METIS/D3.3

**Date:** 25/02/2015

**Security:** Public

**Status:** Final

**Version:** 1

---

[TKBH12] L. Thiele, M. Kurras, K. Börner and T. Haustein, "User-Aided Sub-Clustering for CoMP Transmission: Feedback Overhead vs. Data Rate Trade-off", Signals, Systems and Computers (ASILOMAR), Conference Record of the Forty Sixth Asilomar Conference on, Nov. 2012.

[YG06] T. Yoo and A. Goldsmith, "On the Optimality of Multiantenna Broadcast Scheduling Using Zero-Forcing Beamforming", Selected Areas in Communications, IEEE Journal on, vol. 24, pp. 528 - 541, Mar. 2006.

## 8 Appendix B: Final results for Task 3.2

### 8.1 T3.2 TeC 1: Multi-node resource allocation under imperfect feedback and backhaul channels [CTH]

The work on this TeC is completed. Please refer to [METIS14-D32] for the most updated results.

### 8.2 T3.2 TeC 1b: Non-coherent joint processing CoMP for energy-efficient small cell networks [CTH]

#### 8.2.1 General Overview

The concept of heterogeneous dense networks, which is based on the idea of dense deployment of low-cost and low-power access points coexisting with the traditional macro BSs, has been considered as a key technique to increase the spectral efficiency and energy efficiency for future wireless communication systems. By creating a large number of small cells, these low-power access points have the potential to offload traffic from macro BSs, reduce the average distance between users and transmitters, and increase the system capacity and reduce the transmit power.

Different from the traditional cellular system, the densely deployed access points will be heterogeneous in the number of transmit antennas, transmit power, and coverage area, etc. Moreover, the knowledge of the CSI at each BS is highly likely to be different and imperfect. In this complex scenario, a major research problem is to design low-complexity and robust multi-BS cooperative schemes that improve the overall energy efficiency, at the same time, satisfying QoS expectations of the users. The total power consumption of the network can be modelled with a static part that depends on the transceiver hardware and a dynamic part which is proportional to the transmit signal power. Adding more low-power BSs or more transmit antennas can reduce the dynamic power consumption, but require more hardware, thus, it will increase the static part. Note that the static power consumption also depends on the operation mode of each BS, i.e., whether the BS is active or in the sleep mode [EAR12D23].

Our previous work in [METIS14-D32] mainly focused on the design of CoMP transmission in homogeneous networks. In this work, we study the joint precoding and load balancing problem in the downlink of a heterogeneous network, as illustrated in Figure 8-1. The network consists of different types of BSs, differ in terms of the number of transmit antennas, the power consumption model and the channel propagation model. A number of single-antenna users are randomly deployed in the network. We assume that the BSs are connected via backhaul links, and all BSs are able to transmit to all users at the same time-frequency resource. However, motivated by the fact that tight phase synchronization between BSs is extremely difficult to achieve in practice, only linear non-coherent joint transmission is allowed: that is, each user can be served by a set of BSs using superposition coding. This scheme can be referred to as spatial multiflow transmission, which allows each user to receive different data streams from multiple BSs. In addition, it is assumed that the channels are imperfectly known to the users and the BSs.

The following important system design questions are investigated in our work:

1. How to design precoding matrix for each BS with imperfect CSI?
2. How to select the transmission nodes for each user?
3. How to decide the operation mode (active or sleep) for each BS?
4. How to reduce the energy consumption, at the same time, satisfying QoS expectations of the users?

The above problems can be formulated into a joint resource optimization problem, which minimizes the weighted total power consumption of the system, while satisfying a set of per-user SINR constraints (rate constraints) and a set of per-BS transmit power constraints. The optimization problem is not convex. In particular, when taking BS operation mode (active or sleep) selection into account, the power consumption function leads to a hard combinatorial problem. However, we show that for each fixed combination of BS operation modes, the optimization problem can be reformulated to a convex problem. Then, the global optimum can be found by an exhaustive combinatorial search over these  $2^M$  convex problems, where  $M$  is the number of BSs in the network. Moreover, in order to reduce the complexity, we propose a heuristic algorithm, which resolves the non-convex problem by iterative convex approximations of the power consumption functions.

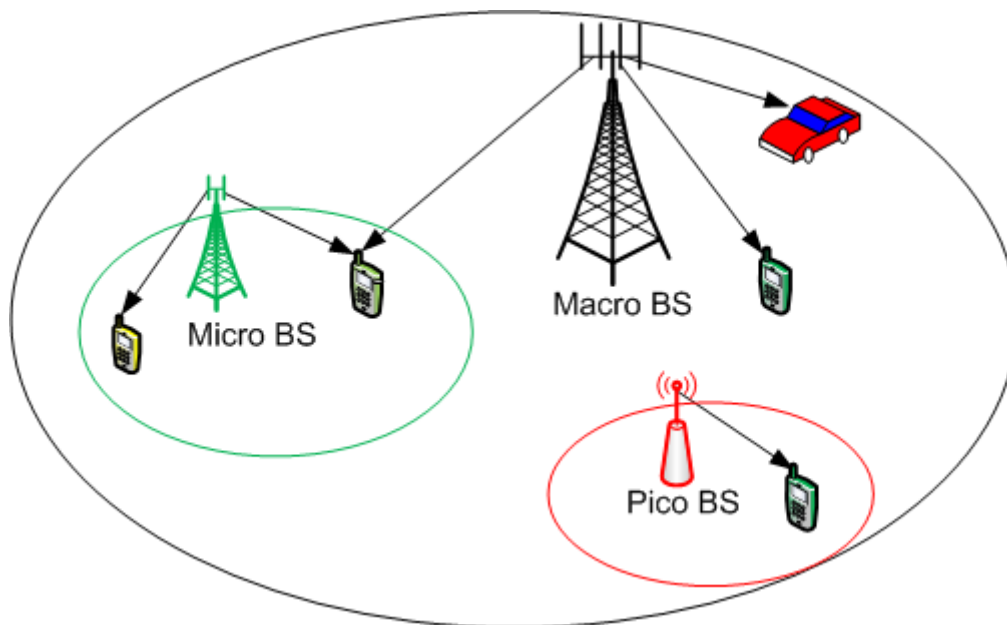


**Figure 8-1: Illustration of a downlink heterogeneous network consisting of macro, micro and pico BSs**

### 8.2.2 Performance Results

System level simulation is performed to illustrate our analytical results and test our proposed algorithms. The environment model is a simplified version of the dense urban information society model (TC2) used in the METIS project, as illustrated in Figure 8-2. The model consists of four square shaped buildings of  $120\text{m} \times 120\text{m}$ , each with 6 floors. A macro BS (MBS) is complemented with 4 small cell BSs (SBSs). The MBS has 4 transmit antennas, and the SBS has 2 transmit antennas each. Five users are randomly and uniformly dropped in the network, with 80% are indoor users and 20% are outdoor users. Here, we adopt the indoor and outdoor propagation models, PS#1-PS#4, identified in METIS. More details regarding network deployment and propagation modes can be found in [METIS13-D61], Table 3.7 and Section 8.1. We assume independent Rayleigh small-scale fading.

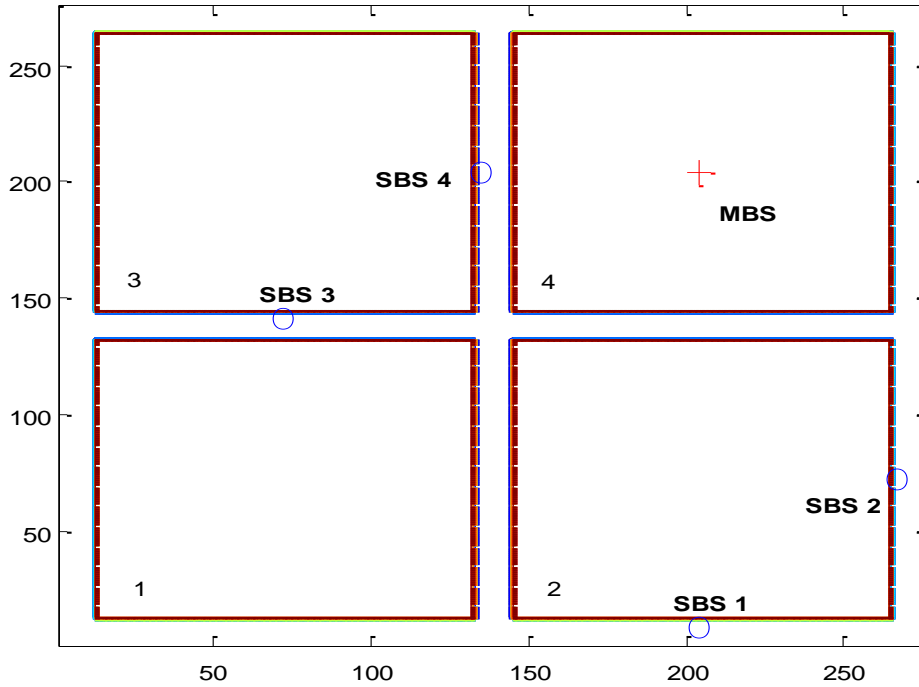


Figure 8-2: The MBS (cross) and SBSs (circles) deployment considered in our simulation

The total power consumption of the network is modelled with a static part that depends on the transceiver hardware and a dynamic part which is proportional to the transmit signal power. Adding more low-power BSs or more transmit antennas can reduce the dynamic power consumption, but require more hardware, thus, it will increase the static part. Note that the static power consumption also depends on the operation mode of each BS, i.e., whether the BS is active or in the sleep mode. In particular, we adopt the linear approximated power consumption model proposed in the EU EARTH project, where the total consumed power of BS  $v$ , is

$$P_v = \begin{cases} N_v P_{\text{active},v} + \Delta_v P_{\text{trans},v} , & 0 < P_{\text{trans},v} \leq P_{v,\text{max}} \\ N_v P_{\text{sleep},v} , & P_{\text{trans},v} = 0 \end{cases} ,$$

where  $N_v$  is the number of transmit antennas at BS  $v$ ,  $P_{\text{active},v}$  is the power consumption at BS  $v$  at the minimum non-zero transmit power,  $P_{\text{sleep},v}$  denotes the sleep mode power consumption of BS  $v$  with  $P_{\text{sleep},v} < P_{\text{active},v}$ , and  $P_{v,\text{max}}$  is the peak transmit power constraint for BS  $v$ . The scaling factor,  $\Delta_v$ , models the impact of the transmit power  $P_{\text{trans},v}$  on the inefficiency of the power amplifiers used at BS  $v$ . Some example values of  $P_{\text{active},v}$ ,  $P_{\text{sleep},v}$ ,  $P_{v,\text{max}}$  and  $\Delta_v$  for different BS types can be found in [EAR12D23]. Table 8.1 shows the power model parameters used in our simulation and is based on [EAR12D23, Table 6 and Table 8].

Table 8.1: Power model parameters for different BS types

BS type	$N_v$	$P_{v,\text{max}}$ [W]	$P_{\text{sleep},v}$ [W]	$P_{\text{active},v}$ [W]	$\Delta_v$
MBS	4	39.8	75.0	130.0	4.7
SBS	2	6.3	39.0	56.0	2.6

Three different joint precoding and load balancing schemes are compared in the scenario depicted in Figure 8-2. We name these three schemes as “Optimal”, “Heuristic” and “All Active” respectively. The “Optimal” scheme obtains the global optimal solution by an exhaustive search over all  $2^5$  possible BS mode combinations. The “Heuristic” scheme follows the proposed iterative heuristic algorithm. The “All Active” scheme is used as our performance

baseline, which solves the optimization problem by assuming that all BSs are active. For each scheme, the performance is average over 1000 independent user drops that provide feasible solutions for our optimization problem. For each user drop, the algorithms are evaluated over 50 independent channel realizations. The power weights are set to 1 for all BSs, implying that the power consumption is equally important among all the nodes.

Define the dynamic part of the total power consumption as the total RF power (i.e.,  $\sum_{v=1}^M \Delta_v P_{\text{trans},v}$ ), and the remaining part of the total power consumption as the circuit power. Figure 8-3 and Figure 8-4 demonstrate the total RF power and the total power consumption as a function of target spectral efficiency per user, respectively. As expected, the total power consumption and the RF power increase as the target spectral efficiency increases. Figure 8-3 shows that the RF power for the “All Active” scheme is less than that of the “Heuristic” and “Optimal” schemes. This is expected since all BSs are active in the “All Active” scheme, whereas for the “Heuristic” and “Optimal” schemes, some BSs are put into the sleep mode. With more BSs being active, the “All Active” scheme provides better energy-focusing and less propagation losses between the users and the transmitters, and will therefore reduce the total RF power. However, as can be seen from Figure 8-4, compared to the “All Active” scheme, the “Heuristic” and “Optimal” schemes can substantially reduce the total power consumption, especially when the target QoS is small. This is because the circuit power consumption under the sleep mode is much lower compared to the one under the active mode, i.e.,  $P_{\text{sleep},v} \ll P_{\text{active},v}$ . For the “All Active” scheme, the increase in the circuit part from the extra power consumed by activating BSs clearly outweighs the decrease in the dynamic part. This implies that putting a BS into sleep mode by proper load balancing is an important solution for energy savings in heterogeneous networks.

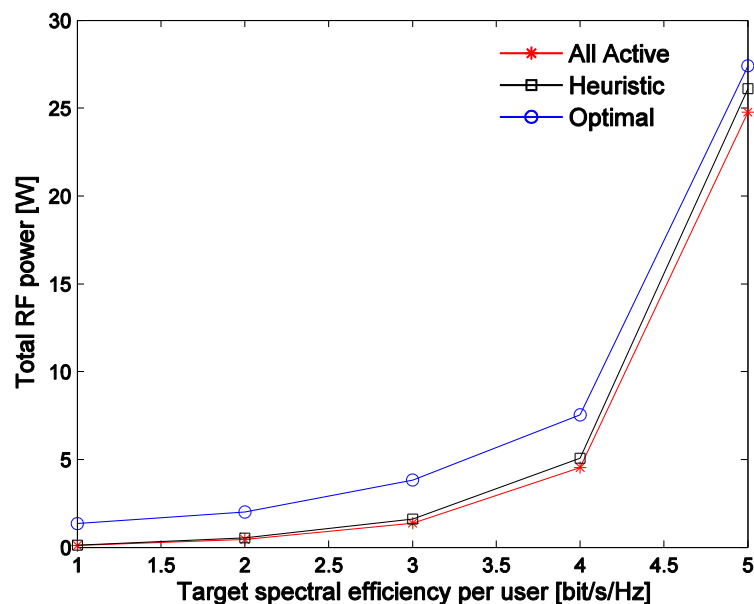


Figure 8-3: Total RF power vs. target spectral efficiency per user

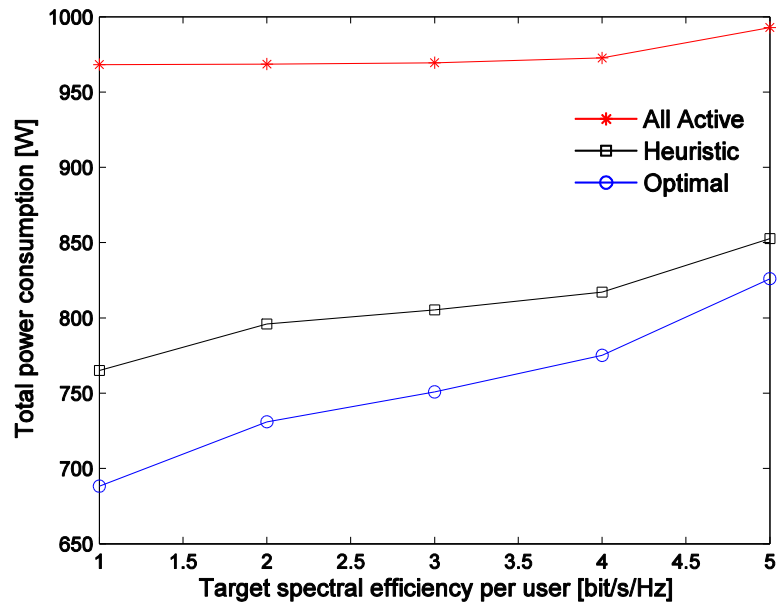


Figure 8-4: Total power consumption vs. target spectral efficiency per user

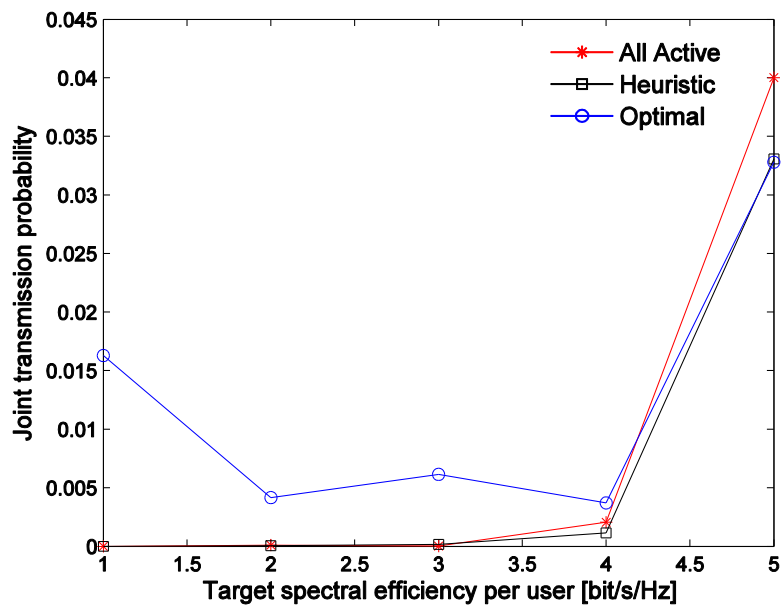
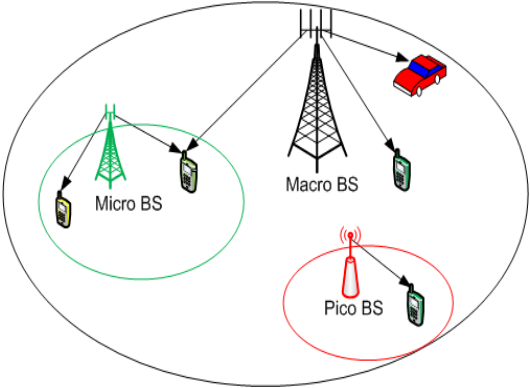


Figure 8-5: Joint transmission probability vs. target spectral efficiency per user

In Figure 8-5 the joint transmission probability has also been evaluated over different targets of spectral efficiency, i.e., for 1,2,3,4,5 bits/s/Hz. Although the system allows all BSs to transmit to all users at the same time-frequency resource, our simulation result shows that the probability that a user is served by multiple BSs is less than 4% for all considered schemes over the considered range of target spectral efficiency per user.

### T3.2 TeC 1b – Non-Coherent Joint Processing CoMP for Energy-Efficient Small Cell Networks

<b>Main Idea</b>	
	<p>This work considers the downlink of a heterogeneous network, where different types of multi-antenna BSs communicate with a number of single-antenna users. We assume that imperfect channel state information is available at both BSs and users. Multiple BSs can serve the users by joint non-coherent multiflow beamforming. Each user performs successive interference cancellation on its own information symbols, and treats both channel errors and co-user interference as Gaussian noise. The precoding, load balancing, and BS operation mode (active or sleep) are jointly optimized for improving the energy efficiency of heterogeneous networks.</p>
Considered SoA solution	Not applicable
KPIs considered and achieved gain	Energy efficiency
Performance evaluation approach	System level evaluation
System model considered	WP3 Task Simulation Baseline
Deviation compared to Simulation Baseline	<p>Minor</p> <ul style="list-style-type: none"> <li>Deployment model: a simplified model consisting of four square shaped building 120m × 120m, each with 6 floors.</li> </ul>
Brief update of the results with respect to D3.2	<p>new KPI: energy efficiency</p> <p>new scenario: heterogeneous networks</p> <p>updated simulation results based on a simplified model of the dense urban information society model (TC2) proposed in [METIS13-D61, Section 8.1].</p>
Association to the TeC Approach	Tech Approach 1: CoMP with Advanced UE Capabilities
Targeted TCs	TC2
Impacted HTs	UDN
Required changes for the realization with respect to LTE Rel. 11	Minor: BSs are connected via backhaul links for control information sharing.
Trade-off required to realize the gains	Control information sharing via backhaul links between BSs.

#### 8.2.3 Impact on Horizontal Topics

T3.2 TeC 1b - HT.UDN	
Technical challenges	imperfect CSI, improve energy efficiency while satisfying QoS requirements at users.



TeC solution	non-coherent joint processing CoMP joint precoding, load balancing, and BS operation mode optimization.
Requirements for the solution	reliable backhaul connectivity between BSs joint control/coordination of BSs
KPIs addressed and achieved gain	energy efficiency
Interaction with other WPs	<b>WP1 (Small):</b> Implications of channel measurements for heterogeneous networks. <b>WP4 (High):</b> Architectural and signaling implications for multi-node coordination. <b>WP6 (Moderate):</b> Non-coherent joint transmission CoMP relies on the feedback and backhaul parameters provided by WP6.

### 8.2.4 Addressing the METIS Goals

T3.2 TeC 1b	
1000x data volume	Under the assumption that the increased area spectral efficiency requirement will be (partly) met by network densification using heterogeneous network nodes, this study targets the resulting energy efficiency challenge.
10-100 user data rate	Under the assumption that the increased area spectral efficiency requirement will be (partly) met by network densification using heterogeneous network nodes, this study targets the resulting energy efficiency challenge.
10-100x number of devices	
10x longer battery life	
5x E-E reduced latency	
Energy efficiency and cost	Putting a BS into sleep mode by proper load balancing for energy savings in heterogeneous networks.

### 8.2.5 References

- [EAR12D2.3] INFISO-ICT-247733 EARTH, Deliverable D2.3, “Energy efficiency analysis of the reference systems, areas of improvements and target breakdown,” Jan. 2012.
- [METIS13-D61] METIS D6.1, “Simulation Guidelines”, Oct. 2013.
- [METIS14-D32] METIS D3.2, “First performance results for multi-node/multi-antenna transmission technologies”, Apr. 2014.

## 8.3 T3.2 TeC 1c: Precoder design with limited information in CoMP networks [CTH]

### 8.3.1 General Overview

In an FDD system, centralized joint transmission (JT) CoMP requires the CSI to be available at a central coordination node to mitigate interference for the cell-edge users. The CSI feedback overhead and its corresponding overhead in the backhaul is reduced with relative thresholding, where the users feedback the CSI from a set of BSs that fall within a threshold relative the best link. Those links that do not fall under this window are not feedback. Such inactive links were previously modelled as zeros in [DOI+12], [LBS12], [PBG+08], [PBG+11].

The limited information for designing the precoding weights can be approached via layered design, such as a PHY layer precoder design, or a MAC layer scheduling approach or a joint design. In our earlier contribution to METIS in [LLB+13] where a MAC layer approach was proposed where a simple ZF precoder is used, and the complexity is moved to the MAC layer for scheduling the best subset of BSs and UEs. In this regard, constrained, unconstrained and block diagonal scheduling schemes were considered. These approaches aim at having a suitable channel matrix for the ZF precoder to function without numerical problems. In the PHY layer approach, the precoder is designed for any set of users that need to be scheduled without any need for a well-conditioned channel matrix. Prior art was based on [LBS12] where a stochastic precoder such as particle swarm optimization (PSO) was introduced that is not only able to design the precoder with limited information but also achieve efficient backhauling. By this we mean that the number of CSI coefficients being fed back by the users is equal to the number of precoding weights for the corresponding active links.

The novel contribution of this work is to use the long term channel statistics already available in the legacy networks as RSSI. This can be used to model the missing CSI coefficients during precoder design at the central coordination node. In particular, this results in a pessimistic precoder design, as these long term channel coefficients show up in the interference terms. In this regard, we propose a successive second order cone programming (SSOCP) with the objective of maximizing the weighted sum rate with the constraint of using limited information and the RSSI as side information under per-antenna power constraint.

### 8.3.2 Performance Results

A homogenous cluster of three BSs cooperate in serving three cell-edge users located at the cluster center. The channel model is based on the 3GPP pathloss model,  $128.1+37.6 \log_{10} r$ , where  $r$  is the distance in kms. Log normal shadowing was used with a shadow fading of 8 dB and the wireless channel also experiences Rayleigh fading. A cell edge SNR of 15 dB was considered. The noise bandwidth is 10 MHz operating at a temperature of 290 K, with a noise figure of 0 dB. The number of channel realizations performed is  $10^3$ .

The Figure 8-6 below shows the CDF of the weighted sum rate of the users at the cell-edge for a relative threshold of 6 dB. The left subplot shows the rate that can be obtained with limited information when designing the precoder at the central coordination node. When there is full CSI feedback and backhauling, it is marked by SSOCP and PSO, while the curves with limited feedback and limited backhauling are marked by SSOCP<sub>0</sub> and PSO<sub>0</sub>. When the RSSI is included naively in the interference terms, it is denoted as SSOCP<sub>PL,0</sub>, and when the RSSI is included as a second order cone (SOC) constraint we have SSOCP<sub>λ,PL,0</sub>. The pessimistic design is prominent when designing the precoder with lower throughput. However, the actual weighted sum rate due to the transmission to the user is capture on the right subplot, where the proposed approach SSOCP<sub>λ,PL,0</sub> outperforms the case with limited information using the RSSI available in existing networks. Also, a reference curve for ZF is provided for the case of full feedback and full backhauling. The results shown here are for single antenna BSs and UEs. The proposed SSOCP algorithm scales with the number of antennas at the BSs in a fully loaded system.

The use of side information in the design of the precoder, as in  $\text{SSOCP}_{\lambda, \text{PL}, 0}$ , provides a relative gain of ~16% when compared with the case when the side information is not used, as in  $\text{SSOCP}_{\text{PL}, 0}$ , for a cell-edge SNR of 15 dB and a threshold of 6 dB. These thresholds are typically observed at the cluster centre, where the cell-edge users are prone to interference.

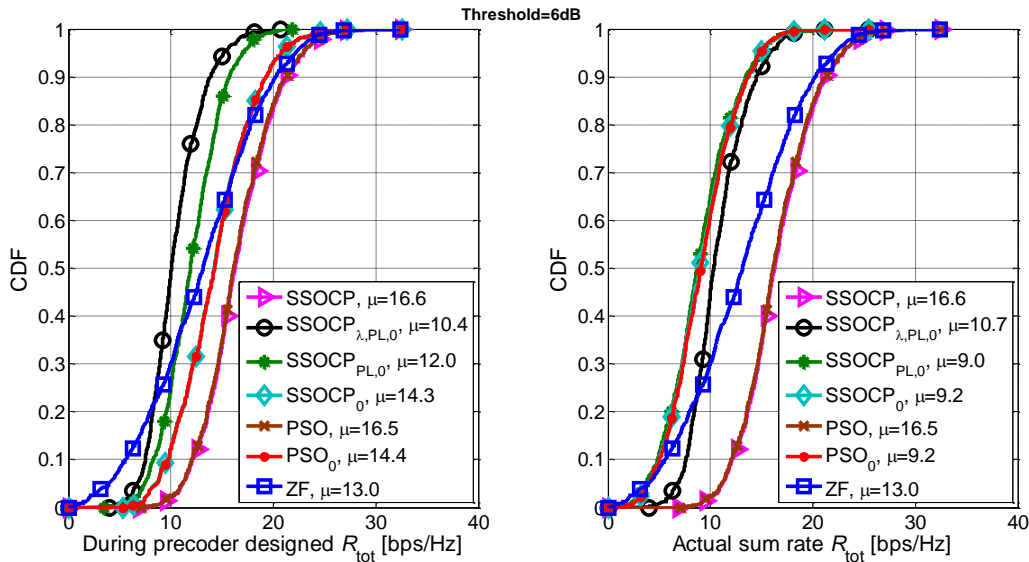
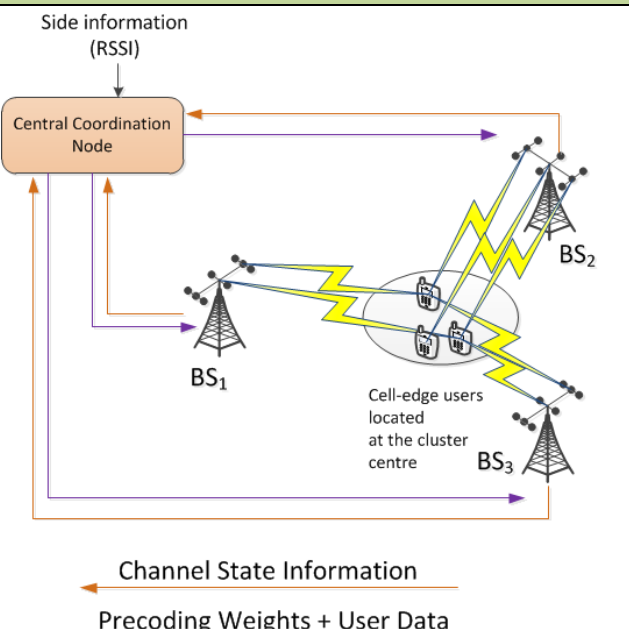


Figure 8-6: CDF of the weighted sum rate when 3 single antenna BSs are cooperating to serve 3 single antenna users

T3.2 TeC 1c – Precoder design with limited information in CoMP networks	
	<p><b>Main Idea</b></p> <p>Precoder design with limited information can be improved with the use of side information such as RSSI that is already available in the existing cellular networks.</p>
<p>Considered SoA solution</p>	<p>Particle swarm optimization was used under limited feedback conditions. The proposed algorithm is compared with this. However, the use of RSSI in the PSO can only be implemented naively as in <math>\text{SSOCP}_{\text{PL}, 0}</math>, whose actual performance is poor, compared to the proposed <math>\text{SSOCP}_{\lambda, \text{PL}, 0}</math>.</p>

KPIs considered and achieved gain	CDF of the weighted sum rate: ~16% gain on average compared to the state of the art. See the results provided above.
Performance evaluation approach	Mainly simulation based and the system design is backed up analytically.
System model considered	Other
Deviation compared to Simulation Baseline	Some: <ul style="list-style-type: none"> <li>• Model of environment: Macro-cellular environment</li> <li>• Spectrum assumptions: 10 MHz bandwidth is used to model the receiver noise power.</li> <li>• Propagation model: 3GPP pathloss model with log-normal shadowing of 8dB and Rayleigh fading is accounted.</li> <li>• Deployment model: Homogenous cluster of BSs</li> <li>• User/Device distribution: Focus on only the cell-edge users</li> <li>• Traffic model: Full buffer</li> </ul>
Brief update of the results with respect to D3.2	New TeC.
Association to the TeC Approach	T3.2 Tech Approach 2: CoMP with limited backhaul capabilities.
Targeted TCs	TC2
Impacted HTs	UDN
Required changes for the realization with respect to LTE Rel. 11	Major. This TeC focuses on intercell interference experienced by the users at the cell-edge. Hence, inter-eNB CoMP is required.
Trade-off required to realize the gains	Nothing additional compared to centralized JT-CoMP in FDD mode, which already expects the users to feedback the CSI typically to its serving BS. In this TeC, the RSSI already available in existing cellular networks is being used.

### 8.3.3 Impact on Horizontal Topics

T3.2 TeC 1c - HT.UDN	
Technical challenges	UDN: RC1
TeC solution	Improved precoder design with limited CSI feedback. Simple precoders such as ZF perform poorly with ill-conditioned channel matrices at the central coordination node. While, PSO can solve the problem of achieving efficient backhauling. However, the RSSI available as side information cannot be used directly, and PSO falls short with the increase in problem size, and also the power constraint is suboptimal. Hence, the proposed technique SSOCF overcomes all these limitations.
Requirements for the solution	Perfect and limited CSI was considered in this



	precoder design.
KPIs addressed and achieved gain	CDF of the weighted sum rate: ~16% gain on average compared to the state of the art. See the results provided above.
Interaction with other WPs	

### 8.3.4 Addressing the METIS Goals

T3.2 TeC 1c	
1000x data volume	
10-100 user data rate	16% improvement in the data rate for the cell-edge users when using the long term statistics.
10-100x number of devices	
10x longer battery life	
5x E-E reduced latency	
Energy efficiency and cost	

### 8.3.5 References

[DOI+12] K. Donghyun, S. Oh-Soon, S. Illsoo, L. Kwang, "Channel Feedback Optimization for Network MIMO Systems," IEEE Trans. Veh. Technol., vol. 61, no. 7, pp. 3315–3321, Sep. 2012.

[LBS12] T. R. Lakshmana, C. Botella, and T. Svensson, "Partial Joint Processing with Efficient Backhauling using Particle Swarm Optimization," EURASIP J. of Wireless Commun. and Netw., vol. 2012, 2012.

[LLB+13] T. R. Lakshmana, J. Li, C. Botella, A. Papadogiannis and T. Svensson, "Scheduling for Backhaul Load Reduction in CoMP," in Proc. IEEE Wireless Communications and Networking Conference (WCNC), Apr. 2013

[PBG+08] A. Papadogiannis, H. Bang, D. Gesbert, and E. Hardouin, "Downlink overhead reduction for multicell cooperative processing enabled wireless networks," IEEE Personal, Indoor and Mobile Radio Commun., 2008

[PBG+11] A. Papadogiannis, H.J. Bang, D. Gesbert, and E. Hardouin, "Efficient Selective Feedback Design for Multicell Cooperative Networks," IEEE Trans. Veh. Technol., vol. 60, no. 1, pp. 196–205, Jan. 2011.

## 8.4 T3.2 TeC 2: Exploiting temporal channel correlation to reduce feedback in CoMP scheme [FT]

The work on this TeC is completed. Please refer to [METIS14-D32] for the most updated results.

## 8.5 T3.2 TeC 2b: DoF and net DoF of recent schemes for the MIMO IC and BC with delayed CSIT and finite coherence time [FT]

### 8.5.1 General Overview

The first part of the work was to evaluate how existing schemes cope with feedback delay. A new metric was defined in order to fairly evaluate the effect of feedback delay. It is called net DoF, and it measures the degrees of freedom (DoF) available taking into account both feedback and training overheads. This net DoF proved to be a judicious metric as some schemes for delayed channel state information at the transmitter (DCSIT) rely on extensive channel information sharing which can severely degrade the performances, for instance [MT10] which is optimal in terms of DoF for completely outdated CSIT requires all the receivers to know their channel and the channels of all other receivers.

This approach allowed us to find interesting techniques that efficiently deals with feedback delay. Among them is one developed for the MISO broadcast channel [LH12] that is singled out as it was the very first solution that allowed preserving the optimal DoF for small feedback delay.

Noticing its potential in [LSY13b] we then extend this technique to multiple cell configurations and to MIMO configurations. More precisely in MIMO configuration we make use of the multiple antennas at receiver to preserve the optimal DoF for longer feedback delay than with single antenna receivers in [LSY13c].

In order to maximize the net DoF another feedback scheme was proposed based on the finite rate of innovation channel models introduced in [LSY13a]: foresighted channel feedback (FCFB). It allows to have constant knowledge of the CSIT at the cost of an increase of training/feedback rate.

Finally, in the context of the Interference Channel (IC), a new scheme is proposed, based on the idea of ergodic interference alignment (IA) [NGJ+12], it allows to approach the full DoF of the SISO IC (and square MIMO IC) for feedback delays up to half the channel coherence time without extra overheads. Basically, the channel realization pairing is modified so that in a coherence block, CSIT are only needed during the second half of the block, hence the robustness to feedback delay up to half the channel coherence time.

### 8.5.2 Performance Results

So far the metric employed to evaluate the different transmission techniques are the DoF and net DoF. The DoF is another appellation of the so called multiplexing gain, it is the prelog of the sum rate. In order to take into account the feedback cost, we define the feedback overhead. Let  $R(P)$  be the ergodic (sum) throughput of a system with transmit power  $P$  and  $F(P)$  the total feedback rate then  $DoF = \lim_{P \rightarrow \infty} \frac{R(P)}{\log_2(P)}$  and  $DoF_{FB} = \lim_{P \rightarrow \infty} \frac{F(P)}{\log_2(P)}$ . The DoF used for training are also taken into account, in the end the net DoF are the DoF available for data transmission. According to this definition they represent the slope of the data sum rate at high SNR.

1) Intermediate results included [METIS14-D32]:

Extension of STIA [LH12], for the MISO BC was identified and extended to MIMO BC and MIMO IC allowing preservation of the optimal DoF of the network for longer feedback delays. Going from MISO to MIMO (both in BC and IC) allow to preserve the sum DoF for feedback delay up to  $1/(N_r/N_t+1) = N_r/(N_t+N_r)$  of the channel coherence time.

The finite rate of innovation (FROI) channel model [LSY13a] allows doing foresighted channel feedback which at a cost of a training/feedback overhead increase gives constant CSIT. The main characteristic of FROI channel models is that they closely approximate stationary band limited signals. This means that if a FROI channel model is a good model, so is an arbitrary time shift of the FROI model. It can be exploited to overcome the feedback delay and have CSIT available all the time, with a channel prediction error SNR proportional to the general SNR. However due to the increase rate of feedback and training net DoF gains are more limited than expected.

2) A new scheme is proposed for the IC which does not require extra overheads and it is robust to feedback delay.

By modifying the channel realization pairing ergodic IA [NGJ+12] in [LSY14a], CSIT are only needed during the second half of the block. The new pairing is illustrated in Figure 8-7.

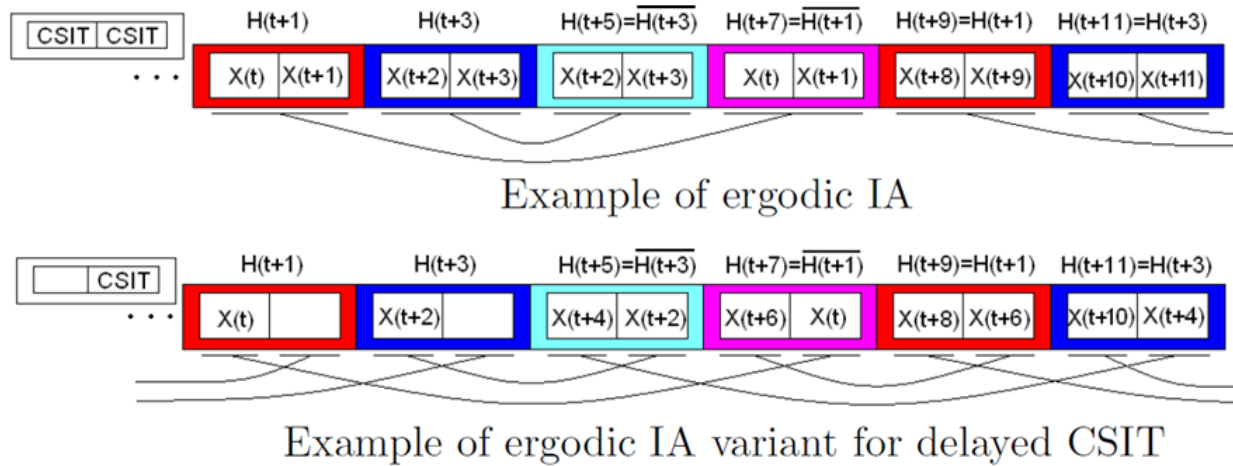


**Figure 8-7: Original and modified pairings**

The variant of ergodic IA proposed works for feedback delay of half the channel coherence time but also for any shorter feedback delay without any modification. The case of longer feedback delay can be dealt with by doing time sharing between the variant we propose and time division multiple access (TDMA) transmission or any technique designed for the SISO IC with completely delayed CSIT. In Figure 8-8, we plot the sum DoF that can be achieved (solid lines) in the K-user SISO IC as a function of the ratio feedback delay/coherence time.

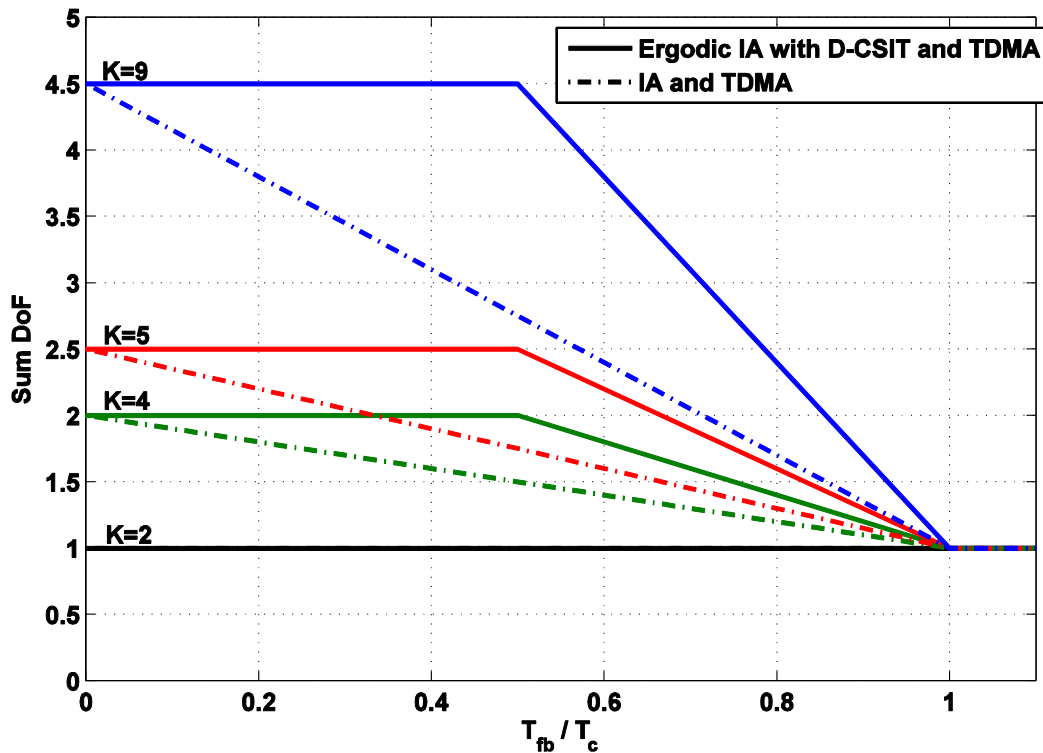
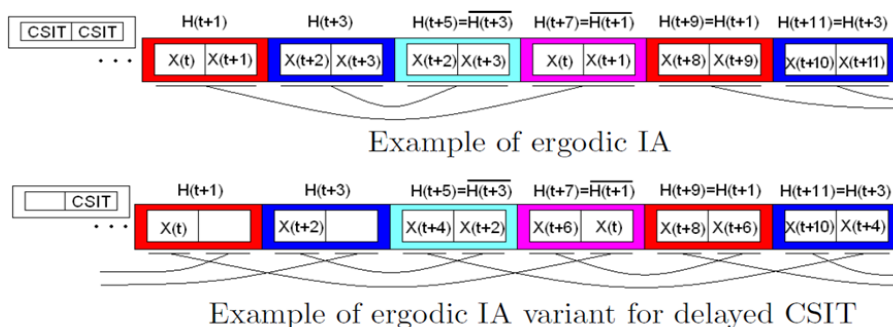


Figure 8-8: Feedback delay-DoF tradeoff in the SISO IC

The dashed lines corresponds to time sharing between IA (when current CSIT is available) and TDMA (otherwise). We observe that the proposed ergodic IA variant significantly improves the sum DoF. The proposed scheme performs also very well in terms on net DoF, i.e., when overheads are taken into account since it does not require any additional overhead compared to traditional ergodic IA. The net DoFs and more details can be found [LSY14b] and confirm that the scheme also brings significant gain when accounting for overheads.

### T3.2 TeC 2b – DoF and net DoF of recent and new schemes for the MIMO IC and BC with delayed CSIT and finite coherence time



#### Main Idea

Modify the ergodic IA scheme so that current CSIT are needed only in the 2nd half of each block.



Considered SoA solution	In [LSY14a] SOA is described and performances are compared
KPIs considered and achieved gain	<ul style="list-style-type: none"> <li>Cell throughput in DoF, gain up to 100%</li> <li>Feedback delay supported without DoF loss, from 0 to half of channel coherence time</li> </ul>
Performance evaluation approach	Analytical
System model considered	Other
Deviation compared to Simulation Baseline	Not Applicable. General theoretical result on IC.
Brief update of the results with respect to D3.2	New scheme for the IC, preserving the full sum DoF for feedback delays up to half of the channel coherence time.
Association to the TeC Approach	Not Applicable
Targeted TCs	Test Case 2 - Dense urban information society
Impacted HTs	UDN
Required changes for the realization with respect to LTE Rel. 11	Major, theoretical results, achievable scheme not easily deployable.
Trade-off required to realize the gains	The scheme proposed was carefully designed to not require extra overheads, however being based on ergodic interference alignment, it requires long decoding delays.

### 8.5.3 Impact on Horizontal Topics

T3.2 TeC 2b - HT.UDN	
Technical challenges	Increase spectral efficiency.
TeC solution	A new transmission scheme is proposed, it significantly increases the spectral efficiency by transmitting at full DoF even when channel state information are not yet available at the transmitter
Requirements for the solution	Backhaul supporting high data rates
KPIs addressed and achieved gain	Cell throughput in DoF, gain up to 100% Feedback delay supported without DoF loss, from 0 to half of channel coherence time
Interaction with other WPs	WP4: interference management is an important topic in WP4.  WP5: frequencies considered below 6 GHz where interference is the limiting factor

### 8.5.4 Addressing the METIS Goals

T3.2 TeC 2b	
1000x data volume	DoF increases means throughput increase at high



	SNR hence possible data volume increase
10-100 user data rate	DoF increases means throughput increase at high SNR hence possible user data rate increase
10-100x number of devices	Decomposability of the proposed scheme means that multiple single-antenna devices can be served as a single multiple-antenna device
10x longer battery life	
5x E-E reduced latency	
Energy efficiency and cost	

### 8.5.5 References

[MT10] M. Maddah-Ali and D. Tse, "Completely stale transmitter channel state information is still very useful," in Proc. Allerton, Monticello, IL, USA, Oct. 2010.

[NGJ+12] B. Nazer, M. Gastpar, S. Jafar, and S. Vishwanath, "Ergodic interference alignment," IEEE Transactions on Information Theory, vol. 58, no. 10, pp. 6355–6371, Oct. 2012.

[LH12] N. Lee and R. W. Heath Jr., "Not too delayed CSIT achieves the optimal degrees of freedom," in Proc. Allerton, Monticello, IL, USA, Aug. 2012.

[LSY13a] Y. Lejosne, D. Slock, and Y. Yuan-Wu, "Finite Rate of Innovation Channel Models and DoF of MIMO Multi-User Systems with Delayed CSIT Feedback", in Proc. ITA, San Diego, CA, USA, Feb. 2013.

[LSY13b] Y. Lejosne, D. Slock, and Y. Yuan-Wu, "Net degrees of freedom of recent schemes for the MISO BC with delayed CSIT and finite coherence time," in Proc. WCNC, Shanghai, China Apr. 2013.

[LSY13c] Y. Lejosne, D. Slock, and Y. Yuan-Wu, "Space Time Interference Alignment Scheme for the MISO BC and IS with Delayed CSIT and Finite Coherence Time", in Proc. ICASSP, Vancouver, Canada, May 2013.

[LSY14a] Y. Lejosne, D. Slock, and Y. Yuan-Wu, "Achieving Full Sum DoF in the SISO Interference Channel with Feedback Delay", IEEE Communications Letters, vol.18, no.7, pp.1202-1205, July 2014.

[LSY14b] Y. Lejosne, D. Slock, and Y. Yuan-Wu, "Net degrees of freedom of decomposition schemes for the MIMO IC with delayed CSIT," in Proc. ISIT, July 2014.

[METIS14-D32] METIS D3.2, "First performance results for multi-node/multi-antenna transmission technologies", Apr. 2014.

## 8.6 T3.2 TeC 3: Distributed precoding in multicell multiantenna systems with data sharing [HWDU]

### 8.6.1 General Overview

The concept of precoders utilizing data sharing (e.g., by caching) and local channel knowledge was introduced in [METIS13-D31], and further developed in [METIS14-D32] (cf. also [LVS14]). The main goal was to enable a form of “light” coordinated multi-point (CoMP) transmission, in the sense of significantly reducing the requirements on the backhaul links’ latencies. The imperfect backhaul is recognized as one of the key issues in fast multi-cell cooperation, especially in the context of small cells and ultra-dense networks. The proposed scheme benefits from the envisaged possibility of smart end-user data sharing/caching in future wireless access networks (cf. e.g. [GMD+13]). The precoding is distributed with respect to the channel state information (CSI) availability, which is assumed to be local for a time-division-duplex (TDD) system. The interference at the users is (approximately) cancelled by a predefined, offline agreement among the base stations (BSs).

For this TeC, the mathematical background was developed and the evaluations in a simplified, 2-cell setting were performed in [METIS13-D31, METIS14-D32]. In this deliverable we focus on further evaluations of the TeC regarding the following aspects:

- It is examined, what performance improvement can be achieved if the cluster size is increased to be more than 2. Increasing the cluster size has several implications. On one hand, the expected performance gains should be evaluated as the proposed DIA scheme in its basic form does not assume constructive addition of the desired signals, but rather focuses on increasing the number of degrees-of-freedom (DoFs) by eliminating the interference. Further, larger coordinated groups of base stations, mean also weaker out-of-cluster interference, which essentially increases the operating system SNR point.
- The simulation evaluation in the previous reports was done using normalized Rayleigh channel models. Here, we first utilize a more sophisticated system-level simulator with 3GPP-like hexagonal deployment and channel parameters, following the first T3.2-RC1 baseline. For this model, we apply a selected “triangle-based” clustering scheme. Further, we evaluate the results on the reduced METIS TC2 (Dense Urban Information Society) model, following the agreed METIS T3.2 baseline [METIS14-D32].

### 8.6.2 Performance Results

Although the DIA approach results in no multi-user interference from inside the cluster, it does not guarantee a constructive addition of the desired signal components like distributed MRT or cooperative multicell precoding (CMP [BZG+10]). Previous results [LVS14] have evaluated DIA under the assumption of two base stations cooperating in one cluster. If the number of cooperating base stations increases, DIA is still able to guarantee no intra-cluster interference. However, the increased cluster size will impact the effective channel of the desired signal, since it will consist of a larger number of components. In order to assess the impact of the number of cooperating base stations, we have extended the previous presented setting [LVS14] consisting of three single-antenna users in an isolated cluster with two cooperating base stations, each equipped with two antennas, to a larger number of cooperating base stations. To this end, we depict in Figure 8-9 for the previous setting the average sum rate with DIA assuming 2, 3, 4 and 10 base stations.

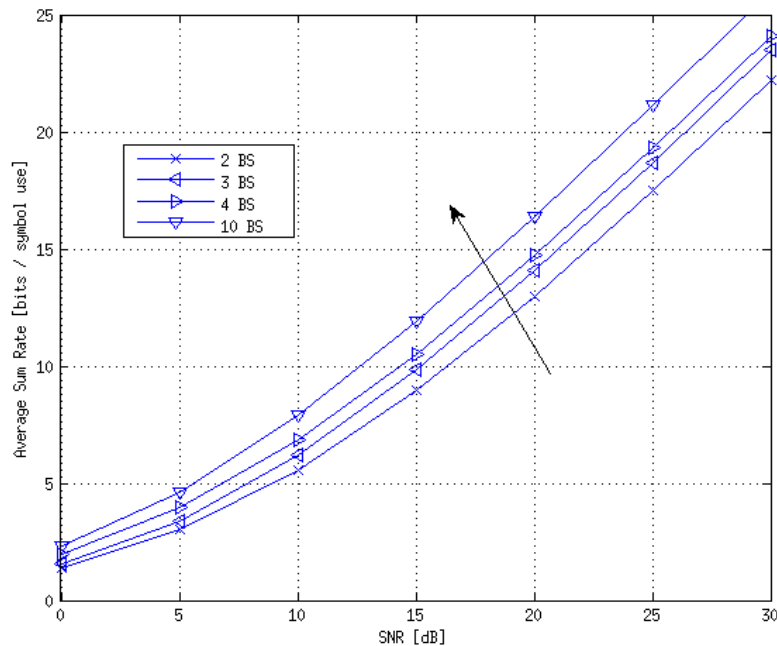


**Figure 8-9: Effect of Increased Cluster Size with DIA. Configurations {2,3,4,10}-2-3-1.**

From the plot, we can observe a performance increase since the effective channel of the desired signal consists of a larger number of components. Despite the fact the increased number of cooperating base stations leads to a diversity gain for the desired signal, note that the DoF, i.e. the slope of the curve, remains unchanged. Although we have disregarded the out-of-cluster interference, we point out that considering more cooperating base stations, indirectly also implies a reduction of the out-of-cluster interference which would be experienced in a cellular network deployment. Besides these issues, we have yet to consider the higher complexity involved with a larger cluster size. However, the optimum operating point taking into account the previous issues and resulting tradeoffs is out of the scope of this work.

Our previous presented results are based on normalized Rayleigh fading channel models. In order to align our simulation results with the first T3.2-RC1-baseline, in this deliverable we employ a more elaborate and realistic system-level simulator referred to as MIDAS (Matlab-based Interference Simulator for Distributed Antenna Systems). MIDAS is a Winner/3GPP-like deployment developed at the Huawei European Research Center, featuring a geometric multipath channel model assuming a ring of scatterers around the users. It offers a simplified albeit flexible system-level platform for evaluating heterogeneous networks consisting of hexagonal sectors with three co-located base stations at a site as shown in Figure 8-10, where the red circles represent the positions of the sites.

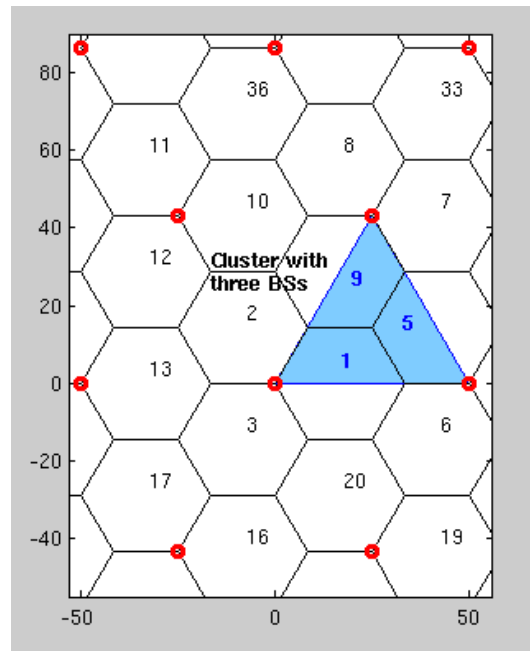


Figure 8-10: Cellular network deployment in MIDAS

In order to implement DIA in the deployment described before, we assume a cluster consisting of the three closest base stations belonging to different sites. With such a clustering scheme, the coverage area of the cluster is described by a triangle as shown in Figure 8-10. We consider such triangular clusters since they reflect better the given cellular hexagonal deployment. Furthermore, we assume the users in this triangle will be served only by the three BSs in the cluster. The numbers in the figure represent the index of the hexagonal sector.

To observe the performance of DIA in a more realistic scenario, we plot in Figure 8-11 the average sum rate of the cluster as a function of cell edge SNR for an isolated cluster (highlighted in Figure 8-10) with base stations that are equipped with two antennas. In addition, we assume there are three single-antenna users uniformly distributed in the cluster and an ISD of 50 meters. We refer to cell edge SNR as the average SNR that a user would experience in the middle of the triangular cluster (where the three sectors of a cluster intersect). We perform 1000 Monte Carlo simulations to compute the average sum rate of the cluster. For a comparison we also include the performance with distributed MRT, distributed ZF and cooperative multicell precoding (CMP) [BZG+10], which represent the state of the art assuming distributed CSI to be available at each of the cooperating BSs. We can clearly observe that:

- DIA outperforms all of the schemes at high SNR and hence, the performance of DIA in the normalized Rayleigh fading channel model [LVS14] can be translated into a more realistic scenario.
- as expected, CMP converges to distributed MRT at low SNR and to distributed ZF at high SNR.
- at low SNR, DIA is outperformed by distributed MRT and CMP. In such a regime, the multi-user interference, which DIA is able to completely null out, is not significant and in fact the optimum strategy is to maximize the strength of the desired signal component, which DIA, in contrast to distributed MRT and CMP, does not consider.
- at high SNR, DIA achieves the maximum DoF, while the other scheme saturates due to the multi-user interference.

- similarly as in our previous results [LVS14], DIA UPC is able to perform better than DIA at low SNRs but is not able to achieve the DoF at high SNR.

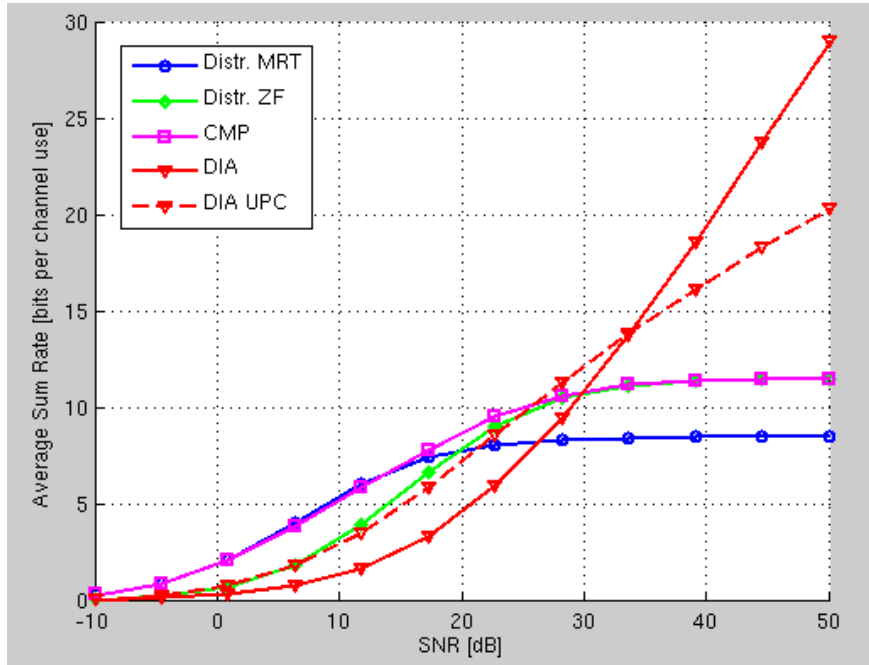


Figure 8-11: Average Sum Rate for different schemes with distributed CSI

As a last comment to this simulation scenario, we point out that at high SNRs, the other distributed schemes can opt to drop one user and serve instead only two users to avoid the sum rate saturation. However, due to the higher DoF being exploited by DIA with three users, DIA is still able to outperform the other distributed schemes with two users at high SNRs.

In order to obtain a more comprehensive view of the performance gain, we plot in Figure 8-12 the CDF of the sum rate of an isolated cluster for different distributed schemes under the previously described scenario with the following system parameters: carrier frequency 3 GHz, bandwidth 10 MHz and available transmit power per BS of 25dBm. Even though one user would not be served over the entire 10 MHz, we assume the ratio of the power to the bandwidth assigned to a user will be the same as the ratio of the total transmit power to the total available bandwidth. For this setting, DIA is able to achieve a gain of about 30%, 45% and 54% in the 10<sup>th</sup> percentile, 50<sup>th</sup> percentile and 90<sup>th</sup> percentile, respectively, with respect to state of the art schemes. Notice that with the given transmit power, the average sum rate with CMP and distributed ZF has already saturated due to the multiuser interference resulting from serving three users with the two antennas per cooperating BS.

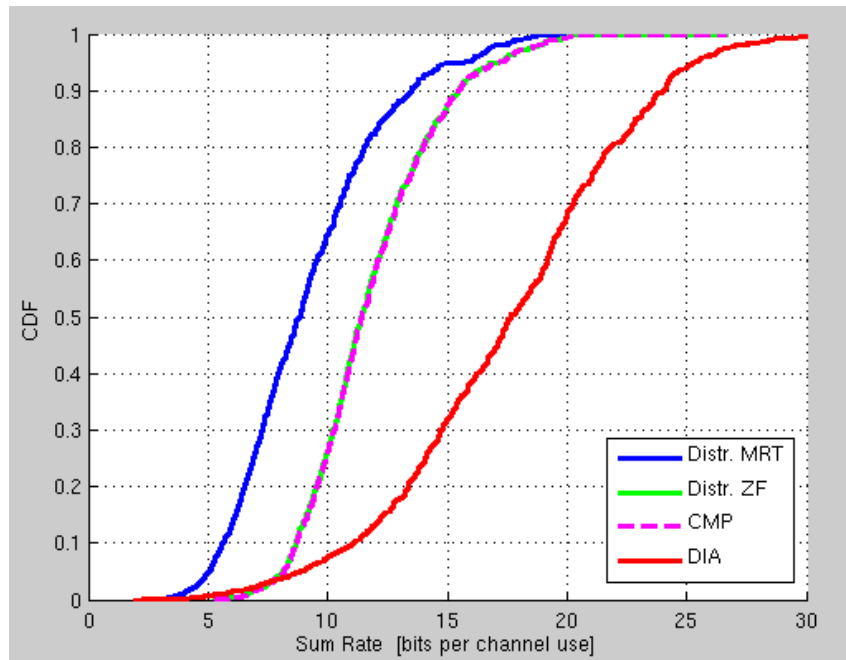


Figure 8-12: CDF of Sum Rate for Different Distributed Schemes

Let us now consider the effect of the out-of-cluster interference, i.e. when the cluster is no longer isolated. In this case, we can expect the performance of DIA to saturate with increasing transmit power due to the uncontrolled interference resulting from outside the cluster. For the other schemes, the interference would now result not only from the multiuser intra-cluster interference but also from the out-of-cluster interference. In order to implement the clustering scheme described by the triangular clusters (see Figure 8-10), we first point out that each sector is involved in two clusters. This implies that the resources of one BS (transmit power, transmit antennas, etc.) must be shared between two clusters. To address this issue, we propose to orthogonalize the two clusters involved with one BS and separate them, for instance, in time or frequency. Hence, only every second cluster would be active over a given resource block as shown by the highlighted clusters in Figure 8-13. With the previous simulation setting, this means only three users would be served by each base station at each resource block.

The effect of the out-of-cluster interference can be observed in Figure 8-14, where we have plotted the CDF for the sum rate under the same setting as Figure 8-12, i.e. three single-antenna users per cluster, two transmit antennas per cooperating BS, carrier frequency 3 GHz, bandwidth 10MHz and available transmit power per BS of 25dBm. Figure 8-14 depicts the CDF of the sum rate with DIA and DIA UPC for an isolated cluster as well as with one, two and three neighbouring interfering clusters.

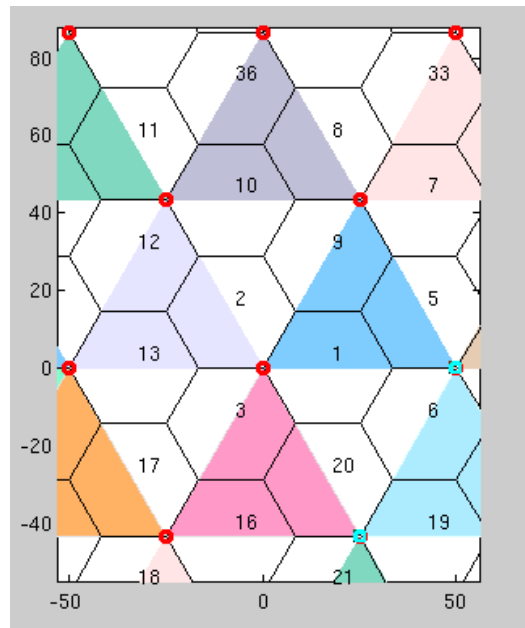


Figure 8-13: Clustering and orthogonalization in the hexagonal model

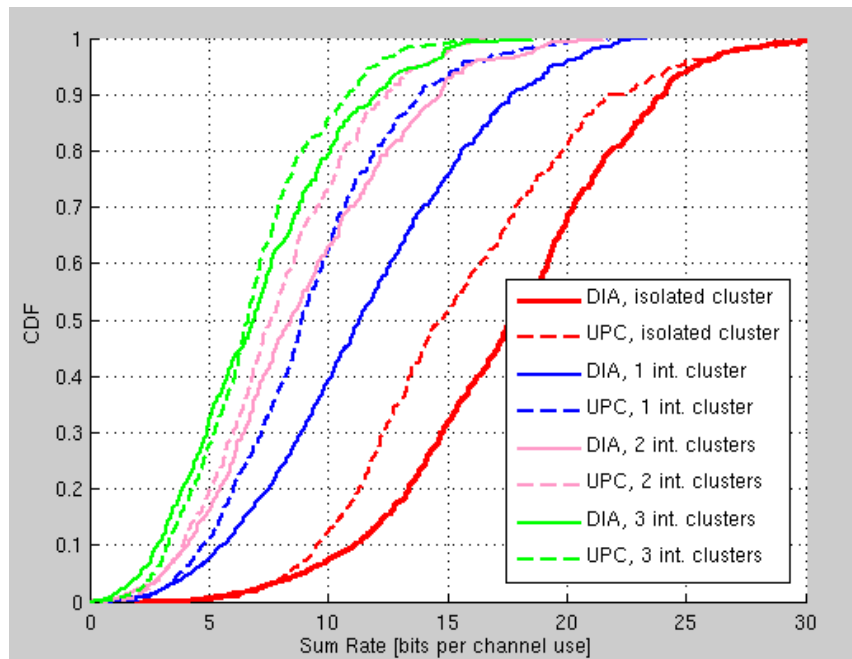


Figure 8-14: CDF of Sum Rate for Different Distributed Schemes

In addition, we present in Table 8.2 the sum rate of DIA and the best SoA solution (CMP, distributed ZF or distributed MRT) in the 10<sup>th</sup> percentile, 50<sup>th</sup> percentile and 90<sup>th</sup> percentile for the different number of interfering clusters. Note that DIA is able to outperform the SoA at the 90<sup>th</sup> percentiles with the out-of-cluster interference.

**Table 8.2: Sum Rate in bits per channel use for different percentiles and number of interfering clusters for the homogeneous dense scenario**

Percentile	Isolated Cluster		1 Interfering Cluster		2 Interfering Clusters		3 Interfering Clusters	
	DIA	SoA	DIA	SoA	DIA	SoA	DIA	SoA
10 <sup>th</sup>	13.42	9.61	5.75	6.55	4.04	5.62	2.93	4.82
50 <sup>th</sup>	17.66	11.47	11.36	8.91	8.45	8.05	6.96	7.62
90 <sup>th</sup>	24.12	15.51	17.78	12.15	14.75	11.92	12.01	10.86

We can observe that although DIA performs well even when considering some of the uncontrolled out-of-cluster interference, it is important to point out that for the simulation results we assume that all the clusters are performing DIA and hence, not all BSs are transmitting at full power. In practice, it might hold that not all the clusters are performing DIA and thus, that all BS are transmitting with full power. In this case, the performance with DIA would degrade due to the larger out-of-cluster interference. However, in that case, we can consider DIA UPC as an alternative, since with such a scheme all the BSs are transmitting with full power.

In order to compare the results with the partners in the METIS project, the METIS Test Case 2 – Dense Urban Information Society was implemented in a simplified version, which was agreed in METIS WP3-T32 [METIS14-D32] for the purpose of testing multi-cell multi-antenna technologies.

An illustration of the considered test case is given in Figure 8-15. The scenario encompasses 9 square-shaped buildings, and the focus is only on the outdoor users on the streets. The maximum transmit powers of the BSs sectors (in total 3 of them) and the 9 micro BSs (each having 2 sectors, not depicted in Figure 8-15) are 46 dBm and 30 dBm, respectively. Each BS sector and micro BS is equipped in total with 4 antennas. As BS clustering and scheduling are for the moment outside of our work scope, we apply the simple macro BS sector-based clustering scheme (“pie” model) shown in Figure 8-15. Notice that the clusters 1, 2, and 3 have 4, 3, and 5 BSs, respectively (the number of BSs in these clusters should be reduced by one for the homogeneous dense case). In all clusters, the number of supported users per RB is 5 (underdetermined systems with 4 antennas per BS). The large scale fading effects are calculated based on the available METIS implementation [METIS14-D32]. The fast fading is implemented following the Rice model with the K-factor of 10 dB for the line-of-sight (LOS) component.

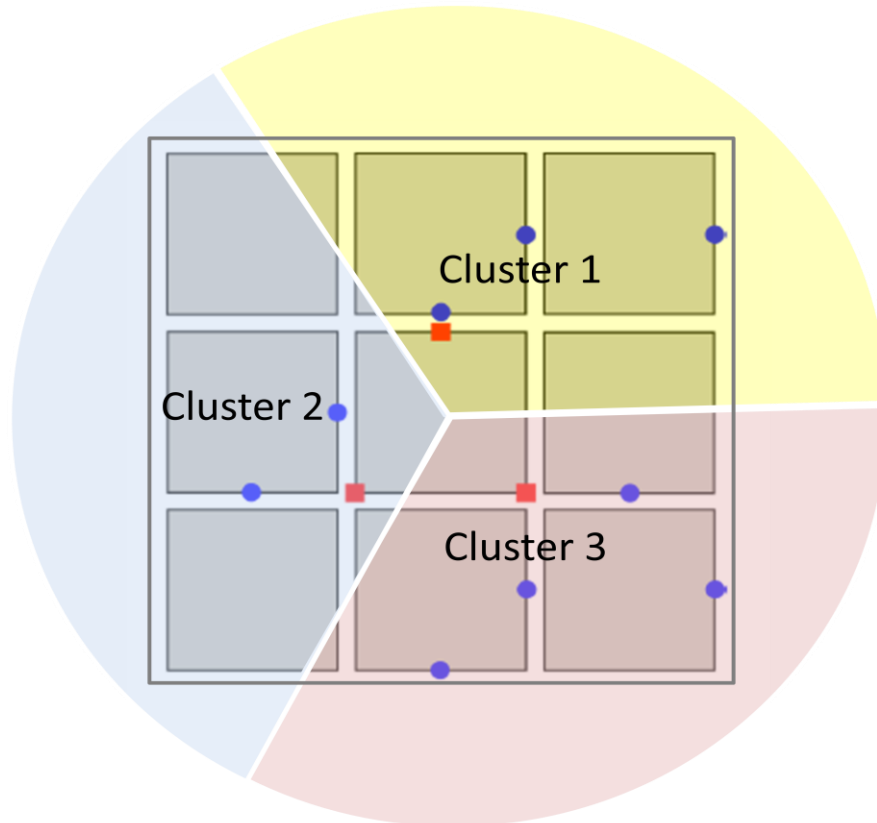


**Figure 8-15: Test Case “Dense Urban Information Society”.** The buildings are depicted as square shaded areas. The small squares denote the positions of the macro BS sectors, while the small circles denote the positions of the micro BSs [METIS14-D32]

In Figure 8-16, we plot the CDFs for 4 schemes: distributed MRT, CMP, DIA, and DIA-UPC. The graph on the left side refers to the case where only micro BSs support the users (related to the above explained simulation in a MIDAS homogeneous environment with pico cells), while the graph on the right side shows the case where macro BSs are also turned on.

It can be seen that all distributed precoding schemes with data sharing significantly outperform the MRT scheme. The performance of the studied distributed schemes also significantly depends on the adopted clustering scheme. Interestingly, it can be seen that the introduction of macro BSs does not always lead to better performance for all schemes, which can be attributed to the uncoordinated out-of-cluster interference. Handling out-of-cluster interference (including optimal clustering), as well as the user assignment and scheduling procedures, can be considered as interesting topics for the future work.

The numerical results corresponding to Figure 8-16 are shown in Table 8.3. Similarly to Table 8.2, DIA boosts the performance for the higher percentiles (depending on the scenario), while CMP is generally better for guaranteeing (lower) data rates, so the techniques can be used in a complementary fashion. Compared with the MRT approach, the gains of the best decentralized strategy (DIA or CMP) range from 195% until 212%. DIA outperforms the CMP for 7.3% and 18.8% in the 50<sup>th</sup> and the 90<sup>th</sup> percentile, respectively, in the homogeneous dense case.

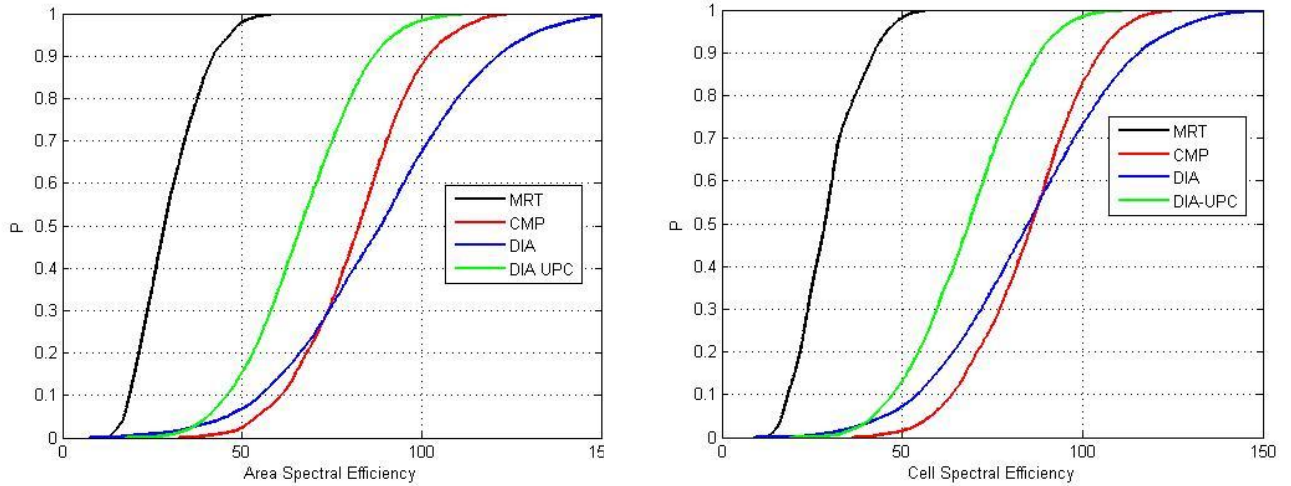
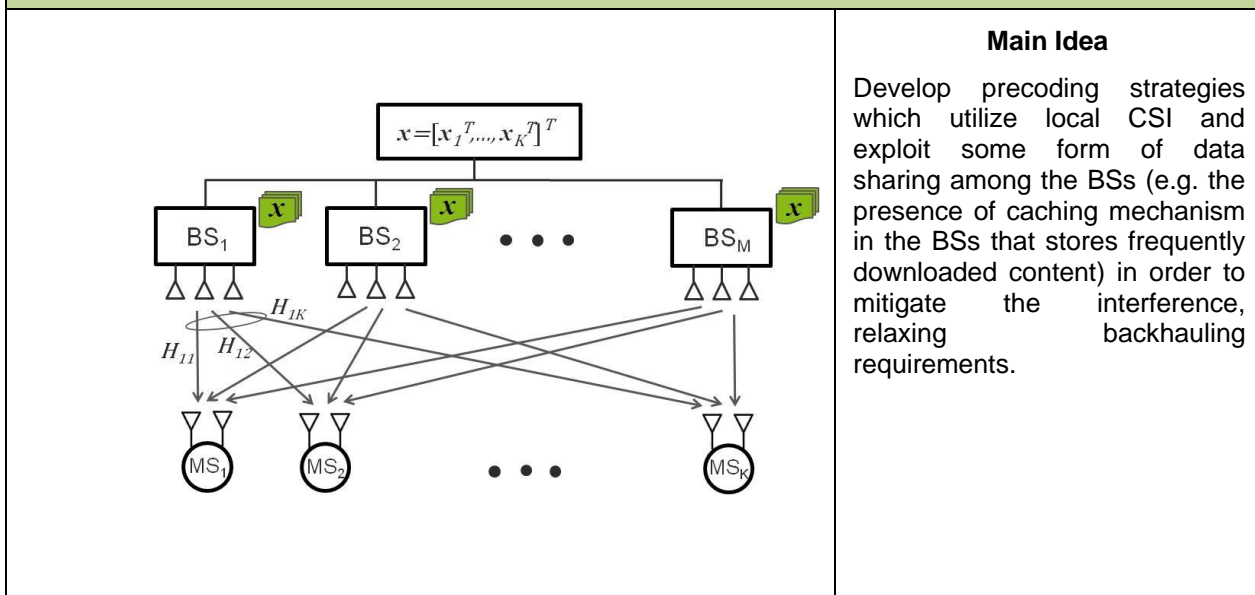


Figure 8-16: Area/cell (the terms can be used equivalently in the studied scenarios) spectral efficiencies in bits per channel use for the cases where macro base stations are turned off (left hand side) and on (right hand side).

Table 8.3: Percentiles for area/cell spectral efficiency (bits per channel use) in the homogeneous small cell and heterogeneous cases for the 4 analyzed schemes.

Percentile	Homogeneous Case (micro BSs)				Heterogeneous Case (micro and macro BSs)			
	MRT	CMP	DIA	DIA-UPC	DIA	CMP	DIA	DIA-UPC
10 <sup>th</sup>	18.70	61.02	55.13	45.86	18.39	63.89	54.17	47.47
50 <sup>th</sup>	28.43	82.65	88.67	66.44	28.59	85.96	84.88	68.55
90 <sup>th</sup>	41.88	101.92	121.11	86.83	42.09	104.94	115.72	88.23

### T3.2 TeC 3 – Distributed Precoding in Multicell Multiantenna Systems with Data Sharing





Considered SoA solution	Distributed maximum ratio transmission (MRT), distributed zero-forcing (ZF), coordinated multicele precoder (CMP).
KPIs considered and achieved gain	Cell spectral efficiency gains between 195% and 212% in the TC2 model (10 <sup>th</sup> percentile, 50 <sup>th</sup> percentile and 90 <sup>th</sup> percentile of CDF calculated), w.r.t. the MRT solution. 7.3% and 18.8% gains over the best SoA solution CMP, for the 50% and the 90% percentile, respectively (CMP is not a part of the LTE baseline) for the homogeneous dense scenario.
Performance evaluation approach	Simulation-based
System model considered	WP3 T3.2-baseline for TC2 (reduced Madrid grid)
Deviation compared to Simulation Baseline	In accordance with the WP3-T3.2 baseline for TC2.
Brief update of the results with respect to D3.2	Evaluation of clustering effects. Evaluation of the DIA scheme in more complex system and realistic setups, using more sophisticated simulation environments.
Association to the TeC Approach	CoMP with Limited Backhaul Capabilities
Targeted TCs	TC2,TC9
Impacted HTs	UDN
Required changes for the realization with respect to LTE Rel. 11	Minor for the PHY layer
Trade-off required to realize the gains	End-user data sharing (e.g. by smart caching) must be enabled.

### 8.6.3 Impact on Horizontal Topics

T3.2 TeC 3 - HT.UDN	
Technical challenges	Fair provision of services with practical (non-ideal) backhauling irrespectively of the user's geographic location.
TeC solution	Interference mitigation with relaxed backhauling requirements by an offline agreement on the placement of the interference components.
Requirements for the solution	Synchronization corresponding to the requirements for CoMP. New architecture which can support efficient data sharing or caching at the level of a radio access point. Moderate mobility to enable reliable estimation of local channels.
KPIs addressed and achieved gain	Cell spectral efficiency gains between 195% and 212% in the TC2 model (10 <sup>th</sup> percentile, e 50 <sup>th</sup> percentile and 90 <sup>th</sup> percentile of CDF calculated), w.r.t. the MRT solution. 7.3% and 18.8% gains over the best SoA solution CMP, for the 50% and the 90% percentile, respectively (CMP is not a part of the LTE baseline) for the homogeneous



	dense scenario.
Interaction with other WPs	Complementing the considered model with the backhaul outage model from TeC1. Complementing the considered scenario with the imperfect (delayed) CSI from TeC1 and TeC2. Complementing the scheme with advanced UE interference mitigation capabilities from T3.2. Utilization of new waveforms from WP2 for relaxing the synchronization requirements. Complementing the scheme with slow multi-cell interference management methods from WP4.

**8.6.4 Addressing the METIS Goals**

T3.2 TeC 3	
1000x data volume	Cell spectral efficiency gains between 195% and 212% in the TC2 model (10 <sup>th</sup> percentile, 50 <sup>th</sup> percentile and 90 <sup>th</sup> percentile of CDF calculated), w.r.t. the MRT solution. 7.3% and 18.8% gains over the best SoA solution CMP, for the 50% and the 90% percentile, respectively (CMP is not a part of the LTE baseline) for the homogeneous dense scenario.
10-100 user data rate	
10-100x number of devices	
10x longer battery life	
5x E-E reduced latency	
Energy efficiency and cost	Approximately 60% transmit power saving for DIA compared with SotA methods, for the homogenous hexagonal scenario.

**8.6.5 References**

[METIS13-D31] METIS Deliverable D3.1, “Positioning of multinode/multi-antenna transmission technologies”.

[METIS14-D32] METIS Deliverable D3.2, “First performance results for multi-node/multi-antenna transmission technologies”.

[LVS14] Y. Long, N. Vucic, and M. Schubert, “Distributed precoding in multicell multiantenna systems with data sharing,” Proc. EW’14, May 2014, Barcelona, Spain.

[GMD+13] N. Golrezaei, A. F. Molisch, A. G. Dimakis, and G. Caire, “Femtocaching and device-to-device collaboration: A new architecture for wireless video distribution,” IEEE Comm. Magazine, vol. 51, no. 4, pp. 142-149, Apr. 2013.

[BZG+10] E. Björnson, R. Zakhour, D. Gesbert and B. Ottersten, “Cooperative Multicell Precoding: Rate Region Characterization and Distributed Strategies with Instantaneous and Statistical CSI,” IEEE Trans. on Signal Processing, vol. 58, no. 8, pp. 4298-4310, Aug 2010.

## 8.7 T3.2 TeC 4: Real world interference alignment [ALU]

### 8.7.1 General Overview

Interference management in cellular networks is a well known issue which limits the performance of the cellular networks. Interference Alignment (IA) is one of the solutions to manage the interference efficiently by using “align” and “suppression” strategy. With the help of multiple antennas at the transmitters, the spatial dimension can be used for interference alignment. Similarly, with the help of multiple antennas at the receivers, the spatial dimension can be used for interference suppression. In cellular multi-antenna, multi-user (MU-MIMO) systems the users suffer not only from the inter-cell interference (ICI) but also from the intra-cell (multi-user) interference (MUI). The contribution in [AW13] addresses the issue of MUI and the applicability of IA to deal with both types of interferences in the system. The idea in [AW13] is to use partial and outdated ICI information for the alignment with MUI. The authors in [AW13] refer this precoding scheme as Multi User Inter Cell Interference Alignment (MUICIA). The partial ICI information is based on the direction of maximum average ICI which is represented by the eigen-vector corresponding to the maximum eigen value of the ICI covariance matrix estimated by the UE. Estimating the ICI covariance for current transmission is coupled problem therefore, outdated information based on the estimation of ICI from the last transmission is used. For this purpose, the BS requires only the local information i.e. no inter-BS coordination is required. Each user estimates and sends the required information only to its serving BS.

Many low complexity sub optimal user selection algorithms like in [YG06]-[JJY+12] have been presented in literature. However, they mostly deal with MISO multi user single cell systems with Zero-Forcing based precoding. We deal here with a MIMO multi user and multi cell system which is affected by both ICI and MUI and employ alignment based precoding.

In this contribution, our objective is to improve the system spectral efficiency. At first we used a **Standard** multi user selection algorithm [SS04] to select the users for transmission. However, the gains with the standard algorithm are very marginal. Therefore, we have proposed three new algorithms for user selection in a MU-MIMO system which can be categorized based on their feedback requirements and computational complexity. We refer to [AMW13] for the details of the algorithms, however, a brief introduction of each algorithm is given below:

- Based on Transmit Side Colinearity (**Min-TxColinearity**): Similar to [SS04], our objective in this method is to find a mutually orthogonal pair using the serving channel matrices. Two matrices which exhibit nearly spatial orthogonal structure should have minimum colinearity. Therefore, we use colinearity between transmit correlation matrices as a metric and find the pair with minimum colinearity.
- Based on Maximum ICI (**Max-ICICondNum**): The ICI is *colored* when the UE faces strong interference from one or more interfering BSs. The presence of strong interferers can be detected with the help of the ratio of maximum to minimum eigenvalue of the ICI covariance matrix. The condition number of the ICI covariance matrix represents this ratio. For this purpose, we consider it as a metric and find the users with maximum condition numbers.
- Based on Estimated Rate (**Max-ERate**): In this method, the selection is based on the post receiver SINR estimation and the rate by the serving BS. For this purpose, the BS estimates the rates of all possible combinations of the UEs with the help of outdated ICI and UE-category information.

In this contribution we show with the help of extensive simulations that our proposed algorithms provide considerable gains in the performance of IA based precoding schemes. The algorithms are also compared with a standard pair selection algorithm. The results show that our algorithms outperform the standard selection. We also assess the performance of IA based precoding with user selection by comparing it with baseline precoding in three cellular

network scenarios. The three scenarios differ with respect to the ICI characteristics in the network. The comparison shows that when the ICI is strong in the network, IA based precoding outperforms the baseline precodings using our proposed selection algorithms.

### 8.7.2 Performance Results

We consider an OFDM based closed loop downlink multiuser MIMO cellular system which consists of multiple cells each equipped with  $M$  transmit antennas. Each cell is serving  $R$  active UEs ( $R \geq M$ ). Each UE is equipped with  $N$  antennas. Only  $K$  out of  $R$  UEs are selected simultaneously on the same time-frequency resource for transmission. In order to limit the search space, we assume  $K=2$  (pair selection) and single stream transmission for each UE. We assume a block fading channel in time and frequency over an allocated OFDM physical resource block.

Let UE 'j' and UE 'k' be selected for transmission on the same resource by the  $i$ th cell using a selection algorithm. As they are co scheduled so each of them will cause MUI on the other. Each UE will also suffer from ICI due to the transmission to the scheduled UEs by the other cells. The serving cell designs the transmit precoding vectors for the two selected users as given in [AW13]. Interference rejection combining receiver algorithm is used at the receiver side. Please refer to [AW13] for the details of transceiver design.

We have used the drop based system level simulation methodology as guided by 3GPP in [TR36814]. The realization of all time and frequency selective spatial channels between the cells and the UEs is done according to the channel model given in [TR25966]. Perfect channel estimation and instantaneous error-free feedback of CSI is assumed (please refer to [AMW13] for the details of CSI required for each selection method). Further propagation and antenna related parameters can be referred from [TR36814]. As the focus of this work is to analyse the qualitative impact of different selection algorithms therefore, some of the simulation features like retransmissions and link adaptation are disabled on purpose. Moreover, the performance metric of mean cell rate is evaluated by output SINR using Shannon formula.

One complete simulation cycle consists of several Monte Carlo drops. Each drop consists of certain number of transmission time intervals (TTI). Full buffer traffic and a user speed of 3 km/h is simulated. The total frequency bandwidth is divided into  $B$  physical resource blocks (PRB) [TR36814]. Each PRB contains  $W$  consecutive subcarriers with a frequency spacing of 15kHz (here in 10MHz including band gap: 576 subcarriers,  $B = 50, W = 12$ ). With the user speed of 3 km/h, we have slow time variant and nearly frequency flat channels within a single PRB. However, we have frequency diversity due to high number of PRBs within a TTI. We have the possibility of  $B$  different pair selections within a TTI if the number of active users is very high. The output SINR after the receive-processing is evaluated for each PRB as given in [AW13] and [AMW14] depending upon the considered network scenario. This output SINR is then used to calculate the mean cell rates in bits/sec/Hz. Please refer to [AW13] and [AMW14] for further details.

We have simulated three cellular scenarios. The initial two scenarios are based on the homogenous network whereas the third scenario is based on heterogeneous network (low power small cells overlaid on macro coverage layer). The results in Figure 8-17 and Figure 8-18 are the outcome of the 3-cells scenario modelled by a site with co-located 3-sectorized antennas where each sector corresponds to a cell. Whereas in Figure 8-19, we show the results of 21-cells scenario modelled by a hexagonal grid of 7 sites each with co-located 3-sectorized antennas which corresponds to a large cellular network. Figure 8-20 presents the results of a co-channel heterogeneous network modelled by a hexagonal grid of 7 sites. Each site is based on 3 macro cells and 1 pico cell is overlaid in each macro cell coverage area.

#### **Performance in Homogenous Network:**

For homogenous network scenarios, the UEs are dropped in the coverage area according to the given downlink wide band average SINR ( $\sigma$  in dB). This input SINR depends upon the average receive signal level from the serving cell, upon the average receive signal from all

other cells and upon the thermal noise. Typical values of  $\sigma$  lie between  $-5$  to  $17$  dB for a frequency reuse-1 cellular system. Lower values of  $\sigma$  indicate that the UEs are close to the cell border and facing a high ICI, representing ICI-limited region. Although MUI exists in the region but just to emphasize the strong influence of ICI at cell border we explicitly term the region as ICI-limited. Similarly, higher values of  $\sigma$  represent MUI-limited region i.e. the UEs are very close to the cell center. Middle order values of  $\sigma$  represent a region where both ICI and MUI have significant influence on the performance of the system.

Figure 8-17 presents the performance improvements in cell spectral efficiency using MUICIA transmit precoding with different selection algorithms over the increasing number of active users in ICI-limited ( $\sigma = 0$ dB) and MUI-limited ( $\sigma = 14$ dB) regions. Notice that our proposed algorithms provide considerable gains in the performance as compared to the standard selection algorithm. The Max-ICICondNum which is an alignment based user selection method, outperforms classical orthogonality based user selection Min - TxColinearity in both cases of  $\sigma$ . This is because Max - ICICondNum increases the alignment gain for MUICIA and suppression gain at the receiver by selecting active UEs experiencing strong ICI. Moreover, the gains of Max - ICICondNum are higher in ICI-limited region due to the highly coloured (strongly directed) interference in ICI-limited region. The selection with Max - ERate outperforms all other algorithms. It shows that with UE-category information and with slow time variant channels, transmission rate estimation can be done with high accuracy at the serving cell which helps to select maximum rate UEs. Hence the system can gain in the performance with advance UE capabilities. Table 8.4 lists the percentage performance gains of the user selection methods over the standard selection with MUICIA. We can see higher gains of Max-ICICondNum in ICI-limited region ( $\sigma=0$ dB) and higher gains of Min-TxColinearity in MUI-limited region ( $\sigma=14$ dB).

Now, we intend to compare the performance of MUICIA in homogenous network scenarios with a non-alignment based multi-user transmit precoding scheme. This scheme is based on the optimization of Signal to Leakage and Noise Ratio (SLNR) [STS07]. Figure 8-18 shows the results when both precodings are using Max - ERate based selection in 3-cells scenario. With this selection, MUICIA outperforms SLNR with very high gains for all the number of UEs as well as for all interference regions. With 21-cell scenario as shown in Figure 8-19, as the overall network ICI characteristics change due to large number of cells, we see a little different performance picture than Figure 8-18. At  $\sigma = 0$ dB, with increasing number of UEs, MUICIA shows relative gains over SLNR. This trend continues also for  $\sigma = 8$ dB. However, with  $\sigma = 14$ dB, SLNR outperforms MUICIA till very large number of active UEs.

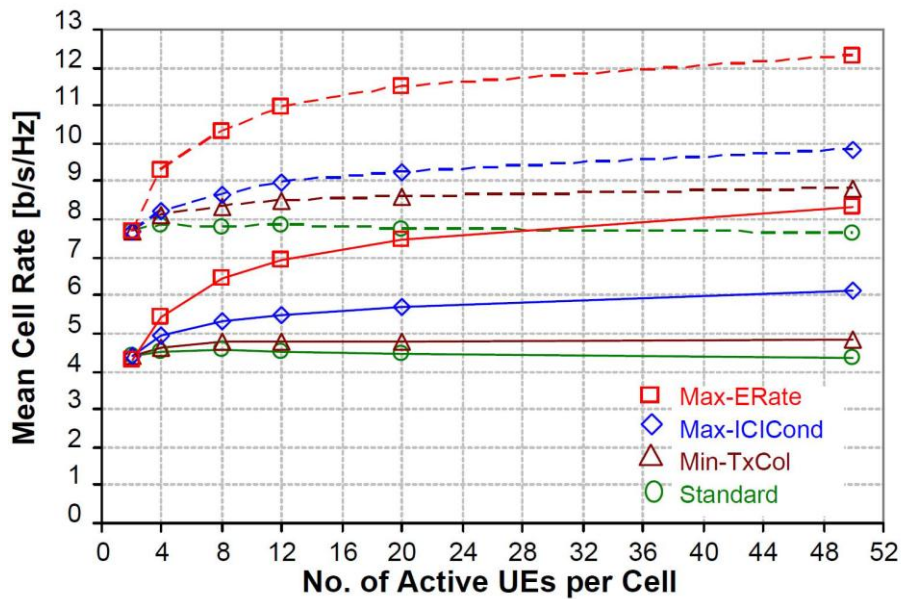


Figure 8-17: Performance of MUICIA precoding with different user selection algorithms in ICI limited ( $\sigma = 0$ dB; Smoothed lines) and MUI limited ( $\sigma = 14$ dB; Dashed lines) regions, in a scenario with 3-cells

Table 8.4: Performance gains over standard user selection method for 3 Cells, 20 UEs active/cell

User Selection Methods	SINR = 0 dB	SINR = 14 dB
Max-ERate	~68%	~46%
Max-ICICondNum	~28%	~17%
Min-TxCOLinearity	~6 %	~10%

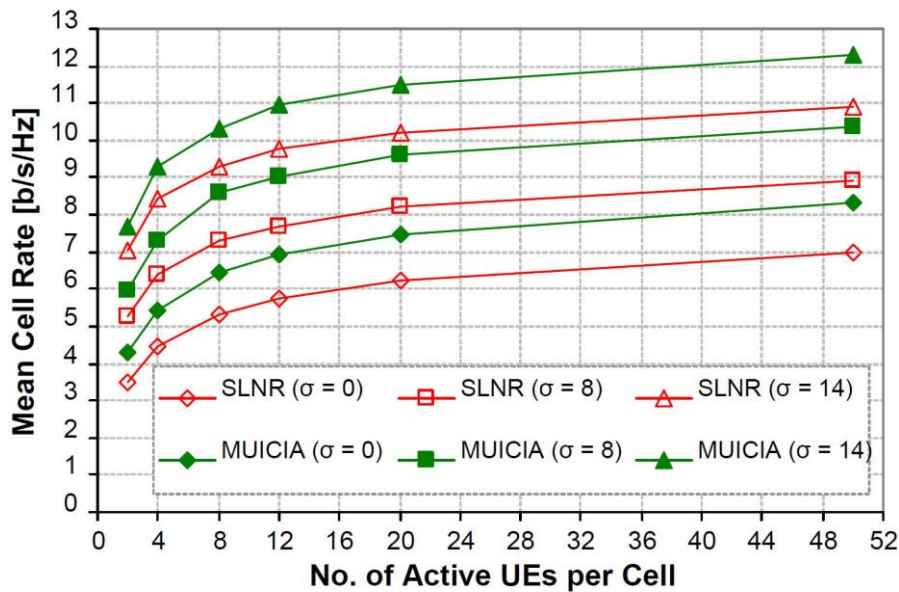


Figure 8-18: Comparison of the performance of MUICIA with SLNR using Max - ERate as selection algorithm in a scenario with 3-cells

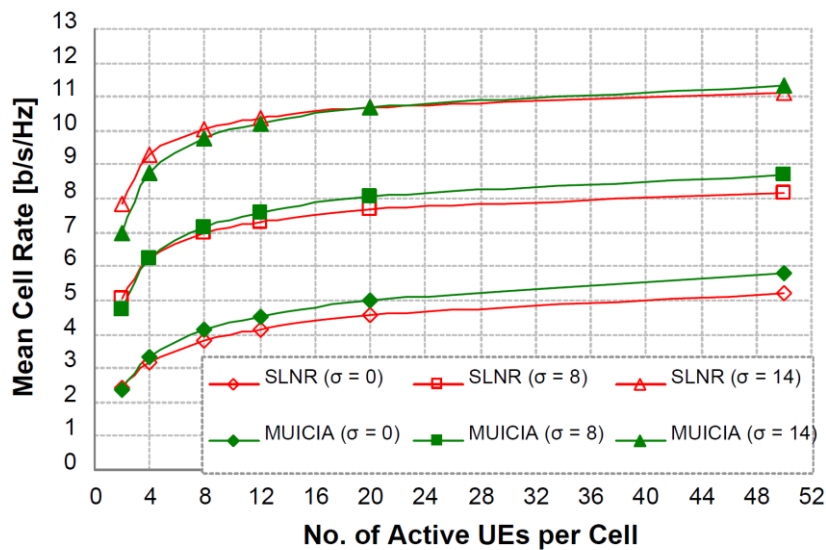


Figure 8-19: Comparison of the performance of MUCIA with SLNR using Max – ERate as user selection algorithm in a homogenous network scenario with 21-cells.

### Performance in Heterogeneous Network:

For the modelling of heterogeneous networks, one low-power pico cell is placed under the coverage of each high-power macro. The pico cell is positioned at a distance of 0.3 ISD (150 m) and along the bore-sight direction of the antenna array of the macro which depicts a scenario where ICI management is highly required. Users are randomly dropped over the simulation area with the help of a uniform distribution. We refer to [AMW14] for further details on simulation assumptions and parameters.

We have compared the mean cell rate performance of alignment and non-alignment based transmission schemes with user selection in heterogeneous networks. Here we have considered an additional state of the art non-alignment based scheme known as Effective Zero Forcing (EFZF) which nullifies the multi user interference [BHT07]. Figure 8-20 presents the performance comparison with Max-ERate user selection. The figure depicts an overall superior performance of MUCIA in comparison with other precodings.

With the help of system simulations, we have not only evaluated the individual performance of MUCIA but also compared it with state of the art MU-MIMO precodings (e.g. SLNR and EFZF). Our results indicate that with respect to the overall system performance, MUCIA provides higher gains in heterogeneous networks due to the specific ICI characteristics of heterogeneous networks. Moreover, it serves two purposes at a time. First, as a transmit precoding scheme and second as an interference management scheme without any additional effort or requirements. With these results, we infer that interference alignment can also be considered as a candidate interference management technique for 5G in parallel with enhanced interference coordination schemes introduced by 3GPP for co-channel heterogeneous network scenarios. The uncoordinated interference management approach through interference alignment has a prime advantage over coordinated approaches.

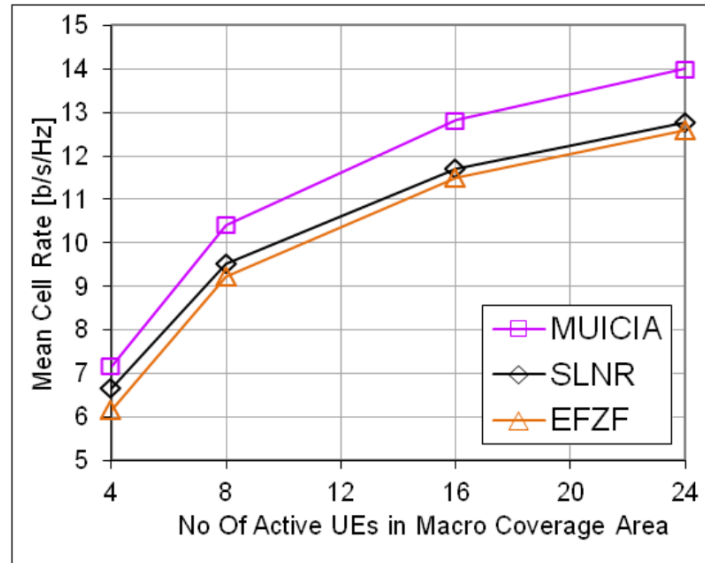
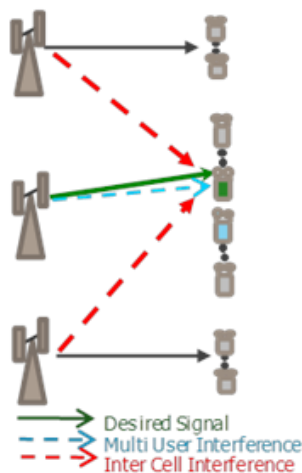


Figure 8-20: Comparison of the performance of MUICIA with SLNR and EFZF using Max – ERate as selection algorithm in a heterogeneous scenario with 21 macro cells each with 1 pico cell

T3.2 TeC 4 – Real world interference alignment	
 <p> <span style="color: green;">→</span> Desired Signal  <span style="color: blue;">- - -</span> Multi User Interference  <span style="color: red;">- - -</span> Inter Cell Interference         </p>	<p style="text-align: center;"><b>Main Idea</b></p> <p>The main idea is to find algorithms for user selection that maximises the performance of multi user IA based transmit precoding, in order to maximise the system spectral efficiency.</p> <p>The approach is to find a pair of users that can benefit most from the alignment technique that aims to align intra-cell and inter cell interference. Such a pair provides high system performance when IA is applied as transmission technique.</p>
Considered SoA solution	Comparison with SoA user selection [SS04] and non-alignment based MU-MIMO transmit precoding schemes SLNR [STS07] and EFZF [BHT07].
KPIs considered and achieved gain	Spectral efficiency: average gain of IA based precoding with proposed user selection method up to 70% in homogenous network scenario with 20 UEs per cell with ideal channel estimation and instantaneous error-free CSI feedback.
Performance evaluation approach	Simulation-based: system level evaluation
System model considered	Other



Deviation compared to Simulation Baseline	<p>Some:</p> <ul style="list-style-type: none"> <li>• Model of environment: Urban Macro Area</li> <li>• Spectrum Assumptions: 2.0 GHz</li> <li>• Propagation model: 3GPP SCM</li> <li>• Deployment model: Hexagonal Grid</li> <li>• User/Device Distribution: Geometry Based (Homogenous Network) and Uniform Random (Heterogeneous Network)</li> <li>• Traffic model: Full Buffer</li> </ul>
Brief update of the results with respect to D3.2	<ul style="list-style-type: none"> <li>• Simulation results for 7-Sites homogenous network scenario</li> <li>• Simulation results for 7-Sites co-channel heterogeneous network scenario</li> <li>• Performance comparison with other state of the art transmit precoding schemes both in homogeneous and heterogeneous scenarios.</li> </ul>
Association to the TeC Approach	Proposed to be considered in "CoMP with Advanced UE Capabilities"
Targeted TCs	TC2 (Dense urban information society)
Impacted HTs	UDN
Required changes for the realization with respect to LTE Rel. 11	<p>Minor:</p> <ul style="list-style-type: none"> <li>• Feedback for ICI information</li> </ul>
Trade-off required to realize the gains	The performance gains of alignment based user selection over standard selection with interference alignment based precoding come without extra overhead. However, higher gains can be achieved with Max-ERate selection method at the cost of high computational complexity at the transmitter.

### 8.7.3 Impact on Horizontal Topics

T3.2 TeC 4 - HT.UDN	
Technical challenges	<ul style="list-style-type: none"> <li>• Optimize user selection and interference management.</li> <li>• Increase system spectral efficiency.</li> </ul>
TeC solution	The main idea is to find algorithms for user selection that maximises the performance of multi user IA based transmit precoding, in order to maximise the system spectral efficiency. Important gains are observed in TC2, which is very relevant for UDN.
Requirements for the solution	<ul style="list-style-type: none"> <li>• Channel and Interference information at the BS</li> <li>• Low variation in ICI</li> </ul>
KPIs addressed and achieved gain	Spectral efficiency: average gain from 10% to 70%.
Interaction with other WPs	<ul style="list-style-type: none"> <li>• WP2: TeC developed by assuming</li> </ul>



	<p>OFDM, no major change expected when other air interfaces like UFMC are employed. Some interaction is possible with MAC and RRM solutions in WP2.</p> <ul style="list-style-type: none"> <li>• WP4: Interference identification (TeC1: New interference estimation techniques) in WP4 are essentials for interference alignment and cancellation</li> <li>• WP6: For system level evaluations</li> </ul>
--	--

### 8.7.4 Addressing the METIS Goals

T3.2 TeC 4	
1000x data volume	Increase in the achieved cell throughput and spectral efficiency (up to 70% gain) allows the increase of the data volume per area
10-100 user data rate	
10-100x number of devices	With proposed user selection methods, higher number of active devices can be served.
10x longer battery life	
5x E-E reduced latency	
Energy efficiency and cost	

### 8.7.5 References

[AW13] D. Aziz, A. Weber: "Transmit precoding based on outdated interference alignment for two users multi cell MIMO system", Proceedings of IEEE ICNC, San Diego, USA, Jan 2013.

[YG06] Taesang Yoo, Andrea Goldsmith, "On the Optimality of Multiantenna Broadcast Scheduling Using Zero-Forcing Beamforming," Communications, IEEE Journal on , vol.24, no.3, Mar 2006.

[ZO09] Min Zhi, T. Ohtsuki; "An improved user selection algorithm in multiuser MIMO broadcast," PIMRC, 2009 IEEE 20th International Symposium on , vol., no., pp.192-196, 13-16 Sept. 2009.

[JJY+12] Junling Mao; Jinchun Gao; Yuanan Liu; Gang Xie; "Simplified Semi-Orthogonal User Selection for MU-MIMO Systems with ZFBF" Wireless Communications Letters, IEEE, vol.1, no.1, Feb. 2012.

[SS04] Q. Spencer and A. Swindlehurst, "Channel allocation in multi-user mimo wireless communications systems," in Communications, 2004 IEEE International Conference on, vol. 5, june 2004, pp. 3035 – 3039 Vol.5.

[TR36814] 3GPP, "Further Advancements for E-UTRA - Physical Layer Aspects," TR 36.814, V 9.0.0, March 2010.

[STS07] M. Sadek, A. Tarighat, and A. Sayed, "A leakage-based precoding scheme for downlink multi-user mimo channels," Wireless Communications, IEEE Transactions on, vol. 6, no. 5, pp. 1711 –1721, may 2007.

[BHT07] F. Boccardi, H. Huang, and M. Trivellato, "Multiuser eigenmode transmission for mimo broadcast channels with limited feedback," in Signal Processing Advances in Wireless Communications, 2007. SPAWC 2007. IEEE 8th Workshop on, june 2007, pp. 1 –5.



**Document:** FP7-ICT-317669-METIS/D3.3

**Date:** 25/02/2015

**Security:** Public

**Status:** Final

**Version:** 1

---

[AMW13] D. Aziz, M. Mazhar and A. Weber: “Performance Enhancement of Multi User Multi Cell Interference Alignment with Pair Selection”, IEEE 78th Vehicular Technology Conference, IEEE VTC-Fall 2013, Las Vegas, USA., Sep. 2013.

[AMW14] D. Aziz, M. Mazhar and A. Weber: “Multi User Inter Cell Interference Alignment in Heterogeneous Cellular Networks”, IEEE 79th Vehicular Technology Conference, IEEE VTC-Spring 2014, Seoul, South Korea, May 2014.

## 8.8 T3.2 TeC 5: Semi-distributed IA algorithm for MIMO-IC channel, with power control convergence speed up [FT]

The work on this TeC is completed. Please refer to [METIS14-D32] for the most updated results.

## 8.9 T3.2 TeC 5b: Distributed interference alignment techniques under imperfect channel state information [FT]

### 8.9.1 General Overview

Interference alignment schemes rely heavily on channel state information. Analytical solutions for Interference alignment presented in [CJ08] require global CSI. Distributed algorithms presented in [GCJ11] have the property to achieve interference alignment with only local channel knowledge at each node. This permits to reduce the overhead of CSI acquisition. In all cases, the requirement of perfect CSI by the IA scheme is practically unrealizable for a time variant or frequency selective channels.

In this work, we investigate the impact of CSI imperfection on the iterative IA based techniques. In particular, we consider as a reference the interference leakage minimization (LM) problem proposed in [GCJ11] where, based on reciprocity, in each algorithm' iteration, receivers updates their suppression filters to minimize their total leakage interference. Other objectives are considered equivalently such as maximizing the SINR or minimizing the total sum MSE. Regardless of the subspace selection rule, the general framework considered for transmit/ receive filters design with reciprocity under imperfect CSI proceeds as follows:

1. Forward link training where transmitters send pre-coded pilot symbols using a set of initial pre-coders. Receivers estimate forward channel parameters principally their interference covariance matrix and compute receive filters that optimize a predefined objective ( least interference for LM);
2. Reverse link training where receivers send pre-coded pilot symbols using the receive filters computed from step 1 as transmit pre-coders. Transmitters, in turn, compute their pre-coders that optimize also the same objective. Then, a second training phase is initiated by the transmitters with the new pre-coders;
3. Transmitter / receiver pairs iterate the previous steps for fixed predefined iteration (or until convergence);
4. Data transmission where payload data is communicated from the transmitters.

These four steps are valid for perfect and imperfect channel estimation where CSI acquisition is based on reciprocity which is valid for TDD systems. With perfect CSI, it has been shown that this algorithm converges [GCJ11]. However, we show that under imperfect CSI the previous processing does not converge, in general, basically since a new independent estimation noise is added at each step. This issue has not been yet treated for iterative IA under imperfect CSI. Most existent works rely on a predefined channel model to study the IA performance (BER or spectral efficiency) as presented for example in [XLM+13]. Another technique is based on first estimating only the channel, then this estimated channel will be used through the previously iterative steps to compute the transmit/receive filters as presented in [TG09]-[AH12]. The idea behind our work is to give an insight of the performance of iterative IA in the interference channel under a practical assumption related to the availability of a noised CSI at each step. This solution aims also at reducing the overhead since we combine the algorithm iterations with the channel estimation steps.

We investigate, in this work, a new perspective for the proposed schemes in [MET14-D32] where perfect CSI is considered.

### 8.9.2 Performance Results

We consider a  $K$ -user narrowband MIMO interference channel where there are  $K$  APs equipped with  $M_T$  transmit antennas and  $K$  users equipped with  $M_R$  receive antennas. Each AP is paired with a single user in a one to one mapping and interferes with all the  $(K-1)$  receivers it is not paired with. We assume a block fading channel, i.e. all the links in the network are constant for one transmission frame and change from one frame to another. The transmitted signal  $\mathbf{x}_j \in \mathbb{C}^{M_T \times d_j}$  from AP  $j$  is given by  $\mathbf{x}_j = \mathbf{V}_j \mathbf{s}_j$ .  $\mathbf{V}_j \in \mathbb{C}^{M_T \times d_j}$  is the pre-coding matrix at the  $j$ -th transmitter and  $d_j$  is the number of streams transmitted on link  $j$ . At the reception, each user  $k$  decorrelates the received signal by applying the decorrelation matrix  $\mathbf{U}_k \in \mathbb{C}^{M_R \times d_k}$ . We have presented in [MET14-D32], the design of  $\mathbf{V}_j$  and  $\mathbf{U}_k$  based on target SINRs at all streams of all the links.

Here we are interested in evaluating this communication scheme and the reference technique under partial CSI. Therefore, at each step, each receiver (or transmitter on the reverse link) should have an accurate estimate of  $\mathbf{H}_{kj} \mathbf{V}_j$  (or  $\widehat{\mathbf{H}}_{kj} \widehat{\mathbf{V}}_j$  on the reverse link), the effective CSI.  $\mathbf{H}_{kj} \in \mathbb{C}^{M_R \times M_T}$  is the channel between the transmitter  $j$  and the receiver  $k$ . The estimation model considered is given by  $\widehat{\mathbf{H}}_{kj} \widehat{\mathbf{V}}_j = \mathbf{H}_{kj} \mathbf{V}_j + \mathbf{E}_{kj}$ , where  $\widehat{\mathbf{H}}_{kj} \widehat{\mathbf{V}}_j$  is the estimated effective channel at the receivers.  $\mathbf{E}_{kj} \in \mathbb{C}^{M_R \times d_k}$  is the estimation error at the receiver  $k$  at the link  $j$ . For the minimum leakage problem, based on the effective CSI, each receiver will be able to estimate its covariance matrix and thus compute the interference suppression matrix following the same original LM algorithm at each step. This technique permits to reduce the overhead for the iterative IA techniques with imperfect CSI since the channel estimation phase is combined with the algorithm iterations phase. Other distributed algorithms are considered also for comparison such as the SINR maximization and the sum-MSE minimization problems. In these cases, both receivers and transmitters will alternating the optimization of the users' SINR or the total sum-MSE at the final receivers respectively for Max-SINR and min-MSE problems.

For the simulations a 3-user 2x2 MIMO IC with one stream transmitted from each AP is considered. All the elements of  $\mathbf{H}_{kj}$  and  $\mathbf{E}_{kj}$  are i.i.d.  $\text{CN}(0,1)$  and  $\text{CN}(0, \sigma_e^2)$  respectively where  $\sigma_e^2$  reflects the CSI error. Figure 8-21 and Figure 8-22 illustrate the average sum-capacity evolution of LM and MAX-SINR algorithms for different errors. For constant noise variance, the sum-rate level for the different algorithms saturates when SNR becomes high. This behavior remains even if we have perfect CSI. The sum-rate saturation disappears for adaptive estimation error (that depends on the operating SNR).

We are interested also in studying the convergence of the total interference leakage for the LM algorithm. In this case, we consider for the problem relaxation that the transmitters can be aware of the effective channels. Simulations show that the algorithm does not converge but oscillates after a certain number of iterations to a certain value that depend on the SNR and the error power. This has motivated us to study analytically the average interference leakage. This metric indicates the mean convergence of the interference at each user. Figure 8-23 shows the mean convergence of the interference for one user. Figure 8-24 shows the convergence of the average sum MSE when MSE algorithm is considered.

Simulations show that average interference (or sum- MSE) converges after some number of iterations. In this case, with a fixed power budget, it is more preferable to reliably estimate the channel by giving more power for pilot transmission in reduced number of iterations than continue on iterating. This technique aims at having accurate channel estimation for reliable transmission.

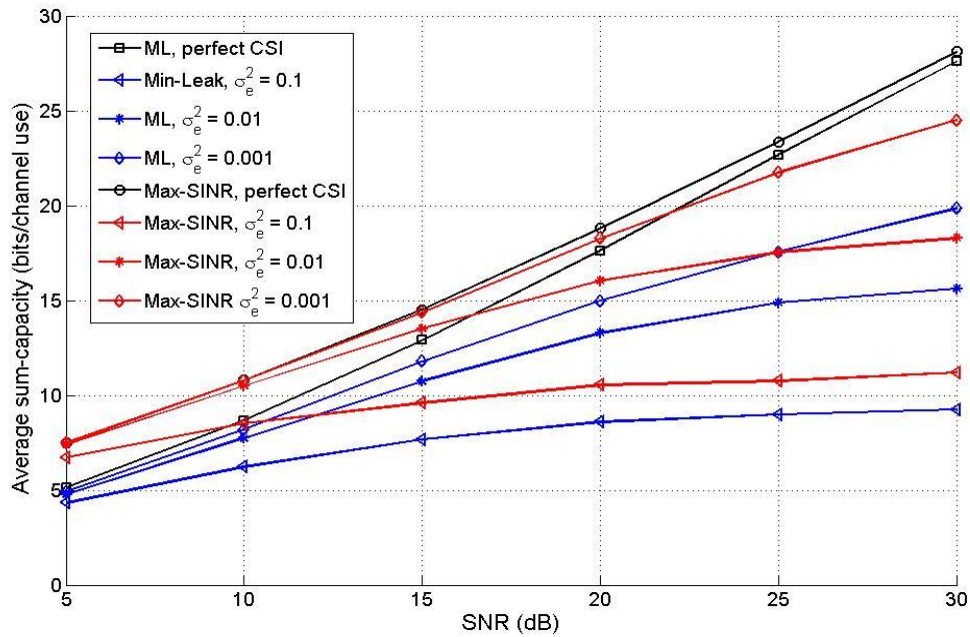


Figure 8-21: Average sum-capacity of the minimum leakage and Max-SINR algorithms with different constant levels of error powers for the 3-user 2x2 MIMO IC with  $d_k = 1, \forall k = 1, 2, 3$

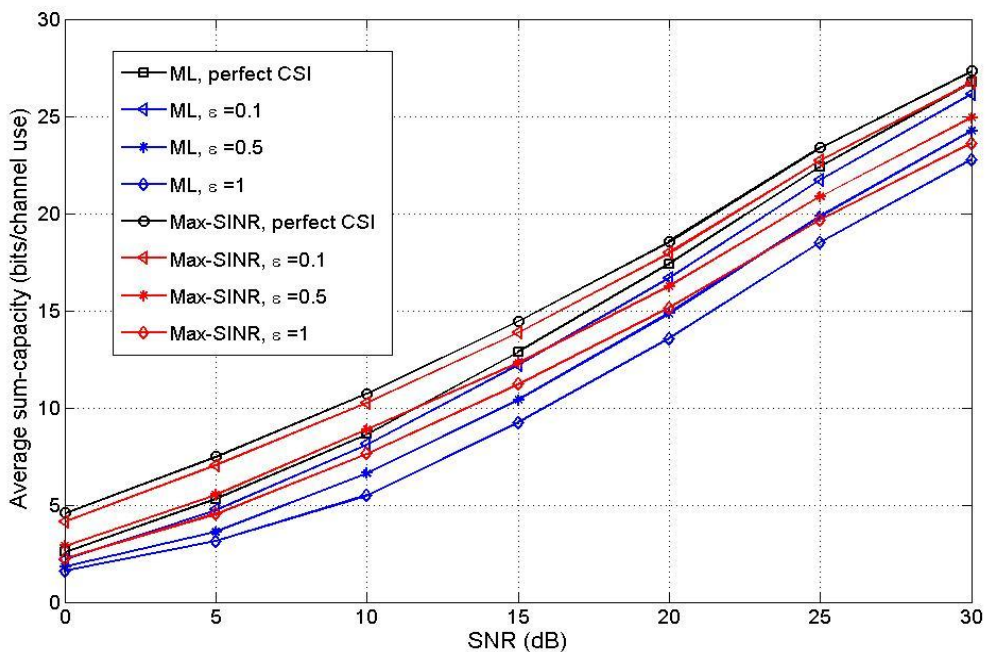


Figure 8-22: Average sum-capacity for the minimum leakage and Max-SINR algorithms with different variable levels of error powers:  $\sigma_e^2 = \epsilon/SNR$  for the 3-user 2x2 MIMO IC with  $d_k = 1, \forall k = 1, 2, 3$

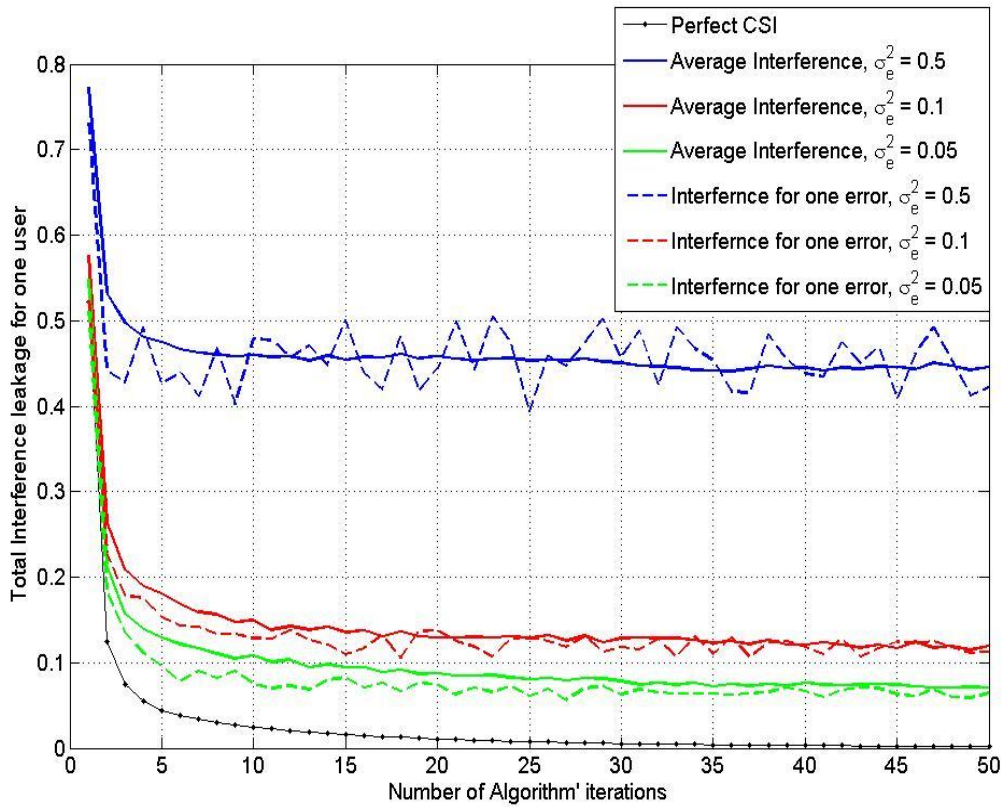


Figure 8-23: Average interference leakage (straight lines) vs interference leakage when new estimation error is generated at every algorithm's iteration (dash lines). The system is 3-user 2x2 MIMO IC with  $d_k = 1$  and SNR = 0dB.

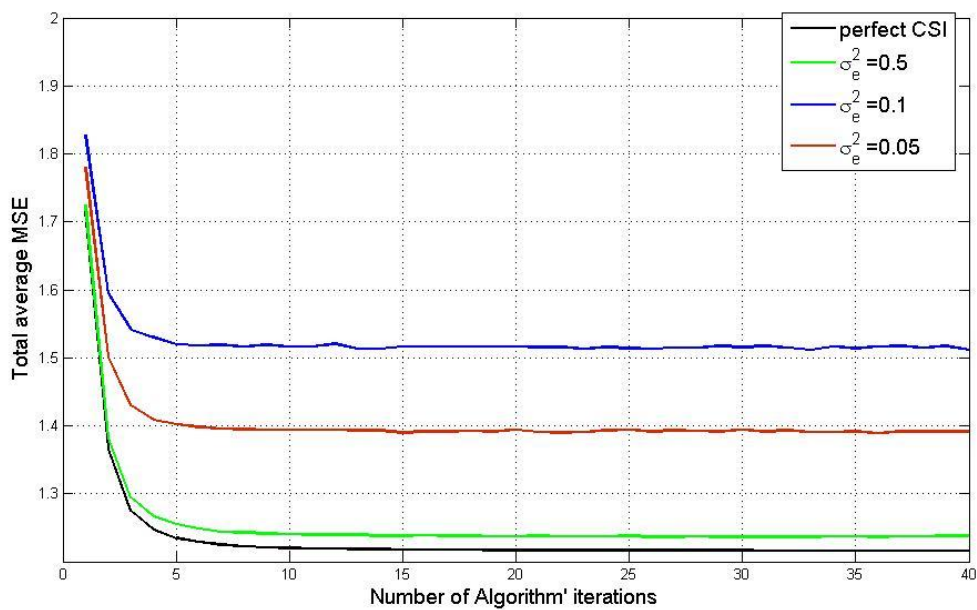
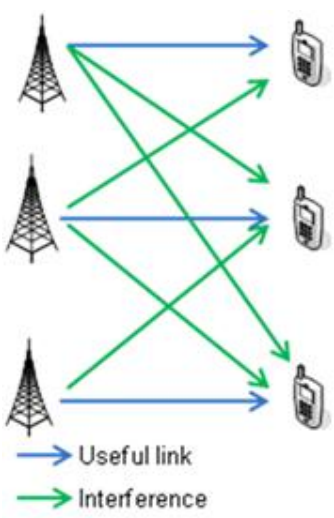


Figure 8-24: Average sum MSE for different estimation error powers. The system is 3-user 2x2 MIMO IC with  $d_k=1$  and SNR =0dB.

### T3.2 TeC 5b – Distributed Interference Alignment techniques under Imperfect Channel State Information

<p style="text-align: center;">System Model</p> 	<p style="text-align: center;"><b>Main Idea</b></p> <p>The main idea is to study the performance of distributed iterative IA algorithms for the interference channel under imperfect CSI.</p> <p>Our approach is based on combining the channel estimation phase and IA iterations phase into one phase where at each step the effective SNR is estimated and the receive filters are optimized. This approach reduces the overhead and permits to more time for data transmission phase.</p>
<p>Considered SoA solution</p>	<p>The SoA solution is the Minimum leakage algorithm [GCJ11] with perfect CSI</p>
<p>KPIs considered and achieved gain</p>	<p>Average sum-capacity</p>
<p>Performance evaluation approach</p>	<p>Analytical / Simulation-based (system level evaluation)</p>
<p>System model considered</p>	<p>Other</p>
<p>Deviation compared to Simulation Baseline</p>	<p>Not Applicable.</p> <p>A simplified system model is considered that consists of a <math>K</math>-user MIMO IC, with narrowband flat fading.</p>
<p>Brief update of the results with respect to D3.2</p>	<p>We provide simulation results with of distributed IA with imperfect CSI at APs and UEs.</p> <p>No contribution in this topic in [MET14-D32].</p>
<p>Association to the TeC Approach</p>	<p>CoMP with limited backhaul capabilities</p>
<p>Targeted TCs</p>	<p>TC2 (Dense urban information society)</p>
<p>Impacted HTs</p>	<p>UDN</p>
<p>Required changes for the realization with respect to LTE Rel. 11</p>	<p>Minor:</p> <ul style="list-style-type: none"> <li>• TDD system</li> <li>• Clustering (groups of links where IA is feasible)</li> <li>• Training phases for IA algorithm iterations</li> </ul>
<p>Trade-off required to realize the gains</p>	<p>The solution presented aims at reducing the overhead phase duration in the interference channel by combining channel</p>



	estimation and IA phases. We show that it is preferable to reliably estimate first than continue on iterating.
--	--

### 8.9.3 Impact on Horizontal Topics

T3.2 TeC 5b - HT.UDN	
Technical challenges	<ul style="list-style-type: none"> <li>• Interference management with imperfect CSI</li> <li>• Decreasing the overhead</li> </ul>
TeC solution	The effect of imperfect CSI is an important issue to study the real gains of Interference alignment based techniques in terms of spectral efficiency. The potential gains can be observed for TC2.
Requirements for the solution	<ul style="list-style-type: none"> <li>• CSI acquisition model at APs and UEs</li> <li>• TDD system</li> </ul>
KPIs addressed and achieved gain	Spectral efficiency: the average gain depend on the CSI error power
Interaction with other WPs	<ul style="list-style-type: none"> <li>• WP4: interference management addressed in Tec1 is closely related to our work</li> </ul>

### 8.9.4 Addressing the METIS Goals

T3.2 TeC 5b	
1000x data volume	With reduced overhead phase duration, more time is allocated to data transmission which increases the total users' throughput and the spectral efficiency.
10-100 user data rate	With reduced overhead phase duration, more time is allocated to data transmission which increases the average users' data rates.
10-100x number of devices	
10x longer battery life	
5x E-E reduced latency	
Energy efficiency and cost	The total power allocated to the pilot transmission can be minimized resulting in some energy efficiency.

### 8.9.5 References

[GCJ11] K. Gomadam, V. R. Cadambe, and S. A. Jafar, "A distributed numerical approach to interference alignment and applications to wireless interference networks", IEEE Transactions on Information Theory, vol. 57, no.6, pp 3309-3322, June 2011.

[CJ11] V. R. Cadambe, and S. A. Jafar. "Interference alignment and degrees of freedom of the-user interference channel", IEEE Transactions on Information Theory, vol. 54, no. 8, pp 3425-3441, Aug. 2008.



[TG09] R. Tresch and M. Guillaud. "Cellular interference alignment with imperfect channel knowledge", ICC Workshops, 2009.

[AH12] O. El Ayach and R.W. Heath. "Interference alignment with analog channel state feedback", IEEE Transactions on Wireless Communications, vol. 11, no. 2, pp 626-636, 2012.

[XLM+13] B. Xie, Y. Li, H. Minn, and A. Nosratinia, " Adaptive Interference Alignment with CSI Uncertainty", IEEE Transactions on Communications, vol. 61, no. 2, pp 792-801, 2013.

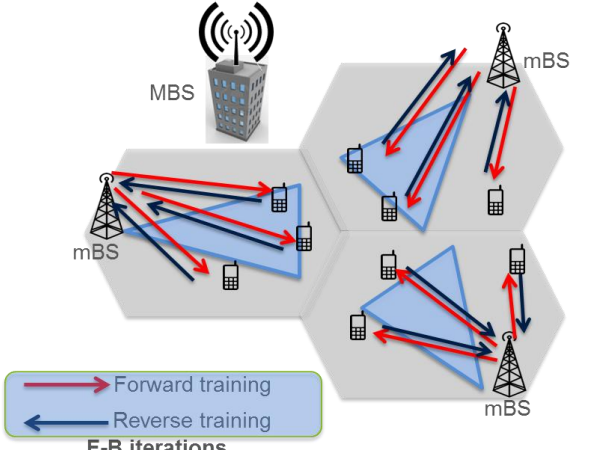
[MET14-D32] METIS consortium, "D3.2 – First performance results for multi-node/multi-antenna transmission technologies," project report, Apr. 2014.

## 8.10 T3.2 TeC 6: Distributed low-overhead schemes for MIMO Interference Channels [KTH]

### 8.10.1 General Overview

The main focus of the proposed TeC is to greatly enhance the spectral efficiency of DL and UL transmission in dense heterogeneous networks – which constitute the core of the network densification paradigm. The proposed schemes advocate the use of *training via UL / DL pilots in a TDD network (also known as forward-backward (F-B) or “ping pong” iterations)*, to iteratively optimize the transmit / receive filters, in a fully distributed manner. In the DL phase of each F-B iteration, users estimate their effective signal and interference covariance matrix (using DL pilots), and accordingly optimize their receive filters based on this local CSI only. Similarly, in the UL phase, mBSs estimate their effective signal and interference covariance matrix, using UL pilots to obtain local CSI and optimize their transmit filters. The procedure is illustrated in Table 8.5. The latter algorithm is an extension to our earlier proposed method in [METIS14-D32] (described in [GKB+15]), where we now *accommodate multiple users within each cell*. Furthermore, while the aforementioned algorithm used a suboptimal metric such as the interference leakage, *the proposed algorithm optimizes both the interference-plus-noise, and the signal subspace, resulting in largely superior performance with respect to its predecessor.*

Table 8.5: Proposed Algorithm Structure

	<p><b>F-B iteration structure</b></p> <p><u>Forward Training:</u></p> <ul style="list-style-type: none"> <li>• mBSs send DL pilots</li> <li>• each user estimates desired and interference covariance matrix</li> <li>• each user updates its receive filter</li> </ul> <p><u>Reverse Training:</u></p> <ul style="list-style-type: none"> <li>• users send UL pilots</li> <li>• each mBS estimates desired and interference covariance matrix</li> <li>• each mBS updates its receive filter</li> </ul>
---	--

Although this F-B iterations structure has been employed in many earlier works (e.g., [GCJ08]), the resulting algorithms require hundreds of such F-B iterations – a prohibitively high communication overhead. In our work, *we investigated the regime where the number of such F-B iterations is relatively small (i.e. less than 5), resulting in algorithms with small associated overhead.* Note that each F-B iteration consists of one subframe, and perfect channel estimation at BSs and UEs is assumed: though static users are used in the simulations, the results are still relevant for slow-moving UEs. The chief advantage of such schemes is that they *alleviate the need for feedback* (while still keeping the communication overhead associated with F-B iterations at a minimum level), and for a backhaul (micro BSs do not need to exchange information, since only local CSI is needed at each mBs). As opposed to “pure IA” schemes that are only aimed at reducing / suppressing interference, the proposed schemes optimize both the signal and interference, thus resulting in far better

performance than pure IA methods. Finally, the *proposed schemes are ideal for cases where multi-stream transmissions are needed*, i.e., where a relatively high spectral efficiency is desired for each user (as we will see from the simulation results).

### 8.10.2 Performance Results

#### Simulation Setup and Evaluation Procedure:

We follow standard baseline for TC2, outlined in [METIS14-D32], Sect. 8.2, consisting of 210 outdoor users of the “reduced Madrid Grid”. Exploiting the fact that each mBS has two sectors, we assign 4 orthogonal resource blocks to the area in question, resulting in every two mBS sectors, covering a specific area, that we dub super-cell (as shown in the figure below).  $K_u = 26$  users are dropped randomly in each sector (following a uniform distribution), for a total of approximately 210 outdoor users. The path loss value at each user location follow the PS#3 calculations provided in [METIS13-D61, Section 8.1.3], and were computed using the supporting material provided in [M13]. All the parameters follow the simulation guidelines in [METIS14-D32, Section 8.2].

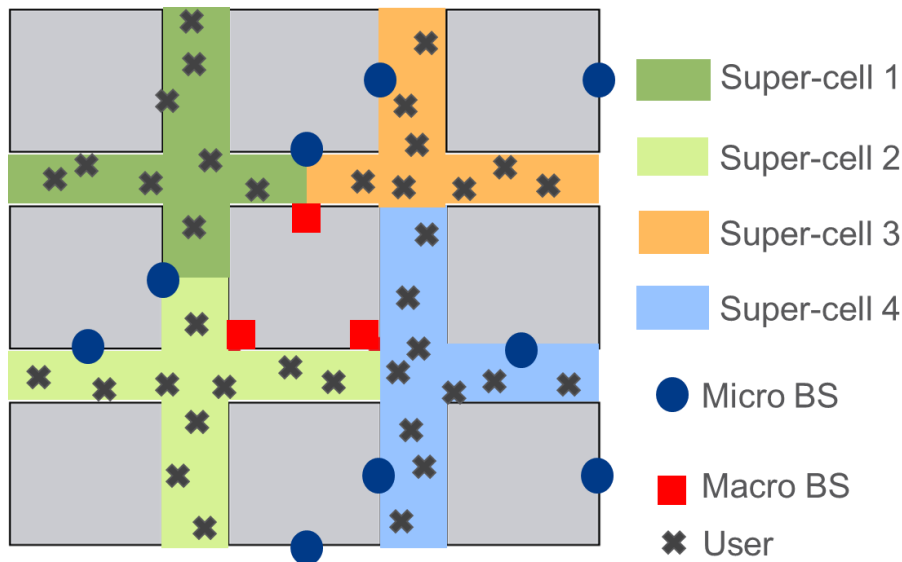


**Figure 8-25: Simulation setup as per the guidelines given in [METIS14-D32, Section 8.2]**

Since channels are assumed to be unknown at this point, we opted not to use any channel specific scheduling (such as proportional fair queuing), and since scheduling is somewhat outside the scope of our evaluation, we opted to use a simple round robin scheduler. In each of the two sectors,  $K$  out the  $K_u$  users ( $K < K_u$ ) are scheduled for transmission, and the proposed algorithm is run to optimize the filters at the mBS, and users. Then the achievable rate of communication over  $T_s = K_u/K$  blocks, for each super-cell is given by,

$$R_{prop} = \frac{1}{T_s} \sum_{t=1}^{T_s} \sum_{l=1}^L \sum_{k=1}^K \log_2 |I + \rho_{l,k}(U_{l,k}^* S_{l,k} U_{l,k})(U_{l,k}^* Q_{l,k} U_{l,k})^{-1}|$$

where  $\rho_{l,k}$ ,  $U_{l,k}$ ,  $S_{l,k}$  and  $Q_{l,k}$  are the received power, receive filter, signal covariance matrix, and interference-plus-noise covariance matrix of user  $k$ , in cell  $l$ , respectively.

The baseline scheme is one using orthogonal access (e.g. TDMA), where each user in each sector is assigned a separate transmission block, thereby removing interference from any transmission. Capacity-achieving single user eigen-beamforming based on the SVD of the channel is used for the latter transmission (we assume that the channel is known perfectly for

that case): this technique is simplified version of transmission mode 9 in LTE, to achieving full spatial multiplexing. The achievable rate of communication for  $T_s$  scheduling block is,

$$R_{orth} = \frac{1}{KLT_s} \sum_{t=1}^{T_s} \sum_{l=1}^L \sum_{k=1}^K \log_2 \left| I + \frac{\rho_{l,k}}{\sigma^2} (U_{l,k}^* S_{l,k} U_{l,k}) (U_{l,k}^* U_{l,k})^{-1} \right|$$

for each super-cell.

### Simulation Results:

We pick a user at random, with rate  $R$ , and evaluate the corresponding CDF as,  $F_\gamma = Prob[R > \gamma]$ , for both our proposed schemes, and the benchmark. Figure 8-26 shows this results for a “typical” network configuration (4x4 MIMO links, with  $d=2$  stream), as a function of the operating SNR. As we can see, there is a significant gap between the proposed schemes and the benchmark.

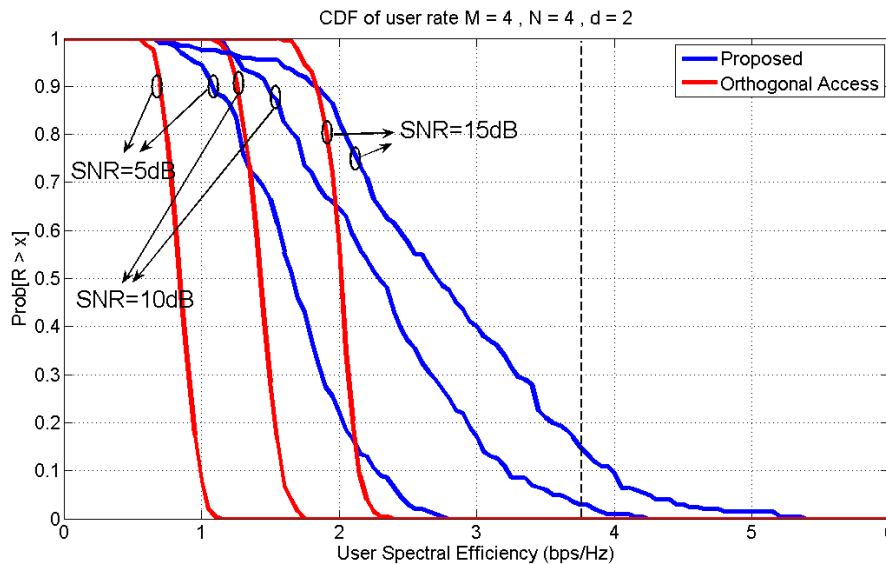


Figure 8-26: CDF of user rate as function of SNR (M=N=4, d=2)

The main KPI of TC2 clearly states that a user data rate of 300 Mbps in DL, should be maintained for 95% of the time: following the simulation parameters set in [METIS14-D32, Section 8.2], *this requirement translates into a 3.75 bps/Hz in spectral efficiency*. It can be seen from that above figure that this KPI is far from met (shown as dashed vertical line). Next we investigate the effect of varying antenna configurations, by increasing the number of transmit antennas. It can be clearly seen from Figure 8-27, that *when the number of transmit antennas is gradually increased, the performance of our proposed scheme increases massively* (around 200% gain for  $M=10$ ), while improvement of the benchmark scheme is quite insignificant. Furthermore, we note that for  $M=10$ , the 3.75 bps/Hz threshold is satisfied around 97% of the time, thereby implying that the KPI would be met.

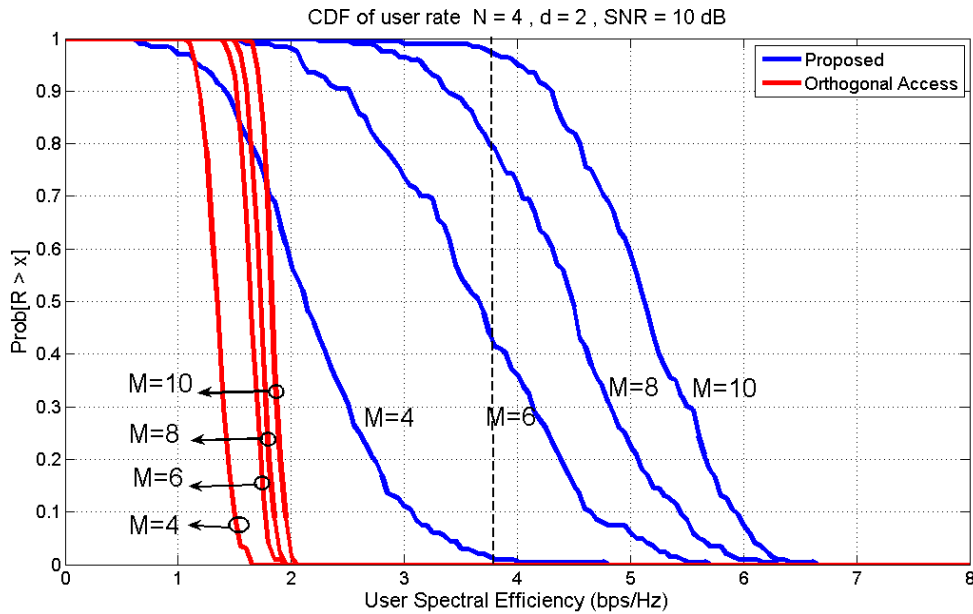


Figure 8-27: CDF of user rate as function of number of transmit antenna (N=4, d=2)

Next we evaluate the area-wide performance of the proposed scheme, i.e. the average area spectral efficiency (in bps/Hz) for both our proposed scheme and the benchmark, as well as the robustness of the performance of our method, by the variance of the area spectral efficiency metric (all the results are divided by the number of used resource blocks, i.e. 4). As we can see from the table below, though the performance delivered by our schemes seems to have more variability than the benchmark, the average area-wide performance is largely superior, and ranges from 80% to 200% over the benchmark.

Table 8.6: Mean and Standard deviation of area spectral efficiency

		<i>Area spectral efficiency (bps/Hz)</i>				
<b>Prop.</b>	<i>mean</i>	14.233	20.947	26.474	29.964	32.501
	<i>std. dev.</i>	0.262	0.377	0.304	0.331	0.305
<b>Orth.</b>	<i>mean</i>	8.583	9.611	10.336	10.847	11.327
	<i>std. dev.</i>	0.0534	0.0401	0.0331	0.0337	0.0338
		<b>4x4, 2</b>	<b>6x4, 2</b>	<b>8x4, 2</b>	<b>10x4, 2</b>	<b>12x4, 2</b>

In Figure 8-28 and Figure 8-29 we provide, for both our scheme and the benchmark, the 5<sup>th</sup>, 50<sup>th</sup> and 90<sup>th</sup> percentile of the user’s spectral efficiency. As before, we can see that although our scheme has slightly less robustness in performance than the benchmark, it does offer significantly better performance (2 - 3 times better).

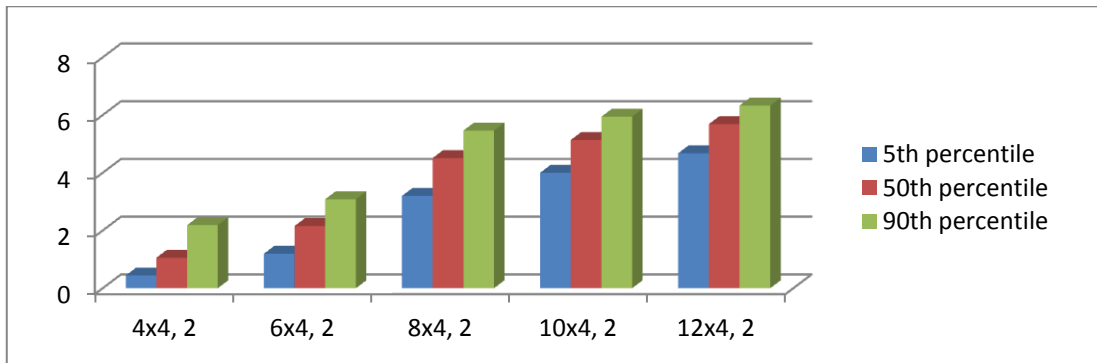


Figure 8-28: Statistics of user rate, for proposed scheme

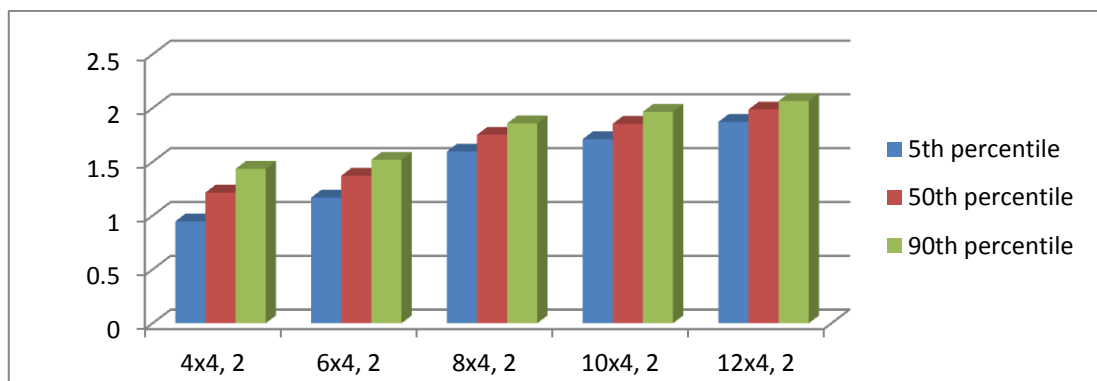


Figure 8-29: Statistics of user rate, for benchmark scheme

Finally, we investigate the net effect of the particular schemes, by comparing the gain of our proposed scheme with respect to the benchmark,  $G = R_{prop} / R_{orth}$ , against the associated increase in overhead,  $F = O_{prop} / O_{orth}$ , where  $O_{prop}$  and  $O_{orth}$  are the communication overhead required by the proposed scheme, and the benchmark, respectively (measured by the number of required pilot transmissions). It can be shown, that by fixing the number of F-B iteration to some value, then  $F$  is constant. Interestingly, it can be seen from the figure below, that as the system dimensions are increased, the gains in spectral efficiency will offset the required increase in overhead.

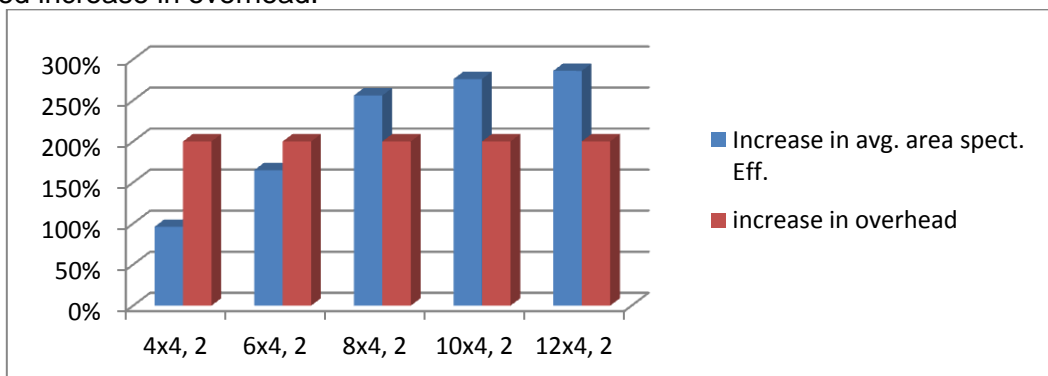
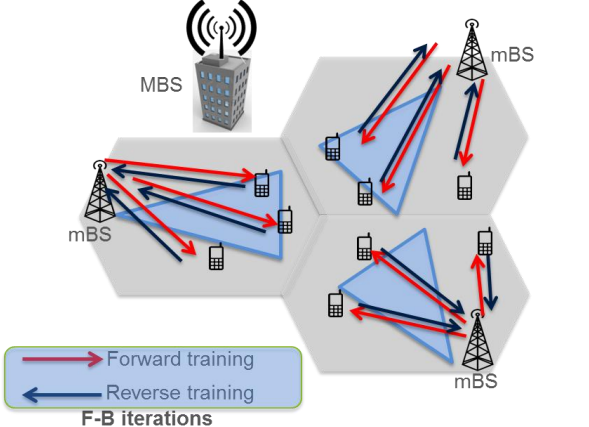


Figure 8-30: Gain in area spectral efficiency, vs increase in overhead

The presented above seem to imply that a decentralized network architecture, employing TDD operation, can deliver significantly higher performance compared to a centralized FDD architecture (since it alleviates the need for feedback, while requiring a minimal amount of overhead for F-B iterations), for delivering high spectral efficiency.

### T3.2 TeC 6 – Distributed low-overhead schemes for MIMO ICs

	<p><b>Main Idea</b></p> <p>Group of algorithms that iteratively refine transmit filters (at mBSs) and receive filters (at users) in a fully distributed manner, using uplink-downlink pilots (to maximize the area spectral efficiency). Exploiting channel reciprocity in TDD systems, such algorithms have the distinct advantage of alleviating the need for feedback, backhaul (cooperation is implicit), requiring only local CSI at each node (acquired through pilots), and a relatively low communication overhead.</p>
<p>Considered SoA solution</p>	<p>The benchmark solution is orthogonal access (e.g. TDMA), where each user in each cell, is assigned a separate transmission block. Optimal single user eigen-beamforming (somewhat similar function as transmission mode 9 in LTE Rel 11) is then used for each transmission block, to achieve high multiplexing gain.</p>
<p>KPIs considered and achieved gain</p>	<ul style="list-style-type: none"> <li>• <u>Total spectral efficiency of area:</u> <ul style="list-style-type: none"> <li>- Average gain: 80% ~ 180% (Table 8.6)</li> <li>- Gain for 5<sup>th</sup> / 50<sup>th</sup> / 90<sup>th</sup> percentile: 80% ~ 200% (Figure 8-28, Figure 8-29)</li> </ul> </li> <li>• <u>CDF of user spectral efficiency:</u> directly related to the “300 Mbps DL , 95% of the time” KPI, required by TC2 (refer to Figure 8-26 and Figure 8-27 and accompanying discussion) <ul style="list-style-type: none"> <li>- 50% ~ 150% gain</li> </ul> </li> </ul>
<p>Performance evaluation approach</p>	<p>Link-level simulation</p>
<p>System model considered</p>	<p>WP3 Task Simulation Baseline</p>
<p>Deviation compared to Simulation Baseline</p>	<p>Minor. The only signification deviation from the simulation baseline is regarding the spectrum assignment assumption, where we divide the overall area into <math>B=4</math> super-cells, each with a different resource block / spectrum band (Figure 8-25 and accompanying discussion). Note that all our results are renormalized by <math>B</math>, to account for this fact, i.e. the area spectral efficiency in actually in bps/Hz, per resource block.</p>
<p>Brief update of the results with respect to D3.2</p>	<p>Prior simulation results presented in [METIS14-D32] we not aligned with simulation baseline. Furthermore, we used here an extended version of the algorithm used in [METIS14-D32]. The results presented here are the most accurate and relevant.</p>
<p>Association to the TeC Approach</p>	<p>CoMP with limited backhaul capabilities</p>
<p>Targeted TCs</p>	<p>TC2</p>
<p>Impacted HTs</p>	<p>UDN</p>
<p>Required changes for the realization with respect to LTE Rel. 11</p>	<p>Minor changes in LTE frame structure, to allow for the pilot transmission phase</p>



Trade-off required to realize the gains	Proposed TeC incurs increase in pilot overhead for coordination and channel estimation, with respect to benchmark solution. However, the gains in performance outweigh the increase in overhead for some specific antenna configurations (Figure 8-30 and accompanying discussion).
---	---

### 8.10.3 Impact on Horizontal Topics

T3.2 TeC 6 - HT.UDN	
Technical challenges	<ul style="list-style-type: none"> <li>Densification is the core concept of UDN</li> <li>Densification → high interference conditions → low throughput.</li> <li>Densification → high feedback and backhaul overhead.</li> </ul>
TeC solution	<ul style="list-style-type: none"> <li>Proposed TeC greatly boosts the throughput, via simple coordination schemes.</li> <li>Proposed TeC bypasses the need for feedback and backhauling, while keeping the commutation overhead low (by coordinating clusters of small size).</li> </ul>
Requirements for the solution	TDD network architecture, reliable channel estimation, low-to-medium mobility of users
KPIs addressed and achieved gain	Average gain in area spectral efficiency (80% ~ 180%)
Interaction with other WPs	WP4

### 8.10.4 Addressing the METIS Goals

T3.2 TeC 6	
1000x data volume	
10-100 user data rate	As simulations showed, the proposed TeC offers a 2 - 3 increase in average user data.
10-100x number of devices	
10x longer battery life	
5x E-E reduced latency	
Energy efficiency and cost	

### 8.10.5 References

[GCJ08] K. S. Gomadam, V. R. Cadambe and S. A. Jafar, "Approaching the Capacity of Wireless Networks through Distributed Interference Alignment", Proceedings of IEEE GLOBECOM, New Orleans, LA, Dec. 2008.

[GKB+15] H. Ghauch, T. Kim, M. Bengtsson, M. Skoglund, "Distributed Low-Overhead Schemes for Multi-stream MIMO Interference Channels", IEEE Trans. on Signal Processing, accepted for publication, Jan. 2015.

[M13] METIS test cases following the simulation guidelines, <https://www.metis2020.com/documents/simulations/>.

[METIS13-D61] METIS D6.1, "Simulation Guidelines", Oct. 2013.



**Document:** FP7-ICT-317669-METIS/D3.3

**Date:** 25/02/2015

**Security:** Public

**Status:** Final

**Version:** 1

---

[METIS14-D32] METIS D3.2, "First performance results for multi-node/multi-antenna transmission technologies", Apr. 2014.

## 8.11 T3.2 TeC 7: Dynamic clustering with multiple receive antennas in downlink CoMP systems [ALU]

### 8.11.1 General Overview

Most of the works on CoMP focus on systems where UEs are equipped with only one antenna, although already with LTE-Advanced UEs may be equipped with up to eight antennas [BCG+12]. Although this number seems a bit optimistic, the technological innovation may allow in the near future manufacturing smartphones and tablets equipped with several antennas. Moreover, different types of UEs will be served by the cellular networks in 2020: for instance, vehicles will be probably part of the cellular infrastructure, and, due to their size, they can be quite easily equipped with multiple antennas [METIS62]. Hence, it has been recognized the importance of developing algorithms for CoMP-JP that explicitly take into account these additional UE capabilities [HCL+13]: clusters should be organized by considering that multiple antenna UEs can either use an interference rejection combiner (IRC) [Win84] to partially suppress the residual inter-cluster interference (ICI) or be served by means of a multi-stream transmission.

In this work we consider a downlink CoMP-JP scenario, i.e., a scenario where CSI and data to be sent to the UEs are shared among the BSs. We assume that a CU coordinates the BSs and the backhaul links have zero latency and are error free. In this setup, we propose an algorithm to jointly perform dynamic BS clustering and UE scheduling, under the assumption of multi-antenna UEs. We assume that UEs perform SIC with IRC. By observing that most of the interference at each UE comes from the closest BSs and with the aim of reducing the implementation complexity of the algorithm, we assume that only a set of candidate BS clusters, which depends on the large scale fading, is considered by the CU. As this candidate BS cluster selection depends on the large scale fading component of the channel, the list of candidate BS clusters is updated on a long-term time interval, for instance every hundreds of milliseconds.

Then, depending on the fast-fading component of the channel, i.e., every few milliseconds, the CU organizes BS clusters and schedules UEs in each cluster by applying the following two-step scheme.

1. For each candidate BS cluster, a weighted sum-rate is estimated by optimizing precoders, powers, transmission ranks and scheduled UEs. In particular, we use the multiuser eigenmode transmission (MET) scheme [BH07], with equal power allocation among the streams and a greedy iterative eigenmode selection algorithm. Note that MET has been proven to outperform in a MIMO broadcast channel other linear precoding schemes, whereas the assumption of equal power allocation among the scheduled streams is asymptotically optimal at high SNR.
2. Once the weighted sum rate has been computed for all the candidates, the CU selects the set of non-overlapping BS clusters to be used for transmission by maximizing the system weighted sum rate. As the optimization problem is shown to be NP-hard, we propose a greedy iterative algorithm to reduce the implementation complexity.

We highlight that the proposed dynamic solution allows the flexibility of scheduling a given UE in different BS clusters across successive blocks and with different transmission ranks, depending on the SNR conditions. More details about the developed technology can be found in [BBB14].

### 8.11.2 Performance Results

We consider the WP3 task 3.2 simulation baseline where 3 macro sectors and 18 micro sectors, for a total of 21 BSs, are deployed in a grid of 3x3 buildings and serve 210 outdoor UEs [METIS32, Fig. 8.1]. Several details regarding the position of the BSs and the model for the large scale fading component of the channel can be found in [METIS32, Sect. 8.2]. Regarding the fast fading, we consider (a) a MIMO Rice model with a Rice factor of 10 dB for

the LOS case and (b) a MIMO Rayleigh model for the NLOS case. Moreover, we assume that each macro BS is equipped with 4 antennas with a maximum transmit power of 46 dBm, whereas each micro BS is still equipped with 4 antennas but with a maximum transmit power of 30 dBm. The carrier frequency is 2.6 GHz and the system bandwidth is 10 MHz. Then, we implement proportional fair scheduling to provide fairness among the UEs, which employ SIC with IRC. Perfect detection is also assumed.

We compare the developed scheme based on dynamic clustering (DC) by assuming a maximum cluster size of 3 BSs against a baseline denoted single cell processing (SCP), where each UE is served by its anchor BS and no cooperation is allowed among the BSs in the network.

In Figure 8-31 and Figure 8-32 we report in terms of the number  $N$  of UE antennas the average cell rate and the 5th percentile of the UE rate, respectively. By adding antennas at the UE, we observe an important performance improvement. For instance, with SCP by increasing  $N$  from 1 to 4 there is an improvement of about 80% in terms of 5th percentile of the UE rate. Two factors mainly contribute to this gain: (a) UEs with lower SINR use IRC to limit the impact of residual ICI not managed at the transmit side and (b) UEs with higher SINR can be served by multiple streams of data. From Table 8.7, where we report the distribution of the transmission rank with  $N = 4$ , we note that with SCP more than 80% of the transmissions are rank-1. On the other hand, with DC, as the interference level suffered by the UEs is lower, about 35% of transmissions are multi-stream. This shows that in general most of the gain is due to the IRC and multi-stream transmission plays a non-negligible role only with DC. Moreover, we also observe that the performance gain achieved by DC over SCP decreases by adding more antennas at the UE side. In fact, as the gain of using multiple antenna UEs is mainly due to the IRC which cancels ICI, the benefits of increasing  $N$  are seen more in a non-cooperative scenario, where the residual ICI is higher with respect to DC. In detail, the performance gain in terms of the average cell rate achieved by DC over SCP drops from about 70% with  $N = 1$  to about 25% with  $N = 4$ , while the performance gain in terms of the 5th percentile of the UE rate achieved by DC over SCP drops from about 160% with  $N = 1$  to about 100% with  $N = 4$ .

Then, two important comments should be made when we compare these results with the ones already shown in a homogeneous hexagonal scenario [BBB14, Fig.s 5-6]. First, we observe that much higher rates are achieved in the WP3 task 3.2 simulation baseline considered here: for instance, the average cell rate is almost doubled. Second, we observe that the gain achieved by CoMP over the baseline are much higher here than in the homogeneous hexagonal scenario: for instance, in terms of the 5<sup>th</sup> percentile of the UE rate, in [BBB14] this gain varies from about 15% when  $N=4$  to about 50% when  $N=1$ , whereas here this gain varies from about 100% when  $N=4$  to about 160% when  $N=1$ . These two effects can be explained by observing that the WP3 task 3.2 simulation baseline is an heterogeneous scenario with an higher density of BSs. Therefore, the UEs are typically closer to their anchor BS, they measure a better SINR and, as a consequence, the achieved rates are also higher. Then, in Heterogeneous networks the *structure* of the interference is typically different with respect to the one in a homogeneous scenario: in Heterogeneous networks the interference comes mainly from few strong interferers, typically the macro BSs. Hence, CoMP schemes provide more benefits in this setup, even if the maximum cluster size is rather small (only 3 BSs).

Besides previous results obtained in the WP3 task 3.2 baseline, further studies and simulations have been conducted in the homogeneous hexagonal grid scenario by investigating the effects of imperfect CSI at the BSs. In particular, we have considered a TDD system where channels are estimated at the BSs by assuming that orthogonal training sequences are transmitted by the UEs, thus avoiding interference on channel estimation. In Figure 8-33, we plot the fifth percentile of the UE rate versus the pilot overhead, i.e., the percentage of resource elements allocated to pilots, for the extended typical urban (ETU) channel model, characterized by a root mean-square delay spread of 991 ns and a Doppler

frequency of 5 Hz [STB09, Ch. 21]. Further simulation parameters can be found in [BBB14]. The dashed lines are the rates computed by assuming perfect CSI at BSs. We observe that the rates increase with the increase of the number of pilots up to a maximum and then decrease. In fact, increasing the pilot overhead has two conflicting effects: (a) a more reliable CSI is collected at BSs thus improving performance and (b) a lower number of resource elements is allocated to data transmission thus obviously reducing the achievable rate. Clearly, for lower values of the pilot overhead, the effect of a better channel estimation dominates, whereas for higher values of the pilot overhead, the CSI is reliable enough for the SINR level of the UEs, and a further increase of the number of pilots represents only a waste of resources. Even if we consider a low mobility scenario, due to the higher frequency selectivity of the ETU channel model, no scheme reaches the rates achieved with perfect CSI. Then, the fraction of resources allocated to pilots necessary to reach the peak in performance is lower for SCP than that for DC: in fact, while with SCP only the channels between a BS and its anchored UEs are used for precoding design, with DC precoders are optimized on the basis also of the channels between some other auxiliary BSs and these UEs. By choosing for each scheme the value of the pilot overhead which provides the best rate, the performance gain achieved by DC over SCP decreases with respect to the perfect CSI case to about 16%. More results and studies on the effects of imperfect CSI at both the BSs and the UEs can be found in [BBB14].

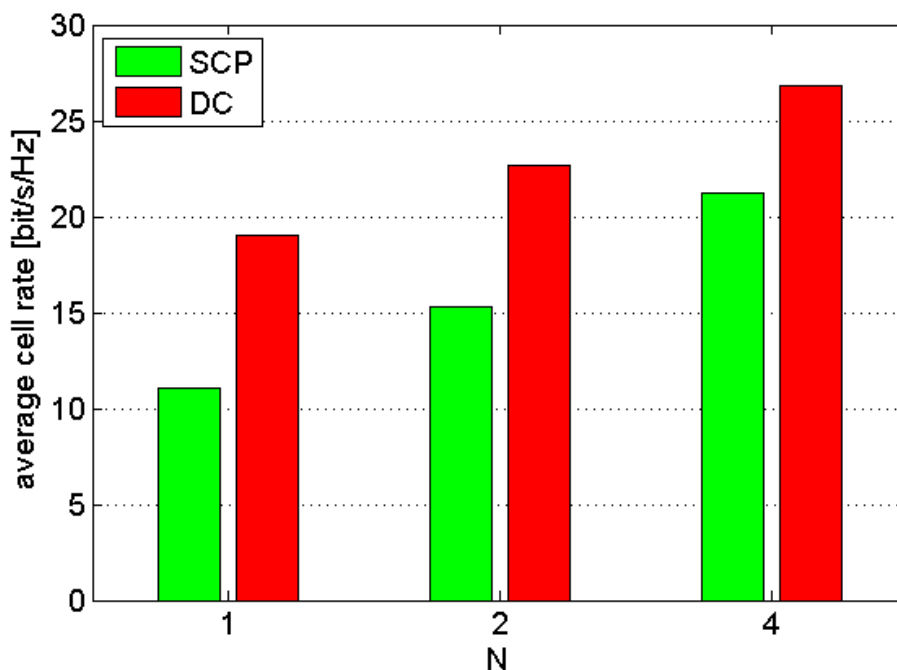


Figure 8-31: Average cell rate with respect to the number N of UE antennas

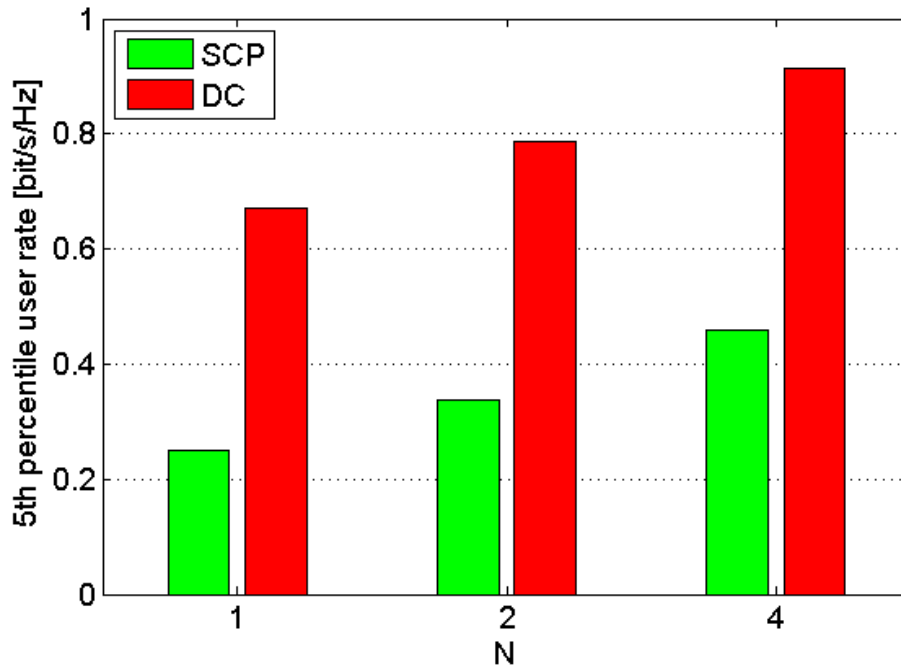


Figure 8-32: 5th percentile of the UE rate with respect to the number N of UE antennas

Table 8.7: Distribution (%) of the transmission rank with N=4

	Rank-1	Rank-2	Rank-3	Rank-4
SCP	82.0	15.6	2.2	0.2
DC	65.2	22.3	9.2	3.3

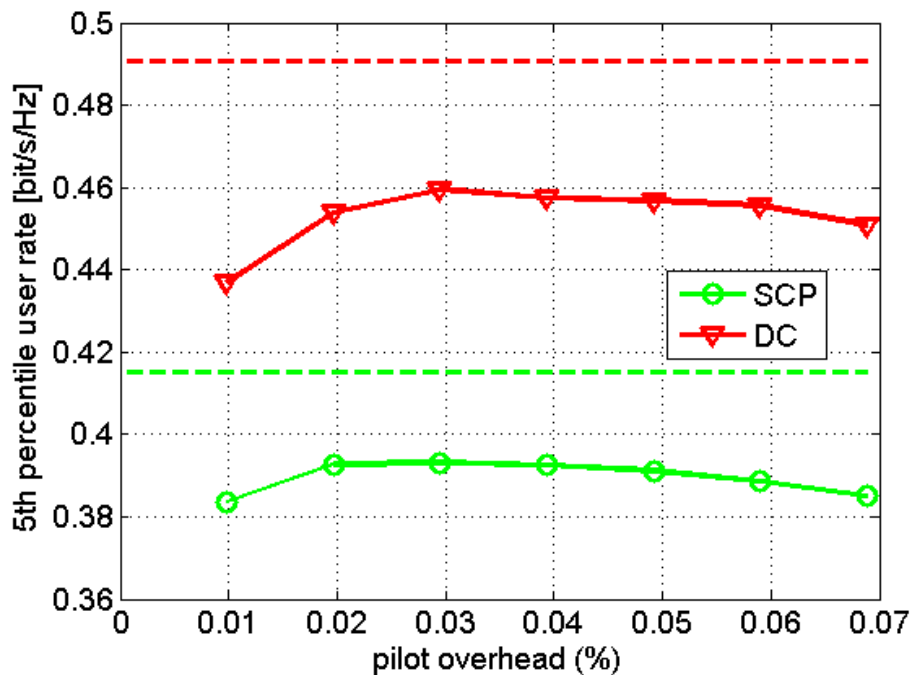
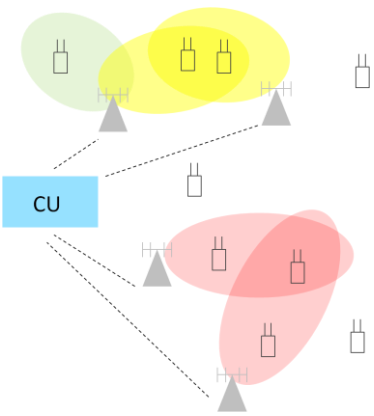


Figure 8-33: 5th percentile of the UE rate versus pilot overhead with N = 4 and for the ETU channel

### T3.2 TeC 7 – Dynamic clustering with multiple receive antennas in downlink CoMP systems

	<p style="text-align: center;"><b>Main Idea</b></p> <p>The work considers a downlink CoMP-JP system and proposes a dynamic BS clustering and UE scheduling algorithm. The algorithm allows a dynamic optimization, in each time slot, of the set of non-overlapping clusters and the UEs scheduled within each cluster, maximizing the network weighted sum rate. The approach is extended to the case where the UEs are equipped with multiple antennas and exploit them either to implement an interference rejection combiner or to be served by multi-stream transmission.</p>
---	--

Considered SoA solution	Adapted LTE Release 11
KPIs considered and achieved gain	<ul style="list-style-type: none"> <li>Cell throughput: average gain up to 70%.</li> <li>User throughput: 5<sup>th</sup> percent. gain up to 160%.</li> <li>Spectral efficiency: average gain up to 70%.</li> </ul>
Performance evaluation approach	Simulation-based: system level evaluation
System model considered	WP3 task 3.2 simulation baseline
Deviation compared to Simulation Baseline	None
Brief update of the results with respect to D3.2	<ul style="list-style-type: none"> <li>Simulation results for the WP3 task 3.2 simulation baseline</li> <li>Simulation results with imperfect CSI at BSs and UEs for the hexagonal grid scenario</li> </ul>
Association to the TeC Approach	CoMP with Advanced UE Capabilities
Targeted TCs	TC2 (Dense urban information society)
Impacted HTs	UDN
Required changes for the realization with respect to LTE Rel. 11	Minor: <ul style="list-style-type: none"> <li>Backhaul supporting high data rates and with strict latency requirements</li> <li>High precision oscillators for a tight synchronization among the BSs</li> </ul>
Trade-off required to realize the gains	Cost: The gains achieved in throughput and spectral efficiency are obtained thanks to a higher cost of the backhaul infrastructure

### 8.11.3 Impact on Horizontal Topics

T3.2 TeC 7 - HT.UDN	
Technical challenges	<ul style="list-style-type: none"> <li>• Short term radio resource and interference management (ST-RRM)</li> <li>• Nodes activation and clustering techniques (NA&amp;C)</li> </ul>
TeC solution	A novel dynamic BS clustering scheme is developed for downlink CoMP-JP with multiple antenna UEs. Important gains are observed in TC2, which is relevant for UDN.
Requirements for the solution	<ul style="list-style-type: none"> <li>• Backhaul supporting high data rates and with strict latency requirements</li> <li>• High precision oscillators for a tight synchronization among the BSs</li> <li>• Low UE mobility</li> </ul>
KPIs addressed and achieved gain	<ul style="list-style-type: none"> <li>• Cell throughput: average gain up to 70%.</li> <li>• User throughput: 5th percent. gain up to 160%.</li> <li>• Spectral efficiency: average gain up to 70%.</li> </ul>
Interaction with other WPs	<ul style="list-style-type: none"> <li>• WP2: TeC developed by assuming OFDM, no major change expected when other air interfaces like UFMC are employed</li> <li>• WP4: close alignment needed with WP4 where interference management is an important topic</li> <li>• WP5: TeC targets frequencies below 6 GHz</li> </ul>

### 8.11.4 Addressing the METIS Goals

T3.2 TeC 7	
1000x data volume	Increase in the achieved cell throughput and spectral efficiency (up to 70% gain) allows the increase of the data volume per area
10-100 user data rate	Increase in the fifth percentile of the user rate (up to 160% gain)
10-100x number of devices	Increase in data rates can be translated to an increase in the number of connected UEs
10x longer battery life	
5x E-E reduced latency	
Energy efficiency and cost	



### 8.11.5 References

[BCG+12] F. Boccardi, B. Clercks, A. Ghosh, E. Hardouin, K. Kusume, E. Onggosanusi and Y. Tang, "Multiple-Antenna Techniques in LTE-advanced", IEEE Communications Magazine, vol. 50, no. 3, pp.114-121, March. 2012.

[METIS62] METIS consortium, "D6.2 – Initial report on horizontal topics, first results and 5G system concept," project report, Mar. 2014.

[HCL+13] I. Hwang, C.-B. Chae, J. Lee, and R. W. Heath, "Multicell cooperative systems with multiple receive antennas," IEEE Wireless Commun. Mag., vol. 20, no. 1, pp. 50–58, Feb. 2013.

[Win84] J. Winters, "Optimum combining in digital mobile radio with cochannel interference," IEEE J. Sel. Areas Commun., vol. 2, no. 4, pp. 528–539, Jul. 1984.

[BH07] F. Boccardi and H. Huang, "A near-optimum technique using linear precoding for the MIMO broadcast channel," in Proc. IEEE International Conference on Acoustics, Speech and Signal Processing (ICASSP), Honolulu (HI), Apr. 2007.

[BBB14] P. Baracca, F. Boccardi, and N. Benvenuto, "A dynamic clustering algorithm for downlink CoMP systems with multiple antenna UEs," EURASIP journal on wireless communications and networking, 2014:125, Aug. 2014.

[METIS32] METIS consortium, "D3.2 – First performance results for multi-node/multi-antenna transmission technologies," project report, Apr. 2014.

[STB09] S. Sesia, I. Toufik, and M. Baker, "LTE: The UMTS Long Term Evolution", John Wiley & Sons, 2009.

## 8.12 T3.2 TeC 8: Studies on non-orthogonal multiple access (NOMA) [DOCOMO]

### 8.12.1 General Overview

The main idea is to combine Non-Orthogonal Multiple Access (NOMA) schemes with multi-antenna transmission schemes. One example is to use multiple antennas at the transmitter to form multiple beams and within each beam, multiple users are multiplexed using a non-orthogonal multiple access based technique. This idea can also be extended to multi-site operations by introducing inter-site interference coordination (e.g. in frequency, space and/or power domains). NOMA can also be combined with single user MIMO (SU-MIMO) where multiple beams intended for a single user are multiplexed in the spatial domain and users are multiplexed in the power-domain. The benefits of NOMA (i.e. OFDMA plus power-domain user multiplexing) compared to OFDMA are:

- Improved spectrum efficiency/system capacity/cell-edge user performance in both macro-cells and small cells (~ 30 % gain);
- The number of simultaneously served users can be almost doubled (up to 2 users multiplexed in power-domain);
- Spectrum efficiency/system capacity/cell-edge user performance can be improved even in high mobility scenarios.

### 8.12.2 Performance Results

NOMA combined with MU-MIMO was studied for 2x2 MIMO in [HK13] and NOMA with 1x2 SIMO was studied in [BL13]. Here, we describe our proposed extension of NOMA to SU-MIMO for 2x2 MIMO ( $N_t = N_r = 2$ ) [BL14]. Figure 8-34 illustrates SU-MIMO (left side) and NOMA combined with SU-MIMO (right side), where the maximum number of multiplexed users  $m = 2$ . UE1 and UE2 represent cell-interior and cell-edge users, respectively, and are paired together on the same time/frequency resources. Similarly to the 1x2 SIMO case, the BS simultaneously superposes with different transmit powers the signals of UE1 and UE2. However, differently from 1x2 SIMO case, SU-MIMO is applied to each UE independently with up to 2-layer per UE. As a result, for 2-UE multiplexing case ( $m=2$ ), using only 2 transmit antennas we are able to perform 4-layer transmission (4-beam multiplexing).

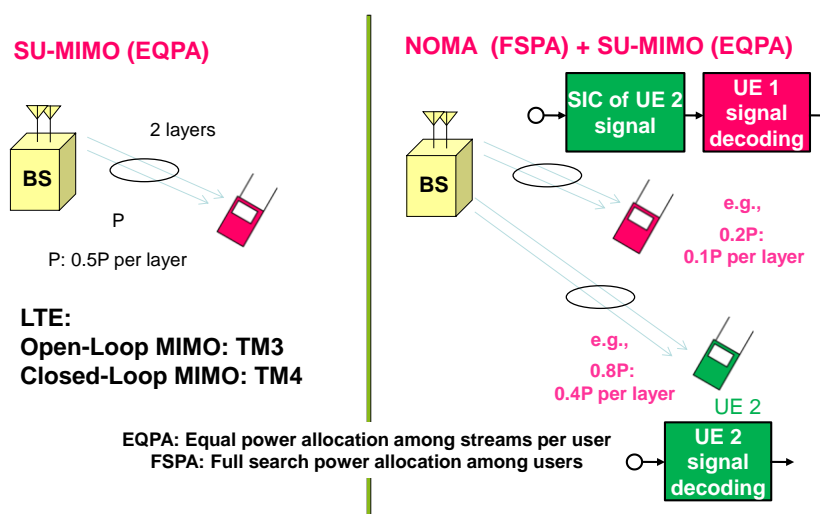


Figure 8-34: NOMA combined with SU-MIMO (2x2 MIMO & 2-UE) (cf. Eqs. (1) and (2))

For orthogonal multiple access (OMA) with SU-MIMO, equal power allocation (EQPA) is applied to split the power between transmission layers. For NOMA with SU-MIMO, the total

power is equally split among transmission layers to a single UE (EQPA) and full search power allocation (FSPA) is applied among multiple users. For FSPA, the best power split is exhaustively searched among all candidate power sets (i.e., combinations of power allocations to NOMA multiplexed users). For instance, let  $P_1$  be the candidate transmit power of cell-center user and  $P_2$  be the candidate transmit power of cell-edge user, with  $P_1$  and  $P_2$  chosen from a discrete set of values [MET14-D23]. As shown in Figure 8-34, assuming that  $P$  is the total transmit power and  $(0.2P, 0.8P)$  is the best power set chosen by FSPA, where  $0.2P$  is allocated to the cell-center user (UE1) and  $0.8P$  is allocated to the cell-edge user (UE2), and both users are multiplexed in the power-domain, the allocated power to each user is split equally among the layers (streams) sent by each user, i.e., the transmit power per layer is  $0.1P$  for the cell-center user (UE1) with two layers case and allocated power of  $0.2P$ .

▪ **Signal model:**

The received signal  $Y_n$  at UE <sub>$n$</sub>  for 2x2 SU-MIMO is described by

$$\mathbf{Y}_n = \mathbf{H}_n \cdot \mathbf{W}_n \cdot \sqrt{P} \cdot X_n + \mathbf{N}_n \quad (1)$$

where  $\mathbf{H}_n$  denotes the channel matrix,  $\mathbf{W}_n$  denotes precoding matrix,  $X_n$  denotes data symbol transmitted for UE <sub>$n$</sub> ,  $\mathbf{N}_n$  denotes inter-cell interference plus additive white Gaussian noise at UE <sub>$n$</sub> , respectively. For each UE <sub>$n$</sub> , the modulation symbols corresponding to one or two transport blocks are first mapped to  $N_L$  layers. The number of layers is referred to as Rank. The Rank is decided by the UE semi-statically and is identical over all subbands. After layer mapping, the symbols of  $N_L$  layers are mapped to transmit antennas by precoding matrix  $\mathbf{W}_n$ . The following two MIMO transmission modes: open-loop (TM3) and closed-loop (TM4) are considered [3GPP06-25814].

As shown in Figure 8-34, for NOMA combined with SU-MIMO, the BS simultaneously transmits a superposed signal to UE<sub>1</sub> and UE<sub>2</sub> and up to 2-layer transmission is supported for each user. From (1), the received signal  $\mathbf{Y}_n$  at UE <sub>$n$</sub>  ( $n = 1, 2$ ) can be expressed as

$$\mathbf{Y}_n = \mathbf{H}_n \cdot (\mathbf{W}_1 \cdot \sqrt{\beta_1 P} \cdot X_1 + \mathbf{W}_2 \cdot \sqrt{\beta_2 P} \cdot X_2) + \mathbf{N}_n \quad (2)$$

where  $\beta_i$  denotes the power ratio for UE  $i$  and  $\beta_1 + \beta_2 = 1$ ,  $P$  denotes the transmit power of BS.

Therefore, both UE1 and UE2 receivers receive the transmit signals designated to UE1 and UE2 multiplexed in the power-domain.

▪ **UE receiver:**

For data detection at receiver side, UE<sub>1</sub> conducts minimum mean-squared error (MMSE) detection as  $\mathbf{U}_{MMSE} \cdot \mathbf{Y}_1$  where  $\mathbf{U}_{MMSE}$  denotes the MMSE weight at UE<sub>1</sub>. UE<sub>1</sub> conducts SIC to remove the data signal of UE<sub>2</sub> then detect its own signal. Similarly, the UE<sub>2</sub> conducts MMSE with weight  $\mathbf{V}_{MMSE}$  to its received signals as  $\mathbf{V}_{MMSE} \cdot \mathbf{Y}_2$ . Treating the signal of UE<sub>1</sub> as interference, UE<sub>2</sub> conducts MMSE detection for its own signal.

▪ **BS scheduler:**

Figure 8-35 illustrates the scheduling steps for multi-user scheduling, multi-user power allocation and NOMA SINR calculation for the case of NOMA combined with SU-MIMO.

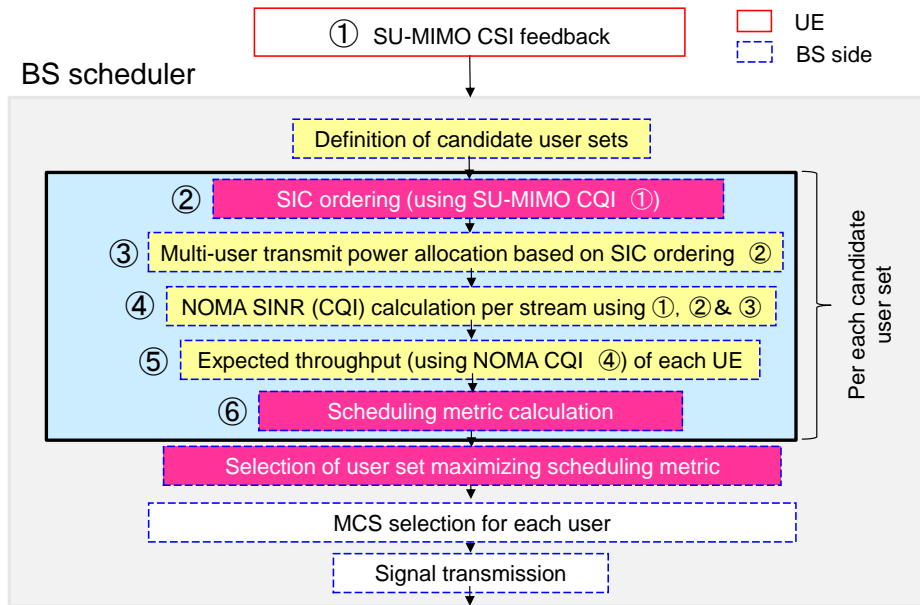


Figure 8-35: Scheduling steps for NOMA combined with SU-MIMO

NOMA gains compared to OMA for TM4 and TM3 for different granularities of MCS selection and scheduling are summarized in Figure 8-36.

Assuming 3GPP LTE simulation parameters, for case 2 (3GPP compliant MCS selection), around 20% cell throughput gains and 30% to 40% for cell edge user throughput gains are achieved. This provides upper bound performance as genie-aided NOMA SINR estimation (UE received SINR after BS scheduling/data transmission perfectly known at BS side before scheduling) is assumed. The improvements are the result of improving spectrum efficiency/system capacity/user fairness improvements by exploiting power-domain user multiplexing at the BS side and SIC receiver at UE side.

However, the genie-aided estimation of NOMA SINR, which is used at the BS side to compute expected user throughput, cannot be perfectly derived at BS from SU-MIMO CQI feedback from UE. In Figure 8-37, we evaluated NOMA performance with NOMA SINR approximation derived at BS side based solely on SU-MIMO CQI (no CSI feedback enhancement) feedback from UEs [BL14].

This, however, cannot be derived from SU-MIMO CQIs reported by UE1 ( $CQI_{SUMIMO}^1$ ) and UE2 ( $CQI_{SUMIMO}^2$ ). Using P1, P2 and SU-MIMO CQI only, we can approximate NOMA SINR for each spatial layer of UE1 and UE2 as follows:

$$CQI_{NOMA}^1 = P_1 CQI_{SUMIMO}^1 \quad CQI_{NOMA}^2 = \frac{P_2 CQI_{SUMIMO}^2}{P_1 CQI_{SUMIMO}^2 + 1}$$

In Figure 8-37, because of the proposed approximation, some performance degradation is observed when we compared Figure 8-36 and Figure 8-37, but a hefty portion of the gains can still be maintained even without CSI feedback enhancements (using SU-MIMO CQI feedback).

### Genie-aided NOMA SINR estimation @ BS

	2x2, MIMO TM3			2x2, MIMO TM4		
	OMA (m=1)	NOMA (m=2)	Gain	OMA (m=1)	NOMA (m=2)	Gain
Case 1: Subband scheduling, subband MCS selection						

Cell	21.37	27.05	26.56%	21.97	27.86	26.84%
Cell-edge	0.47	0.63	34.11%	0.54	0.77	42.83%
Case 2: Subband scheduling, wideband MCS selection						
Cell	21.59	26.29	21.77%	22.29	27.49	23.36%
Cell-edge	0.47	0.62	30.25%	0.55	0.76	39.31%
Case 3: Wideband scheduling, wideband MCS selection						
Cell	19.06	24.89	30.55%	19.57	25.51	30.33%
Cell-edge	0.40	0.53	34.16%	0.45	0.64	43.90%

Figure 8-36: Performance evaluations for NOMA combined with SU-MIMO (2x2).

### NOMA SINR approximation @ BS using SU-MIMO CQI feedback from UE

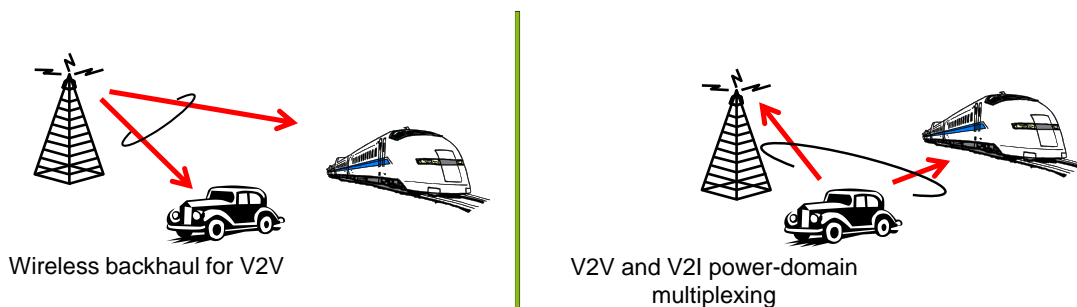
	2x2, MIMO TM3			2x2, MIMO TM4		
	OMA (m=1)	NOMA (m=2)	Gain	OMA (m=1)	NOMA (m=2)	Gain
Case 1: Subband scheduling, subband MCS selection						
Cell	21.37	24.95	16.73%	21.97	25.69	16.96%
Cell-edge	0.47	0.60	28.81%	0.54	0.72	33.46%
Case 2: Subband scheduling, wideband MCS selection						
Cell	21.59	24.30	12.57%	22.29	25.43	14.09%
Cell-edge	0.47	0.59	25.63%	0.552	0.72	30.43%
Case 3: Wideband scheduling, wideband MCS selection						
Cell	19.06	23.37	22.57%	19.57	24.19	23.60%
Cell-edge	0.40	0.52	31.17%	0.45	0.63	40.58%

Figure 8-37: Performance evaluations for NOMA combined with SU-MIMO (2x2).

To maximize the performance of NOMA combined with SU-MIMO, enhancements for NOMA SINR approximation at BS and CSI feedback from UE should be subject to further study. BS scheduling and power allocation, receiver design and signalling aspects for NOMA are studied in WP2 Task 2.3 (TeC11.1.1).

### NOMA for moving networks (MN)

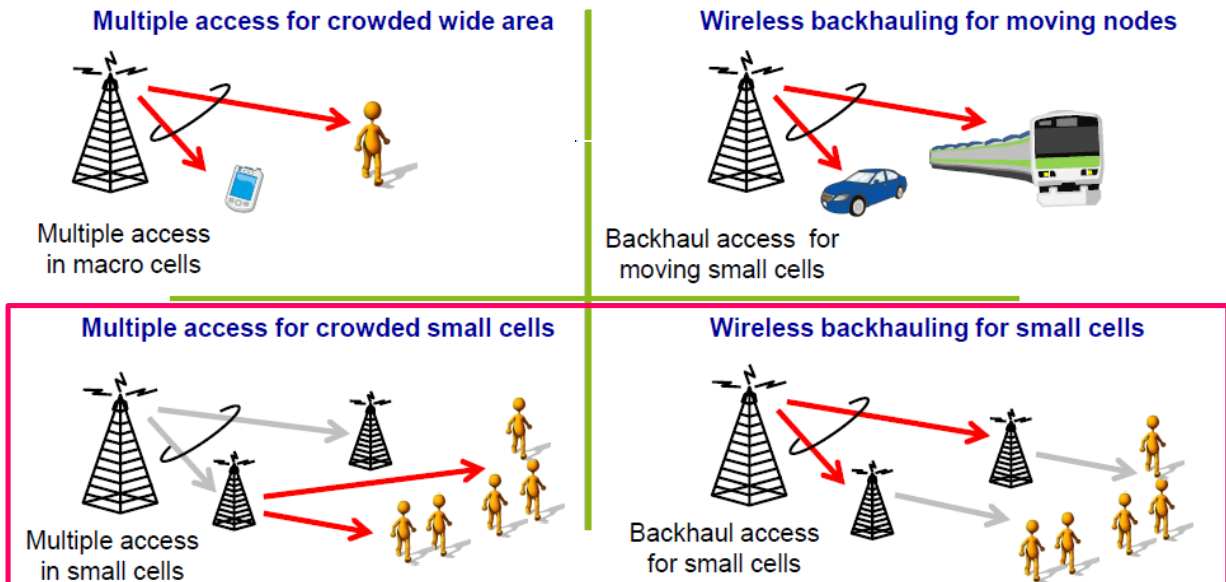
### NOMA for V2X



**NOMA can enable the power-domain multiplexing in V2X scenarios**

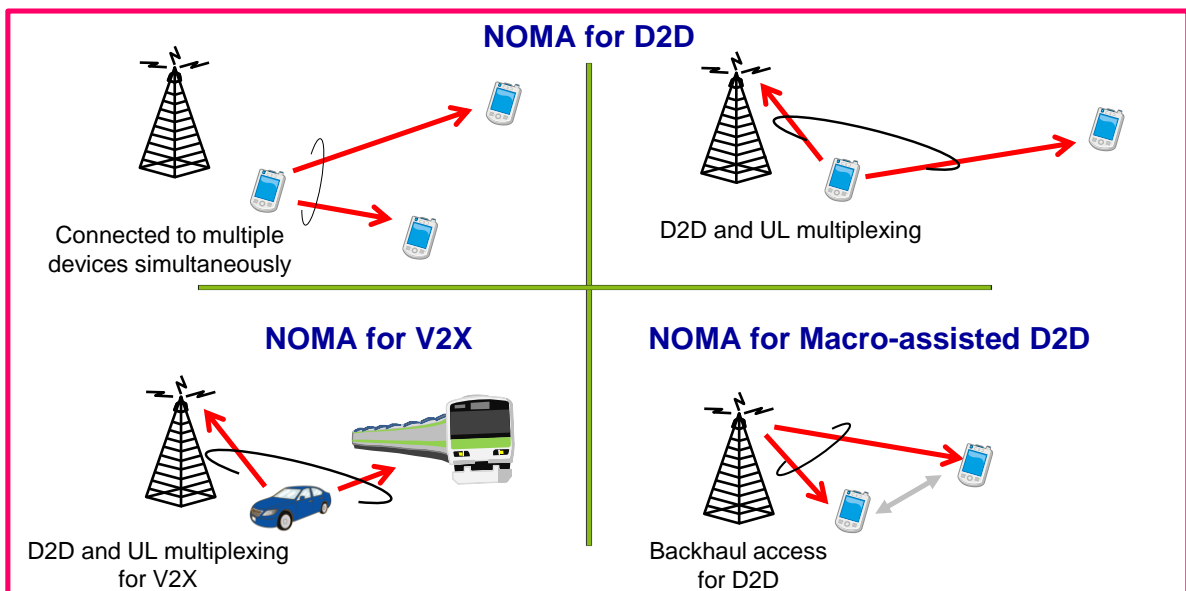
- NOMA is robust to mobility and can exploit the SNR difference between V2V link and V2I link in order to multiplex both links in the power domain.

**NOMA for ultra-dense networks (UDN)**



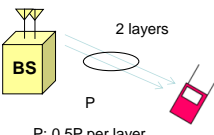
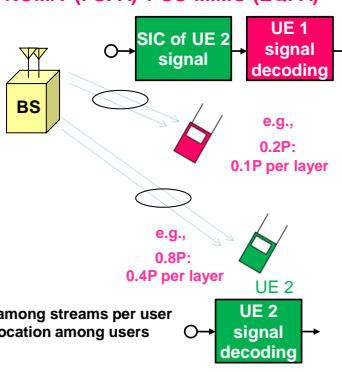
- NOMA can be applied as multiple access for users under small cells or it can be applied as backhauling access from macro cells to small cells.

**NOMA for device-to-device (D2D) communications**



- NOMA can also be applied to D2D and V2X scenarios.
- The benefits of NOMA compared to spatial multiplexing (i.e., MU-MIMO) are summarized as follows:
  - User multiplexing is conducted in the power-domain by exploitation of SNR difference among multiple links or devices; therefore,
    - Multi-user transmission is enabled with no need to increase the number of transmit antennas;

- Robustness to high mobility since it does not rely much on CSI feedback from the receiver for user multiplexing at the transmitter.

T3.2 TeC 8 – Non-Orthogonal Multiple Access (NOMA) antenna transmission schemes		
<p><b>SU-MIMO (EQPA)</b></p>  <p>P: 0.5P per layer</p> <p><b>LTE:</b>  <b>Open-Loop MIMO: TM3</b>  <b>Closed-Loop MIMO: TM4</b></p> <p>EQPA: Equal power allocation among streams per user          FSPA: Full search power allocation among users</p>	<p><b>NOMA (FSPA) + SU-MIMO (EQPA)</b></p>  <p>e.g., 0.2P: 0.1P per layer</p> <p>e.g., 0.8P: 0.4P per layer</p> <p>UE 2 signal decoding</p>	<p><b>Main Idea</b></p> <p>The main idea is to combine Non-Orthogonal Multiple Access (NOMA) schemes with multi-antenna transmission schemes. One example is to use multiple antennas at the transmitter to form multiple beams and within each beam, multiple users are multiplexed using a non-orthogonal multiple access based technique. This idea can also be extended to multi-site operations by introducing inter-site interference coordination (e.g. in frequency, space (beam) and/or power domains). Here, we focus on the combination of NOMA with SU-MIMO for intra-site user multiplexing.</p> <p>In the left side we combine NOMA with SU-MIMO (2x2) where up to two beams are multiplexed in the spatial domain and up to two users are multiplexed in the power-domain..</p>
Considered SoA solution	OFDMA (LTE rel. 8 parameters)	
KPIs considered and achieved gain	<ul style="list-style-type: none"> <li>• End user data rate, ~ 50% gain for cell edge user throughput.</li> <li>• System capacity, About 30% gain</li> <li>• User Mobility</li> </ul>	
Performance evaluation approach	System-level simulation	
System model considered	Other	
Deviation compared to Simulation Baseline	<ul style="list-style-type: none"> <li>• Model of environment: Urban Macro, MIMO 2x2</li> <li>• Spectrum Assumption: Carrier frequency 2 GHz. System Bandwidth 20 MHz</li> <li>• Propagation model: 3GPP Spatial Channel Model (SCM) Urban Macro, ITU Urban Micro, Correlated shadowing.</li> <li>• Deployment model: Hexagonal grid, 19 sites, 3 cells per site, ISD 500m, ISD=200m.</li> <li>• User distribution: uniform random, UE speed 3 km/h~250km/h.</li> <li>• Traffic model: full buffer traffic</li> </ul>	
Brief update of the results with respect to D3.2	NOMA is multiplexed with SU-MIMO for the cases of open-loop (TM3) and closed-loop (TM4)	
Association to the TeC Approach	Although NOMA was not associated with the most	



	promising technology approach of WP3, NOMA can be combined with Massive MIMO to enable multi-user multiplexing gains in both spatial and power domains.
Targeted TCs	TC2, TC8
Impacted HTs	MN, UDN, D2D
Required changes for the realization with respect to LTE Rel. 11	The modifications signalling and MCS scheduling is needed to be changed with respect to the current LTE Rel. 11.
Trade-off required to realize the gains	Complexities of user paring, including transmission power allocation for the user scheduling

### 8.12.3 Impact on Horizontal Topics

T3.2 TeC 8 - HT.MN, HT.UDN, HT.D2D	
Technical challenges	MN, UDN, D2D
TeC solution	NOMA
Requirements for the solution	CSI feedback enhancements would improve performance (cell throughput/cell-edge user throughput)
KPIs addressed and achieved gain	<ul style="list-style-type: none"> <li>• End user data rate, ~50% gain for cell edge user throughput.</li> <li>• System capacity, About 30% gain</li> <li>• High User Mobility</li> </ul>
Interaction with other WPs	WP2, WP6

### 8.12.4 Addressing the METIS Goals

T3.2 TeC 8	
1000x data volume	Up to 1.5x
10-100 user data rate	Up to 1.5x (even at high mobility)
10-100x number of devices	Up to 2x
10x longer battery life	
5x E-E reduced latency	
Energy efficiency and cost	

### 8.12.5 References

[3GPP06-25814] 3GPP, "Physical layer aspects for Evolved UTRA," TR 25.814,V7.1.0, Oct. 2006.

[MET14-D23] METIS D2.3. "Components of a new air interface - building blocks and performance". *ICT-317669 METIS Deliverable 2.3 Version 1*, May 2014.

[HK13] K. Higuchi and Y. Kishiyama, "Non-orthogonal access with random beamforming and intra-beam SIC for cellular MIMO downlink," *IEEE VTC Fall 2013*, Sept. 2013.



**Document:** FP7-ICT-317669-METIS/D3.3

**Date:** 25/02/2015

**Security:** Public

**Status:** Final

**Version:** 1

---

[BL13] A. Benjebbour, A. Li, Y. Saito, Y. Kishiyama, A. Harada, and T. Nakamura, "System-level performance of downlink NOMA for future LTE enhancements," IEEE Globecom 2013, Dec. 2013.

[BL14] A. Benjebbour, A. Li, Y. Kishiyama, H. Jiang, and T. Nakamura, "System-Level Performance of Downlink NOMA Combined with SU-MIMO for Future LTE Enhancements," IEEE Globecom 2014, Dec. 2014.

### 8.13 T3.2 TeC 9: Coordination scheme for medium range interference with message splitting to facilitate efficient SIC [EAB]

Please refer to [METIS13-D31] for the most updated results.

### 8.14 T3.2 TeC 10: Hierarchical precoding for ultra dense networks with enhanced multi-antenna receive processing [HHI]

#### 8.14.1 General Overview

The need for cell densification leads to inter-cell interference mitigation techniques known as CoMP transmission and reception. In this work, we demonstrate the limits of joint regularized zero-forcing precoding within a cluster of several macro and small-cell base stations. While studying the effects of heterogeneous power constraints in such a cluster of transmission nodes, we develop a hierarchical precoding solution which mitigates the inter-cell interference from the macro-cells caused at the users mainly served by the small-cells. Due to significantly reduced transmit power budget, both inter-small-cell interference as well as interference from small-cells caused at the macro users is of less importance and hence is not taken into account within the precoding algorithm. This assumption is justified by using a cell-range extension (CRE) factor of 6 dB which ensures that users connected to the macro are not located close to the small-cell BS.

We consider a macro-cellular OFDM downlink system where a central site is surrounded by multiple tiers of sites, each partitioned into three 120° sectors. Within each sector, additional small cells are deployed for capacity extension. Each macro sector and each small-cell constitutes an own cell with own cell-id such that the system model covers a set  $\mathcal{M}$  consisting of  $M = |\mathcal{M}|$  macro- and small cells in total. The set  $\mathcal{M}_c \subset \mathcal{M}$  constitutes a coordinated cluster with size  $M_c = |\mathcal{M}_c|$  and joint processing will only be possible between BS belonging to the same cluster. Since we assume full frequency reuse within  $\mathcal{M}$ , BSs outside the cluster are not coordinated and cause residual inter-cluster interference. A set  $\mathcal{K}$  of UE are placed into the region covered by all  $M$  cells, where  $\mathcal{K}_m \subset \mathcal{K}$  and  $m \subset \mathcal{M}$  denotes the set of user connected to the  $m$ -th BS. The number of transmit antennas at each BS is denoted as  $N_t^m$ , whereas the mobile terminals are equipped with  $N_r$  receive antennas. The received downlink symbol  $\mathbf{y}_k$  per resource block is given by

$$\mathbf{y}_k = \underbrace{\mathbf{H}_{m,k} \mathbf{s}_{m,k}}_{\text{Desired signal}} + \underbrace{\sum_{j \in \{\mathcal{K}_m \setminus k\}} \mathbf{H}_{m,k} \mathbf{s}_{m,j}}_{\rho_k} + \underbrace{\sum_{n \in \{\mathcal{M}_c \setminus \{m\}\}} \sum_{j \in \{\mathcal{K}_n\}} \mathbf{H}_{n,k} \mathbf{s}_{n,j}}_{\vartheta_k} + \underbrace{\sum_{l \in \{\mathcal{M} \setminus \mathcal{M}_c\}} \sum_{j \in \{\mathcal{K} \setminus \mathcal{K}_l\}} \mathbf{H}_{l,k} \mathbf{s}_{l,j}}_{\mathbf{z}_k} + \mathbf{n}, \quad (1)$$

where  $\mathbf{H}_{l,u} \in \mathbb{C}^{N_r \times N_t^l}$  denotes the channel matrix between the  $l$ -th BS and the  $u$ -th UE. The vector  $\mathbf{s}_{l,u} = \mathbf{b}_{l,u} \sqrt{p_{l,u}} x_u \in \mathbb{C}^{N_t^l \times 1}$  denotes the pre-coded signal  $x_u$  and  $\mathbf{b}_{l,u}$  the respective precoding vector. We emphasize that the rank 1 transmission assumption is only made to simplify the notation. This assumption can easily be extended to the more general case of sending multiple independent streams to a subset of scheduled users. The vector  $\mathbf{n}$  denotes the  $\mathbb{C}^{N_r \times 1}$  vector of AWSCGN samples at the receiver with covariance  $\mathbb{E} \{\mathbf{n} \mathbf{n}^H\} = \sigma_n^2 \mathbf{I}_{N_r}$ . The transmit covariance matrix is given by  $\Phi = \mathbb{E} \{\mathbf{s}(\mathbf{s})^H\}$ , where the appropriate selection of the precoding entries is typically subject to a *per-BS* or *per-antenna* power constraint. The resulting per-user SINR is given by the following expression:

$$\text{SINR}_k = \frac{|\mathbf{w}_k^H \mathbf{H}_{m,k} \mathbf{b}_{m,k} \sqrt{p_{m,k}}|^2}{\underbrace{|\mathbf{w}_k^H \rho_k|^2}_{\text{Inter Stream IF}} + \underbrace{|\mathbf{w}_k^H \vartheta_k|^2}_{\text{Intra Cluster IF}} + \underbrace{|\mathbf{w}_k^H \mathbf{z}_k|^2}_{\text{Inter Cluster IF}}}, \quad (2)$$

with  $\mathbf{w}_k$  the receiver weight vector (receive beam-former) at the  $k$ -th UE. Thus, the desired data stream  $x_k$  is distorted by inter-stream interference, caused by spatial multiplexed users at

BS  $m$ , intra-cluster interference which is caused by BS within the same cluster  $\mathcal{M}_c \setminus \{m\}$  and inter-cluster interference caused by the surrounding network  $\mathcal{M} \setminus \mathcal{M}_c$  plus thermal noise, as marked in (2).

In order to offload multiple UE to the small-cells even though the transmit power is less compared to macro BS, 3GPP introduced a so-called CRE. This functionality can be considered as a bias for handover procedures with respect to the small-cells. Figure 8-38 visualizes the impact of a CRE of 0 dB and 6 dB on the effective SINR after biased handover.

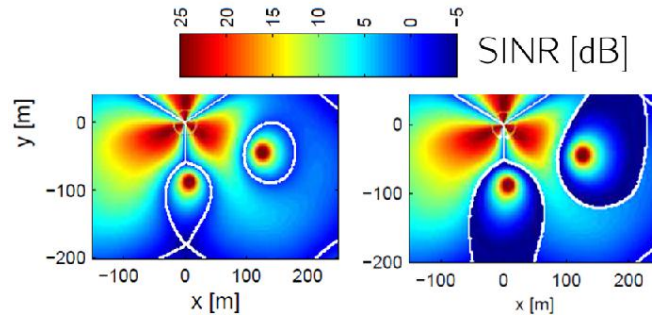


**Figure 8-38: CRE controls off-loading from macro- to small-cells. A large CRE introduces bad SINR locations for small-cell UEs, but also protects macro-cell UEs from interference. (Left) is the coverage plot with CRE of 0 dB, (right) is CRE of 6 dB.**

#### 8.14.2 Performance Results

Here we consider a coordinated cluster  $\mathcal{M}_c$  to constitute three macro-sectors and the respective small-cells which are allocated within the coverage area of the macro BS. The set of users  $\mathcal{K}_c$  within the cluster  $c$  are divided into macro user  $\mathcal{K}_m$  and small-cell user  $\mathcal{K}_u$ , such that  $\mathcal{K}_c = \mathcal{K}_m \cup \mathcal{K}_u$  as illustrated in Figure 8-39.

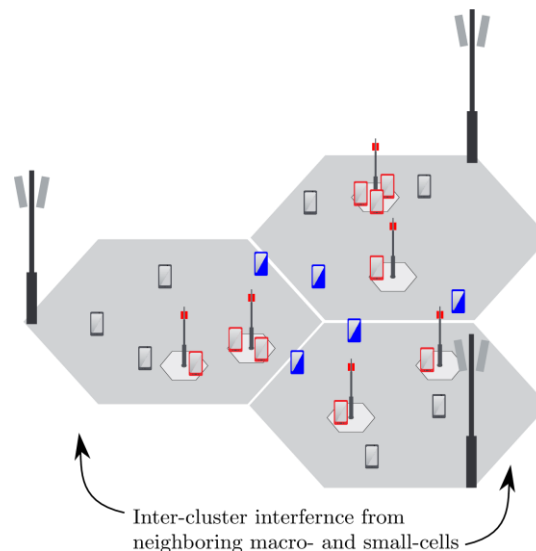


**Figure 8-39: Inter-site CoMP of macro-sectors facing to each other. In addition, we add 2 small-cells per macro sector footprint. Red UEs are attached to small-cells, blue UEs will benefit most from the joint transmission of macro sectors, and gray UEs may be served independently from all other.**

This macro/small-cell overlay is considered a typical deployment strategy within LTE-A networks, i.e. a macro-cell deploys *basic* coverage for a specific area whereas optional small-cells with reduced cell-radius provide additional capacity within a specific region and can be activated optionally. Since small-cells are deployed within the coverage zone of a macro-cell, interference needs to be coordinated between macro and small cells in order to ensure

efficient transmission. In this section, spatial interference management schemes are proposed taking advantage from high number of Tx-antennas at the macro BS-site. As a baseline, we consider each cell  $c \in \mathcal{M}_c$  to transmit independently in an uncoordinated fashion by using a regularized ZF-based SMUX [WC12] - approach, i.e. each macro and each small cell schedules associated UE without influencing the interference introduced from other cells, which corresponds to an uncoordinated transmission.'

Since small cells are assumed to be deployed within the coverage zone of the macro cell, associated small cell UE will suffer strongly from macro interference if no interference management is employed. In the following, methods for hierarchical precoding are suggested to exploit a large amount of transmit antennas at macro-site to protect small cell UE from macro-cell interference.

### **Channel Feedback for Multi-Antenna UEs**

Each UE is assumed to provide CSI and CQI feedback under the assumption of its own dominant eigenmode vector with respect to the cluster  $\mathcal{M}_c$ .

In essence, the channel feedback is assumed as MISO CSI, in particular focusing on a so-called multi-user eigenmode transmission (MET) [BH07] strategy. The MET strategy is an extension of the block-diagonalization concept. In particular, channel decomposition is done according to  $\hat{\mathbf{H}}_k = \mathbf{U}_{c,k}^H \mathbf{H}_{c,k} = \mathbf{U}_{c,k}^H \mathbf{U}_{c,k} \boldsymbol{\Sigma}_{c,k} \mathbf{V}_{c,k}^H = \boldsymbol{\Sigma}_{c,k} \mathbf{V}_{c,k}^H$ .

In general, this feedback method can be considered as reporting of virtual receive antennas enabling the UE to utilizing full beam forming gain already with a single MISO feedback vector. Note, there are other methods for receive beam forming also enabling IRC feedback [TWH+09, NMK+07].

### **Semi-Orthogonal User Grouping**

Based on the conveyed downlink user CSI, a greedy and central scheduling entity, denoted as GRA, selects the appropriate users from  $\mathcal{K}_c$ , refer to [TKBH12]. One characteristic of this metric is an adaptive loading of spatial layers. It stops adding a new data streams when the approximated sum-rate decreases. Thus, it is clear that a sufficiently large set of users is required in order to exploit the multi-user diversity. Merging users with correlated MIMO channels will cause a significant reduction in channel norm after precoding. A brute-force user grouping is infeasible since each user constellation changes the precoding weights and thus the achievable SINR per UE. We use a greedy projection-based user selection criteria

$$\Psi_k = \mathbf{I} - \underbrace{\hat{\mathbf{H}}_k^H (\hat{\mathbf{H}}_k \hat{\mathbf{H}}_k^H) \hat{\mathbf{H}}_k}_{=\mathbf{V}_{c,k} \mathbf{V}_{c,k}^H, \text{ in case of MET}},$$

being the projector of user  $k$ . The projection matrix  $\tilde{\Psi}_k$ , which combines all users' null-space except the  $k$ -th UE, can be approximated by repeatedly applying

$$\tilde{\Psi}_k = [\Psi_1 \cdot \dots \cdot \Psi_{k-1} \Psi_{k+1} \cdot \dots \cdot \Psi_{K_c}]^n,$$

with  $n \rightarrow \infty$  as the projection order. The achievable link-rate is approximated based on

$$R_k = \log_2 \left( 1 + \frac{p_{c,k}}{\sigma_n^2} \|\hat{\mathbf{H}}_k \tilde{\Psi}_k\|_F^2 \right)$$

Once the sum-rate is not increasing further, we stop adding more users for downlink service. This ensures that we do not overload the coordinated antenna system by means of spatial degrees of freedom.

Note, this metric is clearly sum-rate maximizing. In order to allow certain degree of fairness we add an additional GBR to the pool of UE: If a user's achieved data rate is exceeding its bit rate target we remove this specific user from the pool of active users and hence this UE is not requesting further resources.

### **Uncoordinated SDMA per BS**

Here, we assume that each BS  $c \in \mathcal{M}_c$  within the cluster performs autonomous transmission towards its connected UE. To be more specific, we consider SMUX by considering the RZF precoding satisfying a MMSE constraint.

$$\mathbf{B}_{m,RZF} = \hat{\mathbf{H}}_m (\hat{\mathbf{H}}_m \hat{\mathbf{H}}_m^H + \mathbf{R})^{-1} \quad (3)$$

where  $\hat{\mathbf{H}}_m$  constitutes the compound channel matrix of all selected users with respect to the  $m$ -th BS. The regularization matrix  $\mathbf{R}$  includes the thermal noise plus wideband interference measured at each user  $k$

$$r_{k,k} = \frac{1}{N_{PRB}} \sum_{i=1}^{N_{PRB}} \text{trace}(\mathbf{Z}_{k,i}) \quad (4)$$

where  $\mathbf{Z}_{k,i}$  is the inter-cell interference covariance matrix of user  $k$  on RB  $i$  and  $N_{PRB}$  is the number of RBs.

Each base station equally distributes the transmit power  $P_m$  among all antenna elements. In order to meet this constraint, we determine  $\sqrt{\mathbf{P}_c}$  according to [ZD04]:

$$\sqrt{\mathbf{P}_c} = \left\{ \min_{n=1, \dots, N_t} \sqrt{\frac{P_{m,n}}{\|\mathbf{B}_{m,n}\|_2}} \right\} \cdot \mathbf{I}_{[N_t \times N_t]}$$

### **Joint Transmission with SDMA**

Here, we assume that all BS  $m \in \mathcal{M}_c$  within the cluster  $c$  perform joint transmission towards its connected UE. This is done by joint RZF precoding satisfying a MMSE constraint.

$$\mathbf{B}_{c,RZF} = \hat{\mathbf{H}}_c (\hat{\mathbf{H}}_c \hat{\mathbf{H}}_c^H + \mathbf{R})^{-1} \mathbf{D} \quad (5)$$

where  $\hat{\mathbf{H}}_c$  constitutes the compound channel matrix of all selected users with respect to all transmit antenna elements. The regularization matrix  $\mathbf{R}$  is obtained according to (4). With the *diagonal* matrix  $\mathbf{D}$  we can control the *power demands* per user. So far, we assumed equal demand, i.e. equal per-stream power constrained, which works perfectly for symmetric base-station-to-user constellations. The work in [AS14] introduces a so called demand matrix  $\mathbf{D}$  and indicates that it will play an important role for non-symmetric cases which dominantly appear in the scenario of ultra-dense networks with joint signal processing among heterogeneous base stations.

Again each base station equally distributes the transmit power  $P_m$  among all antenna elements. In order to meet this constraint, we determine  $\sqrt{\mathbf{P}_c}$  among all BS jointly:

$$\sqrt{\mathbf{P}_c} = \left\{ \min_{m=1, \dots, M_c} \left\{ \min_{n=1, \dots, N_t} \sqrt{\frac{P_{m,n}}{\|\mathbf{B}_{m,n}\|_2}} \right\} \right\} \cdot \mathbf{I}_{[|\mathcal{I}_s| \times |\mathcal{I}_s|]}$$

### **Macro-Interference Coordination**

Since we aim to reduce the interference introduced by the macro cell  $m \in \mathcal{M}_c$  to the small cell UE  $j \in \mathcal{K}_u = \{\mathcal{K}_c \setminus \mathcal{K}_m\}$ , we exploit some degree of Tx-antennas at the macro-site to *protect*  $N_t^m - K_m$  small-cell UE by calculating the RZF approach per cell hierarchy: Small-cells act uncoordinated, while macro-cells perform joint transmission and take the whole set of  $\mathcal{K}_c$  users into account. In the power allocation step for the macro layer, small-cell UE are not receiving any power budget, i.e. the matrix  $\mathbf{D}$  from (5) is of binary structure: equal power per macro UE and zero power for small-cell UE.

### **MMSE-Optimized MIMO Interference Alignment**

Based on the idea from [DKTH14] where BD is combined with the iterative IA algorithm from [ABW12, APJ12] we are using MMSE optimization in the iterative pre- and post-coder design. In [DKTH14] no results on data rates are provided leaving an open question on quantifying the

overall system efficiency by reducing the interference at the small-cell users and at the same time sacrificing efficiency for the macro users. Here we compare the schemes from [DKTH14] and an extended approach with MMSE optimization for the post- and pre-coders. The following acronyms correspond to the three cases:

1. BD: Uncoordinated case where each node is uses the BD precoding independently
2. BDIA: Hierarchical precoding as in [DKTH14] where small cell users are protected from macro-interference
3. BDIA MMSE: Extension of the scheme shown in [DKTH14] with MMSE transmit and receive filter design.

In the third case, also the channels between the small-cell users and small-cell BSs have to be known at the macro BS, but there is no joint precoding of user data shared among the macro and small-cell BSs.

The effect on the interference from the macro BS received at the small-cell users after post-coder is shown in Figure 8-40 (a). We assume that two users at the macro BS and one user per small-cell BS are served. Here we observe an average gain of more than 20 dB using the IA techniques with and without the MMSE modification in the single-cell scenario, labeled with 'SC'. However, in the multi-cell scenario labeled with 'MC' there is a lower bound from inter-cell interference (ICI) which limits the gains achieved in the single-cell scenario. The impact on signal power received at the macro users is given in Figure 8-40 (b) we observe the expected loss for both IA schemes compared to 'BD' which maximizes the signal power.

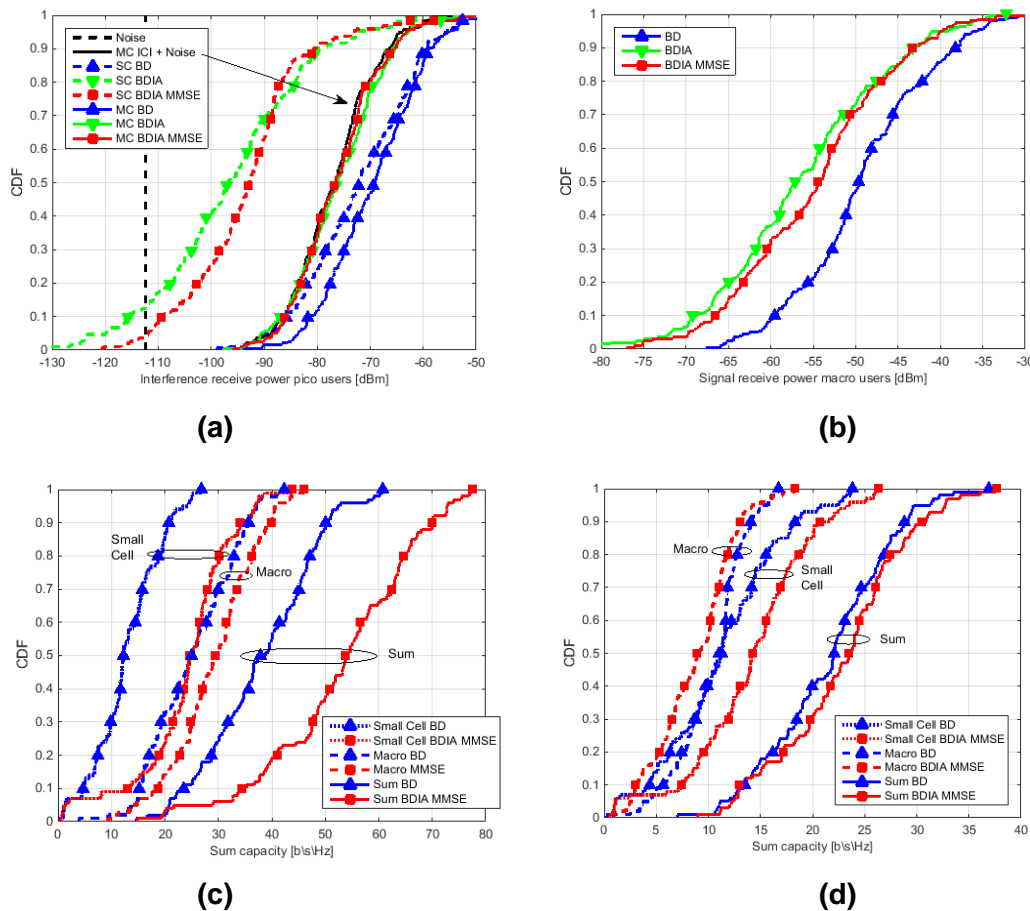


**Figure 8-40: (a) Impact of interference coordination on perceived macro-cell interference at small-cell users. (b) Impact of signal power perceived at macro-cell users. (c) Results in sum spectral efficiency for a single macro-sector and its corresponding 2 small-cells (d) Results in sum spectral efficiency in multi-cell environment.**

The results on capacity in the single-cell scenario are shown in Figure 8-40 (c). Compared to the uncoordinated case we can achieve a gain of 16 bit/s/Hz with the joint BDIA MMSE approach by increasing the performance for interference limited small-cell users. The gain achieved at the macro users despite the loss in the receive signal is caused by the interference suppression from small cells. In Figure 8-40 (d) the corresponding multi-cell results are shown where the overall gain is reduced to 3 bit/s/Hz originating from the small cells.

We expect another improvement by using channels weighted with the transmit power to further optimize the SINR, especially for small-cell UE. Future work will study this algorithm in presence of remaining multi-cell interference on system-level. We expect another improvement by using channels weighted with the transmit power to further optimize the SINR, especially for small-cell UE. Future work will study this algorithm in presence of remaining multi-cell interference on system-level.

### **Conclusion and Discussion of Results**

Figure 8-41 shows the system-level simulation results for different assumptions on the infrastructure side<sup>1</sup>: First we show (green triangle) the performance of a system where only macro-cells are available and 3 sectors perform the joint transmission. In this case, we can only guarantee the given bit rate target for 67% of users.

As next step, we add small-cells into the coverage area and assume a full joint transmission among all nodes in the cluster, i.e. 3 macro sectors and 6 small-cells in total (right-pointing triangle and circle) as indicated in Figure 8-39. We observe severe degradation in peak and user rates under a realistic PAPC. This is attributed to the small power budget at small cells which results in the fact that also macro BS transmit with 27 dBm instead of 46 dBm. As a proof, Figure 8-41 shows the CDF of the distributed transmit power budget in the cluster. 100% attributes to  $3 \times 46$  dBm +  $6 \times 27$  dBm and is achieved in the non-feasible pool power constraint (light blue) case, where all BS can share their transmit power budget. The red bound is based on the assumption of  $9 \times 27$  dBm transmit power allocation.

Next, we compare these results with the assumption that 3 macro-sectors perform joint transmission and small-cells operate independently in the same band (red triangle), which improves the the peak performance significantly. However, user satisfaction is only slightly better. Finally, we provide the results of macro-interference coordination and highlight that we coordination trades peak performance with higher user satisfaction ratio (black square).

By adding more antennas at the macro-cells and at the users (red star), we show that both peak and user rates can be improved even without any coordination between macro- and small-cell layer. This clearly indicates that massive MIMO has to become a mature technology component for future 5G in order to guarantee certain bit rate targets per user and serve the tremendous peak data rate requirements of the future. Our suggested transmit coordination scheme from BDIA MMSE shows promising results in a limited scenario.

The open question for future is: What is the right coordination scheme and how does it scale with large number of small-cells and massive MIMO at the macro-cell level?

<sup>1</sup> The user distribution is always: uniform distribution of 10 users per macro sector and 2 dense user crowds (each with 10 UEs) co-located with the position of the small-cell per sector.

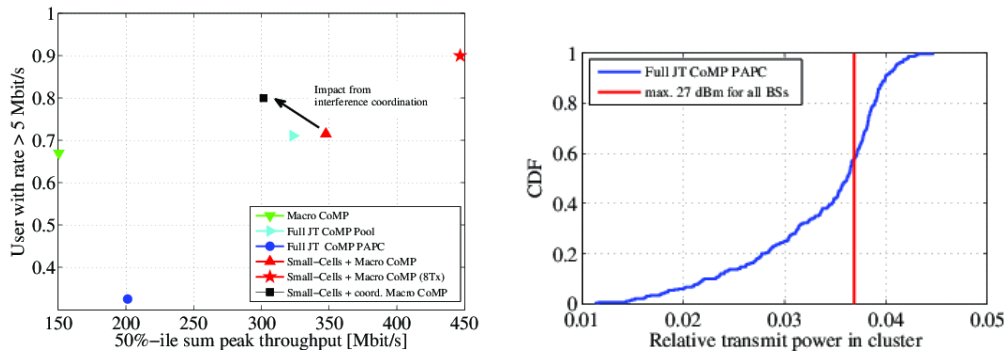
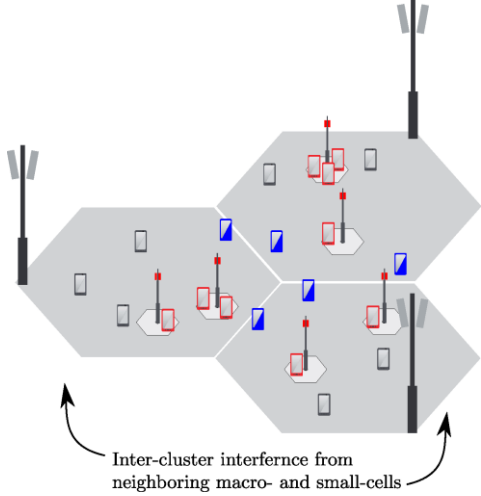


Figure 8-41: (a) The x-axis depicts the 50%-ile sum data rates under a full-buffer assumption for user data traffic. Therefore, we call it peak data rate. The y-axis plots the fraction of users achieving their bit rate target of 5 Mbit/s (the higher the better). Note, we cannot achieve both metrics at the same time. The data point (red star) assumes  $N_t=8$  at the macro sites and  $N_r=4$  elements at UE, while all other results assume  $N_t=4$  and  $N_r=2$ . (b) Depicts the power allocation in the joint precoding case, i.e. Full JT CoMP PAPC.

T3.2 TeC 10 – Hierarchical precoding for ultra dense networks with enhanced multi-antenna receive processing	
 <p>Inter-cluster interference from neighboring macro- and small-cells</p>	<p style="text-align: center;"><b>Main Idea</b></p> <p>In this work, we demonstrate the limits from joint regularized zero-forcing precoding within a cluster of several macro and small-cell base stations. While studying the effects of heterogeneous power constraints in such a cluster of transmission nodes, we develop a hierarchical precoding solution which mitigates the inter-cell interference from the macro-cells caused at the users mainly served by the small-cells.</p>
Considered SoA solution	<ul style="list-style-type: none"> <li>CoMP in LTE-A release 11</li> </ul>
KPIs considered and achieved gain	<ul style="list-style-type: none"> <li>Cell edge throughput: gain up to 34 %</li> <li>Cell throughput: median gain up to 200 %</li> <li>Spectral efficiency: average gain up to 200 %</li> </ul>
Performance evaluation approach	Simulation-based: System level evaluation
System model considered	Hexagonal layout
Deviation compared to Simulation Baseline	<p>Medium:</p> <ul style="list-style-type: none"> <li>Model of environment: WINNER urban macro</li> <li>Spectrum Assumption: 18 MHz bandwidth (100 RBs) at a centre frequency of 2.68 GHz</li> <li>Propagation model: Fast fading with QUADRIGA 100% NLOS [JRBT14]</li> <li>Deployment model: 3 BS per site in a hexagonal grid</li> </ul>



	<p>with an ISD=500m without small cells</p> <ul style="list-style-type: none"> <li>• User distribution: uniform random</li> <li>• Traffic model: full buffer</li> </ul>
Brief update of the results with respect to D3.2	Results for hierarichal precoding over macro and small cell base stations
Association to the TeC Approach	CoMP with Advanced UE Capabilities
Targeted TCs	TC2 “Dense urban information society”
Impacted HTs	Ultra Dense Networks (UDN)
Required changes for the realization with respect to LTE Rel. 11	Backhaul with sufficient data rata New feedback protocol for MET feedback
Trade-off required to realize the gains	The gains achieved in throughput and spectral efficiency are obtained by increased feedback and higher backhaul requirements.

### 8.14.3 Impact on Horizontal Topics

T3.2 TeC 10 - HT.UDN	
Technical challenges	<p>Short term radio resource and interference management (ST-RRM).</p> <p>Node clustering.</p>
TeC solution	We develop a hierarchical precoding solution which mitigates the inter-cell interference from the macro-cells caused at the users mainly served by the small-cells.
Requirements for the solution	Backhaul supporting CSI and user data exchange between BSs
KPIs addressed and achieved gain	<ul style="list-style-type: none"> <li>• Cell edge throughput: gain up to 34 %</li> <li>• Cell throughput: median gain up to 200 %</li> <li>• Spectral efficiency: average gain up to 200 %</li> </ul>
Interaction with other WPs	<p>WP2: OFDM is assumed for this TeC. The impact from new air interface on MIMO transmit and receive beamforming needs to be further studied.</p> <p>WP4: Interference inside the cluster of BS is managed on a short term time scale. A major part of WP4 is interference management but on a larger time scale. Mutual dependence has to be studied in a common framework.</p> <p>WP5: New spectrum changes the channel propagation conditions and requires new studies. This TeC considers frequencies below 6 GHz.</p>

### 8.14.4 Addressing the METIS Goals

T3.2 TeC 10	
1000x data volume	Increase in cell throughput and spectral efficiency up to 200 %



10-100 user data rate	Increase in user data rates up to 200 %
10-100x number of devices	The increase in system throughput corresponds to an increase in the number of devices
10x longer battery life	
5x E-E reduced latency	
Energy efficiency and cost	

### 8.14.5 References

[ABW12] Danish Aziz, Federico Boccardi, and Andreas Weber. System-level performance study of interference alignment in cellular systems with base-station coordination. 23rd IEEE Intern. Symp. on Personal, Indoor and Mobile Radio Communications (PIMRC 2012), September 2012.

[APJ12] Omar El Ayach, Steven W. Peters, and Robert W. Heath Jr. The practical challenges of interference alignment. CoRR, abs/1206.4755, 2012.

[AS14] Rikke Apelfröjd and Mikael Sternad. Design and measurement-based evaluations of coherent JT CoMP: a study of precoding, user grouping and resource allocation using predicted CSI. EURASIP Journal on Wireless Communications and Networking, 2014.

[BH07] F. Boccardi and H. Huang. A near-optimum technique using linear precoding for the MIMO broadcast channel. IEEE International Conference on Acoustics, Speech and Signal Processing (ICASSP), 3:III-17-III-20, April 2007.

[BHL+14] F Boccardi, R.W. Heath, A. Lozano, T.L. Marzetta, and P. Popovski. Five disruptive technology directions for 5G. Communications Magazine, IEEE, 52(2):74-80, February 2014.

[BLM+14] N. Bhushan, Junyi Li, D. Malladi, R. Gilmore, D. Brenner, A. Damnjanovic, R. Sukhavasi, C. Patel, and S. Geirhofer. Network densification: the dominant theme for wireless evolution into 5G. Communications Magazine, IEEE, 52(2):82-89, February 2014.

[DKTH14] J. Dommel, P.-P. Knust, L. Thiele, and T. Haustein. Massive MIMO for interference management in heterogeneous networks. In Sensor Array and Multichannel Signal Processing Workshop (SAM), 2014 IEEE 8th, pages 289-292, June 2014.

[JRBT14] S. Jaeckel, L. Raschkowski, K. Borner and L. Thiele, "QuADriGa: A 3-D Multi-Cell Channel Model With Time Evolution for Enabling Virtual Field Trials", Antennas and Propagation, IEEE Transactions on, vol. 62, pp. 3242-3256, June. 2014

[LETM14] E. Larsson, O. Edfors, F. Tufvesson, and T. Marzetta. Massive MIMO for next generation wireless systems. Communications Magazine, IEEE, 52(2):186-195, February 2014.

[NMK+07] M. Noda, M. Muraguchi, Tran Gia Khanh, K. Sakaguchi, and K. Araki. Eigenmode tomlinson-harashima precoding for multi-antenna multi-user mimo broadcast channel. In 6th International Conference on Information, Communications Signal Processing, pages 1 -5, 10-13 2007.

[TKBH12] Lars Thiele, Martin Kurras, Kai Börner, and Thomas Haustein. User-aided sub-clustering for CoMP transmission: Feedback overhead vs. data rate trade-off. 46th Asilomar Conference on Signals, Systems and Computers, November 2012. accepted.

[TR09] TR 36.814 V1.0.0. Evolved universal terrestrial radio access (E-UTRA); further advancements for (E-UTRA) physical layer aspects, February 2009.



[TWH+09] Lars Thiele, Thomas Wirth, Thomas Haustein, Volker Jungnickel, Egon Schulz, and Wolfgang Zirwas. A unified feedback scheme for distributed interference management in cellular systems: Benefits and challenges for real-time implementation. 17th European Signal Processing Conference (EUSIPCO2009), August 2009. invited.

[WC12] Zijian Wang and Wen Chen. Regularized zero-forcing for multi-antenna broadcast channels with user selection. IEEE Wireless Communications Letters, 1(2):129–132, April 2012.

[WHG+14] Cheng-Xiang Wang, F. Haider, Xiqi Gao, Xiao-Hu You, Yang Yang, Dongfeng Yuan, H. Aggoune, H. Haas, S. Fletcher, and E. Hepsaydir. Cellular architecture and key technologies for 5g wireless communication networks. Communications Magazine, IEEE, 52(2):122–130, February 2014.

## **8.15 T3.2 TeC 11: Decentralized interference aware scheduling [NOKIA]**

Please refer to [METIS14-D32] for the most updated results.

## **8.16 T3.2 TeC 12: Network-assisted interference suppressing/cancelling receivers and ultra-dense networks [NOKIA]**

### **8.16.1 General Overview**

In cellular networks, particularly in those targeting high system spectral efficiency by deploying frequency reuse 1, the user data rates, especially on the cell border areas, can be severely degraded by the interference caused by the transmissions in neighbouring cells. This co-channel inter-cell interference (ICI) problem has been identified by the research community as a key limiting factor for reaching increased capacity in cellular networks.

Network-centric approaches to resolve the ICI problem include techniques such as the 3GPP Rel-10 enhanced inter-cell interference coordination (eICIC) mechanism [DMW+11, LVD+11], which involves multi-cell resource management function that takes into account information (e.g., the status of traffic load and resource usage) in multiple cells, such that different cells coordinate use of resources in frequency (coordinating resource block allocation) and time (coordinating subframe utilization across cells in time through so called Almost Blank Subframe (ABS) patterns) domains. In Rel-11, the eICIC operation for heterogeneous deployments was further enhanced by providing a UE with assistance information on Cell specific Reference Symbols (CRS) of the aggressor (interferer) cells to enable the victim UE to cancel interference on common control channels of ABSs caused by CRS of high power macro cells. Two aspects in this further enhanced ICIC (feICIC) scheme are worth noting, namely (1) the active role of the UE receiver (w.r.t. Rel-10 eICIC operation) and (2) the employment of non-linear interference cancellation.

Another approach to cope with the co-channel interference issue, targeting boost in network capacity, is to increase the UE receiver role in system design. This path was taken when Release 11 specified UE performance requirements for interference rejection combining (IRC) receiver [3GPP12-36829]. The obtained results were promising showing notable performance gain compared to receivers treating co-channel interference as Additive white Gaussian noise (AWGN) [PIB+13, 3GPP12-36829].

The core idea in T3.2 TeC12 is to make a UE receiver aware of information related to the key parameters characterizing the transmission in the neighbouring cells causing co-channel interference to the victim UE. Depending on the transmission scheme these interference parameters may include, e.g., (but are not limited to) cell ID, reference signal ports, power offset values, precoder selection, transmission rank, modulation order. With the aid of network assistance (NA) (implemented by means of eNB-to-UE higher-layer signalling), the accuracy of the co-channel interference estimation and mitigation performance in terms of suppression (IS) or cancellation (IC) at UE receiver can be improved [3GPP13-RP130404, 3GPP13-36866]. An example of NA-enabled advanced non-linear receiver structures is a receiver that performs symbol-level IC, and is referred to as SLIC. The SLIC receiver performs the following additional processing, in comparison to that of the baseline IRC: interferer parameter extraction (obtained through eNB-to-UE NA signalling and/or blind detection at UE receiver), interferer channel estimation, interferer detection, and interference reconstruction and cancellation at symbol-level. The concept of network-assisted co-channel interference mitigation is depicted in Figure 8-42.

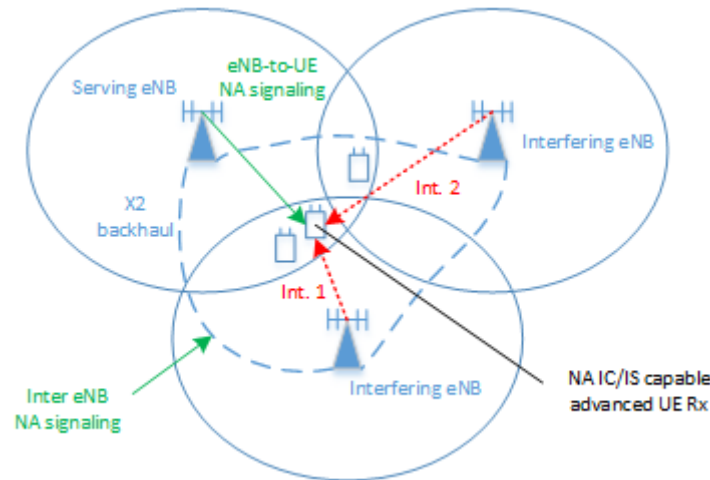


Figure 8-42: Overview concept picture showing the higher-layer NA signaling components

### 8.16.2 Performance Results

To evaluate the performance of T3.2 TeC12, we consider a multi-cell multi-user MIMO system assuming 2Tx – 2Rx antenna configuration (with cross-polarization). For the system-level evaluations, a drop based simulation methodology is adopted. To model the links between cells and UEs, channel realizations are generated according to model in [3GPP10-36814] with the geometry-based stochastic ITU-R Advanced model for fast fading. Quasi-static simulations are assumed, that is, within a given drop the large scale propagation parameters (e.g., path loss and shadowing) remain unchanged whereas Doppler related multi-path parameters change according to UE speed, which is assumed as 3 km/h. Overall, a few tens of drops, each covering a period of few thousand transmission time intervals (TTI) , are simulated.

The simulations are carried out assuming homogeneous network deployment and ITU UMa (Urban macro) environment. Regarding the network topology, a hexagonal grid with inter-site distance (ISD) of 500m is assumed and two tiers (7 sites with co-located 3–sectorized antennas / 3 cells each) are modelled. Bursty (non-full buffer) traffic is modelled using a FTP traffic model characterized by a fixed packet size of 0.5 Mbytes and Poisson distributed packet arrival process with average arrival rate of 1.5 packets/sec/eNB. PF scheduling algorithm is applied. The performance is measured in terms of the mean and 5%-tile user throughputs (UTP), where user throughput is given by the ratio between the amount of data (file size) and the time needed to download data [3GPP10-36814].

The system-level performance of a network-assisted genie-aided SLIC receiver is evaluated and compared to that of the Rel-11 baseline IRC receiver by carrying out simulations under the following assumptions. We consider a carrier frequency of 2 GHz and a system bandwidth of 10 MHz. A 2x2 SU-MIMO operation based on transmission mode (TM) 10 with rank adaptation is assumed as transmission scheme. Practical channel and covariance estimation (associated to both serving and interfering cells) required for demodulation as well as for CSI feedback purposes are assumed. Further, regarding UE feedback we assume subband CQI and wideband PMI reporting and consider 5 ms reporting interval and 6 ms delay in the evaluations. Moreover, HARQ process with maximum of 5 re-transmissions is modelled. Overhead due to reference symbols (incl. 2 CRS Rel-8 legacy overhead, DMRS and CSI-RS) and control channel (assuming 3 OFDM symbols) are taken into account. A BLER target of 10% is set for CQI selection as well as for outer-loop link-adaptation. For SLIC receiver, we have considered the link-to-system (L2S) modelling from [3GPP13-36866].

The obtained system-level results are summarized in Table 8.8, showing the 5%-tile and mean user throughput numbers in Mbps for the Rel-11 baseline IRC receiver and the NA genie-aided SLIC receiver assuming Rel-11 CQI feedback. SLIC receiver can be observed to provide relative gains of 8.7 % and 3.0 % in cell edge and cell average throughputs, respectively.

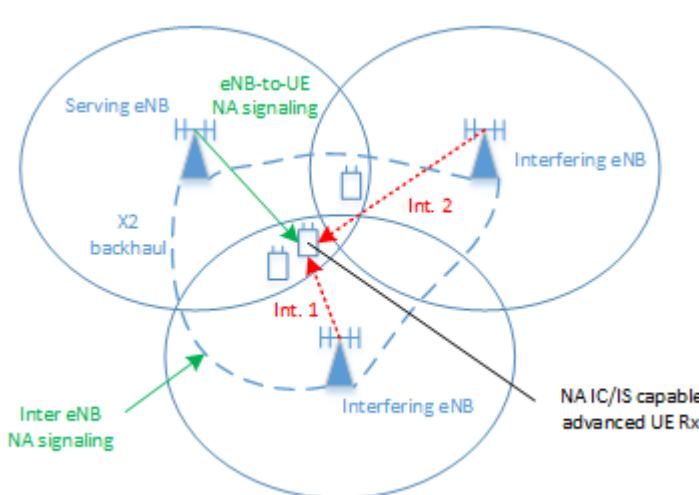
The observed system-level throughput gains are perhaps smaller than those anticipated based on the preceding link-level performance evaluations. There might be a few reasons behind this. One aspect is that the IC efficiency of the SLIC receiver depends heavily on the dominant interferer SINR (DI-SINR) and the combination of the serving cell and interfering cell modulation schemes. Sufficiently high DI-SINR is required for good IC efficiency and to consequent gains over the baseline receiver. Further, the level of DI-SINR required for reasonable IC efficiency is primarily set by the DI cell modulation order, while varying additionally a few dBs as a function of the serving cell modulation. The gain of advanced SLIC receiver seems to be predominantly available when the DI cell is transmitting using low-order modulation such as QPSK whereas gains become less significant more unlikely with increasing DI cell modulation order.

The level of network load (a.k.a. resource utilization (RU)) is expected to affect the gains observed as well. These evaluations were been carried out assuming a relatively low resource utilization level of ~40 %. In case of a higher RU level, the probability for a presence of a strong DI is foreseen to increase, which would make the conditions more favorable for advanced IC receiver operation. Higher gains compared to the baseline could also be expected by allowing for more aggressive load balancing or range extension.

**Table 8.8: The system-level gains of network-assisted SLIC receiver in homogeneous macro scenario in case of moderate network load (resource utilization ~40%)**

	5%-tile UTP [Mbps]	Mean UTP [Mbps]
<b>Rel-11 IRC</b>	3.60 (baseline)	18.25 (baseline)
<b>SLIC /w Rel-11 CQI</b>	3.91 (+8.7 %)	18.80 (+3.0 %)

### T3.2 TeC 12 – Network-assisted interference suppressing / cancelling receivers and ultra-dense networks



**Main Idea**

The work proposes utilization of network assistance (NA) to further enhance the co-channel inter-cell interference mitigation ability of UE receivers.

Network assistance, in forms of signalling of key interference transmission parameters and/or network side transmission coordination, can enhance the interference estimation accuracy and consequently the interference suppression and cancellation (IS/IC) performance of NA-enabled UE receivers. The improved interference robustness, in terms of higher effective post-IS/IC SINRs, enables higher user throughput / network capacity and increased spectral efficiency in co-channel interference limited networks.



Considered SoA solution	LTE Advanced (3GPP Release 11) IS LMMSE-IRC receiver operation (without NA).
KPIs considered and achieved gain	<ul style="list-style-type: none"> <li>• 5%-tile user throughput: a gain of ~9% in homogeneous network scenario in case of non-full-buffer traffic and 40% resource utilization.</li> <li>• Mean user throughput: a gain of ~3% in homogeneous network scenario in case of non-full-buffer traffic and 40% resource utilization.</li> </ul>
Performance evaluation approach	Simulation-based: system-level evaluation
System model considered	Other
Deviation compared to Simulation Baseline	<p>Some:</p> <ul style="list-style-type: none"> <li>• Model of environment: Urban Macro.</li> <li>• Spectrum assumptions: 2 GHz carrier frequency, 10 MHz BW.</li> <li>• Propagation model: ITU UMa, ITU-R IMT-Advanced geometry-based stochastic model.</li> <li>• Deployment model: Hexagonal grid, 500m ISD.</li> <li>• User/Device distribution: Random, uniformly distributed.</li> <li>• Traffic model: FTP, 0.5 Mbyte packets, Poisson distribution with packet arrival rate of 1.5 per sec per eNB.</li> </ul>
Brief update of the results with respect to D3.2	<ul style="list-style-type: none"> <li>• Results for system-level performance assessment in 7-site (21-cell) homogeneous macro scenario.</li> <li>• Performance comparison against the SoA Rel-11 technique.</li> </ul>
Association to the TeC Approach	Tech Approach 1: CoMP with Advanced UE Capabilities
Targeted TCs	TC2 – Dense urban information society
Impacted HTs	UDN
Required changes for the realization with respect to LTE Rel. 11	<p>Major:</p> <ul style="list-style-type: none"> <li>• Inter-eNB exchange of (interference) signal parameters</li> <li>• eNB-to-UE signalling of interference parameters</li> <li>• Blind detection of interference parameters, interfering link channel estimation, MIMO detection of interferer, interference reconstruction and cancellation in a UE receiver (depending on the type of NA UE receiver)</li> </ul>
Trade-off required to realize the gains	The performance gain, over the Rel-11 IRC operation, comes with the cost of additional NA



	<p>signalling overhead (inter-eNB and eNB-to-UE) and higher computational complexity at UE receiver. Inherent trade-off between the eNB-to-UE NA signalling overhead and the blind detection complexity and demodulation performance.</p>
--	---

### 8.16.3 Impact on Horizontal Topics

T3.2 TeC 12 - HT.UDN	
Technical challenges	<ul style="list-style-type: none"> <li>• Optimization of the co-channel interference mitigation in UE receivers</li> <li>• Improving the network capacity and spectral efficiency</li> </ul>
TeC solution	<ul style="list-style-type: none"> <li>• Network assistance (NA), in forms of signalling of key interference transmission parameters and/or network side transmission coordination, can enhance the inter-cell interference estimation accuracy and enable advanced non-linear cancellation (IC) algorithms in NA-enabled UE receivers. The improved interference robustness, in terms of higher effective post-IC SINRs, enables higher user throughput / network capacity and increased cell spectral efficiency in co-channel interference limited networks.</li> </ul>
Requirements for the solution	<ul style="list-style-type: none"> <li>• Knowledge of interference parameters (considered to be obtained through inter-eNB and eNB-to-UE NA signalling and/or blind detection), associated to transmissions in interfering cells, at a victim UE receiver to enable non-linear cancellation of a dominant interferer.</li> <li>• NA signalling matching to the variation rate of the interference in time and frequency.</li> </ul>
KPIs addressed and achieved gain	<ul style="list-style-type: none"> <li>• 5%-tile user throughput: a gain of ~9% in homogeneous network scenario in case of non-full-buffer traffic and 40% resource utilization.</li> <li>• Mean user throughput: a gain of ~3% in homogeneous network scenario in case of non-full-buffer traffic and 40% resource utilization.</li> </ul>
Interaction with other WPs	<ul style="list-style-type: none"> <li>• WP2: TeC12 developed assuming OFDM is deployed. A change in the air interface, such as new waveforms, may imply changes in the implementation specifics of certain UE receiver algorithms, such as channel estimation that is in central role in TeC12. However, the core operation principle and processing requirements on the network and UE sides are considered applicable also to new waveforms without</li> </ul>



	<p>any significant changes.</p> <ul style="list-style-type: none"> <li>WP4: TeC12 targets inter-cell interference limited scenarios. A careful alignment with WP4 TeCs focusing on interference management solutions is required.</li> </ul>
--	--

**8.16.4 Addressing the METIS Goals**

T3.2 TeC 12	
1000x data volume	TeC12 provides increased spectral efficiency which on the other hand translates to support of increased data volume.
10-100 user data rate	TeC12 enables increase in the 5%-tile user rate.
10-100x number of devices	Through enhanced data rates a higher number of UEs can be served within a given time.
10x longer battery life	
5x E-E reduced latency	
Energy efficiency and cost	

**8.16.5 References**

[DMW+11] A. Damnjanovic, J. Montojo, Y. Wei, T. Ji, T. Luo, M. Vajapeyam, T. Yoo, O. Song and D. Malladi, "A survey on 3GPP heterogeneous networks," IEEE Wireless Commun. Mag., 18(3), pp. 10-21, June 2011.

[LVD+11] D. Lopez-Perez, A. Valcarce, G. De La Roche, J. Zhang, "Enhanced intercell interference coordination challenges in heterogeneous networks," IEEE Wireless Commun., Mag., 18(3), pp. 22-30, June 2011.

[3GPP13-RP130404] RP-130404, "Study on network-assisted interference cancellation and suppression for LTE," Mediatek, Renesas Mobile Europe, Broadcom Corporation, Vienna, Austria, Feb. 2013.

[3GPP13-36866] 3GPP TR 36.866, "Network-assisted interference cancellation and suppression for LTE," Release 12, v1.1.0 (2013-11).

[3GPP12-36829] 3GPP TR 36.829, "Enhanced performance requirements for LTE user equipment (UE)," Release 11, v11.1.0 (2012-12).

[PIB+13] P. Papadimitriou, T. Ihalainen, H. Berg and K. Hugl, "Link-level performance of an LTE UE receiver in synchronous and asynchronous networks," WCNC2013, Shanghai, China, April 2013.

[METIS32] METIS consortium, "D3.2 – First performance results for multi-node/multi-antenna transmission technologies," project report, Apr. 2014.

[3GPP10-36814] 3GPP TR 36.814, "Further advancements for E-UTRA physical layer aspects," Release 9, v9.0.0 (2010-03).

## 8.17 T3.2 TeC 13: Extension of IMF-A interference mitigation framework to small cell scenarios and Massive-MIMO – The OP CoMP concept [NSN]

### 8.17.1 General Overview

'1000 times capacity' is the main target of this innovation. There are several well known options to increase capacity (and coverage) for mobile radio networks like interference mitigation, higher modulation and coding schemes, increased RF bandwidth or increased number of cells per area.

Increasing spectrum is quite convenient as long as it is accessible for moderate costs. New spectrum means typically also higher RF frequencies with related lower coverage, which is true especially for the mm-wave range. For that reason it is expected that spectral efficiency (SE) gains in the order of a factor of 10 will be needed in the future for the cm-wave frequency bands and especially for the very precious few GHz RF-bands like 2 to 5 GHz.

Inter cell interference in cellular networks is a well known issue which limits the performance especially for urban areas with low inter site distances of the radio stations. Another important criterion is the rank of the channel matrix per cell as it limits the number of simultaneously spatially supported UEs, which will be always limited to the maximum spatial degree of freedom (SDF) given by the maximum number of Tx-antennas per cell. In case of a 4x2 MIMO system a maximum of four spatial streams per resource use can be supported, while in reality even two spatial streams are difficult to achieve due to strong inter beam interference. This inter beam interference is severe in case the beams are generated by a typical  $\lambda/2$  spaced uniform linear array from a single site due to similar path loss for all beams together with a strong overlap of beams, i.e. a strong correlation between adjacent beams.

In case of very high SINR one might consider higher modulation and coding schemes, but it is well known that in the high SNR regime spatial multiplexing is the superior solution. In addition in the EU FP7 project ARTIST4G [ARTD14] it has been found that even for inter site distances of only 500m indoor users experiencing a strong outdoor to indoor penetration loss (PL) of 20dB are often noise limited instead of interference limited.

To overcome the above mentioned challenges of limited channel rank and UEs in coverage holes with limited SNR two main features are integrated into the available ARTIST4G interference mitigation framework [SGS+13]: massive MIMO antennas at each macro sector as well as a set of randomly placed small cells. Massive MIMO arrays at each macro sector leads to more narrow beams (note here a grid of beam (GoB) concept is being assumed) with less inter beam correlation and consequently a higher rank of the channel matrix. In addition significant beamforming gains help to increase the SNR for each user, and it has been shown that this is true for line of sight (LOS) as well as to quite some extent also for non line of sight (NLOS) scenarios.

As a second mean, small cells (SCs) are considered as these can provide high SNR to close by UEs with low pathloss links and often significantly increase the overall channel rank due to their far off as well as below rooftop placement with respect to the macro site. The distributed placement of macro and small cells ensures that the according radio channels are mainly uncorrelated.

The IMF-A framework includes as main parts a tight cooperation like joint transmission CoMP over e.g. three sites with three sectors each. Interference floor shaping is an essential part, as it decouples adjacent cooperation areas so that these can be optimized individually.

The so-called opportunistic CoMP (OP CoMP) scenario is illustrated in Figure 8-43. It contains a central unit with very good – or here even ideal – backhaul links between all macro as well as small cell radio stations. A similar proposal can be found in [JMZ+14].

Large performance gains can be achieved, but in this most simple type of implementation the according complexity of the system will be extremely high. For that reason the system has to

be setup in an opportunistic way, depending on backhaul availability, strength of channel components to macro or small cell beams, reliability of channel state information, etc. The goal of the accordingly denoted 'OP CoMP' scheme is to get close to the upper performance limits with minimum implementation effort.

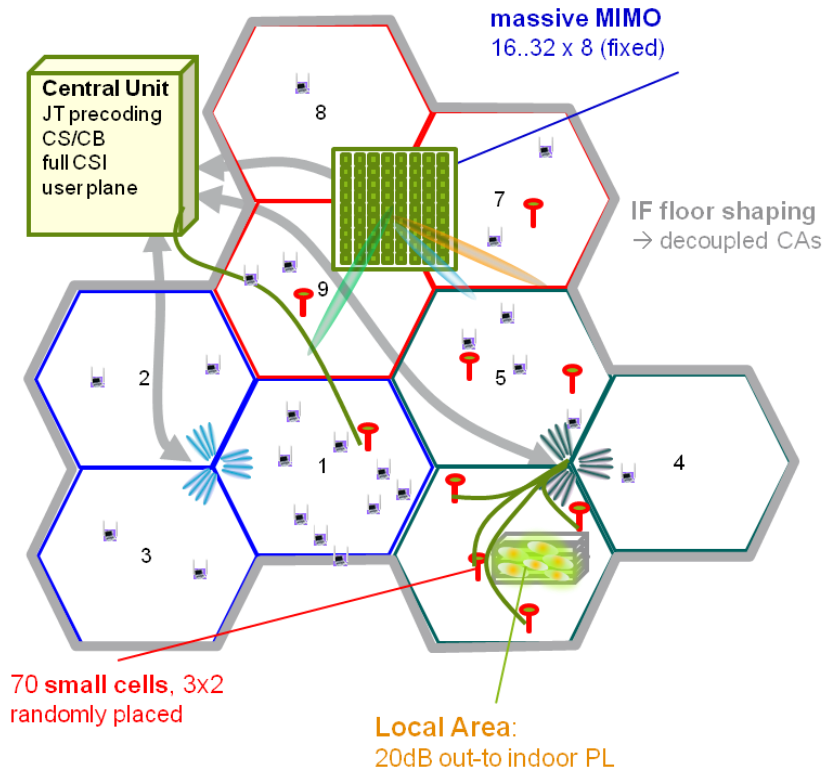


Figure 8-43: Typical OP CoMP scenario

### 8.17.2 Performance Results

So far the achievable performance under some idealized conditions is being investigated to better understand the potential of the combination of massive MIMO and CoMP enhanced by a certain number of small cells. Minimizing of complexity, energy as well as requirements e.g. with respect to the backhaul links will be done in one of the next steps.

We consider an OFDM based closed loop downlink multiuser MIMO cellular system forming cooperating areas over three sites with three sectors each as illustrated in Figure 8-43. We assume perfect interference floor shaping, so that adjacent cooperation areas are fully decoupled so far, i.e. inter cooperation interference is typically below -20dB.

Each sector is upgraded by a massive MIMO array of size 16x16 where the 16 vertical antenna elements are a standard Kathrein antenna with two RF connectors for each polarization, i.e. for the vertical direction only the tilting can be adapted. In the horizontal direction a  $\lambda/2$  spaced uniform linear array (ULA) of size 16 is being formed. By virtual beamforming an equally spaced grid of beam (GoB) is generated, i.e. there are eight beams with beam directions equally spaced over the 120° sector.

In addition there are up to 70 small cells, each using 3 sectors with 2 antennas per sector, randomly placed within the centre of the cooperation area. For illustration a typical radio channel over 100 physical resource blocks (PRB) of 180kHz each can be found in Figure 8-44, which consists of the 72 beams of the 3x3x8 macro beams (index 1 to 72) and the further 70x3x2=420 small cell beams (index 73 to 492). The macro beams are as expected

more frequency selective than the almost flat small cell beams, which is due to the lower SC-UE distance and the below rooftop allocation at a height of 6m.

Some main simulation parameters are:

- height eNB / small cell / UE = 35 / 6 / 1.5m
- antennas eNB / small cell / UE = 16x16 / 3x2 / 1
- RF frontends per macro cell = 16 allowing horizontal beamforming
- single polarization only
- GoB eNB / small cell = 8 / 2 beams equally spaced over 120°
- RF frequency = 2.6GHz
- RF bandwidth = 18MHz plus 2 MHz guard band
- Channel model macro / small cell  
= Quadriga - UMA / Quadriga traces provided by HHI UMI
- Number of randomly placed small cells per CA = 0 ... 70
- Number of randomly placed UEs = 100
- Inter site distance of macro sites is 500m
- Simulated are 3 sites, but tortoise concept ensures CA decoupling → to be verified
- Number of drops: so far only few → low confidence interval so far (for further study)
- Scheduler = round robin of randomly chosen UEs
- Cooperation = JT CoMP over all macro and small cells

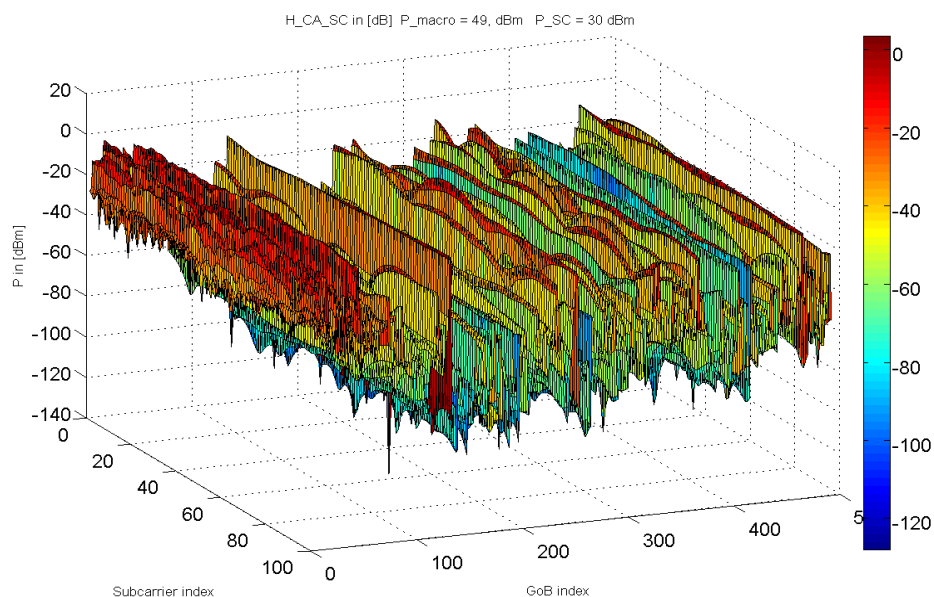


**Figure 8-44: Radio channel for a cooperation area formed over 3 sites**

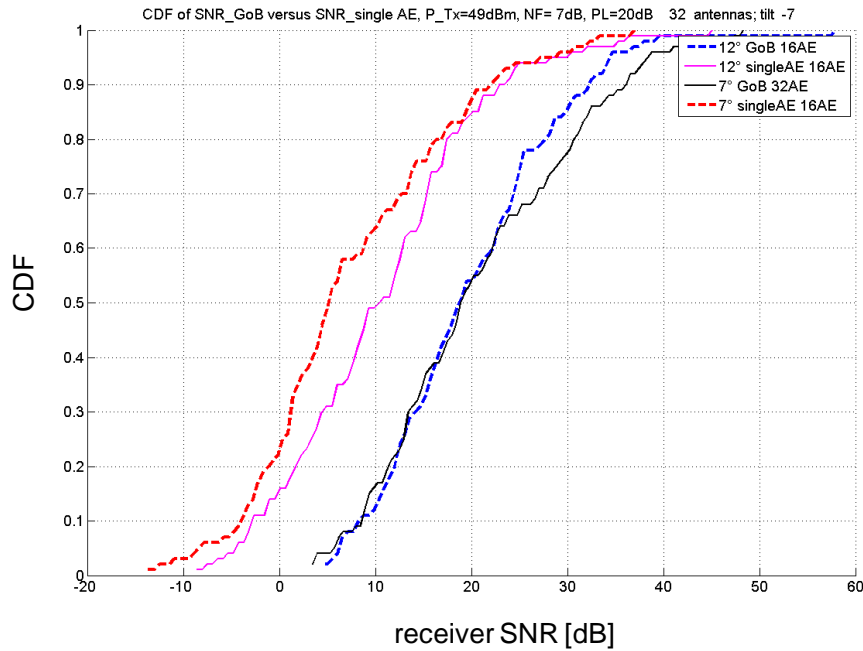


Figure 8-45: CDF of receiver SNR in [dB] for 7 and 12° tilt with 16 and 32 antennas per macro site and no cooperation so far. Compared is the performance of a single antenna of the serving cell versus that of the strongest beam. Note, here are only macro stations active.

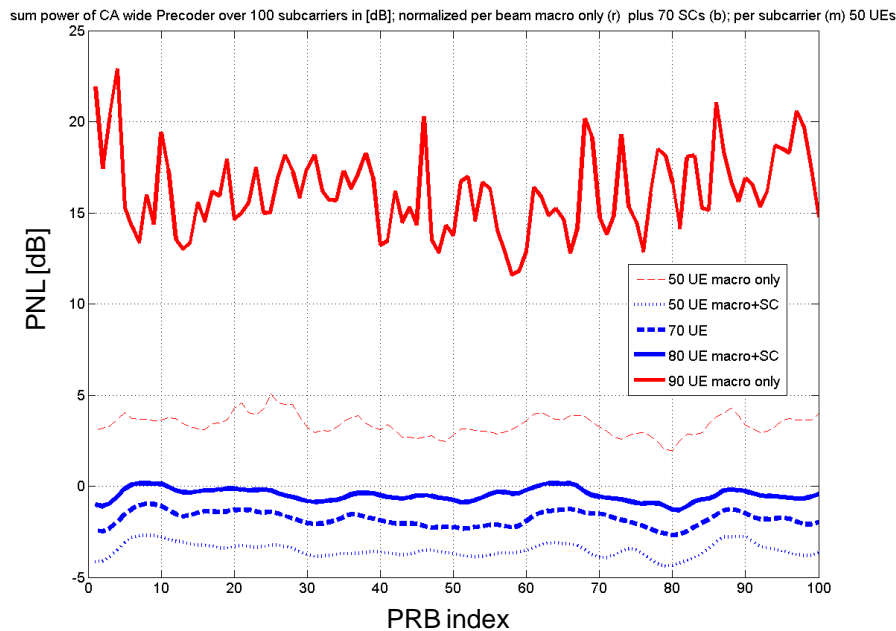


Figure 8-46: Power normalization loss in [dB] for macro cells only (red) versus macro plus small cells (blue). The thickness of the lines indicates the number of UEs (50, 60, 70, 80) per cooperation area (fat line).

Figure 8-45 and Figure 8-46 illustrate some of the available simulation results, which are intended as a verification of the most relevant effects. In Figure 8-45 the SNR with and without massive MIMO beamforming is compared to each other for tilt values of 7 and 12° and it can be observed a strong beamforming gain of about 10dB despite the non line of sight (NLOS) nature of the radio channel. This gain is similar for 16 and for 32 antennas, indicating that for

16 antennas the beamwidth is already in the order of the angle of departure (AoD) of the radio channel. Furthermore it can be recognized that for the very low inter site distance (ISD) of 500m the 12° tilt is by few dB superior to 7° as it steers the Tx-energy better to the UEs, i.e. the centre of the cells.

More interestingly are the results from Figure 8-46, which depict the power normalization loss (PNL) for a JT CoMP cooperation including only macro sites (but with massive MIMO arrays) versus the combination of macro plus small cell sites. The PNL is defined as the sum of the power of the precoding weights over all cells and UEs. It is a key performance indicator for cooperative MIMO systems as for a PNL larger than 1 (=0dB) the Tx power will have to be reduced by the same amount (that why it is called a loss). Assuming for example zero forcing precoding by the Penrose Moore pseudo inverse of the overall radio channel the according Rx signal will be reduced by the same dB value, which directly leads to lower modulation and coding schemes (MCS) and accordingly lower data rate for this UE.

What can be concluded from Figure 8-46 is that macro stations alone - even if enhanced by massive MIMO arrays – have a much higher PNL compared to the combination of macro and small cells. As a remark one should mention that with the IMF-A framework and 4 antennas per eNB one could serve around 2 to 3 UEs per cell, i.e. overall 18 to 27 UEs, where in case of 27 UEs there the PNL was already often significantly above 0 dB. From that it can be concluded that massive MIMO alone is already powerful, but the combination with small cells seems to be by far more promising.

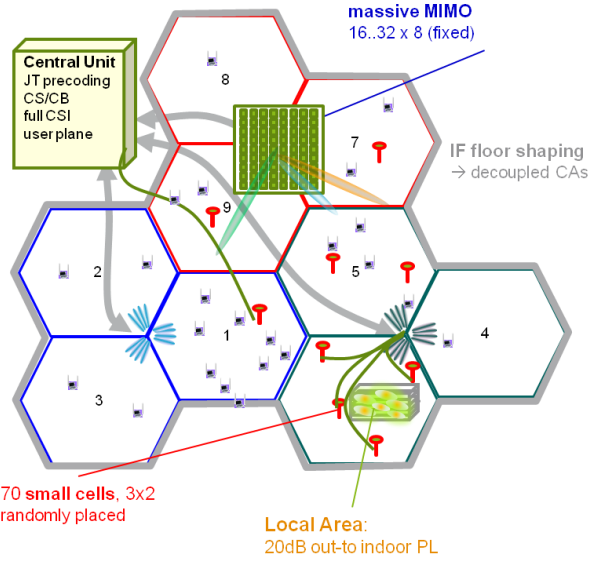
In this case for the macro plus small cell case between 80 to 90 UEs can be served with random scheduling and a PNL close to zero dB. By taking the SINR limits of UEs into account a data rate mapping allows to estimate the achievable overall spectral efficiency of such a system, which is in this case **48bit/s/Hz/cell brutto** or taking an overhead of 47% into account of **23bit/s/Hz/cell netto**, which is a **factor of almost 8** compared to 3GPP LTE Release 10, 4x2 case 1 of 3bit/s/Hz/cell. Note, cell means here macro cell.

Some short remarks: next steps will be to verify results with better statistics. There are several further optimizations possible like using more than one single UE antenna, using some form of per cell scheduling similar to the two stage scheduler of the IMF-A framework, doing some form of network planning for small cells etc.

At the same time the most important next step will be now to reduce the overall complexity to reasonable levels and it seems that there is plenty of room for it as typically UEs see only few macro and even fewer small beams.

More work on fair performance comparison might have to be done for example to classical heterogeneous network approaches like ICIC, eICIC or feICIC.

<b>T3.2 TeC 13 - Extension of IMF-A interference mitigation framework to small cell scenarios and Massive-MIMO</b>	
	<b>Main Idea</b>
	The main idea is to combine massive MIMO with the IMF-A interference mitigation framework and enhance it with small cells to significantly improve the main observed limitations of the IMF-A framework, i.e. low SNR for a significant part of the indoor UEs and limited channel rank per cell

	
<p>Considered SoA solution</p>	<p>Comparison with 3GPP LTE Release 10 performance for 4x2</p>
<p>KPIs considered and achieved gain</p>	<p>Spectral efficiency: in first few simulation runs a SE of 48 bit/s/Hz/cell possible (factor of 8 over LTE Advanced)</p>
<p>Performance evaluation approach</p>	<p>Simulation-based: limited system level evaluation = per CA plus tortoise concept</p>
<p>System model considered</p>	<p>Other</p>
<p>Deviation compared to Simulation Baseline</p>	<p>Some:</p> <ul style="list-style-type: none"> <li>• Model of environment: Urban Macro Area</li> <li>• Spectrum Assumptions: 2.6 GHz</li> <li>• Propagation model: Quadriga - 3GPP SCM</li> <li>• Deployment model: Hexagonal Grid – single CA</li> <li>• User/Device Distribution: Geometry Based (Homogenous Network) and Uniform Random (Heterogeneous Network)</li> <li>• Traffic model: Full Buffer</li> </ul>
<p>Brief update of the results with respect to D3.2</p>	<p>Simulation results for massive MIMO plus small cells</p>
<p>Association to the TeC Approach</p>	<p>Proposed to be considered in “CoMP with Advanced UE Capabilities”</p>
<p>Targeted TCs</p>	<p>TC2 (Dense urban information society)</p>
<p>Impacted HTs</p>	<p>UDN</p>
<p>Required changes for the realization with respect to LTE Rel. 11</p>	<p>To be checked:</p> <ul style="list-style-type: none"> <li>• Feedback</li> <li>• Channel prediction is seen as a main enabler for a simplified implementation</li> </ul>



	<ul style="list-style-type: none"> <li>• Reference signals</li> <li>• Control information</li> </ul>
Trade-off required to realize the gains	The performance gains so far are achieved ignoring overall system complexity, but it is expected that most of the gains can be maintained even with reasonable complexity

### 8.17.3 Impact on Horizontal Topics

T3.2 TeC 13 - HT.UDN	
Technical challenges	<ul style="list-style-type: none"> <li>• Increasing spectral efficiency</li> <li>• Increasing SINR for indoor UEs</li> <li>• Increasing rank of overall channel matrix per cooperation area</li> </ul>
TeC solution	The main idea is to combine massive MIMO and small cells with teh already powerful IMF-A interference mitigation framework
Requirements for the solution	<ul style="list-style-type: none"> <li>• Backhauling between macro and small cell sites</li> <li>• Channel estimation for massive MIMO plus additional small cell sites</li> </ul>
KPIs addressed and achieved gain	Spectral efficiency: first indication for gains in the range of 800% (not optimized so far, but also not verified)
Interaction with other WPs	<ul style="list-style-type: none"> <li>• WP2: TeC developed by assuming OFDM. Other air interfaces like UFMC etc. should add no extra complexity to MIMO transmission. Some interaction is possible with MAC and RRM solutions in WP2.</li> <li>• WP4: Interference identification (TeC1: New interference estimation techniques) in WP4 are essentials for interference alignment and cancellation</li> <li>• WP6: For system level evaluations</li> </ul>

### 8.17.4 Addressing the METIS Goals

T3.2 TeC 13	
1000x data volume	Increase in the achieved cell throughput and spectral efficiency (target is factor of 8...10) allows the increase of the data volume per area
10-100 user data rate	Small cells is part of the solution allowing to increase number of users
10-100x number of devices	Higher number of devices allow for better scheduling decisions
10x longer battery life	RF power reduction can be set as target. It remains open how far there would be overall battery gains



5x E-E reduced latency	
Energy efficiency and cost	RF power reduction can be set as target. It remains open how far there would be overall EE gains

### 8.17.5 References

[ARTD14] ARTIST4G consortium, "D1.4 – Interference Avoidance techniques and system design," project report, July, 2012.

[TR36814] 3GPP, "Further Advancements for E-UTRA - Physical Layer Aspects," TR 36.814, V 9.0.0, March 2010.

[SGS+13] Mikael Sternad, Michael Grieger, Tommy Svensson, Wolfgang Zirwas, Coordinated Multi-Point in Cellular Networks: From Theoretical Gains to Realistic Solutions and Their Potentials, Tutorial at ICC 2013, Budapest, Hungary.

[JMZ+14] Volker Jungnickel, Konstantinos Manolakis, Wolfgang Zirwas, Berthold Panzner, Volker Braun, Moritz Lossow, Mikael Sternad, Rikke Apelfröjd, Tommy Svensson, The Role of Small Cells, Coordinated Multi-point and Massive MIMO in 5G, IEEE Communications Magazine, special issue on 5G, May 2014.

## 8.18 T3.2 TeC 14: Joint dynamic clustering and coordinated scheduling for relaying with physical layer network coding [PUT]

### 8.18.1 General Overview

In this work we apply the coordinated scheduling approach for the two-way relaying with network coding (NC) and MIMO in TDD systems. The main objective is to provide a joint dynamic clustering and coordinated scheduling algorithm to mitigate the increase of co-channel inter-cell interference introduced by colliding RN modes of operation and one-hop transmission.

The considered approach relies on dynamic clustering of nodes depending on the experienced or expected interferences. The set of coordinated entities is selected based on the measured interference level at the selected UEs and possible collisions between the one-hop UEs and the relayed UEs. Then coordinated scheduling is applied within the clusters with the aim to mitigate the interference introduced by time reversed mode of relayed UEs. This can be achieved by restricting the use of available time-frequency resources by grouping the UEs that can use the same resources simultaneously without introducing severe interference, as shown in Figure 8-47.

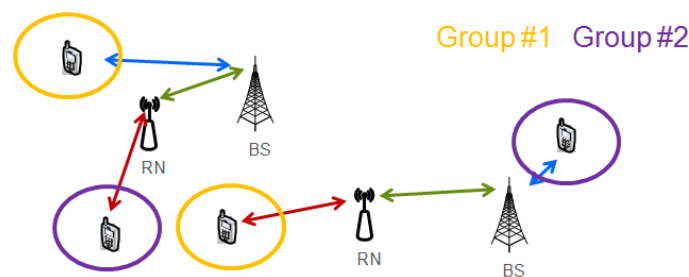


Figure 8-47: Grouping of UEs

Several approaches to joint clustering and coordinated scheduling are possible:

- A simple ideally centralized scheme, where coordination between BSs and several RNs is considered. UEs are assigned into strong interferers groups based on the measured interference level from their neighbours, with a single resource block allocated exclusively to one user from a group of strong interferers. Moreover, an assumption is considered for the two-hop transmission, where for the BS→RN link and UE→RN link the same set of resource blocks has to be allocated.
- Coordinated scheduling (CS) with static clustering, where different set of RBs can be used for the BS→RN link and UE→RN link, with the only constraint being the same transport block size for both links to enable NC.
- CS with dynamic clustering, where coordination clusters are formed depending on the time-domain scheduling of UEs for transmission.

The interference introduced by reverse mode of operation of the relayed users can be completely avoided within the coordination cluster by applying exclusive RB assignment. However, with such approach the available spectrum may be not fully utilized as spatial diversity is not exploited. Therefore, an approach based on interference analysis can be applied to further exploit the spatial diversity within the cluster. Simple approach based on SIR estimation based on path-loss or one based on semi-orthogonal user selection (SUS) [YG06] can be considered.

In the following part only results for the first approach are presented - centralized scheme with UEs division into strong interferers groups based on SIR estimation. Schemes based on fully dynamic clustering and coordinated scheduling are for further study.

### Interference model

The exact interference analysis for two cells separately for multiple-access and broadcast phase is shown in Figure 8-48 and Figure 8-49, respectively. In the analysed scenario we assume that directly connected users and relay connected users in the same cell use orthogonal resource blocks. Therefore, interference can occur only between different cells. In the multiple access phase relays and UEs directly connected to BS (cellular UEs - CUEs) receive signal if scheduled. The interference from another cell can be caused by another BS or relay connected UEs (RUEs). In the broadcast phase BSs and UEs connected to relays receive signal. The interference from another cell can be caused by CUEs or relays. It should be noted, that UEs operating in different mode (directly connected to BS vs. served by relays) experience D2D like interference.

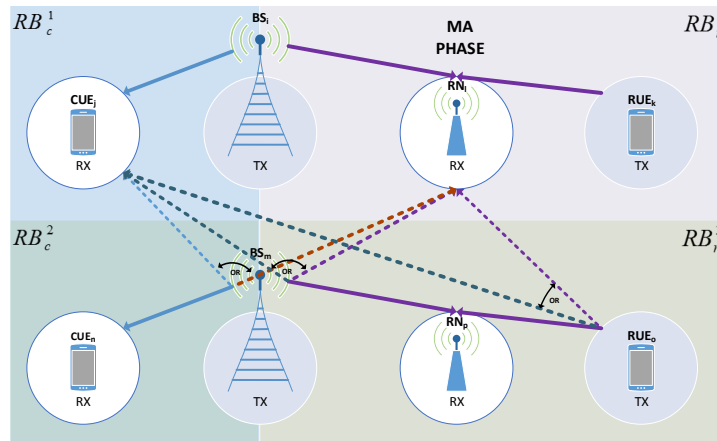


Figure 8-48: Multiple access phase interference

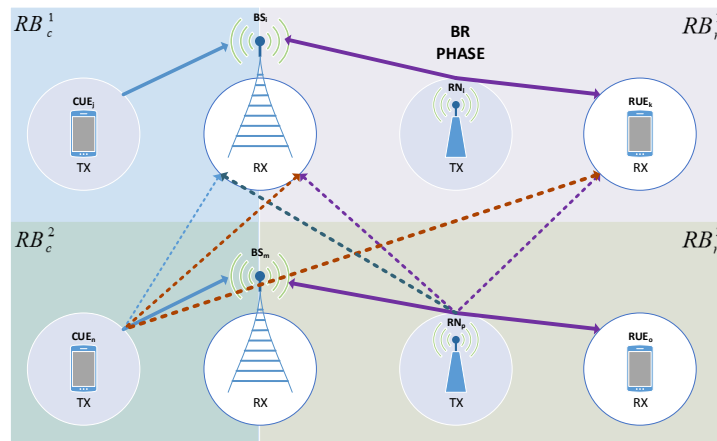


Figure 8-49: Broadcast phase interference

### 8.18.2 Performance Results

We use system-level simulations on an environment that follows standard baseline for TC2, outlined in [METIS14-D32] - the “reduced Madrid Grid”. In this deliverable we provide results with RNs deployed instead of micro BSs, as shown in Figure 8-50. Simulation results in Figure 8-51 present performance comparison of coordinated scheduling schemes with different interference group selection threshold. The grouping algorithm uses large scale fading and

transmitted powers per resource block (with uplink power control and uniform power allocation) to identify a group of users that cause interference to the considered UE stronger than the assumed threshold. Then resource allocation is performed sequentially in each cell considering current allocation of resources and changing the order of cells in each TTI in a Round Robin manner.

In our simulations we assumed physical layer of LTE Rel. 10, therefore the maximal throughput was achieved when SINR on a given link was around 20-25 dB. From Figure 8-52 it is visible that much higher SINR values were possible despite the additional interference introduced by reversed transmission mode of UEs served by relays. On the other hand such high values are not present in real systems due to various implementation impairments (which are not modelled in the used system-level simulator).

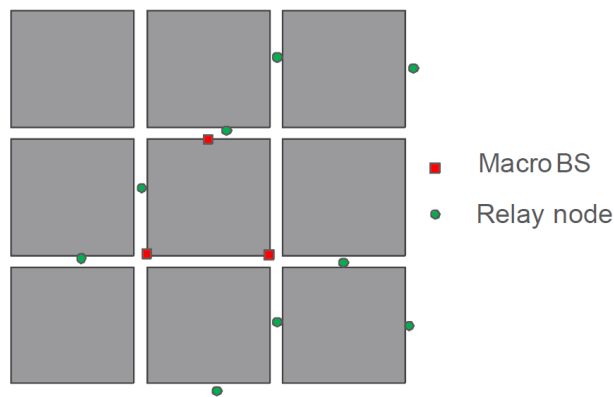


Figure 8-50: Deployment of macro stations and relays

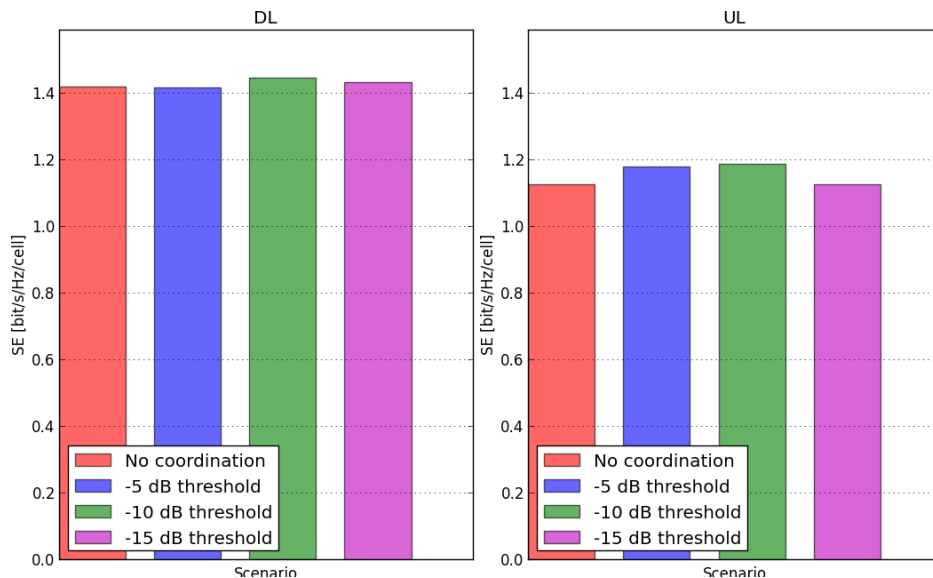
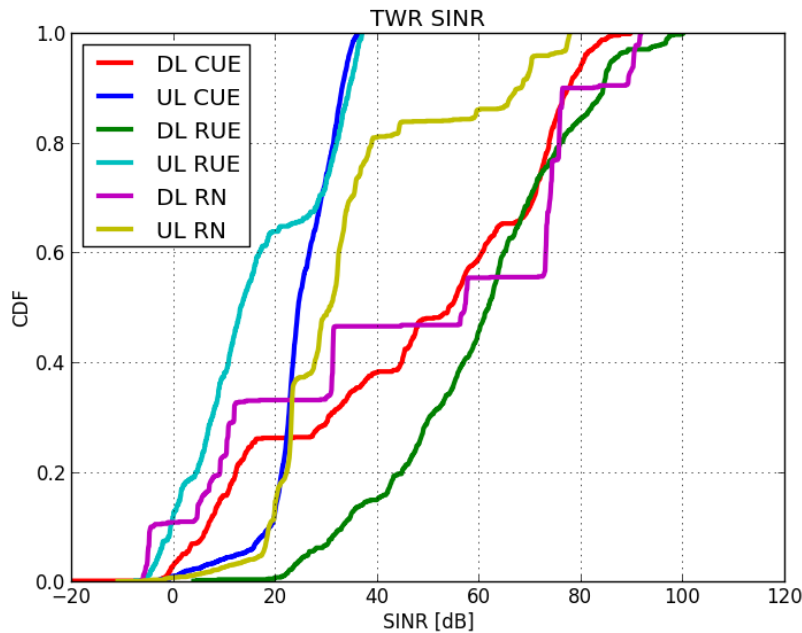
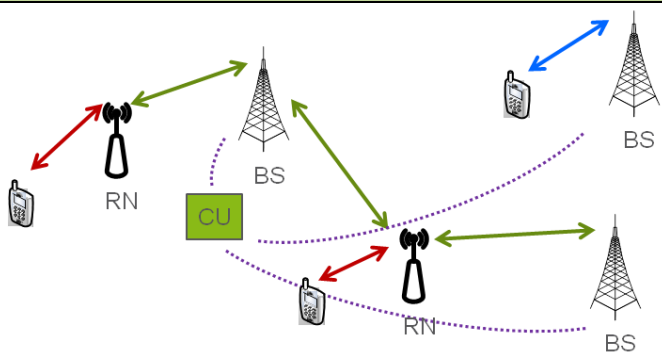


Figure 8-51: Spectral efficiency for different interfering group selection threshold



**Figure 8-52: CDF of SINR for various links in cellular networks with relays nodes performing two-way relaying**

The results presented above demonstrate simulation capability of the considered scenario and some preliminary results. The gains of this TeC are still under investigation with the aim of evaluation of fully dynamic clustering and scheduling scheme.

T3.2 TeC 14 – Joint dynamic clustering and coordinated scheduling for relaying with Network Coding	
	<p><b>Main Idea</b></p> <p>The aim is to jointly schedule users in a dynamic way in a TDD system with MIMO-NC relaying to mitigate the interference introduced by reversed mode of operation of relayed UEs</p>
Considered SoA solution	System based on LTE rel-11 defined as a baseline for TC2 in [METIS14-D32] without RNs or with RNs operating in half-duplex mode. No coordination of BSs.
KPIs considered and achieved gain	UL spectral efficiency: 5%
Performance evaluation approach	Simulation-based (simplified system-level)
System model considered	WP3 Task 3.2 Simulation Baseline
Deviation compared to Simulation Baseline	N/A
Brief update of the results with respect to D3.2	Preliminary results presented



Association to the TeC Approach	Not applicable
Targeted TCs	TC2
Impacted HTs	UDN
Required changes for the realization with respect to LTE Rel. 11	Minor – NC capable receivers
Trade-off required to realize the gains	Increased signalling between BSs and RNs.

### 8.18.3 Impact on Horizontal Topics

T3.2 TeC 14 - HT.UDN	
Technical challenges	Self-backhauling access schemes
TeC solution	Joint dynamic clustering and coordinated scheduling for two-way relaying with MIMO and NC will enable use of self-backhauling with mitigation of interference introduced by reversed mode of operation of nodes using wireless backhaul
Requirements for the solution	<ul style="list-style-type: none"> <li>• UE mobility limited</li> <li>• Hotspots mobility limited</li> <li>• Multiple antennas available at the RN, BS and UE</li> </ul>
KPIs addressed and achieved gain	<ul style="list-style-type: none"> <li>• Cell throughput: Under investigation</li> <li>• User throughput: Under investigation</li> <li>• Spectral efficiency: Under investigation</li> </ul>
Interaction with other WPs	<p>WP4 – impact from interference identification techniques and long-term interference management</p> <p>WP6 – system-level simulations</p>

### 8.18.4 Addressing the METIS Goals

T3.2 TeC 14	
1000x data volume	By reducing the number or required slots the data rate should be doubled but only for a symmetric traffic. The increase should be higher for the cell edge users.
10-100 user data rate	CS for two-way relaying with NC can increase the user data rate by effective mitigation of interference and provisioning of additional nodes
10-100x number of devices	Higher number of devices can be connected simultaneously because of additional RNs introduced
10x longer battery life	Allocation of cell edge UEs to relays should result in lower UE transmission power compared to UE to BS links
5x E-E reduced latency	This TeC reduces latency by enabling exchanging the data between BS and UE through RN only in two slots
Energy efficiency and cost	By introduction of wireless backhaul lower cost of



**Document:** FP7-ICT-317669-METIS/D3.3

**Date:** 25/02/2015

**Security:** Public

**Status:** Final

**Version:** 1

	the access nodes is expected
--	------------------------------

### 8.18.5 References

[YG06] T. Yoo, A. Goldsmith, "On the optimality of multiantenna broadcast scheduling using zero-forcing beamforming," *IEEE J. on Sel. Areas Commun.*, vol. 24(3), pp. 528–541, 2006.

[METIS14-D32] METIS D3.2, "First performance results for multi-node/multi-antenna transmission technologies", Apr. 2014.

## 8.19 T3.2 TeC 15: Adaptive and energy efficient dense small cells coordination [TI]

### 8.19.1 General Overview

The proposed TeC aims to provide a mechanism to reduce the overall power consumption in an over-provisioned network when the traffic is below its peak.

The considered scenario is characterized by a large number of transmitting base stations deployed in a confined space to address a crowd of users. The basic assumption is that by exploiting a non-coherent joint transmission technique the number of nodes that must be kept active to serve a low amount of traffic can be reduced, without impairing the user experience.

In [METISD32] we defined a centralized coordination algorithm that follows a greedy approach in order to dynamically switch on and off the available Base Stations (BSs), based on the amount of traffic that should be served in each transmission time interval (TTI).

In particular, a centralized entity manages a cluster of BSs, collecting from each UE the Channel Quality Indications (CQIs) relative to the  $J$  BSs that are received with higher power (with  $J=3$  in our simulations). Also, an estimate of the overall interference due to the power of the remaining cells is collected. Based on this information, the centralized entity computes a set of proportional fair metrics for each UE, assuming all the possible  $2^J - 1$  configurations where the  $J$  BS reported by the UE are active or deactivated (the configuration where all BS are deactivated is obviously not computed). Depending on the configurations, the metric corresponds to the metric achievable with a non-coherent Joint Transmission (JT) approach (all  $J$  BS are active), or to Dynamic Points Selection with Blanking (DPS/B) (one BS is active, and the other  $J-1$  that would provide the highest interference are deactivated), or to a mix of the two (some BS active, some deactivated). Based on this metrics, and the actual amount of bytes that are stored in the transmission buffer for each UE, the proposed algorithm (that we label "Recursive JT") recursively allocates frequency resources with a greedy approach, thus selecting which UE will be served, and the minimum amount of BSs that should be used to serve that UE, balancing non-coherent Joint Transmission or DPS/B transmission, eventually trying to accommodate user traffic request with a reduced number of active BS. An extended version of the algorithm (labelled "EnEffRec") has also been developed, that further reduces energy consumption by giving higher priority to users that can be served with the remaining resources of Base Stations that have been already activated in the previous step of the algorithm for the considered TTI.

The algorithms were tested in the simplified Test Case 2 scenario agreed as baseline for Task 3.2 and allowed to save up to +27% energy consumption with nowadays nodes power consumption models.

However higher gains were expected with higher small cells density and improved switch off mechanisms. In this deliverable we provide updated results obtained in the more challenging Test Case 4 stadium scenario, where a higher density of small cells is deployed.

### 8.19.2 Performance Results

According to METIS setup [METISD61], the stadium is placed on an ellipse with a minor radius of 105 m and larger radius of 150 m; in the ellipse centre there is a playground of 70 x 100 m. Except for the central playground the rest of the stadium area is covered by a deck placed at an height equal to 33 m. For the simulation purposes we selected a 50 m x 100 m area adjacent to the playground and tilted of 30° degrees out of which only the range of 30 m x 40 m is used to collect the simulation results, in order to limit border effects (see the left part of Figure 8-53).

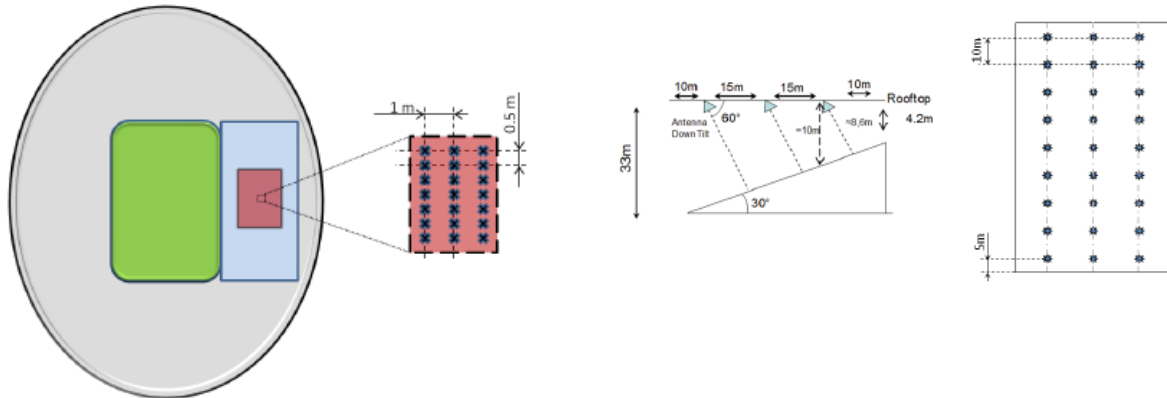


**Figure 8-53: the simulated Stadium area**

The network infrastructure is composed by a dense disposition of small cells deployed on the stadium rooftop and directed toward the audience with a tilt angle equal to  $60^\circ$ . The small cells are connected by means of a backbone network to a centralized controller. In the considered simulations we have 27 small cells regularly deployed on the structure rooftop as is depicted in the right part of Figure 8-53. In the considered area there are potentially up to 8950 users distributed uniformly in the seats, but for simulation purpose we will assume that only 270 are active in a simulation run; the distance between the user is 1 m along the minor stadium axis and 0.5 m along major stadium axis.

A simplified channel model has been included, where pathloss is given according to the Indoor Hotzone scenario with Line of Sight (LOS) provided in [3GPP36814] and small scale fading effect in time is modelled with a Rayleigh distributed fading coefficient. Antenna gain is included as in [3GPP36814], with a main lobe angle set to  $60^\circ$ . Figure 8-54 reports the long term power level (excluding small scale fading effects) that is received from the closest BS in the stadium sector. Note how positions in the highest row of the sector receives a stronger signal, being closer to the transmitting points. Other simulation parameters are summarized in Table 8.9.

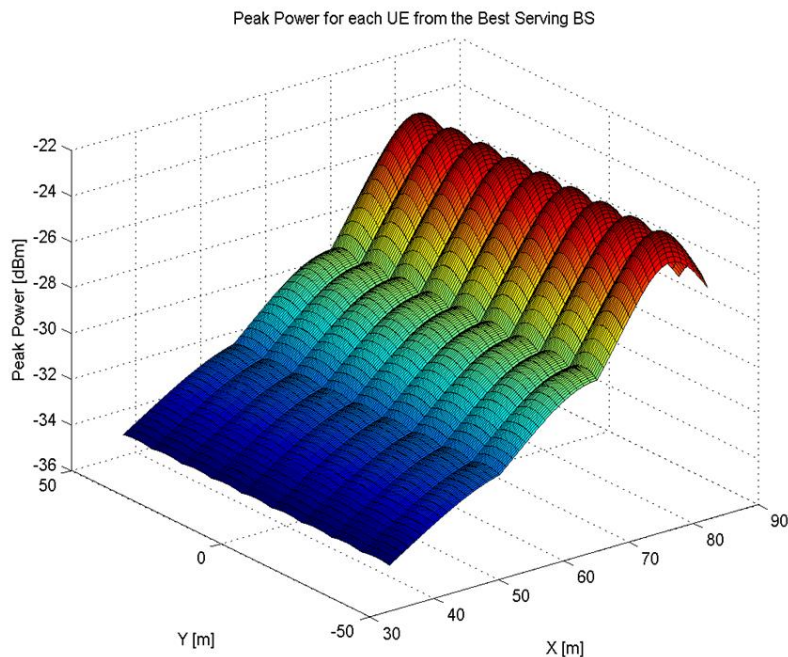


**Figure 8-54: Received power level in the simulated Stadium area**

**Table 8.9: Simulation assumptions**

Parameter	Value
TTI duration	1 ms
Bandwidth	10 MHz
Carrier Frequency	2.6 GHz
Number of Resource Blocks	50
Number of BS	27
Number of BS antennas	1
Number of Active UEs in a simulation drop	270
Number of UE antennas	1
Power BSs	20 dBm (indoor Hotspot)
Physical Layer abstraction	Shannon Law
Traffic type	Constant Bit Rate (CBR) or Full buffer

In this scenario we evaluated the following KPIs:

- The user throughput, defined as the ratio between the total amount of received bits and the amount of time in which the given user had data available on its transmission buffer.
- The system throughput, ratio between the overall amount of bits received by all UEs divided by the amount of time in which at least one cell was transmitting.
- Power consumption, overall amount of power consumed by all the Base Stations during the simulation time. Base station power consumption is estimated on the basis of the radio frequency (RF) transmitted power, according to the power models defined in [EARTH23]. A sleep mode to switch off unused cells is included.
- Energy Efficiency: ratio between power consumption and system throughput

Since the aim of the proposal is to reduce consumption in off-peak traffic condition, simulations were run with a Constant Bit Rate (CBR) traffic source, that allowed to generate fixed size packets in the transmission buffers at different rates, thus varying the network load. As a reference, also full buffer traffic has been considered.

Results for overall power consumption are reported in Figure 8-55(a) as a function of the CBR generated user rate. Note that in general the proposed solutions allow to save energy compared to a classical non coordinated approach. However, if also the overall system throughput is considered, it can be observed that when traffic increases, the proposed algorithms cannot achieve the same level of performance of a non-coordinated approach, as shown in Figure 8-55(b). The proposed schemes give higher priority to save energy rather than provide capacity to the system, so in capacity limited situation they cannot outperform even a non coordinated approach.

Considering the overall energy efficiency (Figure 8-56(a)), it can be seen that in the end proposed solutions enable savings only in the low traffic region, with generated user throughput <0.5 Mbps. However in this region improved energy efficiency up to 33% is possible.

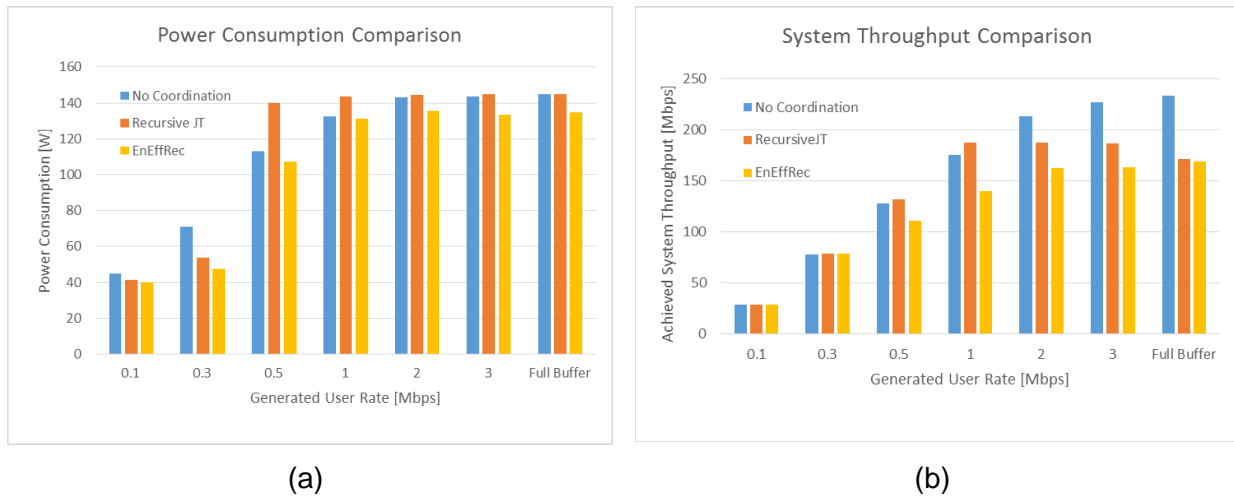


Figure 8-55: Power consumption and achieved system throughput

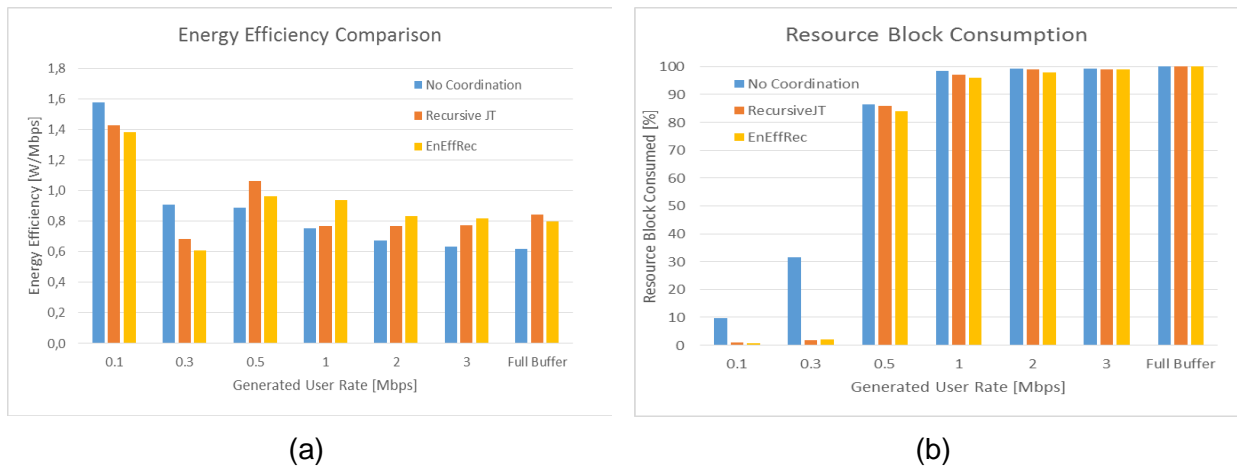


Figure 8-56: Overall energy efficiency and resource block usage

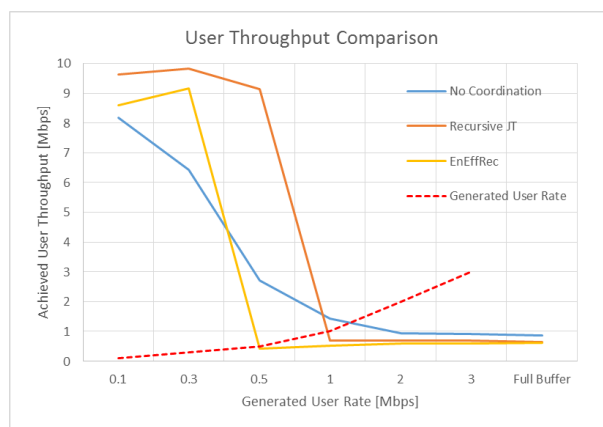


Figure 8-57: Achieved system throughput

It should be noted that as the generated CBR traffic per user goes from 0.1 to 0.5 kbps the amount of resources used by the network to satisfy the traffic request increases steeply, becoming almost the same as in the full-buffer scenario, as highlighted in Figure 8-56(b). So 0.5 kbps can already be considered as an high load situation.

By reducing the number of active nodes and properly manage interference in low load condition, the algorithms not only achieve better energy efficiency, but in this load condition improved user experience is also granted, since the instantaneous achieved user throughput

largely outperforms that available with a non coordinated approach, as it is shown in Figure 8-57.

Note that since the proposed scheme is not efficient when the network load increases, a mechanism operating on a longer time scale could be provided to enable the use of the proposed solution only when the network condition is favourable.

As a final remark, it should be noted that results here obtained assume that small cells consumptions are those presented in the EARTH project, which were however based on hardware implementation in 2012, and that showed limited scalability with the actual amount of resource used, and limited savings when the small cells enter the sleep mode. Since the scope of the METIS project is 2020 it can be expected that future hardware implementation could provide more dynamic power consumption profiles, which could improve the benefit achievable with the proposed solution.

T3.2 TeC 15 – Adaptive and energy efficient dense small cells coordination	
<p>Dense deployment of small cells in a Stadium sector to serve a large number of users</p>	<p style="text-align: center;"><b>Main Idea</b></p> <p>Design of a CoMP based scheduling algorithm that allows to reduce power consumption in a dense network when traffic is below the peak.</p> <p>The algorithm recursively allocates frequency resources with a greedy approach, thus selecting which UE will be served, and the minimum amount of BSs that should be used to serve that UE, balancing non-coherent Joint Transmission (JT) or Dynamic Points Selection with Blanking (DPS/B), eventually trying to accommodate user traffic request with a reduced number of active BS</p>
Considered SoA solution	<ul style="list-style-type: none"> <li>Deployment of small cells in the stadium environment without centralized coordination.</li> </ul>
KPIs considered and achieved gain	<ul style="list-style-type: none"> <li>Energy Efficiency: +33%</li> <li>Achieved instantaneous user throughput: from +5% to +40%</li> <li>(Note <u>results applies only in low traffic condition</u>)</li> </ul>
Performance evaluation approach	Simulation-based: System Level Evaluation
System model considered	Other (Results based on WP3 Task Baseline are available in [METISD32])
Deviation compared to Simulation Baseline	Significant: <ul style="list-style-type: none"> <li>Model of environment according to TC4 Stadium</li> <li>10MHz bandwidth @2.6GHz</li> </ul>



	<ul style="list-style-type: none"> <li>• Propagation model, Deployment model, User/Device distribution according to TC4</li> <li>• Traffic model: Constant Bit Rate, with varying rate levels (from 0.1 to 3 Mbps). Full-buffer results provided as reference</li> </ul>
Brief update of the results with respect to D3.2	The scheme proposed in [METISD32] has been tested in the ultra dense environment foreseen by Test Case 4 Stadium.
Association to the TeC Approach	Not Applicable
Targeted TCs	TC4. (Results for TC2 provided in [METISD32])
Impacted HTs	UDN
Required changes for the realization with respect to LTE Rel. 11	Minor, mainly to enable the CQI feedback collection
Trade-off required to realize the gains	Not applicable

### 8.19.3 Impact on Horizontal Topics

T3.2 TeC 15 - HT.UDN	
Technical challenges	Reduce energy consumption in deployments with a large number of transmitting nodes with good overlapping in coverage areas
TeC solution	Allow cooperation between transmitting nodes to dynamically switch off unnecessary nodes in low load condition and improve performance of the remaining nodes with Joint Transmission or Dynamic Point Selection/Blanking
Requirements for the solution	Centralized architecture with centralized scheduling, power saving features in transmitting nodes to enable sleep mode.
KPIs addressed and achieved gain	Energy saving up to 33% in low traffic condition with nowadays nodes power models.
Interaction with other WPs	Targets interference limited-scenarios so it is closely related with WP4 studies on interference management. Moreover some studies on WP4 also exploit sleep modes in small cells.

### 8.19.4 Addressing the METIS Goals

T3.2 TeC 15	
1000x data volume	
10-100 user data rate	
10-100x number of devices	
10x longer battery life	
5x E-E reduced latency	
Energy efficiency and cost	Increase energy efficiency up to +33% in low load network condition.



### 8.19.5 References

[METISD61] METIS consortium, "D6.1 – Simulation guidelines", project report, Oct. 2013.

[EARTH23] EARTH project, "D2.3 - Energy efficiency analysis of the reference systems, areas of improvements and target breakdown," <https://www.ict-earth.eu/publications/publications.html>.

[METISD32] METIS consortium, "D3.2- First performance results for multi-node/multi-antenna transmission technologies", project report, April 2014.

[3GPP36814] 3GPP, "Further Advancements for E-UTRA - Physical Layer Aspects," TR 36.814, V 9.0.0, March 2010.

## 8.20 T3.2 TeC 16: Non-coherent communication in coordinated systems [UPVLC]

### 8.20.1 General Overview

Current cellular technologies are based on the concept of coherent communication, in which the channel matrix used for demodulation is estimated via reference or pilot signals. Coherent systems, however, involve a significant increase of the signaling overhead necessary for training, especially when the number of transmission points (TP) increases or when the mobile channel changes rapidly. This fact motivates the research on non-coherent techniques, which carry out data detection without knowing the particular channel coefficients at neither the transmitter nor the receiver side.

This TeC investigates non-coherent communication techniques for open-loop transmission in multiple-input multiple-output (MIMO) channels. Following the existing theoretical studies on this topic, the main focus of this approach is to bring non-coherent techniques into practical systems with multiple transmission points (TP). As a first step, a comparison between non-coherent and coherent MIMO communication in Rayleigh block-fading channels was included in [METIS13-D31], where imperfect channel state information (CSI) was considered for the coherent schemes. Other practical aspects such as the impact of the power imbalance among different TP and the correlation among the transmitter antennas were evaluated and reported in [RCC+14a]. There, it was shown that non-coherent transmission is robust within a wide range of power imbalance values. Since already proposed non-coherent schemes only allowed single-user (SU) communication, in this TeC we also proposed a multi-user (MU) transmission scheme based on superposition coding and Grassmannian constellations, where, after weighting each user signal by a different power sharing factor, the arithmetic sum of all the users' signals is transmitted. At the receiver side, we derived the maximum likelihood (ML) detection rule that enables the MU communication in the proposed MU non-coherent setup. Another related contribution was the development of a reduced-complexity MU detector. The proposed MU non-coherent setup was shown to outperform SU non-coherent communication in terms of sum-rate. More details about this activity can be found in [METIS14-D32] and [RCC+14b].

It is well-known that, in practical scenarios, the block-fading assumption is often unrealistic due to the relative speed between transmitter and receiver. Although there are an extensive number of contributions on the performance analysis of coherent schemes in time-varying channels, the impact of the speed on the error performance of non-coherent schemes is still an open issue. In fact, some efforts have been carried out to investigate non-coherent time-selective Rayleigh-fading channels, but the non-coherent capacity is still unknown even for the Single-Input Single-Output (SISO) case. To date, Liang and Veeravalli derived only the pre-log capacity for the SISO case [LV04] and Koliander et al. for the MIMO case [KRD+13].

In this deliverable, we include a performance comparison between coherent and non-coherent SU communication schemes under practical channel conditions, such as user mobility. In particular, the performance analysis has been undertaken over a LTE link level simulator with an Extended Vehicular A 3GPP channel model. Considering 2x2 and 4x4 MIMO systems, we have compared a non-coherent approach based on Grassmannian signaling with its equivalent coherent block in LTE, that is the open-loop space-frequency block coding scheme (SFBC) based on the Alamouti code. It will be shown that the non-coherent schemes are meaningful alternatives to training-based communication as the rate and the number of transmit antennas increases in the considered scenario.

### 8.20.2 Performance Results

Simulations have been carried out in a LTE link-level simulator calibrated according to 3GPP. The simulation was run for 6 resource blocks over an Extended Vehicular A 3GPP channel model at a frequency of 2.6 GHz, considering uncorrelated antennas. We evaluated the throughput as a function of the SNR for different user speeds, ranging from 50 km/h to 300

km/h. The LTE baseline to compare the proposed approach with was the open-loop SFBC transmission mode based on the Alamouti code. For the SFBC coherent baseline we considered a channel estimator based on Wiener filtering in frequency and in time domain. The channel estimator was supposed to know the frequency and time correlation, as well as the noise power, and it used the standardized LTE reference signals for channel estimation (10% of reference signals in the 2x2 MIMO system and 15% of reference signals in the 4x4 MIMO system).

To include the Grassmannian codewords in the LTE simulator, we considered an LTE-based resource mapping, i.e. the codewords were mapped to the resource elements first over frequency and then over time. In this case, the whole resource grid was filled with codewords, since reference signals are not necessary for non-coherent communication.

Figure 8-58 shows the results for the 2x2 setup. It can be observed that the SFBC scheme outperforms the Grassmannian signalling in all cases. Although the Grassmannian scheme is, in fact, quite robust to mobility, its throughput is almost always below the one of the SFBC.

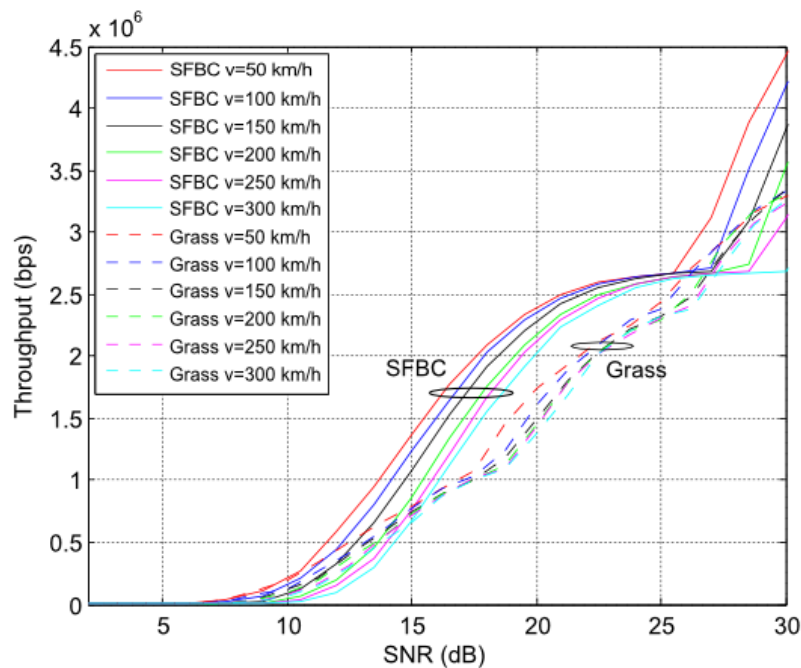


Figure 8-58: Link-level throughput for the LTE SFBC and Grassmannian codes in a 2x2 MIMO system

Figure 8-59 shows the results for the 4x4 setup. In this case, the Grassmannian scheme outperforms the SFBC baseline and it is the best choice for this scenario. Grassmannian signaling is again very robust to mobility but the SFBC is highly degraded with the user speed. The main reason for the SFBC degradation is that two out of the four antennas of the system are using poorer channel estimates, as these antennas are only assigned 50% of the pilot symbols of the other two antennas. In fact, for a channel estimation equivalent to the one in the 2x2 system, in the 4x4 system the percentage of pilot symbols should be 20% instead of 15%.

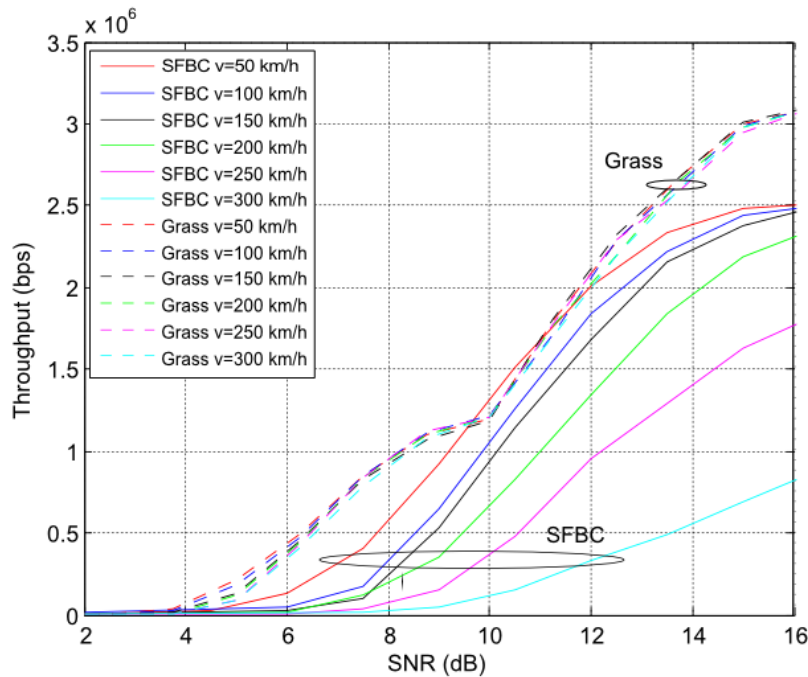
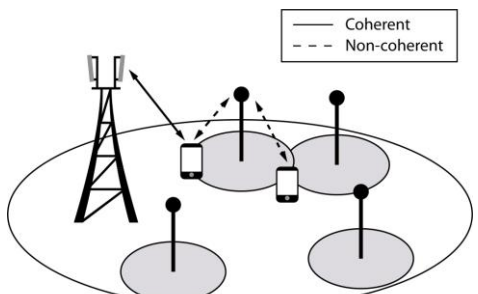


Figure 8-59: Link-level throughput for the LTE SFBC and Grassmannian codes in a 4x4 MIMO system

Overall, non-coherent communications and, in particular, Grassmannian codes are promising techniques for high-rate open-loop communications with more than two transmit antennas in temporally-correlated channels.

T3.2 TeC 16 – Non-coherent communication in coordinated systems	
 <p>Users with coherent connections with a macro cell and non-coherent connections with a small cell.</p>	<p style="text-align: center;"><b>Main Idea</b></p> <p>This work investigates the use of non-coherent communication schemes, which perform data detection without any knowledge of the channel coefficients, to minimize the waste of resources due to the use of reference signals in pilot-based channel estimation.</p> <p>It evaluates non-coherent schemes over architectures where the users can be connected to multiple transmission points (TP) and may receive different kind of information from each TP. In addition, this TeC is evaluated in vehicular networks, where mobility has a deep impact on the performance. In both frameworks, the main goals are to explore the advantages of non-coherent communication under realistic scenarios and, also, to enable multi-user non-coherent communication.</p>
Considered SoA solution	LTE open-loop SFBC mode for 2x2 and 4x4 systems
KPIs considered and achieved gain	Relative velocity: 6-9 dB of link-level gain @300km/h in the 4x4 setup
Performance evaluation approach	Simulation-based (Link level)



System model considered	Other
Deviation compared to Simulation Baseline	Not Applicable. <ul style="list-style-type: none"> <li>• f=2.6GHz</li> <li>• Extended Vehicular A 3GPP channel model</li> <li>• 2x2 and 4x4 MIMO</li> <li>• Uncorrelated antennas</li> <li>• Different constellations evaluated</li> </ul>
Brief update of the results with respect to D3.2	The TeC has been now evaluated in a more realistic setup, with a fair overhead of pilots in the coherent baseline and over a practical vehicular channel model, to study the impact of mobility.
Association to the TeC Approach	This TeC is related to “CoMP with Advanced UE Capabilities” but it has not been selected due to the lack of mature performance results.
Targeted TCs	TC 12
Impacted HTs	MN
Required changes for the realization with respect to LTE Rel. 11	Minor. Non-coherent codebooks should be included within the LTE OFDM grid as in transmit diversity modes like SFBC.
Trade-off required to realize the gains	This TeC increases the complexity of the baseline LTE block (SFBC) due to the decoding of the Grassmannian codewords.

### 8.20.3 Impact on Horizontal Topics

T3.2 TeC 16 - HT.MN	
Technical challenges	<ul style="list-style-type: none"> <li>• Increase supported relative velocity.</li> </ul>
TeC solution	Non-coherent communication enables the communication without any channel state information at the receiver (CSIR), thus avoiding the effect of imperfect CSIR on the system performance.
Requirements for the solution	New signal processing capabilities at the TPs, multi-antenna UEs able to work with non-coherent signaling.
KPI addressed and Expected Gain	<ul style="list-style-type: none"> <li>• Relative velocity: 6-9 dB of link-level gain @300km/h in the 4x4 setup</li> </ul>
Interaction with other WPs	WP6: For system level evaluations

### 8.20.4 Addressing the METIS Goals

T3.2 TeC 16	
1000x data volume	
10-100 user data rate	Non-coherent communication can increase the user data rate by reducing the transmission of pilot signals and increasing the robustness to imperfect CSI.



10-100x number of devices	
10x longer battery life	
5x E-E reduced latency	
Energy efficiency and cost	

### 8.20.5 References

[METIS13-D31] METIS D3.1, "Positioning of multi-node/multi-antenna transmission technologies," Jun. 2013.

[METIS14-D32] METIS D3.2, "First performance results for multi-node/multi-antenna transmission technologies", Apr. 2014.

[RCC+14a] S. Roger, J. Cabrejas, D. Calabuig, J. F. Monserrat, Y. M. Fouad, R. H. Gohary, H. Yanikomeroglu "Non-coherent MIMO Communication for the 5th Generation Mobile: Overview and Practical Aspects", in Waves, vol. 6, 2014.

[RCC+14b] S Roger, D Calabuig, J Cabrejas, J. F. Monserrat, "Multi-user Non-coherent Detection for Downlink MIMO Communication", IEEE Signal Processing Letters, vol. 21, issue 10, pp. 1125-1229, Oct. 2014.

[LV04] Y. Liang and V. Veeravalli, "Capacity of noncoherent time-selective Rayleigh-fading channels," IEEE Trans. on Inf. Theory, vol. 50, no. 12, pp. 3095–3110, 2004.

[KRD+13] G. Koliander, E. Riegler, G. Durisi, V. I. Morgenshtern, and F. Hlawatsch, "A lower bound on the noncoherent capacity pre-log for the MIMO channel with temporally correlated fading," Feb. 2013, available at <http://arxiv.org/abs/1302.2481v1>.

## 8.21 T3.2 TeC 17: Bidirectional signalling for dynamic TDD [UOULU]

### 8.21.1 General Overview

Small cells with very short range can be used in addition to traditional macro/micro-cell coverage in order to satisfy the increase demand of mobile traffic. Time-division duplexing (TDD) systems are well suited to use with small cells since it can provide unbalanced data traffic in uplink (UL) and downlink (DL) by adjusting timeslots in each direction within the TDD frame. In small cell scenarios, the amount of instantaneous UL and DL traffic may vary significantly with time and among the adjacent cells. In such cases, Dynamic TDD allows for resources to be dynamically adapted between UL and DL. Therefore, Dynamic TDD provides vastly improved overall resource utilization. Main challenge in designing dynamic TDD system is handling new type of interference generated in the system. As shown in Figure 8-60, in addition to the normal UL-to-UL and DL-to-DL interference, there are two additional types of interference associated with dynamic TDD in multi-cell operation, UL-to-DL interference (user-to-user) and DL-to-UL interference (BS-to-BS). Numerous studies have been carried out in the literature that mostly considers time-slot allocation algorithms to minimize the cross-link interference in Dynamic TDD. In this research, we aim at jointly optimizing the allocation of resources (space, frequency and time, including the allocation to UL and DL) and coordinated precoder/beamformer (CB CoMP) design across the entire network to maximize various system performance measures.

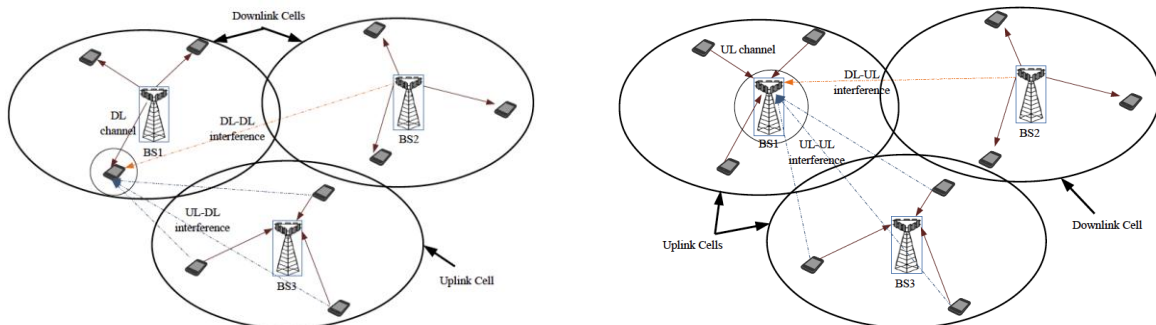


Figure 8-60: Interference types present at UL and DL in Dynamic TDD mode

We assume that each TDD frame is allocated either to UL or DL depending on the instantaneous traffic load of the cell, similarly to the METIS frame structure specified in [Figure 2-1, METIS14-D23]. For the given UL/DL allocation, we propose coordinated iterative algorithms to find precoders/decoders in entire network and proposed corresponding signaling concepts of effective CSI for weighted sum rate maximization [KTJ13]. WSR maximization is considered with per transmitter node power constraints. Furthermore, bi-directional signaling/training is performed for each TDD frame as illustrated in Figure 8-61 [SBH14, KTJ13]. Bi-directional signaling allows *iterative precoder/decoder optimization to be carried out independently* for each transmitted frame in a way that the optimized receivers from the previous backward/forward iteration are used as pilot precoders for the next forward/backward transmission. At the same time it can be *used to carry out implicit user selection* for each frame by letting the iterative algorithm to decide the optimal set of users/streams to be served at any given time instant. Finally, *backhaul information exchange is not anymore required to carry out the precoder coordination*. There is a clear trade-off between the throughput gains

achievable from the TX/RX iterations and the training overhead caused the bidirectional signaling. This training period should be large enough to come up with efficient precoder/decoders while short enough to guarantee sufficient resources for the actual data transmission.

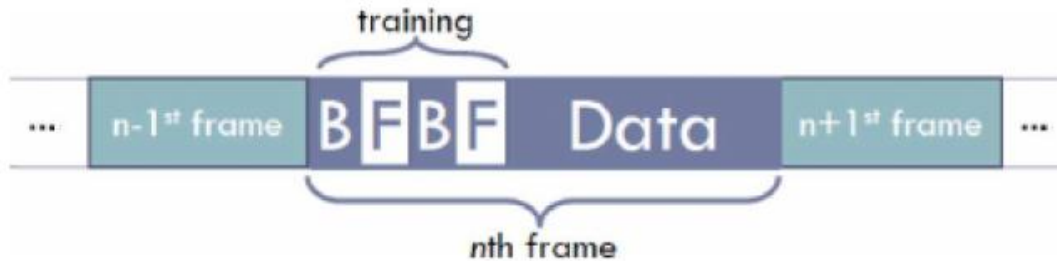


Figure 8-61: Sequence of TDD frames with bi-directional training [SBH14]

### System model

We consider a multi-cell multi-user MIMO system, operates in dynamic TDD mode with traffic aware user scheduling. Multicell network consist with  $B$  BSs and  $K$  users. BS  $i$  has  $M_i$  transmitting antennas and user  $k$  has  $N_k$  antennas. In a given time, subset of base stations  $B_U \subseteq B$  serves uplink traffic and rest of the base stations  $B_D \subseteq B$  are serves downlink traffic. This selection is based on the average traffic demand on the users within that particular base station.

Here, we used linear MMSE receivers in each users and BS to estimate received signal. Optimal transmit precoders are obtain by solving the below weighted sum rate maximization problem using (minimizing WMMSE approach) [SRL11, KTJ13],

$$\min - \sum_{i \in B_D} \sum_{k \in U_k} u_{i,k} \log \det \left( (\tilde{\mathbf{E}}_{i,k}^{DL})^{-1} \right) - \sum_{j \in B_U} \sum_{l \in U_j} u_{j,l} \log \det \left( (\tilde{\mathbf{E}}_{j,l}^{UL})^{-1} \right)$$

$$\text{subject to } \text{Tr}(\mathbf{B}_{i,k} \mathbf{B}_{i,k}^H) \leq P_i \quad \forall i \in B_D$$

$$\text{Tr}(\mathbf{F}_{j,l} \mathbf{F}_{j,l}^H) \leq P_{j,l}. \quad \forall l \in U_j, j \in B_U$$

where the variables are  $\mathbf{B}_{i,k}$  and  $\mathbf{F}_{j,l}$ , whereas  $\mathbf{E}_{i,k}^{DL}$  and  $\mathbf{E}_{j,l}^{UL}$  are their corresponding MMSE matrices [SRL11, KTJ13]. However, this optimization problem is non-convex NP hard problem. Therefore, we reformulate this problem [SRL11, KTJ13] and solve it iteratively by fixing some of the optimization variables until weighted sum rate is converging.

#### 8.21.2 Performance Results

The numerical analysis is carried out for two and three cell scenarios with 4 users in each cell. The power constraint for the DL transmission is fixed to  $P_i=10$  dB and for the UL user power transmission  $P_{j,l}=4$  (UL transmit power constraint is selected such that the maximum sum power of the UL users is equal to the power constraint of the DL BS). All the priority weights are assumed to be 1. The number of antennas at each BS is  $M_i = 4$  and the number of antennas at each user terminal is  $N_k = 2$ . The simulation environment is defined by three types of terminal separations as shown in Figure 8-62. The path loss between the two DL cell edge

users is  $\alpha$ , UL user to DL user  $\beta$  and UL BS to DL BS  $\delta$ . Also, the path loss from a BS to in-cell users is normalized to be 0 dB.

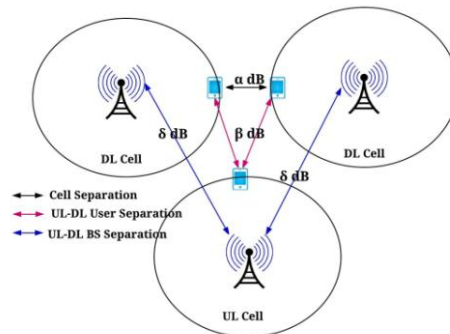


**Figure 8-62: Simulation model**

The actual sum rate for transmit SNRs 10 dB and 20 dB, versus the total overhead for two cell DL only case is shown in Figure 8-63. One BIT iteration is assumed to take two OFDM symbols. Thus,  $\gamma = 0.01$  and  $\gamma = 0.02$  correspond to frame lengths 200 and 100, respectively. Also, uncoordinated beamformer design is considered as the reference case (beamformers calculated locally without considering the inter-cell interference). Algorithm from [KTJ13, Algorithm 3] with the bi-directional signaling can be seen to obtain the peak data rate with less than 10% and 15% overhead for the frame length  $\gamma = 0.01$  and  $\gamma = 0.02$ , respectively. Now, the total signaling overhead is  $\rho = \text{BIT} \times \gamma$ . Thus, the actual achievable WSR can be obtained as  $(1-\rho)R$ , where  $R$  is the achieved WSR from [KTJ13, Algorithm 3].

The actual sum rate improves significantly compared to the uncoordinated system when cell separation is equal to  $\alpha=0$  dB, and it provides considerable performance gain even for larger signaling overhead. However, for the low inter-cell interference scenarios (lower transmit SNR with larger cell separation), the uncoordinated system starts to outperform the proposed beamformer design.

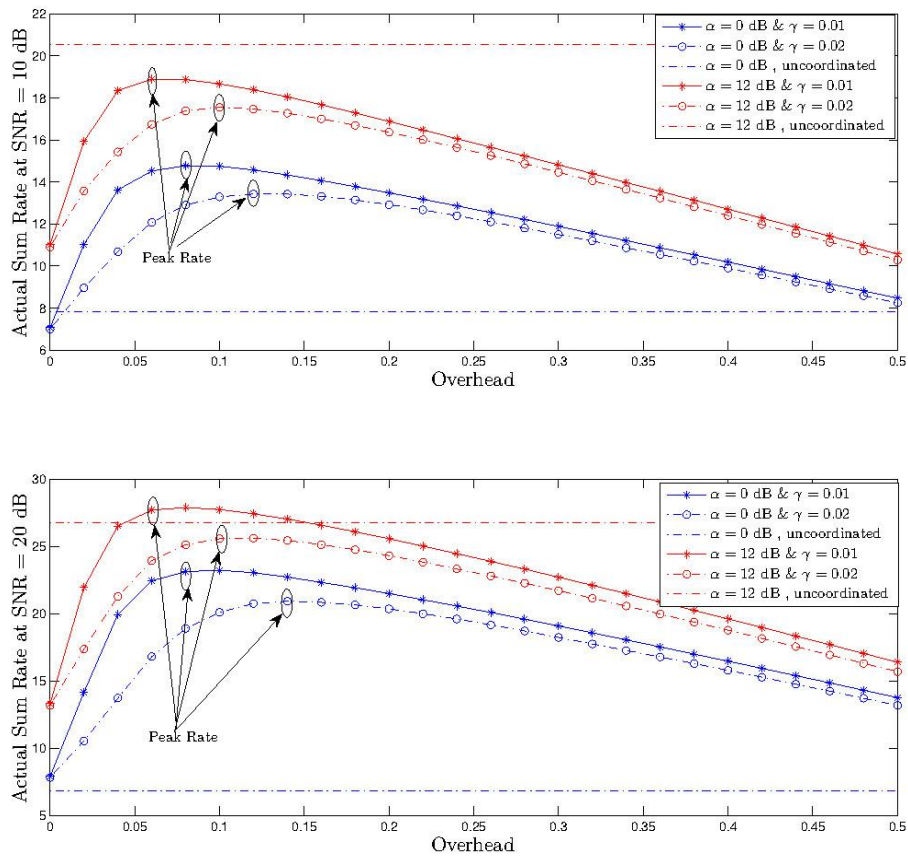


**Figure 8-63: Actual Sum rate vs bidirectional signalling overhead with different SNR (10, 20 dB) values**

Figure 8-64 demonstrates the actual sum rate versus the total overhead of the three cell network with two DL BSs and one UL BS. We consider the TDD frame length 200 ( $\gamma=0.01$ ), and different  $\alpha$ ,  $\beta$  and  $\delta$  values. Similarly to Figure 8-63, the actual sum rate improves significantly for lower  $\alpha$ ,  $\beta$  and  $\delta$  values compared to the uncoordinated system. The peak rate is obtained with less than 12% overhead for all the scenarios and the sum rate improves even with 30% signaling overhead. Therefore, the proposed algorithm performs very well when complex interference conditions are present. Figure 8-65 illustrates the average sum rate of the system versus the transmit SNR with similar BS allocation as Figure 8-64. We vary  $\beta$  (3, 6, 9, 12 dB), while  $\alpha$  and  $\delta$  are fixed, to observe the impact of the UL user transmission on the sum rate. For lower  $\beta$  and high transmit SNR, UL users dominate the sum rate. This is due to the high UL-to-DL interference, which degrades the DL user SINR. However, for large  $\beta$  DL user dominates due to less UL-to-DL interference.

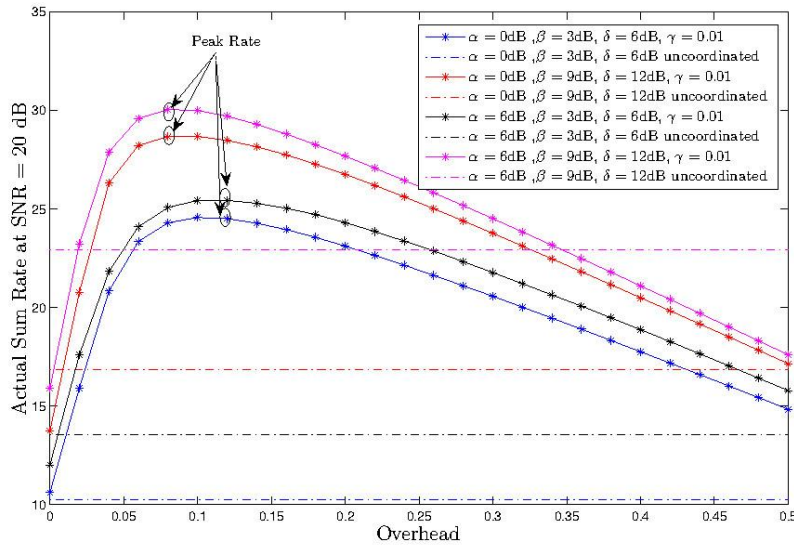


Figure 8-64: Actual sum rate vs overhead at SNR = 20 dB, with different  $\alpha$ ,  $\beta$  and  $\gamma$

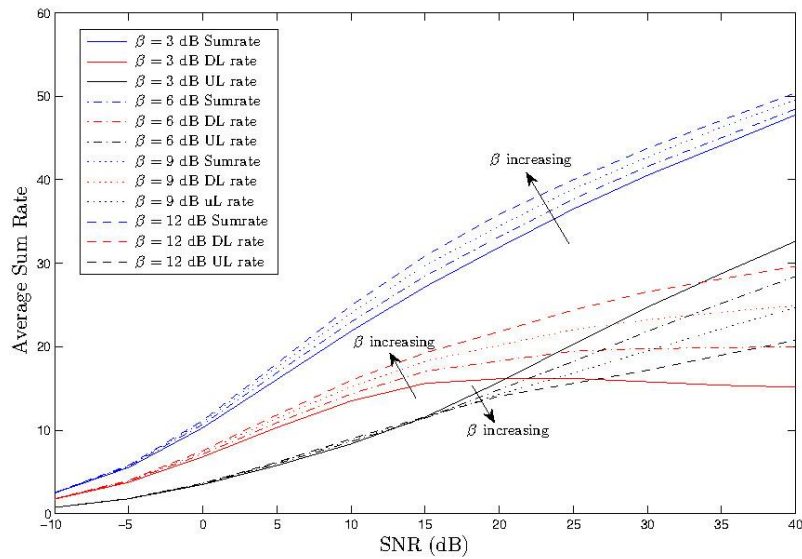
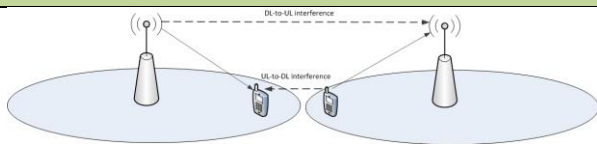


Figure 8-65: Average sum rate vs SNR for different  $\beta$  values

### T3.2 TeC 17 - Bidirectional Signalling for Dynamic TDD



A coordinated iterative beamforming algorithm is considered with bi-directional training.

#### Main Idea

Coordinated algorithm to optimize weighted sum rate of dynamic TDD based multicell multiuser MIMO system.

Bi-directional signaling/training is performed for each TDD which allows iterative precoder/decoder optimization to be carried out independently for each transmitted frame. The optimized receivers from the previous backward/forward iteration are used as pilot precoders for the next forward/backward



	transmission. At the same time it can be used to carry out implicit user selection for each frame by letting the iterative algorithm to decide the optimal set of users/streams to be served at any given time instant.
Considered SoA solution	N/A
KPIs considered and achieved gain	Throughput (both system and user level). Increased rate especially for the cell edge users without any backhaul information exchange. Gains from 35% to 75% in spectral efficiency have been shown for cell edge users, without the need to deploy high performance backhauling in the network.
Performance evaluation approach	Analytical and Simulation-based
System model considered	Multi-cell, multiple users with interferences considered in block fading.
Deviation compared to Simulation Baseline	Minor: <ul style="list-style-type: none"> <li>• Model of environment: N/A (Per user channel model)</li> <li>• Spectrum Assumptions:</li> <li>• Propagation model: N/A (Per user channel model)</li> <li>• Deployment model: multi cell</li> <li>• User/Device Distribution: 4 users in each cell</li> <li>• Traffic model: No traffic model</li> </ul>
Brief update of the results with respect to D3.2	N/A
Association to the TeC Approach	CoMP with limited backhaul capabilities
Targeted TCs	TC 1,2 and 4: Specific Challenge: Reduce energy consumption, backhaul signalling and cost of infrastructure and UEs. Increase availability and reliability.
Impacted HTs	UDN
Required changes for the realization with respect to LTE Rel. 11	Major, new frame structure is required. METIS frame structure proposed in [METIS14-D23] can be adopted. Precoded uplink pilots are also required.
Trade-off required to realize the gains	Bi-directional training requires over-the-air iterations using alternating (precoded) pilot transmissions during the training phase of the data frame.

### 8.21.3 Impact on Horizontal Topics

T3.2 TeC 17 - HT.UDN	
Technical challenges	Coordination in multiple user environment, assignment of sufficient pilot resources, impact of CSI uncertainty
TeC solution	Bi-directional training to allow the implementation of iterative TX-RX algorithms without any backhaul information exchange
Requirements for the solution	New frame structure, similar to the METIS



	structure in [METIS14-D23]
KPIs addressed and achieved gain	Throughput (both system and user level). Increased rate especially for the cell edge users without any backhaul information exchange
Interaction with other WPs	WP4: The proposed scheme targets interference limited-scenarios and a close alignment is needed with WP4 where interference management is an important topic.

### 8.21.4 Addressing the METIS Goals

T3.2 TeC 17	
1000x data volume	Large beamforming and interference reduction gains are available to improve the user rates accordingly, coordinated interference control benefits especially the cell edge users
10-100 user data rate	Large gains are available to improve the user rates, interference control benefits especially the cell edge users
10-100x number of devices	By increasing the number of antennas at the BS by X may increase the number of devices by the same factor.
10x longer battery life	
5x E-E reduced latency	
Energy efficiency and cost	The WSRmax objective can be modified to take into account the the energy efficiency aspects as well. For example, the power allocation among pilot and data resources can be varied to optimize the some energy efficiency specific network utility

### 8.21.5 References

[SKE12] Zukang Shen; Khoryaev, A; Eriksson, E.; Xueming Pan, "Dynamic uplink-downlink configuration and interference management in TD-LTE," *Communications Magazine*, IEEE , vol.50, no.11, pp.51,59, November 2012.

[SBC09] Illsoo Sohn, Kwang Bok Lee, and Young Choi, "Comparison of decentralized time slot allocation strategies for asymmetric traffic in tdd systems," *Wireless Communications*, IEEE Transactions on, vol. 8, no. 6, pp. 2990–3003, 2009.

[SBH14] Changxin Shi; Berry, R.A; Honig, M.L., "Bi-Directional Training for Adaptive Beamforming and Power Control in Interference Networks," *Signal Processing*, IEEE Transactions on , vol.62, no.3, pp.607,618, Feb.1, 2014.

[KTJ13] Komulainen, Petri, Antti Tolli, and Markku Juntti. "Effective CSI signaling and decentralized beam coordination in TDD multi-cell MIMO systems," *Signal Processing, IEEE Transactions on* 61.9 (2013): 2204-2218.

[SRL11] Qingjiang Shi; Razaviyayn, M.; Zhi-Quan Luo; Chen He, "An Iteratively Weighted MMSE Approach to Distributed Sum-Utility Maximization for a MIMO Interfering Broadcast Channel," *Signal Processing*, IEEE Transactions on , vol.59, no.9, pp.4331,4340, Sept. 2011.

[METIS14-D23] METIS D2.3, "Components of a new air interface - building blocks and performance", Apr. 2014.

## 9 Appendix C: Final results for Task 3.3

### 9.1 T3.3 TeC 1: Coordinated multi-flow transmission for wireless backhaul [AAU]

#### 9.1.1 General Overview

One of the core features in 5G, also pursued within METIS, is the deployment of Ultra Dense Networks (UDN). The main ingredient of such deployment is the backhaul. Considering the high cost and inflexibility of wired backhaul deployments, wireless backhaul solutions appear as key enablers of network densification. This is evident in applications where the nodes are nomadic, such as the case with a car acting as a relay [RSF+14].

A wireless backhaul that operates in the same band as the terminal accessing the local access point is an in-band relay, such that we will use the term Relay Station (RS) to mean access point. The systematic use of RSs as architectural elements has not lifted off in the past year. The reason is that wireless transceivers commonly work in a half-duplex mode, such that one-way relaying suffers from a loss in spectral efficiency as RS cannot transmit and receive at the same time. This loss has been mitigated with the introduction of two-way relaying based on wireless network coding (WNC) [PY06a], [ZLL06], and [PY07a]. Various aspects of two-way relaying have been investigated, such as achievable rates [KDM+11]. Paper [WOB+08] extends the optimal broadcasting into multiple-input multiple-output (MIMO) case.

Consider the wired backhaul scenario as shown in Figure 9-1(a). Here the MSs are connected wirelessly to their respective SBSs, while each SBS has a wired connection to the BS. The transmissions are shown in Figure 9-1(b), where the exchange of information takes place over two phases, the Downlink and Uplink phase.

The wireless backhaul scenario, which is the one proposed in this TeC, is depicted in Figure 9-2(a). The wireless channels between each MS and its serving SBS are assumed identical to those in the wired case. The channels between SBS and BS are now wireless, as shown in the figure. The uplink  $R_U$  and downlink  $R_D$  rates are assumed the same as in the wired case. In Figure 9-2(b), the exchange of information also takes place over two phases, but now, the principle of WNC is used. This is possible because in Phase 1,  $MS_i$  and BS transmit to  $SBS_i$ , while in Phase 2,  $SBS_i$  decodes the received signals, and broadcasts the XOR of those signals. The BS and  $MS_i$  can then decode the XOR-ed signal, to obtain the desired signal. The scheme is designed under the assumption that the  $MS_i$  should not undergo any change in the PHY/baseband - it only needs to XOR the received packet with its previously sent packet.

There are two important aspects of the wireless emulated wire (WEW) scheme: First, the BS partitions the downlink data for each MS into two parts, a private and a common part. These three possible options are shown in Figure 9-3. In Figure 9-3(a), the BS transmits the data to the SBS using only spatial ZF. Because each SBS receives only its own data, we refer to this as private data. In Figure 9-3(b), the BS concatenates the data for both MSs, and transmits them using a common beamformer. The WEW scheme is shown in Figure 9-3(c). It is a hybrid between the former two, and we find the optimal partitioning of the data into a private and common part.

The private part for each MS is sent using spatial ZF, so that each SBS can only decode the message intended for it. The common parts for both MSs are concatenated, before being transmitted to both SBSs.

Second, because we want the operation of the scheme to be transparent to the MS, we assume that the MS transmits a rate equal to the capacity of the MS-SBS link. Then, in Phase 1, the SBS receives three signals, the private and common data (which is the downlink data), and the uplink data from the MS. The SBS first decodes the private and common data, while treating the MS's uplink data as noise. After this decoding is done, the SBS decodes the uplink data, without any residual interference from the downlink data.

We find the optimal transmission power at the BS, the optimal beamformer for the common parts of the data. This is detailed in the next section.

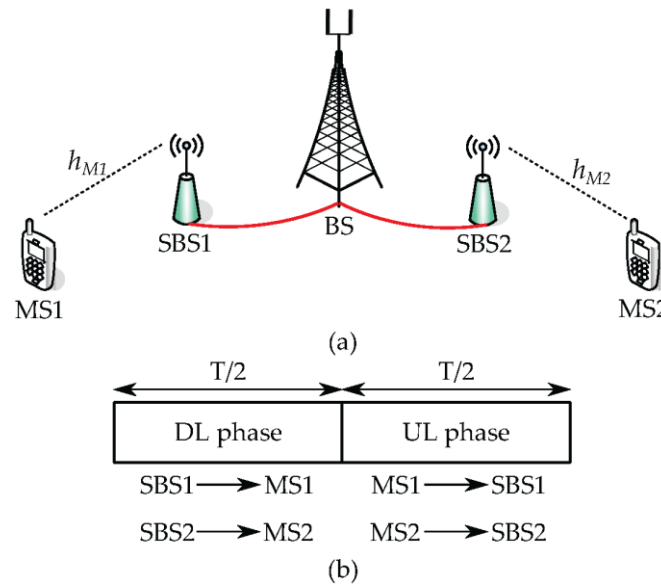


Figure 9-1: System Model for the Wired backhaul (a) and transmissions occurring in the two phases (b)

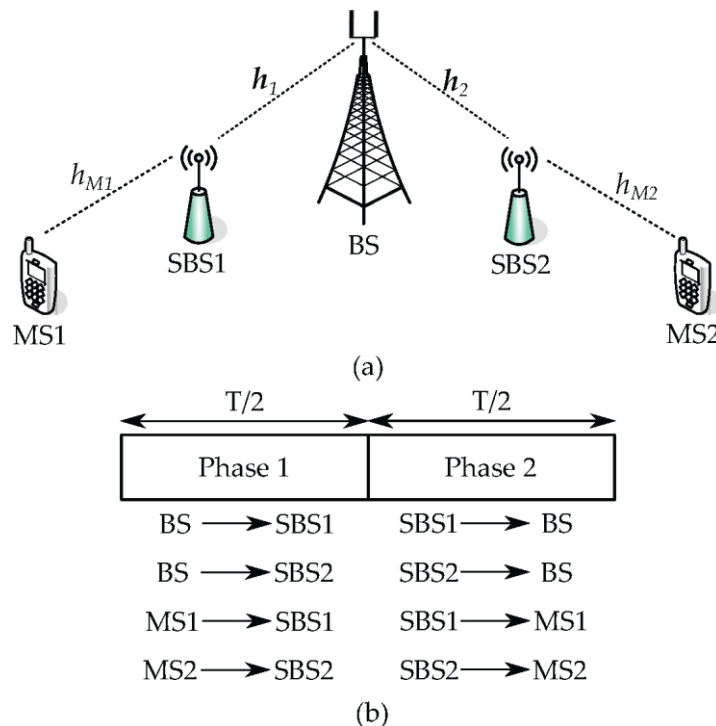


Figure 9-2: System Model for the Wireless backhaul (a) and transmissions occurring in the two phases (b)

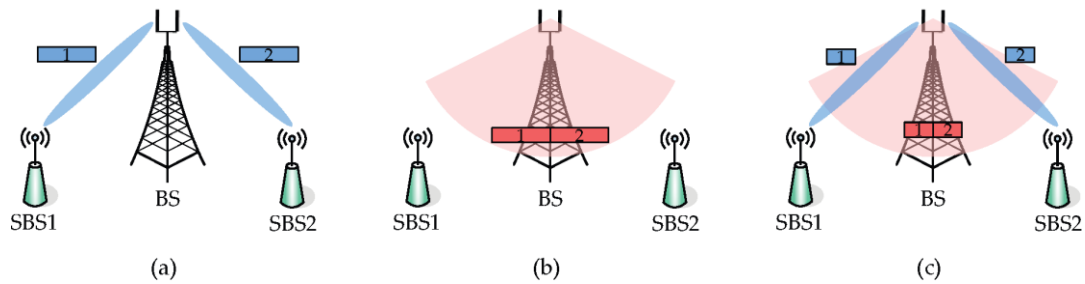


Figure 9-3: The three transmission methods considered in the wireless backhaul solution

### 9.1.2 Performance Results

The simulation baseline considered is the WP3 Task 3.3 simulation baseline, consisting of nine square buildings arranged in a square grid. The buildings are separated by streets. The details of this scenario can be found in [METIS D3.2, Sec. 8.3]. In the model, there are three macro BSs, and nine micro BSs. The deployment of nodes is shown in Figure 9-4. In our simulations, we select one micro BS as the transmitting BS in the WEW scheme. The other micro is set to not transmit. The remaining micro and the three macros are interferers in our scheme. All nodes use the same transmission frequency of 2.6 GHz. The transmission power of the interferers are 42 dBm for Macro and 37 dBm for the micro BSs. Background noise power is set at -95 dBm. In the simulations, we only considered the optimization of the first phase, so we have not dealt with the transmission power of the relay.

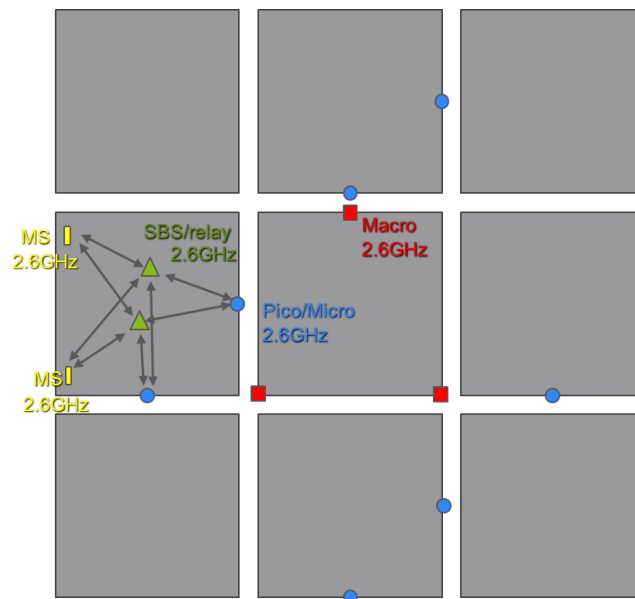


Figure 9-4: Deployment of the nodes in the considered simulation scenario

In the indicated building in Figure 9-4, on floor 3, we deploy two SBSs. The MSs are deployed randomly on the same floor, in the same building. The simulations include path loss of relevant links (both from desired and undesired transmitters), as well as small-scale fading. The pathloss and small scale fading is obtained from the Matlab scripts provided by [M13]. The results are averaged over a sufficient number of fading realizations, and are given in terms of minimal transmission power required by the BS to satisfy the MSs' uplink and downlink rate requirements.

The optimization problem is solved using the software CVX [GB-CVX], where the pathloss, rates and small scale fading are given as parameters. Relevant channel coefficients were obtained from the aforementioned Matlab scripts. The formulation of the optimization problem is given below:

$$\begin{aligned}
 & \min P_1 + P_2 + |\mathbf{w}_C|^2 \\
 & \text{s. t. } R_{Pi} \leq C \left( \frac{\gamma_{Pi}}{1 + \gamma_{Ui} + \frac{I}{\sigma^2}} \right) \\
 & R_C \leq C \left( \frac{\gamma_{Ci}}{1 + \gamma_{Ui} + \frac{I}{\sigma^2}} \right) \\
 & R_{Pi} + R_C \leq C \left( \frac{\gamma_{Pi} + \gamma_{Ci}}{1 + \gamma_{Ui} + \frac{I}{\sigma^2}} \right)
 \end{aligned}$$

Here, the rate of the downlink packet to SBS $i$  is  $R_i = R_{Pi} + R_{Ci}$ , where  $R_{Pi} = \alpha_i R_{Di}$  and  $R_{Ci} = (1 - \alpha_i) R_{Di}$ .  $R_{Di}$  is the rate of the downlink packet sent to SBS $i$ , and  $0 \leq \alpha_i \leq 1$  is the splitting factor of the packet.

The optimization variables are the transmission powers  $P_1, P_2$  for the ZF beamformers, and  $|\mathbf{w}_C|^2$  for the common beamformer, and the splitting factors  $\alpha_1, \alpha_2$ . The constraints mean that each SBS $i$  must decode the entire private packet at rate  $R_{Pi}$ , and the entire concatenated packet at rate  $R_C = R_{C1} + R_{C2}$ . The right hand side of the inequalities are the capacities

$C(x) = \log(1 + x)$ . The SNR of the private packet is  $\gamma_{Pi} = \frac{P_i L(d_i) |\mathbf{h}_i^H \mathbf{w}_i|^2}{\sigma^2}$ , where  $d_i$  is the Euclidean distance between transmitting and receiving node and  $L(d_i)$  is the path-loss function, while the SNR of the common packet is  $\gamma_{Ci} = \frac{|\mathbf{h}_i^H \mathbf{w}_C|^2}{\sigma^2}$ . Here  $\mathbf{w}_i$  is the ZF beamformer, while  $\mathbf{w}_C$  is the common beamformer. Recalling that the SBS $i$  needs to decode the downlink signals while treating the uplink signal as noise, we divide by the equivalent SNR  $\gamma_{Ui}$  of the MS $i$ -SBS $i$  link. The last term  $I$  in the denominators is the aggregated interference from all interfering nodes in the scenario.

In Figure 9-5, we show the results of the simulations, wherein we compare WEW with three other methods: The first is when BS transmits using only spatial ZF, the second one when using only the common beam approach, while the third is when we select the partitioning of the data randomly for each MS. The uplink rates of the MSs are fixed, while the downlink rates vary over the interval shown on the x-axis. The y-axis shows the total transmission power required at the base station, in order to fulfill the given constraints. This transmission power is found using convex optimization. It is observed that the performance of ZF is generally the worst, however the gap in performance between ZF and common beam decreases as the downlink rate requirement (related to the size of the packet) increases. Because high rate requirements translate into high SINR requirements, this is related to the fact that ZF has an advantage at higher SINRs. We also see that the method using the common beam is quite good at low rates (equals small packets), but is not so good at high rates. Recalling that in the Common-only scheme the receivers need to decode the entire concatenated packet, this gives a rather large overhead for the large rates. Furthermore, the optimization of the splitting factors gives an advantage, compared to choosing them at random. This also justifies the optimization of the splitting factors. The WEW scheme is the best of the schemes in terms of transmission power.

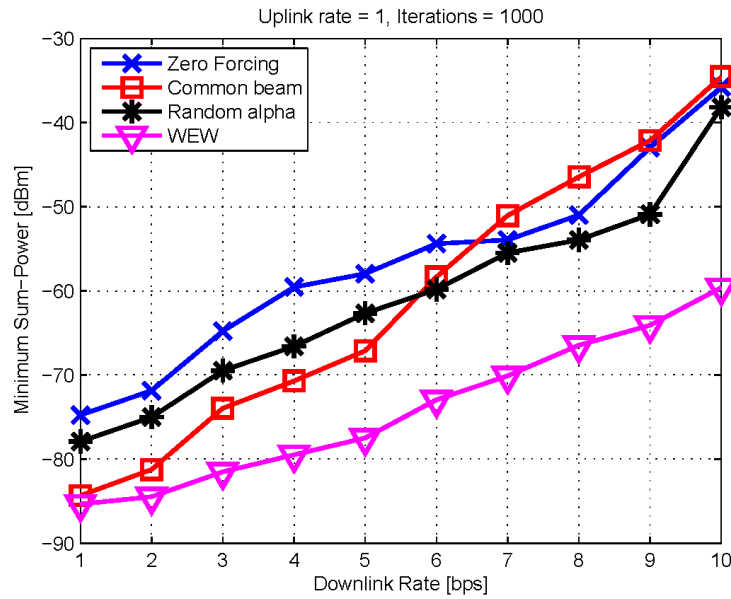
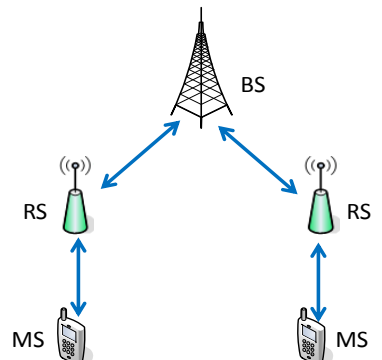


Figure 9-5: Comparison of our proposed method

T3.3 TeC 1 – Coordinated multi-flow transmission for wireless backhaul	
 <p>Antipodal relays, not interfering with each other. One terminal is connected to one relay and has a two-way traffic with the BS.</p>	<p style="text-align: center;"><b>Main Idea</b></p> <p><math>2N</math> flows, <math>N</math> downlink and <math>N</math> uplink, for <math>N</math> relayed users, are served jointly through two transmission phases. In the first phase, the BS broadcasts signals for all terminals to their relays, while each terminal transmits to its relay. The downlink signals for each terminal are partitioned into two parts, a private and public part. In the second phase, each relay broadcasts to its terminal and the BS. Side information at the BS and terminals is used. By coupling all flows, the total service time is decreased or, equivalently, the data rates of all nodes are increased.</p>
Considered SoA solution	Comparing with a small-cell scenario, based on TDD transmission.
KPIs considered and achieved gain	Spectral Efficiency: Achieved gain 100%
Performance evaluation approach	Simulation-based: Link-level evaluation
System model considered	WP3 Task 3.3 Simulation Baseline
Deviation compared to Simulation Baseline	Minor: <ul style="list-style-type: none"> <li>User/Device Distribution: SBSs deployed deterministically and MSs deployed uniformly at</li> </ul>



	<p>random on one floor in one building</p> <ul style="list-style-type: none"> <li>Traffic Model: Full Buffer</li> </ul>
Brief update of the results with respect to D3.2	Simulation results using the Madrid scenario of WP3.
Association to the TeC Approach	Proposed for the Approach: Heterogeneous network at lower frequencies (< 10GHz)
Targeted TCs	<p>UDN:</p> <ul style="list-style-type: none"> <li>TC2, TC4, TC9</li> </ul> <p>MN:</p> <ul style="list-style-type: none"> <li>TC6, TC7</li> </ul>
Impacted HTs	ARCH, UDN, MN
Required changes for the realization with respect to LTE Rel. 11	No changes at the physical layer at the terminal, minor changes at the link layer protocol.
Trade-off required to realize the gains	Requires full CSI and (maybe) additional transmission power at SBSs and BS. The CSI acquisition is assumed to be perfect, and takes place before the exchange of data.

### 9.1.3 Impact on Horizontal Topics

T3.3 TeC 1 - HT.UDN	
Technical challenges	<ul style="list-style-type: none"> <li>Replacing the wired backhaul by a wireless one, while providing equivalent performance for the MSs.</li> <li>Keeping the transmission powers at BS and SBS within reasonable levels.</li> </ul>
TeC solution	Jointly solve the two-way (uplink + downlink) problem instead of treating it as sequence of one-way problems. Use the ideas of wireless network coding to jointly serve multiple communications flows.
Requirements for the solution	<ul style="list-style-type: none"> <li>Channel and Interference information at the nodes.</li> <li>SBS must be able to distinguish between received signals, since the uplink signal is to be decoded last.</li> </ul>
KPIs addressed and achieved gain	<ul style="list-style-type: none"> <li>Spectral Efficiency: 100 %.</li> </ul>
Interaction with other WPs	<ul style="list-style-type: none"> <li>WP6: System Level evaluations.</li> </ul>

### 9.1.4 Addressing the METIS Goals

T3.3 TeC 1	
1000x data volume	
10-100 user data rate	The user data rate can be increased, by using SBSs to serve the users.



10-100x number of devices	Increase the number of devices that can be served, by enabling a larger number of SBSs to be deployed using wireless backhaul.
10x longer battery life	
5x E-E reduced latency	
Energy efficiency and cost	

### 9.1.5 References

[GB-CVX] M. Grant and S. Boyd, "CVX: Matlab software for disciplined convex programming," available at <http://cvxr.com/cvx/>.

[KDM+11] S. J. Kim, N. Devroye, P. Mitran, and V. Tarokh, "Achievable rate regions and performance comparison of half duplex bi-directional relaying protocols," IEEE Transactions on Information Theory, vol. 57, no. 10, pp. 6405 –6418, Oct. 2011.

[M13] METIS test cases following the simulation guidelines, <https://www.metis2020.com/documents/simulations/>.

[METIS D3.2] Metis Deliverable D3.2

[PY06a] P. Popovski and H. Yomo, "Bi-directional amplification of throughput in a wireless multi-hop network," in Veh. Tech. Conf. 2006. VTC 2006-Spring. IEEE 63rd, vol. 2, May. 2006, pp. 588 –593.

[PY07a] P. Popovski and H. Yomo, "Physical Network Coding in Two-Way Wireless Relay Channels", IEEE International Conference on Communication (ICC 2007), Glasgow, Scotland, June, 2007.

[RSF+14] Z. Ren, S. Stanczak, P. Fertl, and F. Penna, "Energy-aware activation of nomadic relays for performance enhancement in cellular networks," in International Conference on Communications (ICC), IEEE, 2014.

[WOB+08] R. Wyrembelski, T. Oechtering, I. Bjelakovic, C. Schnurr, and H. Boche, "Capacity of Gaussian mimo bidirectional broadcast channels," IEEE International Symposium on Information Theory, 2008 , Jul. 2008, pp. 584 –588.

[ZLL06] S. Zhang, S. chang Liew, and P. P. Lam, "Physical-layer network coding," in ACM Mobicom 06, 2006.

## 9.2 T3.3 TeC 2: Interference aware routing and resource allocation in a millimetre-wave ultra-dense network [EAB]

### 9.2.1 General Overview

A medium term resource management scheme for laying out multi-hop wireless routes and allocate resources is considered in this TeC [HA13, METIS-D32]. The resources are taken from a resource pool that is assumed to have been provided by a longer term inter-UDN coordinator (see TeC 09 and TeC 12 of WP5 [METIS-D53]). Several simultaneous flows associated with active users communicating through a local UDN comprising many wireless access nodes and a limited number of wired aggregation nodes, are managed. The flows are assumed having full buffer traffic in one direction, the other direction, or both of them. The resulting routes and allocations are then to be handed off (potentially after some further classification e.g. based on inter route interference) to a faster MAC based RRM operating on individual hops to harvest statistical multiplexing gains when the flows deviate from the full buffer assumption (see TeCC#12.3 in [METIS-D23, Section 2.12.3]).

The routing scheme operates by using an expected throughput metric taking interference of previous laid out routes and hops into account and trading a tuneable fraction of the metric for latency (number of hops). Subsequently routes are alternately widened in frequency and/or time based on their performance relative to what they would achieve if they comprised a sole flow in the UDN. By prioritizing the flow with the worst relative performance, degrees of fairness can be achieved without wasting excessive amount of resources on users that will anyway suffer due to poor channel gain. For more details on the proposed routing/resource allocation scheme we refer to [METIS14-D32].

### 9.2.2 Performance Results

In this TeC the scenario differ substantially from the simulation baseline in Section 8.3 of [METIS-D32] which is a selected subset of TC2 operating at 2.6GHz. Instead, current evaluations adhere closely to the simulation scenario of the cubicle office environment of TC1: Virtual reality office described in [METIS-D61] Section 4.1 and Appendix 9.1 (note the typo that the values in the first column of [METIS-D61] table 9.2 represent permittivity,  $k$ , and the second the conductivity,  $n$ , and not the other way around as listed). Further there is a scaling discrepancy in the x-y dimension as compared to Figure 9.1. The simulated room is 12m x 25m (see Figure 9-6). This scaling also holds for the path-loss maps provided by WP6 after [METIS-D61] release for this scenario on the METIS site [M13].

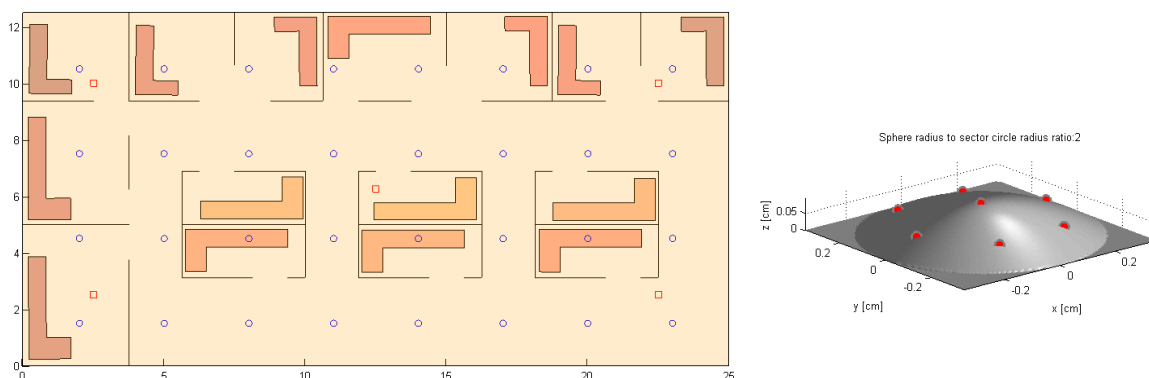


**Figure 9-6: Left: Top view of TC1 layout used. Red squares: AN locations, Blue circles: UE drop positions. Right: AN antenna layout (flip vertically for a ceiling mounted antenna)**

In this TeC we are challenged by the TC1 KPIs of extremely dense traffic demand per subscriber, average data rate during busy hour, as well as traffic volume per area. The assumption is that this cannot be solved easily without wide spectrum which, in agreement with WP5 conclusions, is with the least difficulty believed to be made available in the mmW

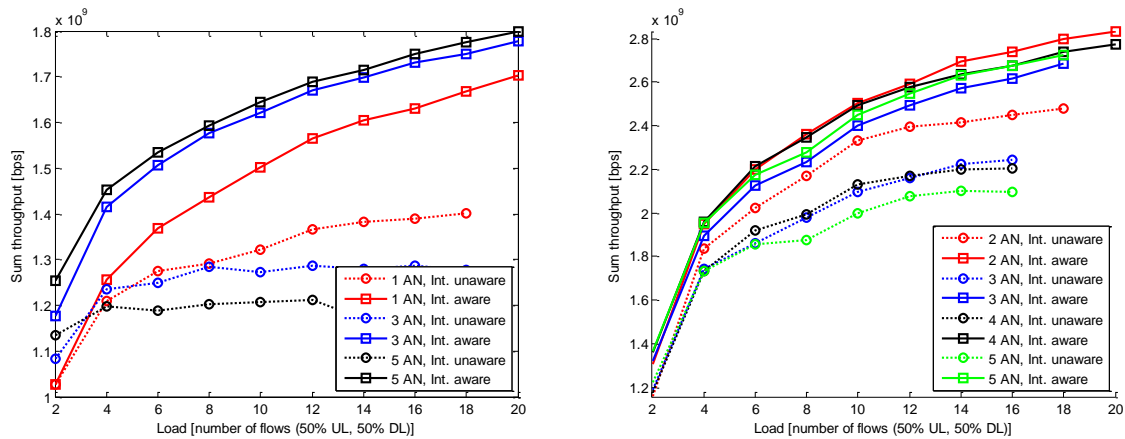
region (we are assuming 60GHz in our evaluations). Propagation aspects of mmWs as well as spatial reuse of extreme densification then eventually lead to needs of enablers of the kind this TeC is providing. So to summarize, the purpose of this TeC is to enable mmW in TC1-like traffic demand scenarios. The shorter dm-wave region TC2 scenario is simply too far from the intended usage. One could perhaps argue that the TeC could have a place in self organizing wireless in-band backhauling also in outdoor densification from Macro at traditional cellular frequencies, but there typically more of manual configuration and out-band backhauling is already an effective alternative (e.g. mmW wireless backhaul for LTE in today's deployments).

In Figure 9-7 we provide simplified system level results assuming full buffer traffic. Some parameters for the simulation setup are listed in Table 9.1.

**Table 9.1: Simulation Parameters**

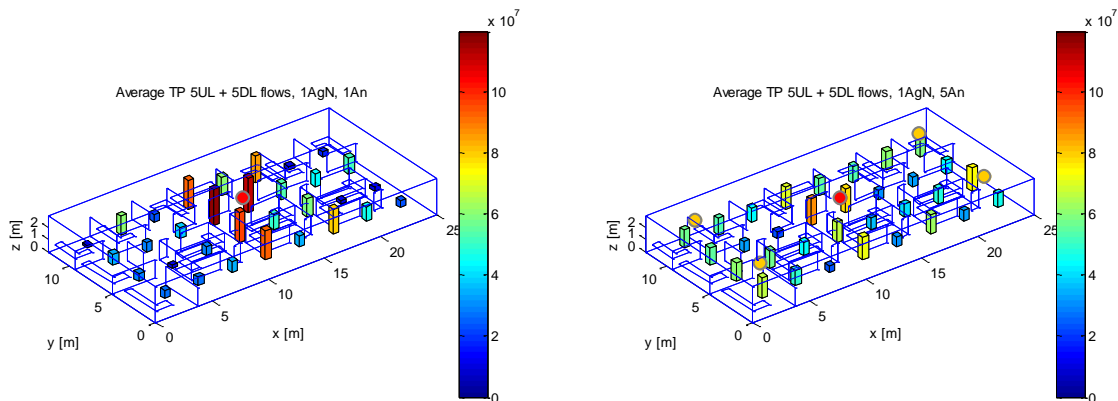
Parameter	Value
Environment	TC1 from [METISD61] (see Figure 9-6, left)
Access Nodes	1-2 wired (AgNs), 0-4 wireless
Access Node Antennas	7 omni element ceiling mounted spherical cap $\sim \lambda/2$ (see Figure 9-6, right), $z=2.85m$
UE Antennas	2 omni element, $\lambda/2$ , random orientation, $z = 0.75m$
Bandwidth	184.32 MHz (0.2GHz), For simulation complexity reasons downscaled a factor of 10 from assumed 2GHz
Carrier Frequency	60GHz
Multiple Access	FDM+TDM, OFDMA, 16 Symbols per subframe, CP=174ns
Subcarrier bandwidth	720KHz
Subframe duration	25us
RX noise figure	6dB
Power control	Full power, 13dBm for AN and 10dBm for UEs
Max number of reflections in channel ray-tracing	2
Reflection loss	5.6dB
Penetration loss	infinite
Stochastic fading power ratio	11.2dB below ray-traced channel component
Routing resources	16 frequency slots, 2 time-slots, per subframe
Receiver	MRC
Precoding	Long term Eigen-precoding.

The left plot of Figure 9-7 illustrates system throughput performance at various loads for the case of a single wired access node (the Aggregation Node, AgN) with zero, two or four additional wireless access nodes (WL ANs). The central red square of Figure 9-6 illustrates the ceiling located wired AgN providing the connection to/from the core network. With an interference unaware version of the TeC (dotted lines), adding wirelessly backhauled access nodes lowers system performance unless load is very low. With interference aware routing, the cost to users close to the AgN of sharing the access medium with wireless backhaul (WLBH) for WL AN is more than compensated for by the higher data rate coverage for users further away from the Wired AgN. The reason for the difference between interference aware and unaware routing also for a single AN (the AgN) is that spatially multiplexed users in UL do not see the MU-MIMO inter-user interference and are hence co-scheduled irrespective of how well they can be spatially separated by the RX beamforming. Simultaneous UL/DL interference is still avoided by the restriction of not having simultaneous UL and DL in any node that typically would lead to RX saturation.



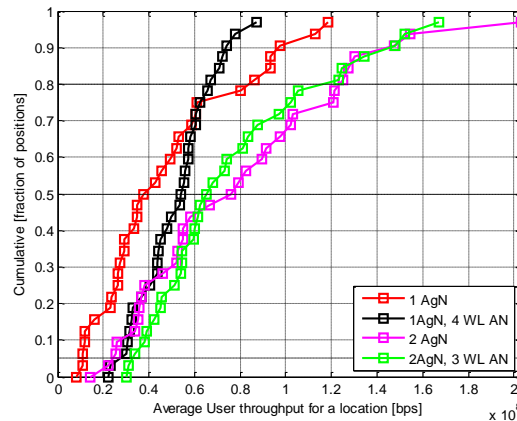
**Figure 9-7: System throughput versus load with increasing number of wireless access nodes for single (left plot) or two (right plot) wired aggregation nodes**

Figure 9-8 illustrates the spatial distribution of average user throughput for the load point of 10 concurrent flows (corresponding to middle x-axis of Figure 9-7, left). Left plot of Figure 9-8 is for zero WL ANs and right plot is with 4 WL AN in addition to the AgN. From these plots it is evident that the UDN performance is experiencing an improved fairness at the same time as the system average performance is improved when the WL ANs are added. It can also be observed that interference between access and backhaul is significantly reducing individual performance for the central users.



**Figure 9-8: Average user throughput (coloured stems) as function of user location for load point 10 in left plot of Figure 9-7, left: Wired AgN (red circle) acting as only access point (red solid line in Figure 9-7) and right: Wired AgN (red circle) assisted by 4 WL AN (orange circles) (black solid line in Figure 9-7)**

If we turn to the right plot of Figure 9-7, system performance is illustrated when the lower left and upper right AN's of Figure 9-6(left) are serving as 2 wired AgNs and the effect of adding one WL AN in the middle, two WLANs in the other corners or all three of them. The fact that there are now two connections to the Core Network significantly increases the general throughput level. The limited directivity of the antennas (aperture of 1/3 wavelength in one random orientation at the UE side and approximately 1/2 and 1.5 wavelengths in elevation and azimuth respectively on the Access node side) is causing a blocking effect in the routing resource allocation when WL access nodes are added to better cover users further from the wired AgNs. Ignoring the interference in the scheme in this case gives a smaller penalty but is still worse than the interference aware version.

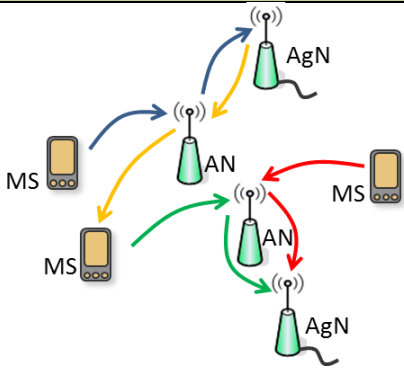


**Figure 9-9: Fraction of the user positions where average user throughput is less than x-axis value. This is for load point 10 in Figure 9-7. Red and black contain same information as Figure 9-8 (left and right respectively). Magenta and green is with two aggregation nodes and two aggregation nodes + 3WLAN, respectively (compare Figure 9-7, right plot).**

In Figure 9-9 we get an overview of the distribution of average throughputs. Adding 4 wireless ANs improves the 95% availability throughput over the single AgN by 145%. With 2 AgNs and 3 WLANs, the corresponding improvement is 195% (out of which 118% can be attributed to the increase of wired AgNs from 1 to 2). The corresponding improvement in median over location is 42% and 71%. Note though that the 20% best performance is reduced significantly under the used simulation assumptions as resources otherwise used for central UE access is given to the WL BH.

Translating the TC1 KPI:s of 0.5Gbps average TP per user during busy hour and 100Mbps/m<sup>2</sup> traffic density to the office area of 312.5m<sup>2</sup>, this gives 62.5 users active on average in both UL and DL. Now, assuming 2GHz spectrum rather than the simulated 200MHz, this would translate to a load point of 12.5 flows in Figure 9-7, assuming links are interference limited rather than power limited. With a single aggregation node we can then read out a system spectral efficiency 170Mbps/200MHz = 0.9bps/Hz and 1.7Gbps/12.5flows = 136Mbps/user in UL and DL respectively, if 4 WLAN are added, and 120Mbps/user without the WL ANs, i.e. a 13% improvement. Similarly for 2 aggregation nodes we can read out 1.3bps/Hz and 2.6Gbps/12.5flows = 208Mbps/user in UL and DL respectively on average. With this setup we conclude that we only reach between 27% and 42% of the targeted average user data rate. We further reflect on the fact that the office is busy indeed. During these busy hours we have more than 4 users per desk each consuming 1Gbps on average. In this scenario, where all ANs are in mutual line of sight and with most UE positions as well, WL BH with this limited beamforming directivity is a challenge compared to the previously studied scenario with rooms and corridor. We expect however that increasing the antenna apertures, in particular at the ANs, will dramatically improve the situation, but likely, a higher density of both AgN and WL AN will be needed to meet the TC1 targets and will be studied next.

Regarding Latency, we finally do the following reflection: From TeCC#1 of WP2 [METIS-D23 Section 2.1] on flexible air interface, TTI is expected to be scaled down from corresponding LTE numerology in a similar way as carrier frequency is scaled up. Assuming 1ms-1.5ms latency in the core network in either direction and a similar latency in UL as in DL within the UDN, a 10ms total latency requirement leaves slightly more than 3ms for the multiple hops for each flow. With 3-4 hops that would mean approximately 1ms per hop. In our simulation as subframe duration of 25us is used, but even if that is increased to 50us or 100us there will be several TTI's of time for processing and potential hop-level re-transmissions. Hence we conclude that a round trip latency of 10ms is not expected to be a problem even with multi-hop WL BH for mmW UDN.

T3.3 TeC 2 – Interference aware routing and resource allocation in millimetre-wave ultra-dense networks	
	<p><b>Main Idea</b></p> <p>To provide high data rate coverage in mmW indoor environments, a denser network than fixed backhaul can provide is required. In order to enhance spectrum efficiency, wireless backhaul and access share spectrum and nodes. The purpose is to develop and evaluate sub-optimal low-complexity routing and resource allocation schemes that take interference into account for several multi-hop flows in the mesh of access nodes, to one or several fibre connected access nodes serving as aggregation nodes.</p>
Considered SoA solution	Single 2GHz bandwidth wired access point operating in 60GHz to mimicking 802.11ad (Red solid lines in Figure 9-7 (left) and Figure 9-8)
KPIs considered and achieved gain	<ul style="list-style-type: none"> <li>• 95% availability user data rate improvement over the considered SOA: 145% to 195%</li> <li>• Median availability throughput improvement of 42%-71%</li> <li>• Average user throughput improvement of 13%</li> <li>• A cost of a lowered 20% availability throughput with current restricted solution in terms of number of Antennas at ANs.</li> <li>• Absolute average user throughput between 27% and 42% of challenging TC1 target. With current setup more Wired ANs or more antennas at WL ANs are needed to meet target. The latter is currently under study and is expected to dramatically improve the above KPIs.</li> <li>• Round trip Latency &lt; 10ms assuming 3-4 hops</li> </ul>
Performance evaluation approach	System Level (simplified)
System model considered	Other, TC1 scenario.
Deviation compared to Simulation Baseline	<p>W.r.t. T3.3 baseline: Significant. W.r.t. TC1 simulation guidelines from WP6: <b>Minor</b></p> <ul style="list-style-type: none"> <li>• Model of environment: TC1 cubicle office</li> <li>• Spectrum assumptions, 2GHz in 60GHz region</li> <li>• Propagation model: Ray-tracing + Statistical fading</li> <li>• Deployment model: See Figure 9-6 (left)</li> <li>• User/Device distribution: Grid based drops according to load, see Figure 9-6(left)</li> <li>• Traffic model: Full buffer</li> </ul>
Brief update of the results with respect to D3.2	Alignment to [METIS-D61] description of TC1. Looking at impact of adding WL ANs rather than comparing wired versus



	wireless BH for fixed number of AN's. Fairness added to scheme.
Association to the TeC Approach	TeC is the key enabler for mmW spectrum in dense deployments with extreme traffic demands and the backbone of the <i>Tech Approach 2: Indoor dense mesh network at mm-wave</i> as wired backhaul is unlikely of sufficient density in foreseen deployments.
Targeted TCs	TC1 is the main TC targeted, see also elaborations in [METISD32]
Impacted HTs	UDN
Required changes for the realization with respect to LTE Rel. 11	Major. Potentially some aspects such as mobility and similar higher layer functionality can be hidden and handled locally in the UDN. Phy and Mac layers need to be modified (see e.g. TeCC# 1 and TeCC#12.3 in WP2), access point association, signalling, mechanisms for CSI acquisition, initial activation procedures and network access, etc. etc.
Trade-off required to realize the gains	Addition of WL AN-hardware. CSI information to routing and routing information to AN. Higher antenna directivity simplifies routing and reduces impact of interference awareness.

### 9.2.3 Impact on Horizontal Topics

T3.3 TeC 2 - HT.UDN	
Technical challenges	Very high data rates for large amount of users
TeC solution	TeC2 contributes to TC1 by addressing how to share resources of dense access points also for WLBH to enable sufficient densification to provide high data rate coverage in mmW
Requirements for the solution	Centralized node responsible for routing/resource allocation in the UDN. Stationary users with reasonably stable traffic demand as link quality needs to be communicated to central node. Large spectrum available in mmW area. Full CSI is assumed in evaluations but feedback of direct and neighbour interfering link quality scalar parameters should be sufficient to harvest most of the performance seen.
KPIs addressed and achieved gain	Wireless backhaul will be needed to support density of nodes required to provide data rate coverage if to support wide spectrum available only in mmW. TeC 2 will contribute significantly to reaching the KPIs of: <ul style="list-style-type: none"> <li>• 36Tbyte/Month/subscriber UL &amp; DL traffic volume</li> <li>• Average Data Rate 0.5Gbps UL&amp;DL</li> <li>• Traffic volume per area 100Mbps/m<sup>2</sup> UL/DL</li> <li>• Experienced user data rate, 95% above 1Gbps, and 20% above 5Gbps.</li> </ul>



	See current performance values in previous table.
Interaction with other WPs	<p>TeCC#1 of WP2 [METIS-D23, Section 2.1] on flexible air interface, in particular frame-structure and numerology for mmW.</p> <p>TeCC#12.3 of WP2 [METIS-D23 Section 2.12.3], Routing and Resource allocation from TeC 2 of Task 3.3 assuming full buffer is expected to be used as input to MAC for adapting the individual hops to traffic variation and harvest statistical multiplexing gains.</p> <p>WP5 has identified mmW as a region with most opportunities for new spectrum. In case of mmW coexistence, spectrum manager of TeC 09 of WP5 [METIS-D53, Section 3.1.2] will provide TeC 2 of Task 3.3 with input on which resources should be masked out in the routing/RA.</p> <p>With increasing antenna aperture towards massive beamforming, TeC 2 of Task 3.1 on pilot coordination strategies will also be relevant</p>

#### 9.2.4 Addressing the METIS Goals

T3.3 TeC 2	
1000x data volume	TeC2 can be seen as a spectrum enabler and densification enabler boosting data volume
10-100 user data rate	TeC2 can be seen as a spectrum enabler and SINR enhancer boosting user data rates.
10-100x number of devices	Enabled spectrum and dense deployment increases spectral and spatial multiplexing gains.
10x longer battery life	UEs closer to AN, enabled by WL AN-deployment, decreases required TX power. High bandwidth enables fast data transfer and device can sooner go to sleep for fixed data size.
5x E-E reduced latency	Numerology on higher carrier enables shorter TTIs reducing latency even if multi-hop backhauling is used.
Energy efficiency and cost	WL BH gives cheaper installation than Wired. Dense Low power AN will have less TX power cost than higher power sparse AN deployment and can be selectively put to sleep in during low load for significant energy savings. Compact design requirements will drive increased integration and thereby lower energy consumption of circuitry.

#### 9.2.5 References

[HA13] Dennis Hui, Johan Axnäs, Joint Routing and Resource Allocation for Wireless Self-Backhaul in an Indoor Ultra-Dense Network, Personal Indoor and Mobile Radio Communications (PIMRC), 2013 IEEE 24th International Symposium on, 8-11 Sept. 2013, London, UK.



[M13] METIS test cases following the simulation guidelines, <https://www.metis2020.com/documents/simulations/>.

[METIS-D23] METIS consortium, "D2.3 – Components of a new air interface – building blocks and performance," project report, April 2014.

[METIS-D32] METIS consortium, "First performance results for multi-node/multi-antenna transmission technologies", project report, April 2014.

[METIS-D53] METIS consortium, "D5.3 – Description of the spectrum needs and usage principles", project report, Aug. 2014.

[METIS-D61] METIS consortium, "D6.1 – Simulation guidelines", project report, Oct. 2013.

## 9.3 T3.3 TeC 3: Virtual full-duplex buffer-aided relaying [KTH]

### 9.3.1 General Overview

Since half-duplex (HD) relaying is based on two-phase operation where a source transmits data to relays in first phase and a relay forwards it to a destination in second phase [LTW04], it inherently causes multiplexing gain loss expressed as one-half pre-log factor in achievable rate. Although several implementable full-duplex (FD) relaying schemes have been recently proposed [CJS10] [JCK+11], they are still premature for cellular communications, which require additional self-interference cancellation gain due to several practical concerns. On the other hand, employing buffer at relays, the loss of multiplexing gain is mitigated and spectral efficiency is improved even in the HD relaying [ZSP11]. Moreover, it is possible to mimic the FD relaying exploiting multiple HD relays with buffer [IKS12]. However, in previous work there was no consideration of inter-relay interference (IRI), which is a crucial issue like the self-interference in the FD relaying.

In this TeC, we consider a virtual FD relaying exploiting more than two HD relays with buffer. More specifically, one relay receives new data from the source while another relay forwards previously received data stored in its buffer to the destination. The main goal is to approach the average end-to-end rate of ideal FD relaying even in the presence of IRI. To this end, we propose transmission schemes based on a joint relay selection and BF design utilizing multiple buffer-aided relays and multiple antennas at the relays. For the joint relay selection and BF design, we first propose a weighted sum-rate maximization using instantaneous channel and buffer states for achieving the average end-to-end rate maximization. Then, we separately design linear BF for each (receiving and transmitting) relay pair, which cancels or suppresses IRI, and optimal relay selection for maximizing the weighted sum-rate based on the beamformers found for each relay pair.

The following joint relay selection and BF schemes have been developed:

1. SINR-based relay selection with BF neglecting IRI – beamformers are determined without consideration of IRI (i.e., MRC at the receiving relay and MRT at the transmitting relay) and then an SINR measure is used at the receiving relay for relay selection.
2. ZFBF-based relay selection – transmit beamformer is determined so that the IRI is perfectly cancelled at the receiving relay while receive beamformer is determined by MRC. Then, effective SNR measures after applying beamformers are used for relay selection.
3. MMSE BF-based relay selection – receive beamformer is determined so that the received SINR is maximized at the receiving relay while transmit beamformer is determined by MRT. Then, effective SNR measures after applying beamformers are used for relay selection. This scheme has been developed after [METIS32] and newly included in this report.
4. Optimal BF-based relay selection – transmit and receive beamformers are optimized through an iterative algorithm between transmitting and receiving relays so that the end-to-end rate is maximized. Then, effective SNR measures after applying beamformers are used for relay selection.

More details about the proposed schemes above can be found in [KB13] and [KB14].

### 9.3.2 Performance Results

#### Simulation Environments and Methodology

In previous, we have considered i.i.d. Rayleigh fading channels for all links in simulation. In this report, we take into account the WP3 T3.3 simulation baseline for TC2 Dense Urban Information Society. Figure 9-10 shows the SINR map of a serving Pico BS in our simulation setup. According to the T3.3 simulation baseline, 3 Macro BSs and 7 Pico BSs generate background interference. The left most Pico BS serves an edge UE placed at inside corner of

the building. We place two relays (RS1 and RS2 in Figure 9-10) in medium SINR range between the serving Pico BS and UE. The pathlosses are determined by PS#1 and PS#2 for Macro-relay and Macro-UE links, and by PS#3 and PS#4 for Pico-relay and Pico-UE links. The pathlosses for relay-UE and inter-relay links are determined by PS#7, indoor propagation scenario. PS#1, PS#2, PS#3, PS#4, and PS#7 are defined in [METIS61]. The small scale fading of interesting links is generated by [ITU09-2135] model referred in [METIS61]. For serving Pico-relay and serving Pico-UE links, the small scale fading follows Urban Micro O2I (UMi O2I) model and for relay-UE and relay-relay links, it follows Indoor Hotspot (InH) model.

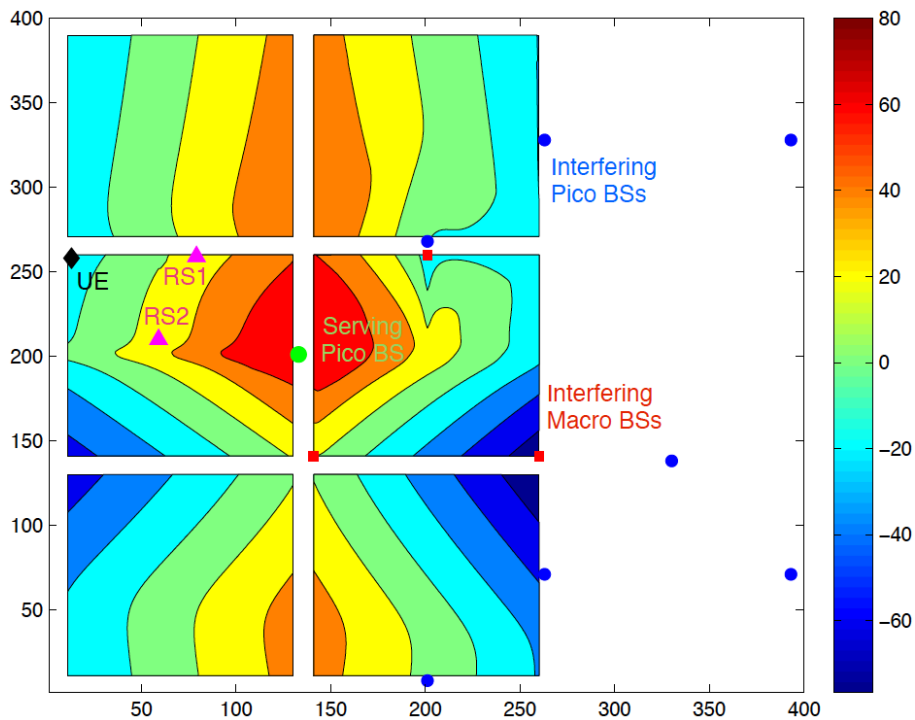


Figure 9-10: Simulation environment and SINR map

The simulation parameters considered are shown in Table 9.2. Basically, the parameters follow the WP3 T3.3 simulation baseline. Since we consider a resource block (RB) based relay selection, bandwidth, transmit power, and noise are taken into account as per subcarrier (e.g., 15 kHz in LTE). We assume that a single RB is used for serving the UE in Figure 9-10. Although multiple UEs can be scheduled using multiple RBs, we consider a single user supported by relays at this moment. Further systematic extensions using whole bandwidth are possible in the future. The BF is applied for each subcarrier and the relay selection is performed in unit of RB based on the effective transmission rate for an RB. We assume that the serving Pico BS has always data to transmit and perfect channel state information at the transmitters (the serving Pico BS and the transmitting relay).

Table 9.2: Simulation parameters

Parameter	Value
Carrier frequency	2.6 GHz
Bandwidth	20 MHz
Transmission power	<ul style="list-style-type: none"> <li>• Macro BS: 42 dBm</li> <li>• Pico BS: 37 dBm</li> </ul>

	<ul style="list-style-type: none"> <li>Serving Pico BS and relay: 22 dBm ~ 40 dBm (variable)</li> </ul>
Noise spectral density	-174 dBm/Hz
Number of total subcarriers	1200 (@20MHz)
Size of resource block (RB)	12 subcarriers x 7 symbols
Channel Model	<ul style="list-style-type: none"> <li>Large scale: PS#1, PS#2, PS#3, PS#4, and PS#7 scenarios [METIS61]</li> <li>Small scale: [ITU09-2135] UMa O2I and InH models</li> </ul>

### **Simulation Results**

We evaluate the performance of the proposed joint relay selection and BF schemes in terms of average end-to-end rate in [bps/Hz], which corresponds to spectral efficiency in KPI.

The following benchmarks are considered for performance comparison:

- Upper Bound (UB): This bound is obtained assuming no IRI. MRC and MRT beamformers for the receiving and transmitting relays are used and then the best relay pair is selected through an exhaustive search.
- SFD-MMRS [IKS12]: SFD-MMRS stands for space FD max-max relay selection representing state-of-the-art in virtual FD (VFD) – buffer-aided relaying (BR). In [IKS12], no IRI was assumed using highly directional antennas at relays. For the sake of comparison, this is modified such that the receiving relay suffers IRI. Thus, this scheme can show effects of IRI and provides a benchmark of conventional performance.
- HD-BRS [BKR+06]: This stands for HD best relay selection. This scheme does not consider buffer at relay and thus the best relay is selected based on a maximum of minimum of channel gains for source-relay and relay-destination links (i.e., max-min relay selection).
- HD-MMRS [IMS12]: This stands for HD max-max relay selection. This scheme considers buffer at relay and the best relay is determined as a relay with maximum channel gain of source-relay link at first time slot and a relay with maximum channel gain of relay-destination link at second time slot.
- Direct communication: The performance of direct communication between the serving Pico BS and UE is compared. The transmission rate is determined by assuming the perfect channel information at the transmitter.

More details about each scheme can be found in references stated above.

Differently from the previous performance evaluation in [METIS32], we examine the proposed ZFBF-based relay selection and MMSE-based relay selection schemes and exclude the optimal BF-based relay selection scheme due to high complexity and SINR-based relay selection scheme due to non-promising performance in overall.

Figure 9-11 shows the spectral efficiency for varying transmission power of the serving Pico BS and relays in case of two relays ( $K=2$ ) with two antennas ( $M=2$ ). We vary the transmit power from 22 dBm to 40 dBm for 20 MHz bandwidth. Thus, the allocated power per subcarrier is determined by multiplying the total power by  $(15k/20M)$ . In the figure, the UB assuming no IRI provides the performance upper limit. As shown in Figure 9-10, since the SINR at the UE is very low, direct communication is almost impossible in this simulation setup. Thus, the achievable end-to-end rate is almost zero even for high transmit power. However, it can still contribute to relay-UE transmission as interference whereas it has been neglected in

the previous theoretical simulation. The conventional SFD-MMRS has always worse performance than the HD relaying schemes due to no consideration of IRI in relay selection while there exists IRI under realistic environments such as the current simulation setup. The HD relaying schemes do not suffer from IRI due to orthogonal transmissions but it has one-half performance degradation due to the orthogonal transmissions, compared to the UB (approximately, the performance of ideal FD relaying). The HD-MMRS scheme exploiting buffer outperforms the HD-BRS scheme thanks to the use of buffering. On the contrary, the proposed ZFBF-based relay selection and MMSE-based relay selection schemes significantly outperform the HD relaying schemes. Even if they have some gap with the UB, the slopes of curves are similar to that of the UB. In the current simulation setup, the proposed ZFBF-based relay selection scheme always outperforms the MMSE-based relay selection scheme. However, the comparison between both schemes depends on relay deployment scenario. Another scenario will be also shown later. In Figure 9-11, the proposed ZFBF-based relay selection scheme achieves the average gains from 60% to 75% compared to the HD-MMRS scheme and from 170% to 440% compared to the SFD-MMRS scheme.

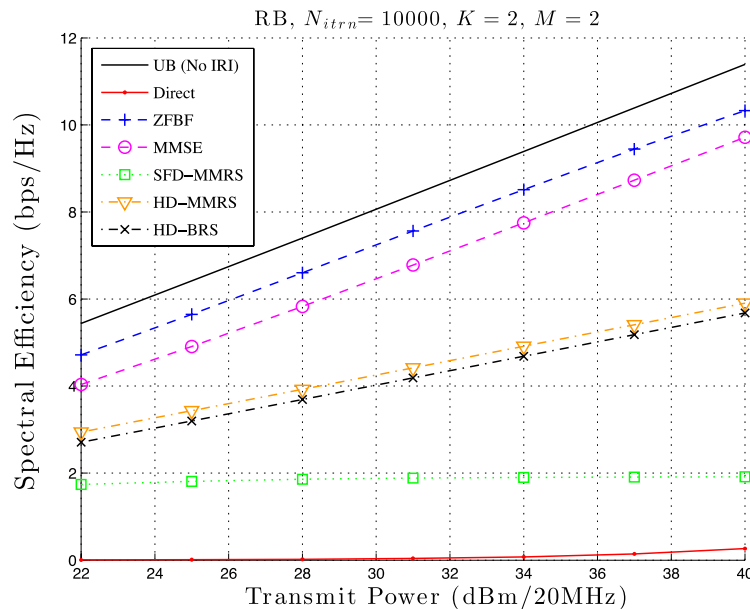


**Figure 9-11: Spectral efficiency for two buffer-aided relays (K=2) with two antennas (M=2) when relays are placed to be closer to the destination**

Figure 9-12 shows the spectral efficiency for two buffer-aided relays (K=2) with four antennas (M=4) under the same simulation setup. In overall, the spectral efficiency is increased for all schemes due to the power gain as the number of antennas increases. Especially, the proposed ZFBF-based relay selection and MMSE-based relay selection schemes are able to approach the UB thanks to the increased degrees of freedom both/either to suppress IRI and/or to increase the effective signal power. Therefore, the proposed ZFBF-based relay selection scheme can achieve the average gain from 80% to 85% compared to the HD-MMRS scheme and from 210% to 460% compared to the SFD-MMRS scheme.

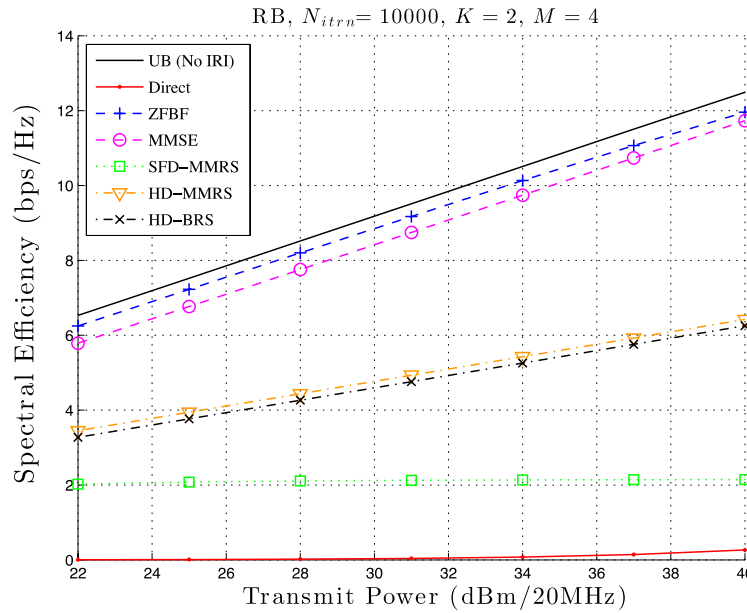


Figure 9-12: Spectral efficiency for two buffer-aided relays ( $K=2$ ) with four relays ( $M=4$ ) when relays are placed to be closer to the destination

In Figure 9-13 and Figure 9-14, we investigate another relay deployment scenario where relays are placed to be closer to the source. Differently from Figure 9-11 and Figure 9-12, the MMSE-based relay selection scheme always outperforms the ZFBF-based relay selection scheme for both two and four antennas cases. In the ZFBF-based relay selection scheme, the bottleneck link becomes the relay-to-destination link since it causes a loss in the effective rate of the link due to IRI cancellation while the other source-to-relay link can achieve the maximum rate by MRC. On the contrary, in the MMSE-based relay selection scheme, the bottleneck link is the source-to-relay link due to a loss in the effective rate of the link for suppressing IRI at the receiving relay.

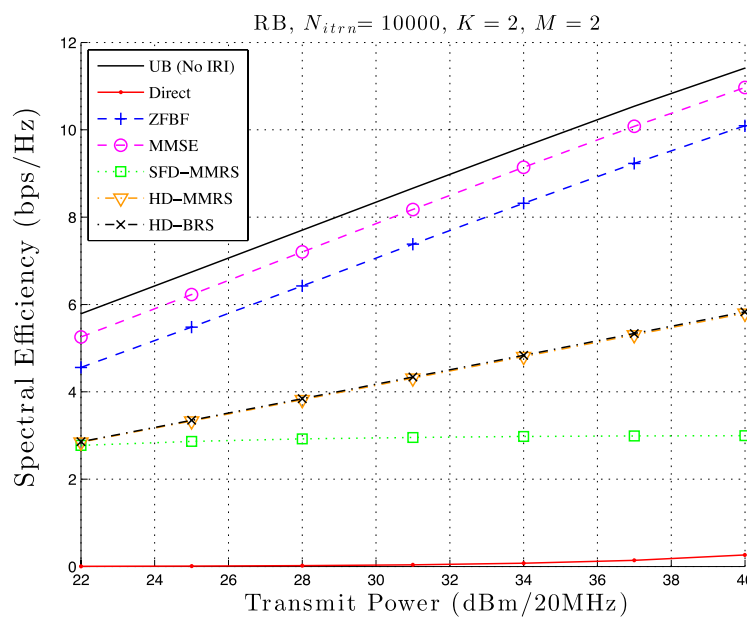
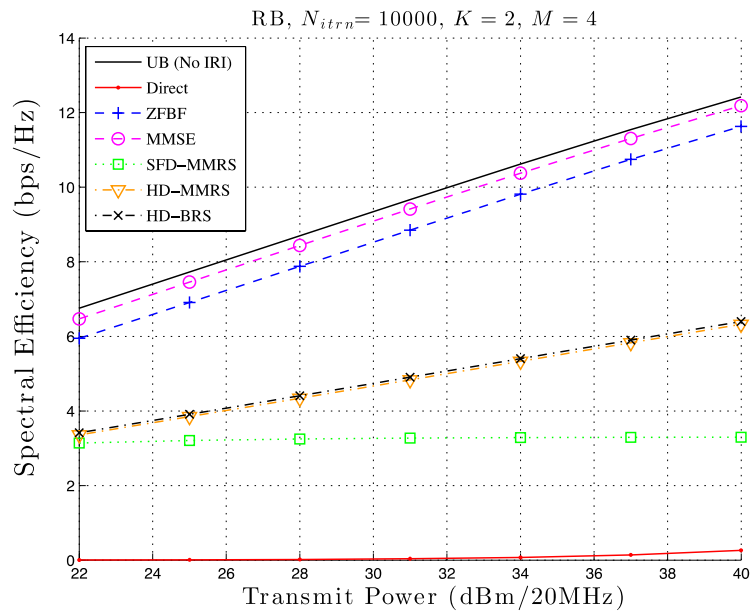


Figure 9-13: Spectral efficiency for two buffer-aided relays ( $K=2$ ) with two relays ( $M=2$ ) when relays are placed to be closer to the source

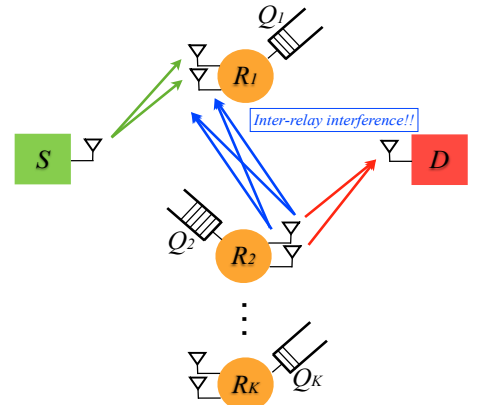


**Figure 9-14: Spectral efficiency for two buffer-aided relays (K=2) with four relays (M=4) when relays are placed to be closer to the source**

Basically, the average end-to-end rate is limited by the minimum of average effective rates of both links. Hence, for the ZFBF-based relay selection scheme, a deployment scenario, where the relay-to-destination link qualities are better than the source-to-relay link qualities, is better because it can provide an extra budget for IRI cancellation at the transmitting relay. On the other hand, for the MMSE-based relay selection scheme, another relay deployment scenario, where the source-to-relay link qualities are better than the relay-to-destination link qualities, is better since it can provide an extra budget for IRI suppression at the receiving relay.

In principle, the proposed VFD-BR schemes can recover the loss of multiplexing gain caused by HD relaying as both/either the number of relays and/or the number of antennas increases. In practice, more than three relays supporting one source-destination pair could be unavailable in many realistic scenarios. However, through the WP3 T3.3 baseline simulation, it is shown that only two relays are enough to recover the loss of multiplexing gain if increasing the number of antennas is available. Compared between the proposed ZFBF-based and MMSE-based relay selection schemes, the ZFBF-based relay selection scheme is more efficient when relays are closer to the destination and the MMSE-based relay selection scheme is more efficient when relays are closer to the source. Therefore, we could selectively use one of the proposed schemes according to relay deployment scenarios.

A summary of the information about this TeC is provided in the following Table.

T3.3 TeC 3 – Virtual Full-Duplex Buffer-Aided Relaying	
	<p><b>Main Idea</b></p> <p>Buffers at the relays enable a virtual full-duplex communication in a network where two relays allow concurrent transmissions with inter-relay interference cancellation. One relay receives the information from the source while the other forwards the information to the destination. The idea is to find the best relay-pair selection for Source-Relay and Relay-Destination links with an efficient beamforming design at both transmitting and receiving relays.</p>
Considered SoA solution	The performance is compared to the HD-MMRS scheme in [IMS12] and SFD-MMRS scheme in [IKS12].
KPIs considered and achieved gain	<ul style="list-style-type: none"> <li>Spectral efficiency, average gain from 60% to 85% compared to HD-MMRS, average gain from 170% to 460% compared to SFD-MMRS, employing two or four antennas at relays.</li> </ul>
Performance evaluation approach	Simulation-based (Simplified system level simulation)
System model considered	WP3 T3.3 Simulation Baseline
Deviation compared to Simulation Baseline	None
Brief update of the results with respect to D3.2	Major updates are the results according to simulation alignment.
Association to the TeC Approach	Heterogeneous network at lower frequencies
Targeted TCs	TC 2
Impacted HTs	UDN
Required changes for the realization with respect to LTE Rel. 11	Minor. A scheduling entity is required to select the source-destination pairs that operate concurrently.
Trade-off required to realize the gains	The gain requires sacrificing delay performance due to buffering. In addition, it requires accurate channel estimations at source and relays, which can be extra overhead.

### 9.3.3 Impact on Horizontal Topics

T3.3 TeC 3 - HT.UDN	
Technical challenges	Increase spectral efficiency of edge users supported by relays.
TeC solution	By allowing concurrent transmissions with interference cancellation, the proposed VFD-BR enables to fully recover the loss of multiplexing gain caused by the HD relaying. Thus, this TeC can provide high spectral efficiency of edge users supported by relays.



Requirements for the solution	A good quality of CSI estimation and feedback is required at relays for precise interference cancellation.
KPIs addressed and achieved gain	Spectral efficiency, average gain from 60% to 85% compared to the state-of-the-art HD relaying (HD-MMSR) and from 170% to 460% compared to the conventional SFD-MMRS with uncontrolled IRI, employing two or four antennas at relays.
Interaction with other WPs	WP4: For further systematic simulations, multiple source-destination pair scheduling considering mutual interference is required. This issue could be related to interference management in WP4.  WP6: Interaction is required for more systematic simulation.

### 9.3.4 Addressing the METIS Goals

T3.3 TeC 3	
1000x data volume	Increase in spectral efficiency can contribute to handle increased data volume.
10-100 user data rate	Increase of edge user data rate supported by relays up to 85% (ideally 100%)
10-100x number of devices	Increase of the number of simultaneously served devices through increase of coverage by the use of relays
10x longer battery life	
5x E-E reduced latency	
Energy efficiency and cost	

### 9.3.5 References

[LTW04] J. N. Laneman, D. N. C. Tse, and G. W. Wornell, "Cooperative diversity in wireless networks: Efficient protocols and outage behavior," *IEEE Trans. Wireless Commun.*, vol. 50, no. 12, pp. 3062 – 3080, Dec. 2004.

[CJS10] J. I. Choi, M. Jain, K. Srinivasan, P. Levis, and S. Katti, "Achieving Single Channel, Full Duplex Wireless Communication", in *Proc. ACM Mobile Computing and Networking (Mobi-Com)*, Dec. 2010.

[JCK+11] M. Jain, J. I. Choi, T. M. Kim, D. Bharadia, S. Seth, K. Srinivasan, P. Levis, and S. Katti, and P. Sinha, "Practical, real-time, full duplexing wireless," in *Proc. ACM Mobile Computing and Networking (Mobi-Com)*, Sept. 2011.

[ZSP11] N. Zlatanov, R. Schober, and P. Popovski, "Throughput and diversity gain of buffer-aided relaying," in *Proc. IEEE Globecom*, Dec. 2011.

[IKS12] A. Ikhlef, J. Kim, and R. Schober, "Mimicking full-duplex relaying using half-duplex relays with buffers," *IEEE Trans. Veh. Technol.*, vol. 61, no. 7, pp. 3025 – 3037, Sept. 2012.

[KB13] S. M. Kim and M. Bengtsson, "Virtual full-duplex buffer-aided relaying – relay selection and beamforming," in *Proc. IEEE PIMRC*, Sept. 2013.

[KB14] S. M. Kim and M. Bengtsson, "Virtual full-duplex buffer-aided relaying in the presence of inter-relay interference," *IEEE Trans. Wireless Commun.*, Aug. 2014 (Submitted).



[METIS61] METIS consortium, "D6.1 – Simulation guidelines", project report, Oct. 2013.

[BKR+06] A. Bletsas, A. Khisti, D. P. Reed, and A. Lippman, "A simple cooperative diversity method based on network path selection," IEE J. Sel. Areas Commun., vol. 24, no. 3, pp. 659 – 672, Mar. 2006.

[IMS12] A. Ikhlef, D. S. Michalopoulos, and R. Schober, "Max-max relay selection for relays with buffers," IEEE Trans. Wireless Commun., vol. 11, no. 3, pp. 1124 – 1135, Mar. 2012.

[ITU09-2135] "Guidelines for Evaluation of Radio Interface Technologies for IMT Advanced", International Telecommunication Union-R, M.2135-1, Dec. 2009.

[METIS32] METIS consortium, "D3.2 - First performance results for multi-node/multi-antenna transmission technologies", project report, Apr. 2014.

## 9.4 T3.3 TeC 4: Distributed coding for the multiple access multiple relay channel [FT]

### 9.4.1 General Overview

One of the promising cooperative communication technologies, network coding, has recently emerged due to its simple concept and vast application potential. The basic idea of the network coding is that intermediate relay nodes perform simple coding operations and forward the coded symbol to a destination. The authors in [CKL06] and [HSO+05] propose network coding schemes with pre-defined network codes to increase the throughput and improve network performance in lossless, i.e., with a deterministic capacity, relay networks, assuming that link states between nodes is not changed over time. However, the assumptions conflict with reality since practical networks have link failures and topology changes.

As a starting point, we consider the Selective Decode and Forward (SDF) relaying function, i.e., the relay forwards a deterministic function of the sources' messages that it can decode error-free. Sending a deterministic function of the received messages at layer 3 of the Open Systems Interconnection (OSI) model instead of routing each received message separately is optimal in the sense that it can achieve the min cut max flow capacity of the underlying network [ACL+00] and is coined network coding. Here, we consider wireless network coding where the network coding is performed at the physical layer. From this viewpoint, the proposed SDF strategy cannot be proven to be optimal anymore, however, it has many advantages: (1) It prevents the error propagation from the relay to the destination; (2) It reduces the energy consumption at the relays and limits the interference within the network (the relay when it cooperates is always helpful); (3) The sources who have poor source-to-relay (S-R) links, with high probability, will not prevent the relays from helping the other sources.

In this document, we show the efficiency of a practical code design for M-users Multiple Access Channel (MAC) assisted by L half-duplex SDF relays, namely Multiple Access Multiple Relay Channel (MAMRC). Different access schemes are considered, ranging from the less efficient orthogonal assignment where sources and relays are given non-overlapping channel uses to the most efficient one where sources and relays are allowed to transmit simultaneously (interfere). Perfect channel state information at receiver and no channel state at transmitter are assumed. Limited feedbacks (ARQ, CQI etc...) may be included in the subsequent phases of our work. In [MVB13a] and [MVB13b], the outage probability of different MAMRC access schemes was derived. The outage probabilities could be seen as a tight upper bound on the achievable Block Error Rate (BLER) of practical codes with finite codeword length (around several hundreds of channel uses) [MAL99]. Hence, in order to evaluate the effectiveness of our proposed coding schemes, we compare the BLER with outage probability bound.

From a pure distributed code perspective, the challenge is to achieve full diversity and to maximize the coding gain. In that respect, we will consider Joint Network Channel Coding at the relay, i.e., the redundancy of the network code is exploited to support the channel code, together with iterative Joint Detection and Network Channel Decoding.

### 9.4.2 Performance Results

#### Proposed schemes description

Relays are assumed to operate in a half-duplex mode mainly for implementation considerations. Due to the half-duplex constraint, the total number  $N$  of channel uses available to transmit a source message (or packet) is divided into two time phases, namely,  $\alpha N$  for the listening phase of the relay and  $(1 - \alpha) N$  for its transmission phase where  $\alpha \in ]0,1]$ . Our reference cooperation scheme is Orthogonal MAMRC (OMAMRC) where each source transmits only during the first phase in  $\alpha N/M$  channel uses, while each relay transmits only during the second phase in  $(1 - \alpha)N/L$  channel uses. By removing gradually the constraint of

orthogonality between the radio links, we obtained three alternative cooperation schemes. The Semi-Orthogonal MAMRC (SOMAMRC) type I is defined as follows. The sources transmit simultaneously during the first phase and stay idle during the second phase where the relays transmit simultaneously. Hence, both the sources and the relays use Non-Orthogonal Multiple Access (NOMA). In contrast, the SOMAMRC type II is defined as follows. The sources use OMA during the first phase (i.e.,  $\alpha N/M$  channel uses allocated to each). During the second phase, the relays and the sources are allowed to jointly transmit using NOMA. This cooperation scheme is particularly interesting for it decreases the receiver complexity at the relay. To the best of our knowledge, it has never been investigated before. Finally, the Non-Orthogonal MAMRC (NOMAMRC) is another benchmark defined as follows. The sources transmit simultaneously during the first phase and also during the second phase together with the relays. All nodes use NOMA. Its derivation is detailed in [MVB13a] for the single transmit and single receive antenna case. This last cooperation scheme provides an upper bound on the  $\epsilon$ -outage achievable rates. Figure 9-15 summarizes all the aforementioned cooperation schemes.

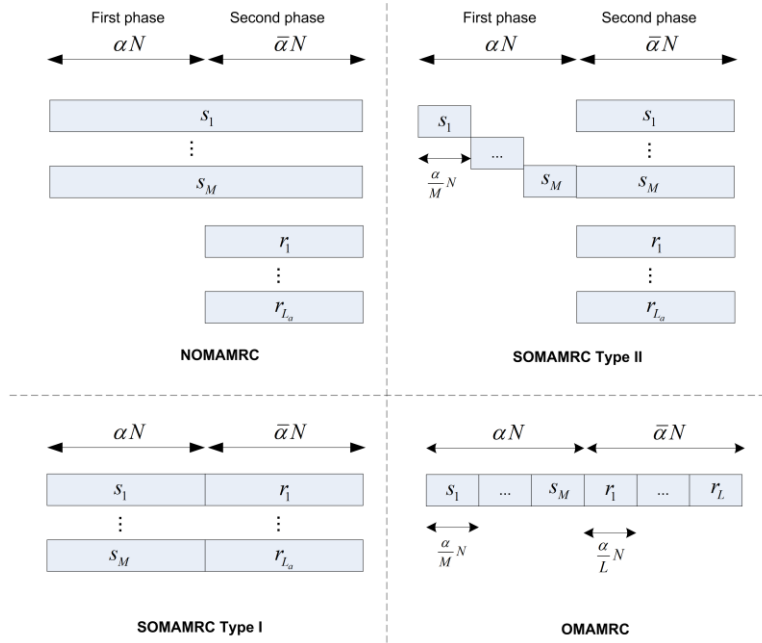


Figure 9-15: Considered cooperation schemes

We denote the Signal-to-Noise Ratio (SNR) between the source-destination, source-relay, and relay-destination by  $\gamma_{sd}$ ,  $\gamma_{sr}$ , and  $\gamma_{rd}$  respectively.

Three network coding schemes are investigated:

1. XOR: The correctly decoded messages are summed up over the binary field.
2. Bit Interleaved XOR (BI-XOR): The correctly decoded messages are first interleaved using random interleaver then summed up over the binary field.
3. Galois Field Network Coding (GFNC): The correctly decoded messages are multiplied by network coding coefficients (chosen from a Galois field of order greater than 2) then summed up.

More detailed description of each coding scheme could be found in [MVB14].

Note 1: the spectral efficiency advantage of NOMAMRC access scheme over OMAMRC for a fixed coding modulation scheme at each source of spectral efficiency  $\rho$  is

$$\beta = \frac{R_{NOMAMRC}}{R_{OMAMRC}} = \frac{\rho}{\frac{\alpha_o}{M} \rho} = \frac{M}{\alpha_o} \quad (1)$$

where  $\alpha_o N$  is the number of channel uses allocated to the listening phase of the OMAMRC. Note that advanced multiuser detection (MUD), e.g., turbo MUD, at the relay and destination allows achieving this spectral efficiency gain at the expense of reasonable performance loss only.

### **Numerical Results**

Due to space limitation, we only show the result for the NO-MAMRC since it is the most spectral efficient access schemes. We fix the number of sources to two, each source is provided by one transmit antenna, the transmission rate is fixed to  $2/3$  bits per channel use (bpcu). In the first simulation, we choose the number of relays to two, each relay is provided by one receive and one transmit antenna. The two sources use identical turbo codes of rate- $1/2$  made of two 4-state rate- $1/2$  Recursive Systematic Convolutional Code RSCC encoders with generator matrix  $G_1 = [1 \ 5/7]$  in octal representation, whose half of the parity bits are punctured and transmitted in the second phase. The GFNC at the relays (when applied) is based on the network coding vectors chosen from MDS code, followed by a 4-state rate- $1/2$  RSCC encoder with generator matrix  $G_r = [1 \ 5/7]$  whose systematic part is dropped)

Figure 9-16 shows the individual outage probability  $P_{out}^{ind}$  and the Individual BLER (IBLER) when the number of receive antenna at the destination is  $m_d = 1, 4$ , the individual spectral efficiency  $R = 2/3$  (b./c.u) (the modulation order at the sources and the relays  $q_r = q_s = 2$  ).

We observe that

- the GFNC achieves the promised full diversity (almost a constant gap from the outage curves),
- the BI-XOR has a very close performance to GFNC and starts to deviate at high SNR,
- as expected, the XOR network coding does not achieve the full diversity (the gap to the outage curves increases with the SNR),
- GFNC in JNCC/JNCD framework is within 3 dB from the outage bound both for  $m_d = 1, 4$  which is significant achievement of our investigations.

Similar observations were made for SOMAMRC Type I, and OMAMRC with higher modulation, up to 64-QAM ( $q_r = q_s = 4$ ), and higher coding rates, up to  $5/6$  at the sources. Results are not shown due to space limitation.

In the second simulation, we vary the number of relays from 1 to 3. Figure 9-17 shows the IBLER of BI-XOR compared to outage bound. We see that the diversity order of BI-XOR increases with the number of the relays. BI-XOR does not achieve the full diversity, except for (2,1,1)-MAMRC. Nevertheless BI-XOR is within 3 dB from the outage in the investigated SNR region. Furthermore, from the result of the first simulation, we could conjecture that in this range of SNR the GFNC with JNCC/JNCD (which is very complex to implement for (2,3,1)-NOMAMRC) will have a very close performance to BI-XOR. On the other hand it is known that the diversity of XOR cannot increase with the number of relays.

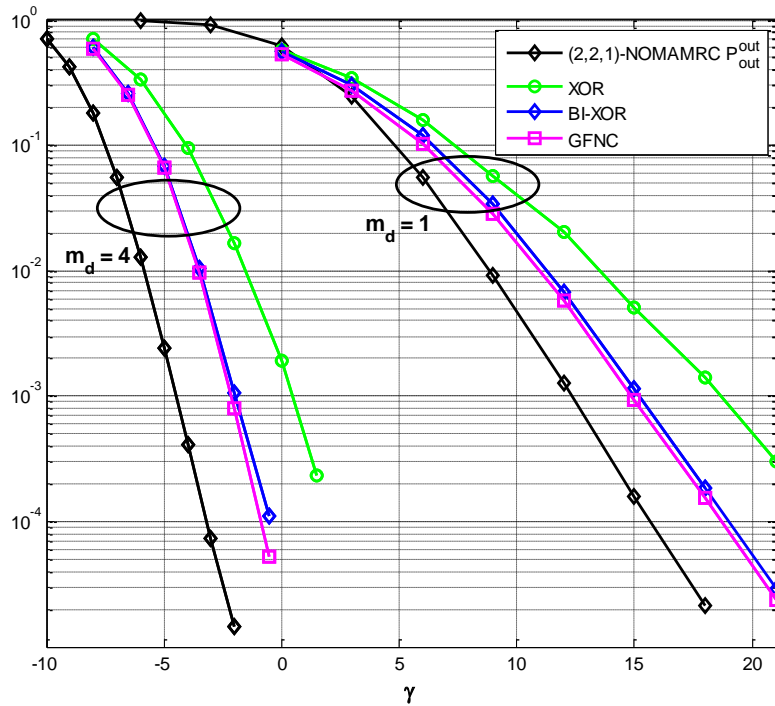


Figure 9-16:  $P_{out}^{ind}$  vs IBLER for (2,2,1)-SOMAMRCm where  $R=2/3$  (b./c.u), and  $\alpha=2/3$ , and  $\gamma_{sd} = \gamma_{sr} = \gamma_{rd} = \gamma$

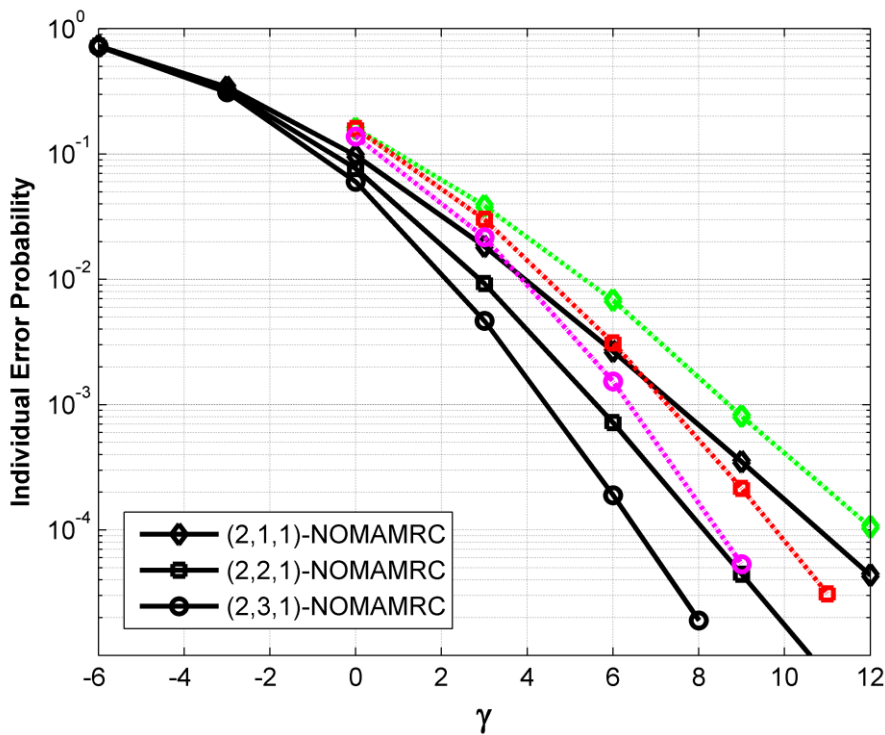
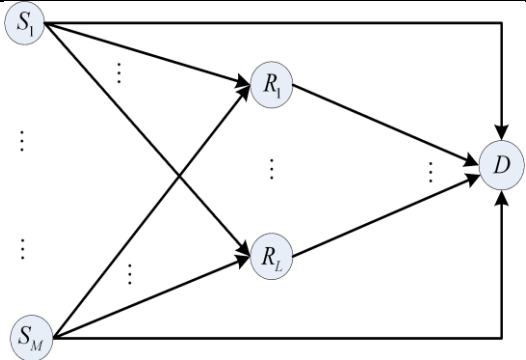


Figure 9-17:  $P_{out}^{ind}$  (full line) vs. IBLER (dashed line) for (2,L,1)-SOMAMRCm where  $L=1,2,3$   $R=2/3$ . (b./c.u),  $\alpha=2/3$  And  $\gamma_{sd} = \gamma_{sr} = \gamma_{rd} = \gamma$

Similar types of simulations require a very high computational power even for a fixed SNR distribution  $\gamma_{sd}$ ,  $\gamma_{sr}$ , and  $\gamma_{rd}$ . Hence, running this simulation for an SINR map like the one adopted in the simulation baselines of [METIS14-D32] is far from being possible for the moment. But the simulation and the theoretical results shows clearly the amount of benefits that can be expected from the proposed relaying solutions in terms of diversity and coding gain.

T3.3 TeC 4 – Distributed Coding for the Multiple Access Multiple Relay channel	
	<p style="text-align: center;"><b>Main Idea</b></p> <p>To reach high spectrum efficiency, non-orthogonal access techniques combined with wireless network coding are considered in a cooperative communication setting. The relaying function denoted Selective Decode and Forward (SDF) is applied at the relay, i.e. the relay gathers the messages that it can decode free of errors and forwards a deterministic function of the sources' messages.</p>
Considered SoA solution	<ul style="list-style-type: none"> <li>Wireless network coding for orthogonal and non-orthogonal transmission relaying schemes.</li> </ul>
KPIs considered and achieved gain	<ul style="list-style-type: none"> <li>Spectral Efficiency: the gain depends on the network topology (number of sources, number of relays, access scheme, etc...). for example the improvement multiplier between the NOMAMRC and OMAMRC is given by (1).</li> <li>Error rate / Energy Efficiency: the gain depends on the network topology (number of sources, number of relays, access scheme, etc...). so it is impossible to give a fixed number.</li> </ul>
Performance evaluation approach	Analytical and Simulation
System model considered	Not based on the WP3. A symmetric S-R, R-D, S-D links are assumed and a symmetric transmission rate of sources.
Deviation compared to Simulation Baseline	<p>Not Applicable.</p> <p>At the moment only preliminary results, with a simplified system model and links distributions, are available.</p>
Brief update of the results with respect to D3.2	<ul style="list-style-type: none"> <li>A network coding strategy other than the GFNC is investigated, namely BI-XOR. It is simple, flexible, and performs close to GFNC at low to moderate SNR.</li> <li>Non-orthogonal MAMRC access schemes are implemented (turbo-MUD at relay and destination) and simulated. The performance of the practical code design is shown to reach the outage bound within 3dB.</li> </ul>
Association to the TeC Approach	Not Applicable.
Targeted TCs	Test Case 2 - Dense urban information society
Impacted HTs	UDN
Required changes for the realization with respect to LTE Rel. 11	<p>Major</p> <p>1) The relay must implement advanced relaying function</p>



	<p>based on turbo-MUD of the sources message</p> <p>2) The destination must perform sophisticated Joint Network Channel Decoding and MUD</p> <p>3)The relay must transmit control information to indicate the messages the relay is cooperating with</p>
Trade-off required to realize the gains	For SDF relaying, M additional bits should be transmitted by each relay to indicate the messages the relay is cooperating with

### 9.4.3 Impact on Horizontal Topics

T3.3 TeC 4 - HT.UDN	
Technical challenges	Increase the reliability of communication and the spectral efficiency.
TeC solution	Network coding with non-orthogonal transmission using multiple relays can dramatically increase the spectral efficiency and the coding gain (energy saving) for dense wireless networks. If relays are devices, natural densification gain could be obtained without the cost of infrastructure deployments.
Requirements for the solution	Fixed or moving relay nodes (which could be mobile UE, vehicular etc...).
KPIs addressed and achieved gain	Spectral Efficiency Energy Efficiency/ Error rate
Interaction with other WPs	

### 9.4.4 Addressing the METIS Goals

T3.3 TeC 4	
1000x data volume	The proposed solution can help many TC to achieve their METIS goals. For example, NOMAMRC can achieve significant spectral and power efficiency gains compare to their orthogonal counterparts (w/o relays) .
10-100 user data rate	Network coding enables to have a wireless backhaul that helps several sources at the same time and thus improve the involved sources data rates
10-100x number of devices	
10x longer battery life	
5x E-E reduced latency	
Energy efficiency and cost	At a fixed reliability (frame error probability) the described solution could achieve part of this goal.

### 9.4.5 References

[ACL+00] R. Ahlswede, N. Cai, S.-Y. R. Li, and R. W. Yeung, "Network information flow," in IEEE Trans. Inf. Theory, vol. 46, Jul. 2000, pp. 1204-1216.



[CKL06] Y. Chen, S. Kishore, and J. Li, "Wireless diversity through network coding," *Wireless Communications and Networking Conference*, vol. 3, pp. 1681- 1686, Apr. 2006.

[HSO+05] C. Hausl, F. Schreckenbach, I. Oikonomidis, and G. Bauch, "Iterative network and channel decoding on a tanner graph," *Proc. Allerton Conf. on Commun. Control and Computing*, Urbana Champaign, IL, Sept. 2005.

[MVB13a] A. Mohamad, R. Visoz, and A.O. Berthet, "Outage Achievable Rate Analysis for the Non Orthogonal Multiple Access Multiple Relay Channel," *Proc. Wireless Communications and Networking Conference (WCNC)*, Shanghai, China, Apr. 2013.

[MVB13b] A. Mohamad, R. Visoz, and A.O. Berthet, "Outage Analysis of Various Cooperative Strategies for the Multiple Access Multiple Relay Channel," *Proc. Personal Indoor and Mobile Radio Communications (PIMRC)*, London, Sep. 2013.

[MVB14] A. Mohamad, R. Visoz, and A.O. Berthet, "Code Design for the Orthogonal Multiple Access Multiple Relay Channel," *Proc. GLOBECOM*, Texas, US, Dec. 2014.

[PGA10] R. Pyndiah, F. Guilloud, and K. Amis, "Multiple source cooperative coding using turbo product codes with a noisy relay," in *Proc. ISTC'10*, Brest, France, Sep. 2010, pp. 98–102.

[MAL99] E. Malkamaki and H. Leib, "Coded diversity on block-fading channel," *IEEE Trans. Inf. Theory*, vol. 45, no. 2, pp. 771–781, Mar. 1999.

[METIS14-D32] METIS D3.2, "First performance results for multi-node/multi-antenna transmission technologies", Apr. 2014.

## 9.5 T3.3 TeC 5: Bi-directional relaying with non-orthogonal multiple access [UB]

### 9.5.1 General Overview

Relaying has been an extensively investigated research topic over the last decades as it allows coping with path loss and fading in mobile radio systems. The main drawback of relaying, however, is the loss in spectral efficiency due to the half-duplex constraint. To overcome this drawback, bidirectional relaying has been investigated considering both transmission directions between two nodes jointly. Applying techniques like network coding (NC) [ACL+00] [FBW06] in the second phase, where the relay broadcasts to both nodes, the overall number of required transmission slots is reduced and, thus, the spectral efficiency is increased.

As soon as a relay supports multiple communication pairs, the question of medium access arises. In order to obtain a highly flexible system concept, especially when considering multiple communication pairs with different rate requirements, non-orthogonal medium access based on IDMA [PLW+06] is applied. The combination of NC with IDMA offers great flexibility in terms of designing MAC and BC phase. Further considering resource allocation and channel coding leads to a system concept supporting high device densities and high spectral efficiencies which is the foundation for a high end user throughput.

One of the crucial parameters of the proposed system is the applied channel code. In [METIS13-D32] Irregular Repeat Accumulate (IRA) codes [JKM00] have been proposed as they allow for a very flexible design at moderate complexity. A code design framework for IRA codes has been developed and IRA codes have been implemented into the general simulation framework. Details regarding the code design framework can be found in [METIS13-D32] and initial performance results have been published in [LBW+13].

In order to get more meaningful results, the simple channel models used thus far have been dropped in favour of more realistic modelling assumptions. Specifically, a concrete simulation model has been developed in which effects as path losses and more realistic small scale fading are incorporated. Within the simulation model, a specific scenario has been investigated which is described in more detail in the following section. Furthermore, an OFDMA-based four-way relaying simulation framework has been developed. In conjunction with LTE-A parameters, this system serves as a legacy solution benchmark for the proposed IDMA-based scheme.

### 9.5.2 Performance Results

The principle system and code optimization assuming a simplified system model has already been presented in [METIS13-D32]. The novelty in the results presented here lie in the adoption of the T3.3 simulation baseline. Figure 9-18 shows the investigated setup within the simplified Madrid grid agreed upon within T3.3. One single relay (orange triangle) is placed indoor 10m apart from the outdoor facing wall to increase outdoor-to-indoor coverage as well as to facilitate indoor device to device communication. In the specific investigated setup the relay supports the communication from an outdoor Pico base station (green dot) to an indoor user UE1 (green rectangle) as well as the communication between two indoor users UE2, UE3 (yellow rectangles). Indoor users are uniformly distributed within a circle of radius  $R$  around the relay.

The overall communication experiences background interference which is caused by macro base stations (red squares) and micro base stations (blue circles) which are deployed as indicated in the figure. The overall background interference and noise pattern is indicated by the underlying colour map. It depends on the positions of the interferers, as well as their transmit powers. Here, macro BSs transmit with 42dBm, whereas micro/pico BSs transmit with 37dBm. The transmit power of the indoor relay is set to 20dBm and the users transmit power to 24dBm, all according to the simulation guidelines described in [METIS13-D61]. Moreover,

the background noise level is set to  $-174\text{dBm/Hz}$  resulting in  $-95\text{dBm}$  for the assumed  $80\text{MHz}$  bandwidth.

The channels between all communicating nodes are determined employing channel models provided by WP6 in [METIS13-D61]. Specifically, the path loss between pico BS and relay as well as relay and UEs is calculated using path loss model PS#4 for outdoor-to-indoor and PS#7 for indoor-to-indoor communication, respectively. Additionally, small scale fading is introduced which is calculated based on the WINNER models suggested by WP6 in [METIS13-D61] using parameters agreed on within T3.3.

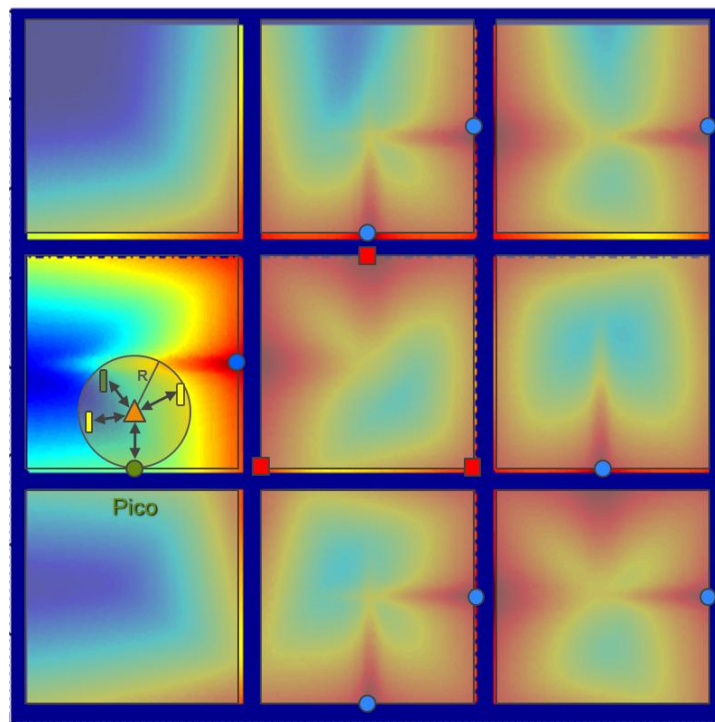


Figure 9-18: Simplified TC2 simulation model with investigated placement of nodes

In order to achieve a meaningful comparison of the proposed IDMA system with an OFDMA based legacy solution we choose  $R_{WP} = 10\text{m}$  as our working point. That means we optimize the system for a distribution of users within a circle of radius  $R = 10\text{m}$  around the fixed position of the relay. The distance between the pico BS and the relay is fixed and set to  $d_{PR} = 10\text{m}$ . Note that the relay is always used, regardless of the position of the users. That means we exclude the case, of a direct transmission between users. Table 9.3 gives an overview of the various link SINRs at the chosen working point. Here, a typical average interference level is chosen to be able to give specific values as example. As can be seen, the link between pico BS and relay in the MAC phase is on average significantly stronger than the links between UEs and the relay. This is mostly due to the difference in transmission power of  $13\text{dBm}$ . Furthermore, it is assumed that the relay is placed in a corridor which introduces a LOS component to the channel model. The relays, however, are assumed to be placed inside offices and, therefore, experience a slightly higher path loss for the same node distance. In the BC phase, the average SINR levels are significantly lower, namely around  $10.35\text{dB}$ . This is due to the rather low transmission power of the relay of  $20\text{dBm}$ . Concluding, the expected power levels at the chosen working point indicate, that the overall performance will be dominated by the low transmit power of the relay in the broadcast phase.

**Table 9.3: Overview of the link SINRs at the working point**

	MAC phase		BC phase	
Tx → Rx	Pico → Relay	UE → Relay	Relay → Pico	Relay → UE
SINR in dB	34.68	16.58	10.35	10.35

The IDMA system is now optimized according to the values given in Table 9.3 and the code optimization process as described in detail in [METIS13-D32]. As benchmark we investigate an OFDMA-based four-way relaying system. Figure 9-19 depicts the average end-to-end-throughput of the optimized two way relaying (TWR) IDMA system and the legacy OFDMA-based solution for different modulation and coding schemes. In this figure, the distance between the relay and UE is the same for all UEs and is exactly  $d_{RU} = R_{max}$ . The distance between pico BS and relay is always fixed as  $d_{PR} = 10m$ . For every investigated scheme, two curves are shown. The solid line depicts the average throughput (up- and downlink) of the pico-UE1 communication and the dashed line the average throughput (up- and downlink) of the UE2-UE3 communication. Up- and downlink here is to be understood with respect to the end users and not with respect to the relay. That means, e.g. for the Pico-UE1 transmission, if the link between Pico and relay is in outage, the throughput between Pico and UE1 is zero and the depicted average is the average between zero and the throughput of the transmission from UE1 to Pico. The throughput curves for pico-UE1 and UE2-UR3 communication are not necessarily identical, since the distance between Pico and relay is fixed and, thus, does not vary with  $R_{max}$ .

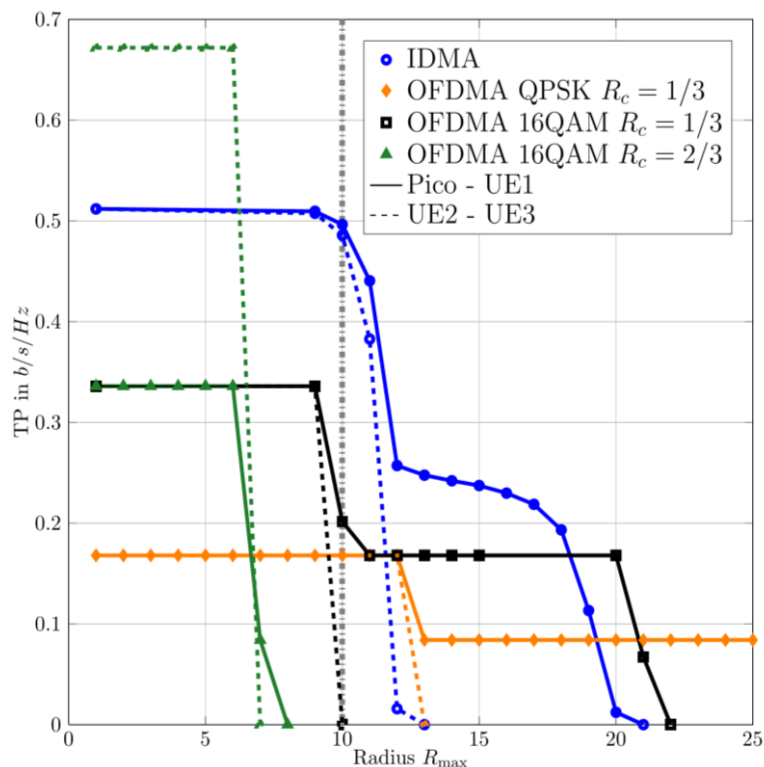


**Figure 9-19: Average end-to-end throughput in bits/s/Hz of optimized TWR IDMA vs. legacy OFDMA-based solution over the distance of the UEs to the relay. Fixed distance  $d_{UR} = R_{max}$ .**

For the optimized IDMA system the achieved throughput at the working point of  $R_{WP} = 10m$  is approximately  $TP = 0.5 \text{ bits/s/Hz}$  for both links. Increasing the distance between relay and UEs  $R_{max}$  leads to a significant drop in throughput. While the communication between UE2 and UE3 fails completely around  $R_{max} = 12m$ , the throughput of the pico-UE1 link is halved.

This is due to the fixed pico-relay link which is independent of the distance of the UEs from the relay. Since UE1 has a slightly higher transmit power than the relay, communication from UE1 to pico is successful until approximately  $R_{\max} = 18m$ . This behaviour is independent of the actual transmission scheme but is due to the chosen setup. The OFDMA-based schemes experience the same behaviour, as can be seen in the figure.

The performance results for the OFDMA-based legacy solution are given for two different modulation schemes and two different code rates. Specifically, QPSK and 16-QAM modulation are shown. Higher order modulation schemes as 64-QAM already fail after a few meters distance between relay and UEs and are, hence, omitted here. The applied code is the LTE turbo code with base code rate of  $R_c = 1/3$  and a punctured version of this code with code rate  $R_c = 2/3$ . As can be seen, the QPSK-based transmission as well as the 16-QAM-based transmission with the base code rate achieve a significantly lower throughput than the optimized IDMA system. At the working point, the throughput of the IDMA system is approximately 150% higher than the best OFDMA-based solution. The 16-QAM-based system with the punctured code of rate  $R_c = 2/3$  achieves a higher throughput than the IDMA system for the UE2-UE3 link, but already fails at the desired working point. Clearly, the IDMA system could then be optimized for a new working point  $R_{WP} = 5m$ , again outperforming the OFDMA system. Note that for most depicted schemes the throughput curves start at the same point for both communication pairs, e.g. TP = 0.5 bits/s/Hz for the IDMA system. For the OFDMA-based solution with 16QAM and the punctured code of rate  $R_c = 2/3$  this is not the case. Here the throughput of the Pico-UE1 transmission is only half of the throughput of the UE2-UE3 transmission. The reason for this behaviour is the fixed distance between Pico and relay of  $d_{PR} = 10m$ . For this distance the combination of modulation and coding fails for the chosen transmit power of the relay of 20dBm such that the transmission from UE1 to Pico is always in outage. The transmit power of the Pico of 37dBm, however, is higher than the transmit power of the relay, such that the transmission from Pico to UE1 is not in outage for small  $R_{\max}$ . Hence, the average throughput of both directions for the pico-UE1 pair is only half of the average throughput of the UE2-UE3 pair for 16QAM,  $R_c = 2/3$  and small  $R_{\max}$ .

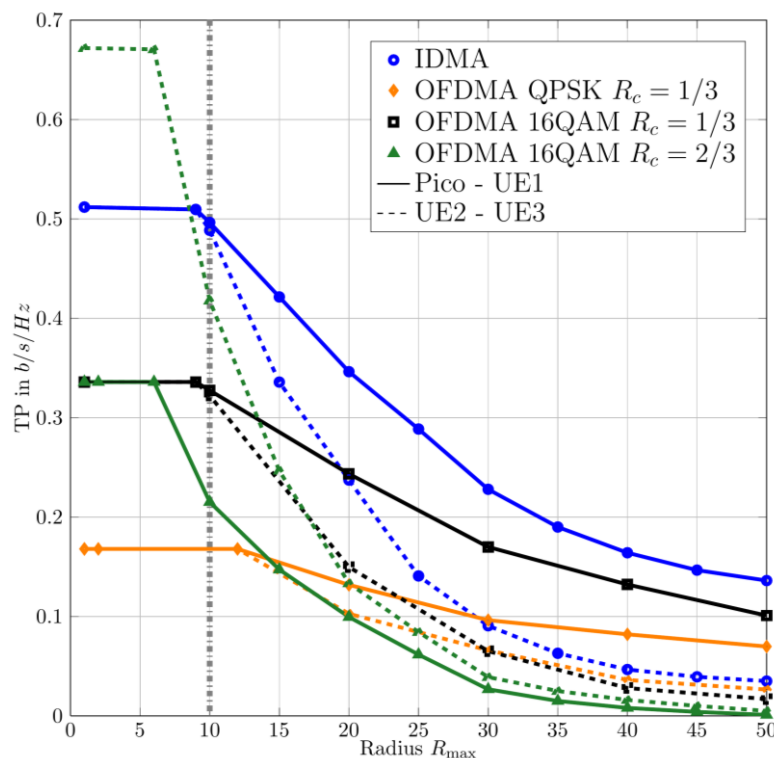
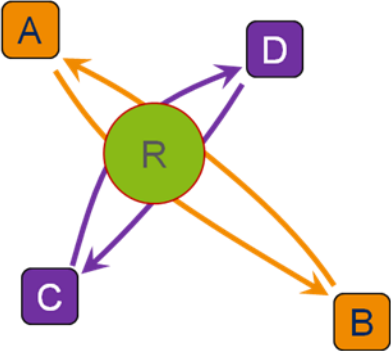


Figure 9-20: Average end-to-end throughput in bits/s/Hz of optimized TWR IDMA vs. legacy OFDMA-based solution over the distance of the UEs to the relay. Random distance  $d_{UR} \leq R_{\max}$ .

Now, the placement of the UEs is loosened. Specifically, the radius  $R_{max}$  is the radius of a circle, in which all UEs are randomly and uniformly distributed. Figure 9-20 again depicts the average end-to-end-throughput of the optimized TWR IDMA system and the legacy OFDMA-based solution for different modulation and coding schemes. Clearly, as the radius  $R_{max}$  is now the maximum distance between relay and UEs, the achieved performance is principally increased for all schemes. The gap between the IDMA solution and the best OFDMA-based solution (16-QAM, base code rate) is now decreased to approximately 50% at the working point. For the 16-QAM based system with the punctured code, the performance gap is decreased to 20% for the UE2-UE3 link at the working point. However, the performance of the OFDMA solution is much more sensitive to the decrease in SINR and, thus, decreases much faster than the performance of the IDMA system. For the pico-UE1 link, the gain of the IDMA system is approximately 177%.

Finally, it is important to point out, that the investigated system highly favours the OFDMA-based solutions as no impairments as, e.g., timing and frequency offsets, Doppler effects, etc. are considered. The IDMA solution is much more robust against these effects and, hence, more realistic simulations would likely lead to even higher gains for the IDMA system compared to the OFDMA solution.

T3.3 TeC 5 – Bi-directional relaying with non-orthogonal multiple access	
	<p style="text-align: center;"><b>Main Idea</b></p> <p>This work focuses on bidirectional relaying with multiple data flows and multiple communication pairs employing Interleave Division Multiple Access (IDMA) as non-orthogonal multiple access. The application of IDMA offers a high degree of flexibility and allows for the combination with known approaches, such as network coding, in order to create efficient combinations of the multiple access (MAC) and broadcast (BC) phases. The impact of IDMA is analysed in combination with network coding to identify efficient strategies regarding MAC/BC structuring, resource allocation and channel coding for bi-directional communication.</p>
Considered SoA solution	“Four-phase” OFDMA-based TWR system with LTE-A parameters.
KPIs considered and achieved gain	Spectral Efficiency/User Throughput: Expected gain > factor 2 compared to legacy OFDMA-based TWR system with LTE-A parameters.
Performance evaluation approach	Semi-analytical / simulation-based
System model considered	WP3 Task Simulation Baseline
Deviation compared to Simulation Baseline	None
Brief update of the results with respect to D3.2	Results have been updated under simulation alignment consideration
Association to the TeC Approach	TeC Approach 1: “Heterogeneous network at lower frequencies (< 10GHz)”



Targeted TCs	TC2
Impacted HTs	D2D (,UDN)
Required changes for the realization with respect to LTE Rel. 11	Major. IDMA is a new air interface and, thus, a potential replacement for OFDMA which is the basis for LTE-A.
Trade-off required to realize the gains	Most of the gains in the proposed IDMA-based system stem from a rather involved receiver processing. Hence, the receivers are required to offer a certain computational power to fully exploit the power of IDMA. A seamless trade-off between receiver complexity and gains is possible.

### 9.5.3 Impact on Horizontal Topics

T3.3 TeC 5 - HT.D2D	
Technical challenges	Very dense deployment of nodes operating on very wide bands in order to increase throughput and capacity.
TeC solution	IDMA as a non-orthogonal channel access scheme in combination with network coding allows for a very flexible design of MAC and BC phase in order to support a dense node deployment and flexible rate requirements.
Requirements for the solution	Limited mobility
KPIs addressed and achieved gain	Spectral efficiency / User throughput: achieved gain > factor 2 compared to legacy OFDMA solution
Interaction with other WPs	<ul style="list-style-type: none"> <li>• WP1: channel models provided by WP1 are used within the T3.3 simulation alignment.</li> <li>• WP2: D2D research activities within WP2 might benefit from developed solutions.</li> </ul>

### 9.5.4 Addressing the METIS Goals

T3.3 TeC 5	
1000x data volume	Due to IDMA in combination with NC and proper system optimization, the overall data volume can be increased significantly.
10-100 user data rate	Layered transmission in combination with system optimization allows to seamlessly adapt the user data rate to the given channel conditions. This helps to increase the user data rate.
10-100x number of devices	
10x longer battery life	
5x E-E reduced latency	
Energy efficiency and cost	



### 9.5.5 References

[PLW+06] L. Ping, L. Liu, K. Wu and W. Leung, "Interleave-Division Multiple Access", IEEE Transactions on Wireless Communications, vol. 5, no. 4, pp. 938-947, Apr. 2006.

[JKM00] H. Jin, A. Khandekar and R. McEliece, "Iregular Repeat Accumulate Codes", Second International Symposium on Turbo Codes, Brest, France, Sep. 2000.

[ACL+00] R. Ahlswede, M. Cai, S.-Y. Li and R. Yeung, "Network Information Flow", IEEE Transactions on Information Theory, vol. 46, no. 4, pp. 1204-1216, Jul. 2000.

[FBW06] C. Fragouli, J. Boudec and J. Widmer, "Network Coding: An Instant Premier", ACM SIGCOMM Computer Communication Review, vol. 36, no. 1, pp. 63-68, Mar. 2006.

[LBW+13] F. Lenkeit, C. Bockelmann, D. Wübben and A. Dekorsy, "IRA Code Design for IDMA-based Multi-Pair Bidirectional Relaying Systems", International Workshop on Broadband Wireless Access (BWA 2013) co-located with IEEE Globecom 2013, Atlanta, GA, USA, 9.-13. Dec. 2013.

[METIS13-D32] METIS D3.2, "First performance results for multi-node/multi-antenna transmission technologies", Apr. 2014.

[METIS13-D61] METIS D6.1, "Simulation Guidelines", Oct. 2013.

## 9.6 T3.3 TeC 6 MIMO physical layer network coding based underlay D2D communication [UOULU]

The work on this TeC is completed. Please refer to [METIS14-D32] for the most updated results.

## 9.7 T3.3 TeC 6b: MIMO PLNC based D2D communication [UOULU]

### 9.7.1 General Overview

Many studies on D2D have considered that D2D communication uses the same frequency spectrum as in the cellular communication. This improves the frequency reuse within the same cell in a more effective manner. A consequence, though, is that the D2D transmit powers need to be constrained to have reliable cellular communication. Accordingly, the D2D communication is only possible, when the devices are located near each other. However, a relay placed in between D2D pair can extend the coverage area with less transmit power. This facilitates longer distance communication through D2D mode. In [JJR+13], we focused on the underlay MIMO relaying based D2D communication. The half-duplexing issue of relay is avoided by performing physical layer network coding (PLNC) at the relay node [ZLL06, ZLL08]. The results have revealed that placing a relay in between the D2D pair allows longer distance communication through the D2D mode. This would be particularly useful near the cell edge. Moreover, since device information does not route through the BS, we can expect a lower level of coordination between BS and D2D pair. This can undermine the secrecy of the communication in unsafe situations, where the possibilities of eavesdropping on the device information can be high.

Recent studies on physical layer security [MS11, WWZ13] have shown advantages of using security features at the physical layer. In particular, they used beamforming techniques to weaken the received signals at the eavesdroppers. Such methods can be also used to prevent eavesdropping on the D2D communication.

Here, we study secure beamforming design to prevent eavesdropping on the MIMO PLNC based D2D communication. Multiple eavesdroppers are attempting to intercept the device information. Since PLNC based two-way relaying (TWR) system performs XOR operation on the device information, a given eavesdropper must successfully decode at least one device message during the multiple access (MA) stage in order to decode the other message during the broadcasting (BC) stage. Therefore, PLNC based TWR have an added security feature which is not available with any other TWR scheme. As discussed in [JJR+13], an accurate PLNC operation requires minimizing mean square error (MSE) at the relay. The secrecy of the D2D communication is enhanced by employing beamforming at the nodes, which generate weak signals at eavesdroppers. Therefore, we consider optimization problems to minimize MSE, and adopt signal-to-noise ratio (SNR) threshold policy to prevent possible eavesdropping. However, the channel state information (CSI) of device-eavesdropper channels is imperfect at the device side. We use ellipsoidal channel uncertainty model, and formulate a robust optimization problem which we solve through an iterative method. Numerical experiments are carried out to investigate the convergence of the proposed algorithm and signal-to-interference-plus-noise ratio (SINR) distribution at a given eavesdropper.

We consider two devices, which communicate in an unsecured environment using a trusted relay node as shown in Figure 9-21. Multiple eavesdroppers attempt to intercept the information of the devices. Bi-directional communication of the devices is assumed with time division duplex (TDD) mode and the relay performs PLNC mapping. The  $i$ th device is denoted as  $D_i$  and the  $k$ th eavesdropper is denoted as  $E_k$  with  $k = 1, 2, \dots, K$ . Single stream transmissions are assumed with perfect synchronization at the relay node.

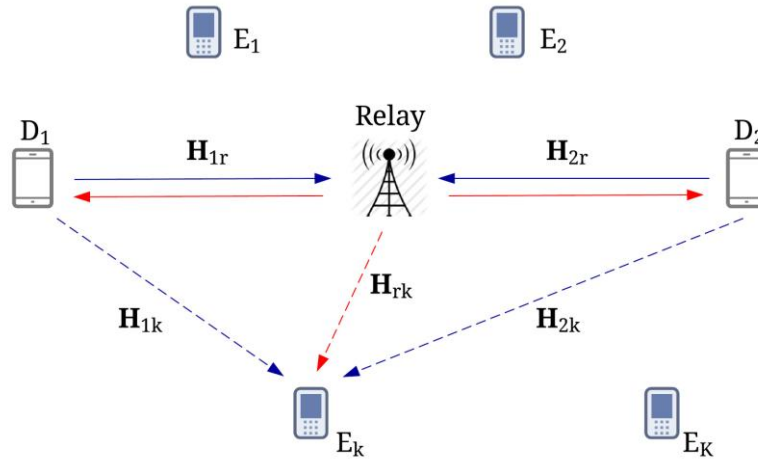


Figure 9-21: A relay assisted D2D communication in unsecured environment. Multiple eavesdroppers.

### 9.7.2 Performance Results

We first analyze the convergence of the proposed secure beamforming Algorithm [JJR+14]. Next, Monte Carlo simulations are used with the proposed algorithm to illustrate the error performance of the D2D communication. Moreover, these simulations are applied to investigate the SINR distributions at a given eavesdropper. We consider TWR system with a single eavesdropper, where all nodes are equipped with two antennas. All channels are assumed to undergo Rayleigh fading with entries  $\sim CN(0,1)$ . The error component of  $\mathbf{H}_{ik}$  is generated using truncated Gaussian distributions with entries  $\sim CN(0,1)$ . The variance of the noise is considered equal at all nodes ( $\sigma^2$ ). Algorithm is used to find beamforming vectors for each channel realization. Furthermore, the device symbols are created with BPSK modulation with unit power. The relay node performs ML estimation to find the XOR of transmitted messages. The numerical examples are performed for 10000 channel realizations.

In Figure 9-22, the convergence of the average MSE is illustrated with the number of iterations. Channel error bound and SINR constraint at the eavesdropper are denoted by  $\varepsilon^2$  and  $\gamma$ , respectively. The maximum transmit power constraint at nodes is considered as  $P_{max}$ . Different  $\varepsilon^2$  and  $\gamma/\sigma^2$  values are considered when  $P_{max}/\sigma^2 = 10 \text{ dB}$ . The algorithm converges with a few number of iterations for all cases. The MSE decreases with  $\gamma/\sigma^2$ . For fixed  $P_{max}/\sigma^2$  and  $\gamma/\sigma^2$ , the MSE decreases with  $\varepsilon^2$ . When  $\varepsilon^2$  is high, the devices are uncertain about the eavesdropper channel. Then, the devices reduce their transmit powers to prevent eavesdropping. In such cases, the received signal power at the relay also reduces, which degrades its performance.

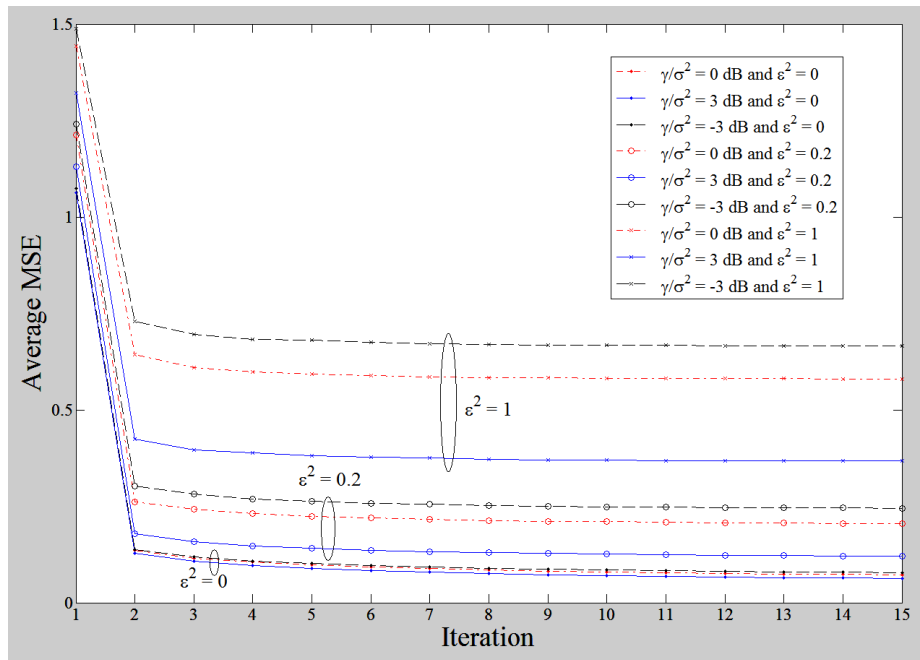


Figure 9-22: Convergence of the Algorithm.  $K = 1$  and  $P_{max}/\sigma^2 = 10 \text{ dB}$ .

Figure 9-23 shows the average BER at the relay versus  $P_{max}/\sigma^2$ . The BER represents the PNC mapping error at the relay node. Two sub-optimal beamforming schemes are compared with the proposed secure beamforming scheme. The first sub-optimal scheme uses zero forcing (ZF) precoding at the devices. The second scheme is the unsecured optimal beamforming scheme, where the design does not consider the SINR policy to prevent eavesdropping. Both are unsecured schemes since they do not prevent the eavesdropping of device information. The unsecured optimal beamforming design provides the best BER performance to the TWR system. The unsecured ZF provides a lower performance than the rest during the low SNR region. There is a maximum error performance level that the secured optimal beamforming designs can achieve. Therefore, we expect ZF to provide better performance in the high SNR region than the proposed beamforming scheme. The eavesdropper SINR threshold  $\gamma/\sigma^2$  is varied from 0 to 3dB in the secured beamforming scheme, where the performance is improved with  $\gamma/\sigma^2$ . However, when the  $\epsilon^2$  is higher, the BER performance degrades. These observations are similar to the Figure 9-22.

Finally, Figure 9-24 shows the cumulative distribution function (c.d.f.) of the received SINR at the eavesdropper. We assume  $P_{max}/\sigma^2 = 10 \text{ dB}$  and  $\gamma/\sigma^2 = 0 \text{ dB}$ . In the perfect CSI scenario, the maximum received SINR at the eavesdropper is limited at the desired level (0 dB in this simulation). However, when  $\epsilon^2$  is higher, the maximum received SINR at the eavesdropper is lower than the desired level (for interception). This reflects that the beamforming design provides higher security even with the imperfect CSI. In the sub-optimal scenarios, it is clear that the SINR is not limited at the eavesdropper. This allows eavesdropper to intercept information.

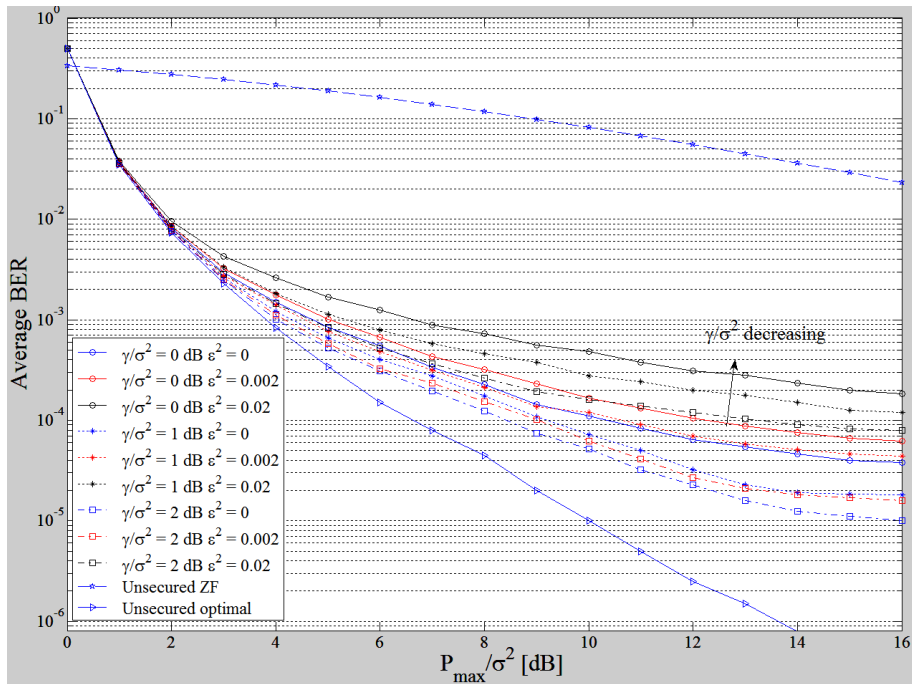


Figure 9-23: Average BER versus  $P_{max}/\sigma^2$

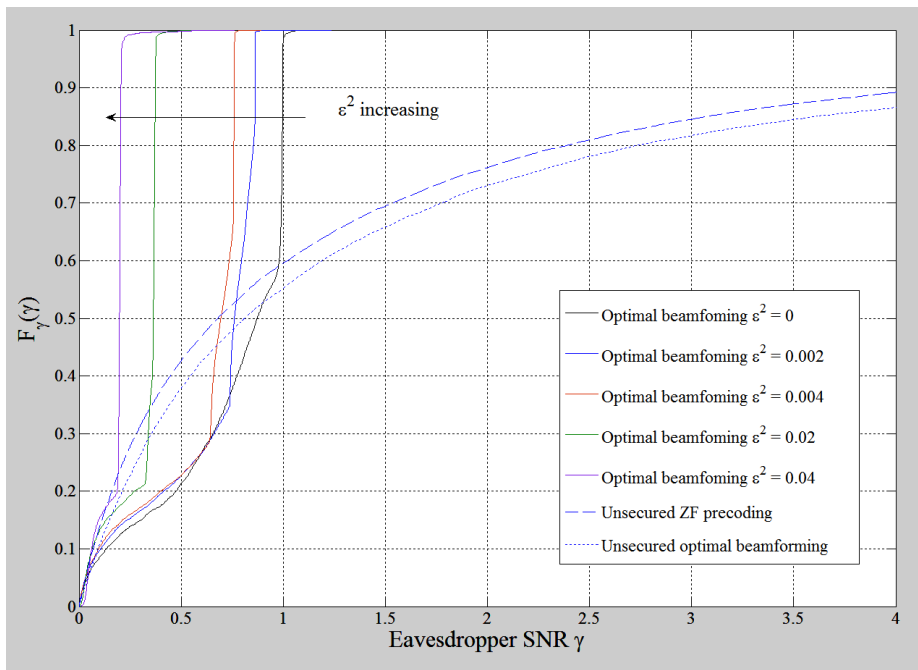
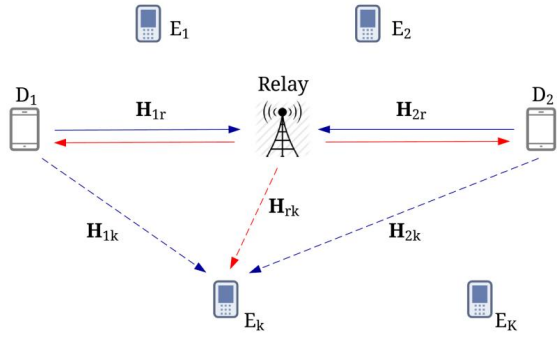


Figure 9-24: c.d.f. of the received SINR at the eavesdropper

### T3.3 TeC 6 – MIMO PLNC based D2D Communication

#### Main Idea

The main idea is to develop multiple antenna techniques at the transmitting or receiving nodes to expand D2D coverage

	<p>and provide reliable communication. The relay node uses physical layer network coding to deliver high spectrum efficiency.</p> <p>During the first transmission phase, the two devices transmit simultaneously. Multiple eavesdroppers are attempting to intercept the device information. Beamformers are designed to provide secure communication between devices.</p>
<p>Considered SoA solution</p>	<p>Comparison with the unsecured beamforming designs.</p>
<p>KPIs considered and achieved gain</p>	<p>Coverage enhancement of D2D communication. 100% expansion. Security of the information. 100% secure in the physical layer.</p>
<p>Performance evaluation approach</p>	<p>Analytical &amp; Simulation-based</p>
<p>System model considered</p>	<p>Other</p>
<p>Deviation compared to Simulation Baseline</p>	<p>Some:</p> <ul style="list-style-type: none"> <li>• Model of environment: Not applicable</li> <li>• Spectrum assumptions: Any</li> <li>• Propagation model: Rayleigh</li> <li>• Deployment model: Single cell</li> <li>• User/Device distribution: Uniform</li> <li>• Traffic model: No traffic model</li> </ul>
<p>Brief update of the results with respect to D3.2</p>	<p>Previously, the coverage expansions of PLNC D2D mode were investigated. New results are considered with secure beamforming designs.</p>
<p>Association to the TeC Approach</p>	<p>Heterogeneous network at lower frequencies (&lt; 10GHz)</p>
<p>Targeted TCs</p>	<p>TC9 : open-air festivals</p>
<p>Impacted HTs</p>	<p>D2D</p>
<p>Required changes for the realization with respect to LTE Rel. 11</p>	<p>Major</p>
<p>Trade-off required to realize the gains</p>	<p>At least imperfect CSI of device-to-relay and device-to-eavesdropper channels are required. Beamforming vectors are exchanged among devices and relay.</p>

### 9.7.3 Impact on Horizontal Topics

<p style="text-align: center;"><b>T3.3 TeC 6 - HT.D2D</b></p>	
<p>Technical challenges</p>	<ul style="list-style-type: none"> <li>• Handle information security issues on the uncoordinated D2D communication</li> <li>• Increase the possible D2D communications via expanding coverage.</li> </ul>



TeC solution	Secure beamforming design is proposed to prevent eavesdropping in MA stage. Utilize PLNC security features to provide secrecy during BC stage.  PLNC based relaying uses low transmit power, which allows far apart devices to communicate via D2D mode.
Requirements for the solution	CSI knowledge. Partial or perfect.
KPIs addressed and achieved gain	<ul style="list-style-type: none"> <li>Coverage enhancement of D2D communication: 100% expansion.</li> <li>Security of the information: 100% secure in the physical layer.</li> </ul>
Interaction with other WPs	None

### 9.7.4 Addressing the METIS Goals

T3.3 TeC 6	
1000x data volume	
10-100 user data rate	
10-100x number of devices	Expand the coverage area for D2D provide higher number of D2D connections.
10x longer battery life	
5x E-E reduced latency	
Energy efficiency and cost	D2D pair transmits with low power saves energy.

### 9.7.5 References

[JJR+13] L.K.S. Jayasinghe, P. Jayasinghe, N. Rajatheva, M. Latva-Aho, "MIMO physical layer network coding based underlay device-to-device communication," in Proc. IEEE 24th Inte. Sym. Per. Indo. and Mob. Rad. Comm. conf. (PIMRC), pp. 89–94, Sep. 2013.

[ZLL06] S. Zhang, S.C. Liew, and P.P. Lam, "Hot topic: physical-layer network coding," in Proc. Mobicomm 2006, p. 365, Sep. 2006.

[ZLL08] S. Zhang, S. C. Liew, and L. Lu, "Physical layer network coding schemes over finite and infinite fields," in Proc. IEEE Global Telecom. Conf. (GLOBECOM), pp. 1–6, Dec. 2008.

[MS11] A. Mukherjee, A.L. Swindlehurst, "Robust beamforming for security in MIMO wiretap channels with imperfect CSI," IEEE Trans. Sign. Proce., vol. 59, no. 1, pp. 351–361, Jan. 2011.

[WWZ13] X. Wang, K. Wang, X. Zhang, "Secure relay beamforming with imperfect channel side information," IEEE Tran. Vehi. Techn. vol. 62, no. 5, pp. 2140–2155, Jun. 2013.

[JJR+14] L.K.S. Jayasinghe, P. Jayasinghe, N. Rajatheva, M. Latva-Aho, "Secure beamforming design for physical layer network coding based MIMO two-way relaying," IEEE Comm. Lett., vol. 18, no. 7, pp. 1270–1273, Jul. 2013.

## 9.8 T3.3 TeC 7: Cooperative D2D communications [KTH]

### 9.8.1 General Overview

Crowded communication environments can easily get congested when the number of radio connections is increased. We propose in this project a cooperative device-to-device (D2D) communications framework in order to combat this problem. The idea is to allow a D2D transmitter to act as an in-band relay for a cellular link and at the same time transmits its own data by employing superposition coding as a form of multiplexing technique in the downlink. This way we can increase the number of connections within the cell without extra radio resources. It could also be beneficial to offload over-loaded cells

Our solution is different from underlay D2D communications where strict interference management is needed. Cooperation between the cellular link and D2D transmitter eases down the requirement on the interference where a better interference control is possible.

We assume that there are  $M$  cellular users (CUEs) that communicate in the conventional way through the base station. Besides,  $N$  transmitter-receiver pairs in the cell operate in the D2D transmission mode. There is no dedicated channel for direct communications between those devices. Therefore, the D2D users cooperate with one of the cellular users in order to transmit their own data while relaying the cellular data simultaneously in the downlink, provided that the cellular user's rate is not degraded.

It is assumed that the D2D transmitter uses the decode-and-forward (DF) relaying protocol. The cooperating D2D transmitter decodes the message broadcasted by the source node, then, transmits the decoded message to the destination. We assume that the D2D transmitter is operating in a half-duplex mode in which it cannot transmit and receive at the same time. The transmission scheme is based on TDMA. Two access schemes are considered in our work. The first access scheme is *superposition coding* where, in case of cooperation, two consequent and equal-sized time slots are used as one transmission frame as illustrated in Figure 9-25. The base station transmits in the first time slot. This signal is received by both the intended cellular user and the D2D transmitter. The signal is decoded and re-encoded by the D2D transmitter. In the next time slot, the D2D transmitter employs superposition coding in order to transmit a linear combination of its own signal and the signal of the cellular user. Here the D2D transmitter splits his power between the two signals. The power splitting should ensure that the link quality of the cellular user is not affected as compared to the regular direct link alone. The second access scheme is based on *orthogonal split of resources*. Here, the frame is divided into three time slots as illustrated in Figure 9-26. The base station transmits in the first time slot. The signal is received by both the cooperating D2D transmitter and the intended cellular user. The signal is then forwarded by the D2D transmitter in the second time slot. The cellular user then employs maximum ratio Combining (MRC) to combine the received signals from the two time slots (direct & forwarded). The third time slot is reserved for direct D2D communications where multiple D2D links can communicate simultaneously. In the orthogonal split access scheme, the D2D links do not experience any interference from the cellular user which is an advantage in comparison with conventional underlay D2D communications. In both access schemes, the main objective is to select the D2D transmitter that can maximize the data rate(s) of the D2D link(s) while ensuring the same or a better link for the cooperating cellular user.

From the two access schemes we can see that superposition coding can double the number of connections per frame within the cell while orthogonal split can increase the number of connections per frame up to  $N+1$  connections.

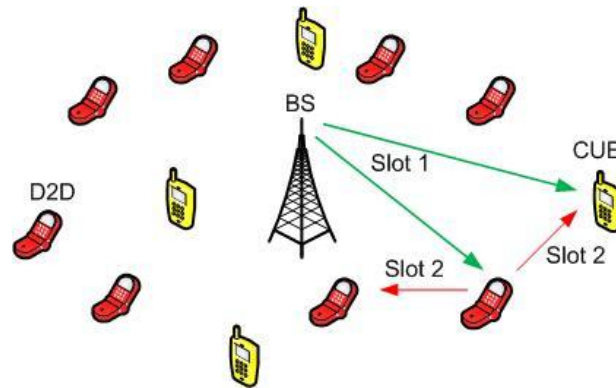


Figure 9-25: Cooperative D2D communications with superposition coding

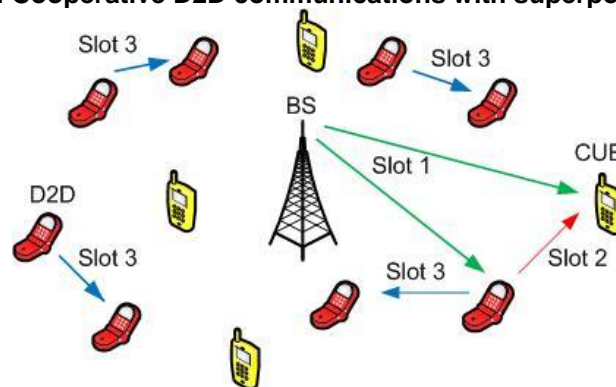


Figure 9-26: Cooperative D2D communications with orthogonal split of radio resources

### 9.8.2 Performance Results

We evaluate the cooperation performance between cellular users (CUEs) and the D2D users within cellular systems. We look at the achievable gain in number of connections for a given radio resource in crowded environments for different system parameters by means of Monte-Carlo simulations. The KPI measure is the achievable rate for the D2D link and the CUE which is measured in bits/s/Hz. For the cooperation with orthogonal split we look at the sum rate of the different D2D links that share the radio resource. A single hexagonal cell with radius  $R$  is considered where the base station lies in the corner of the cell. In each realization,  $M$  CUEs and  $N$  D2D pairs are generated randomly uniformly distributed over the cell area. The distance of the D2D receiver from its transmitter lies in the range  $[20, 50]$  meters. Both base station and D2D transmitter use their maximum power for transmission. The fraction of the D2D transmit power that is assigned to either of the cooperative users is optimized. Simulation parameters are given in the following table.

Table 9.4: Simulation parameters

Description	Parameter	Value
Max. UE TX power	$P_{max}^d$	24 dBm
BS TX power	$P_{max}$	41 dBm
Cell radius	$R$	200, 500 m
Noise power	$N_0$	-118 dBm
Carrier frequency	$f_c$	2 GHz
D2D pair distance	$d_{d2d}$	20 – 50 m

Shadowing (BS and devices)	$\sigma_{sh}$	10
Shadowing (devices)	$\sigma_{sh}$	12
Correlation distance	$d_{corr}$	20 m
Monte-Carlo runs	$MC$	20000

The channel model accounts for the effects of path loss, multi-path fading, and shadowing. The path loss model for D2D communications is based on the model used in [XH10] which is based on the ITU recommendations for micro urban environment [ITU09-2135]. The log-normal shadowing  $X \sim N(0, \sigma_{sh})$  is generated based on a correlated model described in [ZK01]. We use the same shadowing variance for line-of-sight and non-line-of-sight channels. The multi-path fading component is modeled as Rayleigh fading (distributed as  $CN(0,1)$ , where both its real and imaginary components are i.i.d. Gaussian distributed with  $N(0, 1/\sqrt{2})$ ). We assume a Rayleigh block fading channel where the channel is constant during one time slot, but varies over different time slots.

For cooperative D2D communications with superposition coding, the total frame is divided into two equal time slots. Hence, the performance of the two cooperating users (CUE, D2D user) depends on the power allocation in the superposition process, i.e.,

$$\sqrt{\beta}x_{D2D}(t) + (1 - \sqrt{\beta})x_{CUE}(t)$$

In allocating this power we make sure that the performance of the cooperative CUE does not change in comparison to the non-cooperative case (direct link using the whole frame). It is clear that the CUE that gives the lowest  $\beta$  is the best CUE to cooperate with. Figure 9-27 shows the CDF of the fractional of optimal power that is assigned to the D2D links for its own communication versus different number of cellular users in the cell and different number of D2D pairs for the case of cooperation with superposition coding [SB14]. As the results indicate, the cooperation opportunities increase with the number of users. For low density of users, e.g.,  $M = 20$  &  $N=1$ , we see that  $\beta \geq 0.5$  for about 70% of realizations. Having two D2D pairs within the cell increases the possibility of cooperation between the cellular users and the D2D transmitters making  $\beta \geq 0.5$  for about 90% of realizations. Increasing the user density of cellular users within the cell, e.g.,  $M = 100$ , the cooperation can be formed in about 98% of instances. Higher user density eases the pairing of cellular/D2D users for cooperation when superposition coding is employed.

Figure 9-28 illustrates the cumulative distribution function (CDF) of the fraction of time allocated to D2D transmission (third slot) for different number of cellular users and number of D2D pairs when orthogonal split accessing is employed. We notice similar behaviour here as compared to superposition coding. The probability of cooperation increases with the number of users and gets very close to one.

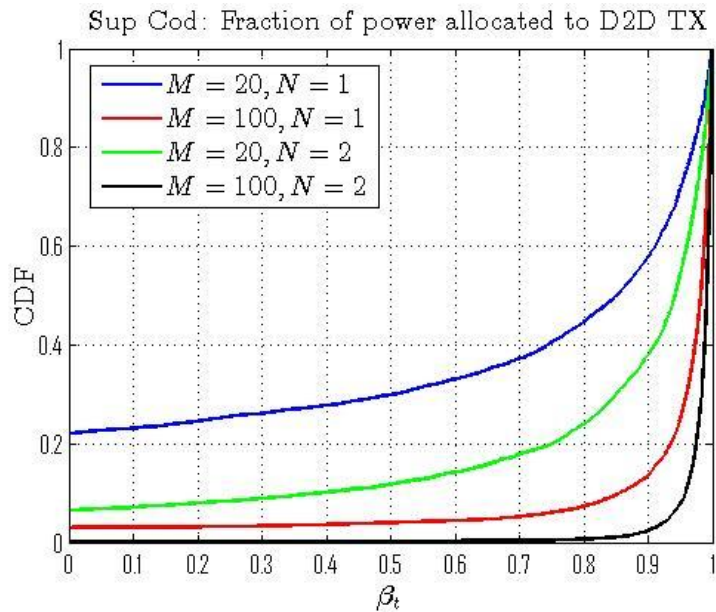


Figure 9-27: CDF of the fractional of allocated power for cooperative D2D communications with superposition coding for  $R=500m$

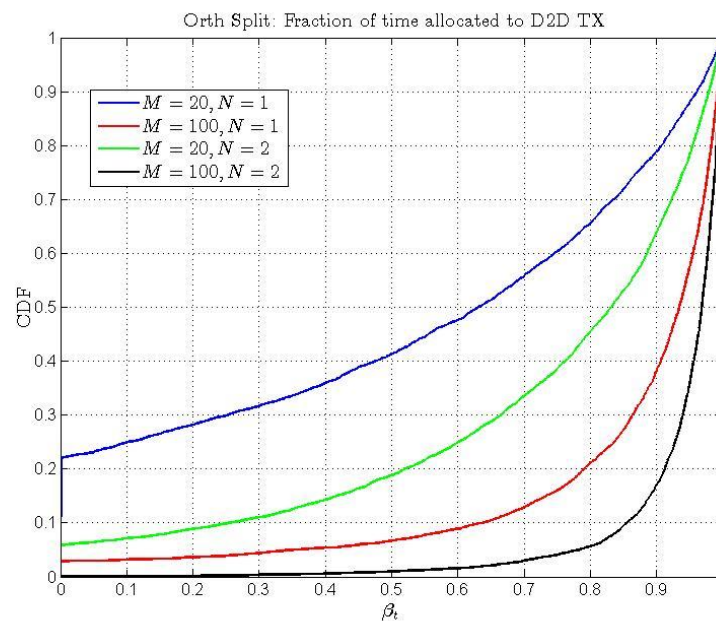
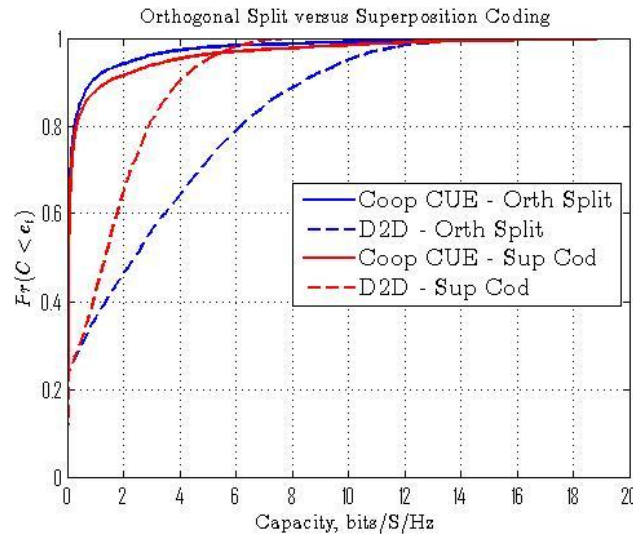


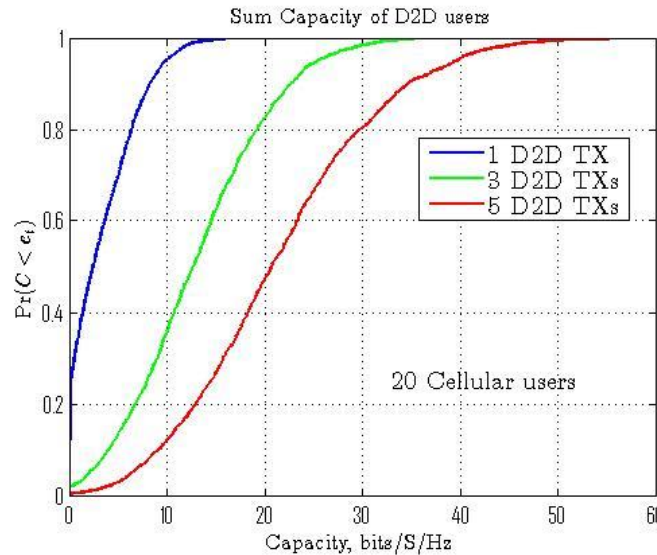
Figure 9-28: CDF of the fractional of allocated time for cooperative D2D communications with orthogonal split for  $R=500m$

Figure 9-29 shows the CDF of the normalized data rate of the cooperating CUE and the D2D link for the two schemes when  $M=20$  and  $N=1$ . As observed, the two schemes ensure that the CUE achieves its direct link data rate while the D2D user can also transmit with high data rate. This leads to an increase in cell throughput. It is also observed that cooperation with orthogonal split performs better than cooperation with superposition coding. This is due to the fact that orthogonal split does not experience any interference from the CUE.



**Figure 9-29: CDF of normalized data rate of the two access schemes in a single cell with  $R=500m$ , when  $M=20$  and  $N=1$**

Figure 9-30 shows how the sum capacity of the D2D users changes with the number of D2D pairs within the cell when  $M=20$  CUEs. As observed, by going from one to 5 D2D pairs, the average D2D sum capacity is increased by more than 8 times. This gain is due to the absence of interference from the CUE and the proximity of D2D communications. Cooperative D2D communications with orthogonal split appear to have good potential especially in areas when proximity communications exist.



**Figure 9-30: CDF of the normalized sum data rate of the D2D users for the orthogonal split scheme in a single cell with  $R=500m$ , when  $M=20$  and  $N=1, 3, 5$**

Figure 9-31 illustrates the average user (D2D and CUE) data rate of the cooperative D2D communications with orthogonal split for different number of D2D pairs. It is observed that the cooperation does not affect the average data rate of the cellular users. Furthermore, the average data rate of the D2D user increases with the number of cellular users. More cellular users give the possibility to the cooperating D2D transmitter to find a good cellular user to cooperate with.

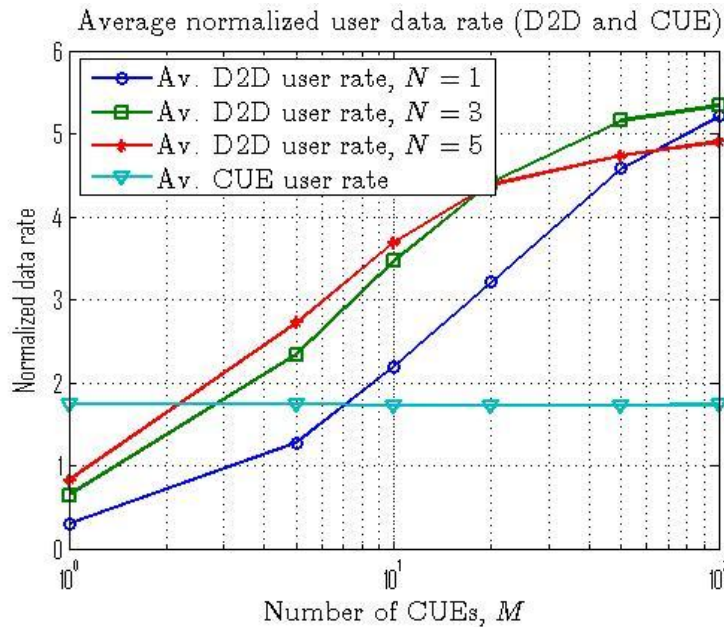
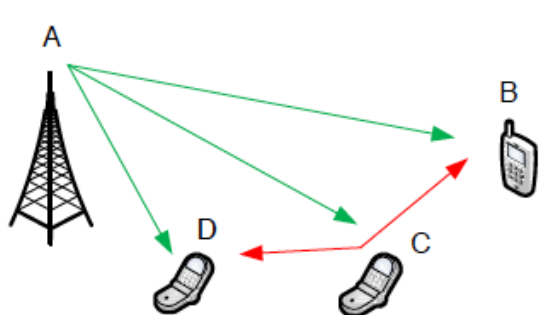


Figure 9-31: Average normalized user (D2D and CUE) data rate of the cooperative D2D communications with orthogonal split as a function of the number of CUEs within the cell,  $M$ , and for different number of D2D pairs

T3.3 TeC 7 – Cooperative D2D Communications	
 <p>Links AB and CD share the same radio resource via cooperation</p>	<p><b>Main Idea</b></p> <p>D2D communication is achieved through cooperation where the interested device relays information from the base station to a mobile user and at the same time gets the opportunity to communicate directly with another device. Hence, by acting as a relay the mobile device can achieve D2D communication with no extra resources. Orthogonal spectrum splitting and superposition coding is considered in the cooperation process.</p>
Considered SoA solution	Comparison with a conventional single cell cellular system with direct links only.
KPIs considered and achieved gain	<ul style="list-style-type: none"> <li>User data rate: Cellular rate unchanged, D2D rate increases in a best effort manner.</li> <li>Cell throughput: Gain equals to or more than 100%</li> <li>Number of connections/radio resource/cell: Gain equals to or more than 100%</li> </ul>
Performance evaluation approach	Analytical & Simulation-based
System model considered	Other
Deviation compared to Simulation Baseline	<p>Minor:</p> <ul style="list-style-type: none"> <li>Model of environment: Urban Macro Area</li> <li>Spectrum assumptions: 2 GHz</li> </ul>



	<ul style="list-style-type: none"> <li>• Propagation model: Based on model in [XH10]</li> <li>• Deployment model: Single cell (Hexagonal)</li> <li>• User/Device distribution: Uniform</li> <li>• Traffic model: Full buffer</li> </ul>
Brief update of the results with respect to D3.2	New results for cooperative D2D communications with orthogonal split as multiple access scheme
Association to the TeC Approach	Heterogeneous network at lower frequencies (< 10GHz)
Targeted TCs	TC3 (Shopping Mall)
Impacted HTs	D2D
Required changes for the realization with respect to LTE Rel. 11	Minor: <ul style="list-style-type: none"> <li>• Support for direct D2D communications</li> <li>• Relaying capability for mobile devices</li> <li>• Possibility for interference cancellation at the mobile device</li> </ul>
Trade-off required to realize the gains	Compared to conventional cellular, one needs to know the transmission mode of each device within the cell, the interference situation of the different link to do the user pairing for cooperation (D2D, cellular).

### 9.8.3 Impact on Horizontal Topics

T3.3 TeC 7 - HT.D2D	
Technical challenges	<ul style="list-style-type: none"> <li>• Increase the number connected devices within the cell</li> <li>• Increase the cell throughput and the data volume</li> </ul>
TeC solution	A cooperative D2D communications scheme that allows coexistence of cellular users and D2D communications without the need for extra radio resources. Important gains are observed in TC2, which is relevant for D2D.
Requirements for the solution	<ul style="list-style-type: none"> <li>• Transmission mode selection for mobile users within the cell.</li> <li>• CSI of cellular links and D2D links.</li> <li>• Low UE mobility.</li> </ul>
KPIs addressed and achieved gain	<ul style="list-style-type: none"> <li>• User data rate: Cellular rate unchanged, D2D rate increases in a best effort manner.</li> <li>• Cell throughput: Gain equals to or more than 100%</li> <li>• Number of connections/radio resource/cell: Gain equals to or more than 100%</li> </ul>
Interaction with other WPs	<ul style="list-style-type: none"> <li>• WP2: The developed TeC assumes perfect link adaptation. Any air interface developed in WP2 can be employed here with no major changes.</li> <li>• WP4: Closer look is needed to see which interference management scheme can be</li> </ul>



	employed. <ul style="list-style-type: none"><li>• WP6: TeC targets frequencies below 10 GHz.</li></ul>
--	--

### 9.8.4 Addressing the METIS Goals

T3.3 TeC 7	
1000x data volume	Increase in number of connections by 100% or more is translated in an increase of the data volume per area
10-100 user data rate	
10-100x number of devices	Increase in number of connections by 100% or more within cell is obtained
10x longer battery life	
5x E-E reduced latency	
Energy efficiency and cost	Direct D2D communications can be translated in less activity at the base station which provides energy saving at the base station

### 9.8.5 References

[Hug87] D. Hughes-Hartog, "Ensemble modem structure for imperfect transmission media", US patent 4 679 227, July 7, 1987

[PPS07] S. Pfletschinger, A. Piątysek and S. Stiglmayr, "Frequency-selective Link Adaptation using Duo-Binary Turbo Codes in OFDM Systems", IST Mobile and Wireless Communications Summit, Budapest, July 2007

[WIN207-D61314] IST-4-027756 WINNER II, Deliverable D6.13.14 Version 1.0 "WINNER II system concept description", November 2007

[3GPP09-36913] 3GPP TR 36.913, "Requirements for further advancements for Evolved Universal Terrestrial Radio Access (E-UTRA) (LTE-Advanced) (Release 9)", Oct. 09.

[XH10] H. Xing and S. Hakola, "The investigation of power control schemes for a device-to-device communication integrated into OFDMA cellular system," in *Proc. IEEE PIMRC*, Istanbul, Turkey, Sep. 2010, pp. 1775–1780.

[ITU09-2135] ITU-R, "Guidelines for evaluation of radio interface technologies for IMT-Advanced," <http://www.itu.int/pub/R-REP-M.2135/>, International Telecommunication Union, Tech. Rep., 2009.

[ZK01] J. Zander and S. L. Kim, *Radio resource management in wireless networks*. Artech House, 2001.

[SB14] S. Shalmashi and S. Ben Slimane, "Cooperative Device-to-Device Communications in the Downlink of Cellular Networks," *IEEE WCNC2014*, Istanbul, Turkey, April 6-9 2014.

## 9.9 T3.3 TeC 8: Open-loop techniques in a network with D2D relaying [UPVLC]

This TeC has been stopped in T3.3. Please refer to [METIS14-D32] for the most updated results.

## 9.10 T3.3 TeC 9a: Studies of deploying moving relay nodes [CTH]

### 9.10.1 General Overview

As moving network (MN) is one of the important technical components to improve the network capacity and the QoS of vehicular UE (VUE), it is essential to understand what could be potential gains of deploying MN in a practical setup. Currently, a significant number of mobile users are vehicular, i.e., they use wireless broadband services while being in public transportation vehicles, e.g., buses, trams, or trains. In addition, it is expected that the number of vehicular users will greatly rise in the near future due to the high penetration of smartphones and the increasing portability of laptops. Hence public vehicles become natural hotspots for wireless data traffics.

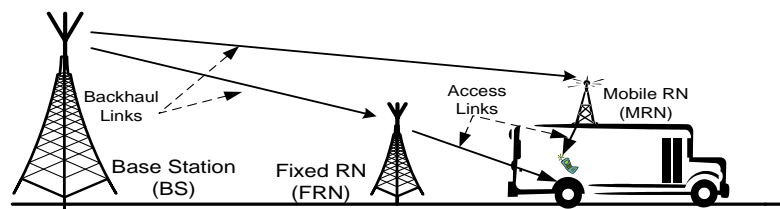
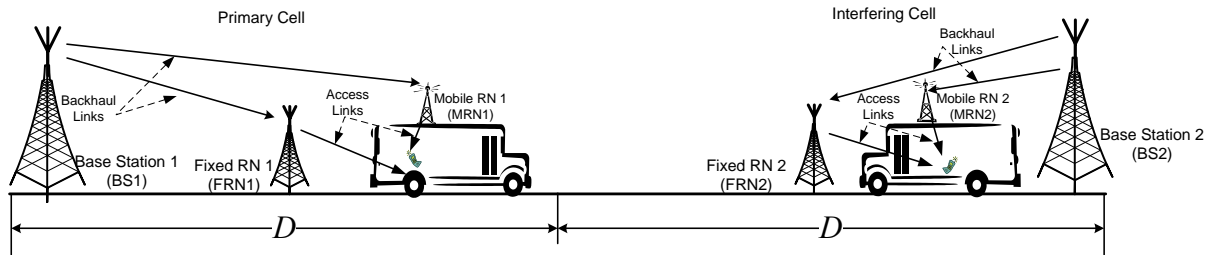


Figure 9-32: Energy efficiency study of MRN assisted transmission in a noise-limited setup

The use of moving relay nodes (MRNs) in cellular systems is still under discussion in the release 11 of the 3GPP LTE [3GPP12-36836]. Studies have shown that by deploying coordinated and cooperative relays on top of trains, the QoS of a user equipment (UE) inside the vehicle can be significantly improved [PHY+10]. In [SPS12], it showed that in a noise limited system, using MRNs can improve the spectral efficiency and lower the outage probability (OP) for vehicular UEs when the average transmit power of the BS and the relay node (RN) is fixed. One of the major advantages of using MRNs is to eliminate the effect of vehicular penetration loss (VPL), which significantly reduces the outdoor to indoor signal strength. Measurements show that VPL can be as high as 25 dB in a minivan at the frequency of 2.4 GHz [TJV+08], and higher VPLs are foreseeable in the well-isolated vehicles of our interest in higher frequency bands. By using two separate indoor and outdoor antennas connected through a cable introducing negligible losses, MRNs can reduce or eliminate VPL, and thereby improve the received signal strength at the vehicular UE. Furthermore, since an MRN can create its own cell within a vehicle, group handover (HO) of UEs served by the same MRN can be performed, which could lower the HO failure probabilities of the vehicular UEs [LZD+12]. Other benefits, such as collective channel state information (CSI) feedback for advanced backhaul design can also be achieved by using MRNs [SGO+12]. Thus, MRNs are potentially very beneficial to serve vehicular UEs.



**Figure 9-33: OP studies of MRN assisted RN transmission in a two-cell setup in the presence of co-channel interference**

In this contribution, we argue that relay nodes in general can significantly reduce the transmit energy of the network and maintain the desired QoS for VUEs. Moreover, we study the OP performance at a vehicular UE when the communication is corrupted by co-channel interference (CCI). The energy efficiency study of using MNRs is conducted in a noise limited system (See Figure 9-32). As the OP in a noise limited system has been studied in [SPS12], in this contribution, we study the OP performance at a vehicular UE when the communication is corrupted CCI (See Figure 9-33). The effects of pathloss, shadowing and small scale fading are taken into account and practical propagation conditions are considered for the links between different nodes. To facilitate our comparisons, in both cases, we optimize the FRN position. We show that as the VPL increases, the total transmit power in the system can be significantly lowered. Moreover, an MRN is better at lowering the OP of vehicular UEs than the BS-to-UE direct transmission as well as the FRN assisted scheme. Hence, we conclude that the use of MRNs is very promising for future mobile communication systems.

### 9.10.2 Performance Results

The channel model for the simulation of energy efficiency study is based on using the 3GPP SCM urban NLOS microcell channel model, and other parameters are summarized in Table 9.5 [3GPP12-25996]. The VUE is assumed to be uniformly distributed with respect to its distance from the BS. The MRN is mounted on top of a vehicle and is assumed to fully circumvent VPL. The positions of the FRN are determined according to the method given in [SPY+13] and plotted in Figure 9-34. An FRN performance lower bound is also simulated based on the study in [SPY+13], where the FRN is placed in a position to minimize the total transmit power in the system assuming the position of the VUE is known beforehand.

**Table 9.5: Simulation parameters**

Parameter	Value
Pathloss model	$PL_{dB} = 34.53 + 38 \log_{10}(d)$
Pathloss break point	$d_{break} = 20 \text{ m}$
Constant power loss K within break point, and between MRN and UE	$34.53 + 38 \log_{10}(d_{break}) = 83.9691 \text{ dB}$
Receiver noise figure for RNs and UE	9 dB
Outage probability target	0.05
Required rate at the UE	$R = 1 \text{ bit/sec/Hz}$

Figure 9-35, Figure 9-36 and Figure 9-37 plot the overall system average transmit power in one time slot, when the VPL is 0 dB, 10 dB, and 20 dB. The OP target is set to 0.05 for all three cases. If there is no power loss due to no VPL (Figure 9-35), the conventional direct transmission (one-hop case) achieves the lowest total average transmit power when the UE is within about 410 meters from the BS. As the use of FRN compensates for the pathloss, the

FRN assisted transmission outperforms the direct transmission when the UE is at a greater distance than 410 meters from the BS. The best energy savings are achieved by the unrealistic FRN lower bound case and this is due to the fact that the optimally placed FRN efficiently compensates for the pathloss.

When the VPL is 10 dB (Figure 9-36), because more transmit power is needed to compensate the VPL, the average transmit power of all the schemes increase, except the MRN assisted transmission. As shown in Figure 9-36, the MRN outperforms the direct transmission and approaches the FRN lower bound. As the VPL keeps increasing, more interesting trends can be observed. Figure 9-37 shows the total average transmit power when VPL is 20 dB. In this case, the MRN assisted transmission requires the lowest overall average transmit power. Furthermore, as the FRN can effectively compensate the pathloss, the FRN assisted transmission requires lower overall average transmit power than the direct transmission, when the VUE is at a distance greater than 300 meters from the BS. We also observe that the overall average transmit power of MRN assisted transmission is even lower than the lower bound of the FRN case. This is mostly due to the fact that the MRN totally circumvents VPL.

**Table 9.6: The expectation of the overall average transmit power  $\bar{P}_D$ ,  $\bar{P}_M$  and  $\bar{P}_F$  of the system**

	$\bar{P}$ [dBm] VPL=0 dB	$\bar{P}$ [dBm] VPL=10 dB	$\bar{P}$ [dBm] VPL=20 dB
Direct Transmission $\bar{P}_D$	-10.38	-0.38	9.61
MRN case $\bar{P}_M$	-8.62	-8.62	-8.62
FRN optimized $\bar{P}_F$	-12.34	-5.93	1.60

In Table 9.6 we calculate the expectation of the overall average transmit power of the system under different values of VPL. When there is no VPL the FRN assisted transmission achieves the lowest expected value of the overall average transmit power, as the FRN can effectively compensate for the pathloss. But as VPL increases, the MRN case begins to outperform both the direct transmission and the FRN assisted transmission. This is because the MRN circumvents VPL while the other two schemes consume more transmit power to compensate for it. From the comparison between Figure 9-36 and Figure 9-37, and the results in Table 9.6, we can observe that the higher the VPL is, the more energy savings the MRN can achieve compared to the other two schemes.

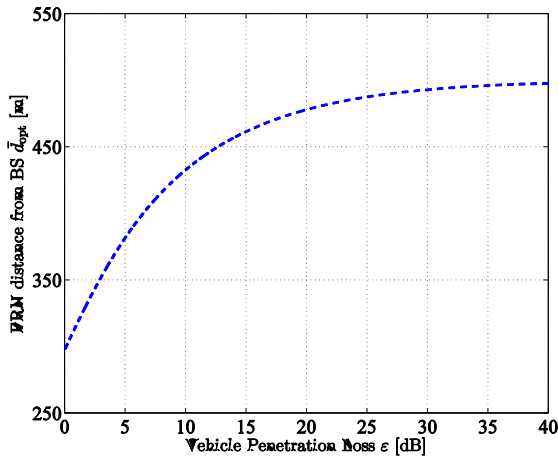


Figure 9-34: Optimal FRN position when the UE is uniformly distributed along the road

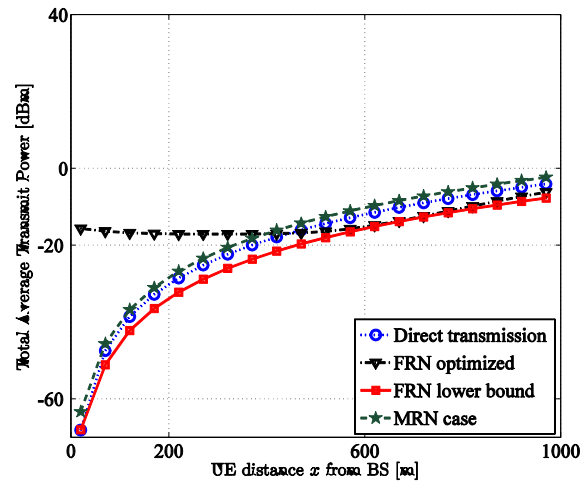


Figure 9-35: Minimum Total average transmit power with outage probability target of 0.05 when VPL = 0 dB

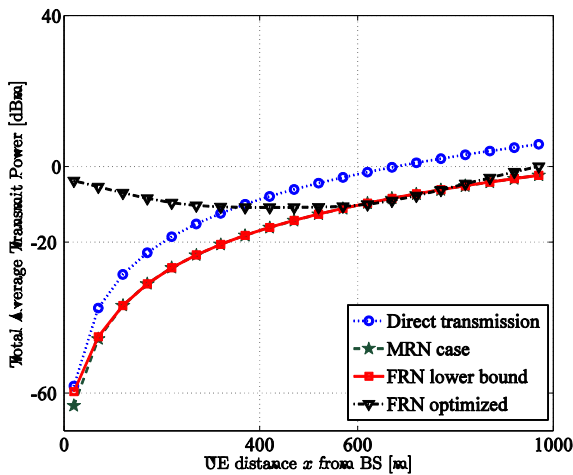


Figure 9-36: Minimum Total average transmit power with outage probability target of 0.05 when VPL = 10 dB

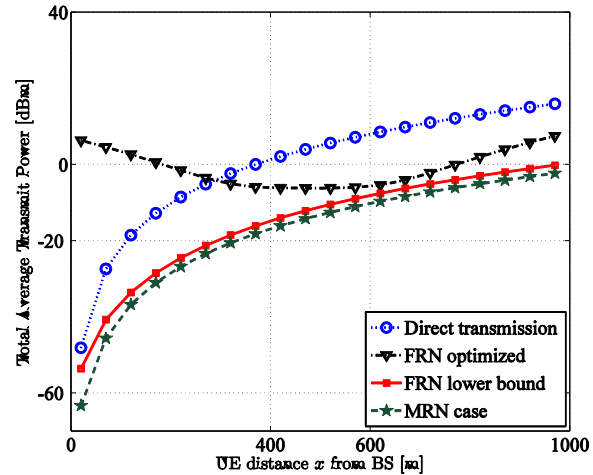


Figure 9-37: Minimum Total average transmit power with outage probability target of 0.05 when VPL = 20 dB

For the OP studies, we evaluate and compare vehicular UE's OP of the considered schemes, i.e., direct transmission and FRN and MRN assisted transmission. The employed evaluation parameters are based on [3GPP09-36814] and summarized in Table 9.7. The MRNs are placed on top of the vehicle and assumed to eliminate VPL.

We move UE1 from its serving BS to the cell edge and plot its OP for the considered setups. As shown from the results (Figure 9-38 - Figure 9-40), the vehicular UE is served by the BS when it is near to the serving BS and handed over to the FRN or MRN afterward. Regarding the MRN assisted transmission, it gives a lower OP at the vehicular UEs when the VPL is moderate to high.

As shown in Figure 9-38 - Figure 9-40, the OP at the UE of the MRN assisted transmission begin to approach the direct transmission when the VPL is 10 dB. But due to the half-duplex loss, there is still a small difference when the vehicular UE is handed over from the BS to the MRN. But the MRN gradually outperforms the direct transmission when the VPL increases. This can be clearly observed from Figure 9-35. The vehicular UE is served by the BS at the

beginning, and due to the HO hysteresis, it will not be handed over to the MRN until it is around 100 meters away from its serving BS. After performing the HO, the OP at the vehicular UE is significantly lower for the MRN assisted transmission compared to the direct transmission.

**Table 9.7: Simulation parameters**

	Value
Inter-site Distance	1732 meters
Average BS transmit power	46 dBm
Average FRN transmit power	30 dBm
Average MRN transmit power	20 dBm
Carrier Frequency	2.0 GHz
System Bandwidth	10 MHz
Receiver noise figure for both RN and UE	9 dB
Normalized Minimum Required Rate R at UE	1 bit/s/Hz

Furthermore, as expected in all the cases, because of the HO between BS and FRN, the FRN assisted transmission shows a better performance compared to the cases without HOs. There is a half-duplex loss of the FRN assisted transmission, but since the FRN can better compensate the pathloss, it serves the vehicular UE more efficiently when the UE is handed over to it. Nevertheless, on average, it still cannot outperform the MRN assisted transmission when the VPL is moderate to high. But since the FRN is not designed to serve vehicular UEs, such a behavior is not unexpected. It is worth mentioning that, we model the backhaul link of the FRN assisted transmission as LOS but its interference is modeled as NLOS. This is the best case one can expect for the FRN assisted transmission, but even with these assumptions, the contribution of FRN to the vehicular UE is very limited at moderate to high VPLs. Another thing that is worth mentioning is that the MRN is assumed to operate at a much lower transmit power than the FRN, but it serves vehicular UEs better than the FRN assisted transmission on average. Thus from an energy efficiency point of view, MRN is also a better choice for serving vehicular UEs.

For the energy saving part, the use of the MRN lowers the energy consumption in the system at moderate to high VPL, i.e., VPL from 10 to 30 dB. For the best case, i.e., when the VPL is 30 dB and the vehicle is at the cell edge, around the use of MRN can lower 80% total transmit power in the system. Detailed results in other situations are presented in Figure 9-35 - Figure 9-37.

For the power outage part, when there is no VPL, i.e., VPL is at 0 dB, there is no gain by using MRN assisted transmission. However, at a VPL of 10 dB, the MRN assisted transmission has almost the same performance as the baseline case. As the VPL keeps increasing, the use of MRN can lower the OP by 65% on average compared to the baseline case.

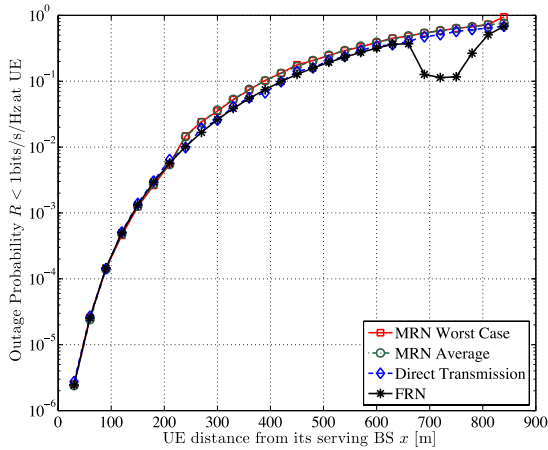


Figure 9-38: OP performance in an always dual-hop system with HO capabilities at VPL = 0 dB

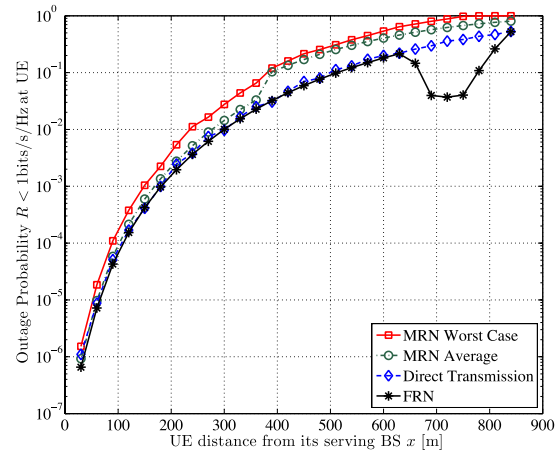


Figure 9-39: OP performance in an always dual-hop system with HO capabilities at VPL = 10 dB

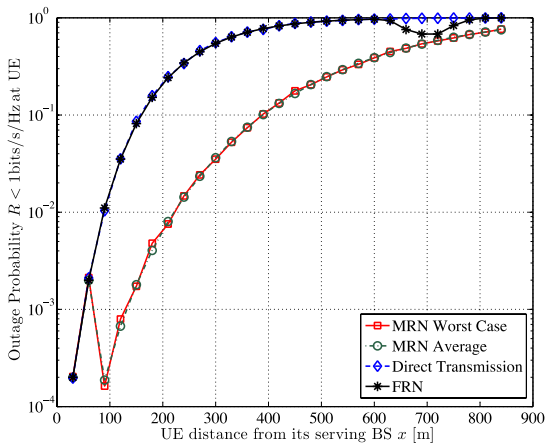


Figure 9-40: OP performance in an always dual-hop system with HO capabilities at VPL = 30 dB

### T3.3 TeC 9a – Studies of deploying moving relay nodes

T3.3 TeC 9a – Studies of deploying moving relay nodes	
	<p><b>Main Idea</b></p> <p>In the present of co-channel interference, the power outage probably of serving VUEs are compared between the use of FRNs, MRNs and direct transmission.</p> <p>The energy efficiency study between different schemes are conducted in a noise limited setup.</p>
<p>Considered SoA solution</p>	<p>VUE directly served by the BS is considered as the baseline case.</p>
<p>KPIs considered and achieved gain</p>	<ul style="list-style-type: none"> <li>Power outage probability at the VUEs. As the VPL keeps increasing, the use of MRN can lower the OP by 65% on average compared to the baseline case</li> </ul>



	<ul style="list-style-type: none"> <li>Total average transmit power in the system. For the best case, i.e., when the VPL is 30 dB and the vehicle is at the cell edge, around the use of MRN can lower 80% total transmit power in the system. Please refer to the explanation in text for details</li> </ul>
Performance evaluation approach	Analytical and Simulation-based (Static System level simulation)
System model considered	Other
Deviation compared to Simulation Baseline	Not Applicable since this is an initial proof of concept study.
Brief update of the results with respect to D3.2	The initial results of using MRNs are summarized both for OP and energy efficiency.
Association to the TeC Approach	Tech Approach 1: Heterogeneous network at lower frequencies (< 10GHz)
Targeted TCs	TC 2 and TC 8
Impacted HTs	MN
Required changes for the realization with respect to LTE Rel. 11	Minor
Trade-off required to realize the gains	A new type of node is introduced to the system, and therefore changes are expected in areas such as control channels, air interface and radio resource management.

### 9.10.3 Impact on Horizontal Topics

T3.3 TeC 9a - HT.MN	
Technical challenges	The QoS at VUEs can be improved, as well as the energy efficiency of the system.
TeC solution	Serving VUEs via MRNs
Requirements for the solution	Deploying MRNs on top of public transportation vehicles.
KPIs addressed and achieved gain	<ul style="list-style-type: none"> <li>Power outage probabilities</li> <li>Total average transmit power in the system</li> </ul>
Interaction with other WPs	<ul style="list-style-type: none"> <li>T2.1 TeC6.3: Air interface for MN - Predictor Antenna System</li> <li>T4.1-TeC8: Resource allocation scheme for moving relay nodes</li> <li>T4.1-TeC13: Interference Management for Moving Networks in Ultra-Dense Urban Scenarios</li> </ul>



**9.10.4 Addressing the METIS Goals**

T3.3 TeC 9a	
1000x data volume	
10-100 user data rate	Higher data rate at VUEs can be supported due to the significant improvement of the received SINR.
10-100x number of devices	
10x longer battery life	
5x E-E reduced latency	
Energy efficiency and cost	The total transmit power in the system can be significantly lowered, especially when the VUEs are affected by high VPL.

**9.10.5 References**

[G10] J. Gozalvez, “Green radio technologies,” IEEE Veh. Technol. Mag., vol. 5, pp. 9–14, Mar. 2010.

[LZD+12] W. Li, C. Zhang, X. Duan, S. Jia, et al., “Performance evaluation and analysis on group mobility of mobile relay for LTE-Advanced system,” in Proc. IEEE VTC 2012-Fall.

[PHY+10] V. V. Phan, K. Horneman, L. Yu, and J. Vihriala, “Providing enhanced cellular coverage in public transportation with smart relay systems,” in Proc. IEEE VNC, 2010.

[SPS12] Y. Sui, A. Papadogiannis, and T. Svensson, “The potential of moving relays—a performance analysis,” in Proc. IEEE VTC 2012-Spring.

[M10] A. F. Molisch, Wireless Communications. West Sussex, UK: John Wiley & Sons Ltd., 2nd edition ed., 2010.

[SPY+13] Y. Sui, A. Papadogiannis, W. Yang, and T. Svensson, “The Energy Efficiency Potential of Moving and Fixed Relays for Vehicular Users,” in Proc. IEEE VTC 2013-Fall.

[3GPP12-25996] 3GPP TR 25.996, “Spatial channel model for Multiple Input Multiple Output (MIMO) simulations,” tech. rep, Sep. 2012.

[3GPP12-36836] 3GPP TR 36.836, “Technical Specification Group Radio Access Network; Mobile Relay for Evolved Universal Terrestrial Radio Access (E-UTRA),” tech. rep, Oct 2012.

[TJV+08] E. Tanghe, W. Joseph, L. Verloock, and L. Martens, “Evaluation of vehicle penetration loss at wireless communication frequencies,” IEEE Trans. Veh. Technol., vol. 57, pp. 2036–2041, Jul. 2008.

[LZD+12] W. Li, C. Zhang, X. Duan, S. Jia, et al., “Performance evaluation and analysis on group mobility of mobile relay for LTE-Advanced system,” in Proc. IEEE VTC 2012-Fall.

[SGO+12] M. Sternad, M. Grieger, R. A. Olesen, T. Svensson, et al., “Using ‘predictor antennas’ for long-range prediction of fast fading for moving relays,” in Proc. IEEE WCNC Workshop, 2012.

[SW88] K. Sowerby and A. Williamson, “Outage probability calculations for multiple cochannel interferers in cellular mobile radio systems,” IEE Proceedings F Radar and Signal Processing, vol. 135, pp. 208 – 215, Jun. 1988.

[STB11] S. Sesia, I. Toufik, and M. Baker, LTE - The UMTS Long Term Evolution: From Theory to Practice. West Sussex, UK: John Wiley & Sons Ltd., 2nd edition ed., 2011.

[DWY+09] K. Dimou, M. Wang, Y. Yang, M. Kazmi, A. Larmo, J. Pettersson, W. Muller, and



**Document:** FP7-ICT-317669-METIS/D3.3

**Date:** 25/02/2015

**Security:** Public

**Status:** Final

**Version:** 1

---

Y. Timner, "Handover within 3GPP LTE: Design principles and performance," in Proc. IEEE VTC 2009-Fall, pp. 1 –5.

[JBT+10] T. Jansen, I. Balan, J. Turk, I. Moerman, et al., "Handover parameter optimization in lte self-organizing networks," in Proc. IEEE VTC 2010- Fall, pp. 1 –5.

[3GPP09-36814] 3GPP TR 36.814, "Evolved Universal Terrestrial Radio Access (E-UTRA); Further advancements for E-UTRA physical layer aspects," tech. rep, Mar. 2009.

## 9.11 T3.3 TeC 9b: Uplink enhancement of vehicular users by using D2D communications [CTH]

### 9.11.1 General Overview

In this study, we present a method to improve the energy efficiency of VUEs by D2D communication. The advantage of using D2D communication is that it demands no additional infrastructure node compared to using MRN. Thus, a quicker roll out can be expected, provided D2D will be supported by VUEs.

In this contribution, we argue that by exchanging data with each other using D2D communications, the VUEs can significantly reduce the radio frequency (RF) transmit energy for their uplink communications. We consider a scenario where several VUEs need to communicate with the BS. They can either communicate with the BS individually, or cooperate with each other for the uplink communication via a D2D service offered by the network. To this end, we compare the required overall RF transmit energy, including the RF energy for D2D communication, of the considered uplink cooperating scheme with individually VUE-to-BS communication. We show that when a public transportation vehicle is far away from the BS, and the communication is affected by high VPL, by cooperating with each other, the expended energy for each VUE is lower than the direct VUE-to-BS communications. This is very beneficial from an energy efficiency point of view, especially for the VUEs that operate with limited battery lives.

We consider a noise limited system with frequency flat fading, where a BS has a fixed coverage of  $D$  meters. This assumption may be extended to wideband systems with frequency-selective fading through orthogonal frequency-division multiple access (OFDMA). In an OFDMA based system, this can be seen as a subchannel or a subchannel group whose bandwidth is much smaller than the coherence bandwidth. We assume  $m$  out of  $n$  VUEs are active and need to send data to the BS. In this study, we assume each active VUE has a reasonable large amount of data to send to the BS, e.g., sending emails with big attachments. The communication takes place in two steps: 1) each VUE exchange its data with all other VUEs by using D2D communication; 2) VUEs cooperate together to send the data to the BS.

We assume all the VUEs are transmitting at their maximum power to communicate with the BS. Then, the objective is to maximize the received signal-to-noise-ratio (SNR) at the BS, so that the total data rate can be increased. Hence, it takes less time for the active VUEs to send the same amount of data. With channel state information at transmitter (CSIT) and in the absence of a per-terminal transmit power constraint, the received SNR can be maximized by employing the maximum ratio transmission (MRT) scheme [Lo99], where a single data stream is transmitted by all the VUEs that participate in the communication. However, MRT tends to allocate most of the power to a few VUEs with better channel conditions, which may violate the power constraints for some of the VUEs [LHW07]. By just regulating the transmit power given by the MRT solution according to the maximum transmit power constraint results in significant performance degradation, since the received SNR is no longer maximized.

In order to satisfy the per-terminal transmit power constraint, we employ a generalized co-phasing scheme introduced in [LNC+09]. With CSIT, the generalized co-phasing scheme aligns the phases of the transmit signals of each of the VUEs with each other, and maximize the received SNR at the BS. The detailed formulation of the optimization problem can be found in [ST13].

### 9.11.2 Performance Results

We evaluate the energy efficiency performance of the considered schemes by using system level evaluations. The employed evaluation parameters are based on [3GPP11-25996], [3GPP13-R1130925], and are summarized in Table 9.8. VUEs are located inside a public transportation vehicle, and several of the VUEs need to send data to the BS. Only VUEs that require uplink communication are assumed to participate in the cooperation. This is a realistic

assumption, as it is difficult to motivate that idle VUEs with no communication should participate in the cooperation. Each of the VUEs could communicate with the BS directly (baseline case), or different number of VUEs can cooperate with each other by using D2D communications. In cooperation, based on the size of an average city bus, we assume a maximum distance of 5 meters between the two furthest VUEs participants. One physical resource block (PRB), which is the smallest scheduling grant, is used for the VUE-to-BS communication, and 10 PRBs are allocated for the D2D communication. This is motivated by the fact that user devices are usually limited by their transmit power, and in practical systems, e.g, the LTE system, user devices can concentrate their power in a small bandwidth to maximize the coverage [STM11, Chapter 18]. However, compared to VUE-to-BS communication, for D2D communication, as VUEs are located near to each other, the communication is unlikely to be limited by power. Thus, wider bandwidth and lower transmit power is assumed in this study for D2D communication.

**Table 9.8: Simulation parameters**

Parameter	Value
Carrier frequency	2.6 GHz
Cell radius	866 meters
VUE to BS pathloss model	$L_{dB} = 39.1 + 35.1 \log_{10}(d)$
D2D pathloss model	$L_{dB} = 41.1 + 16.9 \log_{10}(d_{UE})$
D2D fading margin	20 dB
VUE to BS transmit power	23 dBm
D2D transmit power	10 dBm
Receiver noise figure at the BS	5 dB
Receiver noise figure at the VUE	9 dB
PRB size	180 kHz
Traffic model	Full buffer

Figure 9-41 and Figure 9-42 plot the average expanded energy per information bit when different numbers of VUEs cooperate with each other in the cases of VPL equal to 20 dB, and 30 dB. As we can see from both figures, for the cooperative transmissions, the more VUEs participate in the cooperation, the lower the energy spent on the communication. However, when VPL is 20 dB, the individual direct communication of each VUE with the BS costs less energy than the cooperating transmission. This is because the energy saved by the VUE cooperation is less than the energy overhead introduced by the D2D communication.

Nevertheless, when the communication is affected by higher VPL, i.e, 30 dB, the energy saving of using VUE cooperation can be observed, as the public transportation vehicle is moving away from the BS. This is due to the fact that VUEs are power limited for uplink communications. When the VPL is high, the communications are conducted in a power-limited region, and therefore even if two VUEs cooperate, it results in a significant increase of data rate. Thus, in this case all active VUEs can send their data faster, and spend less energy in total even when including the overhead caused by D2D communication.

There is no gain if the VPL is at 20 dB (see Figure 9-41).

However, when the VPL is at 30 dB, there are gains when the vehicle is more than 500 meters away from the BS. For a cooperation between 2 VUEs, at the cell edge, at most 35% energy saving can be observed compared to the baseline case. For a cooperation involving 8 VUEs,

at the cell edge, up to 70% energy saving can be observed compared to the baseline case. Details of the results are presented in Figure 9-42.

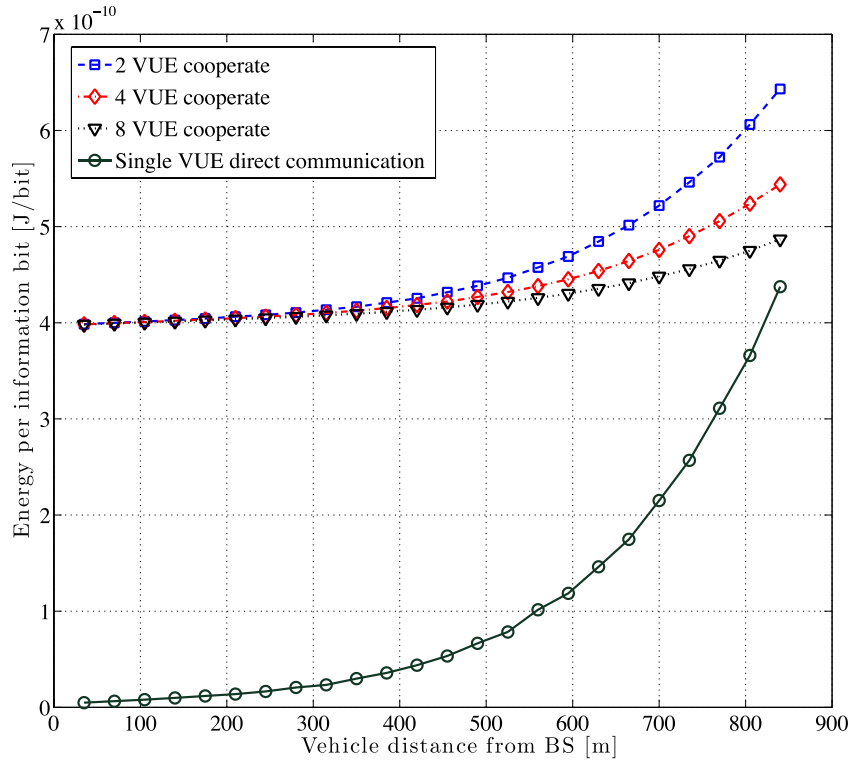


Figure 9-41: Energy per information bit when VPL = 20 dB

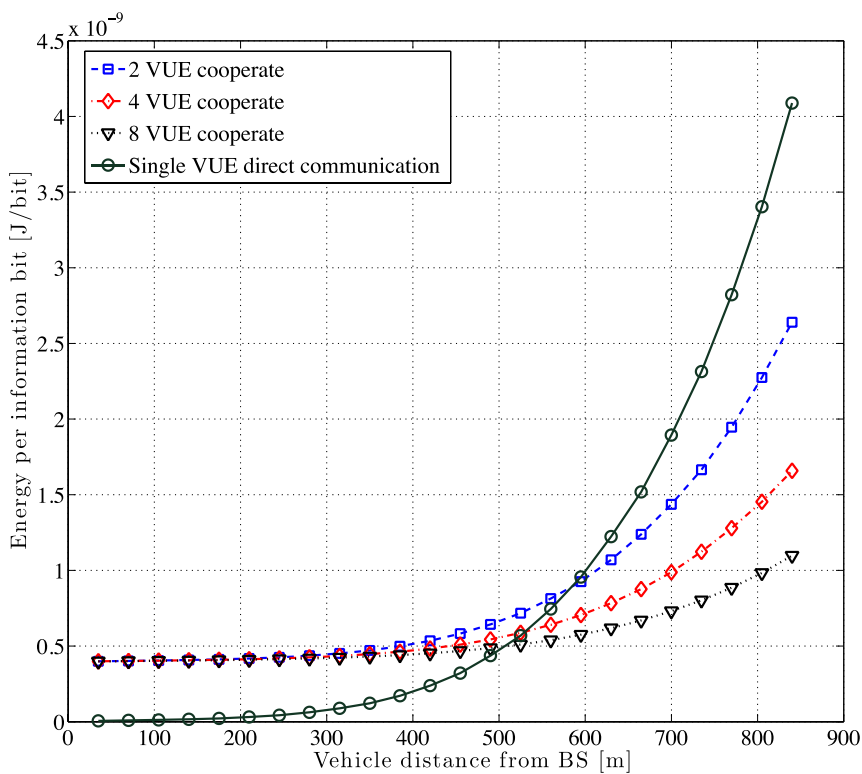
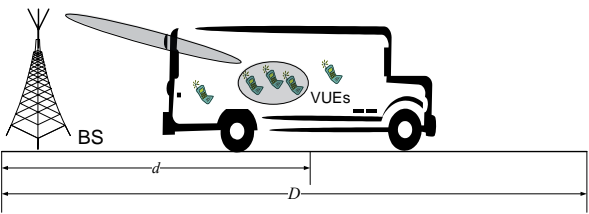


Figure 9-42: Energy per information bit when VPL = 30 dB

### T3.3 TeC 9b – Uplink Enhancement of Vehicular Users by Using D2D Communications

	<p style="text-align: center;"><b>Main Idea</b></p> <p>There are <math>n</math> VUEs in a bus. We assume <math>m</math> out of <math>n</math> VUEs are active and need to send data to the BS.</p> <p>By using D2D communication, the <math>m</math> VUEs can exchange data with each other, and cooperate to communicate with the BS.</p> <p>In this way, less energy is required to send the same amount of data of each active VUE in the cooperative transmission than the individual VUE-to-BS communications.</p>
<p>Considered SoA solution</p>	<p>VUEs communicate with the BS directly without cooperation with each other.</p>
<p>KPIs considered and achieved gain</p>	<p>Energy spent on per information bit [J/bit]. For a cooperation between 2 VUEs, at the cell edge, at most 35% energy saving can be observed compared to the baseline case. Please refer to the explanation in text for details.</p>
<p>Performance evaluation approach</p>	<p>Simulation-based (Static System level evaluation)</p>
<p>System model considered</p>	<p>Other</p>
<p>Deviation compared to Simulation Baseline</p>	<p>Significant As this study is only a proof of concept, we only consider a single cell, noise limited system with frequency flat fading.</p>
<p>Brief update of the results with respect to D3.2</p>	<p>Not Applicable</p>
<p>Association to the TeC Approach</p>	<p>Not Applicable</p>
<p>Targeted TCs</p>	<p>TC8</p>
<p>Impacted HTs</p>	<p>D2D, MN</p>
<p>Required changes for the realization with respect to LTE Rel. 11</p>	<p>Major</p>
<p>Trade-off required to realize the gains</p>	<p>In order to realize the gain, both user and channel information needs to be exchanged between all participated VUEs. Therefore, the overhead of D2D communication needs to be considered.</p>

#### 9.11.3 Impact on Horizontal Topics

<b>T3.3 TeC 9b - HT.D2D</b>	
<p>Technical challenges</p>	<p>QoS at VUEs</p>
<p>TeC solution</p>	<p>The received SNR at the BS can be significantly improved by enabling D2D cooperation between VUEs</p>
<p>Requirements for the solution</p>	<p>Both user and channel information needs to be exchanged between all participated VUEs. D2D</p>



	communication capability of VUEs.
KPIs addressed and achieved gain	Energy spent on per information bit can be lowered significantly.
Interaction with other WPs	Not Applicable

T3.3 TeC 9b - HT.MN	
Technical challenges	Requiring to build new infrastructures
TeC solution	By using D2D communication, no network infrastructures are needed
Requirements for the solution	Both user and channel information needs to be exchanged between all participated VUEs. D2D communication capability of VUEs.
KPIs addressed and achieved gain	Energy spent on per information bit can be lowered significantly.
Interaction with other WPs	Not Applicable

#### 9.11.4 Addressing the METIS Goals

T3.3 TeC 9b	
1000x data volume	
10-100 user data rate	
10-100x number of devices	
10x longer battery life	
5x E-E reduced latency	
Energy efficiency and cost	Energy spent on per information bit can be lowered significantly.

#### 9.11.5 References

[Lo99] T. Lo, "Maximum ratio transmission," *IEEE Trans. Commun.*, vol. 47, pp. 1458–1461, Oct. 1999.

[LHW07] S.Liu, Z.He, and W.Wu, "Transmit diversity method with user 's power constraint for distributed antenna system," in *Proc. 2nd ISWPC 2007*.

[LNC+09] J. Lee, R. Nabar, J. Choi, and H.-L. Lou, "Generalized co-phasing for multiple transmit and receive antennas," *IEEE Trans. Wireless Comm.*, vol. 8, pp. 1649–1654, Apr. 2009.

[ST13] Y. Sui, and T. Svensson, "Uplink Enhancement of Vehicular Users by Using D2D Communications", in *Proc. IEEE Globecom workshop, 2013*.

[3GPP11-25996] 3GPP TR 25.996, "Spatial channel model for Multiple In- put Multiple Output (MIMO) simulations", 2011.

[3GPP13-R1130925] Intel Corporation, "3GPP R1-130925, evaluation methodology for d2d discovery," 2013.

[STM11] S. Sesia, I. Toufik, and M. Baker, *LTE-The UMTS Long Term Evolution: From Theory to Practice*, 2nd ed. John Wiley & Sons Ltd., 2011.

## 9.12 T3.3 TeC 10: MIMO techniques for TDD wireless systems with relaying [PUT]

### 9.12.1 General Overview

In this TeC we consider the two-way relaying system, as shown in Figure 9-43 that comprises one relay station (RS), such that the base station (BS) can communicate through the relay with mobile stations (MSs). As compared to the previous research [RBW14], the number of mobile stations in the considered scheme is increased from one to two. In the proposed scheme two time slots are needed in TDD mode to exchange data blocks between end stations: multiple access slot (MA) and broadcast slot (BR).

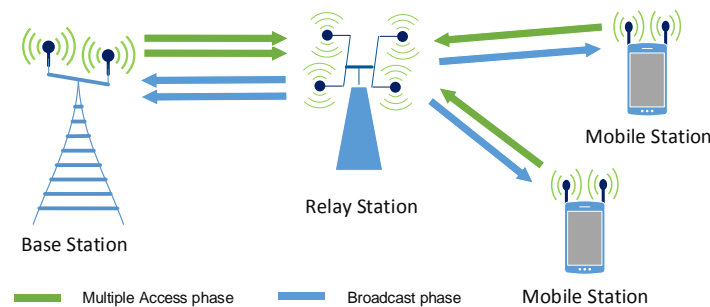


Figure 9-43: Considered two-way relaying scheme

In the MA phase the BS and the MSs transmit their data to RS. All stations use the same time and frequency resources during transmission. The RS jointly detects both data blocks using MIMO (Multiple Input Multiple Output) technique and finds information blocks transmitted by these stations. In the broadcast phase (Figure 9-44) the RS forwards received in the previous phase data blocks to each end station. Two out of four transmit antennas at the RS are used for the transmission to BS (SU-MIMO transmission), another two antennas handle joint transmission to both mobile stations (MU-MIMO transmission). Two separate transmission schemes (SU-MIMO and MU-MIMO) performed on the same time and frequency resources, results in the appearance of interfering signals at each of the receiving nodes. Presented scheme requires the implementation of interference cancellation receivers to enable the correct reception of the data signal.

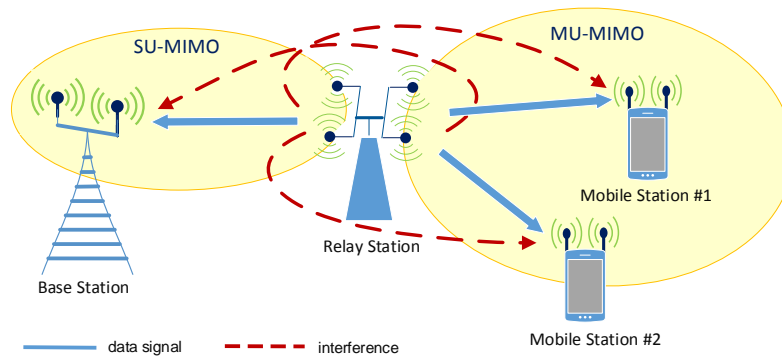


Figure 9-44: Broadcast phase

Several interference cancellation receivers for the BR phase, have been implemented and compared. All implemented interference cancellation receivers, made use of MMSE equalization. In the first verified reception algorithm, we assumed that the receiver knows the interfering signal. The received data signal may be then obtained by subtracting the

interference from the received signal. This idealized receiver is called MMSE-SIC-IDEAL (SIC – Successive Interference Cancellation).

In case of the realistic MMSE-SIC and MMSE-IC (IC – Interference Cancellation) receivers, the interference is unknown. If we assume that the number of receiving antennas is higher or equal to the number of streams transmitted on the same resources, then all streams are decodable. After the MMSE equalization, data symbols and interference symbols are obtained. In case of MMSE-IC algorithm, interference is ignored, and data symbols are processed and decoded. In case of MMSE-SIC algorithm, decoded interfering signal is multiplied by the channel matrix and then subtract from the received signal, giving the pure data signal. The MMSE equalization is then repeated.

In order to obtain better reconstruction of the interfering signal in the MMSE-SIC algorithm, the received interference may be decoded to the vector of bits and then encoded again to the vector of symbols. The algorithm that performs this steps is called MMSE-SCIC (SCIC – Successive Corrected Interference Cancellation). In the proposed scheme MMSE-SCIC is used at the MS receiver (the interference received at the BS is a linear combination of two interfering signal that cannot be decoded to vector of bits).

The last implemented algorithm is called MMSE-ASCIC (ASCIC – Advanced SCIC) and it is the extension of the MMSE-SCIC algorithm. In the described two-way relaying scheme the interfering signal received by the end node in the broadcast phase, consists of the signal that was transmitted by this station during the previous phase. MMSE-ASCIC algorithm makes use of that observation and reconstructs this part of the interference perfectly. MMSE-ASCIC was developed for the BS and MSs, but it works a bit differently depending on the receiver type. In case of the BS all interfering streams are reconstructed perfectly, in case of the MS only one interfering stream.

### 9.12.2 Performance Results

We consider a simplified system model with one base station, one relay station and two mobile stations. Results were obtained for the EPA 5 Hz (Extended Pedestrian A Model) radio channel fading model [3GPP11-36101, Annex B]. The existing 3GPP LTE system (Rel-10/11) with a reasonable density of access points (eNB, Relay, HeNB/WiFi) and certain specified RRM schemes (e.g., proportional fair scheduling, partial frequency reuse, eICIC) can be considered as legacy networks. The considered scheme assumes that the MS is allowed to work in the time reversed mode (it can transmit when other MSs receive and vice versa) and that BS is able to simultaneously receive signals from different subcarrier blocks, modulated both in OFDMA and SC-FDMA mode.

In this section, the performance of the considered scheme will be presented as a result of multi-link level simulations. Two-way relaying in the system with basic features of the LTE system was modelled. QPSK modulation was applied in both transmission directions in which OFDM and SC-FDMA symbols are generated. Results were obtained for the EPA 5 Hz (Extended Pedestrian A Model) radio channel fading model.

The end-to-end performance analysis of the bidirectional relaying is presented in Figure 9-45 to Figure 9-48. Figure 9-45 compares the BLER performance of idealized MMSE-SIC algorithm for different number of receive antennas. With the increasing number of the receive antennas the probability of block errors decreases, as expected. The comparison of the realistic interference cancellation algorithms will be presented for the four receive antennas at the BS and MSs.

Figure 9-46 shows the BLER performance of the MMSE-SIC and MMSE-IC algorithms in comparison to MMSE-SIC-IDEAL receiver. It can be seen that the erroneous reconstruction of the interfering signal degrades the system performance (even 4 dB decrease). Moreover, there is no significant difference between MMSE-SIC and MMSE-IC algorithm.

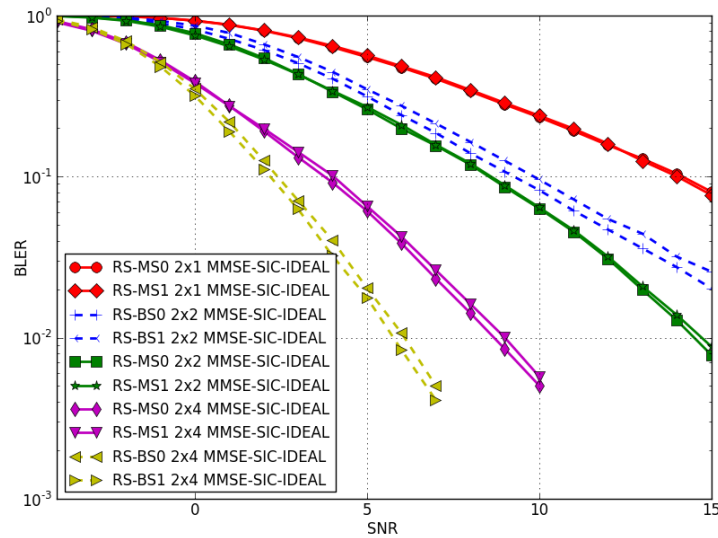


Figure 9-45: Idealized receiver, different number of receive antennas at the BS and MSs

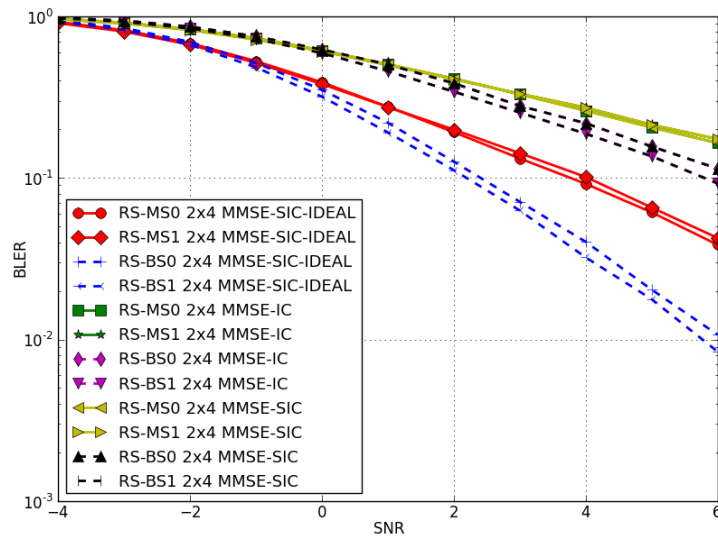


Figure 9-46: Comparison of the idealized receiver and realistic MMSE-SIC and MMSE-IC.

The comparison of all implemented for the MSs' receivers is presented in Figure 9-47. Additional processing incorporated to the MMSE-SCIC and MMSE-ASCIC receivers results in significant system performance increase. The best results achieved for the MMSE-ASCIC receiver.

Figure 9-48 shows the BLER performance of the MMSE-ASCIC receiver in comparison to MMSE-SIC, MMSE-IC and idealized MMSE-SIC receiver at the BS. It can be seen that the performance of the proposed MMSE-ASCIC algorithm outperforms the well-known MMSE-SIC and MMSE-IC algorithms. The BLER of the MMSE-ASCIC is close to MMSE-SIC-IDEAL algorithm – for the SNR higher than -2 dB, there is no significant difference between those two receivers.

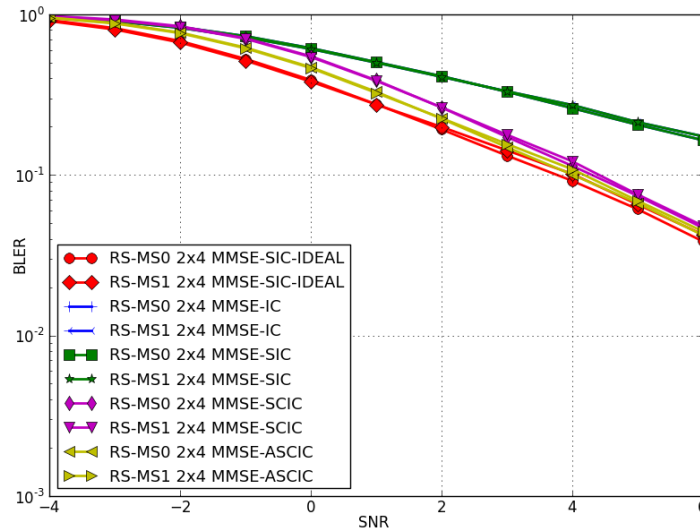


Figure 9-47: Comparison of all IC algorithms at the MSs

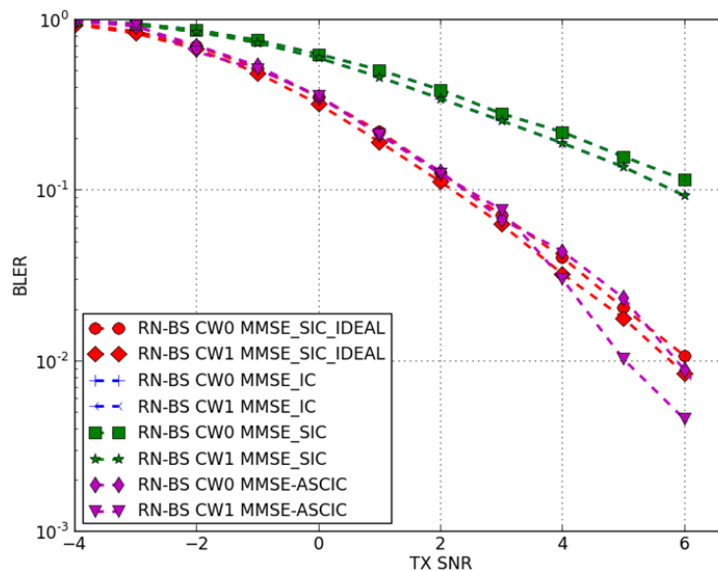


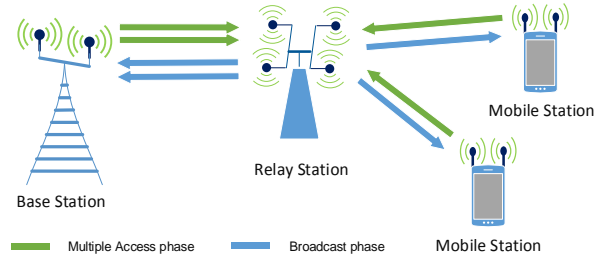
Figure 9-48: Comparison of all IC algorithms at the BS

The classical two-way relaying scheme requires four timeslots to complete messages exchange between BS and MS. When enhanced two-way relaying schemes like Virtual-MIMO and NC/MU-MIMO are applied, the number of required timeslots decreases to two timeslots. Thanks to that, within the same period of time, the number of transmitted messages is doubled. This may result in the throughput increase, by up to 100% (200% of the original value). When an additional MS is served by the two-way relaying scheme, the number of required timeslots remains the same, but the number of exchanged messages increases from two to three, giving up to 50% (150% of the original value) increase in throughput and up to 200% (300% of the original value) in comparison to classical, four timeslots two-way relaying.

### T3.3 TeC 10 – MIMO in TDD system with relaying

#### Main Idea

Two data streams for the base station (BS),

 <p>One relay station with a two-way traffic between base station and two mobile stations. All nodes interfere with each other.</p>	<p>and one data stream for each mobile station (MS) are transmitted jointly through relay station (RS) in two transmission phases. In the first phase, the BS and each MS transmit their data streams to RS. Multiple antennas at the RS are used to separate received data blocks. In the second phase, RS jointly transmits data streams intended for the BS, using two transmit antennas and spatial multiplexing scheme. Two data streams intended for mobile stations are transmitted using another two antennas and MU-MIMO scheme with ZF precoding. The end stations receivers must receive their data signals in the presence of the significant interference.</p>
<p>Considered SoA solution</p>	<p>The existing 3GPP LTE system (Rel-10/11) with a reasonable density of access points (eNB, Relay, HeNB/WiFi) and certain specified RRM schemes (e.g., proportional fair scheduling, partial frequency reuse, eICIC) can be considered as legacy networks.</p>
<p>KPIs considered and achieved gain</p>	<ul style="list-style-type: none"> <li>• User throughput: compared to classical 2-way relaying scheme increases by 300%, and compared to the previously investigated scheme increases by 100%.</li> <li>• Air Delay: compared to classical 2-way relaying scheme decreases by 50% (from 4 to 2 slots) compared to the previously investigated scheme decreases by 0 %.</li> </ul>
<p>Performance evaluation approach</p>	<p>Simulation-based, Multi-link level evaluation</p>
<p>System model considered</p>	<p>Other</p>
<p>Deviation compared to Simulation Baseline</p>	<p>At the moment we consider a simplified system model with one base station, one relay station and two mobile stations. We use channel models such as EPA, ETU and EVA.</p>
<p>Brief update of the results with respect to D3.2</p>	<p>Additional mobile station was added to the previously considered scheme. More data streams need to be transmitted within two transmission phases.</p>
<p>Association to the TeC Approach</p>	<p>Heterogeneous network at lower frequencies (&lt; 10GHz)</p>
<p>Targeted TCs</p>	<p>TC 7 – “Blind Spots”</p>
<p>Impacted HTs</p>	<p>MN</p>
<p>Required changes for the realization with respect to LTE Rel. 11</p>	<p>Minor. The considered scheme assumes that the MS is allowed to work in the time reversed mode.</p>
<p>Trade-off required to realize the gains</p>	<p>The gains achieved in throughput and delay are obtained thanks to multiple antennas in all stations and increased computational complexity of the BS and MSs receivers.</p>

**9.12.3 Impact on Horizontal Topics**

<p style="text-align: center;"><b>T3.3 TeC 10 - HT.MN</b></p>	
<p>Technical challenges</p>	<ul style="list-style-type: none"> <li>• Robust and high-data rate communication links.</li> <li>• Interference management schemes</li> </ul>



	<ul style="list-style-type: none"> <li>• Reduced delay</li> </ul>
TeC solution	In the TeC 10 three end nodes exchange messages via the relay station. Transmission is divided into two phases. Simultaneously transmitted signals during the second phase cause interference to the other nodes. In the proposed solution, interference is suppressed by the advanced interference cancellation receivers. The delay is reduced by applying only two phases.
Requirements for the solution	<ul style="list-style-type: none"> <li>• UE mobility limited</li> <li>• Hotspots mobility limited</li> <li>• Multiple antennas available at the RS, BS and MSs</li> </ul>
KPIs addressed and achieved gain	<ul style="list-style-type: none"> <li>• Latency, Expected Gain 50%</li> <li>• Experienced user throughput, Expected Gain 50-75%</li> </ul>
Interaction with other WPs	<ul style="list-style-type: none"> <li>• WP2 – new waveforms may modify the performance of the proposed techniques,</li> <li>• WP4 – interference management schemes that may be applicable,</li> <li>• WP5 – new spectrum that may be applicable,</li> <li>• WP6 – simulation guidelines for system level simulations of TeC 10.</li> </ul>

### 9.12.4 Addressing the METIS Goals

T3.3 TeC 10	
1000x data volume	
10-100 user data rate	Increase in the achieved user rate (up to 200% gain).
10-100x number of devices	Increase in number of served users (from one to two – x2).
10x longer battery life	
5x E-E reduced latency	The E-E latency reduced from 4 or 3 time slots to 2 time slots.
Energy efficiency and cost	

### 9.12.5 References

[RBW14] K. Ratajczak, K. Bąkowski, and K. Wesolowski, "Two-way Relaying for 5G Systems - Comparison of Network Coding and MIMO Techniques", IEEE Wireless Communications and Networking Conference, IEEE WCNC 2014, 6-9 April 2014, Istanbul, Turkey.

[3GPP11-36101] "User Equipment radio transmission and reception", 3GPP TS 36.101, V10.5.0, Dec. 2011.

## 10 Appendix D: List of Specific METIS Abbreviations

### 10.1 List of METIS WP3 partners

Abbreviation	Full Name
AAU	Aalborg University Denmark
ALU	Alcatel-Lucent Deutschland AG.
CTH	Chalmers University of Technology
DOCOMO	DOCOMO Japan
EAB	Ericsson AB
FT	France Telecom
HHI	Henrich Hertz Institute
HWDU	Huawei Technologies Duesseldorf GmbH
KTH	Royal Institute of Technology Sweden
NOKIA	Nokia Oyi
NSN	Nokia Networks
PUT	Poznan University of Technology
RWTH	RWTH Aachen University
TI	Telecom Italia
UB	University of Bremen
UOULU	University of Oulu Finland
UPVLC	Universidad Politecnica de Valencia
UU	Uppsala University (Third party of CTH)

### 10.2 List of METIS Horizontal Topics

Abbreviation	Full Name
D2D	Direct Device to Device
MMC	Massive Machine Communication
MN	Moving Networks
UDN	Ultra Dense Networks
URC	Ultra Reliable Communications

### 10.3 List of METIS Test Cases

Abbreviation	Full Name
TC1	Virtual reality office
TC2	Dense urban information society
TC3	Shopping mall
TC4	Stadium
TC5	Teleprotection in smart grid network
TC6	Traffic jam
TC7	Blind spots
TC8	Real-time remote computing for mobile terminals
TC9	Open air festival
TC10	Emergency communications
TC11	Massive deployment of sensors and actuators
TC12	Traffic efficiency and safety